



Useful strategy in the design of energy-efficient buildings using innovative daylighting systems

Hyun Joo Han, BSc, MSc

Thesis submitted to the University of Nottingham
for the degree of doctor of philosophy

Department of Architecture and Built Environment

July 2010

ABSTRACT

This research work has been carried out to utilize daylight more effectively for indoor illumination in an energy efficient building without any compromise on indoor environmental quality; especially the visual comfort on task plane. Two different daylighting systems have been designed and constructed, and a series of tests have been performed to assess their photometric characteristics as well as their performance. A typical system considered has an optic concentrator capable of tracking the sun and making high density fluxes of solar rays. It consists of either dish or funnel shaped concentrators followed by optical fiber cables and diffusers at the end. The design of a dish concentrator (diameter less than 30 cm) is prepared by rotating a simple parabolic profile in compliance with the major physical requirements. This geometrical simplicity has also been applied for the design of a funnel shaped concentrator created by combining two parabolas. When the sunlight is highly focused, it is then redirected and undergoes a number of reflections to enter a light guide for its final transmission to the terminal device. The light reaching the terminal device finally gets consumed by the interior of a building for indoor illumination.

The active daylighting system considered in this study offers substantial advantages over conventional solar designs in its fabrication, installation, operation, and utilization of the sun's energy. The proposed daylighting system is durable and suited to economical operation for different schemes of indoor illumination of buildings. Each component of the system could be made from off-the-shelf technology, thus making the generic unit inexpensive to manufacture. Depending on spatial demand or characteristics, the amount of daylight introduced could be controlled without undue difficulties.

To assess the photometric characteristics of a daylighting system, goniophotometer and spectrometer measurements are made, which provided its luminous intensity distribution and

spectral radiance. The spatial distribution of light emerging from the optical cable is examined by monitoring the workplane illuminances for the mock-up spaces in Nottingham (UK) and Jeju (Korea). Six different types of terminal devices (optical lenses, light rod) are also examined experimentally to elicit the most optimal design for use with a daylighting system. Of those tested, the circular shape acrylic rod spreads out the light most widely followed by semi-concave lens whereas the semi-convex lens has shown the smallest light spreading ability. The test results have revealed some distinctive features of the present dish-daylighting system in bringing natural daylight to non-daylit areas or interior spaces too deep for conventional daylighting apertures. Especially, it proved the effectiveness of the system when applied for individualized lighting allowing individual control over the amount of light in space and to suit individual preferences for lighting conditions. Experimental data from measurements are further extended to develop the numerical models with RADIANCE and ECOTECH for theoretical predictions under different situations.

The image of luminance ratio maps generated by RADIANCE and the fish-eye photographs of the sky were conducive to realistic assessment of possible glare reduction and uniformity improvement not just for the task plane but also for its surroundings. There were some appreciable changes made in the indoor luminance distribution thanks to our daylighting system. It has clearly demonstrated its functional reliability and usefulness to control brightness and thus promote indoor visual environment.

TABLE OF CONTENTS

ABSTRACT ----- ii

TABLE OF CONTENTS ----- iv

LIST OF FIGURES ----- vi

LIST OF TABLES ----- xii

NOMENCLATURE ----- xiii

ACKNOWLEDGMENTS ----- xiv

CHAPTER

1.INTRODUCTION ----- 1

 1.1 Background ----- 1

 1.2 Recent Work in Energy Efficient Buildings----- 2

 1.3 Wherefore Daylight ----- 4

 1.4 Daylight for Energy Efficiency ----- 5

 1.5 Daylighting Technologies ----- 6

 1.6 Research Objectives ----- 27

 1. 7 Summary ----- 30

2. DESIGN AND CONSTRUCTION OF THE SYSTEM----- 31

 2.1 Dish Concentrator ----- 31

 2.1.1 Prototype design----- 31

 2.1.2 Optical analysis using PHOTOPA ----- 39

 2.2 Funnel Shaped Concentrator ----- 44

 2.3 System Configuration and Control ----- 46

 2.4 Construction of Prototype Systems ----- 48

 2.5 A Comparative Analysis and Solar Availability ----- 52

 2.6 Summary ----- 59

3. PHOTOMETRY MESURING INSTRUMENTS ----- 60

 3.1 Luminance Meter ----- 60

 3.2 Spectrophotometer ----- 63

 3.3 Spectracolorimeter ----- 64

 3.4 Goniophotometer----- 66

3.5 FLIR i40 Thermal Camera ----- 73

4. PERFORMANCE ASSESSMENT

(MEASUREMENTS AND SIMULATION) ----- 76

4.1 Nottingham Test Chamber ----- 76

4.2 An Office Building Unit ----- 89

4.3 Test Cells in Jeju ----- 97

4.3.1 Construction of the test cells ----- 97

4.3.2 Basic measurements ----- 99

4.3.3 Temperature measurements ----- 104

4.3.4 Illuminance measurements ----- 107

4.3.5 Photometric analysis by RADIANCE ----- 116

4.3.6 Hybrid lighting ----- 140

4.3.7 A comparative analysis using RADIANCE ----- 147

4.4 Summary ----- 167

5. CONCLUSIONS ----- 168

6. BIBLIOGRAPHY ----- 171

7. APPENDIX (Goniophotometer Measurements) ----- 177

7.1 Semi-concave Lens ----- 178

7.2 Concave Lens ----- 197

7.3 Semi-convex Lens ----- 216

7.4 Convex Lens ----- 235

7.5 Acrylic Rod ----- 253

LIST OF FIGURES

FIGURE

1. 1	Research procedure -----	29
2. 1	The design concept of the dish-daylighting system using different second mirrors(reflectors): (a) flat mirror, (b) convex(concave) mirror -----	32
2. 2	Positioning of the second reflector and basic geometry of the dish concentrator -----	34
2.3	Parabola used for the dish concentrator of 30cm -----	34
2.4	Parabola used for the dish concentrator of 15cm -----	35
2.5	Equation of the parabola used for the second reflector -----	36
2.6	Three dimensional design images of the major components and the system (a) (parabolic) dish reflector (b) second reflector (c) concentrator assembly-----	37
2.7	Engagement of the dish reflector (concentrator) with light guides -----	38
2.8	3D modeling by Rhinoceros -----	39
2.9	Modeling of the dish concentrator -----	40
2.10	Convex mirror (model designed for PHOTOPIA simulation) -----	41
2.11	An image of the illuminance distribution at the exit of the homogenizer tube -----	42
2.12	Concave mirror (model designed for PHOTOPIA simulation) -----	43
2.13	A curved profile of the funnel shape concentrator -----	44
2.14	A three-dimensional image of the funnel shape concentrator. -----	45
2.15	Concept of systm configuration -----	46
2.16	Control logic of the dish concentrators -----	47
2.17	Dish reflectors made of aluminum block -----	48
2.18	The second reflector made of aluminum -----	49
2.19	The dish concentrator assembly and tracker (a) the dish concentrator assembly (b) the whole system (c) the tracker (major components are displayed) -----	50

2.20	The funnel shape concentrator and the daylighting system	
	(a) the concentrator and homogenizer (before assembled)	
	(b) the funnel shape concentrator with homogenizer (assembled)	
	(c), (d) different views of the daylighting system -----	51
2.21	Incident solar radiation on a surface element dA from (θ, φ) direction -----	52
2.22	Solar flux on a vertical surface(window) pointed south -----	54
2.23	Ratio of incident solar radiation available on the dish concentrator and window -----	58
3.1	LS-100 Luminance meter -----	60
3.2	Measuring luminance -----	61
3.3	Measuring luminance and illuminance -----	62
3.4	S-3100 system -----	63
3.5	PR-650 Spectracolorimeter -----	64
3.6	Spectral radiance measured -----	64
3.7	Goniophotometer measurements for luminous intensity distribution:	
	(a) test kit with a 50W halogen lamp	
	(b) cylindrical diffuser mounted on goniophotometer -----	66
3.8	Luminous intensity distribution of the convex lens:	
	(a) 2D	
	(b) 3D -----	67
3.9	Luminous intensity distribution of the semi-convex lens:	
	(a) 2D	
	(b) 3D -----	68
3.10	Luminous intensity distribution of the concave lens:	
	(a) 2D	
	(b) 3D -----	69
3.11	Luminous intensity distribution of the semi-concave lens:	
	(a) 2D	
	(b) 3D -----	70
3.12	Luminous intensity distribution of a cylindrical diffuser:	
	(a) 2D	
	(b) 3D -----	71
3.13	Rendered image of light -----	72
3.14	FLIR i40 thermal camera -----	73

4.1	Test chamber at Nottingham	
	(a) built	
	(b) virtual model -----	76
4.2	Interior view of the test module for simulation -----	77
4.3	Luminous intensity distribution for semi-convex lens (lowest 10%) -----	79
4.4	Sensor locations -----	80
4.5	Simulation values of sensors at noon (at the location of sensors) -----	81
4.6	Simulation values of sensors at noon (at nodal points of equal distance) ----	82
4.7	Simulated results by RADIANCE (reflectance=0.1) -----	83
4.8	Simulated results by RADIANCE (reflectance=0.85)-----	84
4.9	Luminance map of the sky when measurements were made (partly cloudy) --	85
4.10	Perspective views of solar availability for the test chamber at different times of the year (equinoxes and solstices) with sun path diagrams -----	87-88
4.11	A picture of the office and its plan view -----	89
4.12	Fisheye photograph and luminance of the sky by RADIANCE -----	90
4.13	Fisheye photograph and luminance of the east wall and the working table near the south window by RADIANCE -----	90
4.14	Fisheye photograph and luminance ratio map of the task plane and its surroundings by RADIANCE -----	91
4.15	(a) task plane, (b) its luminance ratio map (by RADIANCE) -----	92
4.16	(a) luminance values, (b) illuminance ratio map (by RADIANCE) -----	93
4.17	Modeling of the room for simulation -----	94
4.18	Locations of photo sensors -----	95
4.19	Simulated results by RADIANCE (two emitters) -----	96
4.20	Plan view of the test cell-----	97
4.21	Two identical test cells built for performance assessment of daylighting systems :	
	(a) test cells	
	(b) daylighting system with dish concentrator installed on top	
	(c) daylighting system with funnel shape concentrator installed on top ----	98
4.22	Illuminance ratio of daylighting systems with different shapes of solar concentrators : dish, funnel shape-----	100
4.23	Transmitting efficiency of an optical fiber and liquid light guide cable ----	100
4.24	Measuring the beam and diffuse component of illuminance (a)	

	solar radiation (b) -----	101
4.25	Variation of the global total and diffuse illuminance at different times on a cloudy (a) and clear day (b) -----	102
4.26	Global illuminance and irradiance for different sky conditions: (a) clear sky, (b) intermediate sky -----	103
4.27	Results of temperature monitoring on a clear day (10/6) : temperature variation of each sensor at various times of the day (a), temperature sensor(k-type thermocouple) location (b) -----	104
4.28	Thermal image by FLIR camera for two test cells at 9:37 and 11 :35 hours: test cell w/o (a), (c) and with the daylighting system (b), (d) -----	106
4.29	Iso-illuminance contour plots with the convex lens to diffuse sunlight : (a) 2D, (b) 3D -----	107
4.30	Illuminance distribution when two acrylic rods (sand-blasted) are used to diffuse sunlight for indoor illumination: (a) sky condition when measured, (b) light diffused from the rod, (c) and (d) luminance distribution -----	108
4.31	Illuminance at each location of the photo sensor at 13:00 hour on a clear day (10/6): without (a) and with (b) a daylighting system -----	109
4.32	Average illuminance ratio of two test cells at different times of the day on a clear day (10/6) -----	110
4.33	Illuminance ratios at each location of the sensor at different times of the day (10/6) -----	110
4.34	Illuminance at each location of the photo sensor at noon on a clear day (10/4): without (a) and with (b) a daylighting system (slats are adjusted to a horizontal, level position) -----	111
4.35	Illuminance at each location of the photo sensor at 14:00 hours on a clear day (10/5): without (a) and with (b) a daylighting system (tilted upward at 45 degrees for both test cells) -----	112
4.36	Illuminance at each location of the photo sensor at 11:40 hours on a clear day (10/8): without (a) and with (b) a daylighting system (For both cells: venetian blinds on top – rolled up, venetian blinds below - slats closed) ---	114
4.37	Illuminance at each location of the photo sensor at 14:00 hours on a clear day (10/9): without (a) and with (b) a daylighting system (For both cells: venetian blinds on top – closed, venetian blinds below - tilted upward at 45 degrees) -----	115

4.38	Sky luminance map at different hours : 9:00 am, 10:30 am, noon, 2:30 pm--	119
4.39	Luminance and illuminance distributions without [(a),(b), (c), (d)] and with [(c), (d), (e), (f)] at 9:00am -----	121
4.40	Luminance and illuminance distributions without [(a),(b), (c), (d)] and with [(c), (d), (e), (f)] at 10:30am-----	122
4.41	Luminance and illuminance distributions without [(a),(b), (c), (d)] and with [(c), (d), (e), (f)] at noon -----	123
4.42	Luminance and illuminance distributions without [(a),(b), (c), (d)] and with [(c), (d), (e), (f)] at 2:30pm -----	124
4.43	Luminance and illuminance distributions without [(a),(b), (c), (d)] and with [(c), (d), (e), (f)] at 4:00pm -----	125
4.44	A general view of the model image of the test cell for RADIANCE simulation -----	126
4.45	A perspective view of the model image for RADIANCE simulation -----	126
4.46	Luminance and illuminance distribution superimposed on the rendered image by RADIANCE (without the daylighting system) : 9:00am -----	128
4.47	Luminance and illuminance distribution superimposed on the rendered image by RADIANCE (with the daylighting system) : 9:00am -----	129
4.48	Luminance and illuminance distribution superimposed on the rendered image by RADIANCE (without the daylighting system) : 10:30am -----	130
4.49	Luminance and illuminance distribution superimposed on the rendered image by RADIANCE (with the daylighting system) : 10:30am-----	131
4.50	Luminance and illuminance distribution superimposed on the rendered image by RADIANCE (without the daylighting system) : noon -----	133
4.51	Luminance and illuminance distribution superimposed on the rendered image by RADIANCE (with the daylighting system) : noon -----	134
4.52	Luminance and illuminance distribution superimposed on the rendered image by RADIANCE (without the daylighting system) : 2:30pm -----	135
4.53	Luminance and illuminance distribution superimposed on the rendered image by RADIANCE (with the daylighting system) : 2:30pm-----	136
4.54	Luminance and illuminance distribution superimposed on the rendered image by RADIANCE (without the daylighting system) : 4:00pm -----	138
4.55	Luminance and illuminance distribution superimposed on the rendered image by RADIANCE (without the daylighting system) : 4:00pm -----	139

4.56	A test cell built for hybrid lighting (dimming control) : plan view and venetian blinds installed for the window -----	141
4.57	Location of sensors on the floor and dimming control on the ceiling -----	142
4.58	Actual illuminance map of the test cell when lit by the daylighting system: (a) Iso-illuminance contour, (b) sky condition when measured, (c) actual interior view when lit -----	143
4.59	Actual illuminance map of the test cell when lit by the artificial lighting system: (a) Iso-illuminance contour, (b) sky condition when measured, (c) actual interior view when lit-----	144
4.60	A dimmer unit with four light blocking covers : covers 1 , 2 – partial blocking, cover 3-complete blocking, cover 4 – no blocking -----	146
4.61	March 20, 12:00 pm, Seoul (luminance) -----	149
4.62	March 20, 12:00 pm, London (luminance) -----	150
4.63	March 20, 12:00 pm, Seoul (illuminance) -----	151
4.64	March 20, 12:00 pm, London (illuminance) -----	152
4.65	June 21, 12:00 pm, Seoul (luminance) -----	153
4.66	June 21, 12:00 pm, London (luminance) -----	154
4.67	June 21, 12:00 pm, Seoul (illuminance) -----	155
4.68	June 21, 12:00 pm, London (illuminance) -----	156
4.69	September 22, 12:00 pm, Seoul (luminance) -----	158
4.70	September 22, 12:00 pm, London (luminance) -----	159
4.71	September 22, 12:00 pm, Seoul (illuminance) -----	160
4.72	September 22, 12:00 pm, London (illuminance) -----	162
4.73	December 22, 12:00 pm, Seoul (luminance) -----	163
4.74	December 22, 12:00 pm, London (luminance) -----	164
4.75	December 22, 12:00 pm, Seoul (illuminance) -----	165
4.76	December 22, 12:00 pm, London (illuminance) -----	166

LIST OF TABLES

TABLE

1.1	Active daylighting systems	-----	9
1.2	Passive daylighting systems	-----	17
1.3	Building-integrated daylighting systems	-----	21
2.1	Major design variables for the dish concentrator of 30cm	-----	35
2.2	Major design variables for the dish concentrator of 15cm	-----	36
2.3	Major design variables for the second reflector	-----	36
2.4	Available solar radiation and angles on a tilted surface on 01/03/2009	-----	55
2.5	Available solar radiation and angles on a tilted surface on 02/04/2009	-----	56
2.6	Available solar radiation and angles on a tilted surface on 01/03/2009	-----	57
3.1	Some major features of PR-650 SpectraColorimeter	-----	65
3.2	FLIR i49 Specifications	-----	74
4.1	Results(illuminance in lux) comparison at 12:00 P.M.	-----	79
4.2	Surface reflectivity of the room	-----	94
4.3	Comparison between the measured and simulated results	-----	95
4.4	Solar radiation data for Seoul and London at equinoxes and solstices at noon	-----	147

NOMENCLATURE

A	area, m^2
E	illuminance, lux
L	luminance, cd/m^2
x	horizontal distance, cm
y	vertical distance, cm
θ	polar angle measured from normal of surface, angle of incidence
φ	circumferential angle
R	radius, cm
ω	solid angle or hour angle
I	radiation intensity
Q	energy rate, energy per unit time
δ	declination, $-23.45^\circ \leq \delta \leq 23.45^\circ$
ϕ	latitude, $-90^\circ \leq \phi \leq 90^\circ$
β	slope, $0^\circ \leq \beta \leq 180^\circ$
γ	surface azimuth angle, $-180^\circ \leq \gamma \leq 180^\circ$
P	optical path
ρ	reflectivity

Subscripts and superscripts

i	incident
e	emitted or emitting

ACKNOWLEDGMENTS

This doctor's degree thesis could not have been put together if not for the many who cooperated to use their specialties to create it; not unlike how a building is constructed by assembling countless individual blocks.

While I was working to get this degree, I encountered several difficulties. I am thus overwhelmed with joy to receive it at last.

My gratitude goes to Professor Saffa B. Riffat, who provided me with an opportunity to pursue my studies by making it possible for me to get a PhD degree. Further thanks are extended to Dr. Yuehong Sue for his kind support and precious comments.

Dr. Sang Hoon Lim at the National Research Foundation(NRF) went extra distance to help me throughout this work. The researchers at the Electric Energy and Lighting Research Center of KIER, led by Dr. Soo Bin Han, spent their precious time to advise and assist me during my experiment. Further thanks are extended to Prof. Li Shao , who gave me the right direction for its theoretical development at the beginning stage of this work.

Many people among the School of the *Built Environment* at the University of Nottingham and Mr. Spencer Dutton, who recently wrapped up his PhD work, also deserve my appreciation. The technical assistance of those at the *Alternative Energy Research Laboratory* at Cheju National University should not be left out in receiving my gratitude, as well.

Finally I wish to thank my family and especially my beautiful daughter, Isabell, who I love the most. The devoted and constant support of my husband, Wongee, has been vital to the completion of this research. I cannot thank him enough for always being so helpful and encouraging, particularly during the writing of the thesis. He was always there for me when I was going through hard times.

Through all these times, God gave me the strength and courage to carry on, and for that I am grateful. I hope to become a ray of light to those in darkness.

1. INTRODUCTION

1.1 Background

The statistics show that Europe and Asia are responsible for more than seventy percent of the amount of carbon release in the atmosphere. The situation is worsening and there has been little relief done since the Kyoto Protocol in 1997. Burning fossil fuels has steadily increased the carbon dioxide content in the air, which progressively contributed to climate changes around the world causing floods and other natural catastrophes. Global warming has now become a global warning such that everyone agrees on the need for immediate action, especially, by the leading industrialized nations such as UK, USA, China, Japan and etc.

Many can be done to ameliorate the situation by reducing the use of fossil fuels in various areas. Of these, a great deal of contribution could be made in the area of building energy by operating more energy efficient and sustainable buildings. It is estimated that around 80% of the UK electricity is generated by burning fossil fuels and 20% of the electricity generated is used for indoor lighting. The situation is quite similar in Korea except its comparatively heavier dependency on nuclear energy(~20%). Nevertheless, the country still imports about 97% of its total energy needs from abroad.

It is the responsibility of building designers, especially, architecture and lighting engineers to minimize electricity consumption whilst, at the same time, to deliver a high-quality lit environment for the occupant it aims to serve. This clearly requires a progressive design strategy incorporating energy efficiency, renewable energy and sustainable building design schemes, which deem essential in its design of an efficient building. Energy-efficient buildings, generally, reduce both resource depletion and the adverse environmental impacts of pollution generated by energy consumption. They are designed to control, collect, and store the sun's energy to optimum advantage on the basis of establishing an integrated, whole-building design which includes heating, cooling, and lighting.

The most important condition for determining the application domain of a low-energy design is whether it is well matched with the other elements of the system to produce an energy efficient building that satisfies both environmental and functional needs of its users, rather than where it should be installed. In other words, it is not the separate components and materials that matter the most, but the capacity of the various parts to work together to achieve the desired results.

A low-energy design process could begin with energy efficient lighting as it requires concomitant design considerations on heating and cooling. It generally pays particular attention to solar design strategies including building orientation and glazing for indoor illumination. This is because no artificial lighting is as energy-efficient and healthy as natural daylight. There are currently active, passive and hybrid schemes available for daylighting applied in harmony with artificial lighting. Depending on its lighting efficiency, it could consume substantially less electricity without compromising occupant comfort or the building's functionality.

1.2 Recent Work in Energy Efficient Buildings

Owing to the energy crises and urgency of global warming and other environmental concerns, green/sustainable building- the synonym of today's high-performance building [Lerum 2008; Yudelso 2007] – has become a fast-moving movement across most of the world in recent years. (Strictly speaking, the word “green” does not include the full meaning of sustainability as was pointed out in [ASHRAE 2006]. Sustainability is maintaining ecological balance. On the other hand, some characteristics of green design such as indoor environmental quality have no impact on maintaining ecological balance.) The LEED (Leadership in Energy and Environmental Design) rating systems and design guides for green buildings developed by the U.S. Green Building Council (USGBC) were cited and discussed in most new architecture or green building books [e.g., Bonda]. For a building to be rated or certified as green or high-performance, it must score higher than

standard (or code) buildings in several categories such as water and energy efficiencies, indoor environmental quality, and conservation of materials and resources [Yudelso 2007]. Of these, energy efficiency is one of the most significant indicators when evaluating the sustainability performance of an architectural design. Energy and economic considerations are taken into account more rigorously in determining the sustainability of a building.

Large and ever-increasing numbers of books, reports, and papers on energy efficient buildings have been published since 1990s. The major publishers and/or contributors of this topic include EEBA (Energy Efficient Building Association), USGBC, US DOE, and ASHRAE in the United States, and their equivalent institutes or counterpart organizations in other countries. Companies, organizations, or websites with the ancient Greek OIKOS in their names focus on ecology and sustainability, and are also good sources for information about energy -efficient buildings and residential houses. Some educational institutes have published their faculty's notes and work for students interested in improving building energy efficiency. Juodis' book is one of the latest self-study books intended to assist architecture students in designing buildings that meet both efficient energy use and architectural requirements [Juodis 2007].

In the United States, Energy Star (a US government –backed program to identify and promote energy- efficient products [Bonda 2007])-qualified homes must be at least 15 % more energy – efficient than homes built to the 2004 International Residential Code. Each Energy Star rated residential house is estimated to save about 2000 kWh (kilowatt-hours) of electricity annually [Yudelso 2008]. As of the year 2007, there were no international standards established for building energy performance [Lerum 2008]. At present, building annual energy consumptions still vary significantly among developed countries. For instance, the annual specific energy use of educational buildings in the United States was about 250 kWh/m² in 1999. In comparison, school buildings in Norway were required to meet a predicted annual specific energy use of about 110 kWh/m² by the year of 2009 [ASHRAE 1999; Lerum 2008].

A variety of innovative ideas and methods have been developed and tested lately for improving the energy efficiencies of building heating, lighting and air conditioning systems led by BRE and research institutions in UK [BRE 2007; Communities and Local Government Publications 2008]. Architectural designs for reduced heating and cooling loads and illumination costs, such as sun-facing glazing and sunshades and deflectors, have been extensively studied on today's high- performance buildings [ARUP 2001]. Especially, innovative low-energy building designs applying the distributed energy generation concept were developed to improve the energy efficiency and/or reduce greenhouse gas emissions and environmental impacts of existing buildings and residential houses. Much emphases were made to match the energy demand by resorting to renewable resources along with the adaptation of buildings to climate change (e.g., green retrofit-buildings).

1.3 Wherefore Daylight

Daylight has the wavelengths between 350 nm to 700 nm and it is a minor fraction of the solar spectrum which appears visible and naturally-adapted to the human eyes. Thus, daylight is the datum against which how we view things and provides a comparison of colors and brightness. Architecturally, a well-designed building has major consideration for natural light penetration into the interior and, the skillful deposition of daylight into key interior spaces may dictate how the façade of a building is formalized. Hence, the harvesting and deposition of daylight into the interior of buildings is often deemed as a critical element in the design of buildings of high architectural quality.

Daylight is the healthiest and most efficient naturally available light source around us, which is also renewable and free. The provision of daylight in a building is linked to the spatial and architectural design, namely- windows and surfaces are visually expressive and thus, it should be of interest to the architects and building owners. On the other hand, the lack of daylight exposure may cause physical, mental and emotional well-being of a person. For

example, the Seasonal Affective Disorder (SAD) or commonly known as 'Winter Blues', affects many people during the winter period. Daylight exposure is an effective cure for SAD where a patient is simple exposed a bright light environment (about 2500 lux) for an hour or so per day. Domestic or office lighting only provides 200-500 lux on average.

The provision of daylight in a building is strongly linked to the spatial and architectural design. Unlike other environmental services, the elements of daylighting - windows and surfaces - are surely the most visual and expressive. For this reason windows have a long history of attention from Architects; indeed, architectural style has been defined by patterns of fenestration probably more than by any other single characteristic. It should be of interest then, to the architect, that daylighting design also has a strong influence on both the energy use of a building and general comfort and well-being of the occupants.

1.4 Daylight for Energy Efficiency

Throughout human history, daylight has played an essential role for its survival. Daylight was the only source of light and energy before the advent of fire and electricity where humans started to look for other means to supplement daylight. Despite many inventions achieved by human ingenuity, daylight is still considered as one of the most important factors in our daily lives. Daylight is the highest quality and most efficient light and energy source naturally available that is not just free but clean and inexhaustible.

Daylighting can save energy and our environment. If applied appropriately, it could displace the use of electrical energy and fossil fuels that will definitely add more CO₂ in the atmosphere. Almost half the energy spent in the UK is used up in buildings, and one third in non-domestic buildings. As such, reducing the energy use in these buildings is crucial, as many are aware, for lessening the total amount of energy consumed and of CO₂ emitted, and thus the effects of energy use on the environment.

The UK Government's has recently announced its ambitious plan to reduce the national carbon dioxide (CO₂) emissions by 80% till 2050. It has also identified and call for

improvement in energy requirements for buildings as space heating, cooling and indoor illumination make the significant proportion of the country's CO₂ emissions. There has been an even tougher proposition made to reduce CO₂ by 25% (from 2006 levels) before 2010 and 44% reduction by 2013 and for all new homes to be zero carbon by 2016. The "zero carbon" definition has not yet been fully agreed and leaves much room for discussion involving various sectors of society. Nevertheless, it is imperative to take the first step on the journey towards zero carbon buildings.

Daylighting has been a part of built form for a long time to provide heat and illumination for buildings. Although there has been a period of artificial lighting by fluorescent lamps in most buildings thanks to cheap energy prices, the need to use daylight has existed during most of architectural history. Especially, these days where greater emphasis is being laid on sustainable development, the use of daylight has become more important and meaningful for environmental and energy(cost) reasons. Good daylighting not just affects a building's interior spatial characteristics but also increases its energy efficiency and sustainability.

These days, Asian and European countries are leading the way in developing innovative architectural designs that include extensive use of daylighting and passive solar strategies. Increasing energy efficiency and sustainability are clearly the major motivating factors not mentioning the issue of health and well-being of occupants.

1.5 Daylighting Technologies

From a designer's point of view, it is always possible to harvest daylight and introduce deep into a space of a building while controlling the space or target brightness within the users' fields of vision. Such designs could be made with both human comfort and energy efficiency as key design parameters. If there were even daylight distribution throughout a space with constant intensity by controls, one can say that the full benefits of the day-lighting design is realized. The implementation process could be difficulty as there could be solar intensity variation with time of day, leading to over-illumination in some parts of the room.

However, a proper selection of the transmission system would ensure only “cold” light reaching the room spaces and thus eliminating the heating effects from the long waves. The over-illumination by “cold” light may cause unnecessary glare in the space, causing some discomfort to occupant but designers often may use an “iris” design at the harvester for glare control, in particular for wavelength sensitive applications such as the art galleries and museum. In some applications, designers may deliberately incorporate gradual variation in lighting levels to simulate the actual outdoor environment. Many buildings in UK simply use shading controls to cut out direct radiation and allow only diffuse light to enter a room at ambient level. This seems to be quite efficient as sufficient amount of cooling loads are reduced and glares lessened.

As daylighting displaces indoor electric lights for some part of the day, it can save energy. The technology for a complete day-lighting system can be categorized into the following sections:

- (i) The harvester design,
- (ii) The transmission design,
- (iii) The luminaries design.

Within the harvesters, there are both the passive and active systems: Passive systems are generally less efficient but they are comparatively cheaper and simpler to install. For example, a light-tube or light-pipe could be placed on the roof to harvest the diffuse and beam radiation. Active systems are different from passive ones in that passive systems are stationary and do not actively follow or track the sun. They generally require mechanical components and power to drive them, which make them more complex and expensive. Active systems are, however, more efficient and allows flexibility in harvesting sunlight.

There are various ways to transmit sunlight to where it is consumed. The simplest one is to use a duct with shiny inner surfaces. Optical fibers or liquid light guides could also be employed for its transportation without undue difficulties. Depending on its operating temperature, different kinds of optical fibers and light guides are applied with active

daylighting systems.

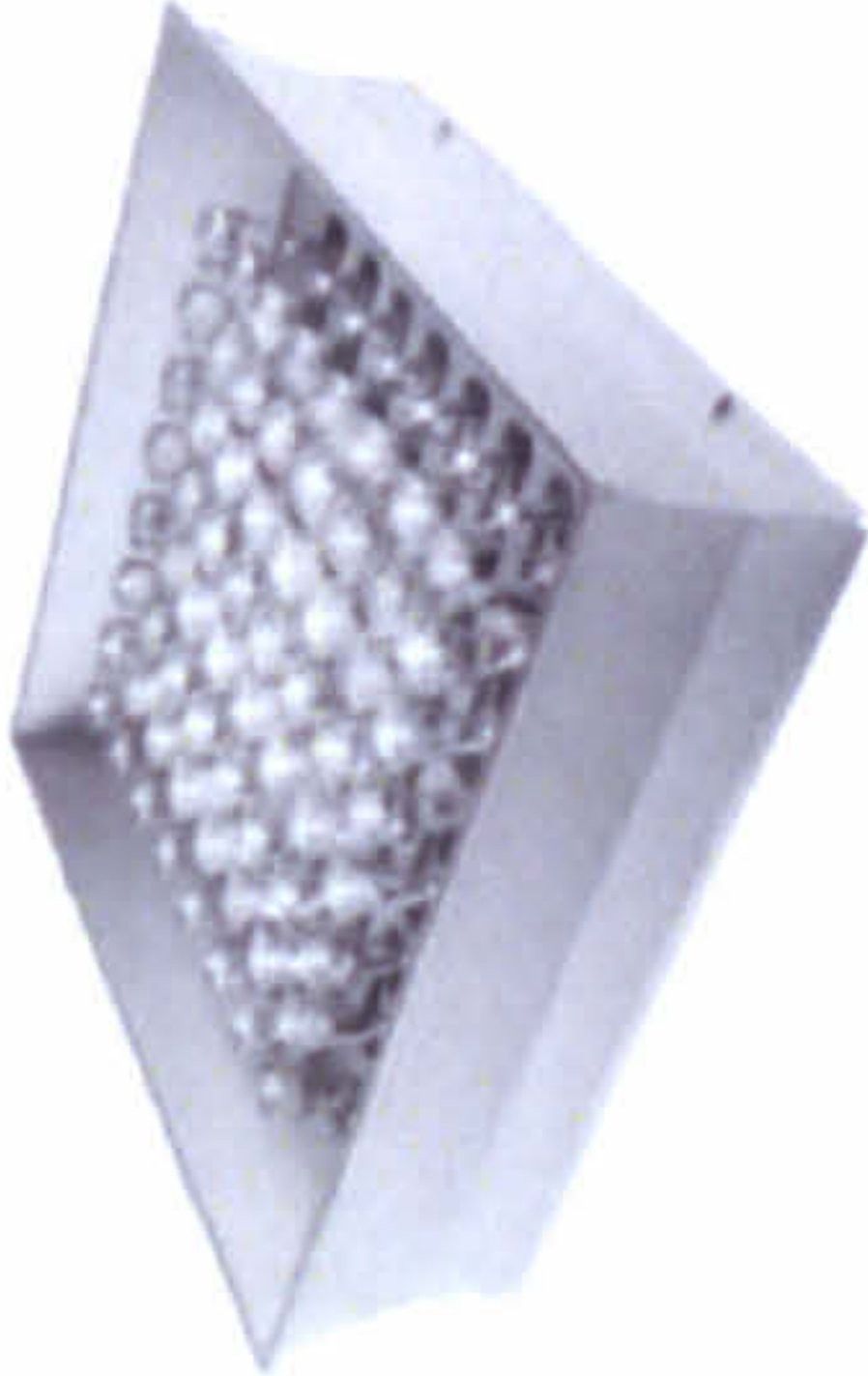
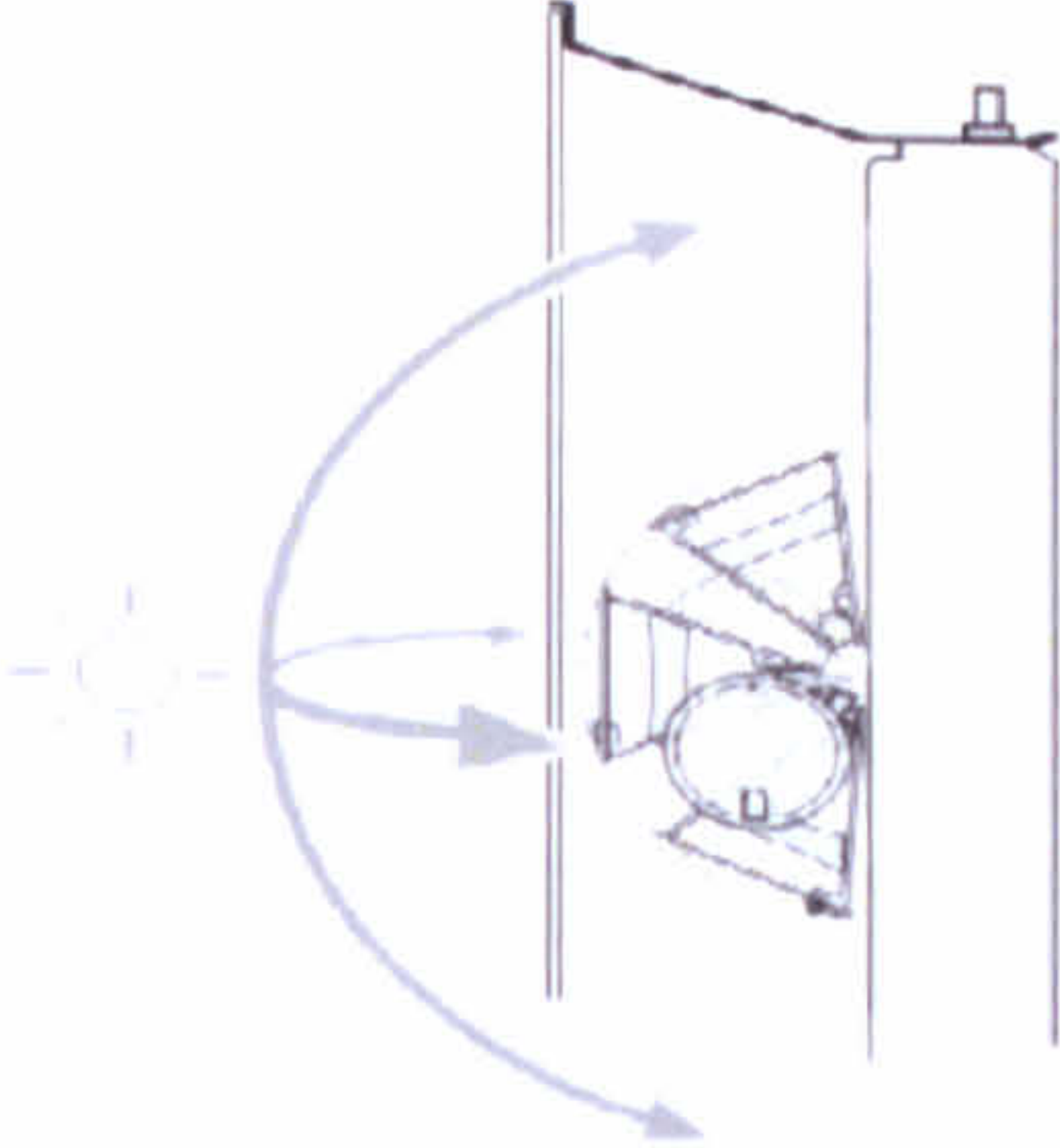

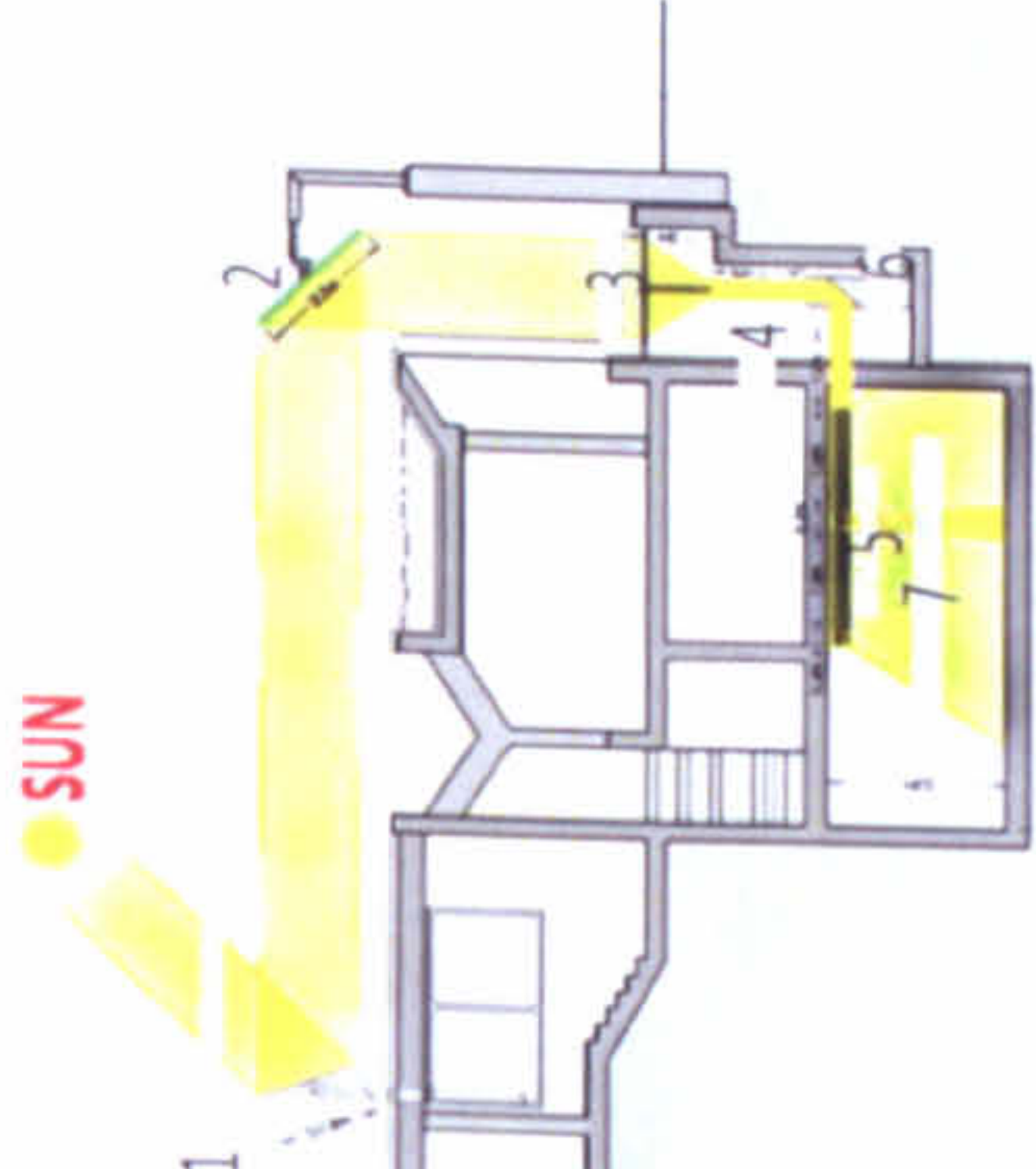
Tables 1.1, 1.2 and 1.3 show different types of daylighting schemes harnessing sunlight for interior illumination. For convenience, the systems are divided into three categories: active, passive and building-integrated daylighting systems. The systems introduced in these tables are mostly commercialized ones and could be found in many literatures.


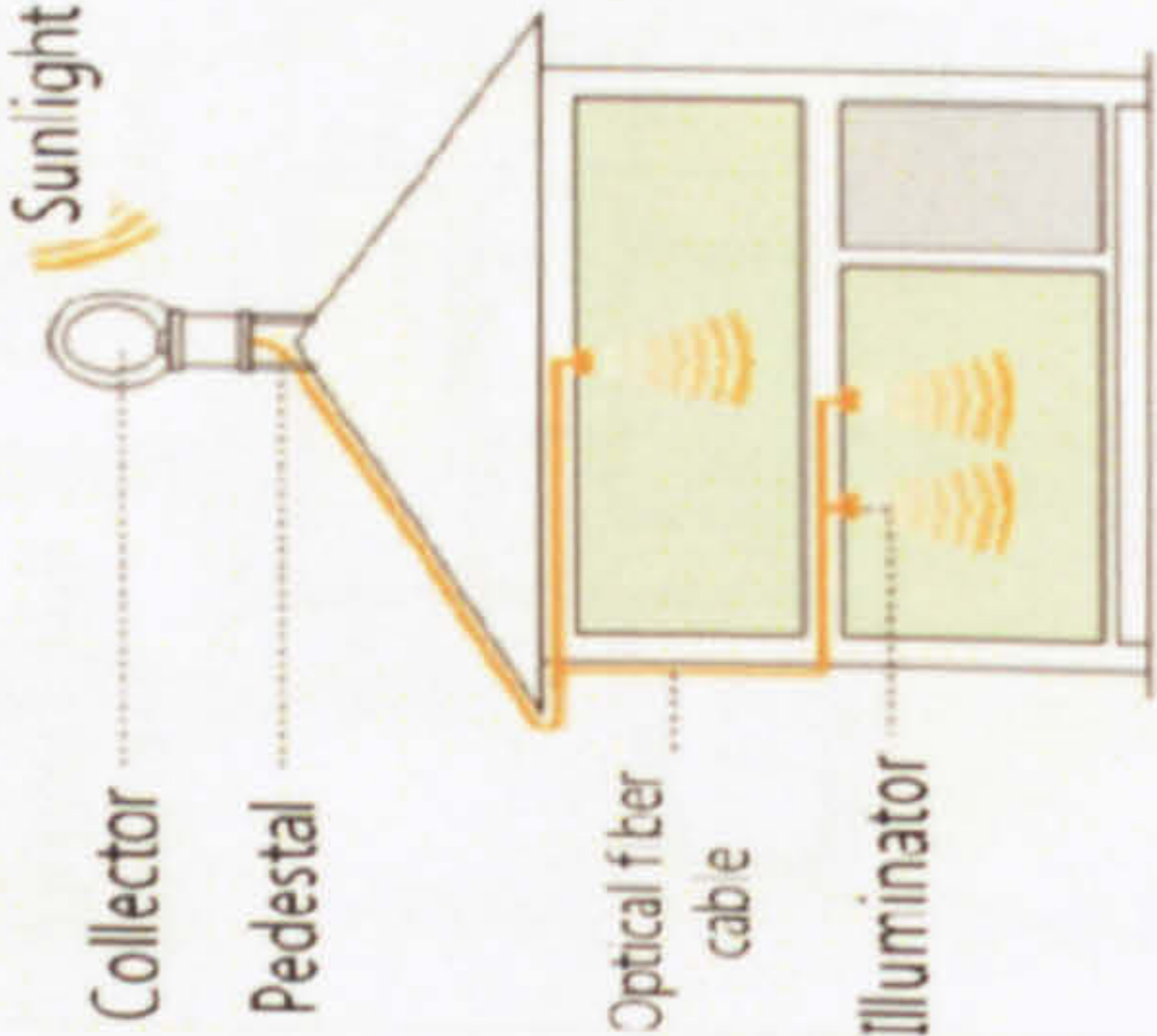

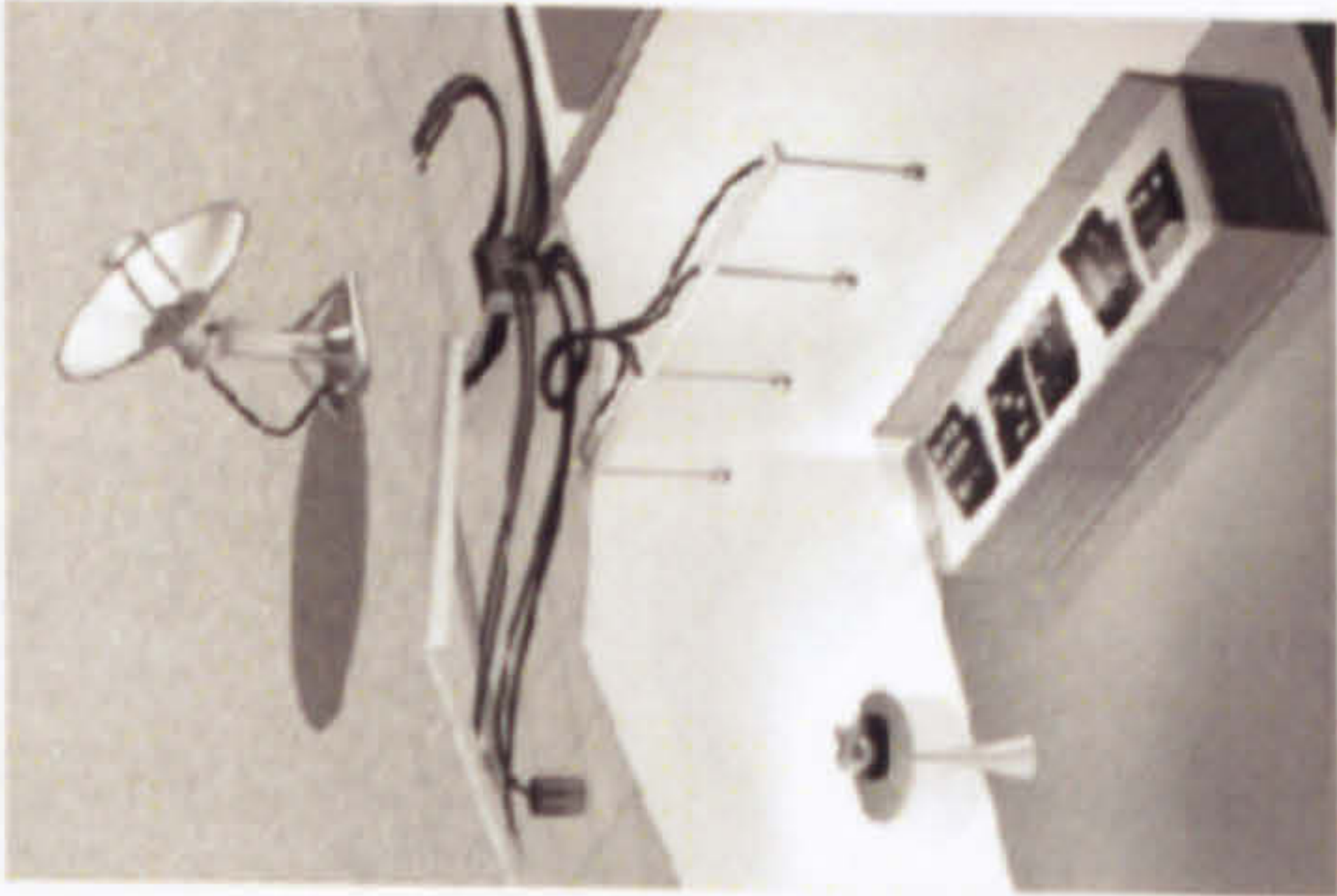
As shown in the Table 1.1, the active designs are based on the solar tracking concept. Although the appearance, dimension and physical components used for the solar concentrator (collector) unit in these systems are different, they all harness the full benefit of the beam straightness of solar radiation and its law of refraction and reflection. Optical lenses such as Fresnel lenses are used to bend and focus sun rays to a targeted area by means of the law of refraction. Or, a series of plane mirrors or combination of concave and convex reflectors could be used to redirect and concentrate sunlight to a high density by applying the law of reflection : When light is reflected from a surface, its angle of incidence is always equal to the angle of reflection where both angles are measured from the path of the light to the normal to the surface at the point at which light strikes the surface. Different types of light guide systems could be applied to transmit (high density) concentrated solar rays to the terminal device for indoor illumination. In many cases, optical fiber cables are used as they are easy to install, lightweight, small in size, and flexible.


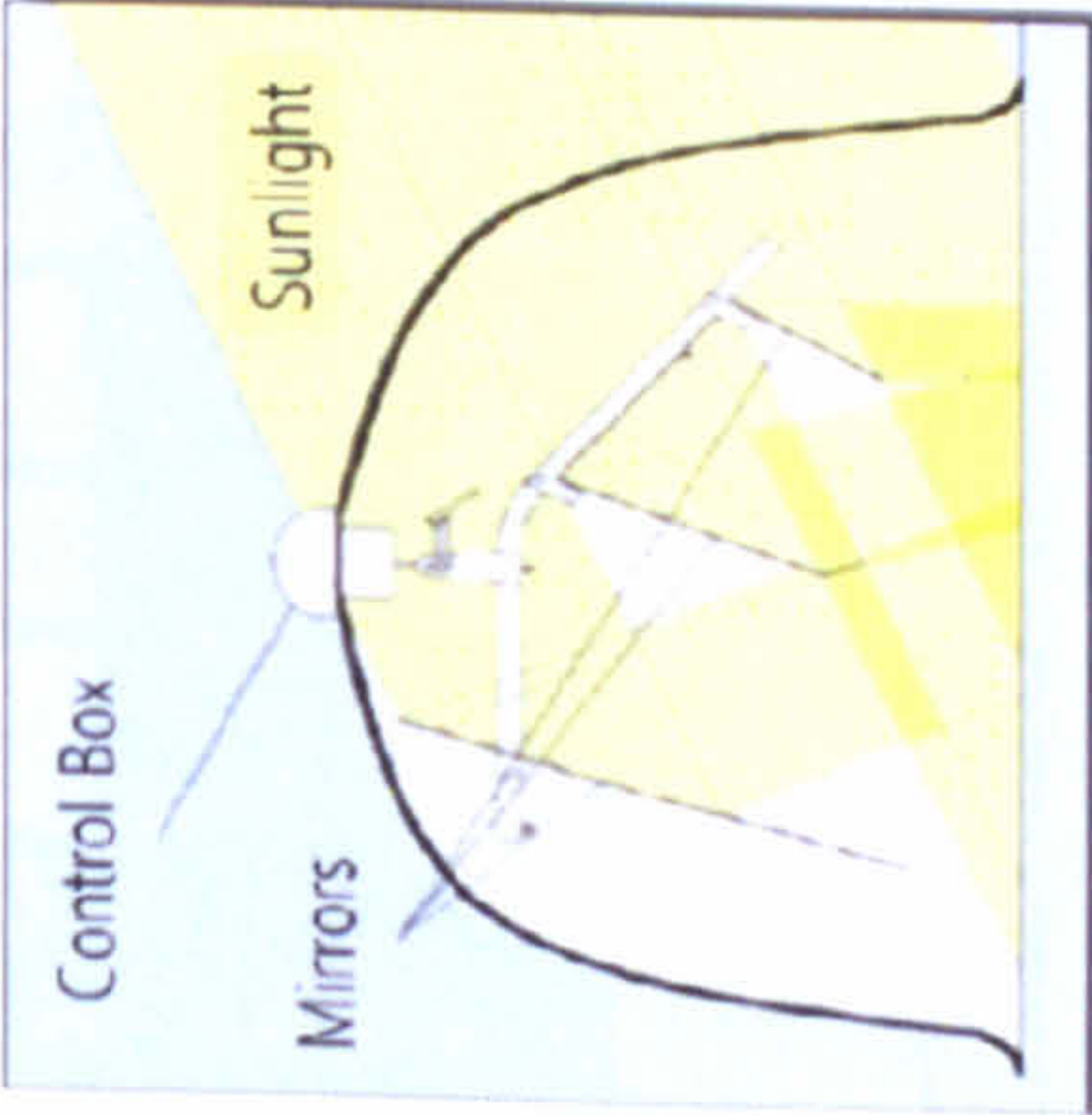
Different from active designs, passive designs are based on static concept in harnessing natural daylight. As shown in Table 1.2, sunlight is collected by non-moving, and non-tracking systems such as light pipes or light ducts. The performance of these systems relies on their position as well as architectural considerations as they directly influence the capturing of sunlight. This becomes more evident in Table 1.3 where daylighting systems are integrated into building designs in introducing natural daylight for indoor illumination.


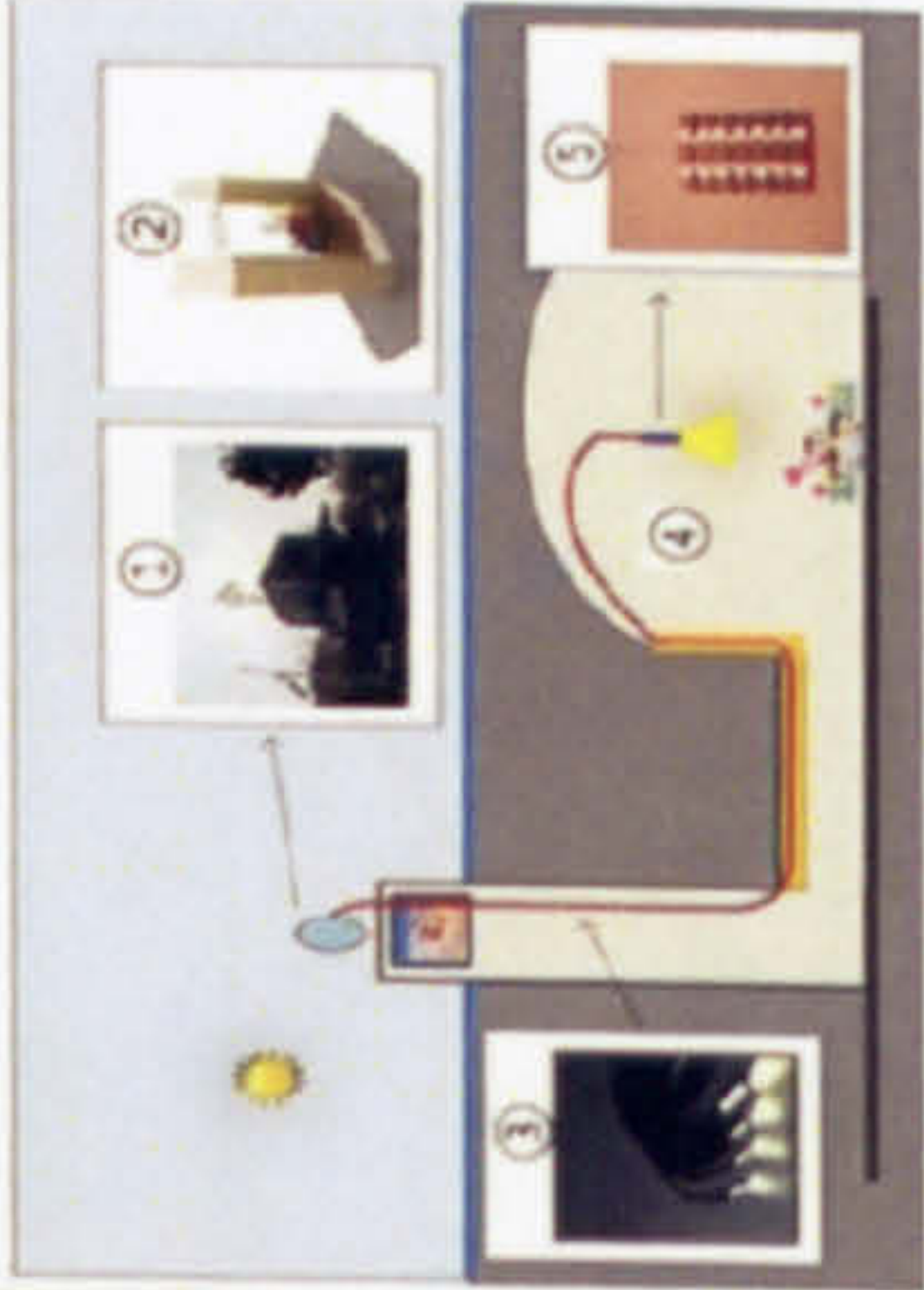


There are currently many other different types of daylighting systems implemented in residential and commercial building. These systems, however, should fall into any one of the three categories introduced here.


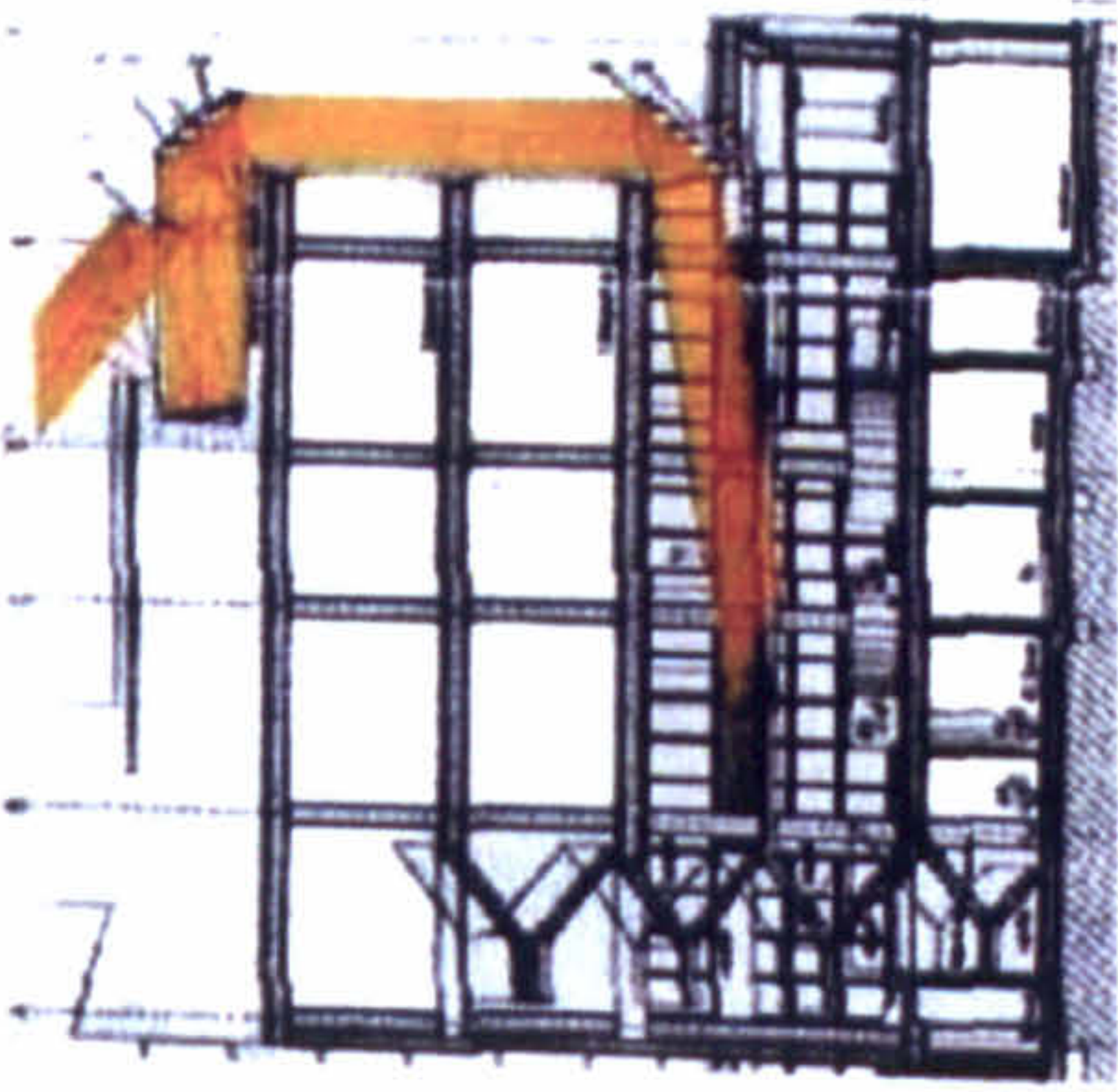

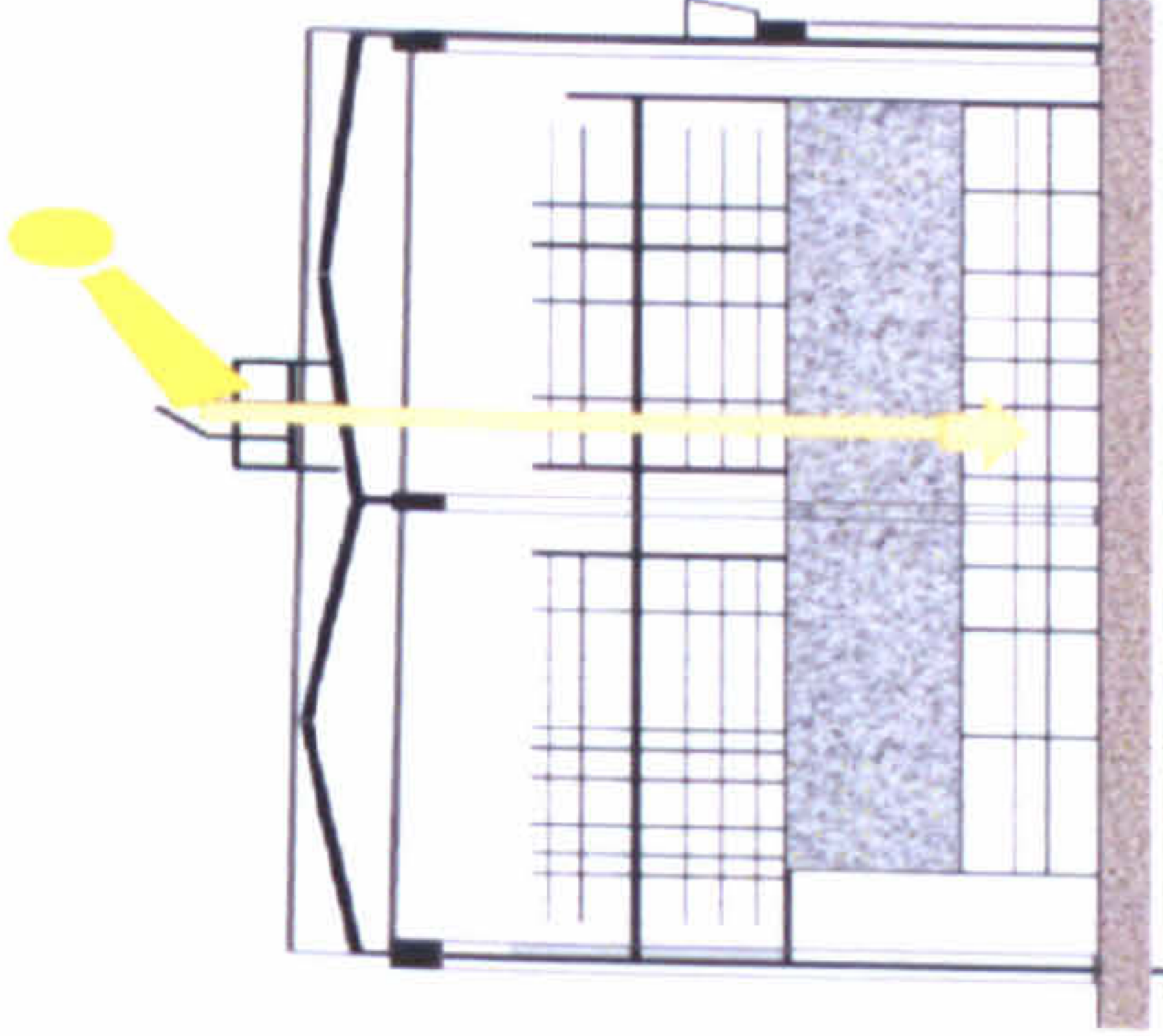
Table1.1 Active daylighting systems

	Name	Picture	Main features (key components)	Operating principle	Installation site	Source
1	Parans SP2 (Parans Sweden)		<ul style="list-style-type: none">-Fresnel lenses-Optical fiber- PSD chip based sensors-A stepping motor- Power supply cable-Communication cable-Dimensions: 980X980X180-Weight solar paner: 30Kg-Luminous Output: 3000 +/- 300lm		<ul style="list-style-type: none">- IKEA, Bilbao, Spain- Museum of Technology, Malmö, Sweden-Viktoria Arena, Fashion Store, Göteborg, Sweden- X-ray Clinic in the Hospital of Södertälje, SwedenWisby Strand Congress & Event, Sweden	www.parans.com/Products/tabid/892/language/en-US/Default.aspx
2	Mirror heliostats (Comfortable Low Energy Architecture, UK)		<p>In contrast to fibre-optic heliostats, plain mirror heliostats don't concentrate the sun light down to a smaller area</p> <ul style="list-style-type: none">- difficult to transmit large amounts of light.	 <ul style="list-style-type: none">1) Heliostat2) Redirection mirror3) Concentrator4) Light pipe5) Sun luminaire6) Glass mirror7) Cellar illuminated with sunlight	Bartenbach Lichtlabor, Austria	sombra.lamatriz.org/heliostatos www.bartenbach.com

3	<p>Himawari Solar Lighting Systems (La Forêt Engineering Co., Ltd. Japan)</p>		<ul style="list-style-type: none"> -Fresnel lens -Acrylic dome -Sun sensor -Optical fiber -Rotation motor -Number of lenses:36 -Lens size(mm):95 -Dome diameter(mm):1,000 -Total luminous flux: 11,520lm 		<ul style="list-style-type: none"> - Underground hall in Okayama city, Japan - Underground promenade, Hiroshima Prefecture, Japan - Underground parking, Niikura, Tokyo - Metropolitan Highway, Japan <p>www.himawari-net.co.jp/e_page-index01.html</p>	
4	<p>Hybrid solar lighting system (Oak Ridge National Laboratory USA)</p>		<ul style="list-style-type: none"> -Plastic primary mirror -Secondary mirror -Receiver Module -Tracking mechanism -GPS navigator 		<ul style="list-style-type: none"> -American Museum of Science and Energy (AMSE) in Oak Ridge, the Sacramento - Municipal Utility District in Sacramento California -Wal-Mart store in McKinney, Texas <p>www1.eere.energy.gov/femp/pdfs/tf_hybrid_solar.pdf</p>	

5	<p>Solar Tracking Skylights (Solar Tracking Skylights, Inc., USA)</p>		<p>Comparing with conventional Skylights,</p> <ul style="list-style-type: none"> - Greater light levels for a longer duration of the day - Generates up to 4x the light levels - Lower initial cost and ongoing expense - Size(mm): 1220X1220X600 	 <p>Major components:</p> <ul style="list-style-type: none"> - Highly reflective mirrors - Clear plastic cover - Precision solar tracking - Utilization of daylight at low solar altitude angles 	<p>YWCA, Downtown Green Bay, USA</p>	<p>http://www.solar-track.com/index.html</p>
---	--	--	---	---	--------------------------------------	--

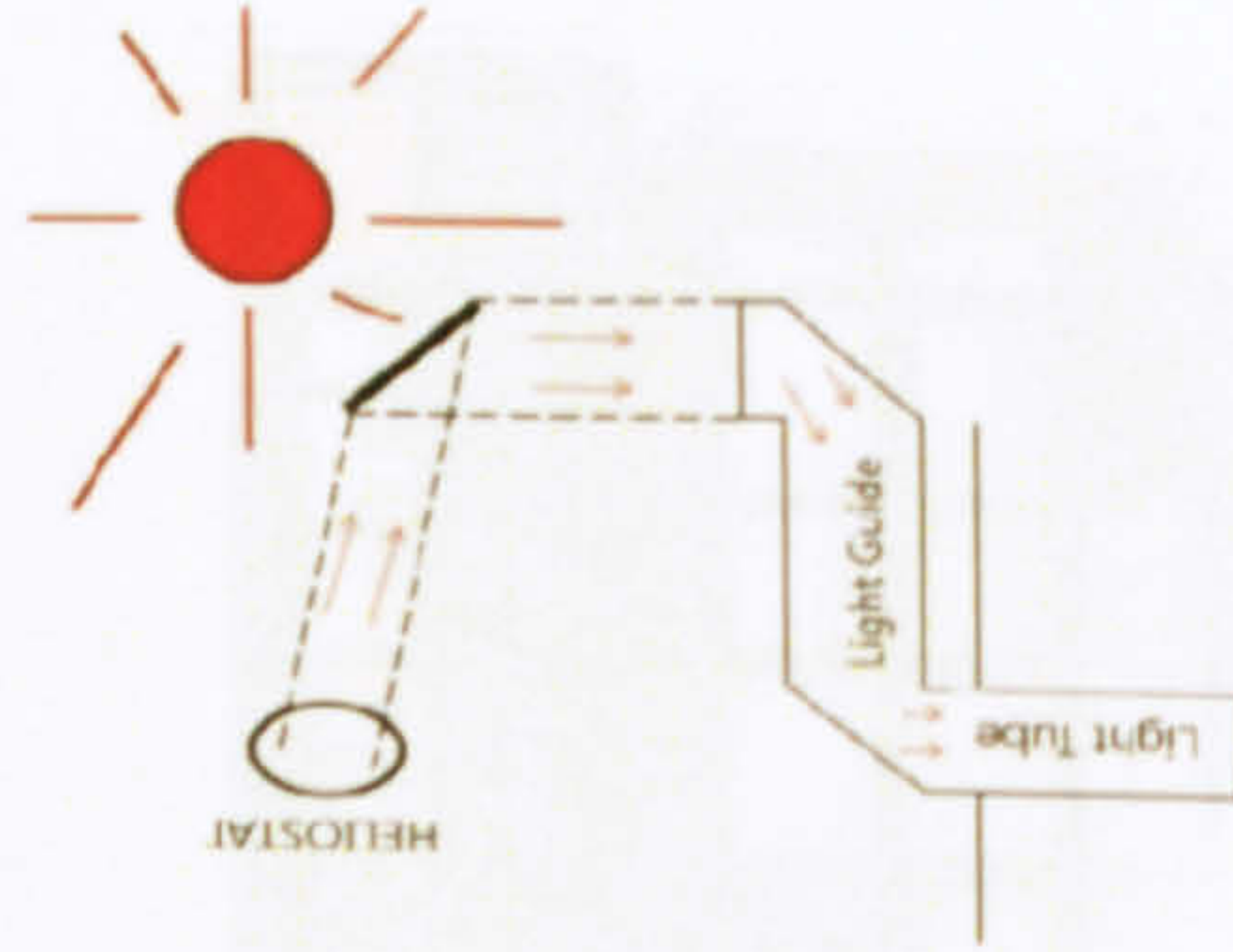
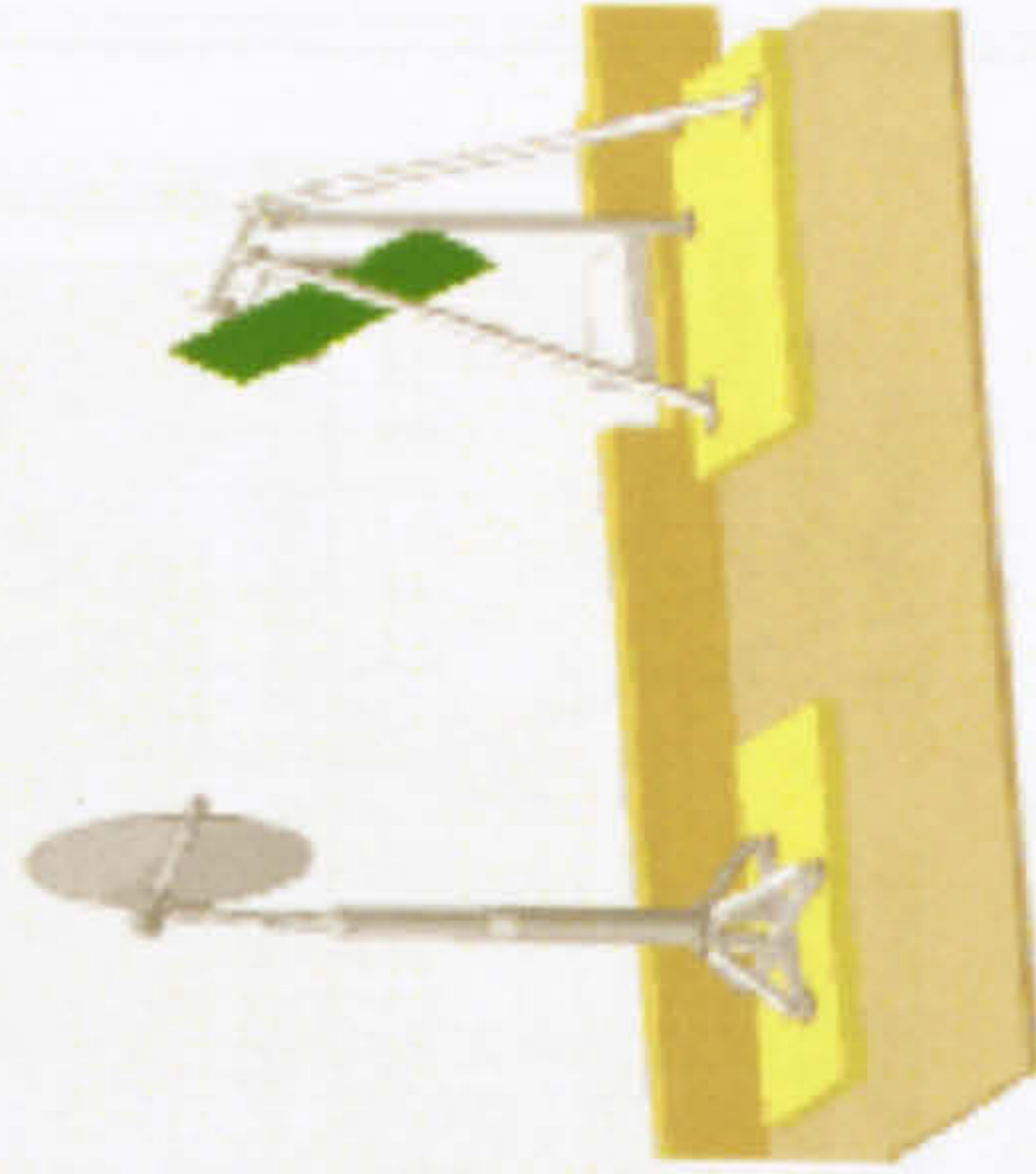
6	<p>WDF 800 (Whilkor, Korea)</p> 	<ul style="list-style-type: none"> - Easily applicable to existing buildings (no limitations on their location and architectural design) - Low transmission losses - Expensive to install 	 <p>① Concentration ② Landscaping ③ Optical cable ④ Waiting Room (Platform) ⑤ Diffusion</p>	<p>Jangahnpyong Station, Seoul, Korea</p> <p>www.whilkor.com</p>	
7	<p>Optical Fibre Type (Whilkor, Korea)</p> 	<ul style="list-style-type: none"> - Multiple stage daylighting - Portable - Solar tracking - Efficient in space utilization - Multiple purpose daylighting system 	 <p>① Sun ray ② AF 95ARF ③ Concentration ④ Transmission ⑤ Diffusion</p>	<p>Children's Dream House, KOEX, Samsung-dong, Seoul, Korea</p> <p>www.whilkor.com</p>	

8	<p>Solar Powered (Whilkor, Korea)</p> 	<ul style="list-style-type: none"> - Continuous transmission of light - Highly efficient 		<p>Diorrich Ville, Jamwon-dong, Seoul, Korea</p> <p>www.whilkor.com</p>	
9	<p>HSR Daylighting (Whilkor, Korea)</p> 	<ul style="list-style-type: none"> - Precision solar tracking - Highly efficient - Transmission capability > 1,000m 		<p>House of Architects, Seoul, Korea</p> <p>www.whilkor.com</p>	

Light Pipe
& heliostat
(Heliobus,
Switzerland)



- Heliostat
- Light tube
- Stepper motor



Wiesengrund
Winterthur,
Switzerland

[http://helio
bus.com](http://helio
bus.com)

11	<div data-bbox="980 2464 1091 2664" data-label="Text"> <p>Universal Fiber Optics (Greece)</p> </div>	<div data-bbox="735 1832 1290 2391" data-label="Image"> </div>	<div data-bbox="845 1466 1214 1796" data-label="List-Group"> <ul style="list-style-type: none"> -Concentrating heliostat -Fresnel lens -Liquid light guide -Artificial fiber light source -Intelligent control system -Prototype sun luminaire </div>	<div data-bbox="385 831 845 1369" data-label="Diagram"> </div>	<div data-bbox="951 535 1098 740" data-label="Text"> <p>Office University of Athens, Greece</p> </div>	<div data-bbox="951 145 1098 438" data-label="Text"> <p>http://new-learn.info/learn/about/doc/ufo_epic2002.pdf</p> </div>
15			<div data-bbox="1145 861 1699 1369" data-label="Diagram"> </div>			


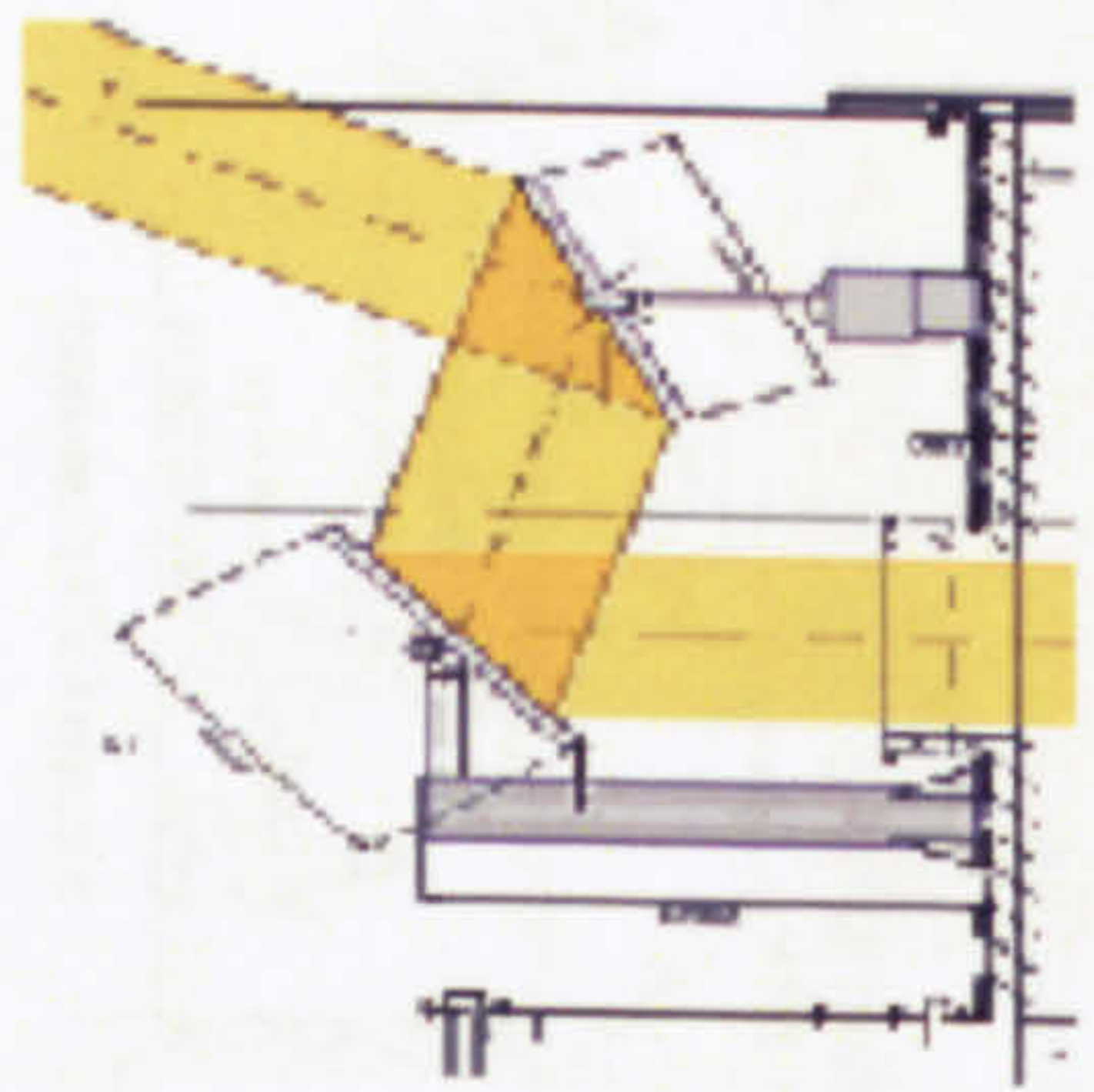

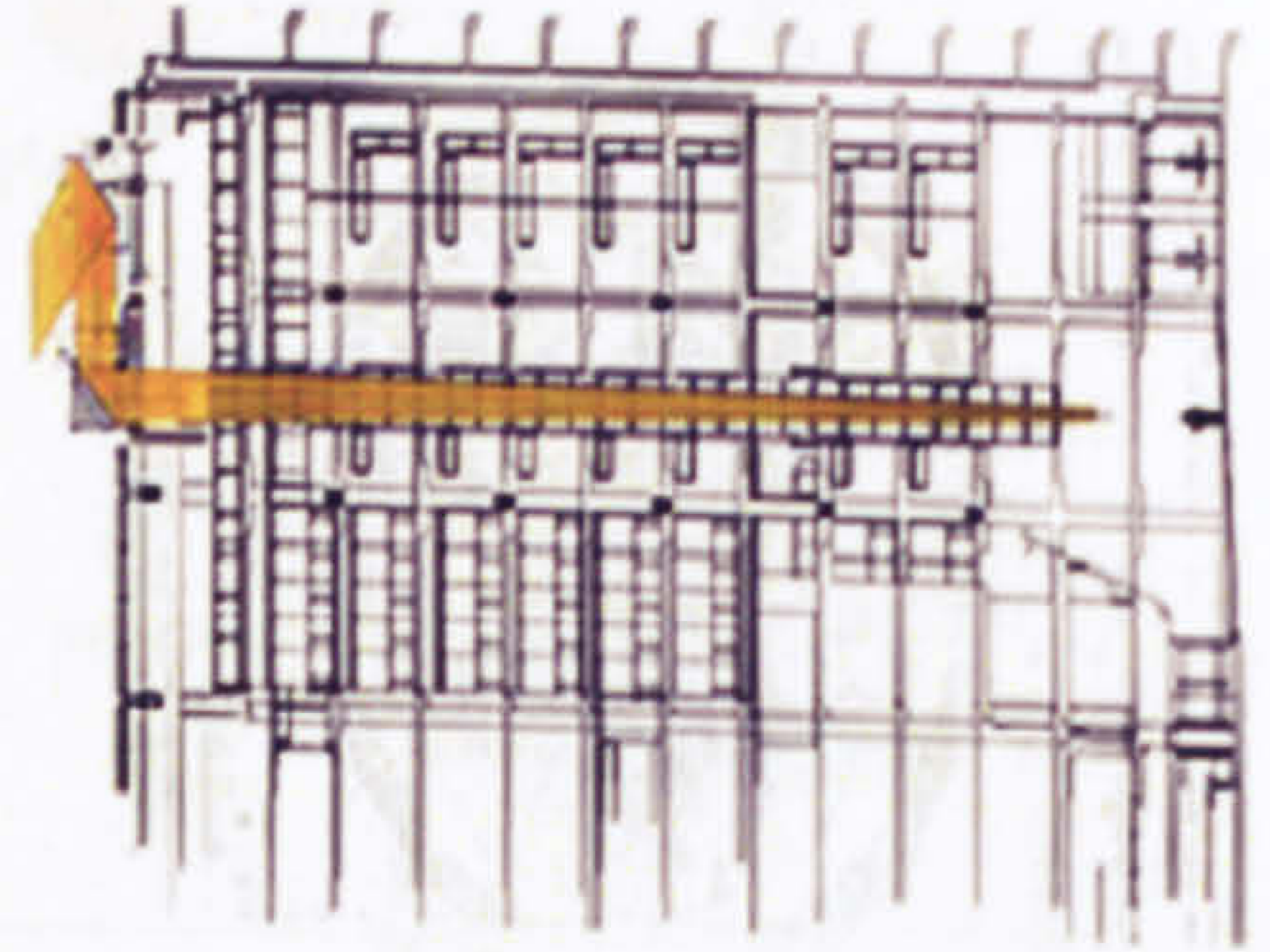


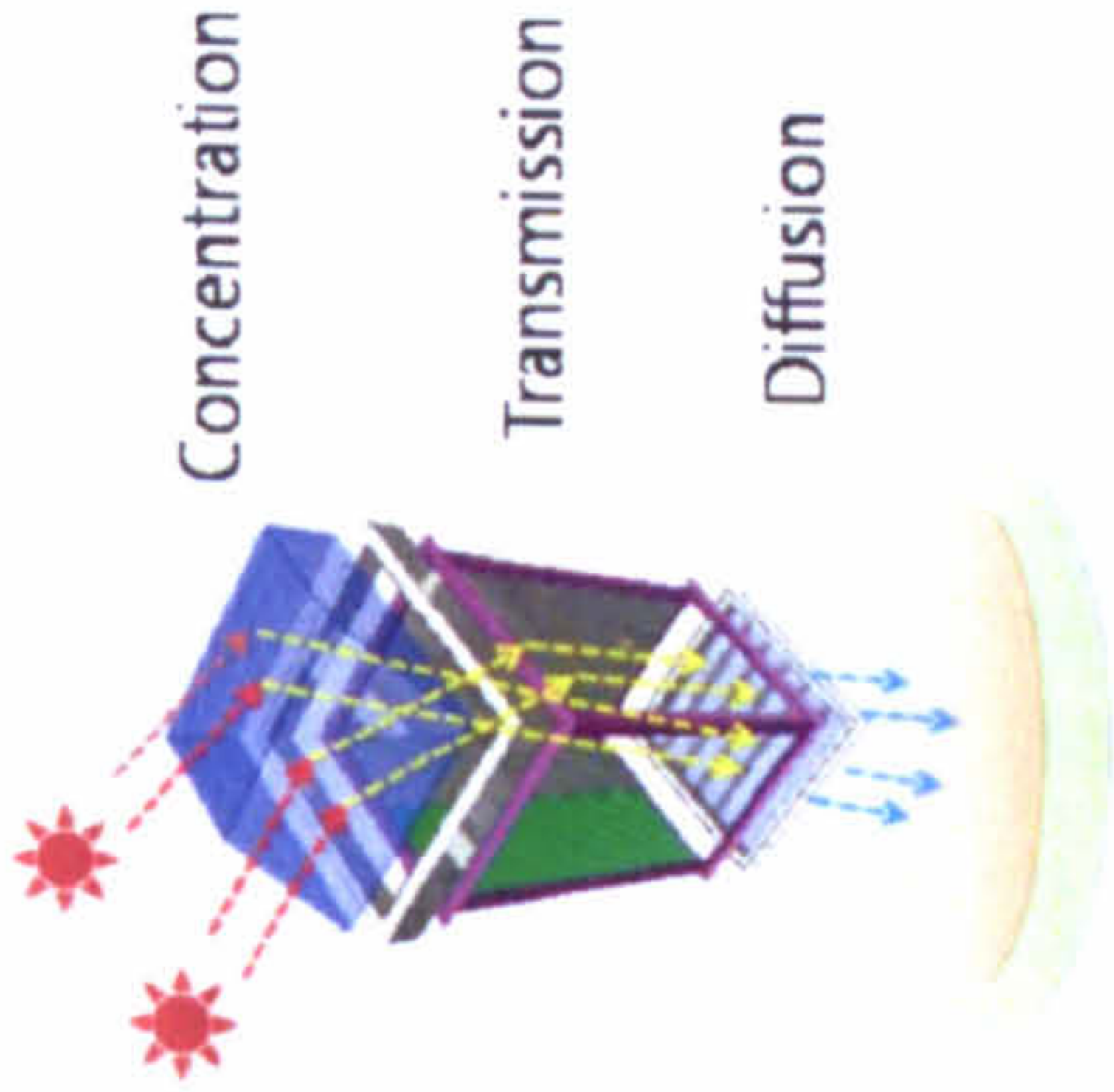
12	<p>Lightron BO 1600 R (Bomin Solar, Germany)</p> 	<ul style="list-style-type: none"> - Heliostats - Solar tracking system - Mirrors - Weight: 300kg - Mirror Dimensions: $\Phi 1,585\text{mm}$ - Surface area: 6.17m^2 		<p>Teadrop Park at Battery Park, New York City, USA</p> <p>Teadrop Park at PT Surya Toto Indonesia</p> <p>Indonesia Jakarta</p> <p>Sonnenhof Munich Germany</p>	<p>www.bomin.de/heliostaten/</p> <p>www.bomin.de/heliostaten/referenzen</p>
13	<p>Lightron BO 2500 (Bomin Solar, Germany)</p> 	<ul style="list-style-type: none"> - Heliostats - Solar tracking system - Mirrors - Weight: 600kg - Mirror Dimensions: $2,485 \times 2,485\text{mm}$ - Surface area: 6.17m^2 		<p>Morgan, Lewis, Brockius Building Washington DC USA</p> <p>Donayang Paragon Apartments Seoul South Korea</p> <p>German Museum Berlin, Germany</p> <p>Hall Nalles, Italy</p>	<p>http://www.bomin.de/Acrobat/Heliostat/LIGHTRON_E.pdf</p>

Table1.2 Passive daylighting systems

	Name	Picture	Main features (key components)	Operating principle	Installation site	Source
1	The Solatube 160DS/290DS (SolaLighting Limited, UK)		<ul style="list-style-type: none">- Double glazed ceiling diffusers- Dome reflectors- Extension tubes- Fasteners and fixings- Size : 530mm diameter- output : Edison screw lamps up to 75 W		Scottish & Southern Energy Eco Cottage (Perth, Scotland, UK)	www.solatube.co.uk/company/mmtech.htm
2	Heliobus Light Pipes (HELIOBUS AG, Germany)		<ul style="list-style-type: none">- Light pipes- Heliostats- Stepper motors		Subterranean train station at Potsdamer Platz, Berlin	http://www.heliobus.com/pages_e/frames.html

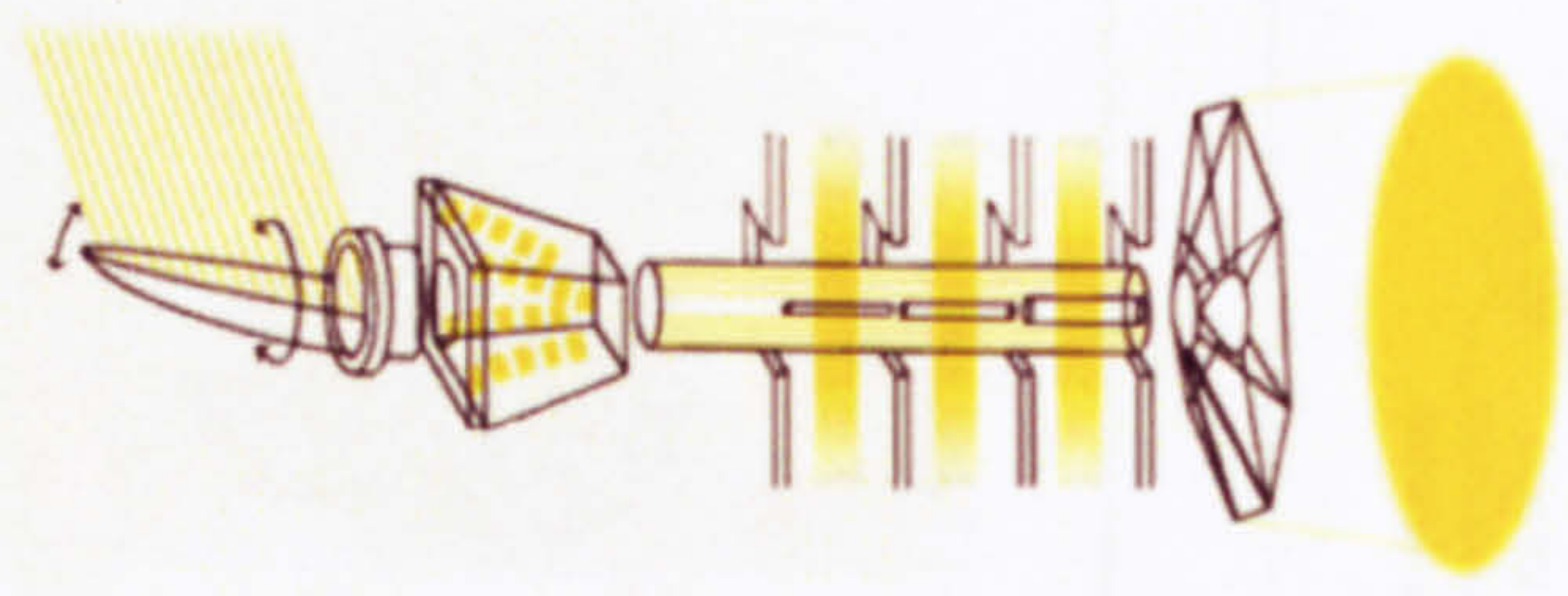
3	<p>SunPipe (Monodraught Ltd, UK)</p> 	<ul style="list-style-type: none"> - Polycarbonate Diamond top dome - ABS flashing plate & weathering skirt - SunPipe Bell end ceiling extension - Ceiling diffuser & ceiling trim - Dome size : 9" (230mm), 12" (300mm), 18" (450mm), 21" (530mm) 		<p>The British School at Abu Dhabi, UAE</p> <p>National Autistic Society, UK</p> <p>Trinity School, UK</p> <p>www.monodraught.com/sunpipe/index.php</p>	
4	<p>SunCatcher (Monodraught Ltd, UK)</p> 	<ul style="list-style-type: none"> - Daylighting with natural air ventilation - Polycarbonate top dome - Highly reflective aluminum tube - Volume control dampers - Temperature and air quality sensors - Cylon digital control panel - Size : 400mm to 1500mm 		<p>St Paul's Catholic College, UK</p> <p>Eco House at Nottingham University, UK</p> <p>BMW Office, UK</p> <p>Wycombe Wanderers Football Stadium, UK</p> <p>http://www.monodraught.com/suncatcher/index.php</p>	

5	<p>Light pipe (Visual Impact Lighting, Inc., USA)</p> 	<ul style="list-style-type: none"> - Use of light pipes - Effectively applicable to storage spaces, hallways - Relatively inexpensive and easily retrofittable 	<ul style="list-style-type: none"> - Highly reflective inner surface for efficient light transmission - Deep light penetration into the building without losing too much of the light. 	<p>YWCA, Downtown Green Bay, USA</p>	<p>www.visualimpactlighting.com/VisualImpactReceiv.html</p>
6	<p>Multi faceted prism light duct (SUN-LES, Korea)</p> 	<ul style="list-style-type: none"> - Multi faceted prism daylighting for extension of daylighting hours - High-efficiency daylighting - Easy maintenance and high durability 		<p>Cleannet, Pangyo, Sungnam, Korea</p>	<p>http://www.sunles.co.kr/html/mn05/mn05_01_02.html</p>

Heliobus
(HELIOBUS
AG,
Switzerland)



- collector (heliostat)
- HLC with SOLF internal prismatic film
- specularly reflecting film
- internal extractors
- diffuser right

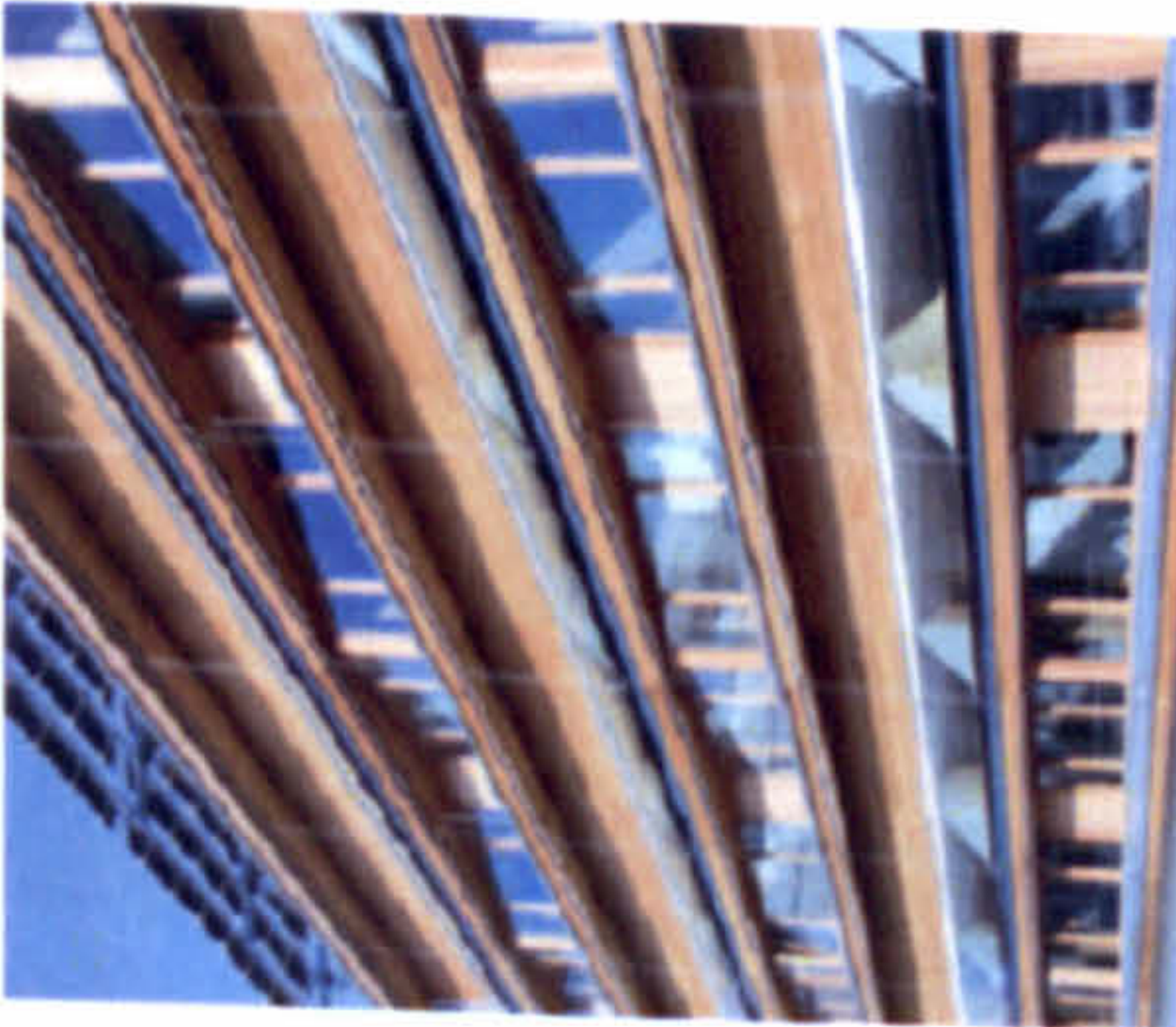
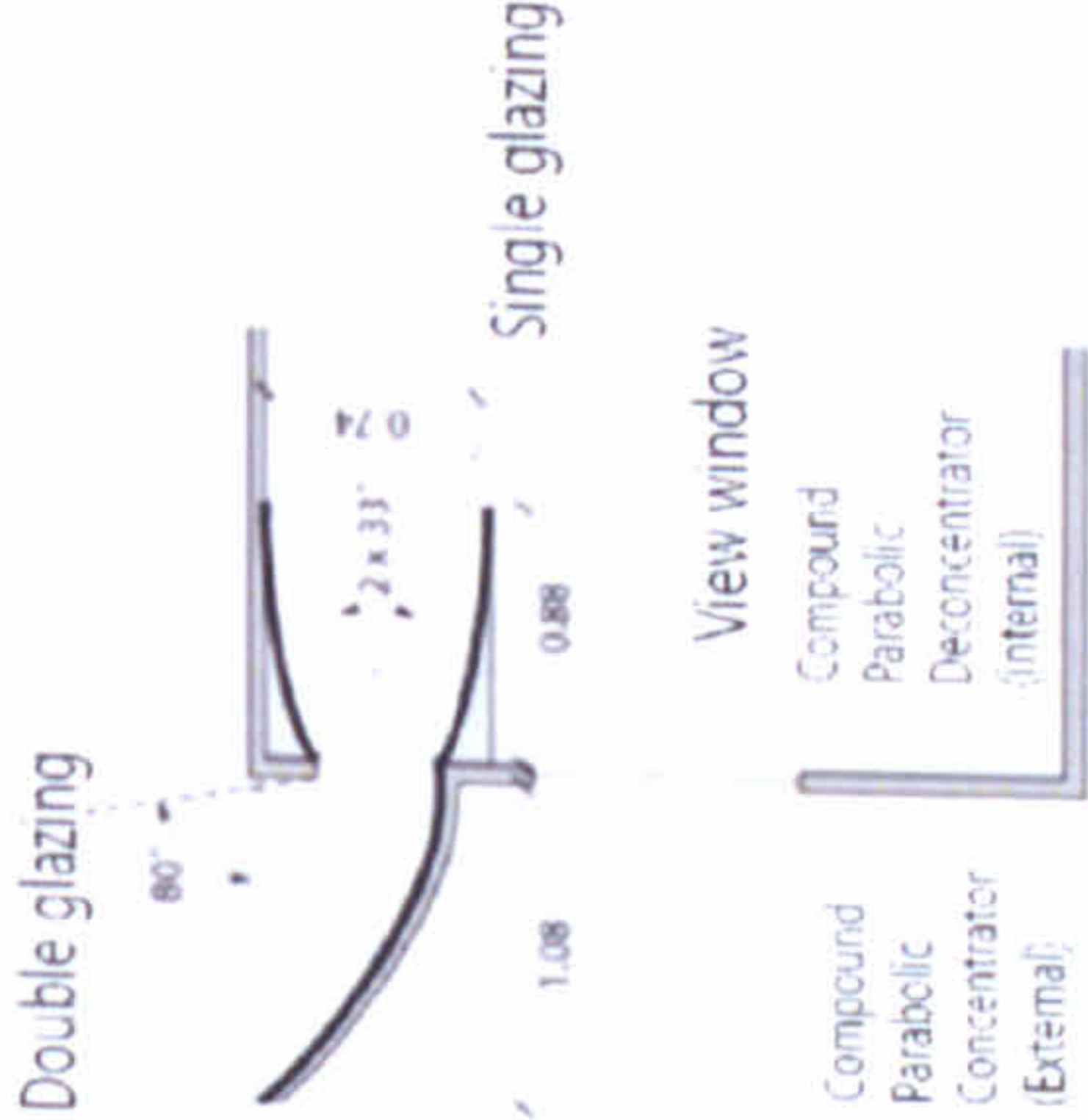

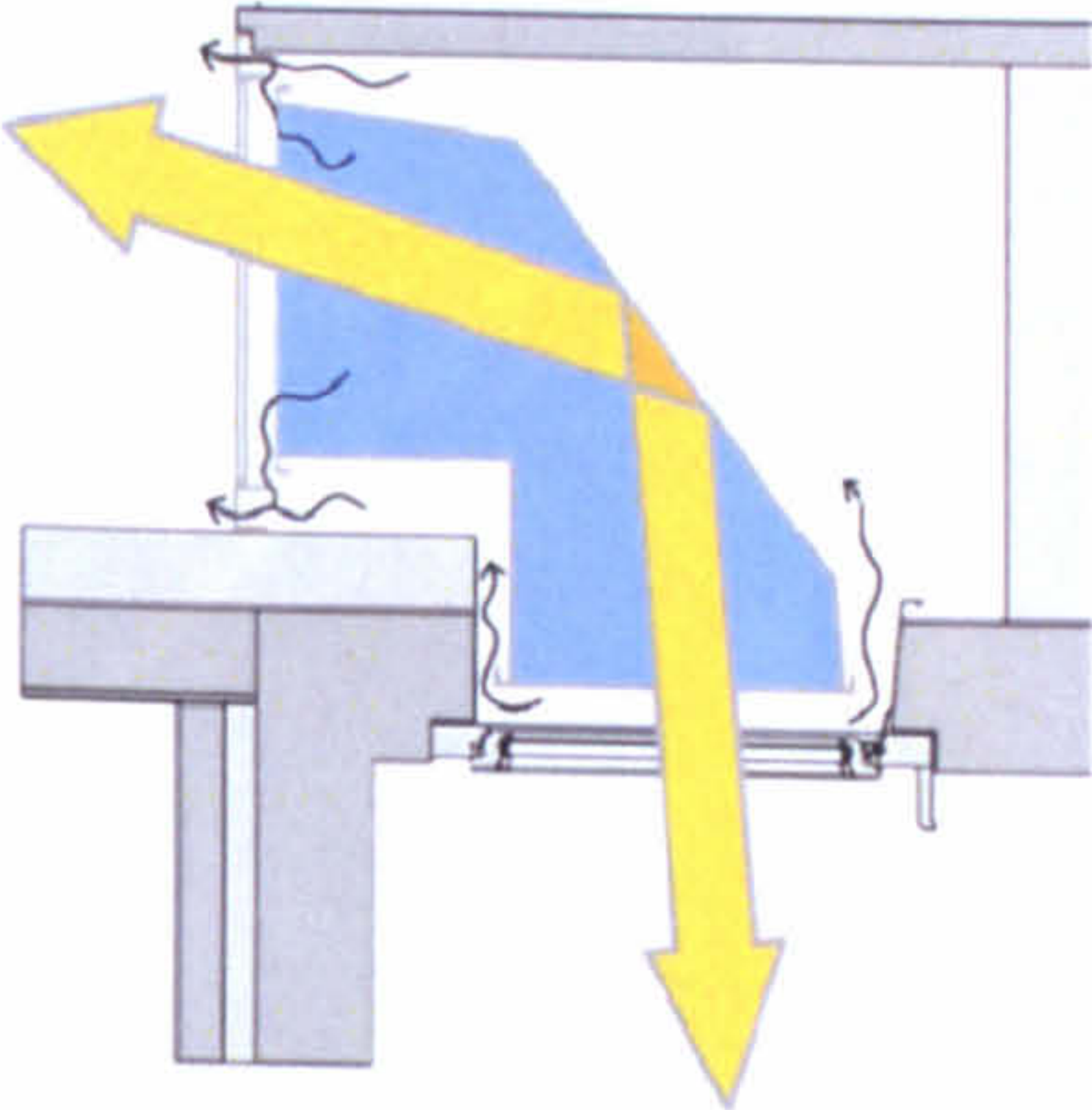



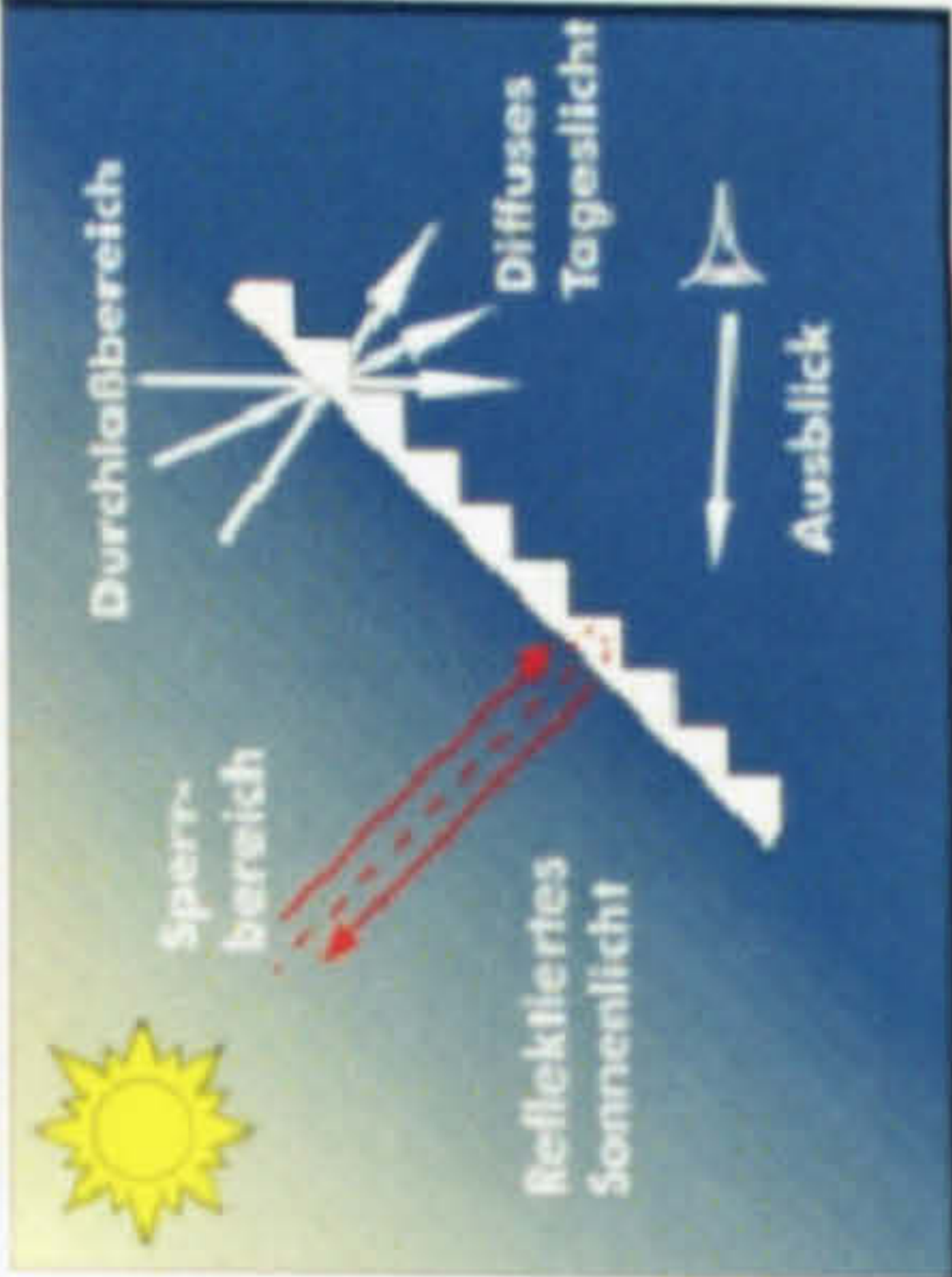

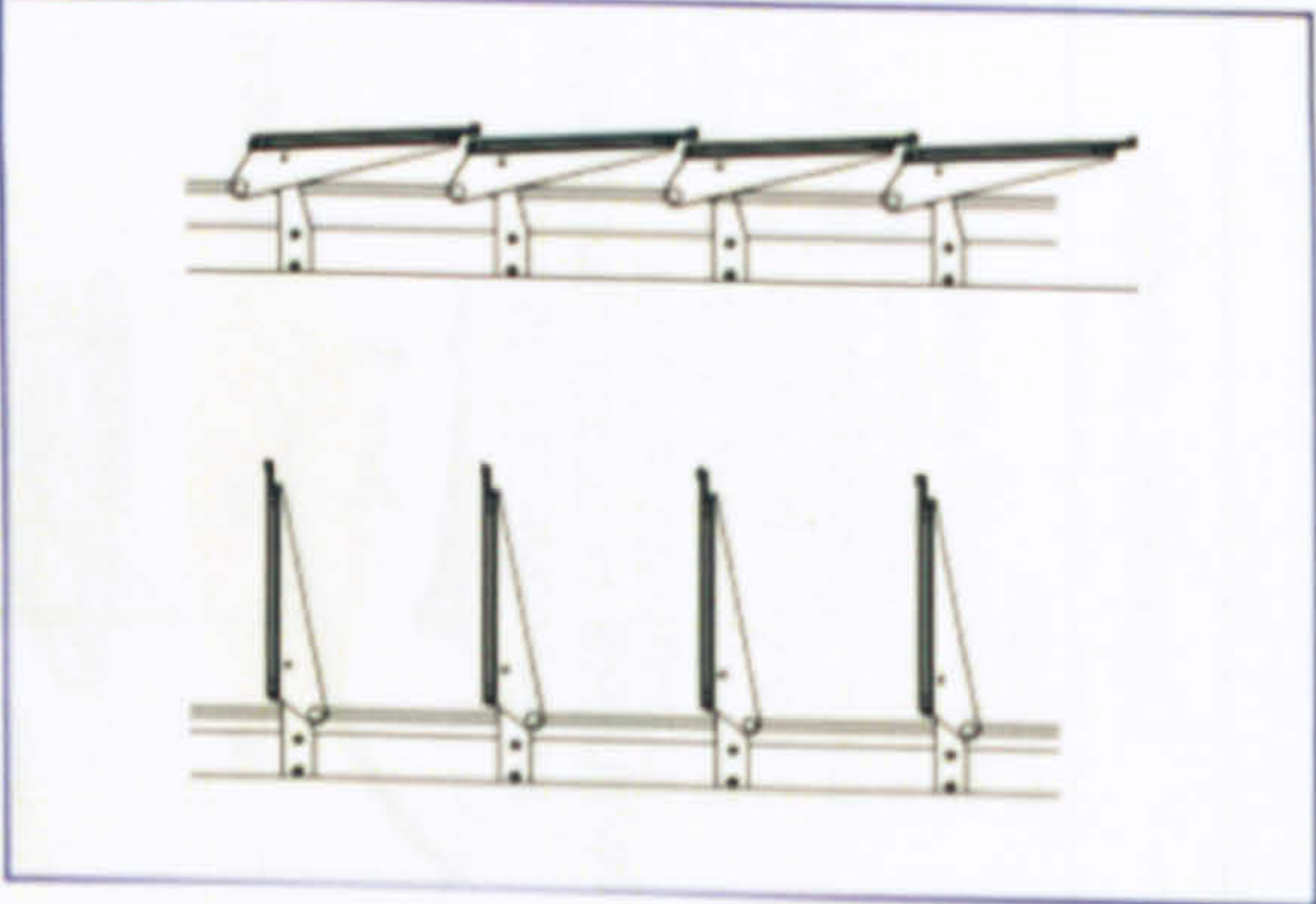
Redirection of light into a vertical prismatic light guide through three floors
Distribution of daylight over the entire surface of the guide allowing each floor to receive small quantities of light by using reflective extractor


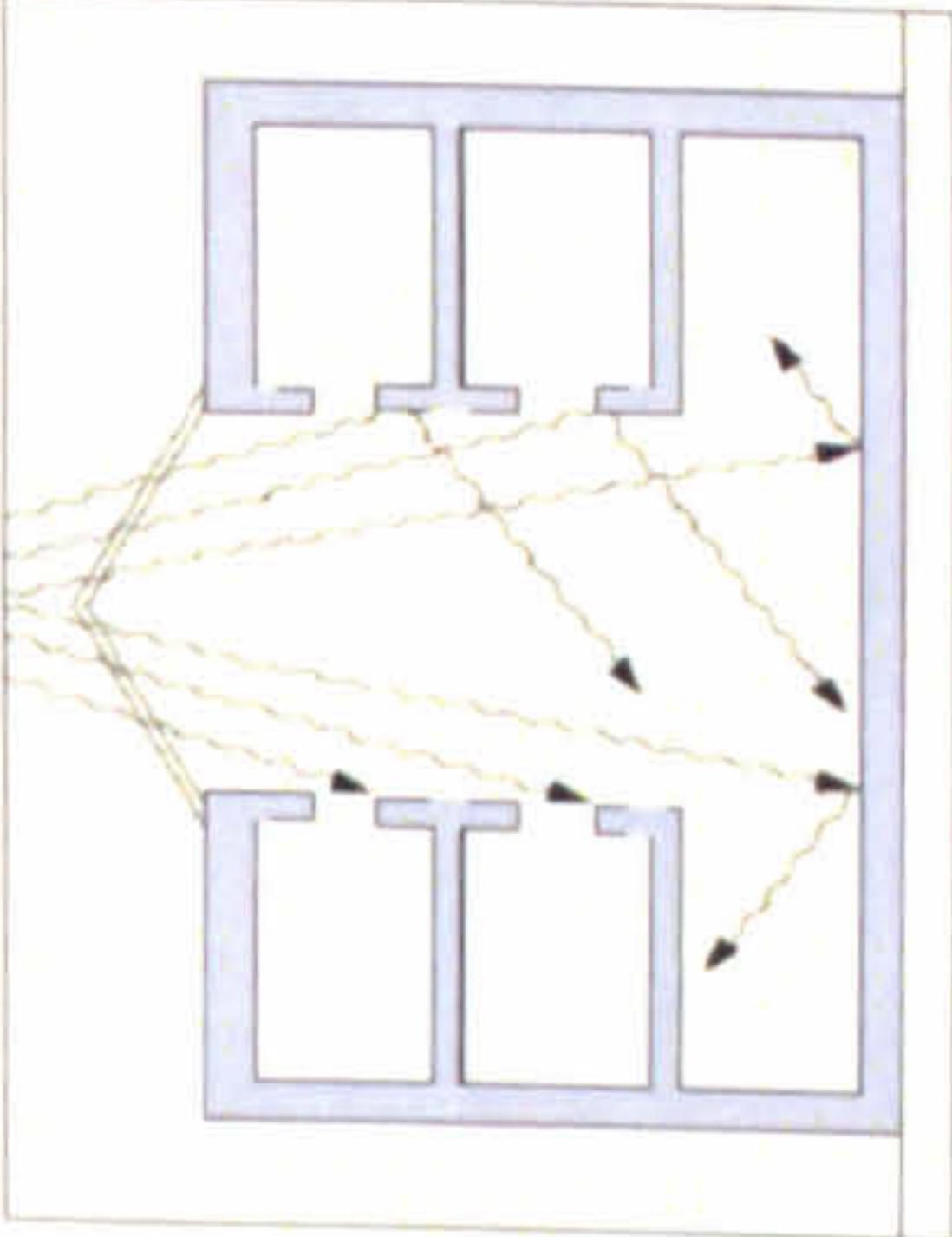

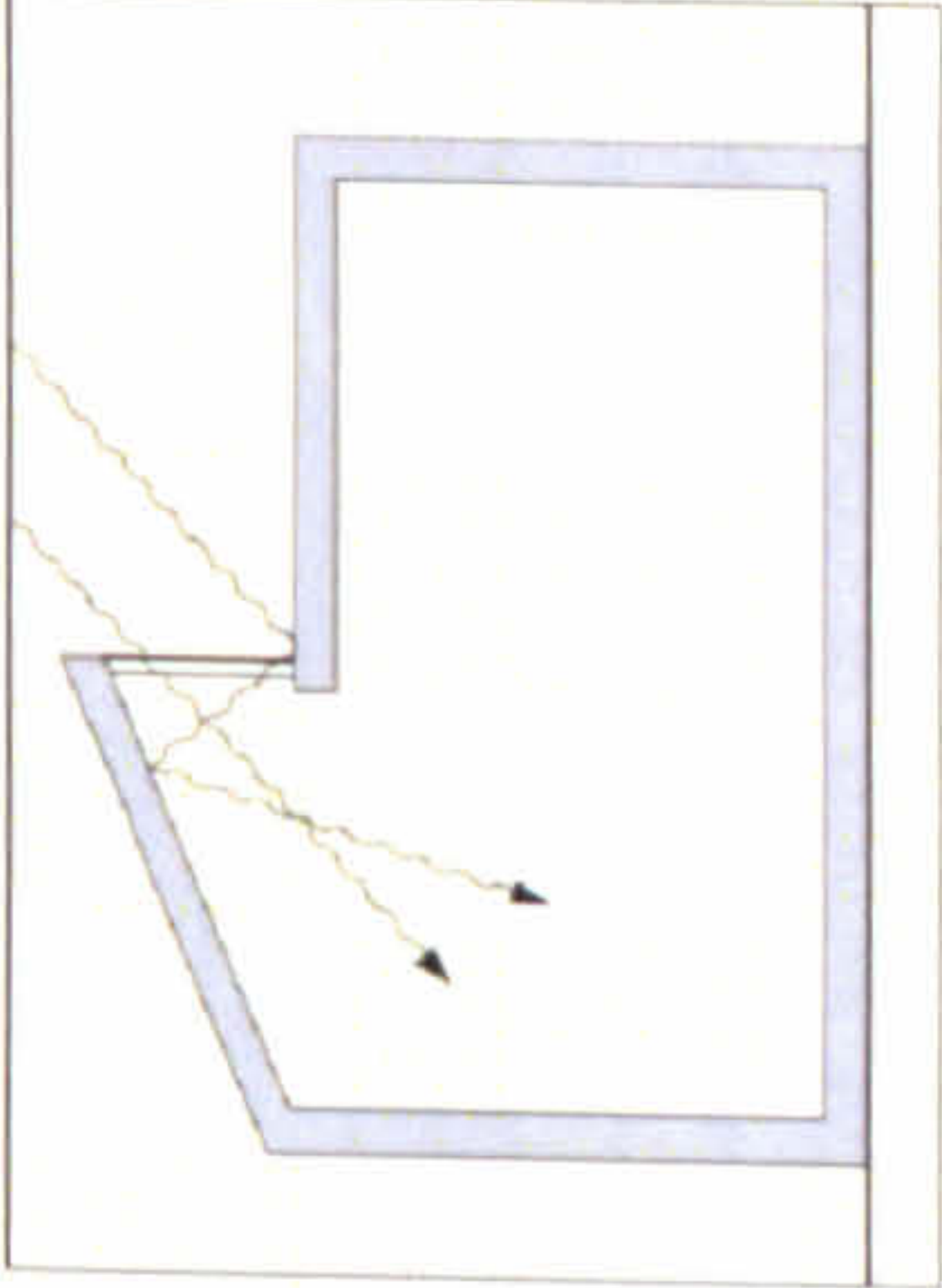
Pilot project in St. Gallen (school building), Switzerland


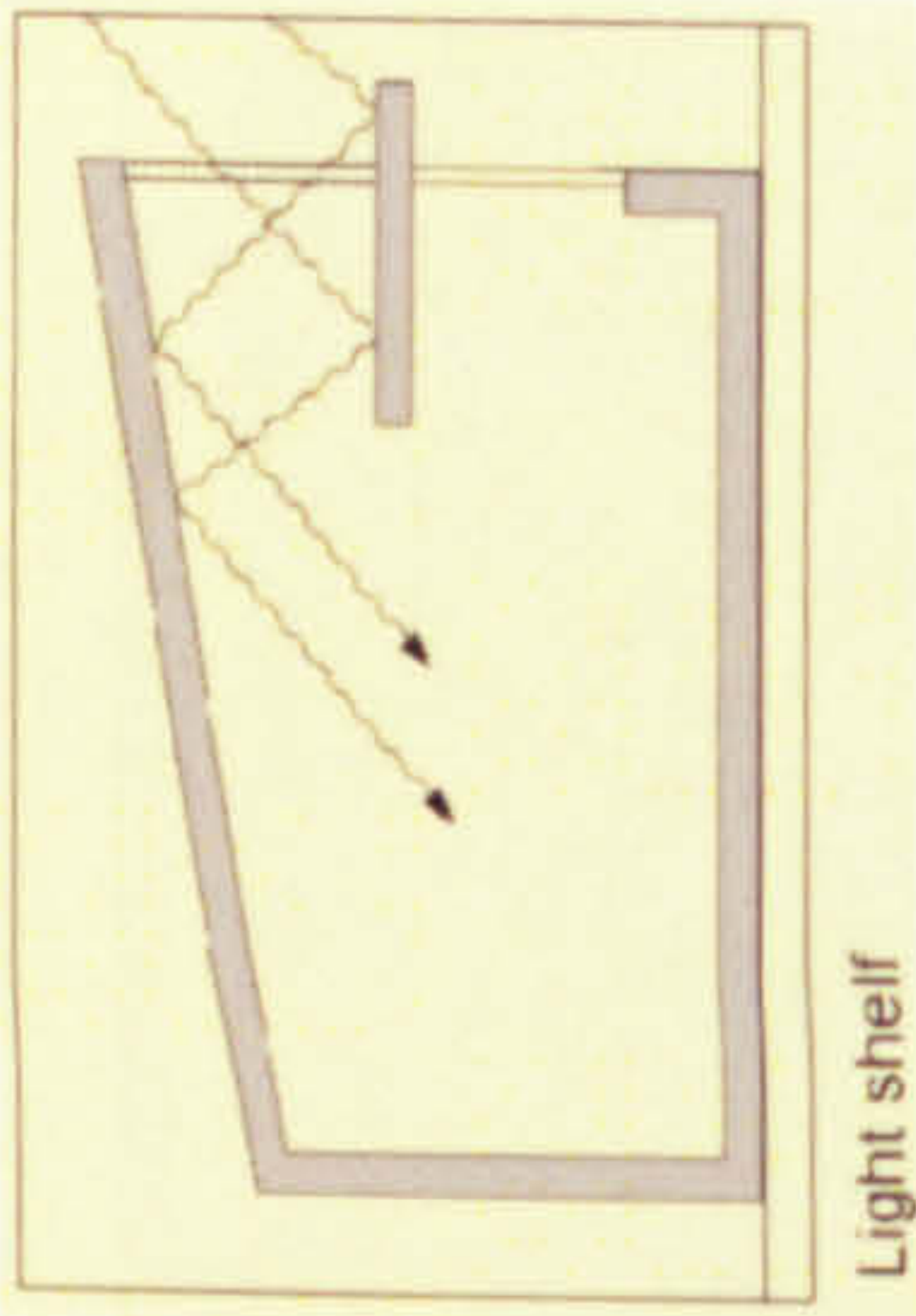

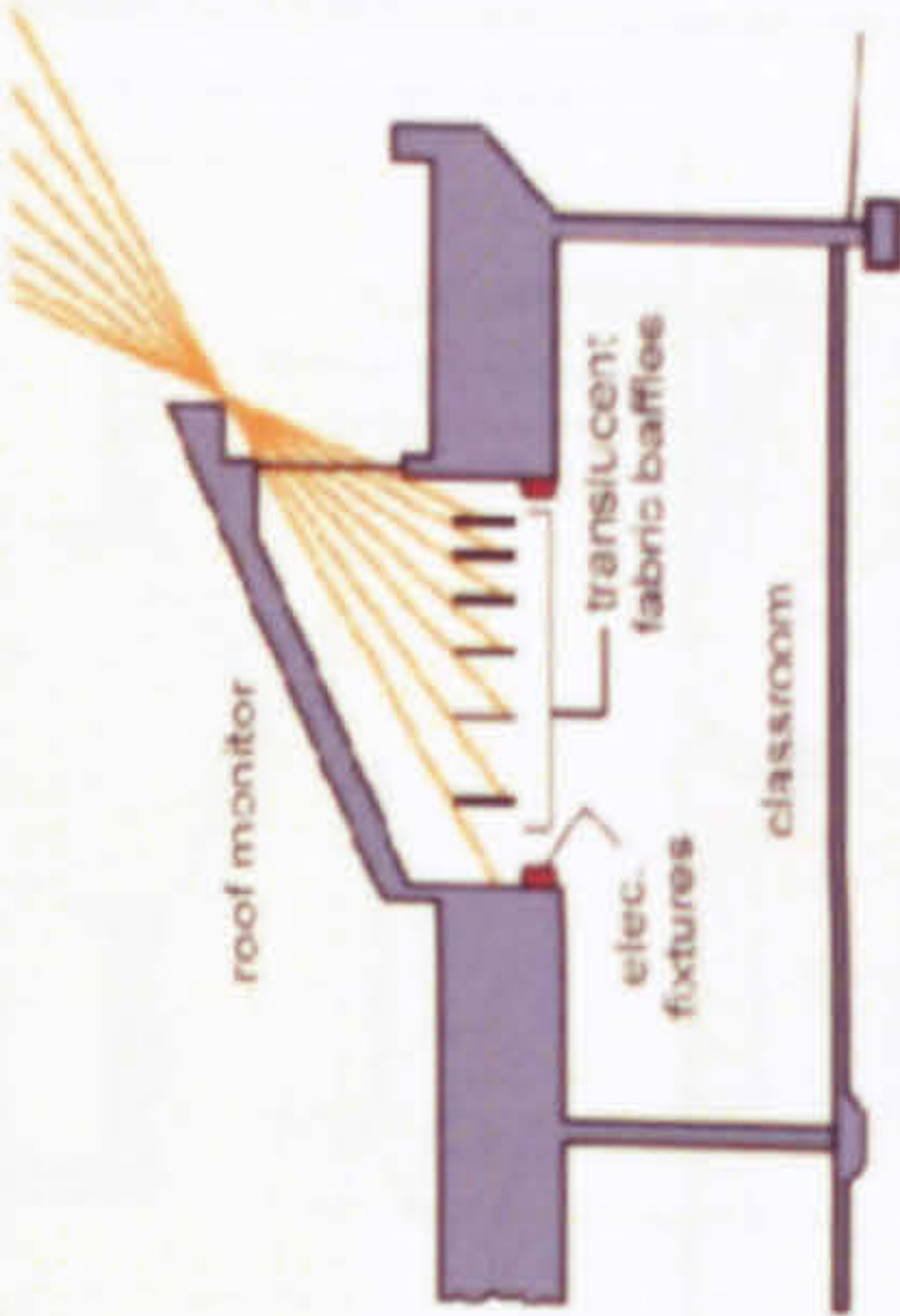
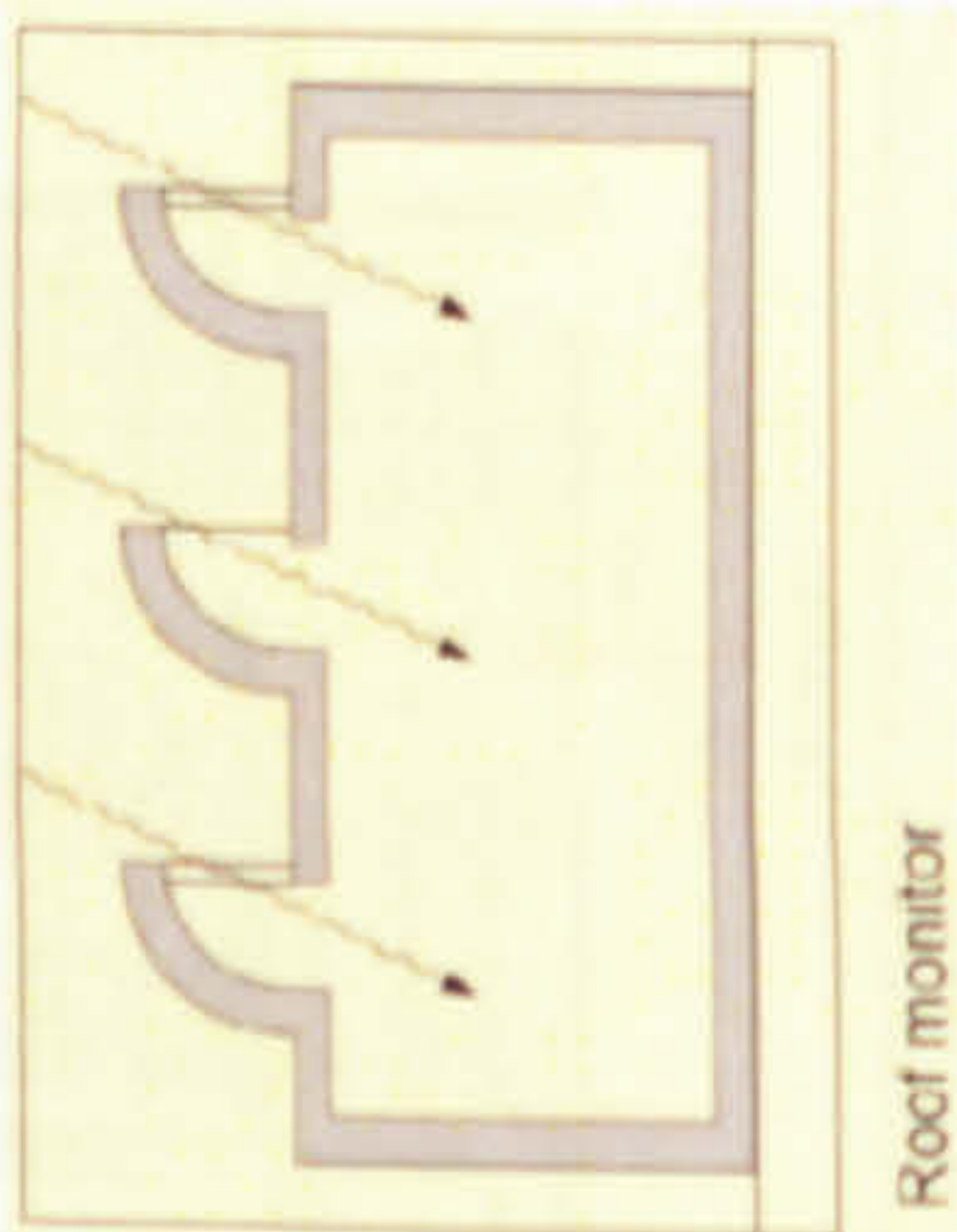
www.heliobus.com

Table 1.3 Building –integrated daylighting systems

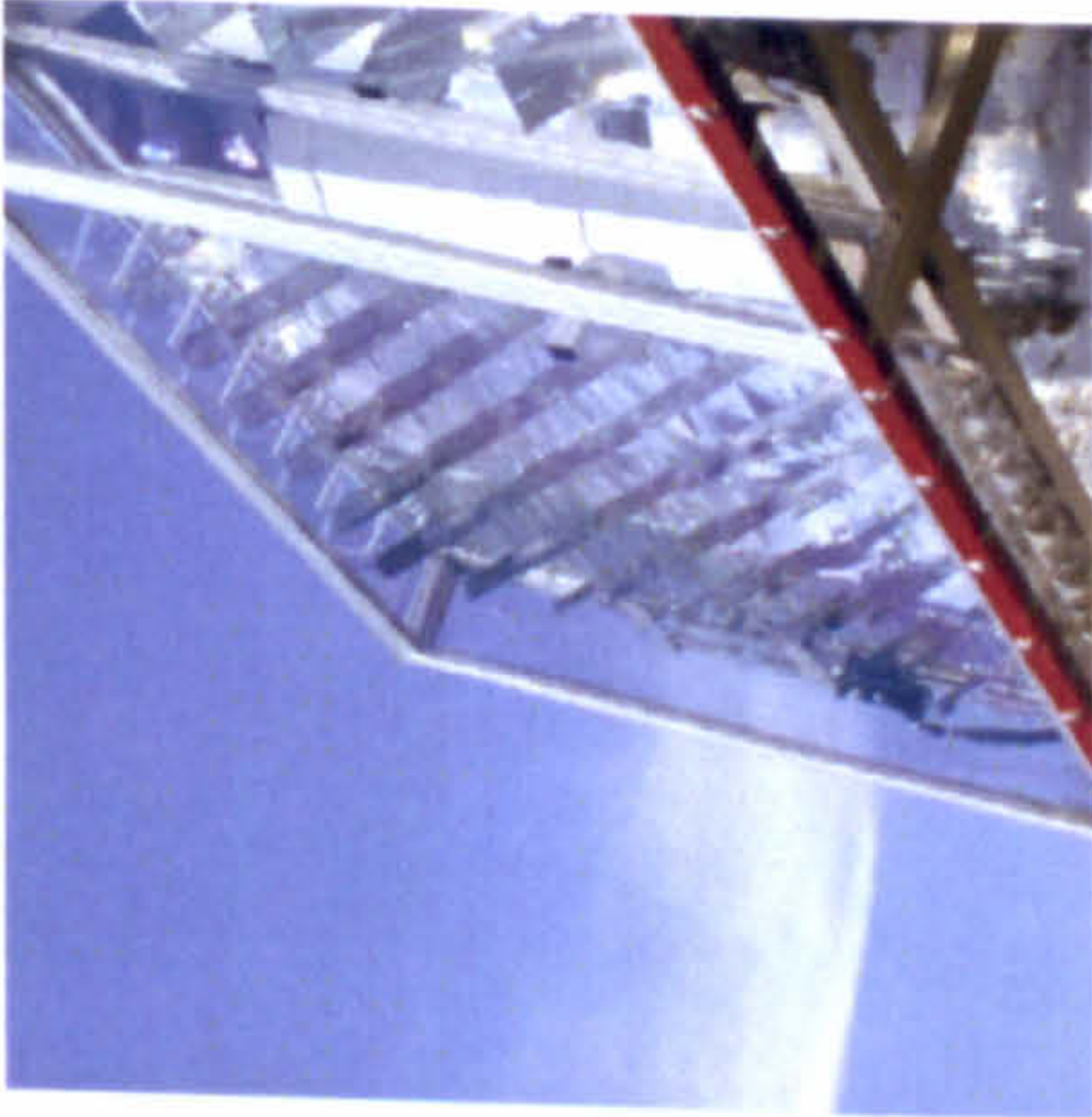
Name	Picture	Main features (key components)	Operating principle	Installation site	Source
1 Anidolic ceiling (Solar energy and building physics laboratory, Switzerland)		<ul style="list-style-type: none">- Double and single glazing- Parabolic deconcentrator- Anidolic element- Roller blind		LESO Solar Experimental Building, Switzerland	http://leso.epfl.ch/e/research_arch_dol_anidolic_facade.html
2 Heliobus Mirror shaft (Heliobus, Switzerland)		<ul style="list-style-type: none">- Aluminium construction- Glass mirrors- Air ventilation- "Tailored" geometry- Distortion-free reflection- Steel frame with powder-coated corrosion protection		Anlage Zollikon ZH MFH Zürich Abtwil SG Unterägeri ZG	http://www.heliobus.com/images/downloads/Lieferprogramm2008_english.pdf

3	<p>Bomin Solar Prism Systems (Bomin Solar, Germany)</p> 	<ul style="list-style-type: none"> - Acrylic plates - Stepper motor with a control system - Support tubes 		<p>German Museum of Technology Berlin, Germany</p> <p>Administration Center Remscheid, Germany</p> <p>Museum of modern art Salzburg, Austria</p>	<p>www.bomin.de/prismenlamellen/</p> <p>http://www.bomin.de/prismenlamellen/referenzen/</p>
4	<p>Bomin Solar Prism Systems (Bomin Solar, Germany)</p> 	<ul style="list-style-type: none"> - Glass plates - Supporting structure with glass holders - Stepper motor with a control system - Size : 520*2700*16mm 		<p>Munich Airport Germany</p> <p>Loffingen School Germany</p> <p>Library of the Bamberg University Germany</p> <p>Centre Municipal de la ville d'Issy Les Moulineaux France</p>	<p>http://www.bomin.de/glasslamellen/glasschuppenlamellen/</p> <p>http://www.bomin.de/glasslamellen/glasschuppenlamellen/referenzen/</p>

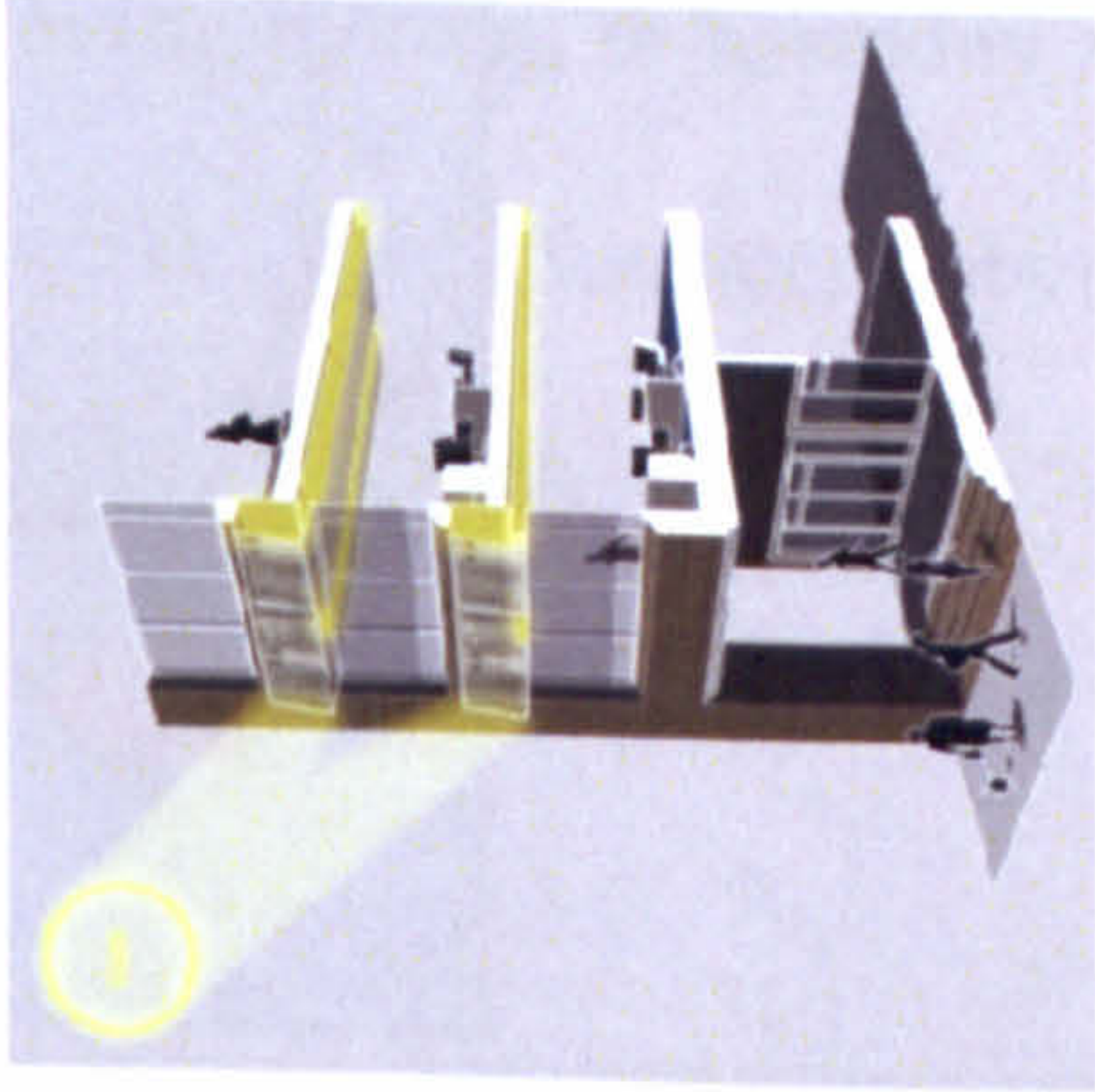
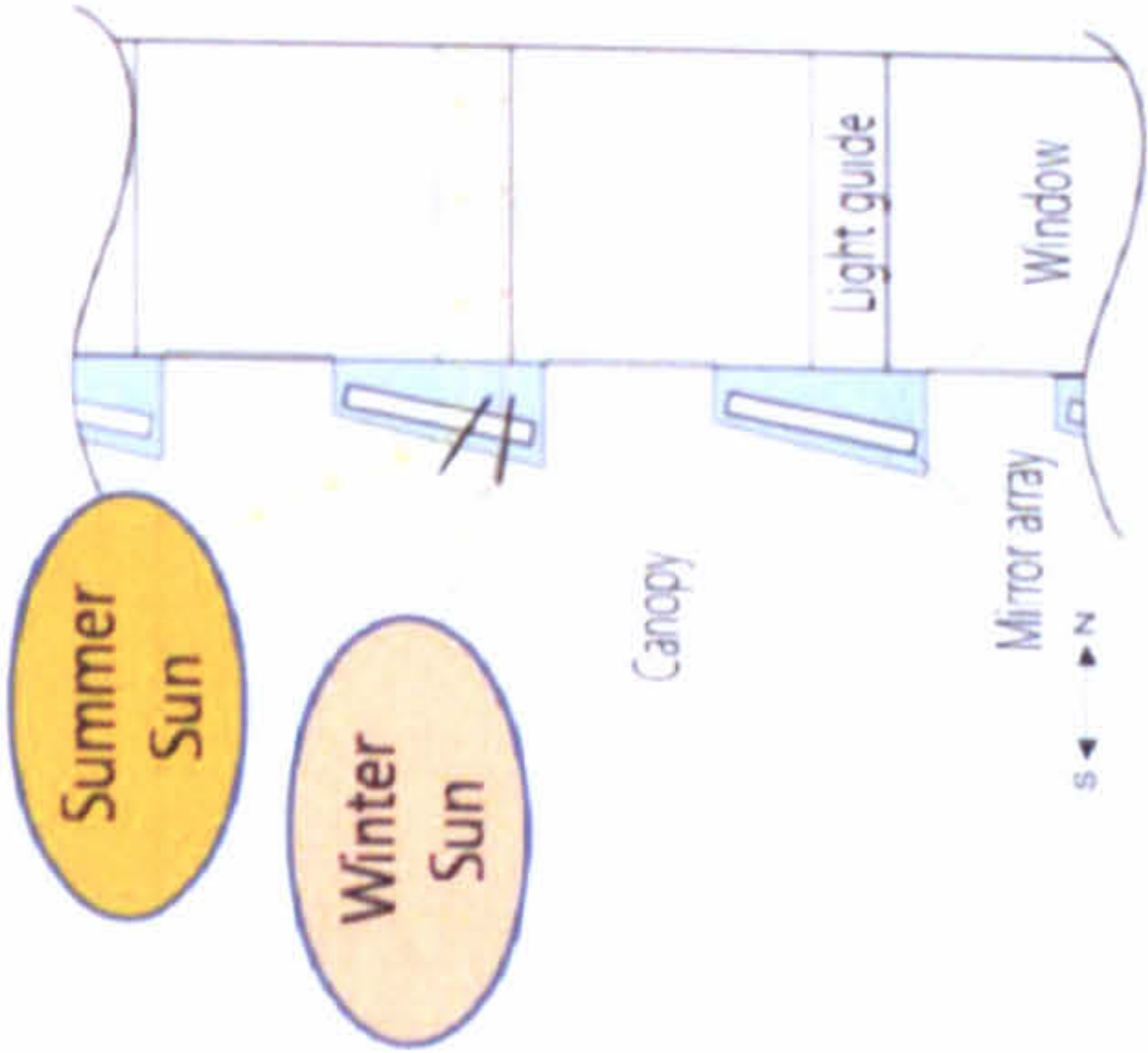
5	<p>Atrium (Behnisch, Behnisch & Partner Architect, USA)</p> 	<ul style="list-style-type: none"> - roof-mounted heliostats - fixed mirror - prismatic louvers - hanging prismatic mobile - reflective panels, reflective light walls - the central atrium functions as a huge exhaust duct and light shaft - saves energy used for lighting as much as 45% <p>Total Electric : 9,908,232 (kWh)</p>	 <p>Atrium</p>	<p>GENZYME CENTER, USA</p> <p>http://www.owl.net.rice.edu/~arch316/2005_genzyme.pdf</p>	
6	<p>Clerestory (Valley Architects, USA)</p> 	<p>Light scoop clerestory daylighting with internal louvers</p>	 <p>Clerestory</p>	<p>Hopland, California, USA</p> <p>http://www.greatbuildings.com/buildings/Fetzer_Winery_Ad_min.html</p>	

7	<p>Light shelf (Guardian Industries Corp., USA)</p> 	<ul style="list-style-type: none"> - Exterior sunshades and interior light shelves - light-colored ceilings - direct daylight deep into the open office environment 	 <p>Light shelf</p> <ul style="list-style-type: none"> - Installation of light weight reflective panel below the transom glass - Distribution of daylight increasing illumination deeper into the building than direct sunlight 	<p>Hoffman Corporation's offices, USA</p> <p>http://continuingeducation.construction.com/article.php?L=88&C=525&P=7</p>	
8	<p>Roof monitor (Corley Redfoot Zack, Inc., USA)</p> 	<ul style="list-style-type: none"> - Lighting controllers - Fabric baffles - Motion sensors - Photo sensors - LRC data loggers - Output : 13.54 (kWh/ft²) - Size : 2' * 4' fixtures 	  <p>Roof monitor</p>	<p>Smith Middle School, located in Chapel Hill, N.C</p> <p>www.lightingresearch.org/programs/daylighting/pdf/SmithCaseStudyFinal.pdf</p>	

The Solar Canopy Illumination System
(University of British Columbia, Canada)



- Redirecting mirrors
- Adaptive Butterfly Array
- Dual Function Light Guide



Transmission of daylight up to 20m into the interior of a building.

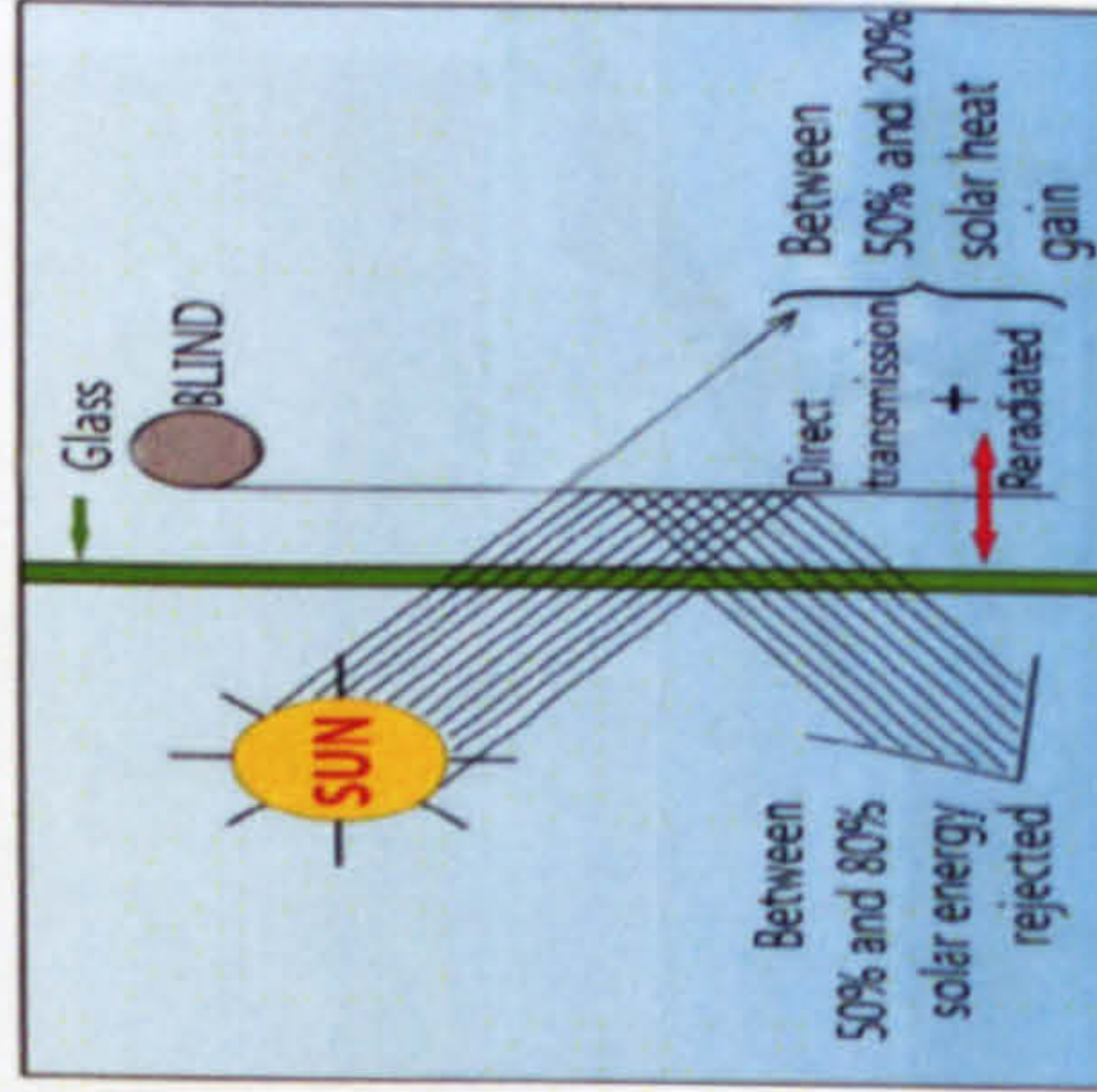
BCIT Campus in Burnaby Canada

<http://solar.calfinder.com/blog/products/the-brilliant-solar-canopy-illumination-system-for-commercial-buildings/>
<http://www.uilo.ubc.ca/advancing/profiles/solar-canopy.html>

Reflective Roller Blinds (Witwork U.S.A)



- reduce the heat of the sun: it's like sitting in the shade
- protect furniture and furnishings from fade
- reduce glare
- give daytime privacy



Reflective Blinds for Air Traffic Control Towers and Maritime Control Towers

<http://www.reflectiveblinds.com.au/roller.html>

As introduced above, there are many ways to distribute daylight according the needs and technical design(specifications) of the system. Depending on the design of a terminal device, which functions as a luminaire(illuminant), sunlight disperses differently in space generating distinct indoor lighting conditions. For those using light guides based on optical fiber cables, for example, various types of optical lenses (convex, semi-convex, concave, etc.) could be simply applied for spot lighting or other forms to create particular lighting conditions.

To fully utilize today's high-tech systems for daylighting in harmony with surrounding architectural environment, it is essential to understand the differences between technological and architectural approaches fully realizing the benefits of each.

1.6 Research Objectives

This study aims at designing a daylighting system for energy efficient buildings without any compromise on indoor environmental quality; especially, the visual comfort by natural daylighting. Good daylighting design is not only advantageous in saving energy and providing a healthier visual environment. It can ease the power shortage problem by shifting peak electrical demand during afternoon hours when utility rates are generally high. It also can improve human working productivity by promoting its natural circadian rhythm and pleasant working atmosphere. When designing a quality lighting environment, one should base it on the simple fact that most people appreciate daylight and also enjoy the outside view that windows provide. To achieve this, it is essential for any good design to get as much daylight as possible deep into a building while controlling the brightness (glare) of surfaces within the occupants' fields of vision.

In this work, we explore the harvesting of outdoor daylight by using an innovative concentrator and transmission system for indoor application. A fully integrated day-lighting system can enhance the visual acuity, comfort, and space aesthetics. The proper design of

daylight system could control the external heat gain and glare and thus, reducing internal heat gain and energy use. When combined with the sustainable design strategies of indoor spaces, daylighting introduced into indoor spaces of building has the effect of improving the work productivity of employees. It has been reported that such system could improve productivity in offices by 16 percent [Edwards and Torcellini, 2002].

Figure 1.1 gives the flow of research procedures taken in the present work. As shown, each step of research development either involves theoretical analysis, physical reasoning, or actual measurements. A rigorous survey has been carried out before embarking on the design of a daylighting system, which deems essential to develop an innovative system different from the existing ones. Especially, the system has to be well suited with other building elements that bring natural daylight into the interior of buildings. Its appearance as well as functional expediency should be considered with the overall architectural integrity of a building. Architectural integrity should not be sacrificed for the sake of functional expediency

Particular attention should be directed to maximize visual comfort in harmony with windows or other openings and reflective surfaces as well as other daylighting devices (systems) such as light pipes. Realization of energy efficient buildings could be simply achieved by the combined effect of the reduced use of artificial (electric) lighting and controlled admission of natural light into a space through windows and various daylighting systems.

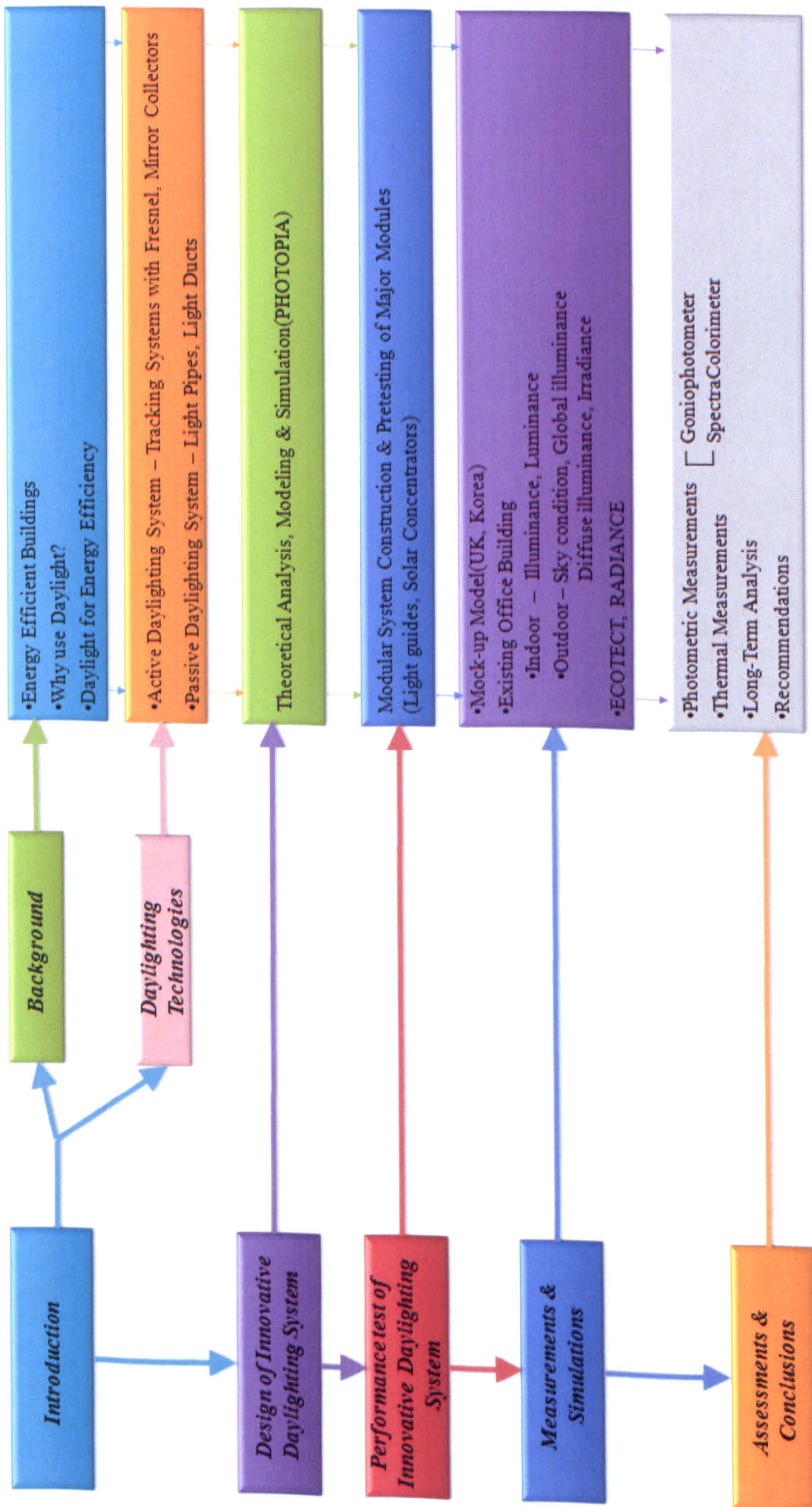


Figure 1.1 Research procedure

1.7 Summary

This chapter has introduced the background and significance of this work in terms of enhancing sustainability and energy efficiency of buildings. Daylight utilization is very important for humans not only because it could save energy but because it boosts healthy and natural ingredients in architectural enclosures. There are currently various types of daylighting schemes harnessing daylight for interior illumination, which could be divided into three categories: active, passive and building-integrated daylighting systems. To harvest natural daylight more aggressively, we explored the possibility of developing an innovative daylighting system well suited with other building elements. Its appearance as well as functional expediency should be considered with the overall architectural integrity of a building as well as other daylighting devices (systems) such as windows and light pipes.

2. DESIGN AND CONSTRUCTION OF THE SYSTEM

Solar concentrators could be designed in various ways. It could assume the shape of a trough, a dish, a cone, a funnel and etc. The shape of a concentrator is very important one should consider many physical limitations in fully implementing its design concept. In addition, its shape should be in harmony with surroundings and endurable against harsh weather elements. In this study, we examined two different types of concentrator design, a dish concentrator and a funnel concentrator, which deem very simple and widely considered in many applications.

2.1 Design Concentrator

When designing a concentrator, considerations should be made to maximize the collection of incoming solar rays and minimize optical losses and any leakage until they are fully delivered to where it is consumed. The following designs fall in this category although they differ in shape and optical approaches.

2.1.1 Prototype design

The dish type solar concentrator is one of the most simple and straightforward ways to harness parallel beams of sunlight. It requires two reflectors; one to concentrate incoming solar rays onto a near focal point of the (parabolic) dish reflector (concentrator) and the other to form and reverse its direction of a stream of high density sunlight as shown in Figure 2.1. In Figure 2.1, major components of the concentrator assembly are given with the paths of parallel beams as they impinge on the surface of a dish reflector (a) and a two-dimensional sectional view (b). A parallel beam of light is first reflected by the dish reflector and directed toward a point near the second reflector, a convex (or concave) mirror. The light is then reflected off the second reflector directed toward a homogenizer tube whose role is to offer a

path till it is admitted to a light guide. The light guide delivers the sunlight to where it is needed by discharging it through a terminal device made with optical lenses (or other materials).

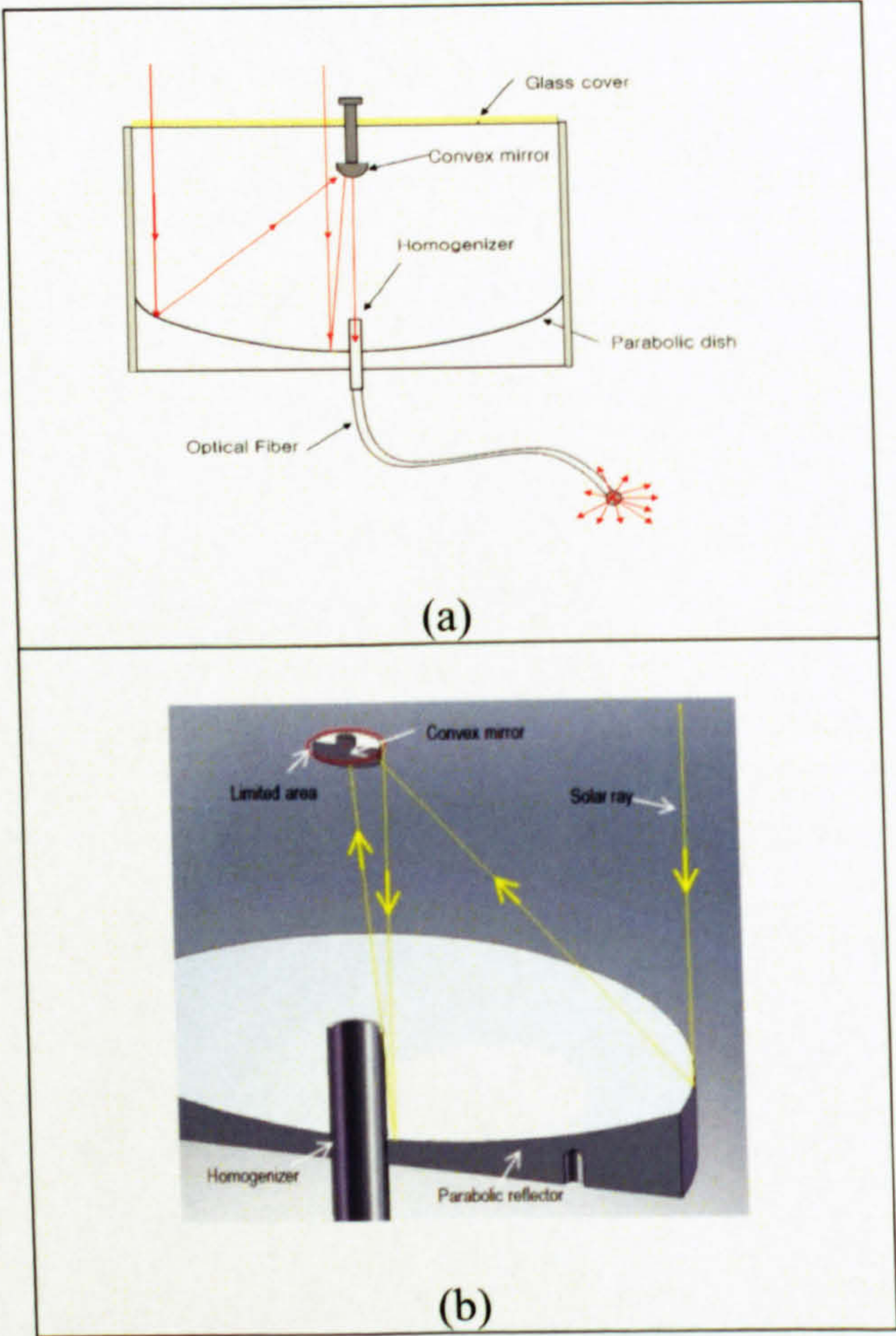


Figure 2.1 Design concept of a dish concentrator for daylighting: (a) light paths and major components, (b) two-dimensional sectional view of the concentrator assembly.

For the second reflector, different shapes of mirrors could be employed as long as they could redirect the sunlight reflected off the dish reflector toward the short homogenizer tube placed at the center of the dish reflector. When placing the second reflector, a transparent cover could be used to hold it at its desired position as shown in Figure 2.1 (a) or other means as long as they provide solid support in maintaining its original position. The transparent

glass cover has an advantage over others as it prohibits dust deposition on the reflector and facilitate cleaning. It, however, could cause some problems in summer or warm sunny climates due to thermal deformation of the cover resulting in misalignment of the second reflector. The position of the second reflector should be carefully determined considering the type a mirror used for the second reflector as shown in Figure 2.2. When a convex mirror is used, it should be placed below the focal point of the dish reflector. This is contrary to the case of a concave mirror where it requires to be positioned higher than the focal point of the dish reflector. For the dish reflector of 300mm in diameter considered in this figure, there is a difference of 39mm in distance between their desired positions. This is because the former enables a parallel beam of high density solar rays to stream downward toward the homogenizer tube whereas the latter forms a converging beam allowing smaller inlet for the homogenizer tube.

In the present study, we used a convex mirror for the second reflector as it facilitates the implementation of the design concept resulting in higher efficiency. The converging beam of sun rays minimizes any leakage entering the homogenizer tube. As sunlight reflects off the dish concentrator and directed toward the second reflector, it becomes quite dense in its flux density such that a small deviation from its original targeted area or blockage caused by an obstacle could lead to a significant loss. Because of this, it is very crucial to design the second reflector as accurately as possible and minimize (or eliminate) any obstacles that might be present along the course of light transmission. In the present study, two different schemes are considered for the positioning of the second reflector at the desired position. One is to use a transparent cylindrical cover and to adhere it at the centre of the circular glass cover. The other is to use slender metal rods to support it at its fixed position. There are cons and pros of both schemes as each has the possibility of causing some minor problems in providing durable and efficient means of positioning the second reflector.

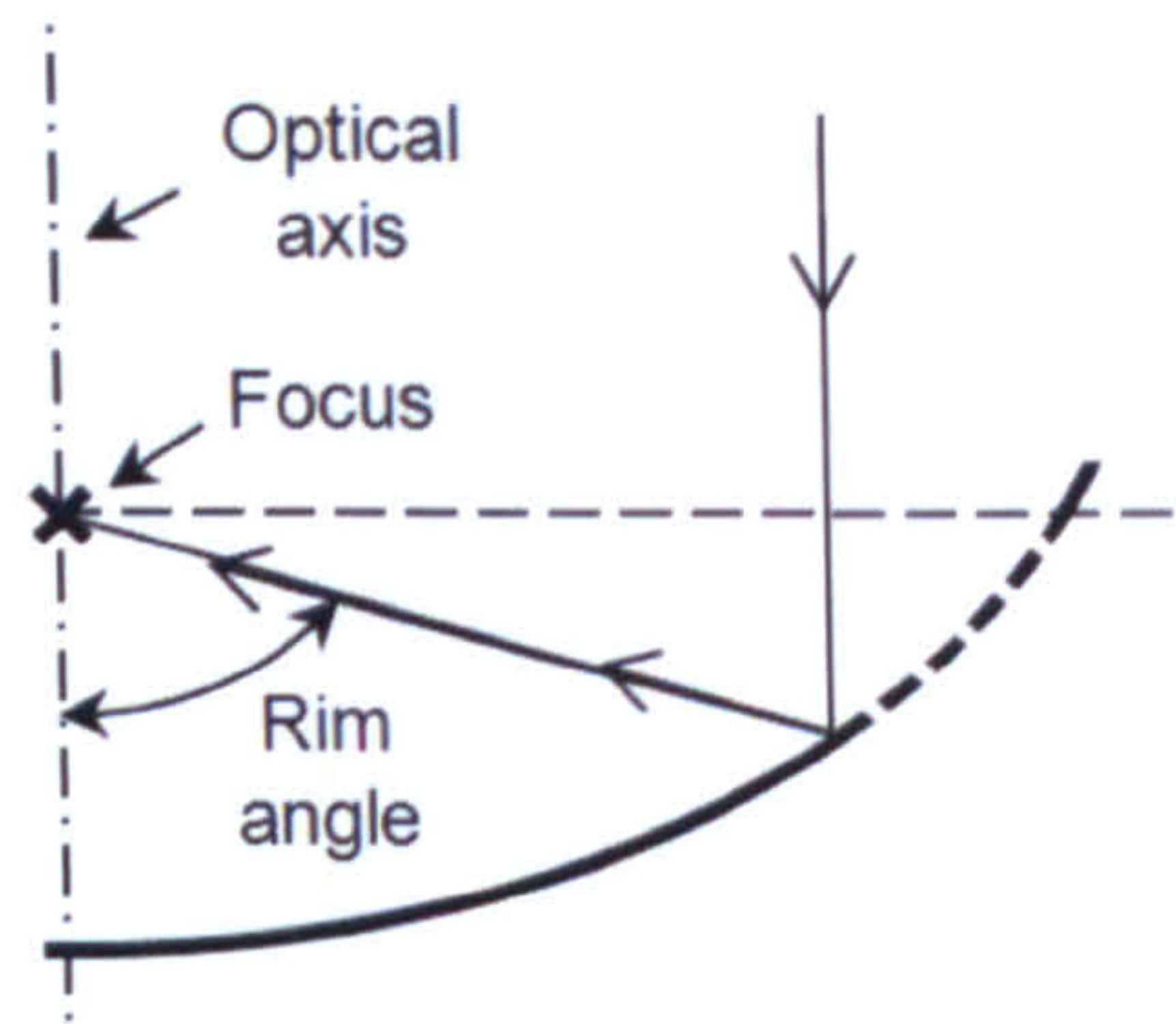
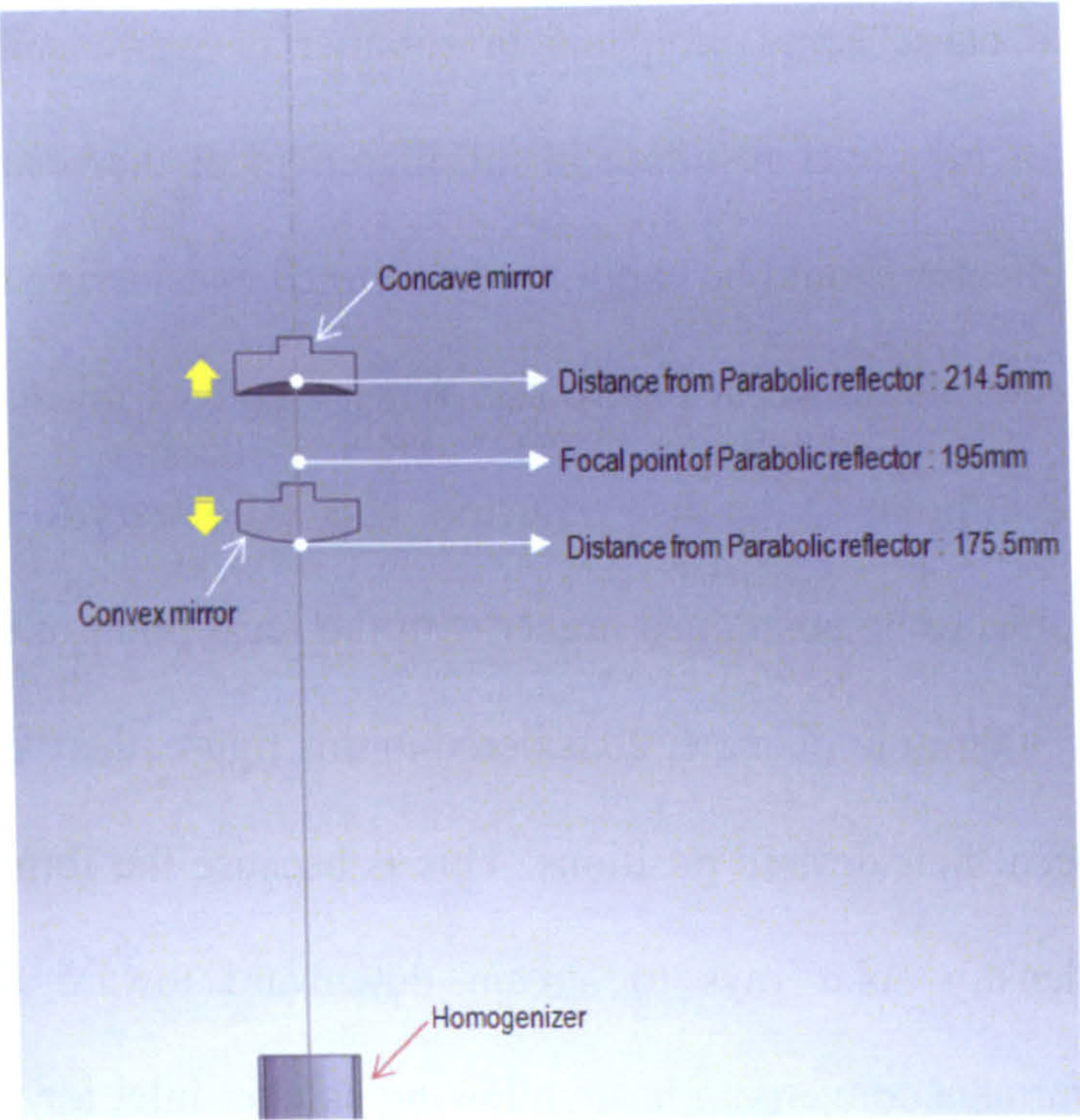


Figure 2.2 Positioning of the second reflector and basic geometry of the dish concentrator

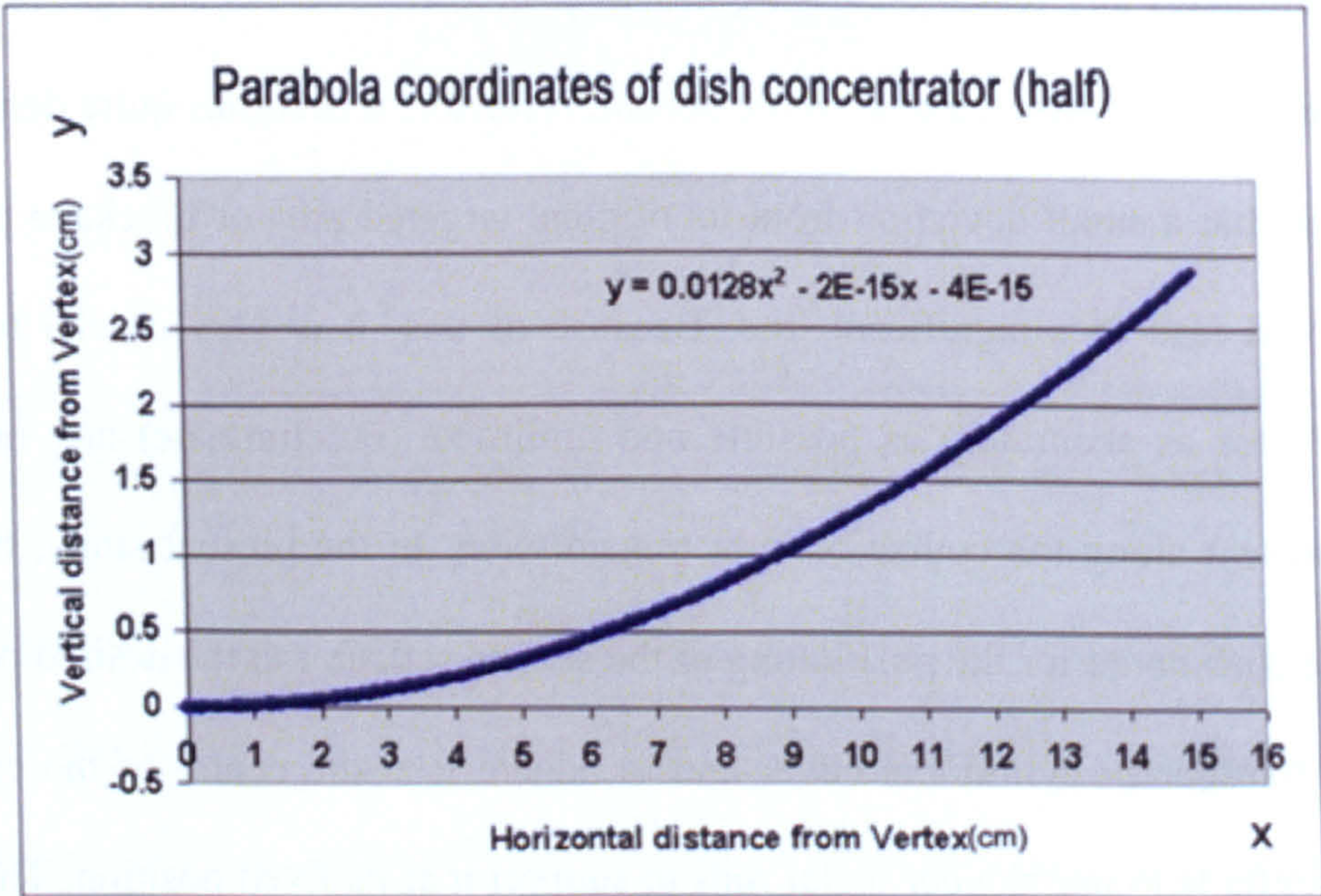


Figure 2.3 Parabola used for the dish concentrator of 30cm

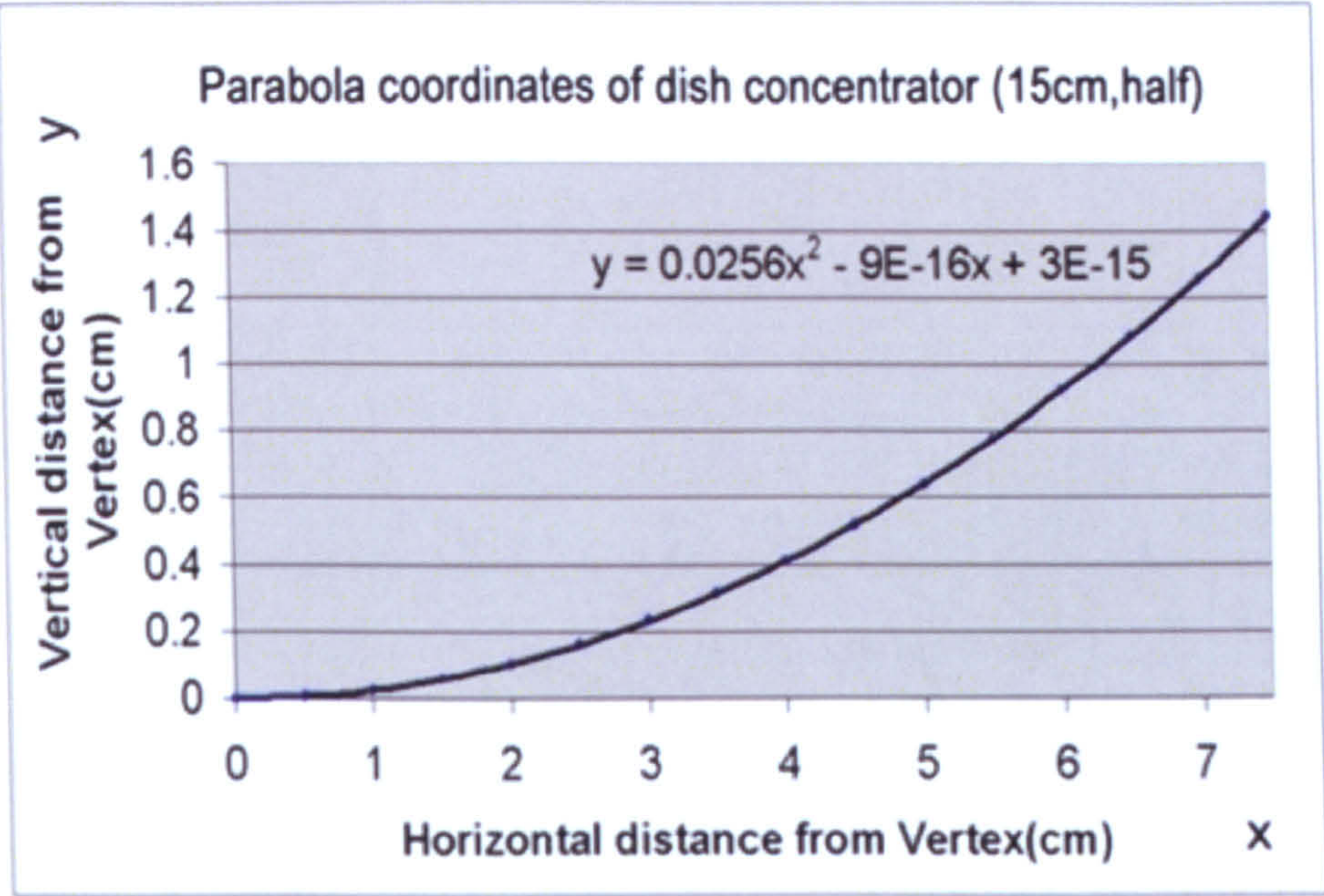


Figure 2.4 Parabola used for the dish concentrator of 15cm

Figure 2.3 and 2.4 show the profile curves of the dish concentrator whose diameters are 30cm and 15cm, respectively. As its area (projection area) is proportionate to the square of the radius, the amount of incident solar radiation doubles each increase in radius. In these figures, the profile curve is given in terms of a quadratic function, which is a parabola. A surface of revolution, i.e., the dish reflector, is simply generated by revolving the curve about the ordinate axis. Depending on its design, the geometrical location of a focal point (where sun rays converge) varies, which determines the overall configuration of the dish-daylighting system.

Table 2.1 Major design variables for the dish concentrator of 30cm

dish diameter (cm)	30.00
focal distance (65% of D, cm)	19.5
dish radius (cm)	15
rim angle (degrees)	42.07506

Major design variables are given in Tables 2.1 and 2.2 for the dish reflectors (concentrators) of 30cm and 15cm in diameter, respectively. As shown, the focal distance from the dish reflector does not change proportionately with the dish diameter. The rim angle, however, remains the same as they are geometrically congruent.

Table 2.2 Major design variables for the dish concentrator of 15cm

dish diameter (cm)	15.00
focal distance (65% of D, cm)	9.75
dish radius (cm)	7.5
rim angle (degrees)	42.07506

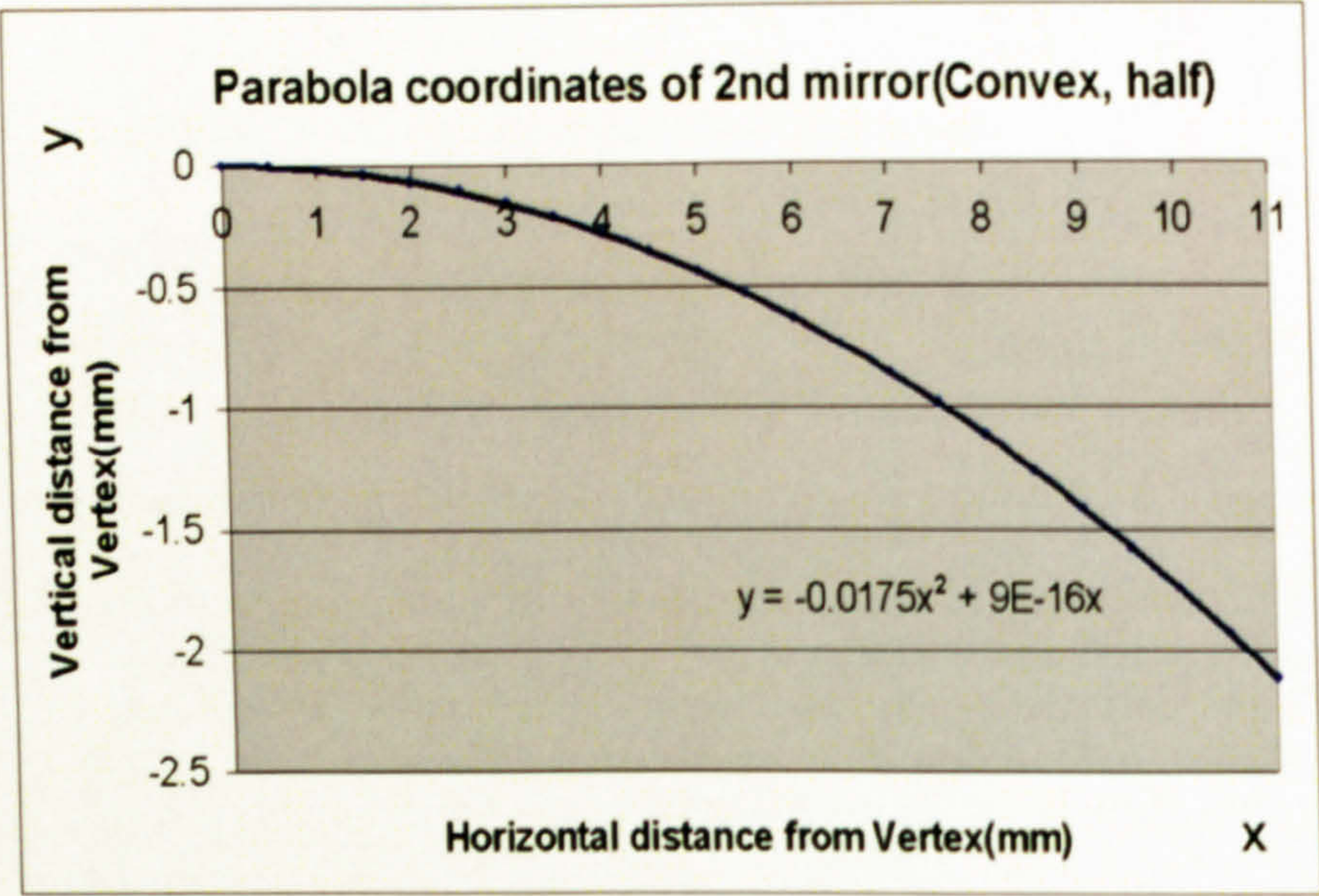


Figure 2.5 Equation of the parabola used for the second reflector

Figure 2.5 gives the parabola equation used to design the second reflector, which is convex in its form in comparison to the dish concentrator designed to be concave. As aforementioned, its shape and dimension are directly related to the dish reflector. An optimization process is required to properly design its overall configuration in relation to the dish reflector. Its diameter is 2.2cm and the rim angle is about 42 degrees; the same as that of the dish concentrator.

Table 2.3 Major design variables for the second reflector

convex mirror diameter (cm)	2.20
focal distance (65% of D, cm)	1.43
radius (cm)	1.1
rim angle (degrees)	42.07506

Again as in Figure 2.3 and 2.4, the profile curve is given by a quadratic function of the horizontal distance measured from the vertex. Table 2.3 gives the major dimensions used in the design of the second reflector.

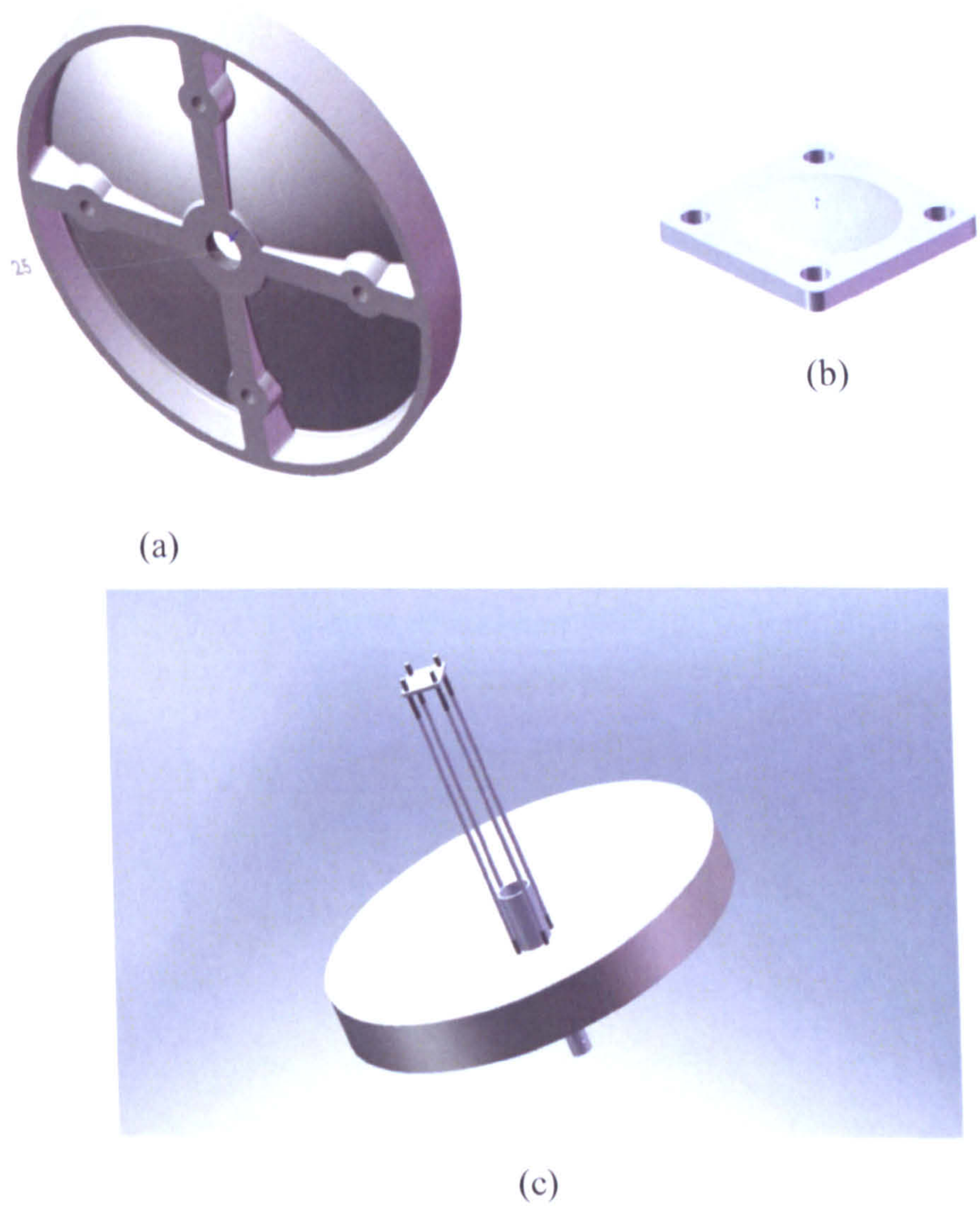


Figure 2.6 Three dimensional design images of the major components and the system:
(a) (parabolic) dish reflector, (b) second reflector, (c) concentrator assembly

Figure 2.6 presents three dimensional design images of the dish reflector, second reflector and concentrator assembly. Each image is actually used for processing of raw materials (aluminum blocks) to make the component (assembly) as shown. Each component is designed such that it is readily eangaged with other components to complete a concentrator

assembly. This enables modular construction of the system and facilitates maintenance. Also, it makes easier for one to change the design of a component for further development if necessary.



Figure 2.7 Engagement of the dish concentrator with light guides

Figure 2.7 shows the scheme used to engage the dish reflector with light guides composed of a homogenizer tube and light guide cable (optical fiber cable and etc.). The homogenizer tube makes the high density sunlight flux to converge before it enters the light guide cable. It is essential to treat the inner surface of the homogenizer tube with highly reflective coatings (aluminum, silver or its equivalent).

To verify the solidness of the present design in collecting and transmitting incoming solar rays for daylighting, a forward raytracing software package, PHOTOPA is used which will be detailed in the next section.

2.1.2 Optical analysis using PHOTOPIA

To investigate the functional appropriateness of the main components, a forward ray tracing technique, PHOTOPIA, has been employed. PHOTOPIA is a 3D modeling and simulation package capable of handling high number of reflections that occur within internally reflecting daylighting systems. It is based on the forward ray tracing algorithm developed from a broad knowledge of luminaire analysis techniques ranging from non-diffuse radiative transfer to non-specular 3D raytracing [PHOTOPIA User's Guide 2002].

This section introduces how PHOTOPIA can be used to draw forth the most optimal conditions in its optical design of a daylighting system with a number of components to reflect and redirect light for indoor illumination. Light intensity and its distribution are calculated at various locations for the major components of the system. This allows one to develop some good intuitions regarding the functional design of major components such as the shape and size of reflectors and light guides. By offering the experimenter to "see" and "quantify" illuminance levels without resorting to very complex experimental investigations, the program makes it possible to efficiently carry out various steps of design calculations without undue difficulties.



Figure 2.8 3D modeling by Rhinoceros

In Figure 2.8, a 3D modeling of our first trial design of the concentrator assembly with a cylindrical transparent cover is given. The modeling is done by Rhinoceros [Cheng 2007] where it is imported to PHOTOPIA domain for 3D performance analysis. Rhinoceros is a stand-alone modeling tool with a very convenient user interface.

Comparisons were made for the concentrator assembly design when different shapes of mirrors are used: convex and concave. Identical reflectance(0.99) and transmittance(0.92) values were assumed for both cases. Mesh densities for critical elements of the designs were incrementally increased until no significant ($<0.1\%$) gains in performance were seen. Small uncertainties in the simulation parameters have a significant impact on the absolute value of the simulation transmission efficiencies. Therefore comparative analysis of the relative performance of two designs is often more informative than the predicted transmission efficiencies themselves. Using ray tracing based simulation of daylighting systems is particularly beneficial when employed to optimize the design of a system.

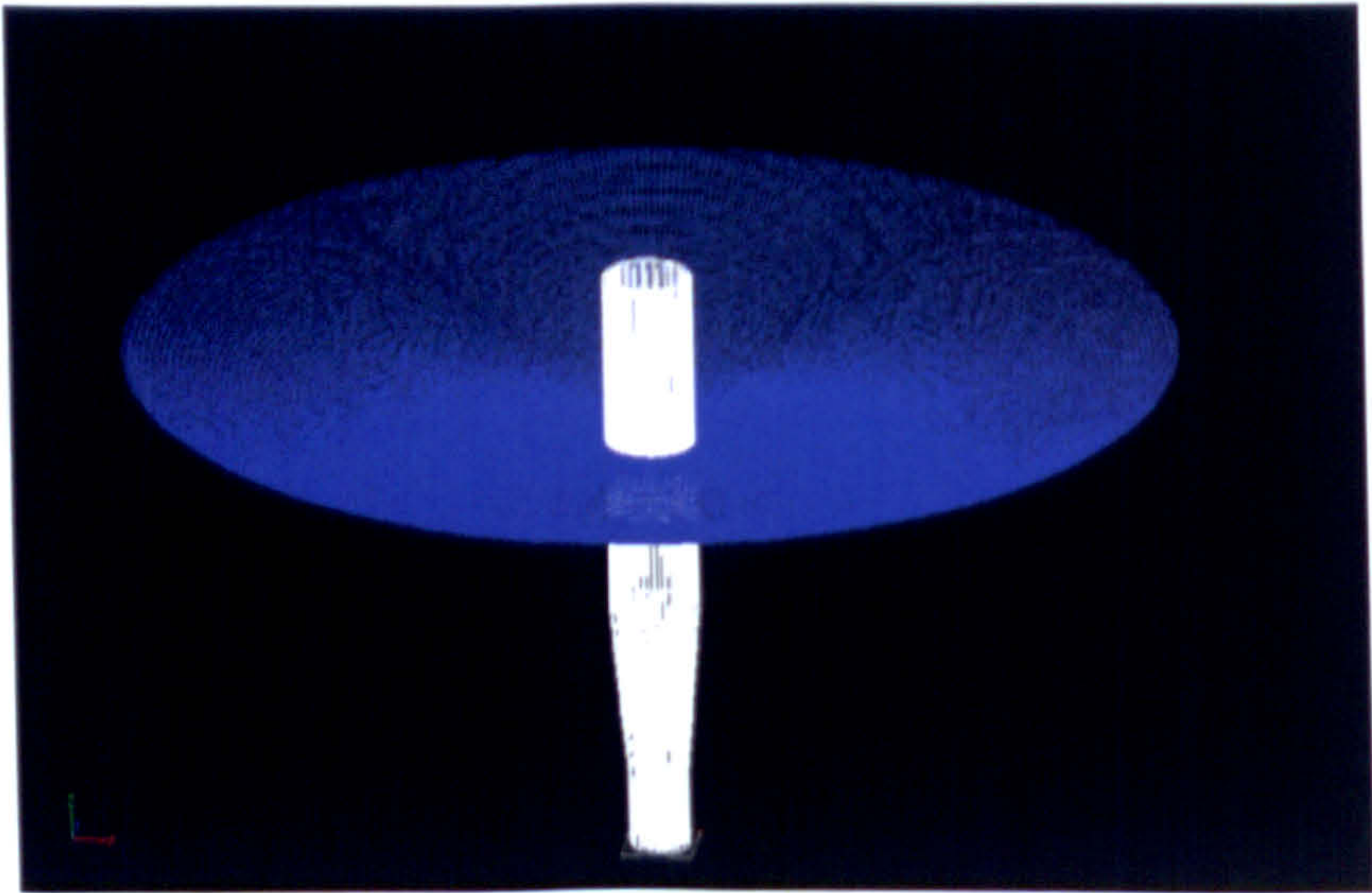


Figure 2.9 Modeling of the dish reflector

Figure 2.9 shows the model of the dish reflector where a minimum initial grid quads (set in the polygon mesh - detailed options) of 10,000 was used. This seems to be enough for PHOTOPIA simulations as finer mesh systems made little difference in its accuracy but

increased the computation time to a greater degree. If not specified by the user, mesh sizes are determined automatically.

Figure 2.10 shows the modeling of a convex mirror used as the second reflector to redirect and concentrate high density fluxes of sunlight into fiber optic bundles. Its geometrical design is determined by a number of optical design constraints, which are imposed for achieving the highest efficiency in transmitting sun rays to the homogenizer tube. The design shown in this figure resulted in the highest efficiency of delivering the sunlight impinged on the dish reflector to the one end (receptacle) of the optical fiber cable. It showed an efficiency of 38.9% with the distance of 175.5mm from the dish (parabolic) reflector. As typical solar tracking daylighting systems show better performance than this, there seems to be much room for improvement requiring a systematic investigation of the major components involved in light transmission. Of these, the transmittance of the cover has to be examined carefully as it is the first barrier that incoming solar radiation encounters.

$$\frac{\text{Total lumens exiting homogenizer}}{\text{Total lumens entering roof above concentrator}} = 38.90\%$$

This indicates some adjustments are necessary to improve its efficiency for the distance suggested in Figure 2.2, which could be done rather easily by installing adjustment screws with the convex mirror.

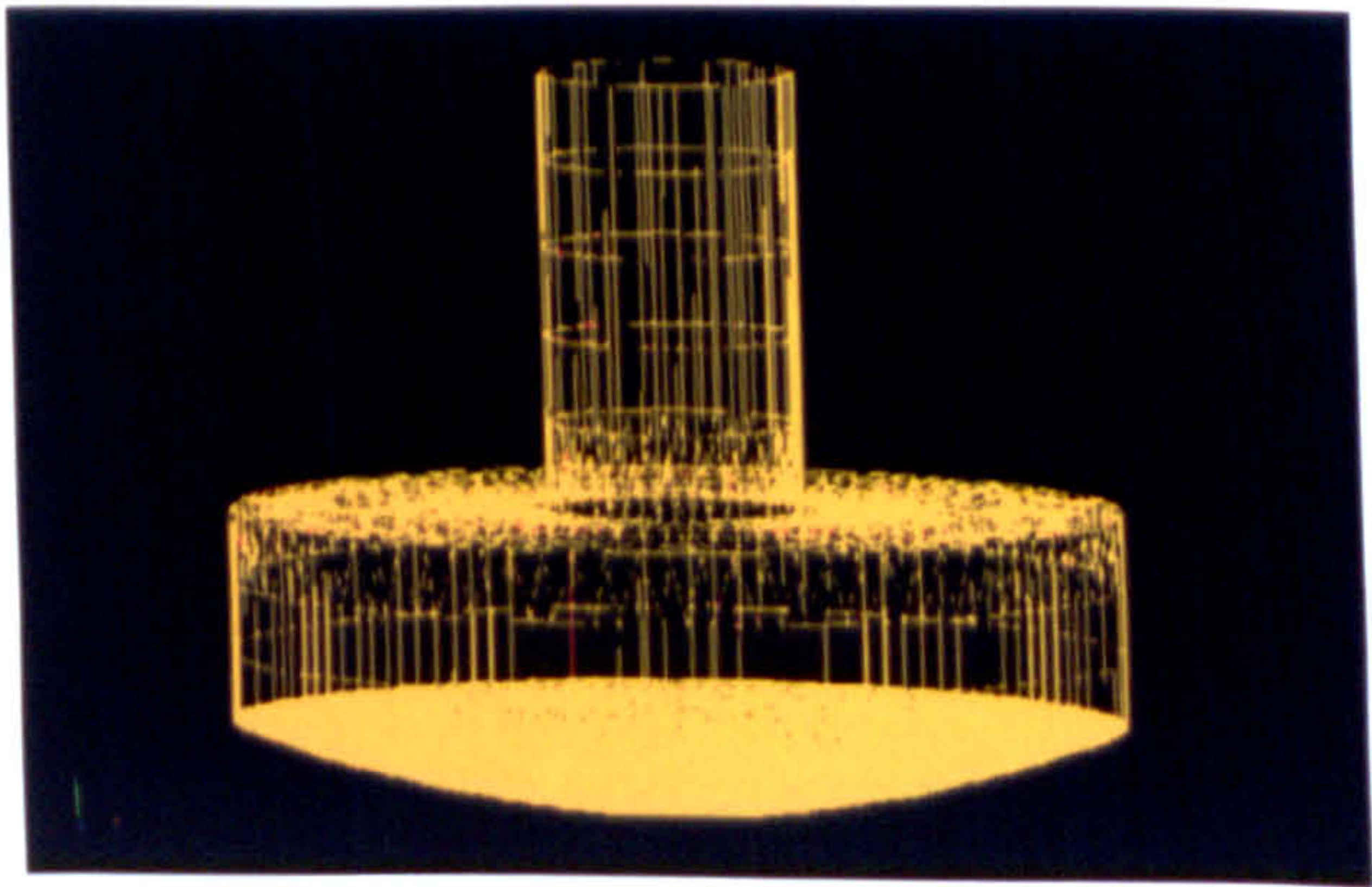


Figure 2.10 Convex mirror (model designed for PHOTOPIA simulation)

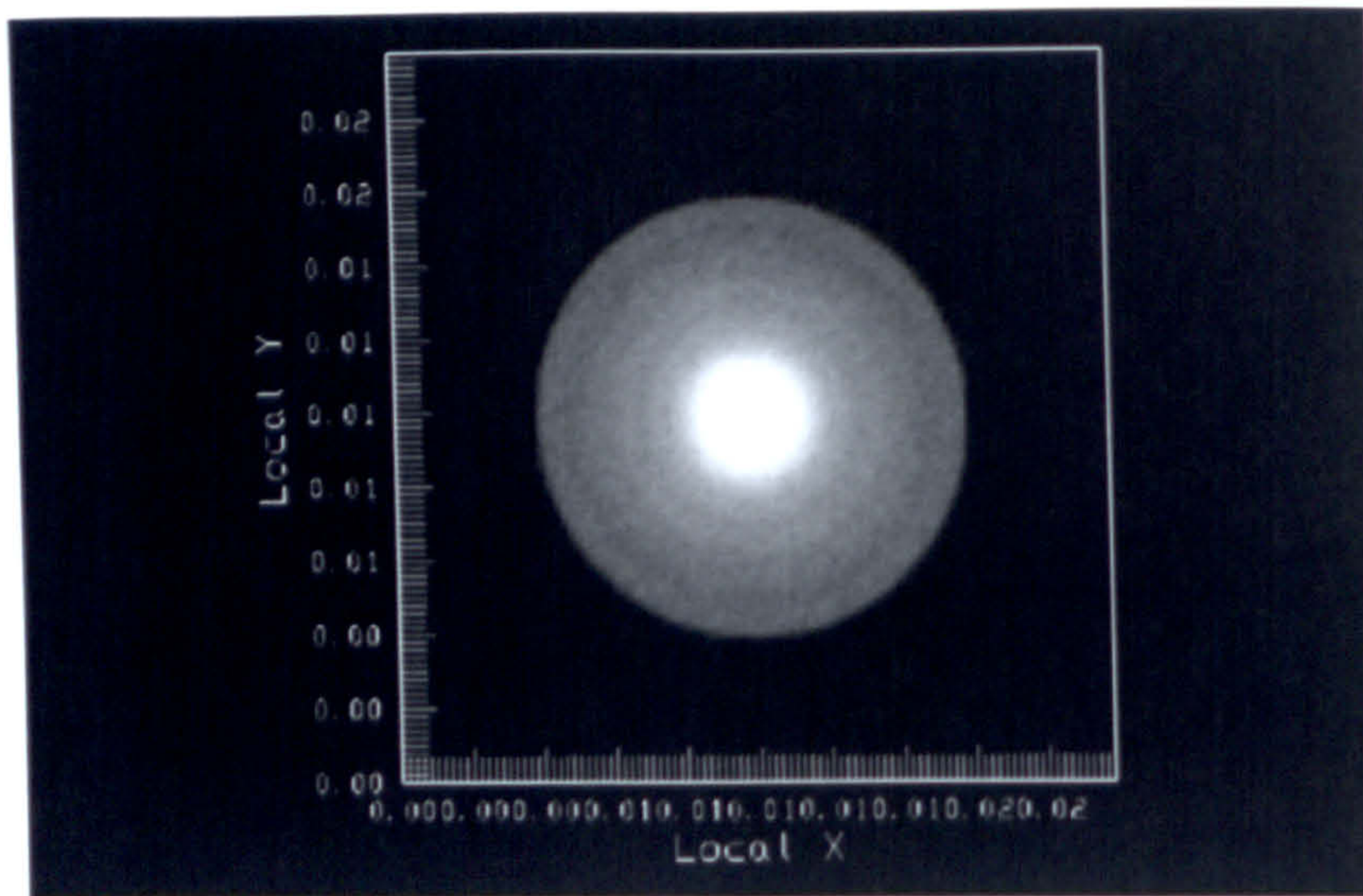


Figure 2.11 An image of the illuminance distribution at the exit of the homogenizer tube

Figure 2.11 shows the illumination distribution at the exit of the homogenizer tube when 50,000,000 rays are assumed to impinge on the dish reflector. The brighter area at the center represents the area of high solar concentration. This implies that the homogenizer is functioning as it is designed. Care should be exercised, however, for the homogenizer tube to have an inner surface with high reflectance which should be also specular. Depending on the smoothness of its design and inner surface optical properties of the homogenizer, light intensity could change quite drastically. It might be desirable to use shorter homogenizer tubes if circumstances permit.

Figure 2.12 shows the modeling of a concave mirror used for PHOTOPIA simulation. That is, the same homogenizer and parabolic (dish) reflector was used as above but with a different distance of 214.5 mm as it should be placed above the focal point of the dish reflector. The concave mirror showed a similar performance as compared to the convex mirror with a transmission efficiency of 37.7%. This again indicates that the focal length of the second reflector is not optimized to maximize the amount of light entering the homogenizer tube. Adjustments could be made manually for its optimal position on the basis of the simulated results in real situations

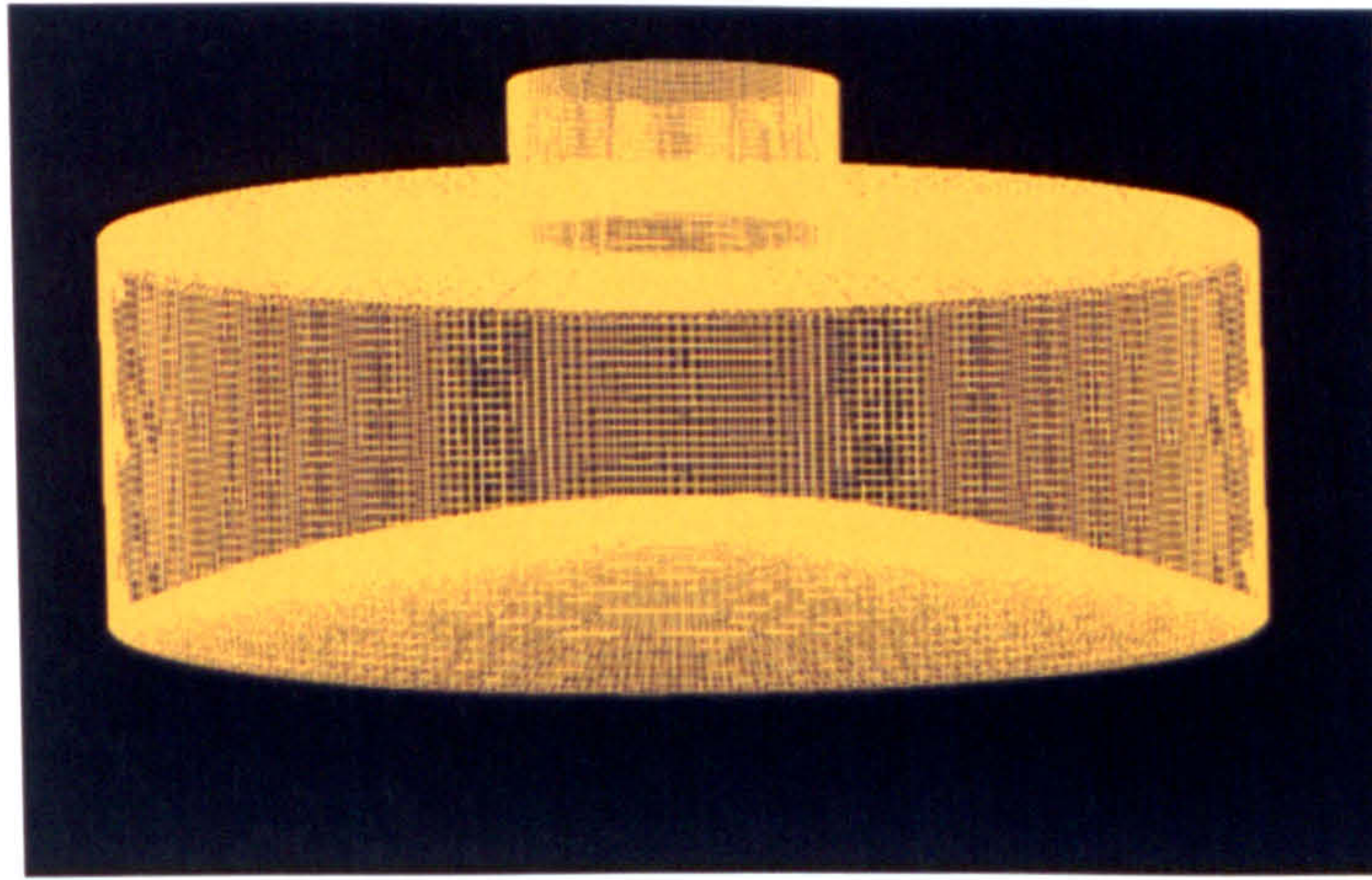


Figure 2.12 Concave mirror (model designed for PHOTOPIA simulation)

All in all, the above simulation results indicate that significant improvements could be obtained in the both convex and concave lenses for the second reflector if is rightly positioned to allow a greater percentage of the light into the homogenizer opening. Although there is no appreciable difference in its efficiency, the convex mirror seems to be more feasible to be used with the dish reflector. This is because light beams converge as they stream downward toward the homogenizer tube. In comparison, the concave mirror produces parallel beams of light toward as they are reflected off its concave surface as shown in Figure 2. 12. It is very important to verify that the inlet of the homogenizer tube is large enough to admit high-density light beams streaming toward its entrance. Because of its light intensity is quite high (up to 100 suns), the peripheral loss at the homogenizer inlet should not be overlooked. Appropriate measures must be taken if some losses take place for any reason. Also, considering the fact that the optical properties used in simulations could have been somewhat exaggerated than the actual ones, it is necessary to examine each of them (if available) for establishing more realistic models in simulation.

2.2 Funnel Shaped Concentrator

Cone or funnel shaped concentrators have been used in many solar applications for a long time. The figure (Figure 2. 13) below shows one of such designs where its geometrical shape is determined by combining two parabolas to form a conical mouth [Xue, 2010]. There are no transparent cover used as compared to one of the designs of dish concentrators simulated using PHOTOPIA in the previous section.

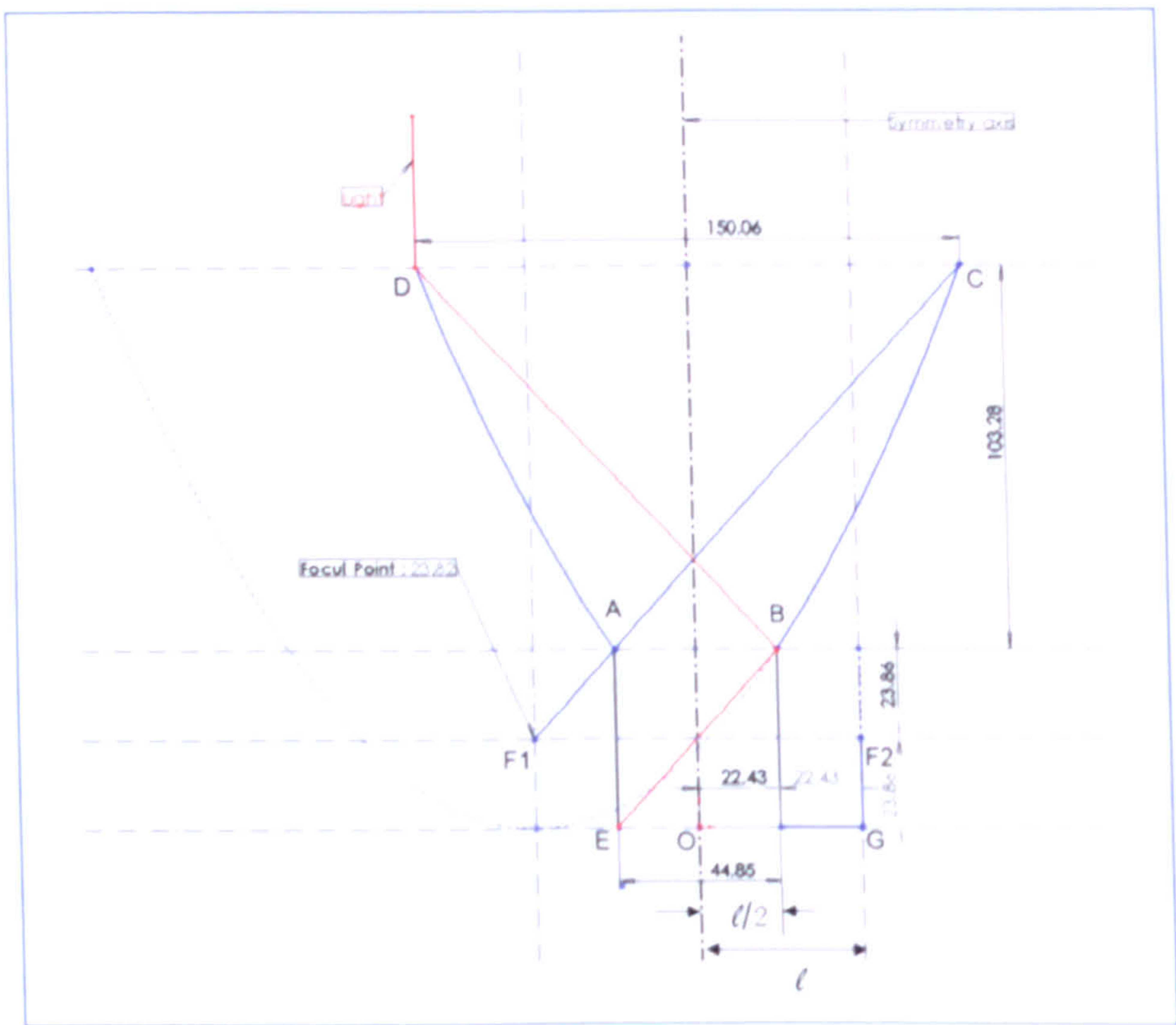


Figure 2.13 A curved profile of the funnel shaped concentrator

The design utilizes segments of two parabolas AD and BC to form its two-dimensional profile curve which are symmetric to each other with respect to the symmetry axis as given in the figure. The straight segment AB is used to truncate the parabolas located above the focal points (F_1 and F_2). A surface of revolution for the funnel shaped concentrator is generated by revolving this curve about the symmetry axis. The design is similar to typical CPC collector designs.

In the present study, the circular inlet diameter of the concentrator was 150.06mm where the distance between the inlet and the end of the curved surface was 103.28mm. A straight tube of 44.85mm in ID and 47.72 mm in height joins the curved surface followed by a homogenizer tube and a light guide. This design eliminates the use of the second reflector but requires an inner surface with very high reflectance(~ 1) as sun rays experience many reflections before they enter the receptacle of a light guide. The funnel shaped inner surface is designed to redirects rays such that they eventually stream downwards toward the narrow straight tube at the bottom. This could be easily done by tracking incident and reflected sun rays continuously for the case of a specular reflection. Similar to the dish concentrators, the funnel shaped solar concentrator is designed to utilize the beam component of solar radiation and requires precise tracking of the sun throughout its operation. The diffuse component of solar radiation is mostly bounced back into the atmosphere.

Figure 2.14 shows a three-dimensional image of a funnel shaped concentrator made by revolving the two-dimensional curve given in Figure 2.13. As mentioned above, funnel-shaped wall concentrates the sunlight admitted by the circular mouth and channels its flow downward until it enters a light guide system via the straight tube portion of the concentrator.



Figure 2.14 A three-dimensional image of the funnel shaped concentrator

2.3 System Configuration and Control

The present overall system could be consisted of one master tracker and a number of slave trackers that are identical to each other. Figure 2.15 shows the concept of system configuration and its operational scheme.

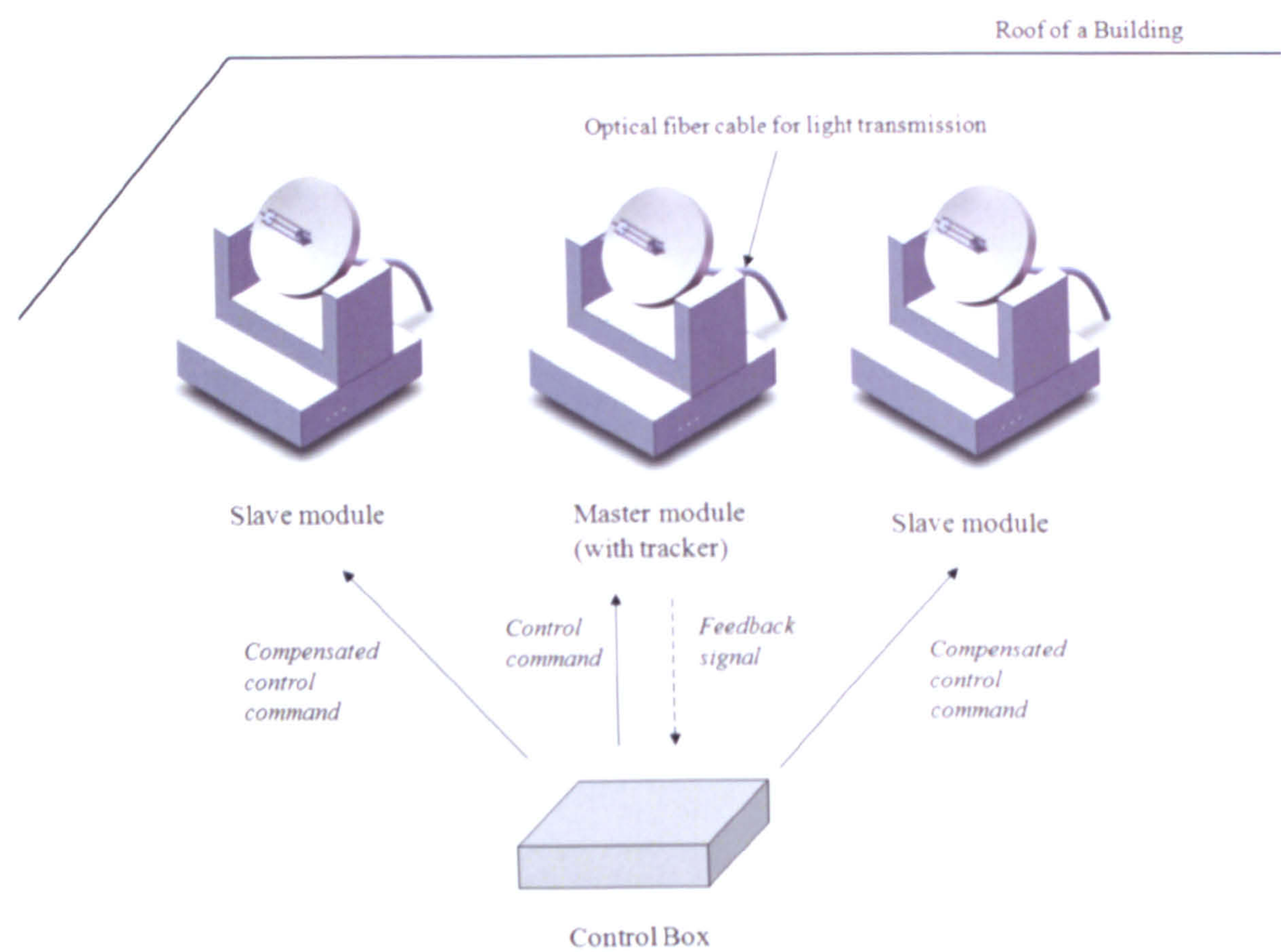


Figure 2.15 Concept of system configuration

Figure 2.16 gives the control logic applied for the operation of the system. As shown, the control system of the master tracker has position sensors to monitor the deviation of the actual position from the desired one by a feedback algorithm. And this deviation signal is used as input to actuate the reflector spindle. In the meantime, the slave tracker has no sensors

All the slaves operate in a parallel motion with the master. Each slave is controlled by the deviation signal that is generated from the master tracker in a feedforward control manner.

The advantage of this strategy is that the overall system configuration is simple and its operation is rather practical. However, it has the drawbacks that the position of each slave may not be the same as that of the master because of the errors associated with its construction and installation.

There are many solutions but the simplest one is the feedforward control by applying the measured disturbance signals to the actuators of slaves. Since the system speed is not fast, an optimal disturbance signals can be defined easily, and by this algorithm, the error can be compensated as desired.

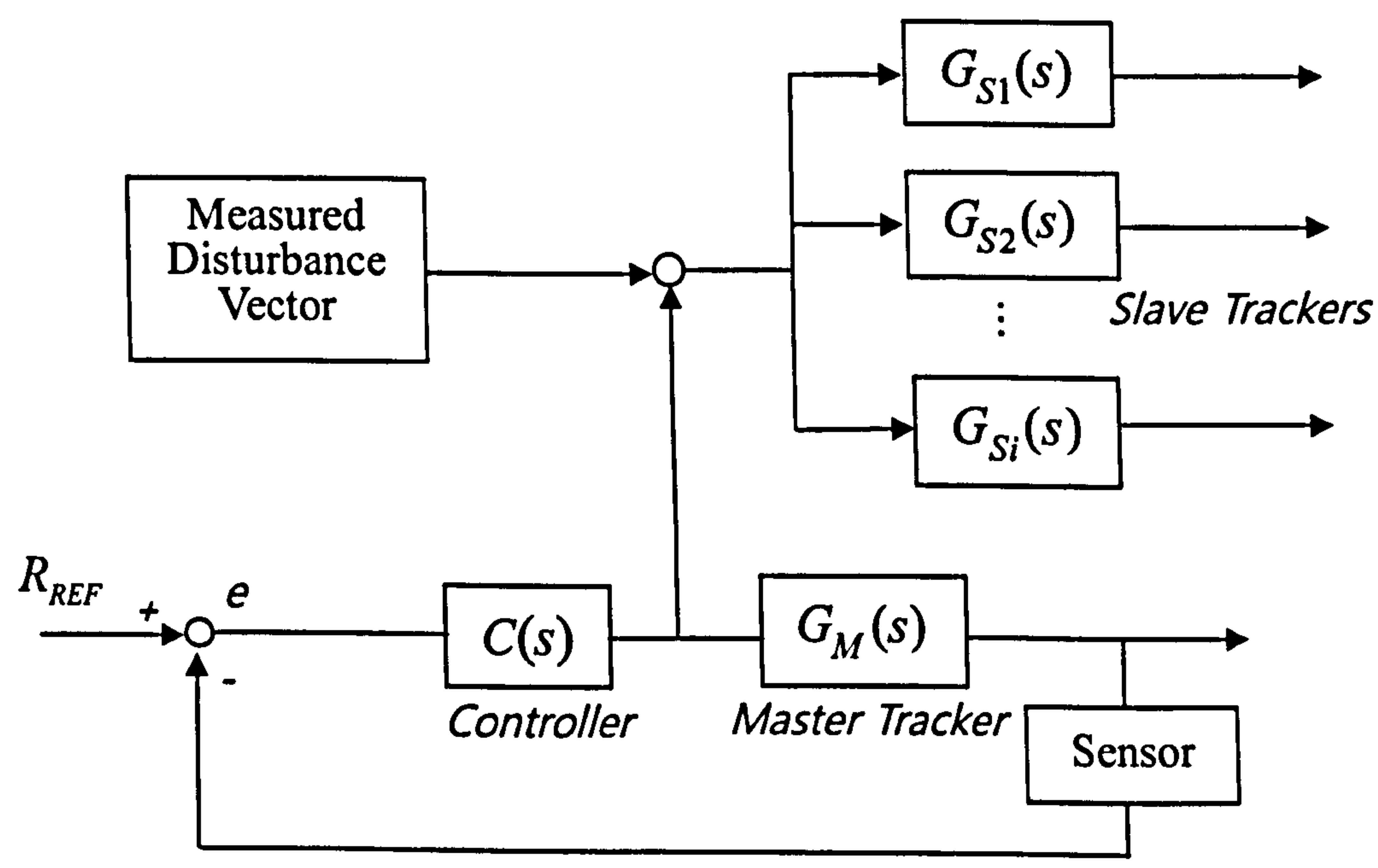
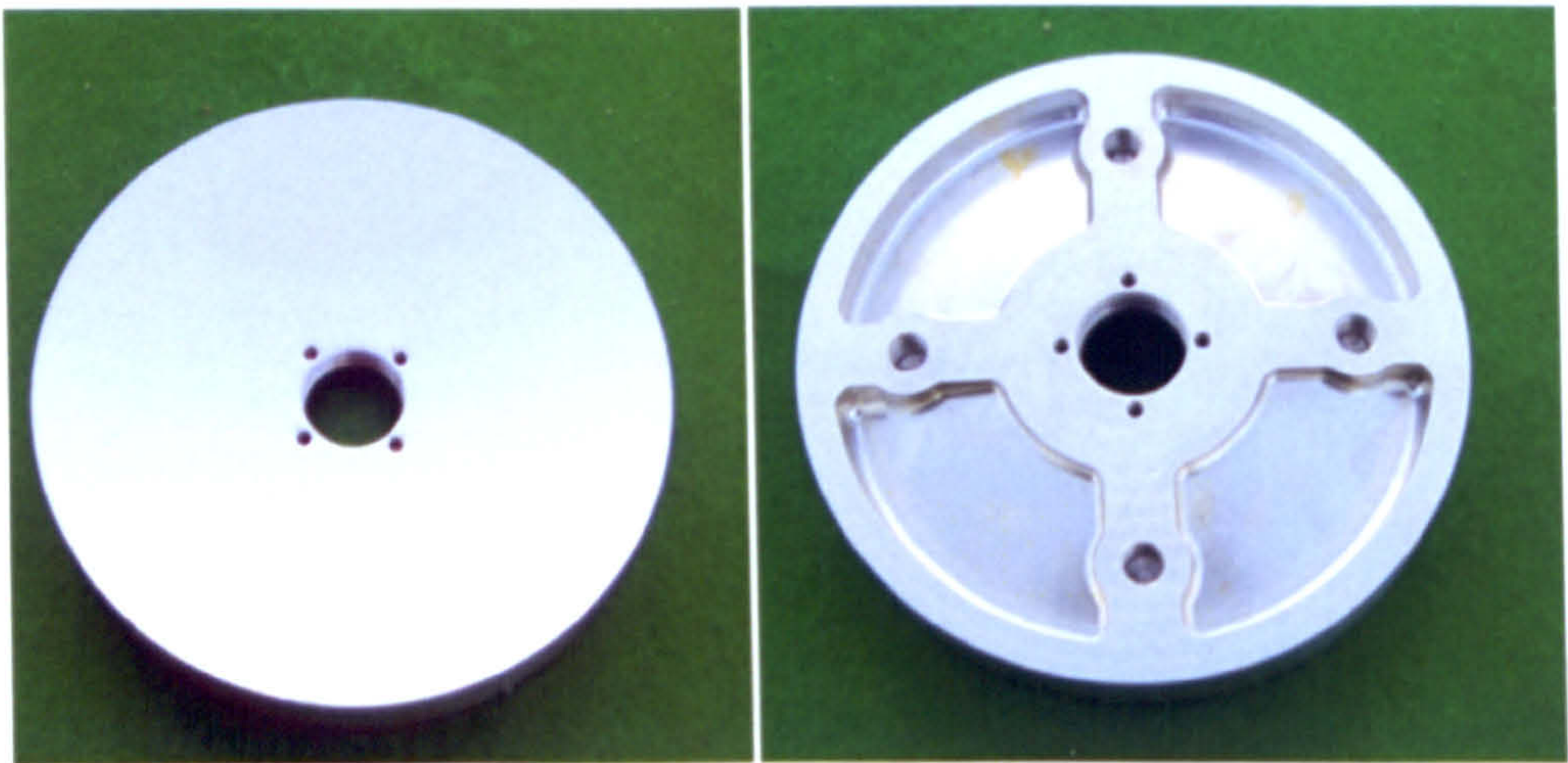


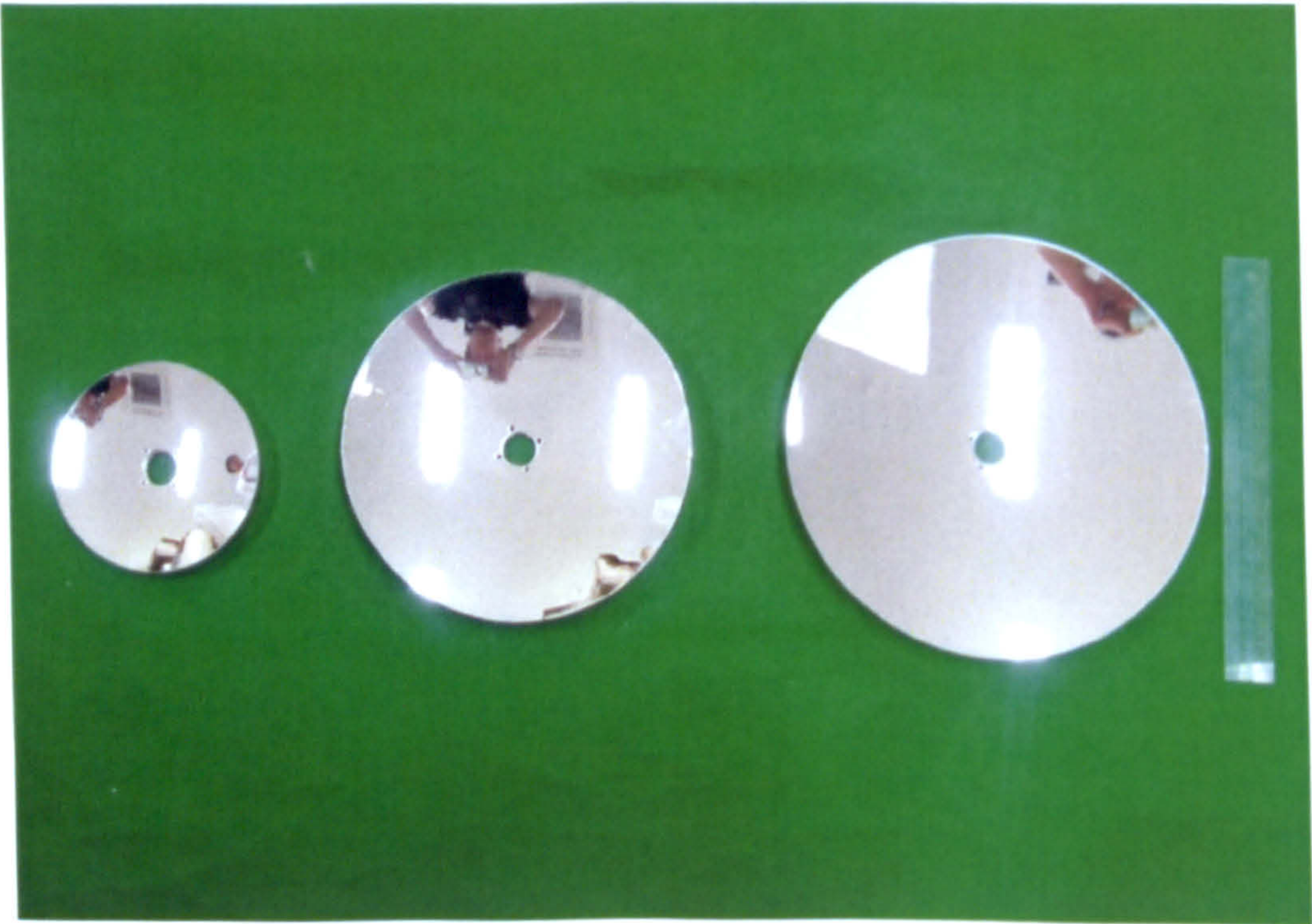
Figure 2. 16 Control logic of the dish concentrators

2.4 Construction of Prototype Systems

The reflectors were made by processing an aluminum block on a CNC milling machine according to the design specifications detailed in section 2.1. Figure 2.17 show the front (a) and rear (b) view of the reflectors as well as three different sizes (15cm, 25 cm and 30 cm in diameter) of the dish reflector (c).



(a) Front view (b) Rear view



(c) Different sizes (15cm, 25cm and 30cm)

Figure 2.17 Dish reflectors made of aluminum block

In Figure 2.17(a), the four small holes near the center is to engage four metal rods to support the second reflector placed around the focal point of the dish reflector. It is very important to design these support rods such that they do not block any crucial amount of sun rays before they arrive at the second reflector. The sun rays near the second reflector are highly condensed and any aberration could greatly affect the efficiency of the system. The large hole at the center is to hold to the homogenizer tube, which runs through it and sticks out some distance toward the second reflector. To reduce its weight, some rear portion of the dish body was removed that doesn't affect the mechanical strength of the reflector body. The four holes near the rim are prepared to mount the dish reflector on the tracker. Three different sizes (diameters) of the dish reflector are considered as shown in Figure 2.17(c). Some details are given in section 2.1.1 for its design specifications.

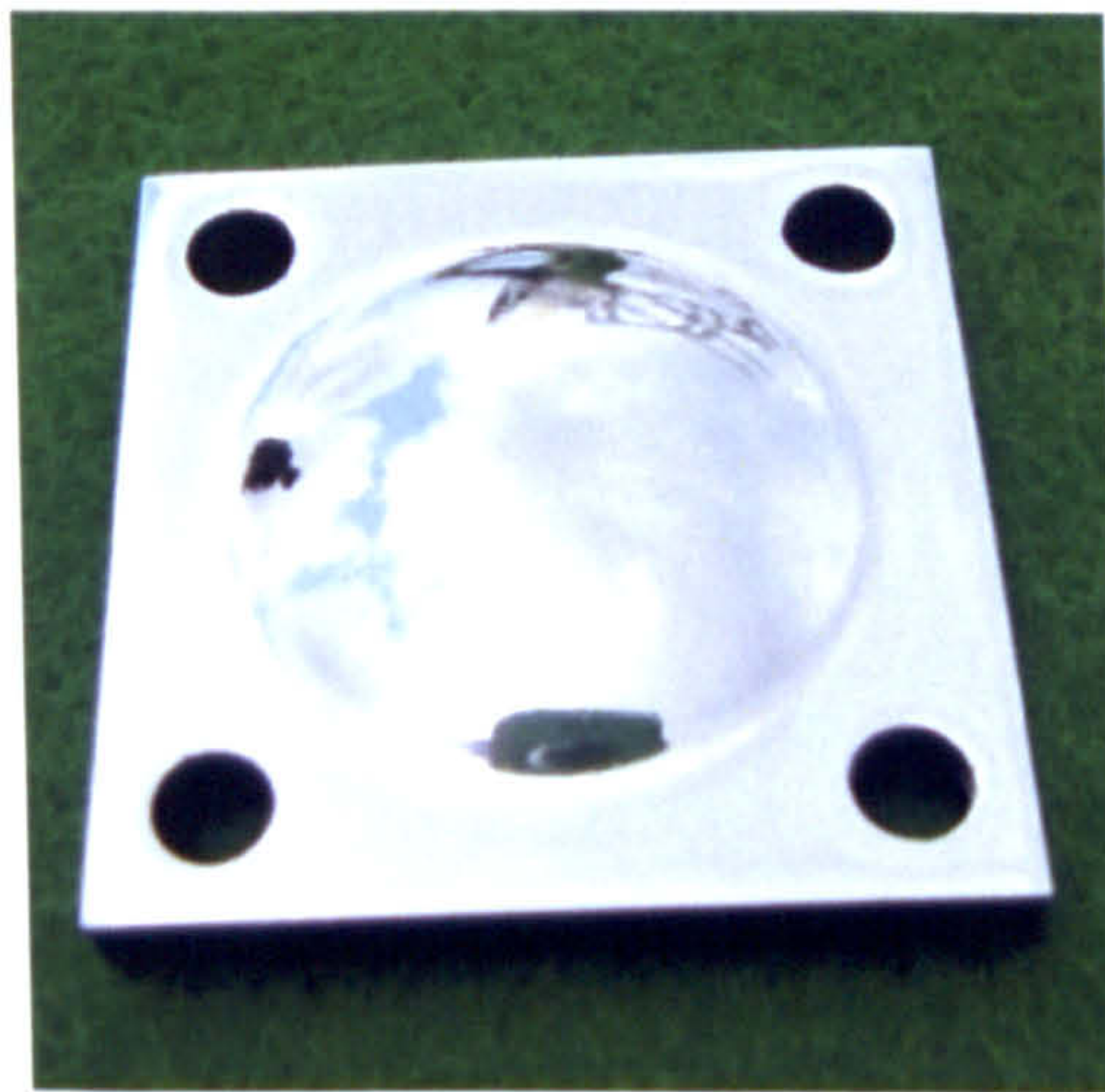


Figure 2.18 The second reflector made of aluminum

Figure 2.18 gives a picture of the second reflector prepared in the same manner as for the dish reflector. It has a shiny convex surface to stream down and concentrate the solar rays reflected off the dish reflector. For its utmost efficiency, it should possess a extremely high luster, exceptional, mirror-like surface, and blemish free surface. The four holes around the convex surface are prepared to place it onto the support made with screwed metal rods.

Accurate adjustments of the second reflector are possible by lowering or raising it through the rods for the right position. Metallic fasteners, such as nuts, are used to hold it in the desired position.

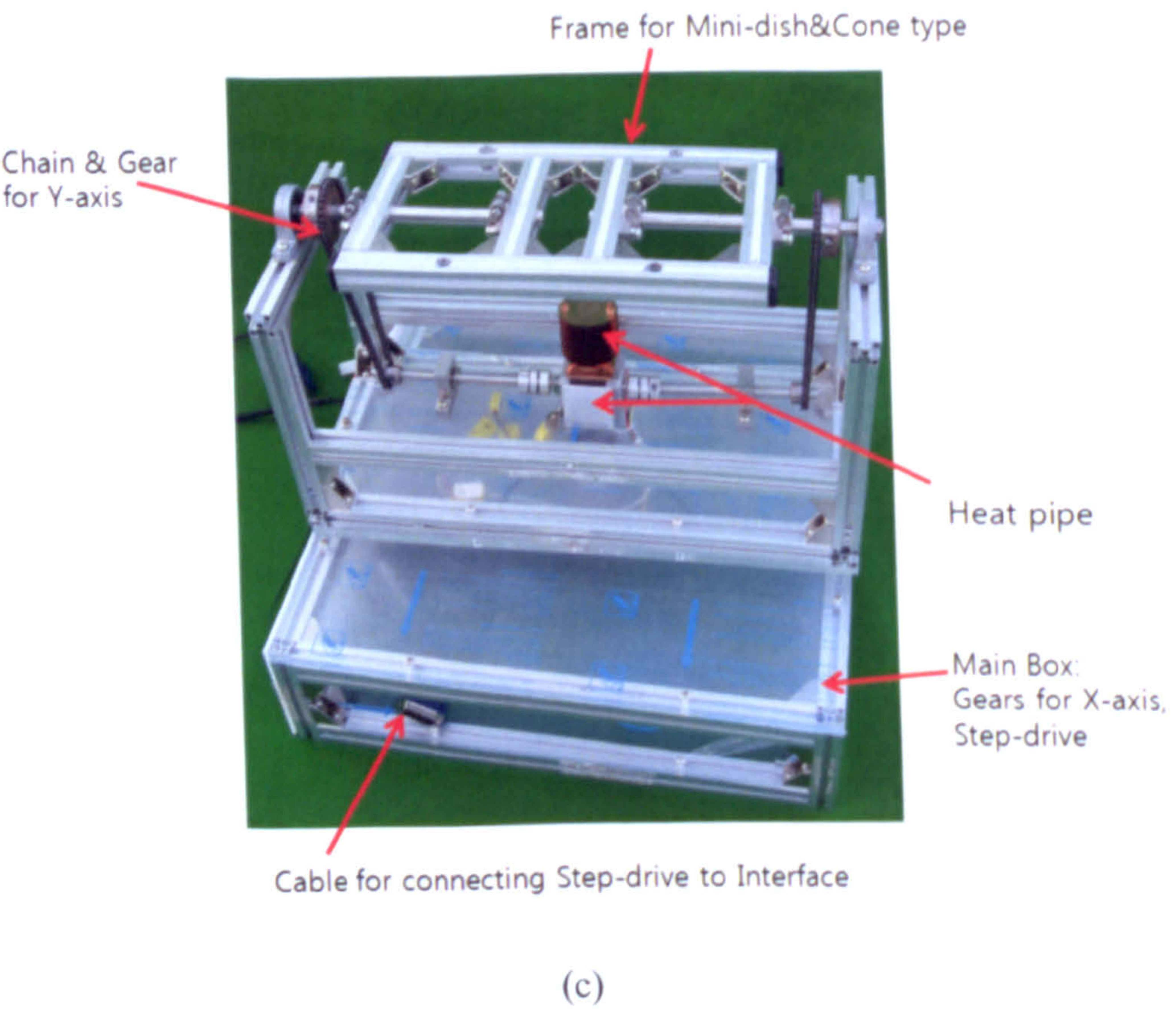
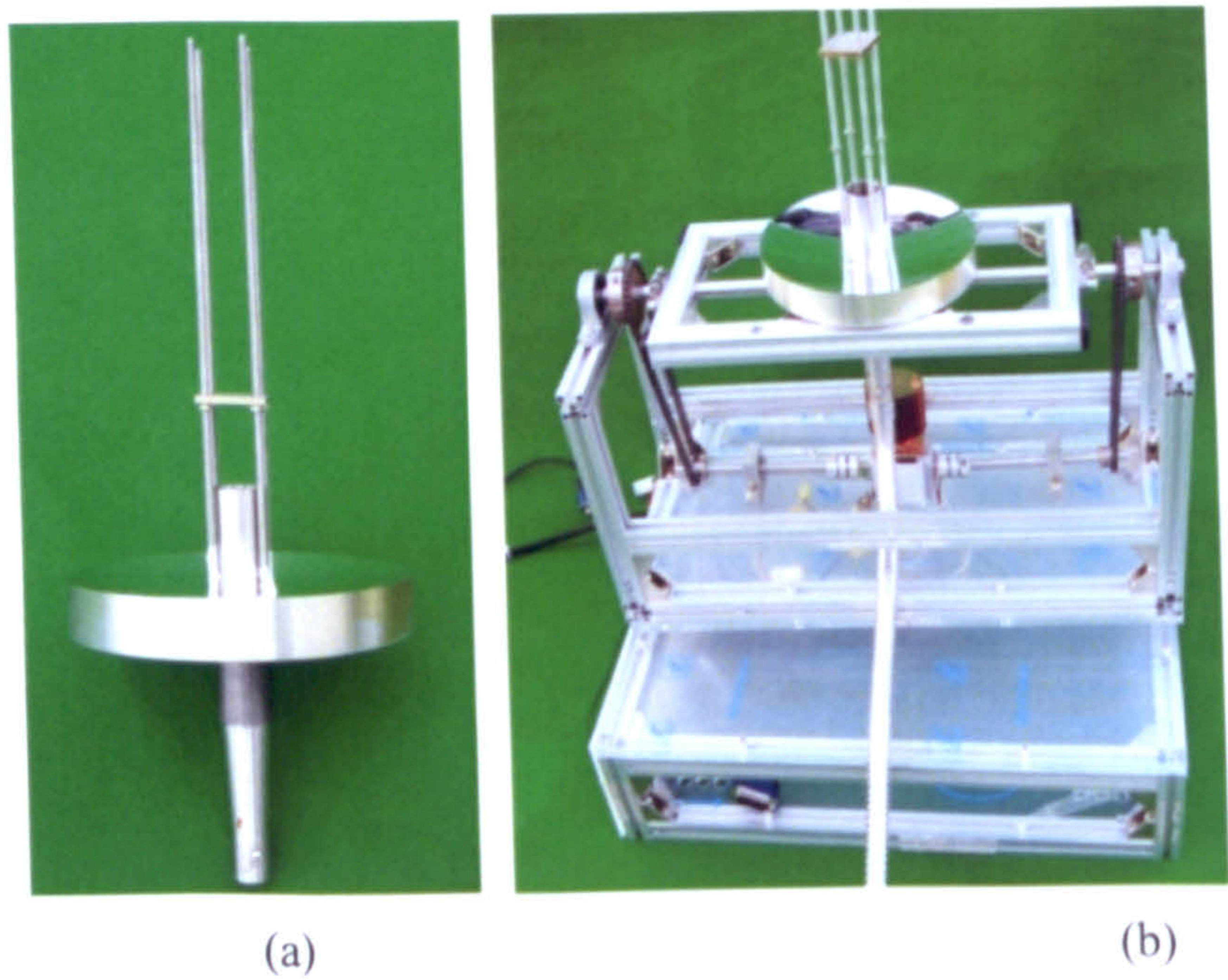
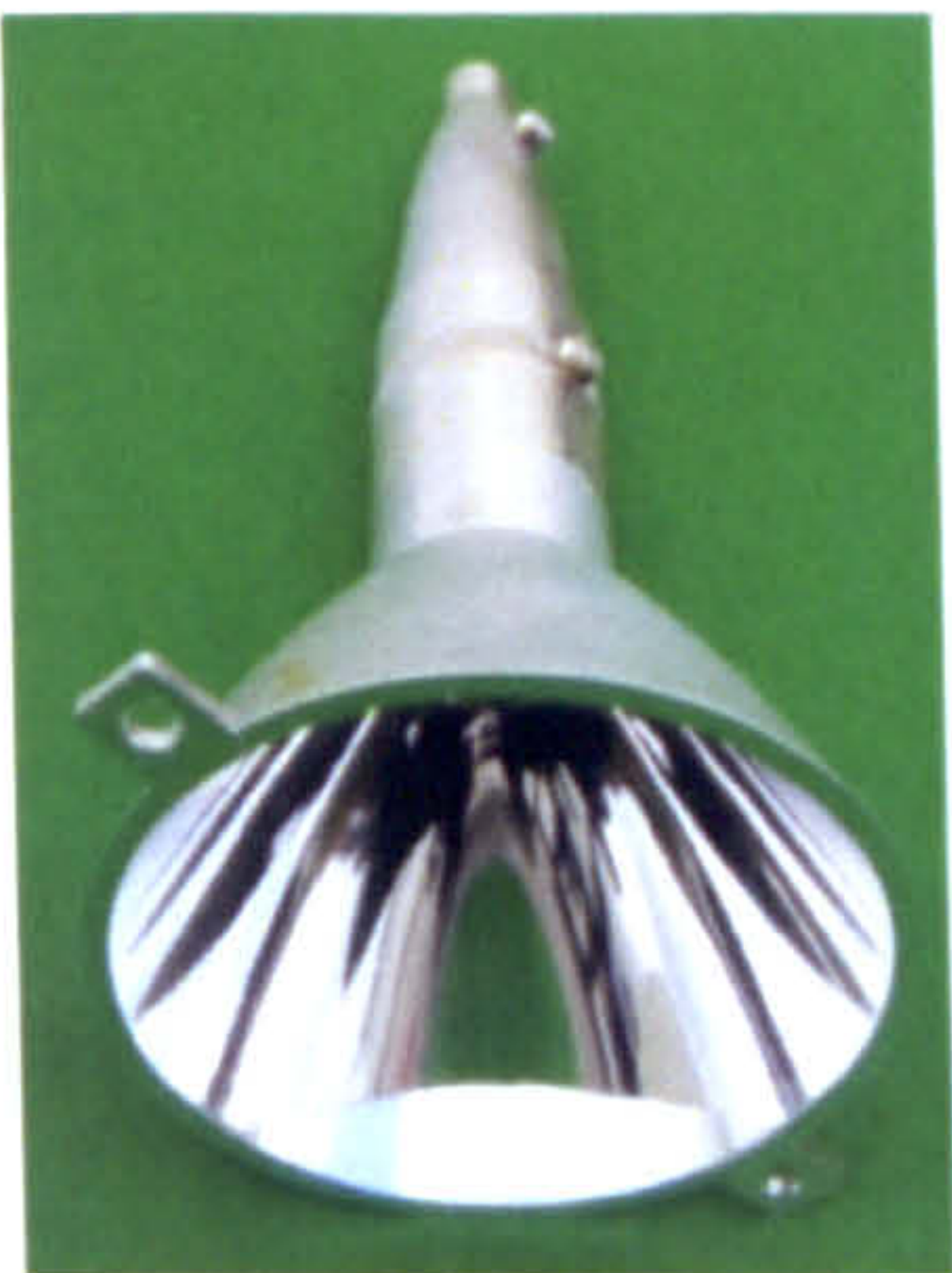


Figure 2.19 The dish concentrator assembly and tracker : (a) the dish concentrator assembly, (b) the whole system, (c) the tracker (major components are displayed)

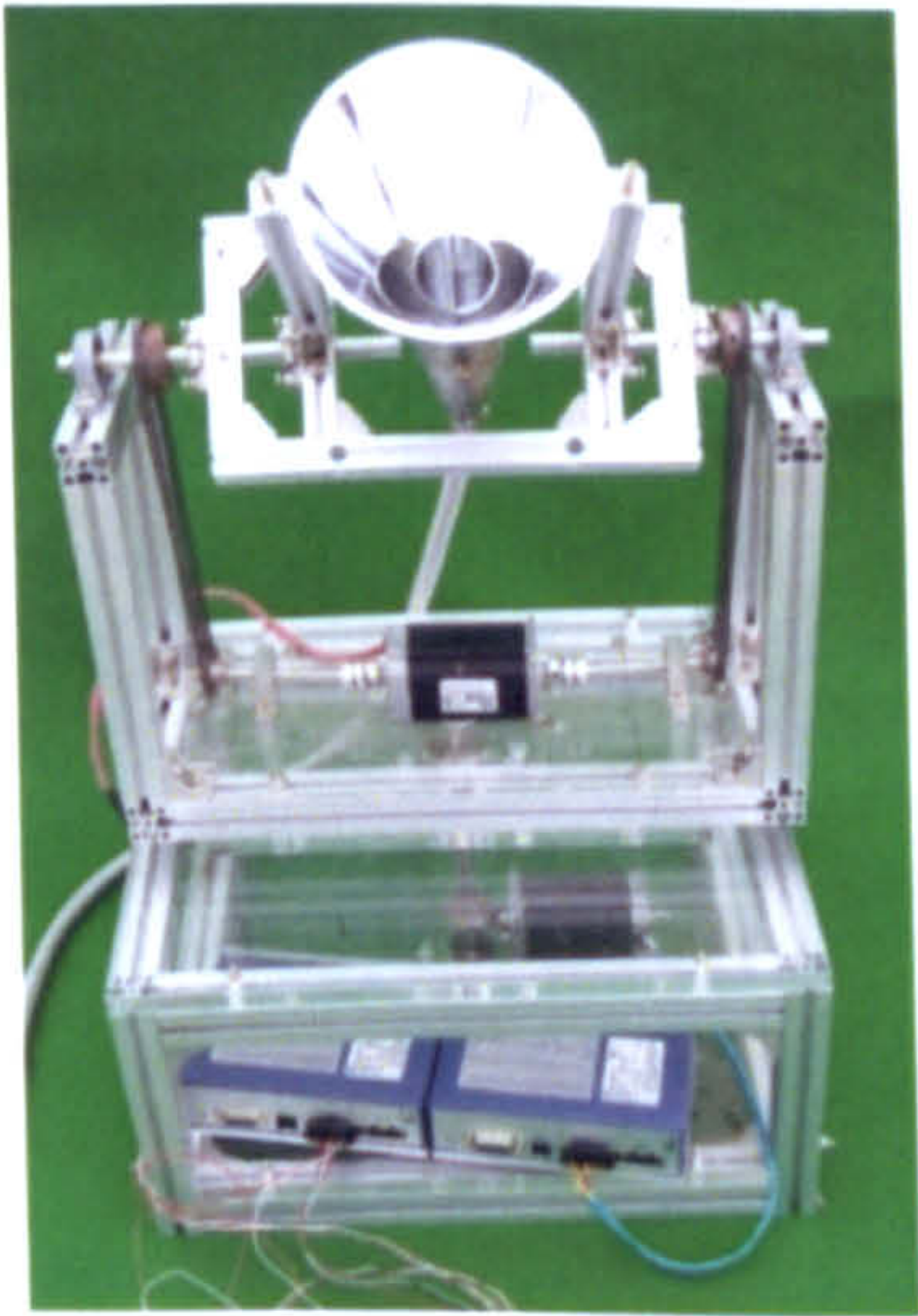
Figure 2.19 shows the concentrator assembly, its solar tracking (double axis tracking) mount and the complete daylighting system. Major components of the tracker (solar tracking mount) are given in Figure 2.19 (c) with labels to briefly illustrate the architecture of the tracker system. As shown, a heat pipe is applied to dissipate the internal heat generated by two stepping motors used for constant and accurate alignment of the concentrator against the sun. Main components of the assembly are contained in the lower compartment (main box) and the whole assembly could be divided into three parts: concentrator, mount and main box.



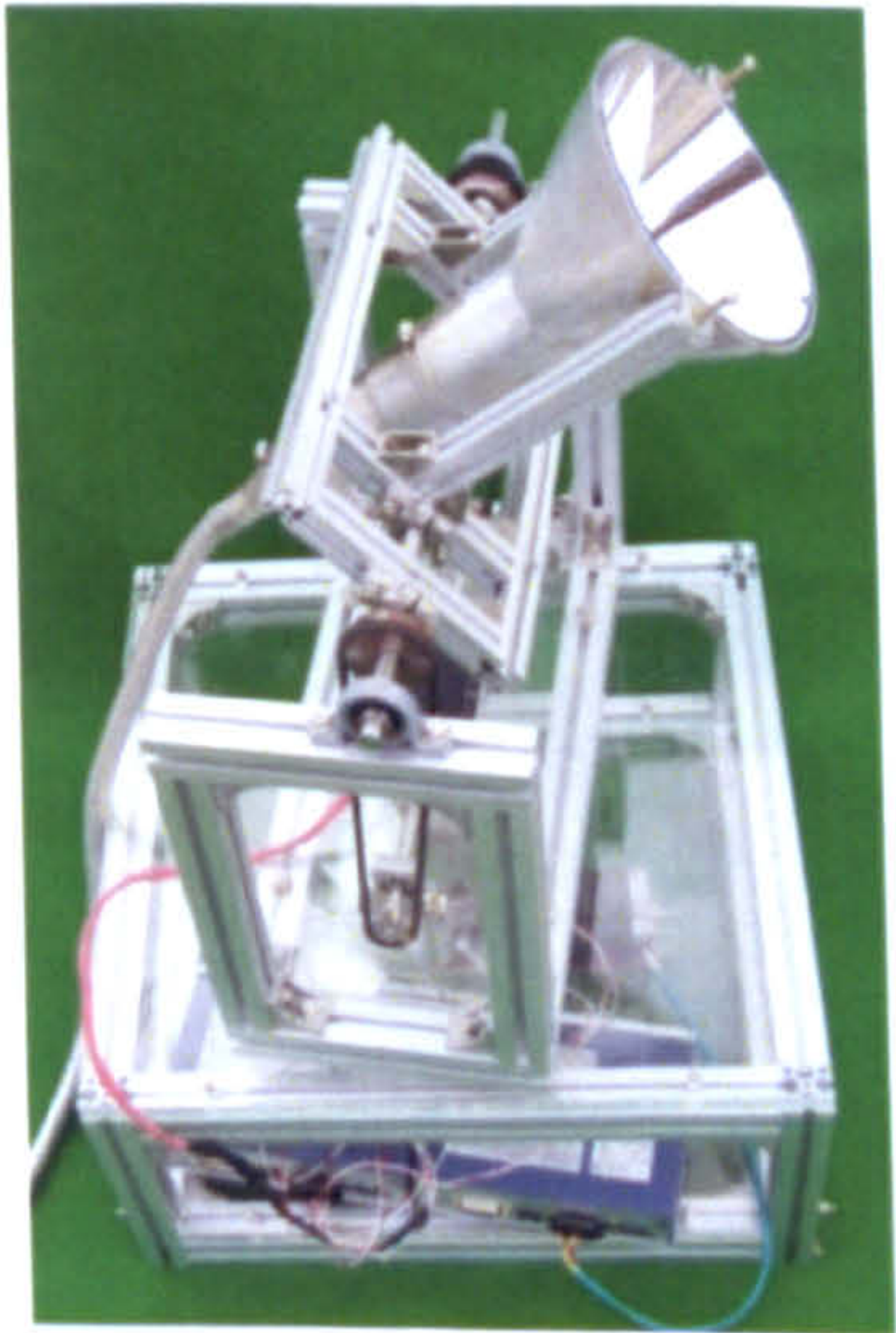
(a)



(b)



(c)



(d)

Figure 2.20 The funnel shaped concentrator and the daylighting system: (a) the concentrator and homogenizer (before assembled) (b) the funnel shaped concentrator with homogenizer (assembled), (c), (d) different views of the daylighting system

One of the advantages using a funnel shaped solar concentrator is the elimination of the second mirror. The sun rays admitted through the wide circular mouth on top bounces of its inner surface repeatedly before they are discharged to a light guide. Figure 2.20 shows the daylighting system with a funnel shaped concentrator considered in this work. As shown, the homogenizer pipe has a different design in comparison to that of the dish concentrator. This is because there was a quite a difference between the inlet areas of the concentrator and the optical fiber cable. Also, to make one with a highly reflective inner surface, two identical halves were prepared separately one at a time and assembled, Figure 2.20(a).

2.5 A Comparative Analysis of Solar Availability

To calculate the illuminance by incoming solar rays on a surface element dA , its direction and distance from a source(an emitter) should be given as shown in Figure 2.21. The flux of rays incident on dA from a source dA_e could be determined by drawing a line from dA to dA_e , which passes normally through dA_e . The distance between dA and dA_e is R and dA_e is assumed to be a hemispherical surface element whose direction is designated by θ and φ . Equations (2.1) and (2.2) are now readily derived for the solar rays incident upon dA within the solid angle $d\omega$ having origin at dA .

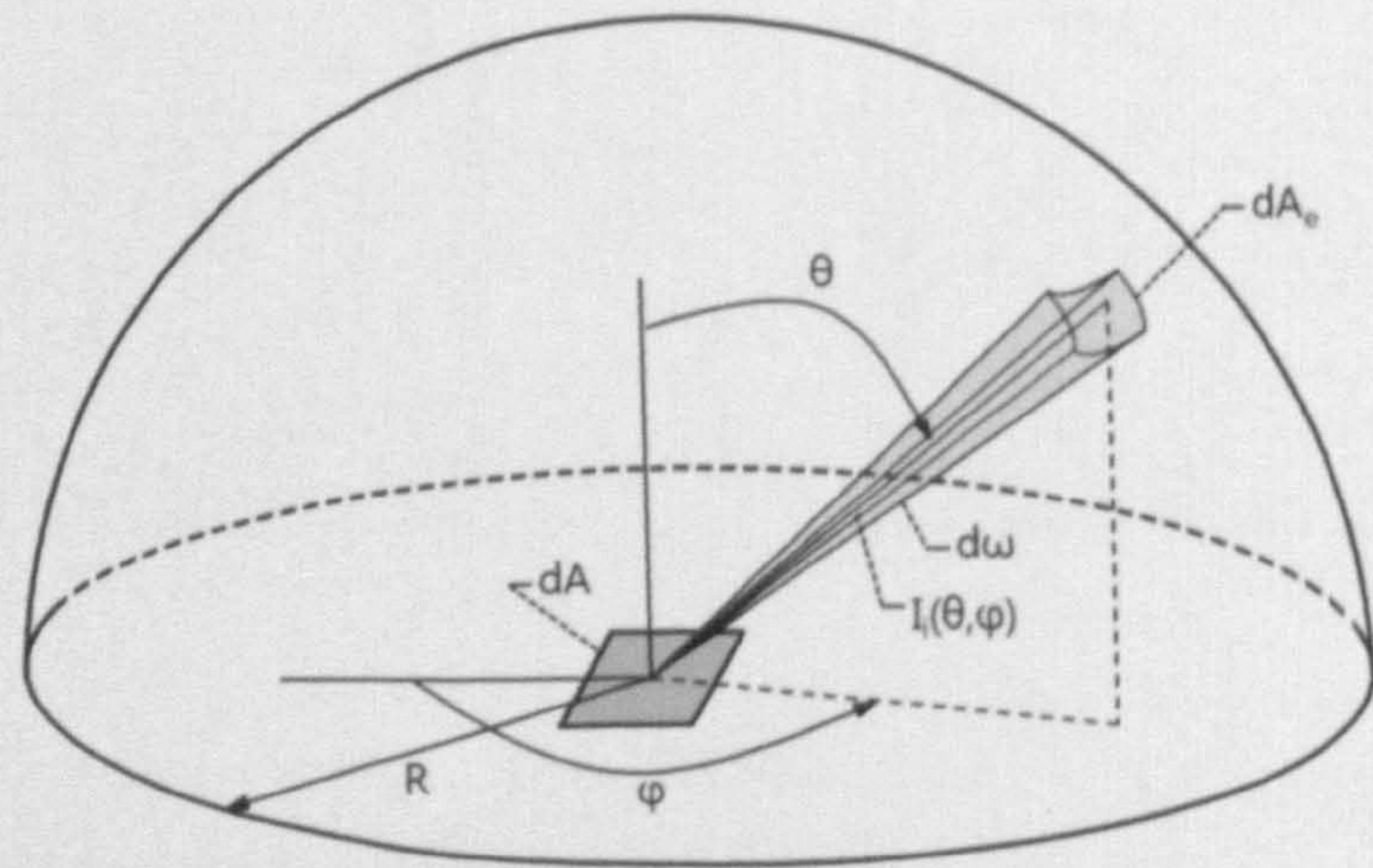


Figure 2.21 Incident solar rays on a surface element dA from the (θ, φ) direction

$$d^2 Q_i(\theta, \varphi) = I_i(\theta, \varphi) dA_e d\omega_e = I_i(\theta, \varphi) dA_e \frac{dA \cos \theta}{R^2} \quad (2.1)$$

$$d^2 Q_i(\theta, \varphi) = I_i(\theta, \varphi) d\omega \cos \theta dA \quad (2.2)$$

Based on the above equations, the amount impinging solar rays on a dish collector (concentrator) and a planar window could be easily calculated. The area ratio, A/A_{sol} , is the required window surface area (A) that would receive the same amount of solar rays to the projected area (A_{sol}) of the dish solar collector normal to the dish collector axis (Since the sun-tracking collector is always perpendicular to the sun, solar rays incident on the collector is equal to the product of solar flux and the projected area). In Figure 2.22, a south facing vertical window (glass panel) is shown whose surface normal is pointed south.

To calculate solar availability and to determine the equivalent area of window comparable to the dish reflector, one could use the light coming out from the exit end of the optic fiber, or just use solar rays impinging on the dish surface. The former is more realistic, but the latter is easier to calculate as shown here. What we need is a illuminance gage mounted on a vertical surface facing south, and record the illuminance over a 8 to 10 hours period from sun rise to sunset on a clear day in each month (for a period of interest). We may also need to figure out how to measure the direct and diffuse components of sunlight incident on the gage surface. The diffuse component may be negligible if the sky is very clear. The sun angle varies with time, but can be calculated if the date and time are specified.

Since the collector surface always faces the sun, the flow rate of solar rays incident on the collector is the integration of solar flux, which is assumed to be parallel to the axis of the dish, over the collector surface. Assuming a uniform solar flux for small dishes, the flow rate of incident solar rays can be calculated from :

$$E_1 = \text{solar flux} * \text{projected area of the collector normal to solar flux} \quad (2.3)$$

Since sunrays come from the same direction, the , the flow rate of incident solar rays is;

$$E_2 = \text{solar flux} * A_w * \cos \theta \quad (2.4)$$

where A_w is the surface area of the glass panel, and θ the angle between the surface normal of the glass panel and the direction of incoming sun rays. Note that, in Eq. (2.3) only the solar flux may vary with time, while in Eq. (2.4) also varies with time as the sun angle changes.

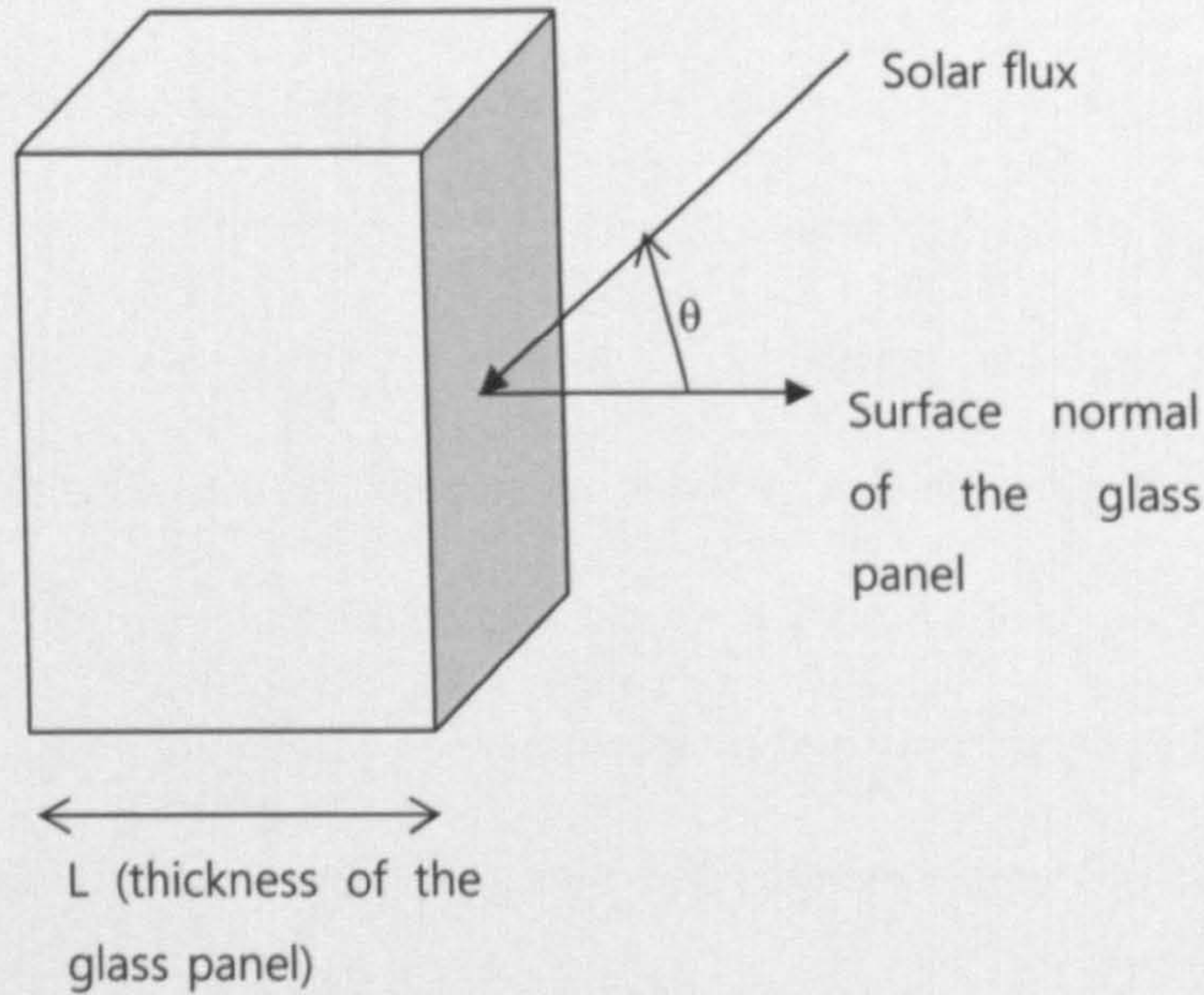


Figure 2.22 Solar flux on a vertical surface(window) pointed south

Equations relating the angle of incidence of beam component on a surface, θ , to the other angle are [Duffie and Beckmann 2006]:

$$\begin{aligned} \cos \theta = & \sin \delta \sin \phi \cos \beta - \sin \delta \cos \phi \sin \beta \cos \gamma \\ & + \cos \delta \cos \phi \cos \beta \cos \omega + \cos \delta \sin \phi \sin \beta \cos \gamma \cos \omega \\ & + \cos \delta \sin \beta \sin \gamma \sin \omega \end{aligned} \quad (2.5)$$

There are several commonly occurring cases for which Eq. (2.5) is simplified. For fixed surfaces sloped toward the south or north, that is, with a surface azimuth angle γ of 0° or 180° (a very common situation in a real practice), the last term drops out.

For vertical surfaces, $\beta=90^\circ$ and the equation becomes [Duffie and Beckmann 2006]:

$$\cos \theta = -\sin \delta \cos \phi \cos \gamma + \cos \delta \sin \phi \cos \gamma \cos \omega + \cos \delta \sin \gamma \sin \omega \quad (2.6)$$

- ϕ Latitude

The angular location north or south o the equator, north positive;
- $90^{\circ} \leq \phi \leq 90^{\circ}$
- δ Declination

The angular position of the sun at solar noon(i.e., when the sun is on the local meridian) with respect to the plane on the equator, north positive; $-23.45^{\circ} \leq \delta \leq 23.45^{\circ}$
- γ Surface azimuth angle

The deviation of the projection on a horizontal plane of the normal to the surface from the local meridian, with zero due south, east negative, and west positive; $-180^{\circ} \leq \gamma \leq 180^{\circ}$
- β Slope

The angle between the plane of the surface in question and the horizontal; $0^{\circ} \leq \beta \leq 180^{\circ}$. ($\beta > 90^{\circ}$ means that the surface has a downward-facing component.)
- ω Hour angle

The angular displacement of the sun east or west of the local meridian due to rotation o the earth on its axis at 15° per hour; morning negative, afternoon positive
- θ Angle of incidence

The angle between the beam radiation on a surface and the normal to that surface

Table 2.4. Available solar radiation and angles on a tilted surface on 01/03/2009

Time	I_{bT} (beam radiation on a tilted surface) [W/m2]	I_{dT} (diffuse radiation on a horizontal surface)[W/m2]	Slope [°]	Declination [°]	Latitude [°]	Surface azimuth angle[°]	Hour angle[°]	Cos θ
8:00	20.69727679	33.64272321	90	-7.6334	33.455	0	-71.5375	0.2838611
9:00	180.1127897	90.9872103	90	-7.6176	33.455	0	-56.5355	0.4119033
10:00	347.0307979	111.4692021	90	-7.6018	33.455	0	-41.5335	0.5194153
11:00	484.8204006	121.1795994	90	-7.586	33.455	0	-26.5315	0.5990509
12:00	583.5236181	128.8763819	90	-7.5701	33.455	0	-11.5295	0.6453627
13:00	614.9797934	136.5202066	90	-7.5543	33.455	0	3.4725	0.6551781
14:00	577.0612267	147.6387733	90	-7.5385	33.455	0	18.4746	0.6278082
15:00	478.6956369	157.4043631	90	-7.5226	33.455	0	33.4766	0.5650995
16:00	356.7573931	154.3426069	90	-7.5068	33.455	0	48.4786	0.4713112
17:00	234.242057	126.757943	90	-7.4909	33.455	0	63.4807	0.3528153

Here the calculation has been carried out for the first clear day of each month in March, April and May. Tables 2.4 – 2.6 show the actual measurements made on March 1, April 2 and May 1. As shown in these tables, solar radiation data are continuously monitored throughout measurements, whose beam and diffuse components are separately recorded as they are used with Eqs (2.3) and (2.4) to determine the amount of solar rays impinging on the dish and window for indoor illumination. It is needless to say that both the dish and funnel shaped solar concentrators utilize only the beam component of incident solar rays.

In addition, here we neglected solar attenuation through the optical fiber cable and glazing material. Our calculation is solely based on solar availability on the collector and window area.

Table 2.5 Available solar radiation and angles on a tilted surface on 02/04/2009

Time	I _{bt} (beam radiation on a tilted surface) [W/m2]	I _{dt} (diffuse radiation on a horizontal surface)[W/m2]	Slope [°]	Declination [°]	Latitude [°]	Surface azimuth angle[°]	Hour angle[°]	Cosθ
8:00	32.64217178	47.24782822	90	4.8776	33.455	0	-69.3575	0.1227029
9:00	127.3044013	87.19559869	90	4.8937	33.455	0	-54.3544	0.2489258
10:00	241.3441394	115.9558606	90	4.9097	33.455	0	-39.3513	0.3533214
11:00	350.2374372	131.8625628	90	4.9257	33.455	0	-24.3482	0.4287564
12:00	428.7957143	143.2042857	90	4.9417	33.455	0	-9.3451	0.4700734
13:00	470.5216201	143.9783799	90	4.9577	33.455	0	5.6579	0.4744417
14:00	427.8775581	147.6224419	90	4.9738	33.455	0	20.661	0.4415479
15:00	372.6022102	135.4977898	90	4.9898	33.455	0	35.6641	0.3736233
16:00	285.0377296	113.9622704	90	5.0058	33.455	0	50.6672	0.275283
17:00	118.8820351	97.31796493	90	5.0218	33.455	0	65.6702	0.153218

Most glass panels are transparent to visible light, thus the attenuation of solar flux through the glass window might be neglected for small values of θ and L. For large θ angles, the optical path in the glass panel varies with θ as:

$$P = L / \cos \theta \tag{2.7}$$

The transmitted radiation is given by :

$$E_3 = E_2 * t$$

(2.8)

where t is the directional-total transmittance of the glass panel. This radiative property must be experimentally determined if not provided by the manufacturer. Generally, the transmittance is an exponential function of optical path such that attenuation is not negligible even for small θ and L (0.85 is the maximum transmittance for a normal glass)

Table 2.6 Available solar radiation and angles on a tilted surface on 01/05/2009

Time	I_{bt} (beam radiation on a tilted surface) [W/m ²]	I_{dt} (diffuse radiation on a horizontal surface)[W/m ²]	Slope [°]	Declination [°]	Latitude [°]	Surface azimuth angle[°]	Hour angle[°]	Cos θ
8:00	35.56135168	42.62864832	90	15.0388	33.455	0	-67.7192	-0.0146257
9:00	85.57200091	63.32799909	90	15.0514	33.455	0	-52.718	0.105816
10:00	157.2951239	95.10487607	90	15.064	33.455	0	-37.7167	0.2042655
11:00	223.6966297	122.2033703	90	15.0766	33.455	0	-22.7154	0.2740026
12:00	267.4016647	139.9983353	90	15.0892	33.455	0	-7.7142	0.3102655
13:00	284.131422	148.868578	90	15.1018	33.455	0	7.2871	0.310575
14:00	250.7643788	148.4356212	90	15.1144	33.455	0	22.2884	0.2749018
15:00	205.3866794	139.2133206	90	15.127	33.455	0	37.2896	0.20567
16:00	152.8037253	101.9962747	90	15.1396	33.455	0	52.2909	0.1075893
17:00	75.86498538	73.03501462	90	15.1521	33.455	0	67.2921	-0.0126615

Figure 2.23 graphically shows the relative amount of solar radiation available on the dish reflector and the south facing vertical window given above. To admit the same amount of daylight through the window as compared to the daylighting system at 9am on March 1, the window area should be about 0.424 m² (six times the area of the dish concentrator).

As the sun changes its position with the time of day and month, the ratio E_1/E_2 varies reflecting the effect of its angle of incidence on the non-tracking surface (i.e., the south facing vertical window). The lower the angle the more spread out and less intense is the solar radiation that reaches the surface.

The figure also shows a pattern of symmetry over the course of a day with respect to noon

arriving at the highest value at 9am and 4pm. Of course, this is due to the diurnal movement of the sun constantly changing its celestial position traveling in a circular path across the sky, reaching its highest point at noon. The seasonal variation of the ratio compared for a day in the months of March, April and May clearly manifests the increase in solar altitude angle as the sun moves toward the summer solstice.

The solar altitude angle also gives an estimation regarding the attenuation of solar rays as they travel through the atmosphere. For example, if the sun is directly overhead, their travel distance becomes the shortest which results in the minimum losses by absorption, reflection and the scattering by the atmosphere reducing intensity at the surface. The air mass (AM), which refers to the ratio of the optical thickness of the beam radiation through a particular path to that when the sun is at zenith (overhead), could be used as one of the important parameters in relation to the performance of any solar tracking daylighting systems. In general, the air mass (AM) is referred to as 1 if the beam radiation traverses through the atmosphere and reach the sea level when the sun directly overhead.

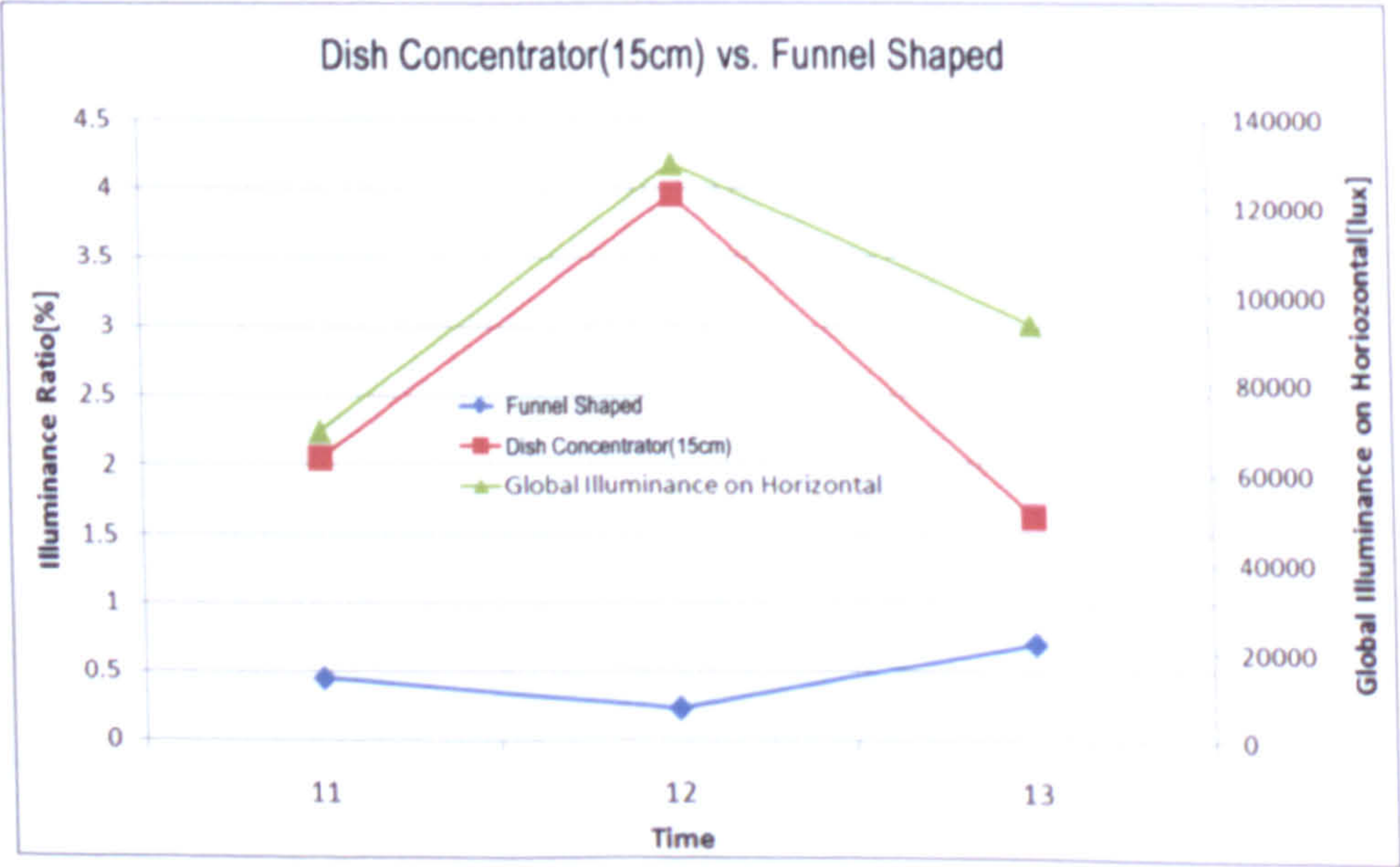


Figure 2.23 Ratio of illuminance available on the dish concentrator and window

2.6 Summary

Some details are given in the design and construction of innovative daylighting systems. To harvest daylight as much as possible, two types of solar concentrators are considered; dish and funnel shaped. Each design has been analyzed for its geometrical justification and functional suitability. Such raytracing simulation software as PHOTOPIA has also been brought in to draw forth the most optimal conditions for its performance. The daylighting system with a dish type solar concentrator is one of the most simple and feasible design to harness parallel beams of sunlight. It consists of two major reflectors; one to concentrate incoming solar rays onto a near focal point of the dish reflector and the other to form and reverse its direction of a stream of high density sunlight delivering it to where it is needed via a series of light guides and a terminal device.

3. PHOTOMETRY MEASURING EQUIPMENTS

To investigate the photometric properties of the daylighting system and other important factors affecting its performance, a series of tests were conducted using different types of photometric instruments : Luminance meter, Spectrophotometer, SpectraColorimeter and Goniophotometer. Each instrument measures distinct features of the optical properties displayed by the daylighting system, luminaires and processed materials.

3.1 Luminance Meter

Luminance measures the amount of light that reaches the eye after being reflected off an object's surface. There are many factors to be considered when determining the luminance of an object as it is influenced by the illumination, the geometrical configuration between the viewer and the light source as well as other photometric properties related to the perception of brightness by a human observer.

To measure the luminance of the light source at various surfaces of a room, a luminance meter (LS-100) was used. LS-100 [Konica Minolta 2008] is small and light such that it offers mobility and convenience in taking luminance measurements of light sources or reflective surfaces. The system employs advanced optics and electronics, which assures accurate and efficient measurements. Above all, it is very easy to operate and store data.



Figure 3.1 LS-100 Luminance meter

The LS-100 has a 1° acceptance angle and its accuracy is $\pm 2\%$ of the measured value at 1 cd/m^2 . It has a through-the-lens viewing system which accurately identifies the area to be measured. It also features an in-view finder display enabling measurements to be seen simultaneously with the subject being measured.

The reflectance of a surface could be determined by measuring and comparing its luminance against two reference surfaces with known reflectance, whose luminance values are to be measured simultaneously as shown below.



Figure 3.2 Measuring luminance

Here two reference surfaces were used, namely, white and gray panel, whose respective reflectance (ρ) was 0.85 and 0.3, respectively. The following shows the luminance values measured by LS-100 Luminance meter (under overcast sky):

$$L_{\text{white}} : 3200 \text{ cd/m}^2$$

$$L_{\text{gray}} : 1989 \text{ cd/m}^2$$

$$L_{\text{surface}} : 2509 \text{ cd/m}^2$$

Finally, the reflectance (ρ_{wall}) of the surface under investigation can be determined:

$$\rho_2 = \rho_{\text{gray}} \times \frac{L_{\text{surface}}}{L_{\text{white}}} \tag{3.1}$$

$$\rho_2 = \rho_{\text{gray}} \times \frac{L_{\text{surface}}}{L_{\text{gray}}} \tag{3.2}$$

$$\rho_{wall} = \frac{\rho_1 + \rho_2}{2} \quad (3.3)$$

This yields $\rho_{wall} = 0.52$.

Alternately, it also could be determined by using illuminance and luminance meters as shown in Figure 3.3

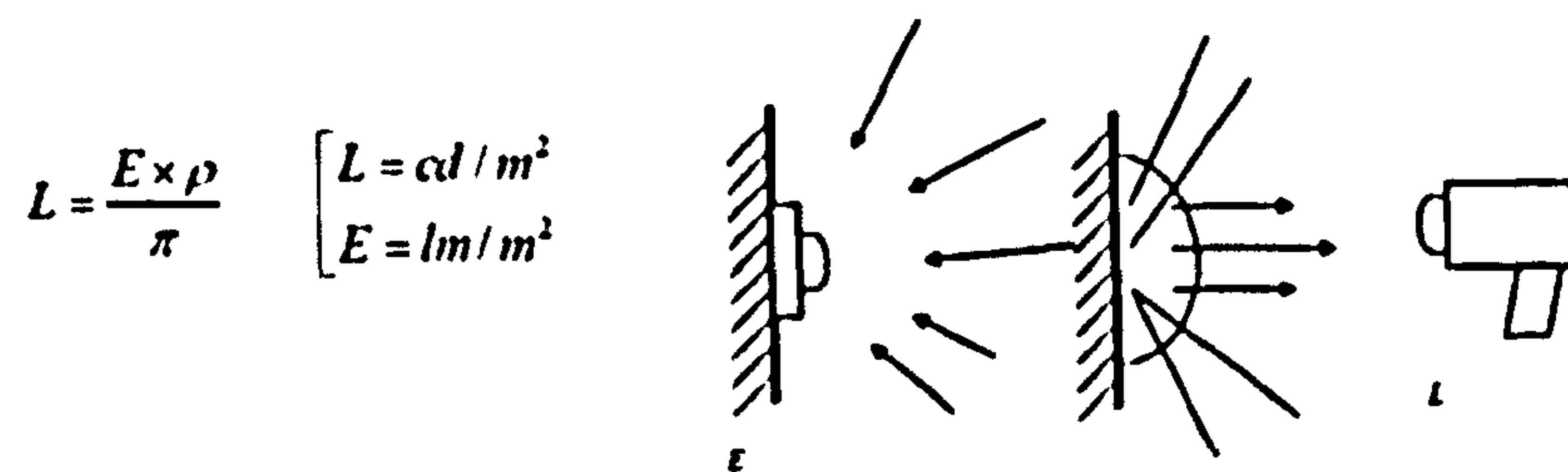


Figure 3.3 Measuring luminance and illuminance

For our surface, these measurements yield:

$$L: 4,348 \text{ cd/m}^2$$

$$E: 23,300 \text{ lm/m}^2$$

The reflectance is now determined by using the following formula:

$$\rho_{wall} = \frac{L \times \pi}{E} \times 100[\%] \quad (3.4)$$

which gives $\rho_{wall} = 0.58$.

It is not difficult to conclude the reliability of both methods when measuring the reflectance of a surface. As illustrated above, each method produced a value not too different from each other.

3.2 Spectrophotometer

When continuous radiation hits the surface of a sample, some is absorbed whilst others could be reflected. An absorption spectrum can be obtained by monitoring the radiation that penetrates the sample and reaches a detector across the wavelengths. For a given surface, the spectra absorption rate varies with the wavelength and temperature of the radiation source and data from such absorption spectra can be used for qualitative and quantitative analyses.

The PDA (Photo Diode Array) Spectrophotometer is equipped with a multi-channel detector controlled by a microprocessor which collects spectral data for several wavelengths simultaneously; while PMT (Photo Multiplier Tubes) Spectrophotometer detects only on a single channel which data collection is performed for a specific wavelength in series. The PDA Spectrophotometer is therefore faster and yet provides better reproducibility data than the PMT Spectrophotometer. The latter sensor depends on a rotating grating or prism operated by a stepper motor to scan across the wavelength bandwidth.

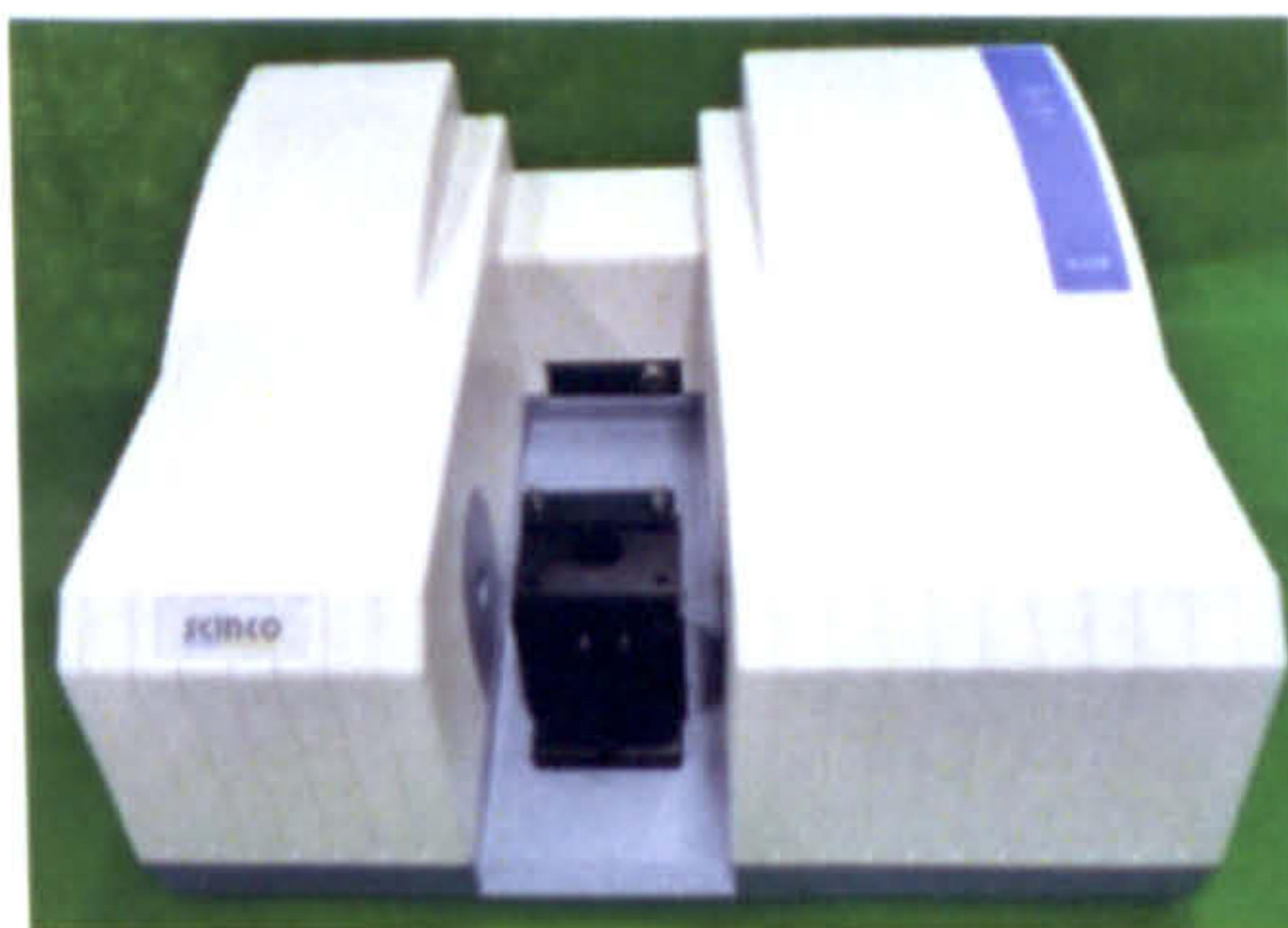


Figure 3.4 S-3100 System

The S-3100 [Sinco 2009] System is a multi-channel spectrophotometer with an array of photodiodes in a 1024 channel, giving optimum wavelength resolution for the readout unit. It has the wave length accuracy as $\pm 0.5\text{nm}$ at 360.95nm and 453.7nm (or $\pm 0.2\text{ nm}$ at 486.0nm and 656.1nm). One feature of a PDA is an integrating photo-detector which integrates charge depending on the light intensity. The advantage of the integrating function is named Felgette's S/N advantage or Multi-channel advantage. The system has been used to measure

the reflectivity of a reference sample used in determining the reflectivity of real surfaces of mockup buildings (test cells).

3.3 SpectraColorimeter

A spectrometer is an optical instrument used to measure optical properties of light sources over a specific portion of the electromagnetic spectrum [Photo Research Inc. 1999]. The PR-650 SpectraColorimeter used to measure spectral distribution of light emitting from the terminal device (optical lens) is one of the latest in the Photo Research family of SpectraScan fast scanning instruments. It is compact, light and capable of carrying out NIST-traceable photometric and colorimetric measurements spectroradiometrically. Figure 3.5 shows a photo of the instrument whereas Figure 3.6 is a plot of the spectral radiance measured by it.



Figure 3.5 PR-650 Spectracolorimeter

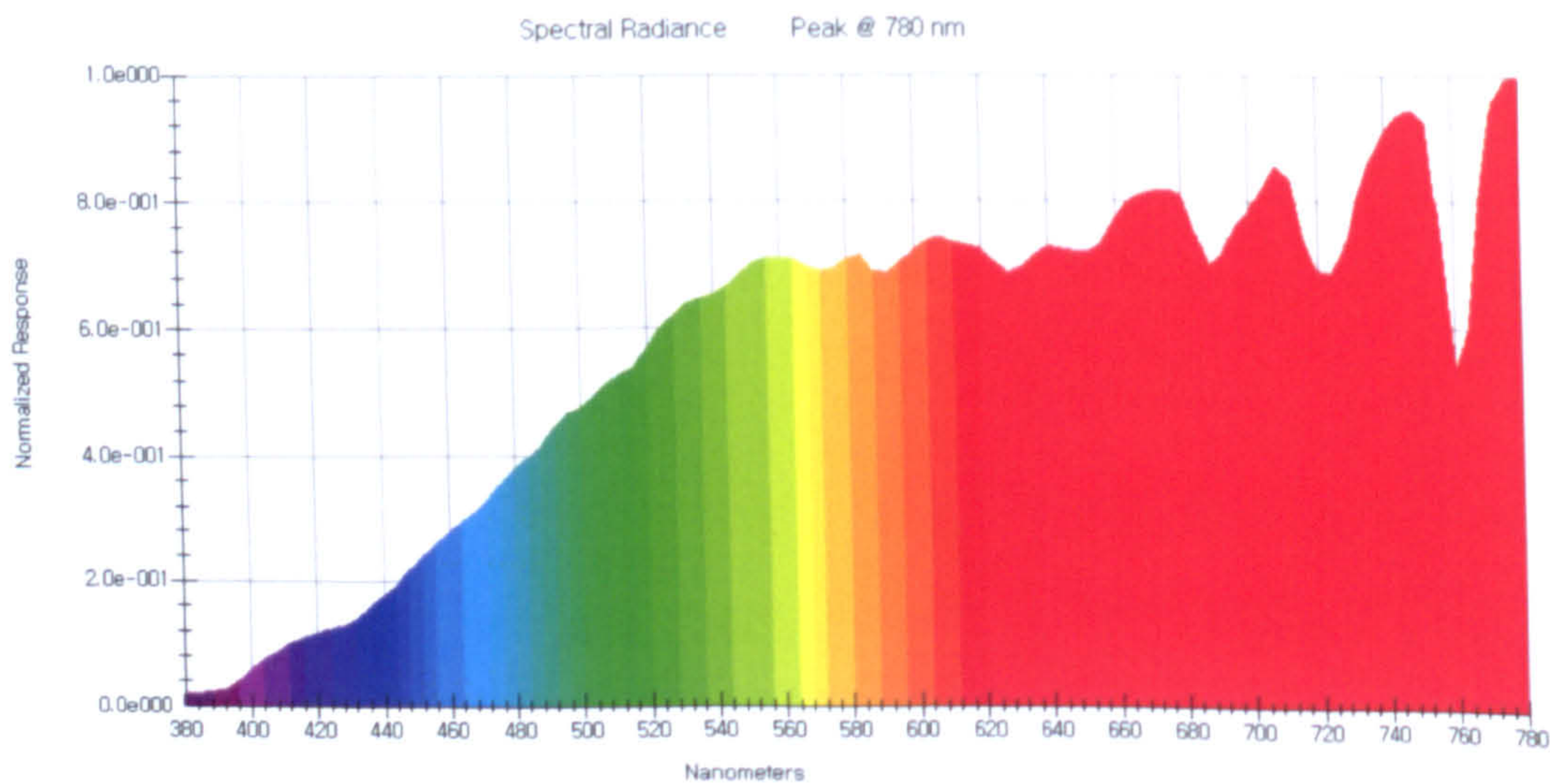


Figure 3.6 Spectral radiance measured

In Figure 3.6, the spectral distribution of light measured by a spectrometer (Spectroscan 650) is shown as it emerges from a convex lens used for the terminal device under a clear sky condition. No appreciable differences were observed with the terminal device.

Table 3.1 Some major features of PR 650 SpectraColorimeter

Spectral Range	380 - 780 nm
Spectral Bandwidth	8 nm
Spectral Accuracy	± 2 nm
Wavelength Resolution	< 3.5 nm / pixel
Luminance Accuracy	± 2% of calculated luminance at 2856K @ 23° C
Color Accuracy when Measuring an Illuminant	±.0015 CIE 1931 x, ± .001 CIE 1931 y (.006 CIE 1931 x, y for CRT's typical)
Digital Resolution	14 bit (1 part in 16,000)
AutoSync Range	40 - 250 Hz
Measuring and Viewing Field	1° (measuring) and 7° (viewing) with MS- 75 lens at infinity focus
Battery	Rechargeable NiCad. Recharge rate - 1.5 hrs. from full discharge with CD-650
Interfaces	RS-232, IEEE-488 (optional)
Operating Temperature	34° to 95° F (1° to 35° C)
Operating Humidity	≤90% non-condensing
Size (approx. including MS-75 lens)	12" (305 mm)L x 7"(178 mm)W x 3" (76 mm) H
Weight (approx.)	4 lbs. 12 oz. (2.15 kg.) with MS-75 lens and battery

3.4 Goniophotometer

A goniophotometer measures the spatial distribution of a radiation source and displays the photometric properties of light [Andersen 2006]. It provides viable information for a radiant source such as light distribution profiles, luminous intensity, luminance and other major photometric data which are essential in designing a luminaire(illuminant) for indoor illumination. Figure 3.7 shows the measurement by a goniophotometer (Model:DP-1600) to obtain the luminous intensity distribution of diffusers (convex, semi-convex, concave, semi-concave lenses and cylindrical luminaires) used at the end of the optical cable for indoor illumination [Optical & Photometric Technology Pty Ltd. 1999]

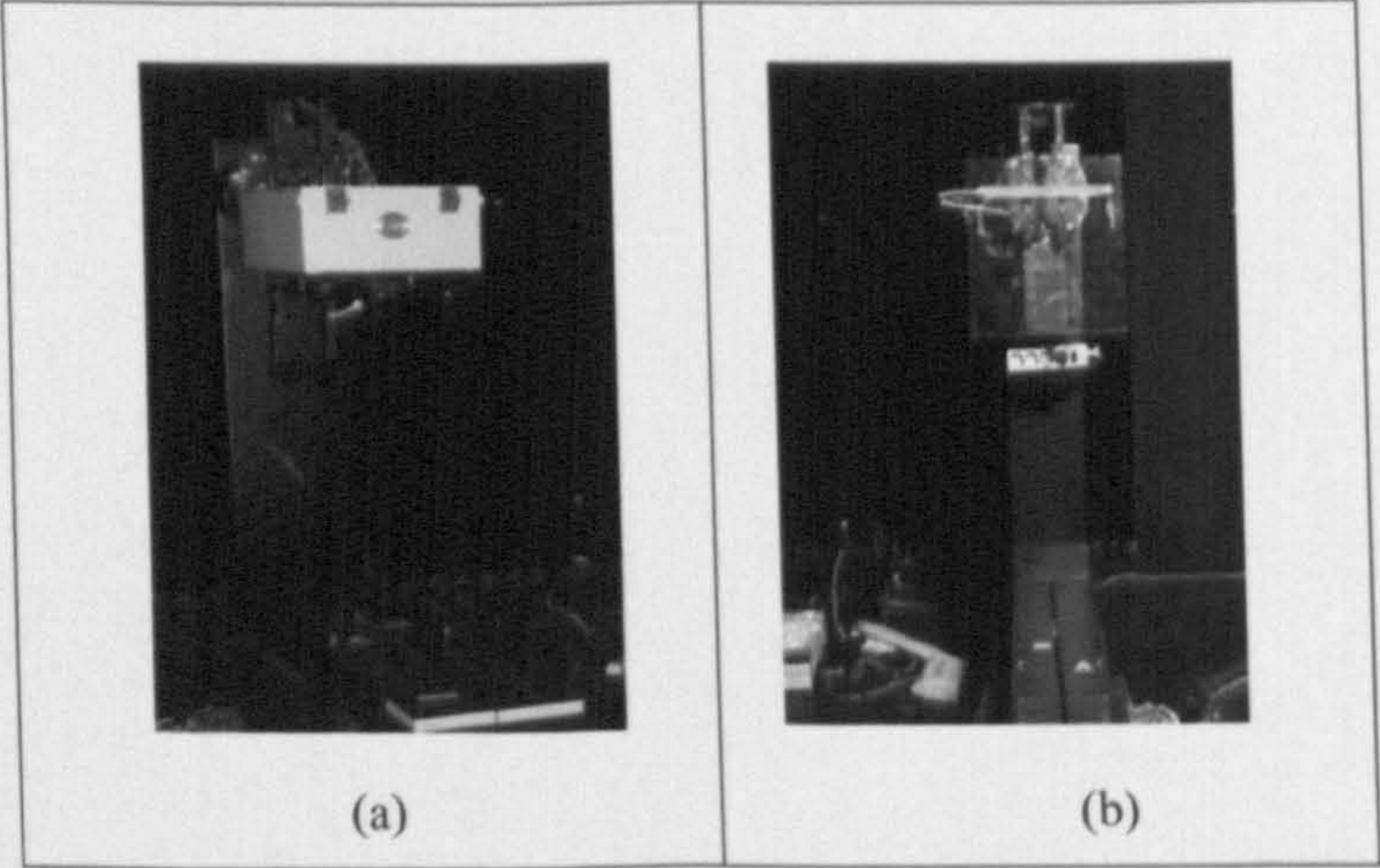
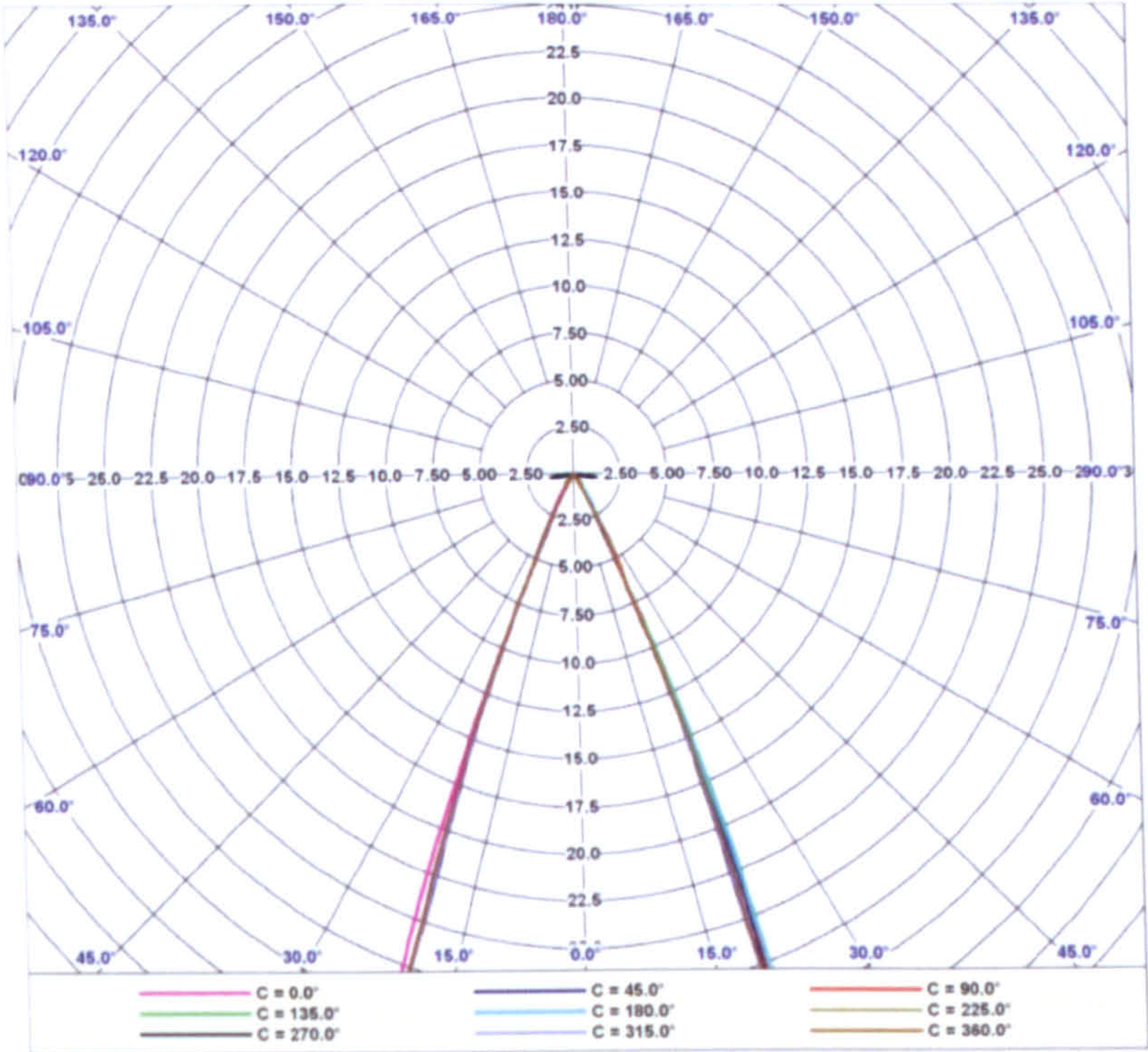


Figure 3.7 Goniophotometer measurements for luminous intensity distribution: (a) a test kit with a 50W halogen lamp, (b) a cylindrical diffuser mounted on goniophotometer

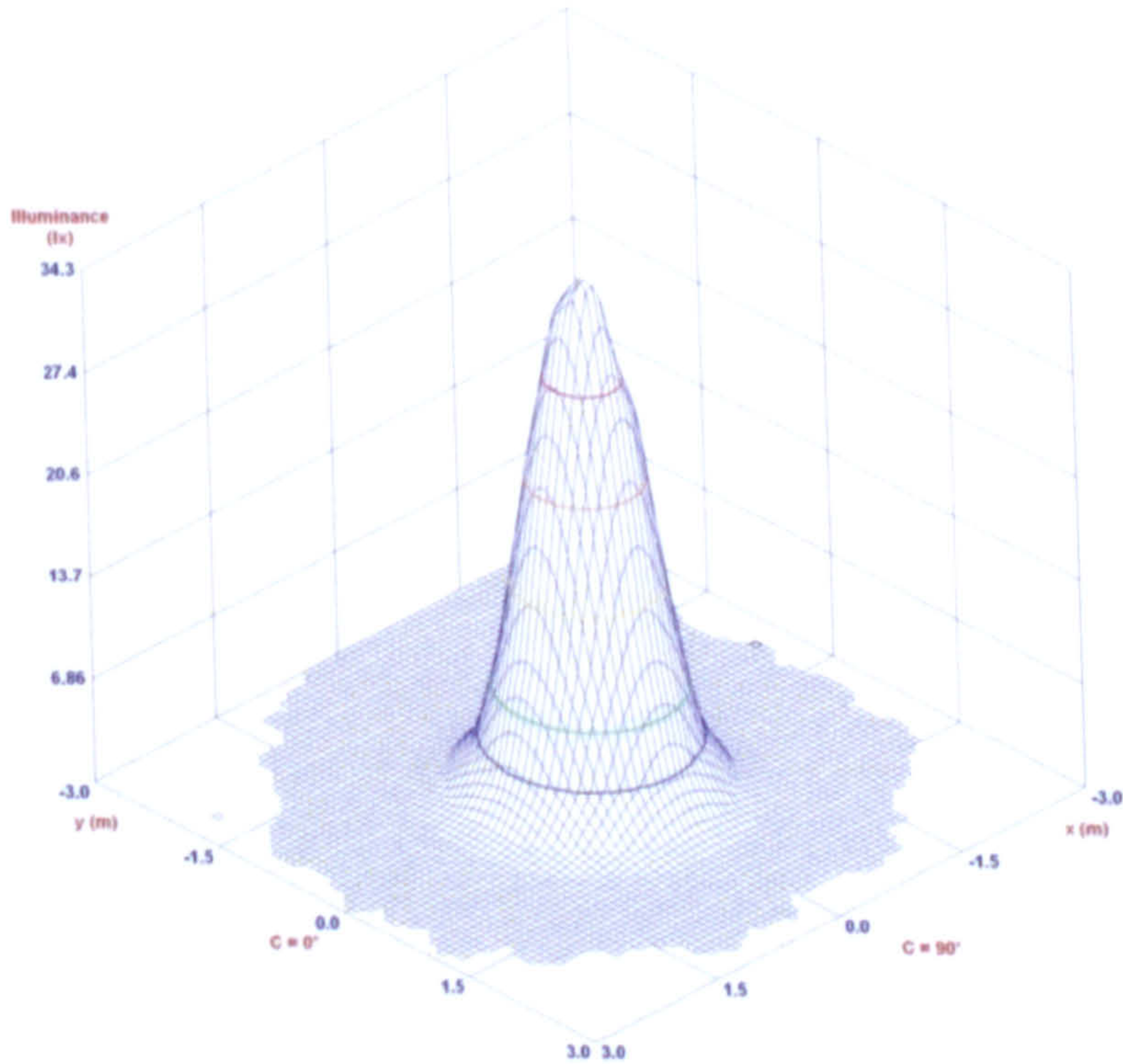
Figures 3.8 to 3.12 present 2D and 3D luminous intensity distributions for different types of diffusers. By examining these figures, the light spreading characteristics of a luminaire (illuminant) could be rather easily obtained. Among the optical lenses tested, the semi-concave lens (Figures 3.11 and 13) has shown the widest spreading angle followed by concave, convex and semi-convex lenses. It, however, is far from the state of uniform illumination and displays suitability for spot lighting. In order to promote uniformity in illumination, a cylindrical shape diffuser should be applied as demonstrated by Figure 3.13.

Luminous Intensity Distribution (Lowest 10%)



(a)

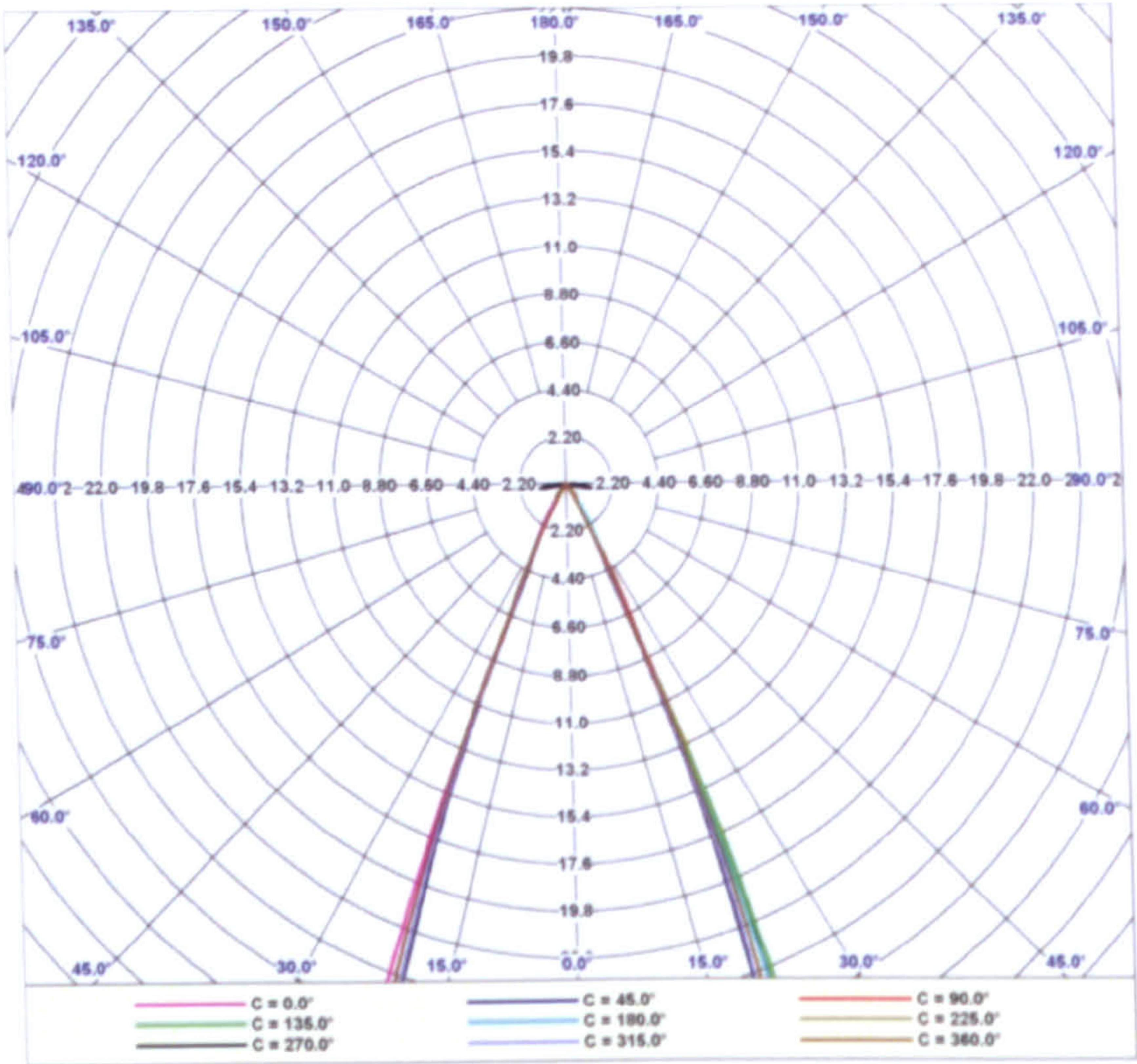
IsoLux 3D



(b)

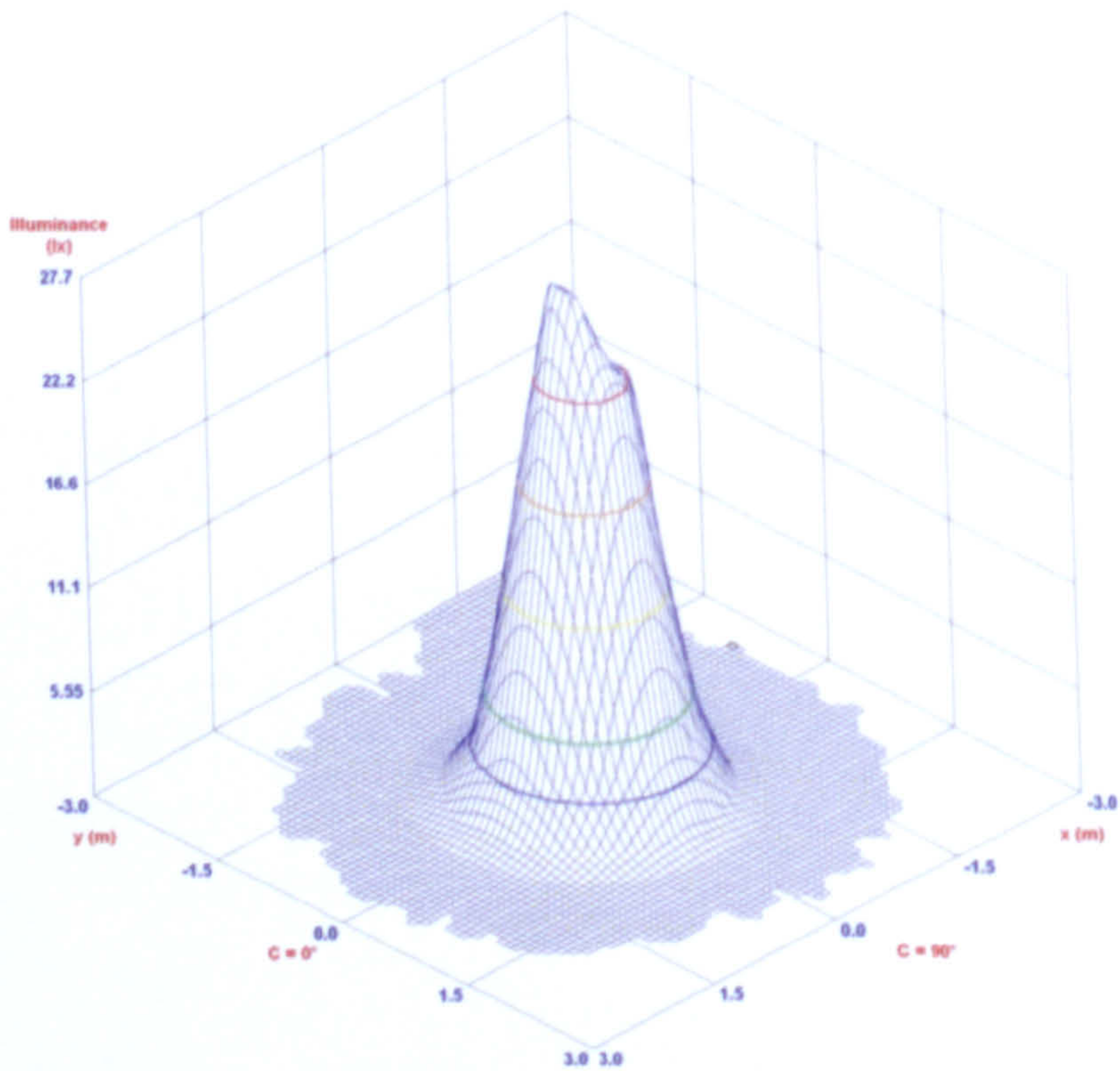
Figure 3.8 Luminous intensity distribution of the convex lens :
(a) 2D, (b) 3D presentation

Luminous Intensity Distribution (Lowest 10%)



(a)

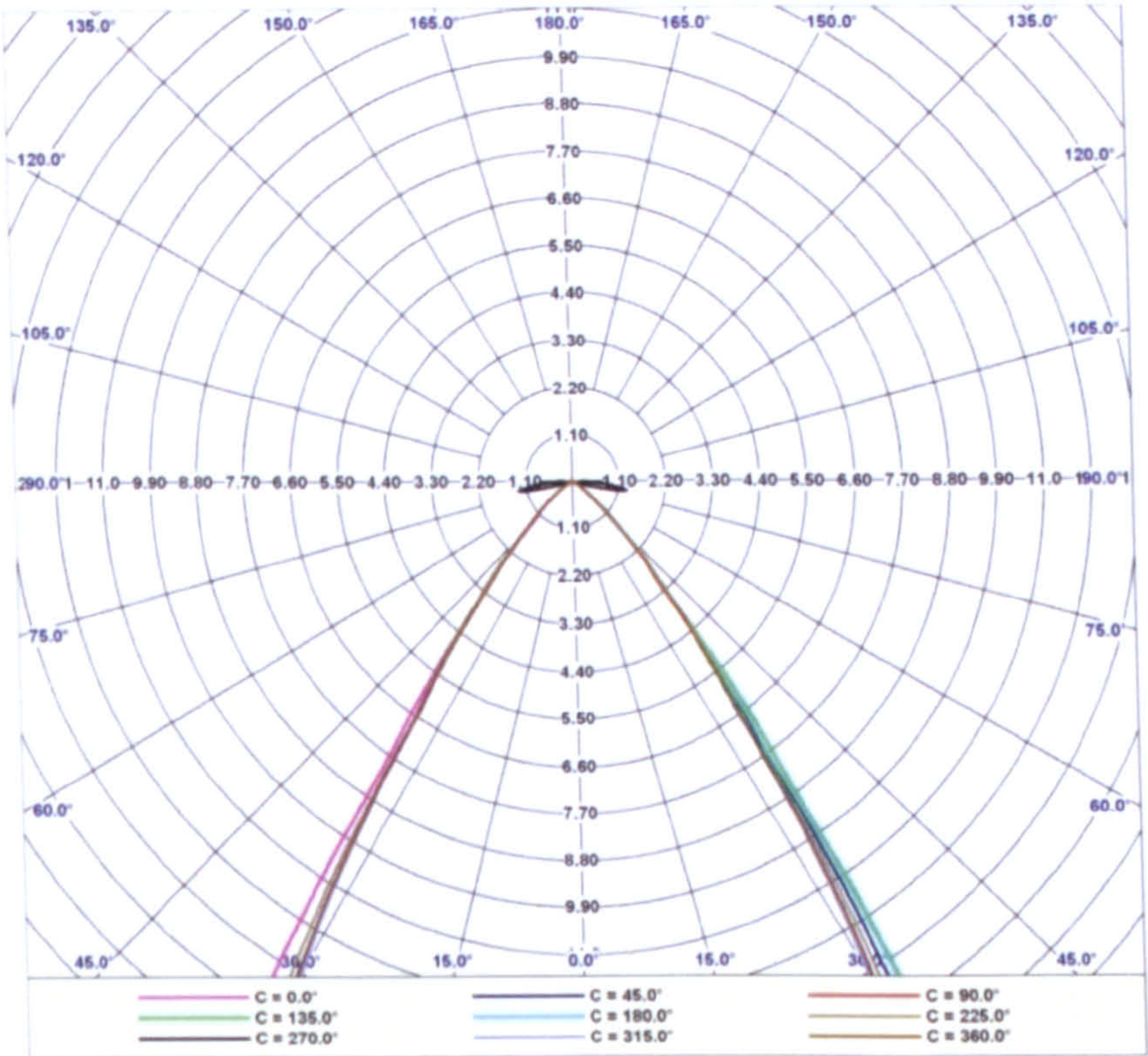
IsoLux 3D



(b)

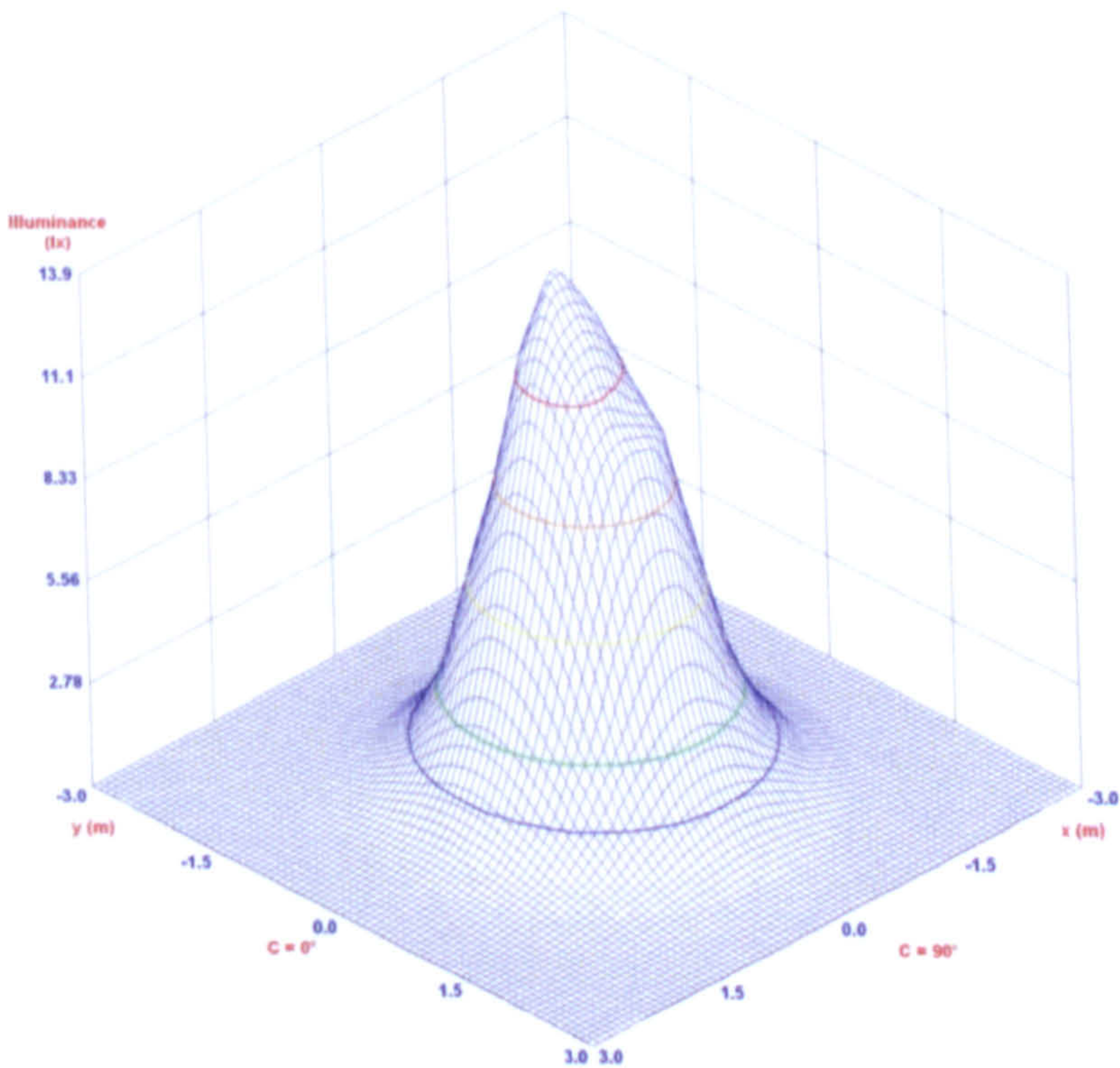
Figure 3.9 Luminous intensity distribution of the semi-convex lens :
(a) 2D, (b) 3D presentation

Luminous Intensity Distribution (Lowest 10%)



(a)

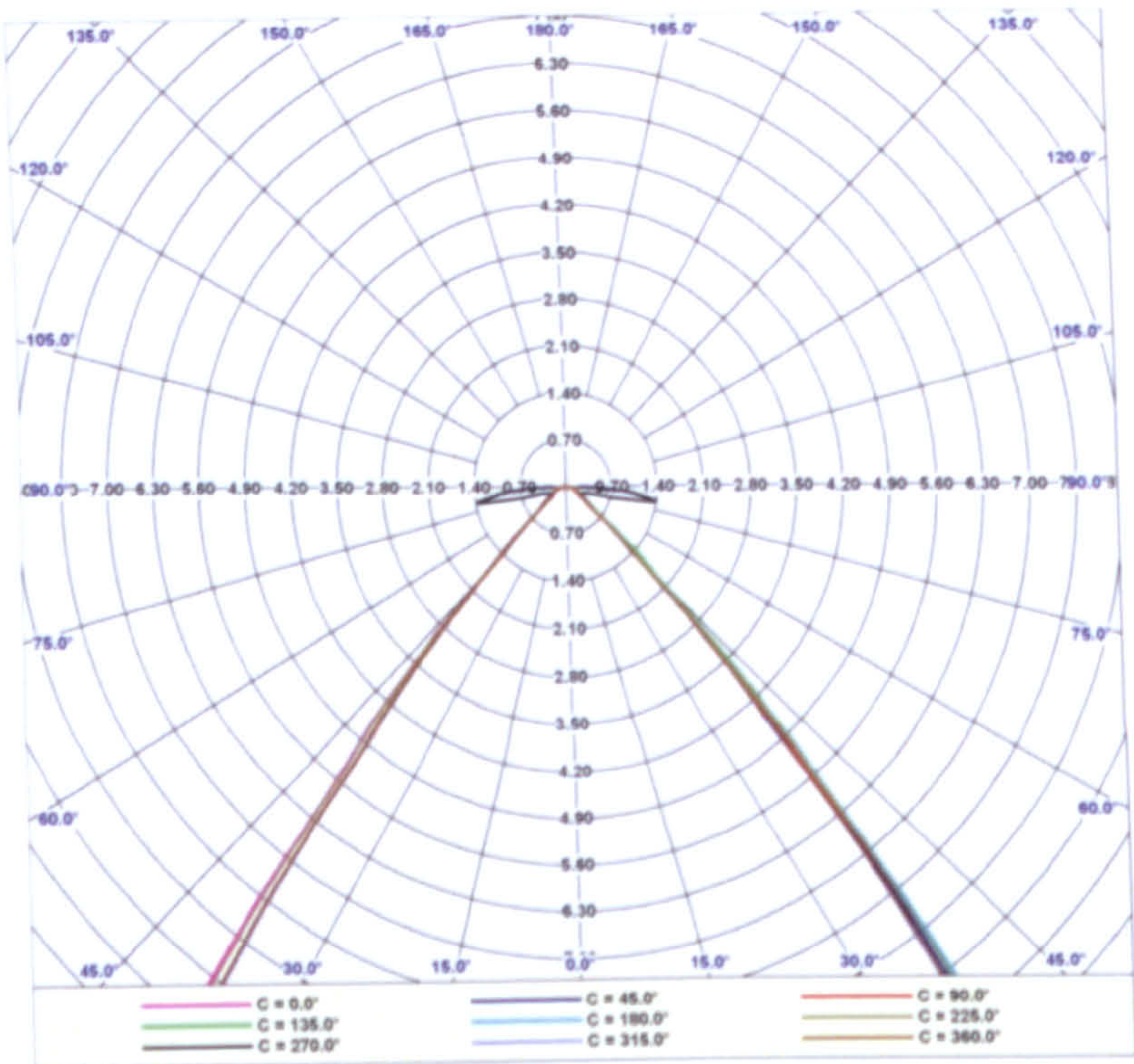
IsoLux 3D



(b)

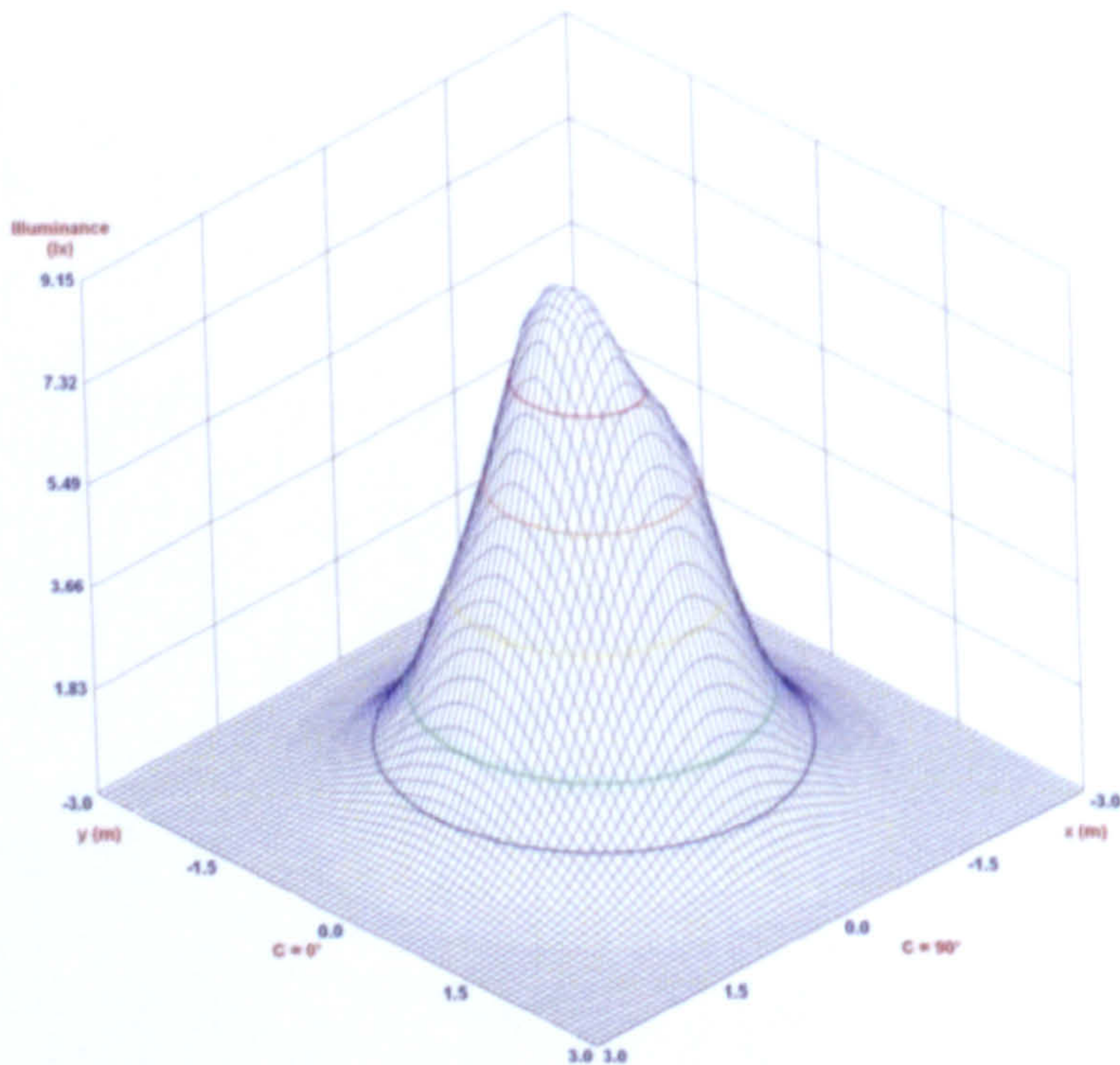
Figure 3.10 Luminous intensity distribution of the concave lens :
(a) 2D, (b) 3D presentation

Luminous Intensity Distribution (Lowest 10%)



(a)

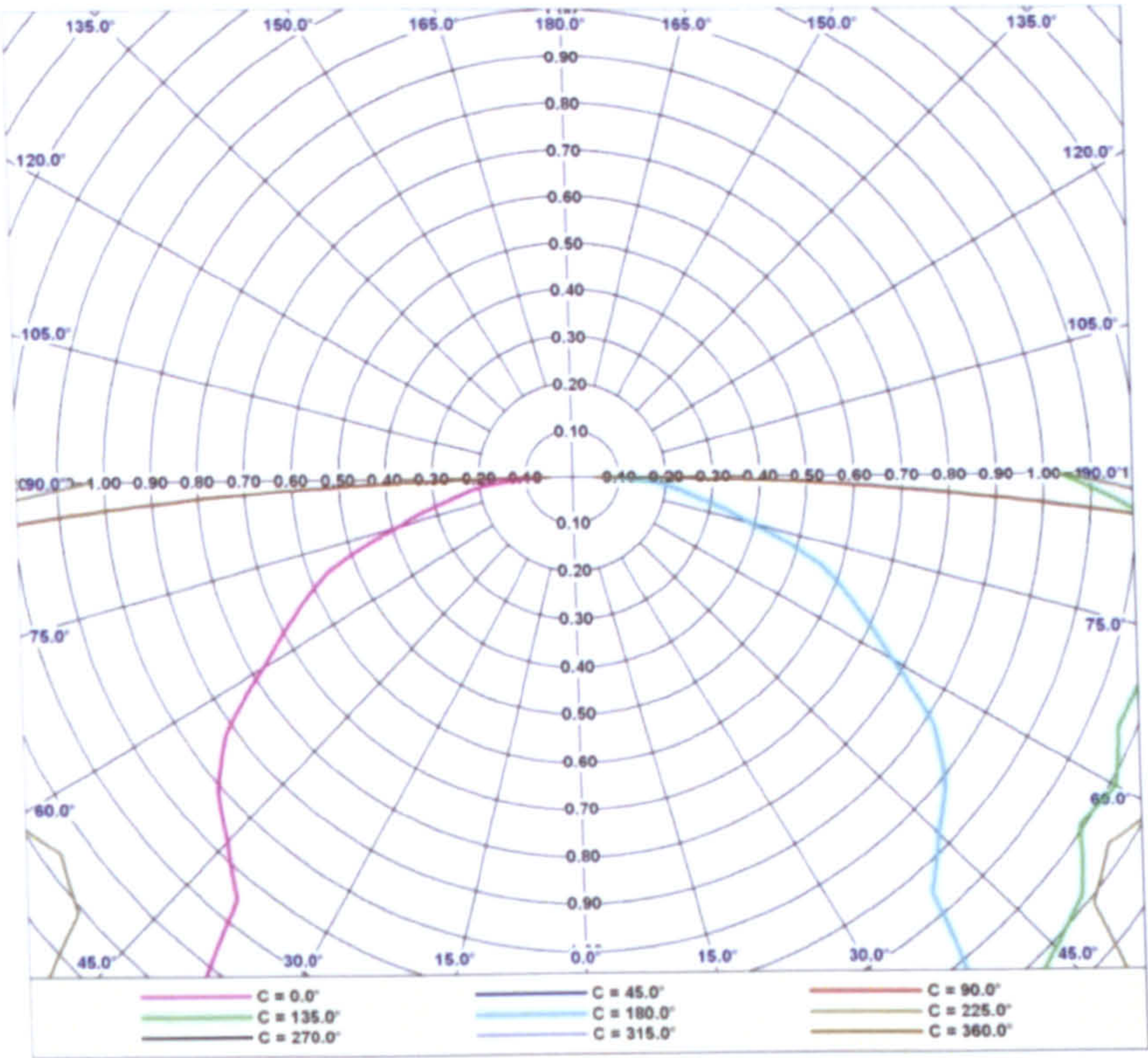
IsoLux 3D



(b)

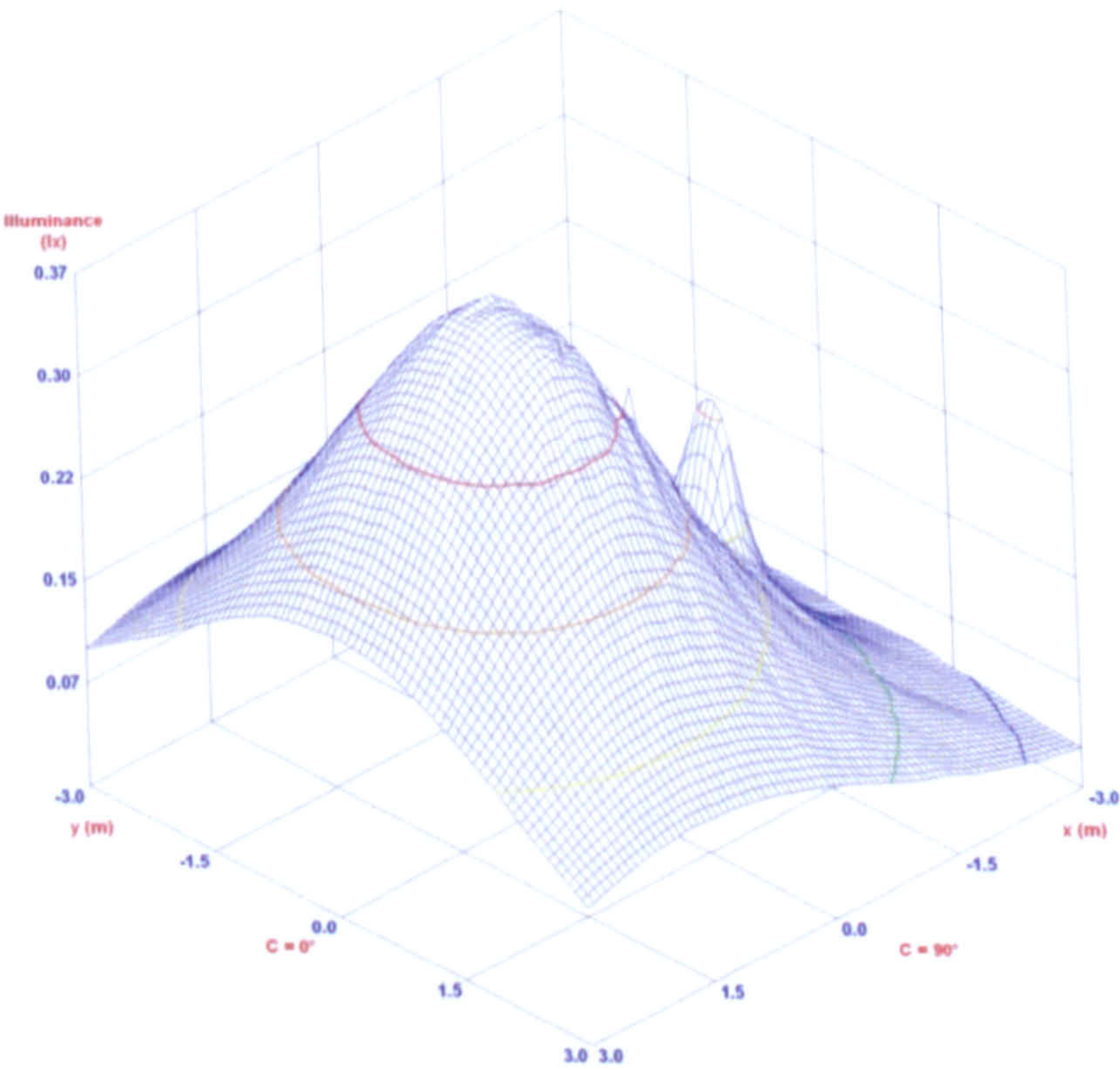
Figure 3.11 Luminous intensity distribution of the semi-concave lens :
(a) 2D, (b) 3D presentation

Luminous Intensity Distribution (Lowest 10%)



(a)

IsoLux 3D



(b)

Figure 3.12 Luminous intensity distribution of a cylindrical diffuser :
(a) 2D, (b) 3D presentation



Semi Concave



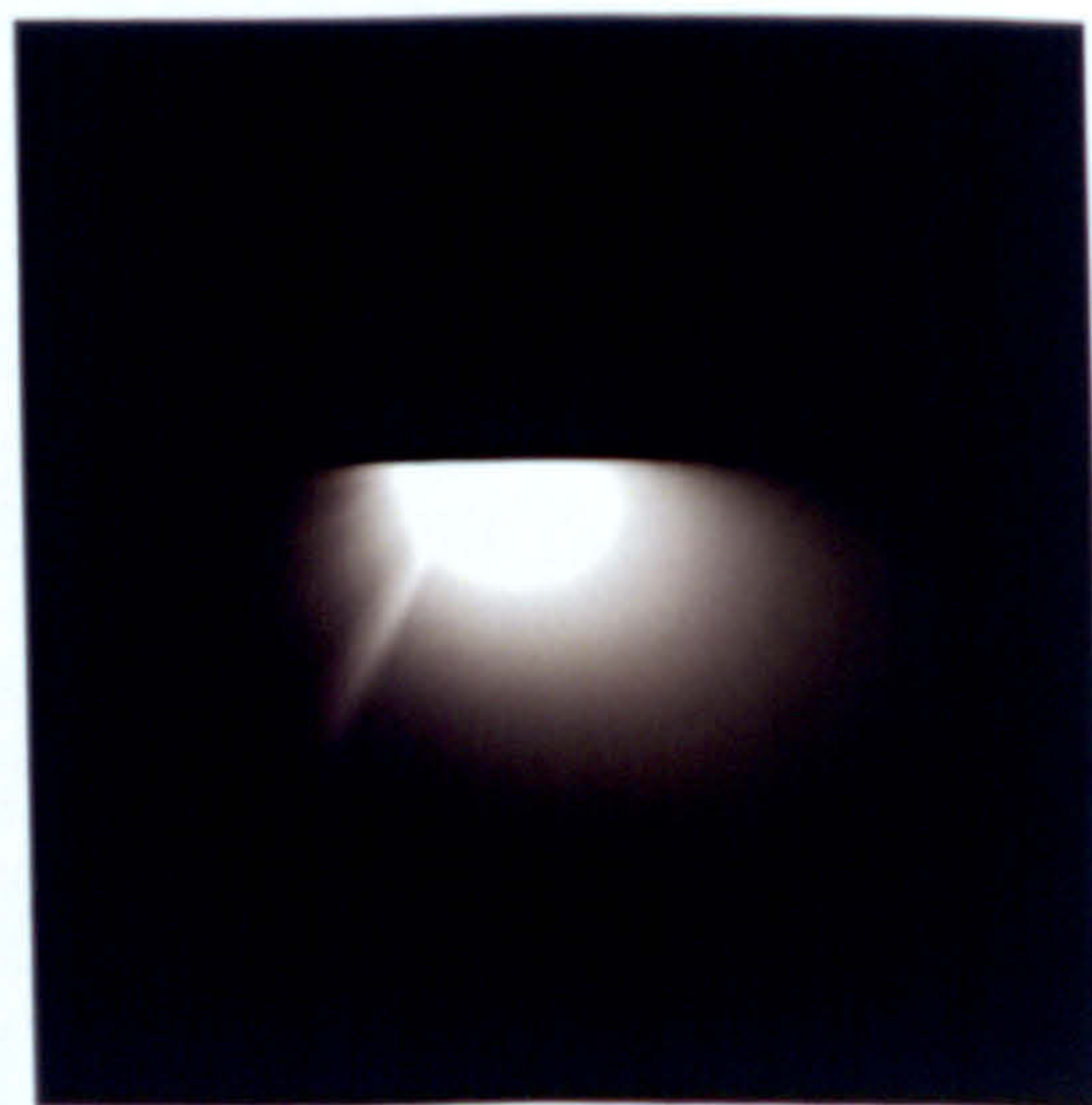
Concave



Semi Convex



Convex

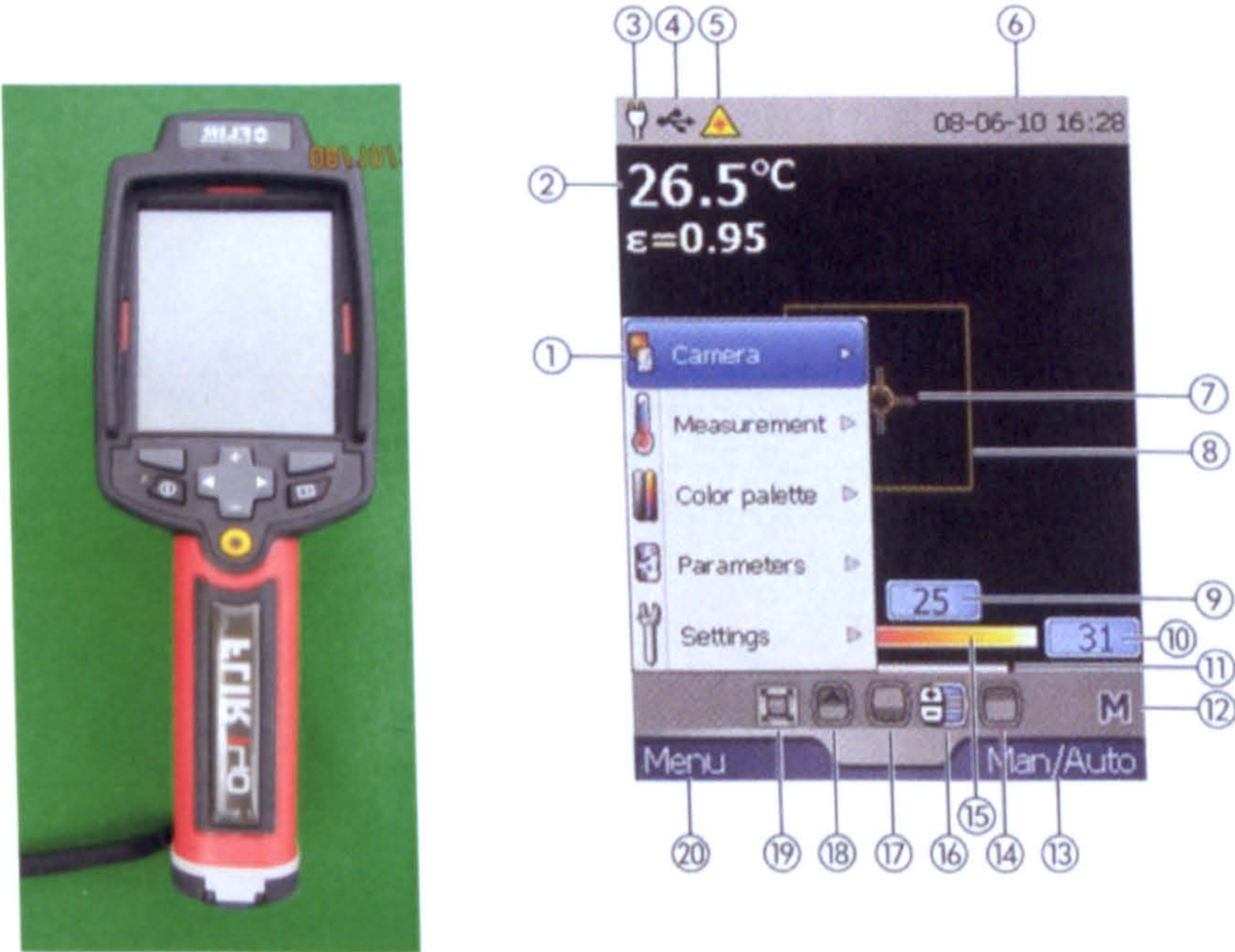


Fluorescent lamp shaped

Figure 3.13 Rendered image of light

3.5 FLIR i40 Thermal Camera

An infrared camera is a very effective tool to detect temperature distribution of an object with some temperature readings. It is designed to generate thermal images or heat pictures displaying small temperature differences [FLIR Inc 2009]. Infrared thermography provides a visual map of surface temperatures in real time. Figure 3.14 shows a picture of the system used in this work with some description regarding the display on its LCD monitor. The system has been used to monitor the temperature change of the interior space at different times of a day.



- ① Menu system
- ② Measurement results table, including information about the emissivity value
- ⑥ Date and time
- ⑦ Measurement spot
- ⑨ Limit value for an isotherm in the temperature scale
- ⑩ Limit value for the temperature scale
- ⑮ Temperature scale

Figure 3.14 FLIR i40 thermal camera

Table 3.2 shows the technical specifications of the system where its accuracy and applicable temperature range is given in detail.

Table 3.2 FLIR i40 Specifications

Features	
Temperature range	-4°F to 662°F (-20°C to 350°C)
Temperature accuracy	±2°C or ±2% of reading
Image Storage	>1000 Images (1GB micro SD memory card)
Emissivity	0.1 to 1.0 (adjustable); Emissivity Table

Imaging Performance / Image Presentation	
Field of view/min focus distance	25° X 25°/0.10m (3.9")
Thermal sensitivity (N.R.T.D)	<0.1°C at 25°C
Detector Type	Focal plane array (FPA) uncooled microbolometer; 14,400 pixels (120 X 120)
Spectral range	7.5 to 13µm
Display	3.5" color LCD
Video output	MPEG-4 via USB
Image Modes	Thermal, Visual, Fusion
Fusion Picture in Picture (PIP)	Fixed
Visible Light Camera Resolution	0.6 Megapixels
Image Controls	Palettes (Iron, Rainbow, and Black/White), level, span, auto adjust (continuous/manual)
Focus	Manual
Set-up controls	Date/time, info, LCD intensity, power down, and 21 languages
Spot (center) Measurement mode	Yes
Area (min/max) Measurement mode	Yes
Battery Type/operating time	Li-Ion/ 5 hours, Display shows battery status
Dimensions/Weight	9.3X3.2X6.9" (235X81X175mm)<1.32lbs (600g), including battery

3.6 Summary

Major photometric properties of the present daylighting system are measured, where a series of tests were conducted using different types of photometric instruments : Luminance meter, Spectrophotometer, SpectraColorimeter and Goniophotometer. Each instrument measures distinct features of the optical properties displayed by the daylighting system, luminaires and processed materials. Some detailed technical specifications are also given along with their output (measured data). Especially, the luminous intensity distributions measured by the goniophotometer for different types of diffusers have revealed the crucial data concerning the light spreading characteristics of various terminal devices. Among those optical lenses tested, the semi-concave lens has shown the widest spreading angle followed by concave, convex and semi-convex lenses. These are, however, far from delivering a state of uniform illumination and deems more suitable for spot lighting. In order to promote uniformity in illumination, a diffuser that is capable of dispersing light in all directions should be employed as shown in the case of a cylindrical shape diffuser.

4. PERFORMANCE ASSESSMENT : MEASUREMENTS AND SIMULATION

To verify its photometric applicability of the high-density daylighting system, a series of measurements and simulations were performed for different operational conditions and architectural environment. Especially, a number of test cells were designed and built to assess its functional suitability in attaining optimum levels of indoor illumination including the case of hybrid lighting. Photometric measurements(and observations) were carried out in Nottingham (United Kingdom) and Jeju (Korea).

4. 1 Nottingham Test Chamber

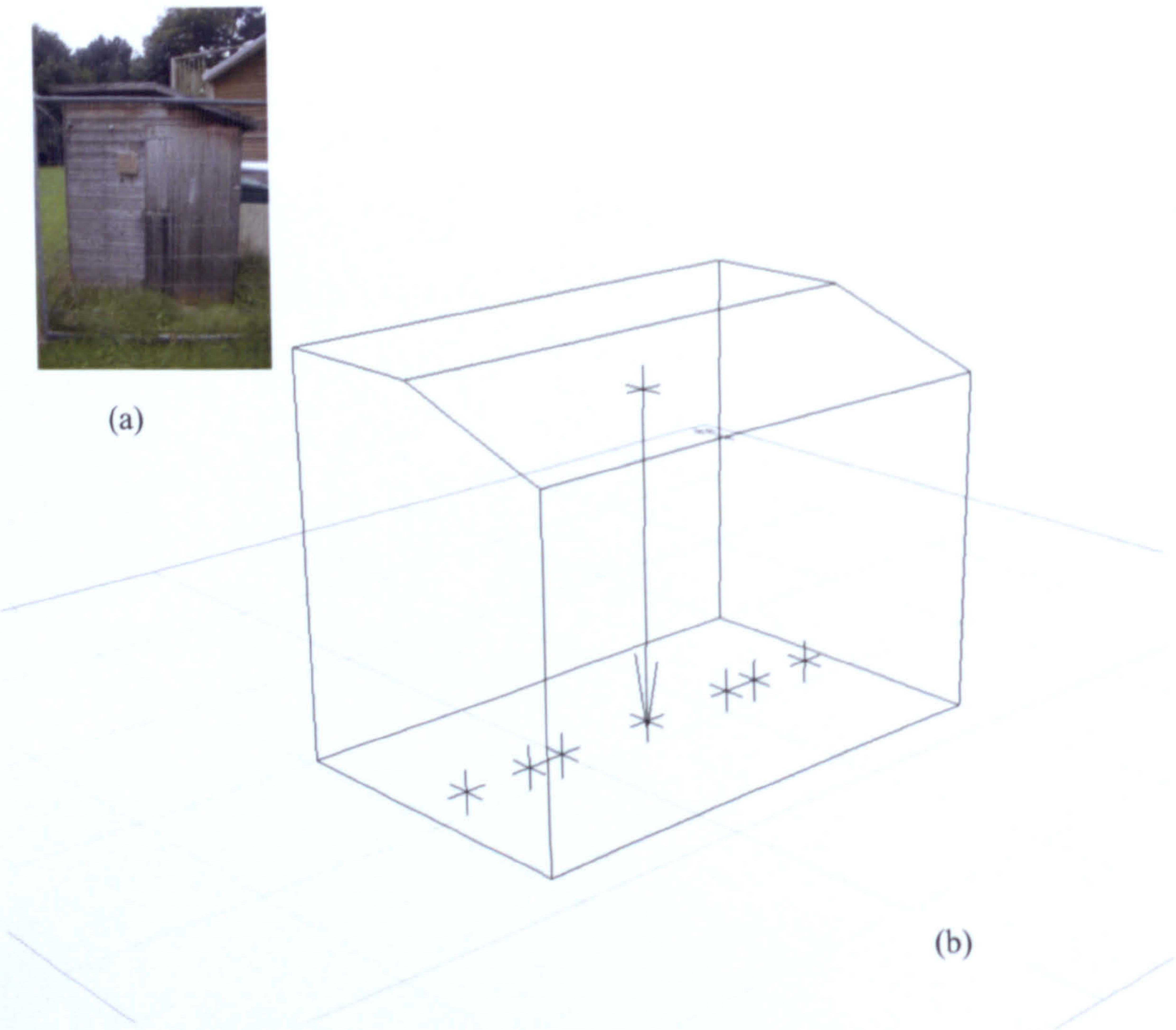


Figure 4.1 Test chamber at Nottingham (Latitude: 52° 58' 0 N, Longitude : 1° 10' 0 W)
(a) Built, (b) Virtual model

Fig. 4.1 shows the actual picture and virtual model of the building (test chamber), which is located in Nottingham, United Kingdom. It is a wooden structure with a partly flat and sloped roof. Its dimensions are 1,670mm(length) x 2,900mm(width) x 2,000m(height-highest) built to the half scale of a real building. The interior of the building is painted black and has no windows making it a dark space.

The photometric properties of the illuminant were based on the experimental measurements given in Chapter 3 where some developments are made to provide the required field data for simulation. Especially, the measured data of goniophotometer were very useful in determining relevant photometric parameters to carry out the simulation. The following are the major photometric properties obtained and used in the analysis when a semi-convex lens is employed:

- Illuminant : semi-convex lens
- Candela output: 4,011 cd
- Available viewing angle of the illuminant (in 2D): 45°
- Solid angle: 0.4783 sr
- Total Lumens: 1,919 lm
- Radius of light source: 32 mm.

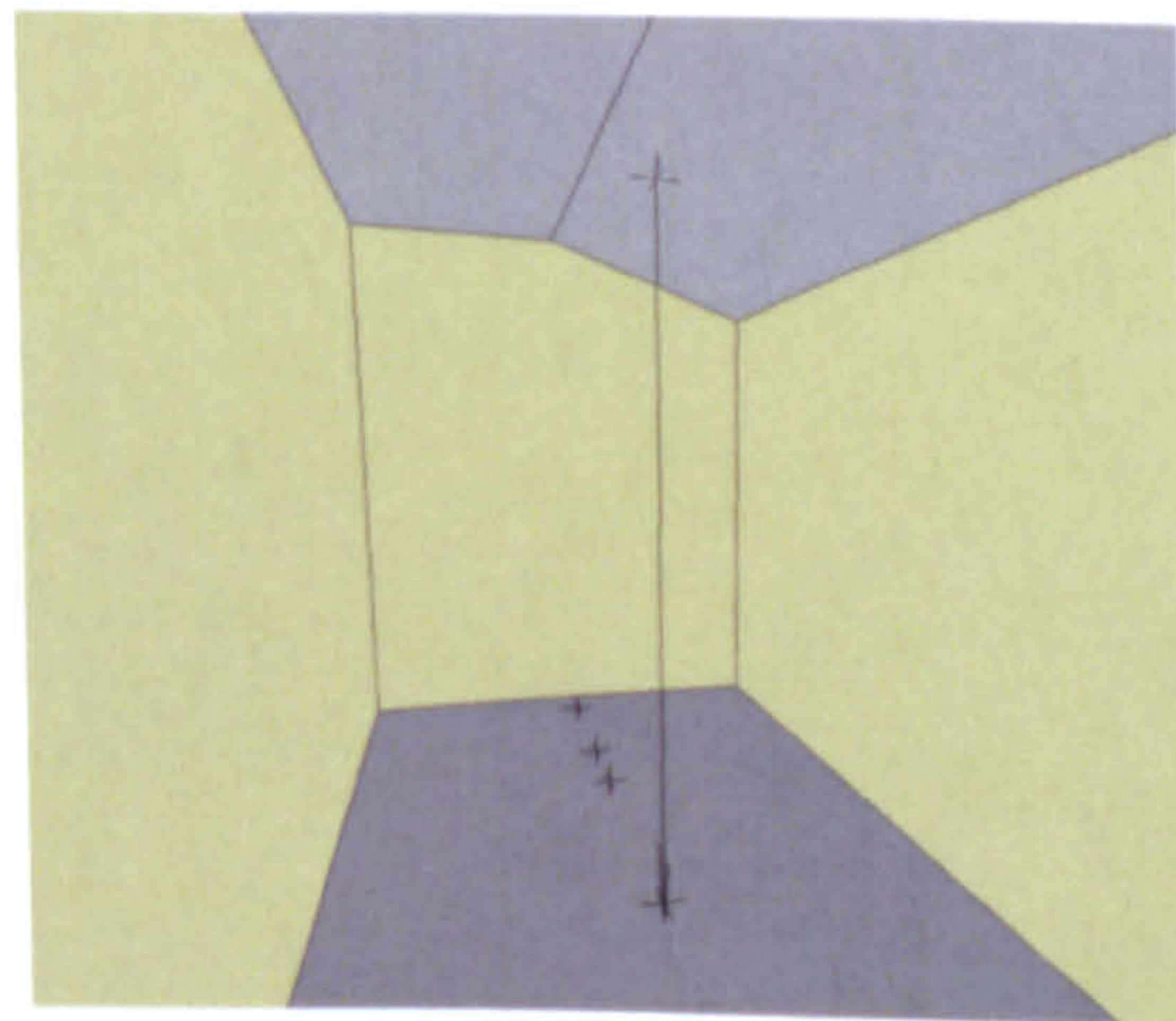


Figure 4.2 An interior view of the test module for simulation

Generally, converting between geometry-based measurement units could be difficult and it should only be attempted when it is impossible to measure in the actual desired units. One must be aware of what each of the measurement geometries implicitly assumes before any conversion is made. The process involved in the present analysis falls in this category where a number of measured data are correlated to obtain key parameters required for performance simulation.

What follows gives some details of the numerical data for the major photometric properties (especially, conversion between lux - lumens per square meter- and lumens) derived from goniophotometer measurements in the previous chapter. The processes shown here for the determination of key variables should be repeated for each case of simulation since the solar intensity changes with time and the IES file will be different depending on the types of optical lenses used for diffusers.

To calculate the illuminance at 1.0 m:

$$E_1 = \left(\frac{d_2}{d_1}\right)^2 \times E_2 \quad (4.1)$$

$$d_1 = 1 \text{ m (reference point to calculate source output)} \quad E_2 = 1,310 \text{ lux}$$

$$d_2 = 1.8 \text{ m} - 0.05 \text{ m} = 1.75 \text{ m (distance between the diffuser and the sensor)}$$

Hence, E_1 (I_v) becomes 4,011 lm/m².

1) Conversion of lm/m² to lm/sr at 1.0 m:

$$4,011 \text{ lm/m}^2 \times 1 \text{ m}^2/\text{sr} = 4,011 \text{ lm/sr}$$

2) Referring to the angular measurements given in Figure 4.3 for θ , where it is measured to be about 45 degrees (indicating that light is blocked 315 degrees) :

$$\begin{aligned}\Omega &= 4\pi \sin^2\left(\frac{\theta}{2}\right) = 2\pi(1 - \cos \theta) \Omega = 2\pi(1 - \cos \theta/2) \\ &= 2\pi(1 - \cos 45/2) \\ &= 0.4783 \text{ [sr]}\end{aligned}\tag{4.2}$$

Using this formula, the solid angle and total luminous flux are now easily obtained.

3) Calculation of the total lumen output:

$$\phi = I_v \times \Omega = 4,011 \times 0.4783 = 1,918.5 \text{ [lm]}\tag{4.3}$$

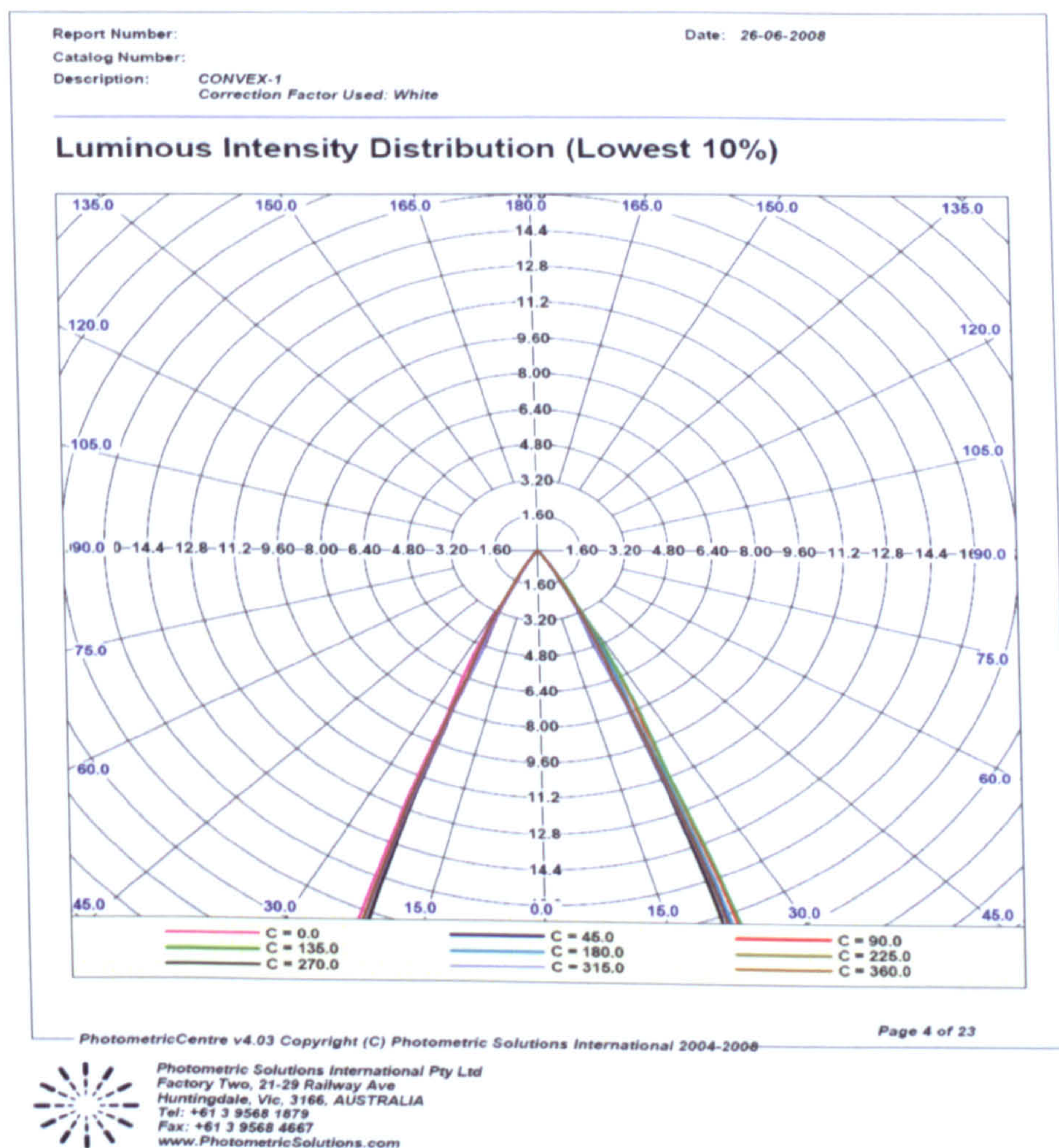


Figure 4.3 Luminous intensity distribution for semi-convex lens(lowest 10%)

The test cell model has dimensions of 2,950mmx1,750mmx1,800mm. The longer side is oriented to the north. Seven photo sensors are installed symmetrically along the centerline at a height of 50mm by using a 100mm wide wooden panel. To prevent any accidental movement of sensors, the rear side of each sensor is treated with an adhesive before it is placed at a specified location. As shown below, the 4th sensor is located at the center directly below the luminaire attached to the optical fiber cable of the dish-daylighting system.

The distances between sensors were

- between #4 and #3(#5) : 60cm
- between #2 and #3(#5 and #6) : 15cm
- between #1 and #2(#6 and #7) : 45cm.

To accurately measure illuminances near the east and west walls away from the center, the sensors were not equally spaced. Also, the sensors 1, 2, 3 and 7, 6, 5 were placed symmetrically with respect to the sensor at the midpoint (sensor 4), respectively. Of course, more sensors could be used for detailed measurements and monitoring of illuminances. The purpose of this measurement, however, was to gather real illuminance data for the test chamber to establish the reliability of its simulation model developed by using ECOTECH (and RADIANCE).

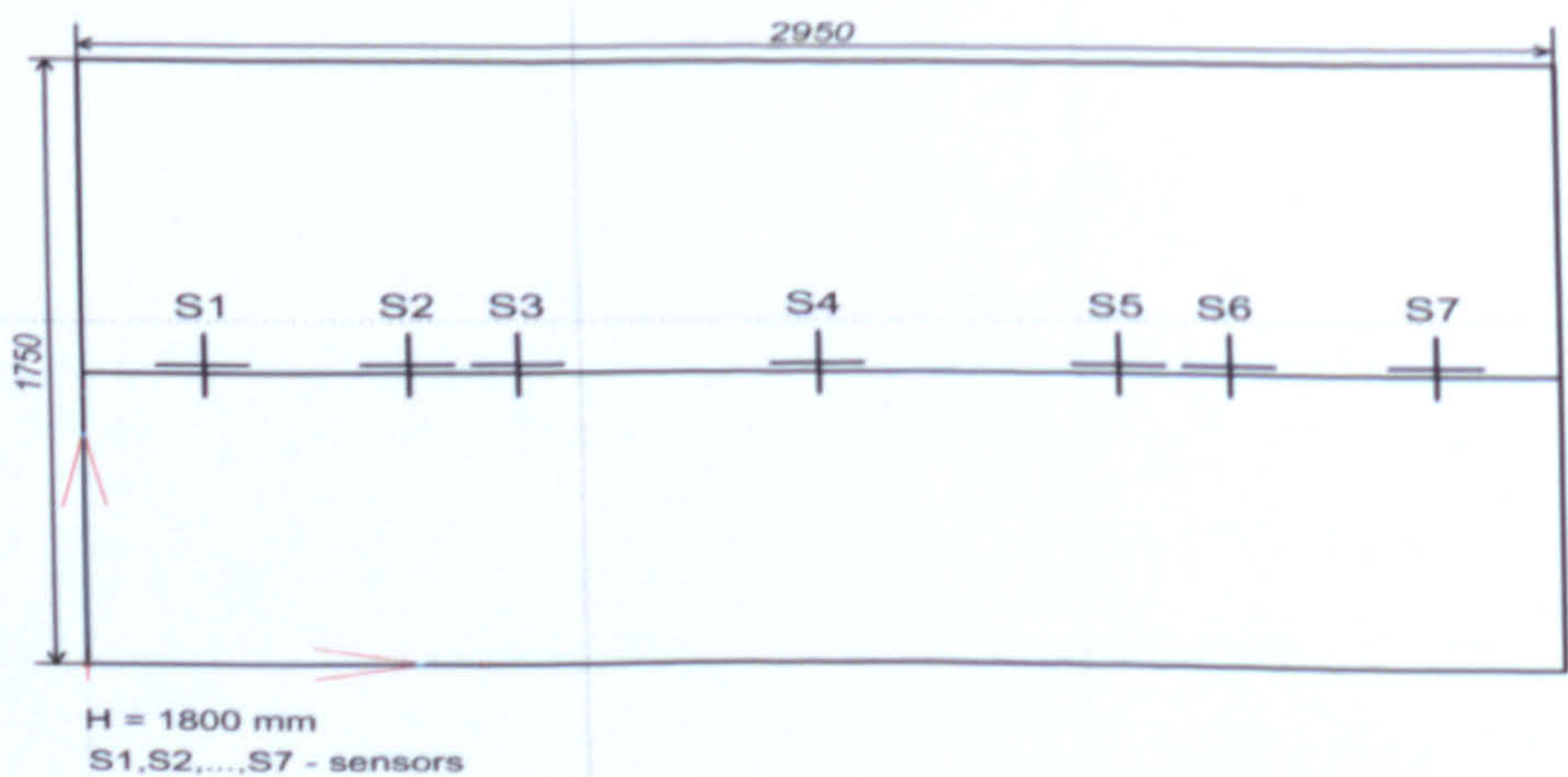


Figure 4.4 Sensor locations

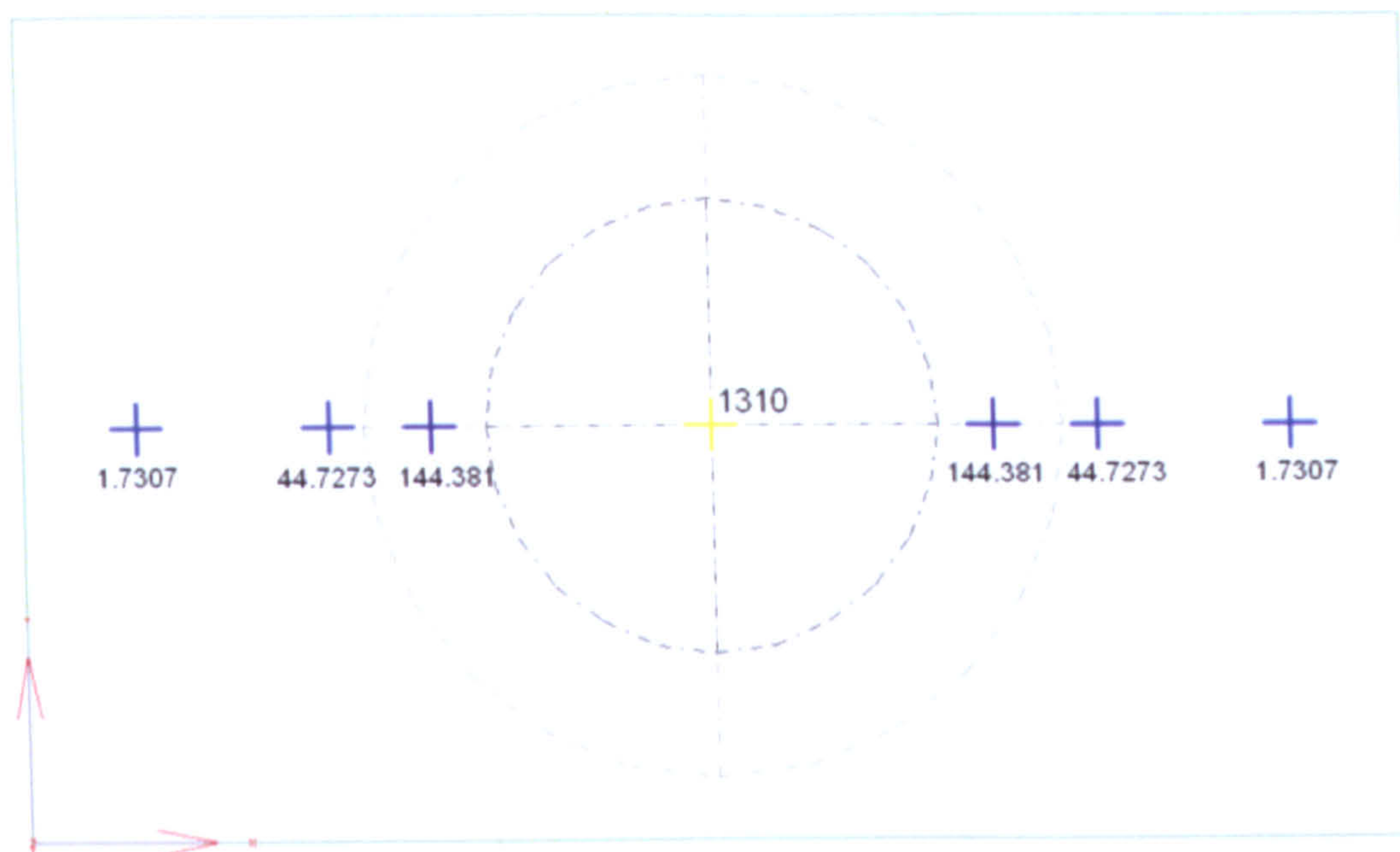


Figure 4.5 Simulation values of sensors at noon (at the location of sensors)

Results of the measurement and simulation for the dish-daylighting system (with a semi-convex lens for diffuser) are comparatively examined to establish the validity of the present investigation and to develop a reliable simulation model applicable to various conditions. Once the model is developed, it could be readily used to make predictions for other cases without undue difficulties. Figure 4.5 gives the simulated values at the exact location of sensors where the direct comparison with the measured ones is possible. As given in Table 4.1 below, there is a good agreement between the two values around bright areas of illumination. Especially, the illuminance predicted for a point directly below the luminaire perfectly matches the experimental one as the candela output (of the luminaire) is based on the measured value. Also, there exists a symmetry with respect to the sensor placed at the center(sensor 4) in both cases. This deems sufficient to establish the reliability of our simulated model.

Figure 4.6 presents the illuminance distribution where its values are given at equally distanced nodal points. A geometrical symmetry is observed in all directions implying the uniformity of illumination by the convex lens. 0.1 is assumed for the surface reflectance as

the interior of the test chamber was painted flat black.

The model provides an excellent tool to examine the effect of a change in physical properties such as surface reflectance and absorptance or the type of an optical lens (diffuser) on the indoor lighting conditions. Without performing a time consuming complex experimentation, one could easily envision what will happen if some photometric properties are changed which clearly demonstrates the full benefit of simulation.

Table 4.1 Results(illuminance in lux) comparison at 12:00 pm

	Sensor #2	Sensor #3	Sensor #4	Sensor #5	Sensor # 6
Measurement	12.7	138	1310	141	15.2
Simulation	44.72	144.38	1310	140.38	44.72

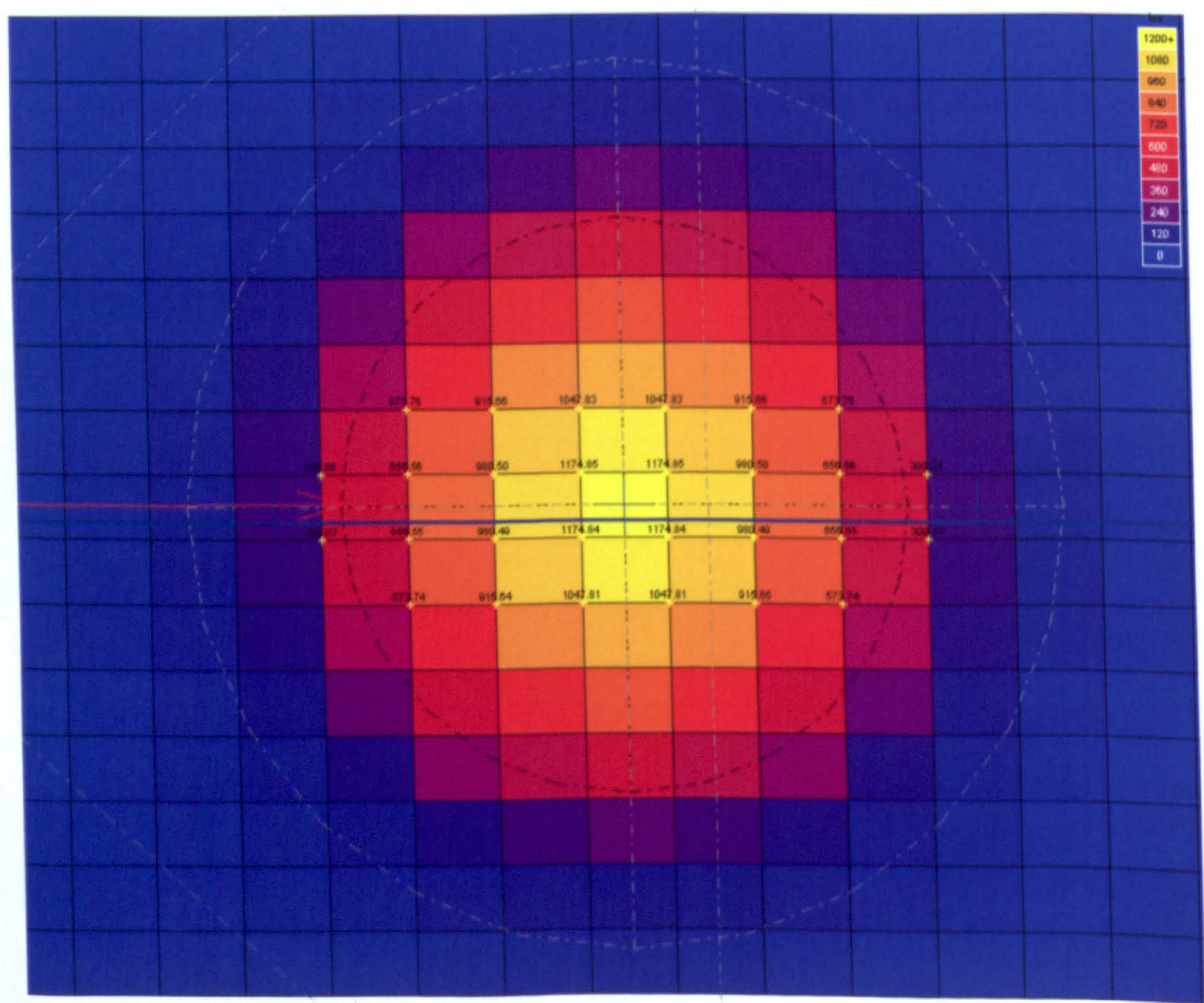
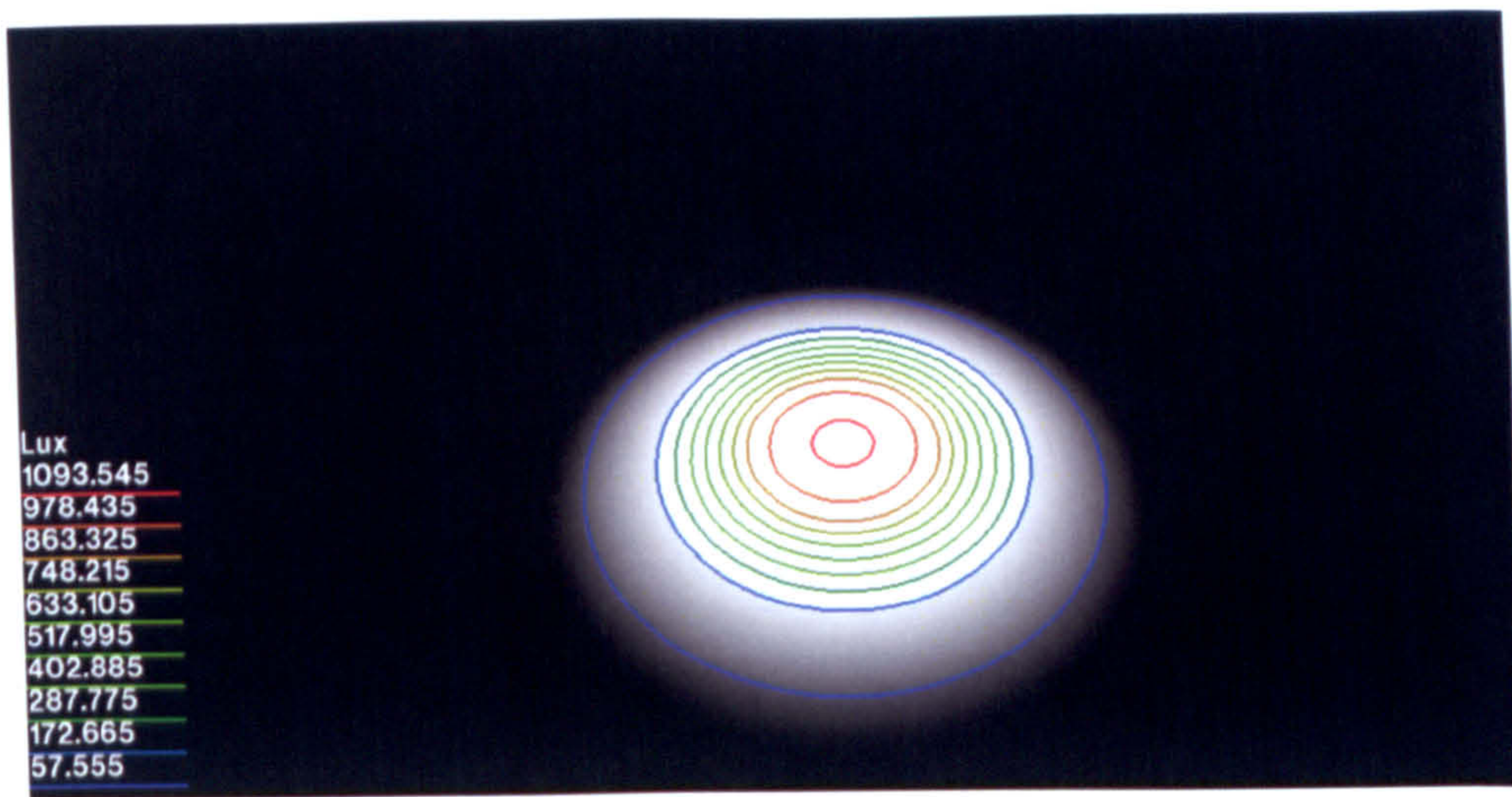
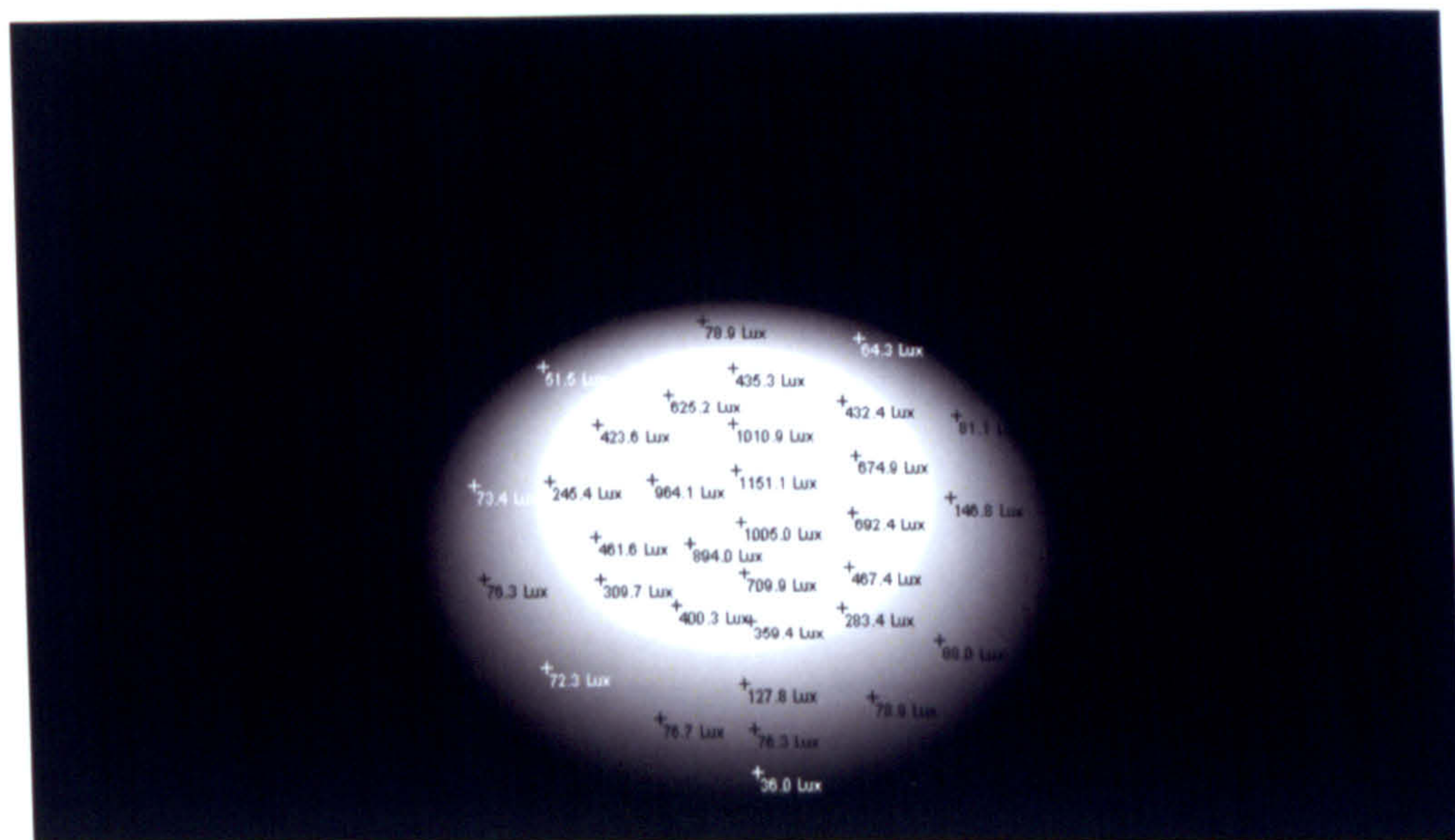


Figure 4.6 Simulation values at sensor locations at noon (at nodal points of equal distance)



(a)



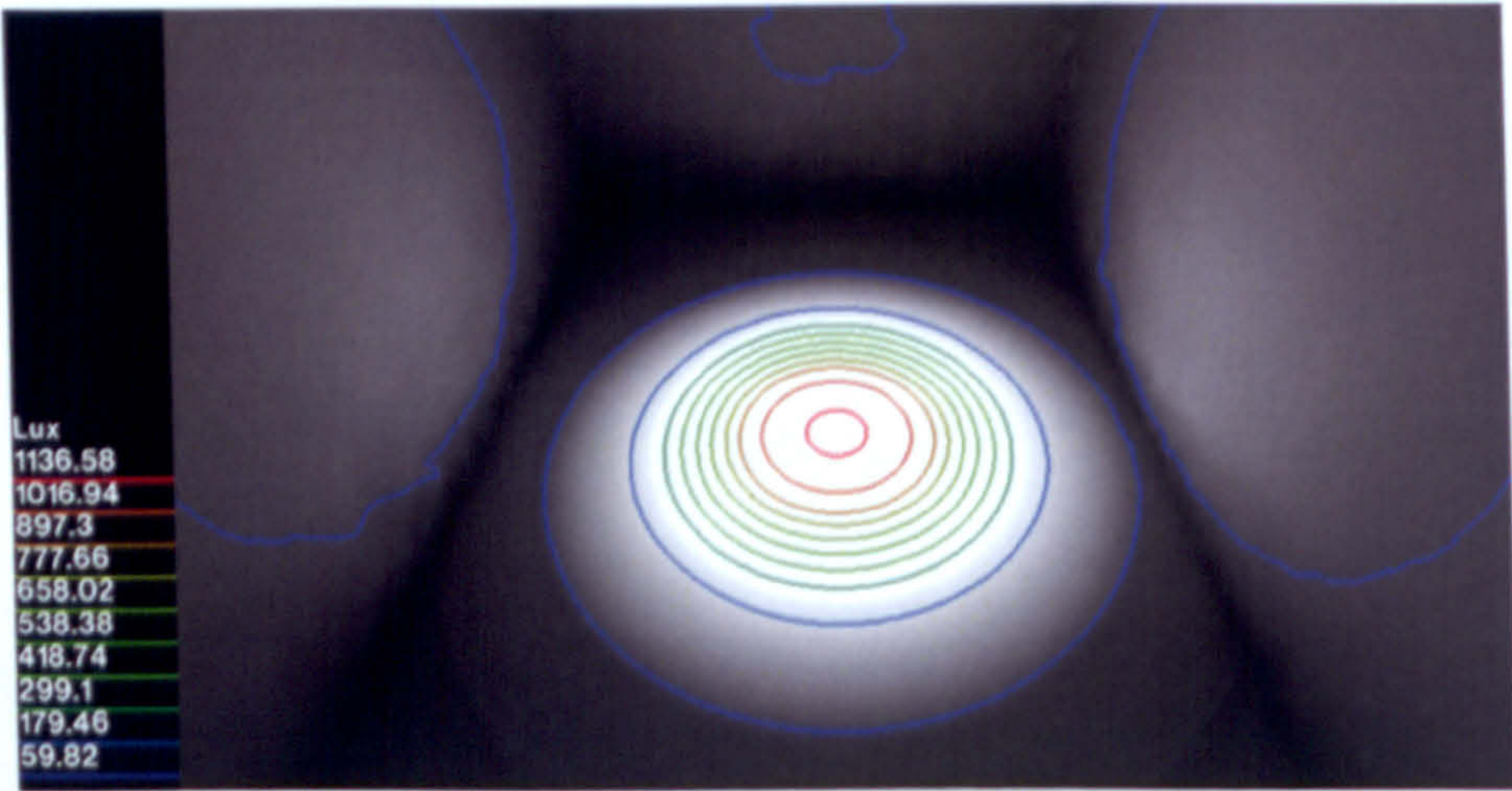
(b)

Figure 4.7 Simulated results by RADIANCE (reflectance = 0.1)

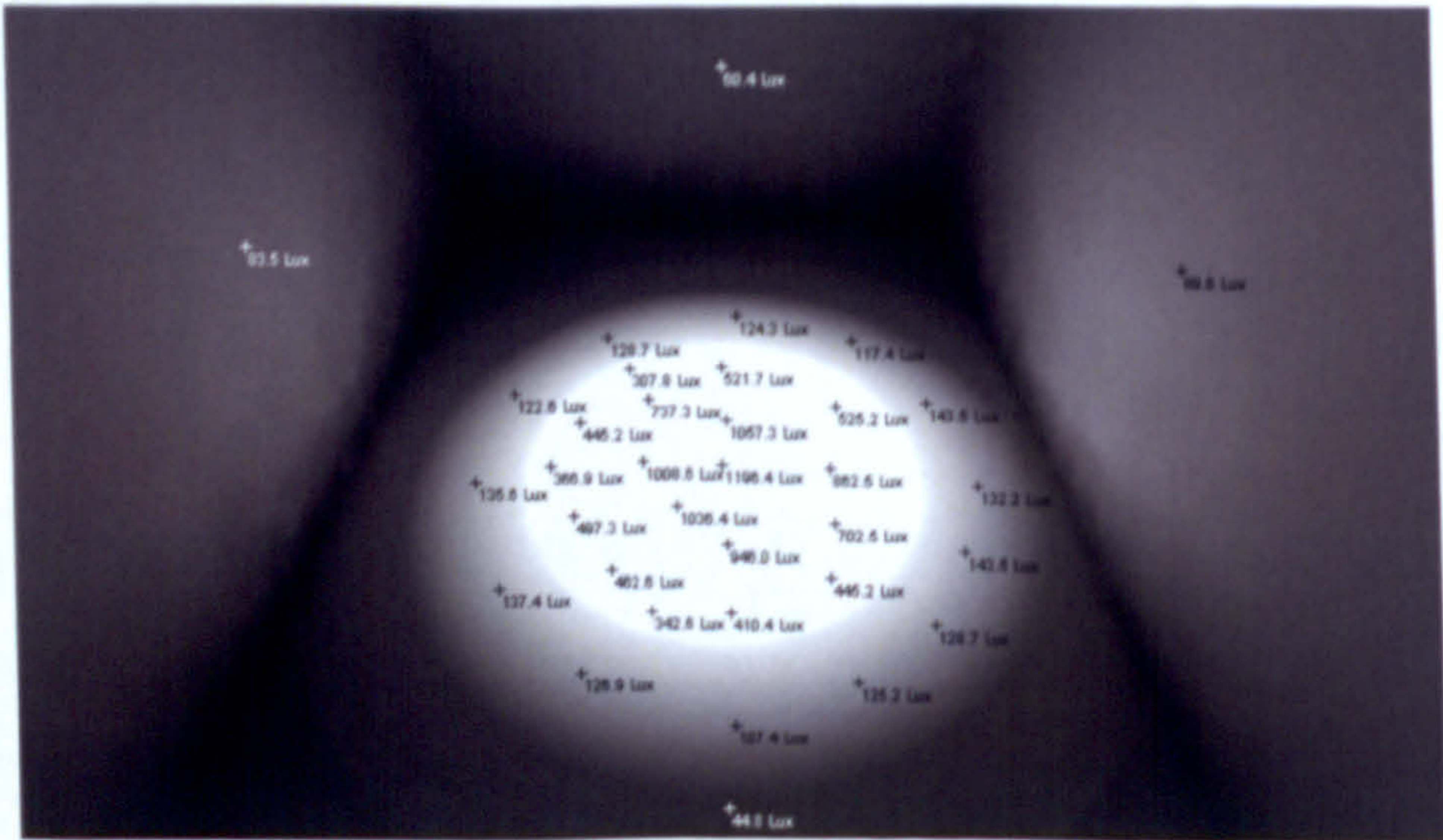
Figure 4.7 shows the simulated results by RADIANCE [Crone 1992], where the illuminance distribution is presented by using concentric circles (a) and values at different locations (b). In both figures, the bright circular area indicates the maximum intensity of solar illumination delivered by the daylighting system at noon. In Figure 4.7 (b), the illuminance of 1151.1 lux corresponds to that at a location near the center of the inner most circle in Figure 4.7 (a).

Figure 4.8 presents the result of RADIANCE simulation with the reflectance of 0.85 for

the interior surfaces of the test chamber. This simulation has been done to examine the effect of internal reflectance on solar illumination. As shown, some improvements are observed throughout the internal space where the illuminance of 1196.4 lux was recorded for the corresponding point value of 1150.1 lux in Figure 4.7. This is, however, much smaller than what's been anticipated considering a rather drastic change in the reflectance to increase the amount of light available for internal reflections which should enhance brightness and overall illuminance.



(a)



(b)

Figure 4.8 Simulated results by RADIANCE (reflectance = 0.85)

Performance of daylighting systems are largely affected by sky conditions. Especially, the active daylighting systems with the solar tracking feature are greatly influenced by the

clearness and air mass of the sun. In Figure 4.9, the actual photo (taken with an 8mm fisheye lens) of the sky condition and its luminance maps are given for the day when the measurements were carried out. As shown, there is a large difference in luminance between the cloudy area near the sun and its surroundings.

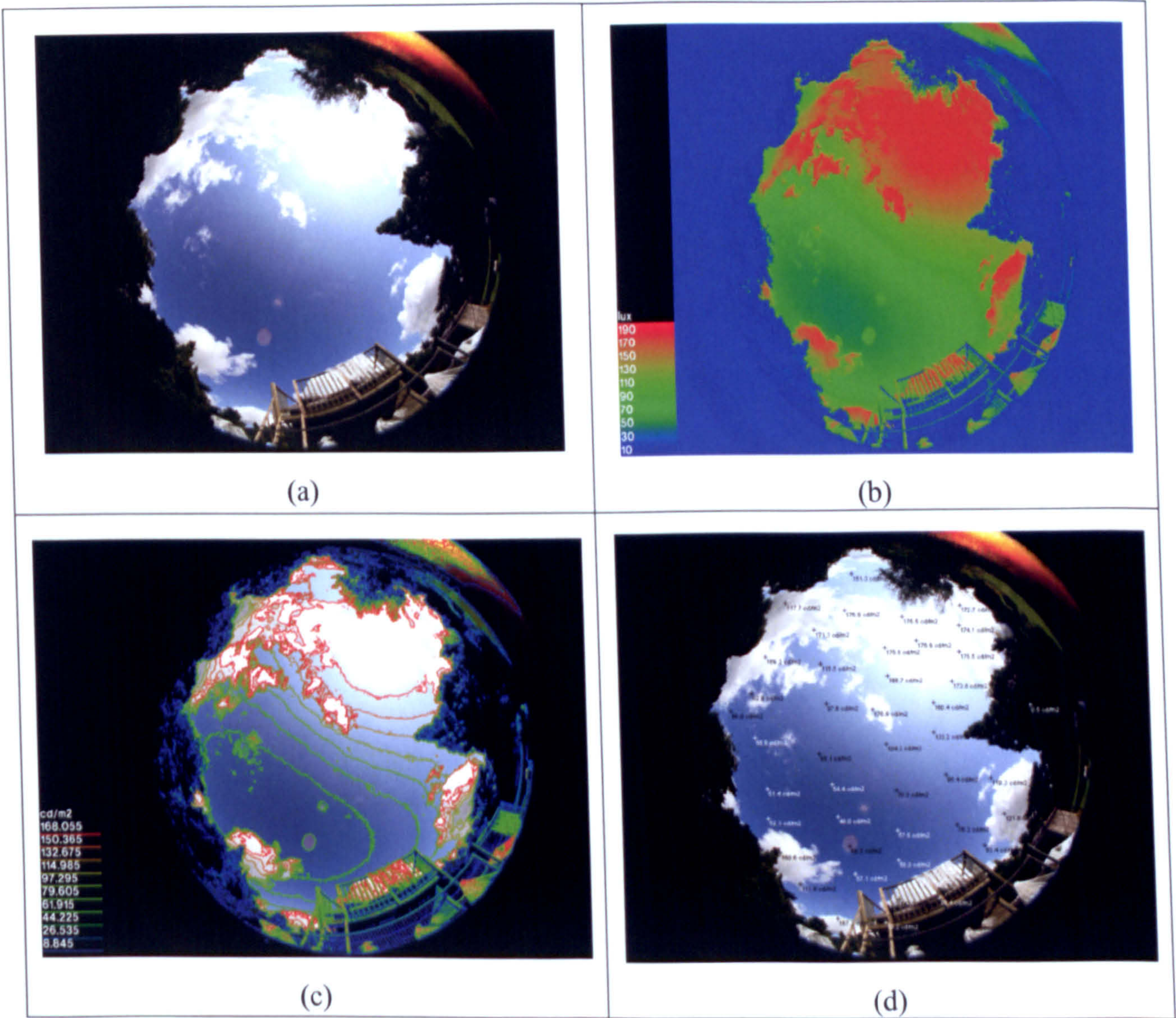


Figure 4.9 Luminance map of the sky when measurements were made (partly cloudy)

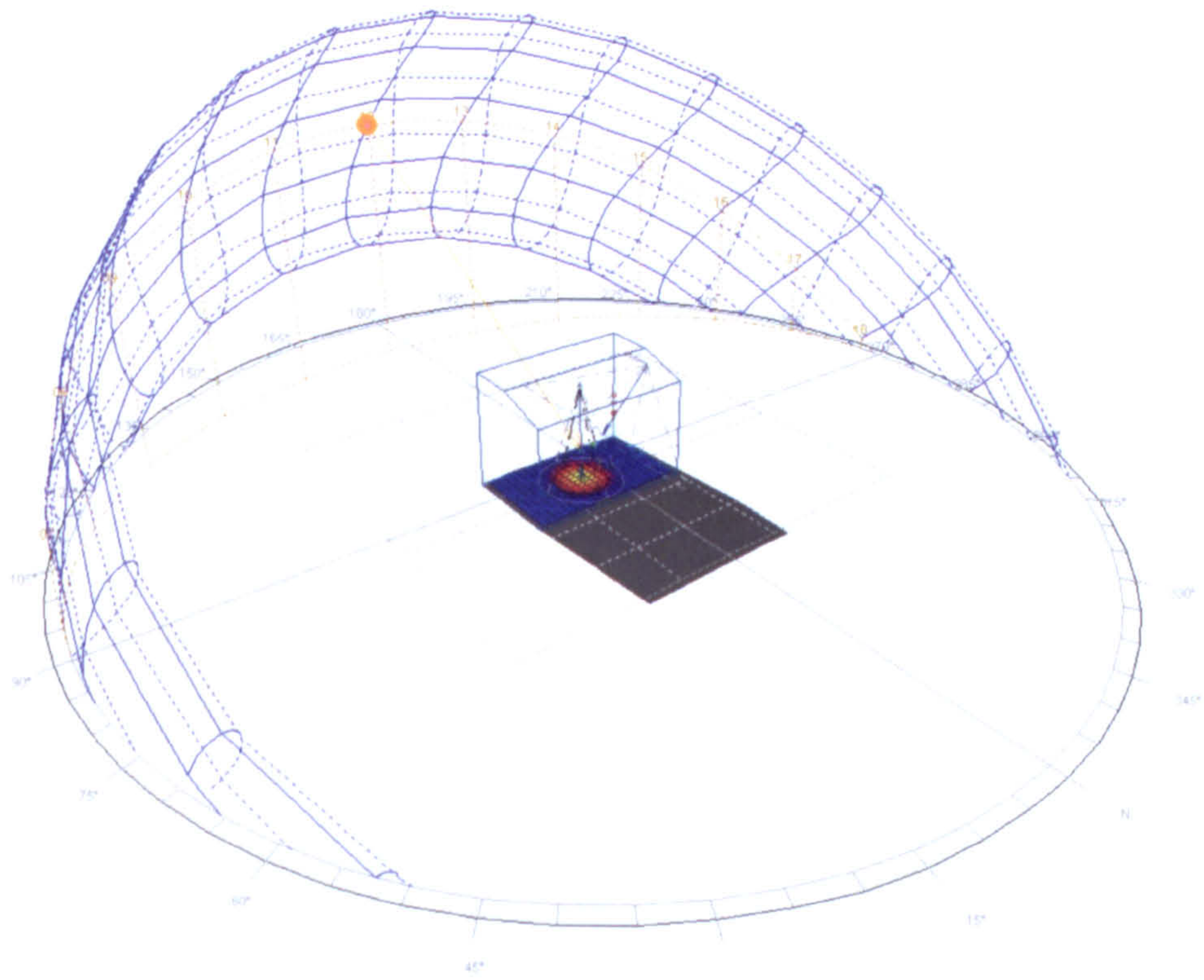
The sun is the only natural source of daylight. The variability of daylight, unfortunately, causes many difficulties for designing buildings that let in ample natural daylight. Daylight that reaches the earth’s surface is composed of both direct beam radiation and diffused

sunlight by dust and other small particles suspended in the atmosphere. Thus, on a bright sunny day with clear skies, solar positions, latitude and local atmospheric conditions have a significant influence on the quantity of natural illumination at any location. It has been observed that pure, brilliant sunlight can increase illumination levels on the ground to over 80,000 lux. Considering its northerly location (Latitude: 52° 58' 0 N), this is quite a sufficient amount of sunlight that could be utilized for indoor daylighting. It is very important for architects and designers to allow the penetration of daylight deep into the space while eliminating excessive glares on work surfaces.

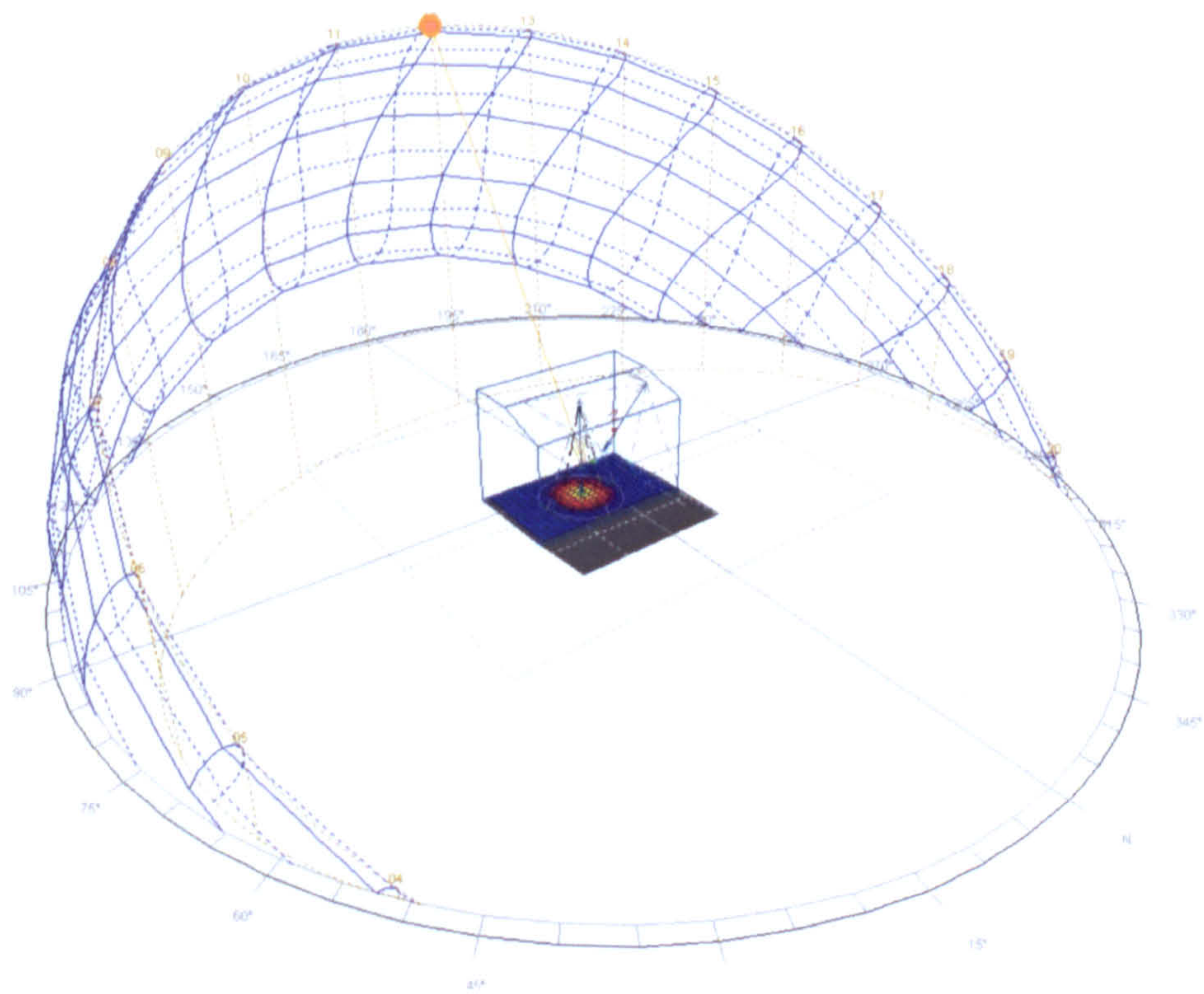
Figure 4.10 shows the effect of the solar altitude angle on the test chamber at different times of the year with the aid of sun path diagrams. By using them, annual changes in the sun's path across the sky can be easily represented on a single 2D diagram. One of the most significant advantages of these diagrams is that one can use them to directly read off the solar azimuth and altitude for any time of the day or the year. Also, designers using them are provided with a unique summary of solar position while considering design options or shading needs.

The sun's changing position in the sky throughout the day and year are frequently represented on stereographic diagrams. These can be compared to a photograph of the sky taken with a 180 fish eye lens looking straight up towards the zenith. Then, the sun's paths at varying times of the year are projected onto this flattened hemisphere for any spot on earth.

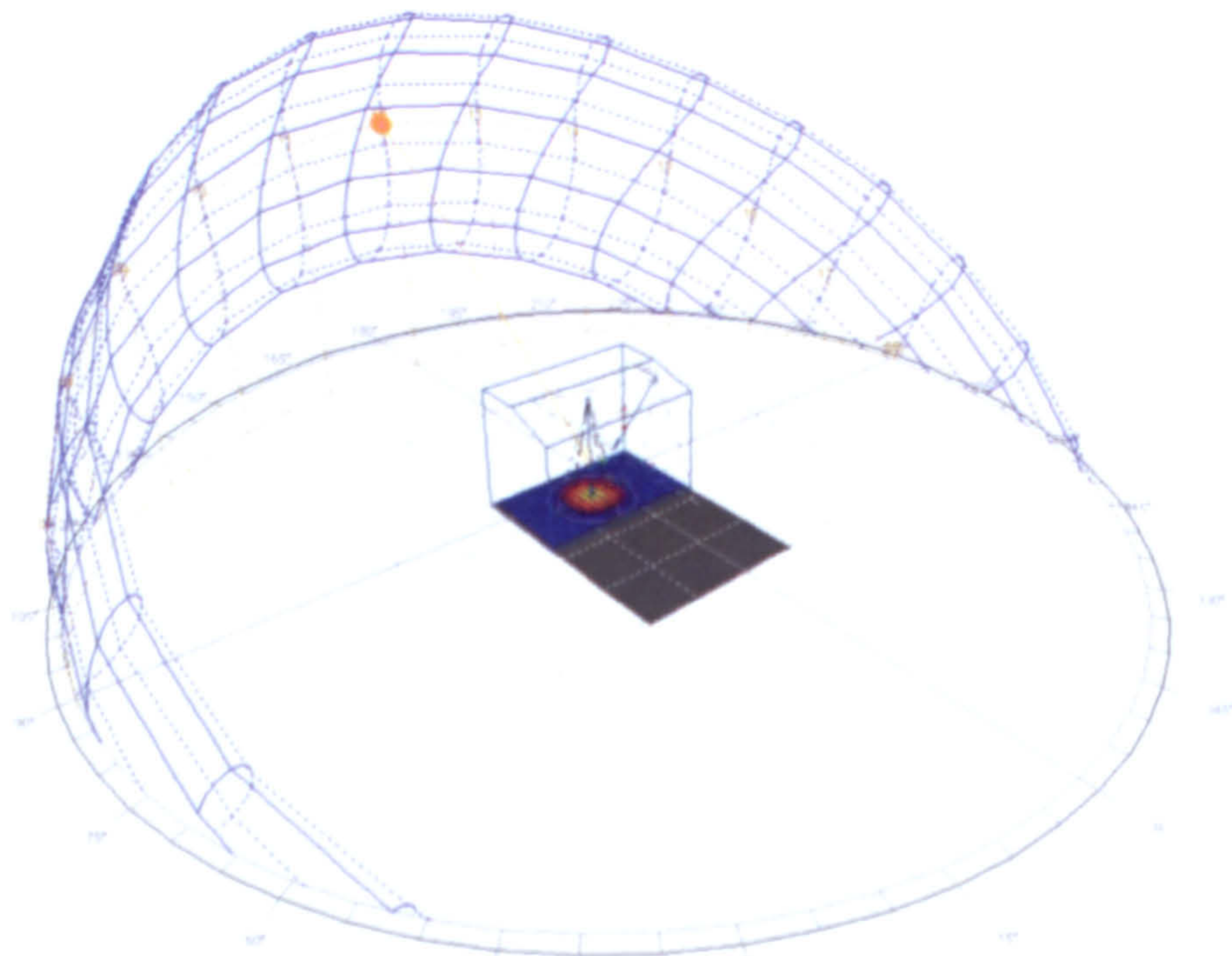
Comparing the length of the shadows projected by the test chamber, seasonal variations of solar altitude are easily comprehensible, especially at equinoxes and solstices. In Figure 4.10, the solar positions in (a) and (c) are almost identical as they present equinotical points: the vernal point and the autumnal point. In contrast, there is quite a difference in the length of the shadows for solstical points as demonstrated by the sun path diagram in (b) and (d): the summer solstice and winter solstice.



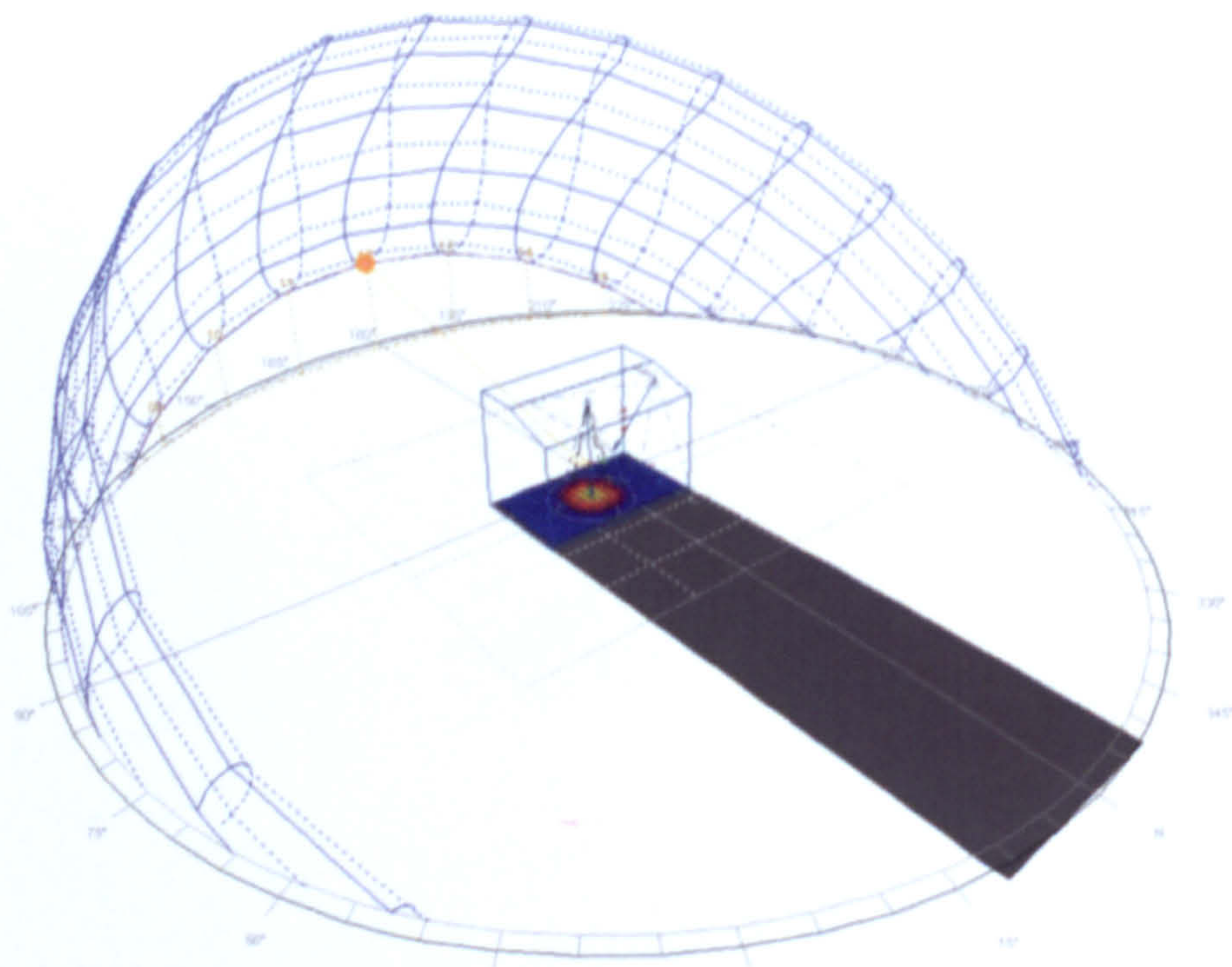
(a) March 20



(b) June 21



(c) September 22



(d) December 21

Figure 4.10 Perspective views of solar availability for the test chamber at different times of the year (equinoxes and solstices) with sun path diagrams.

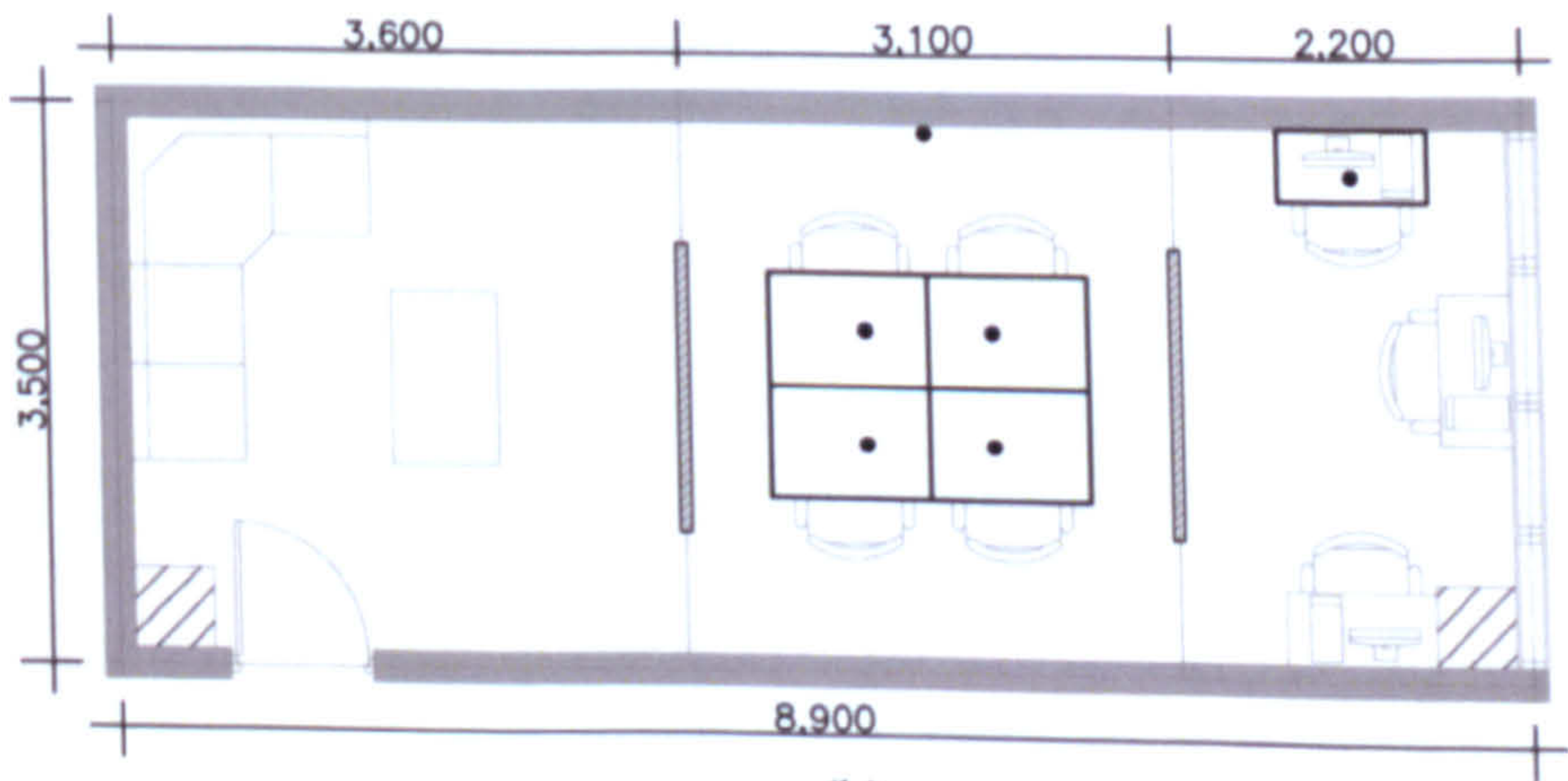
4.2 An Office Building Unit

Designing a lighting system for optimum functionality calls for a perfect balance between visual performance, visual comfort and visual ambience. Especially, the realization of correct lighting for an office space is crucial as it could greatly affect the productivity of people.

Here, a series of measurements were carried out to assess the performance of the dish-daylighting system viewed from this perspective. The office has a tall retaining wall (5.06m) on the south that blocks sunlight through window at lower solar altitude angles. Its ceiling height was 3m slightly higher than a normal office unit of 2.7 m. A large window is located on the south whose respective length and height was 3.2m and 2.25m. Photometric measurements were focused on the meeting table located near the center between a partition wall and a white board.



(a)



(b)

Figure 4.11 A picture of the office and its plan view

Four photo sensors are placed on the table measuring illuminance as sunlight is admitted through the south window and terminal devices (optical lenses) on the ceiling. Measurements were taken on a very clear day as shown in Figure 4. 12. The illuminance level of the east wall and the working table near the south window is also monitored as shown in Figure 4.13. Data are scanned and stored for every second and the sky conditions are monitored by taking pictures with an 8 mm fisheye lens.

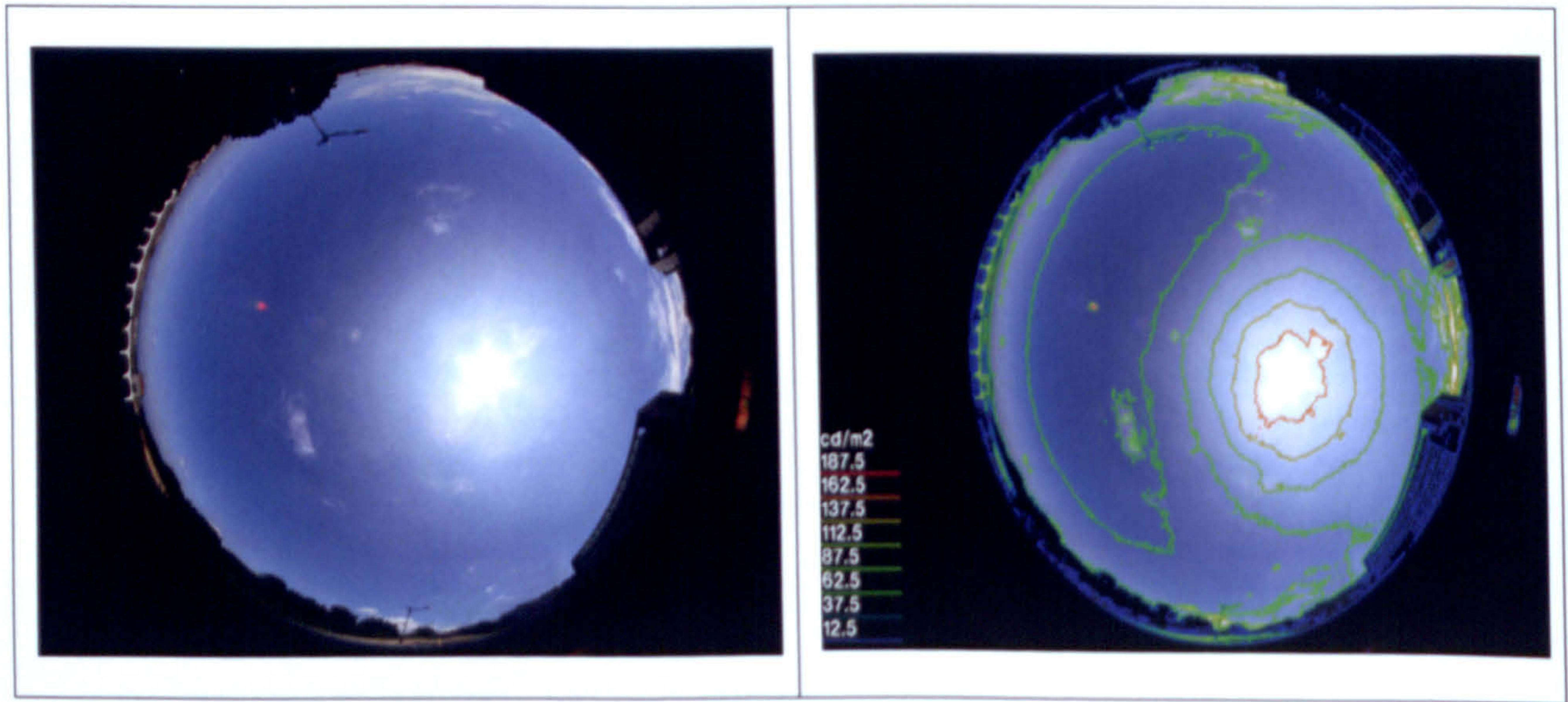


Figure 4.12 Fisheye photograph and luminance of the sky by RADIANCE

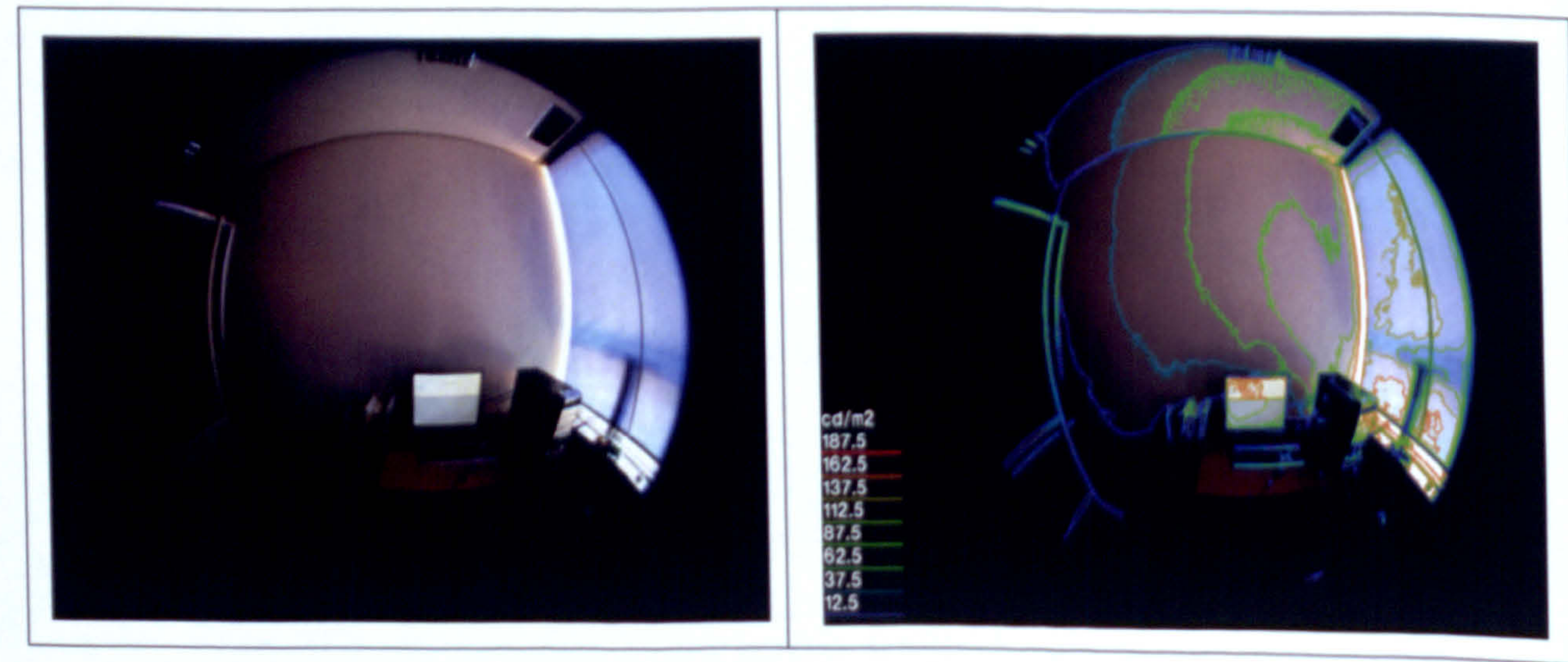


Figure 4.13 Fisheye photograph and luminance of the east wall and the working table near the south window by RADIANCE

The luminance ratio map in these figures indicate that the brightness contrasts of various areas fall within the acceptable range : one to one third between task and adjacent surroundings or twenty to one between luminaires and surfaces adjacent to them. It is unlikely to cause any uncomfortable brightness.

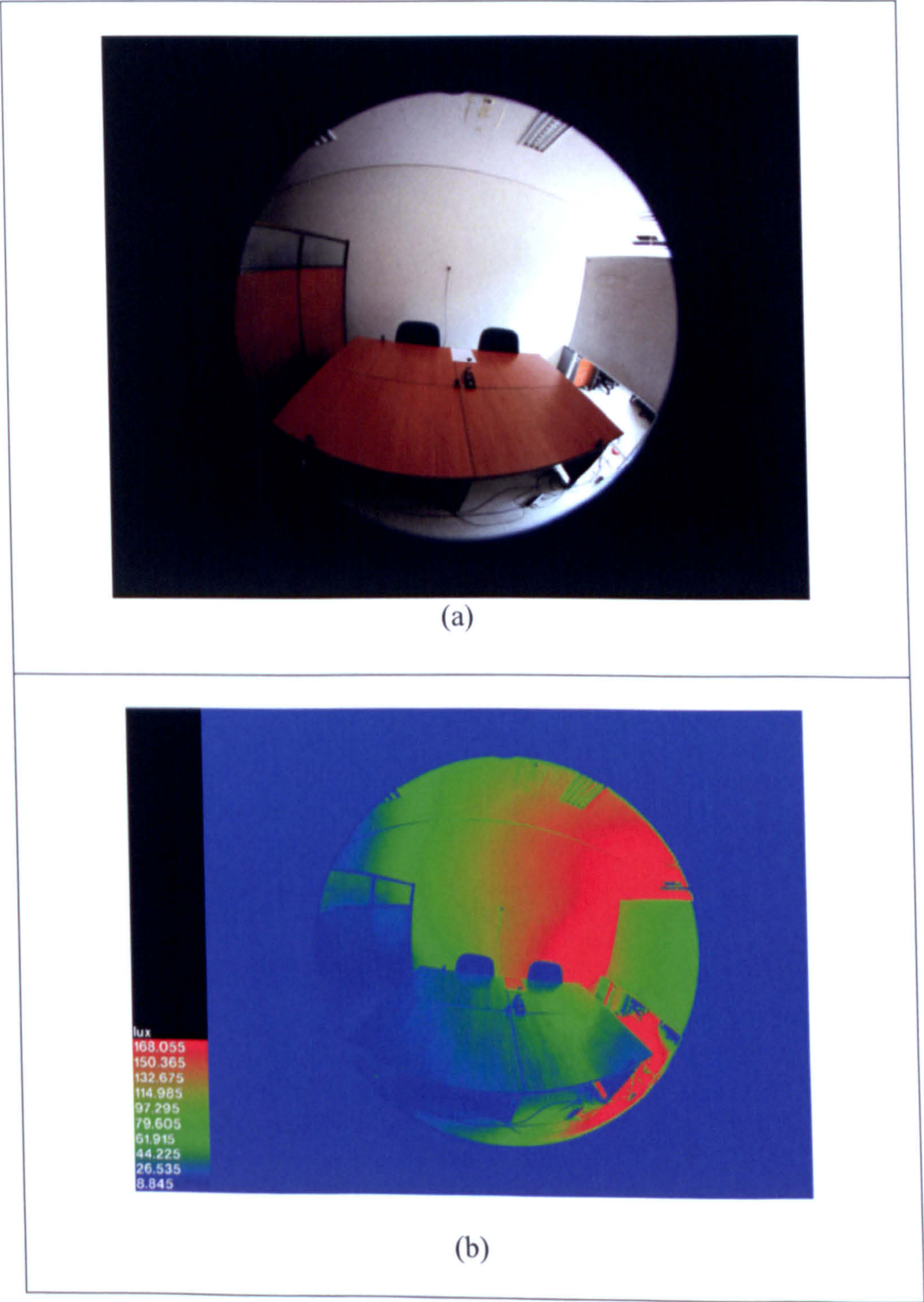


Figure 4.14 Fisheye photograph and luminance ratio map of the task plane and its surroundings by RADIANCE

Figure 4.14 shows the meeting table (i.e., task plane) located near the center (of the room) between a partition wall and a white board. Different from the case above, there is a contrast of brightness beyond the acceptable range, one to one third between the task plane and adjacent surroundings.

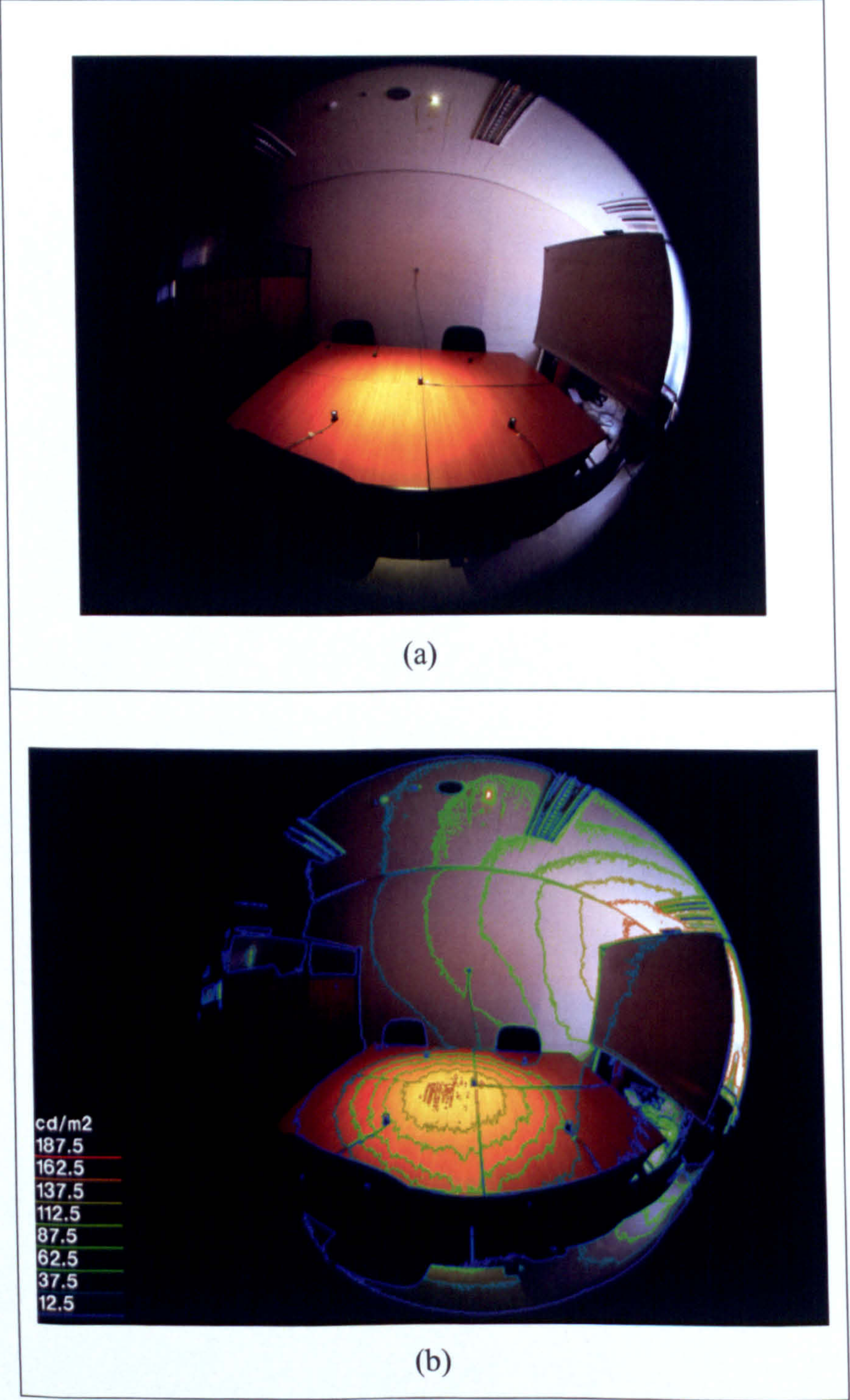


Figure 4.15 Luminance values (a) and illuminance ratio map of the task plane and its surroundings (b) by RADIANCE

The condition can be improved by placing a luminaire on the ceiling as shown in Figure 4.15 (a), where a light diffuser (terminal device) attached to the daylighting system provide natural light for illumination. Figures 4.15 (b) and Figure 4.16 clearly show appreciable improvement in lighting conditions.

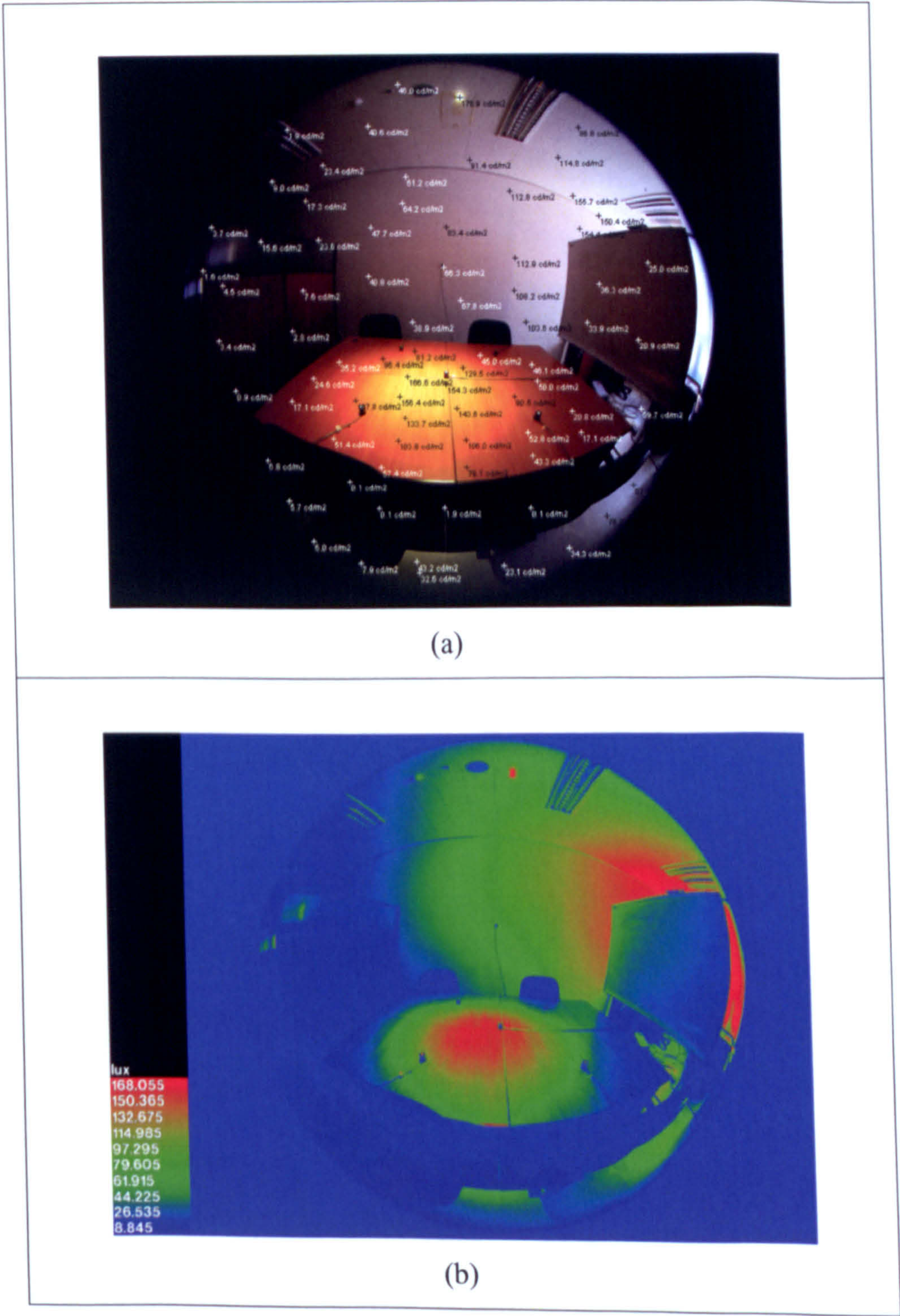


Figure 4.16 Luminance values (a) and illuminance ratio map of the task plane and its surroundings (b) by RADIANCE

Figure 4.17 shows a 3D model of the office for photometric analysis by ECOTECT and RADIANCE. The model has been developed for the case when two daylighting systems are used for indoor illumination of the task plane and its immediate vicinity. Following the actual materials used for its construction , surface reflectances were chosen from the list of materials available by the program. Table 4.2 lists some of the materials and their reflectivity values that closely represent the physical properties of the walls, floor and etc.

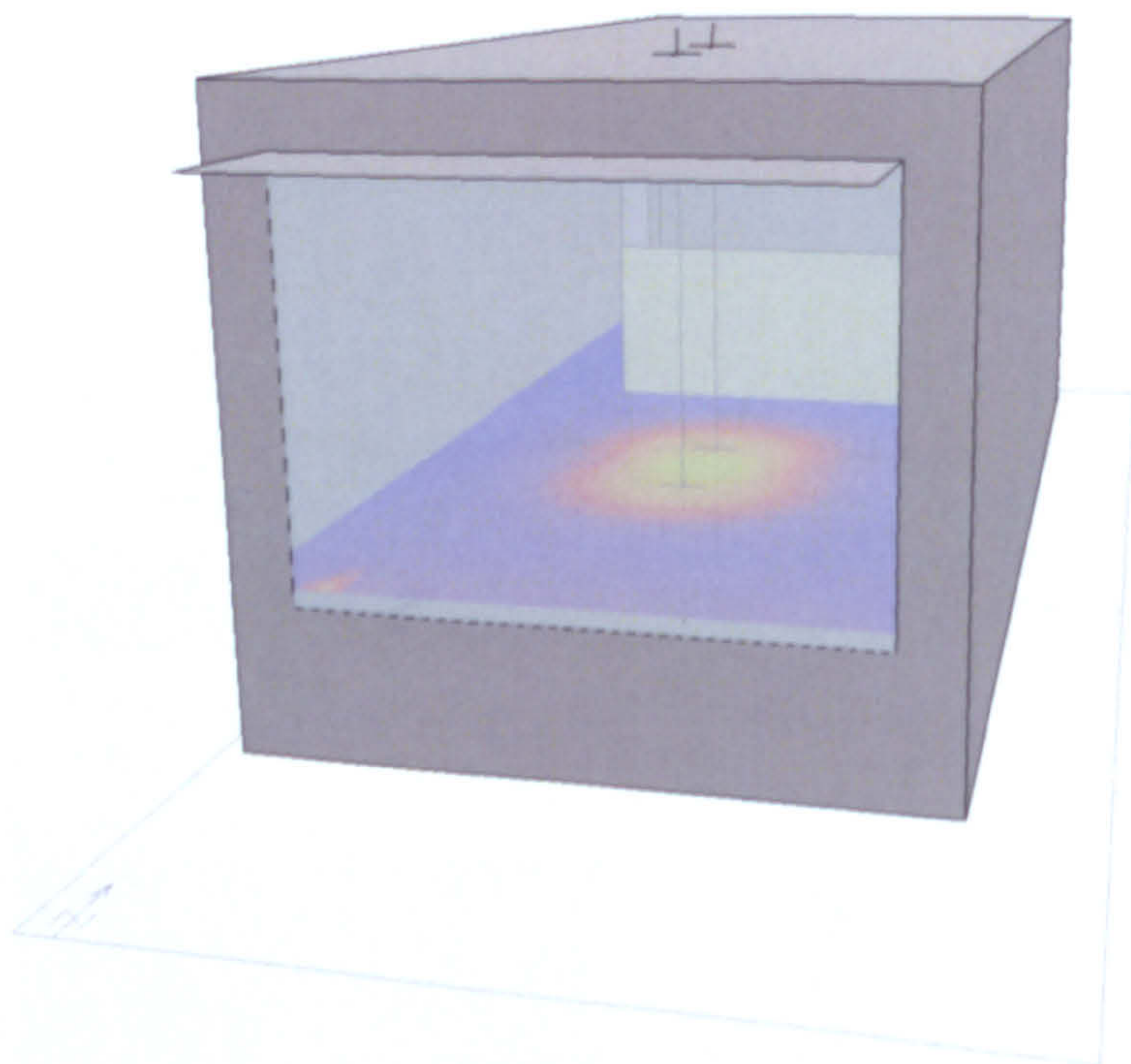


Figure 4.17 Modelling of the room for simulation

Table 4.2 Surface reflectivity of the room

Description	Surface	Reflectivity
walls	white paint	0.561
floor	concrete	0.592
window	glass	0.737
partition A	wooden	0.663
partition B	plaster board	0.835

Simulation results were compared with measurements for a number of points where photo

sensors were located as shown in Table 4.3. It deems the predictions by RADIANCE is much closer to the measurements than those of ECOTECH throughout the comparison. The difference might stem from the different algorithm that ECOTECH and RADIANCE employ for the daylight calculation. ECOTECH uses the split-flux method for daylight factor calculation while RADIANCE calculates the daylight factor using backward ray tracing. In addition, it appears that ECOTECH does not transfer the glazing properties in its domain compatible with the RADIANCE definition.

Table 4.3 Comparison between the measured and simulated results(in lux)

	Sensor 114	Sensor 115	Sensor 116	Sensor 117
MEASUREMENT	924.15	944.74	94.21	167.27
ECOTECH	881.02	907.51	63.08	70.37
RADIANCE	926.13	929.59	127.1	139.45

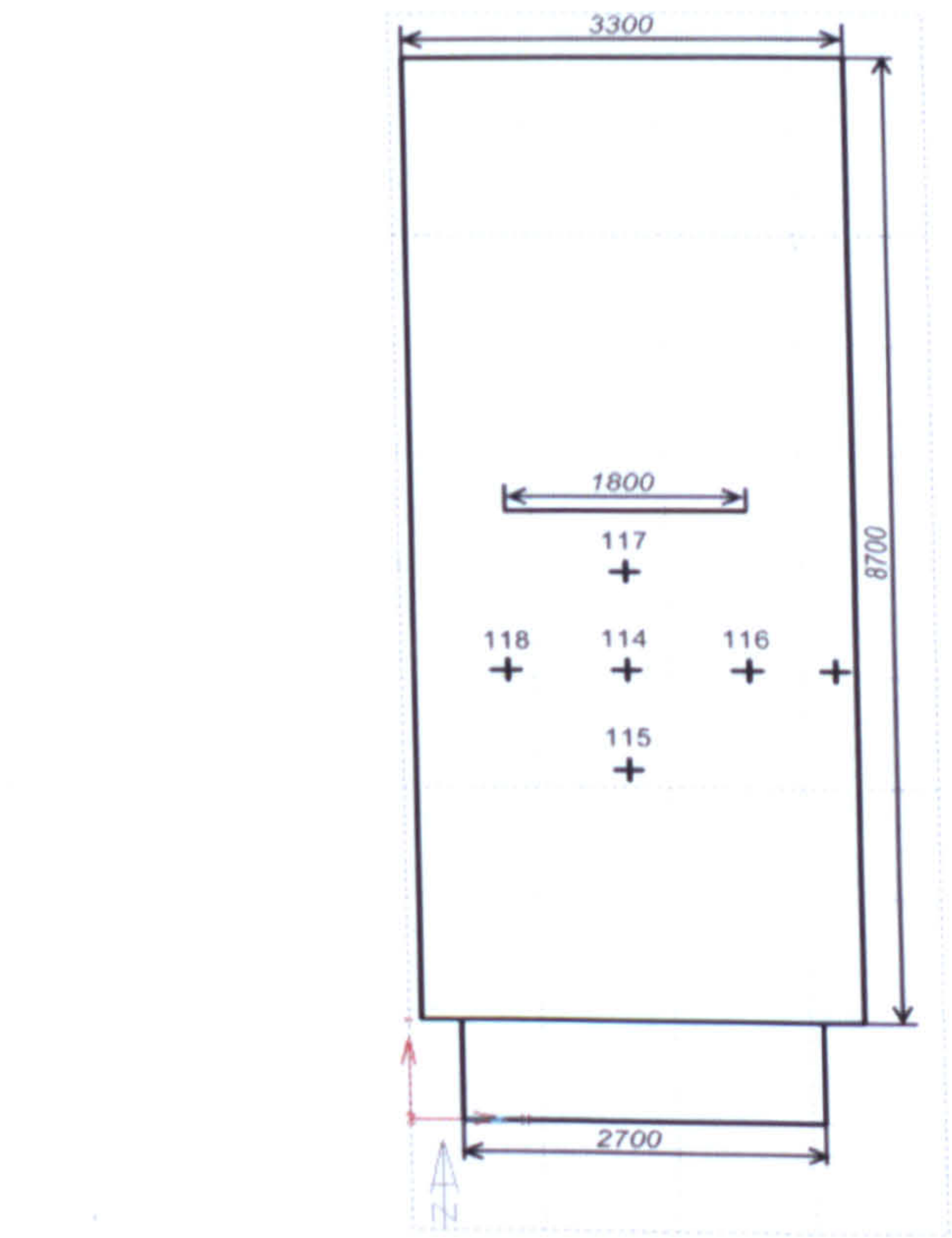
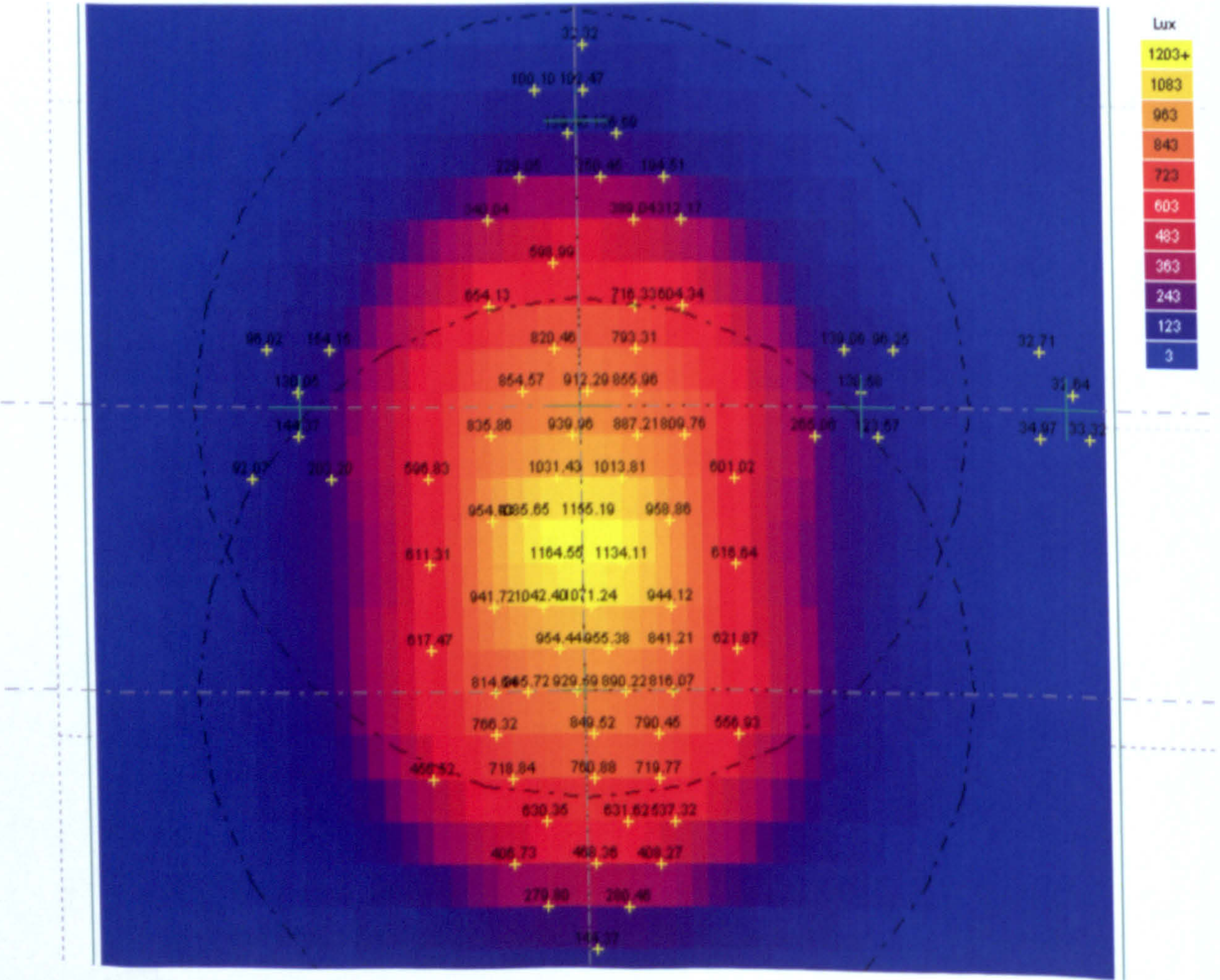


Figure 4. 18 Locations of photo sensors

Figure 4. 18 shows the illuminance distribution by RADIANCE for the case when two

dish-daylighting systems were employed (each dish : 30cm in diameter). As sun rays stream down from two diffusers installed on the ceiling, the task plane and its neighboring area receive sufficient amount of light beyond what might be appropriately needed. Although it depends on the outdoor illuminance, occupant’s preference and specific visual tasks, the relevant illuminance level lies in the range from 500 to 1,000 luxes. As shown in the figure, the overlapping area gives the highest value in illuminance, which could cause some uncomfortable contrast in the visual field. This is because the visual appearance of an object and its surrounding depends on the perception and adaptation by human visual system largely influenced by the luminances of the various elements present in the visual field. For the case considered, it might be more adequate to use one dish instead of two to avoid the aforementioned visual disturbances.



4. 3 Test Cells in Jeju

Two identical test cells were built on Jeju to compare various aspects of daylighting effects on indoor environments. The test cells enable accurate measurements of major variables at different times under identical conditions. Also, the results obtained could be further extended to real buildings in similar situations.

4.3.1 Construction of the test cells

The test cells are built with prefabricated sandwich panels where a 4.7mm polystyrene foam insulation panel is sandwiched in between metal skins of 1.5mm thick. Figure 4. 18 shows its plan view with a south facing window of 1,200mm x 900mm. The length, width and height are 3,000mm, 1,500mm and 1,500mm, respectively. Daylight can enter its interior space only by the window or through the terminal device (optical lens, etc) attached to the dish-daylighting system. A small peep-hole with a cover is prepared at the center of the north wall to take pictures of its interior at any time. It is also equipped with an electric fan to prevent overheating by daylight.

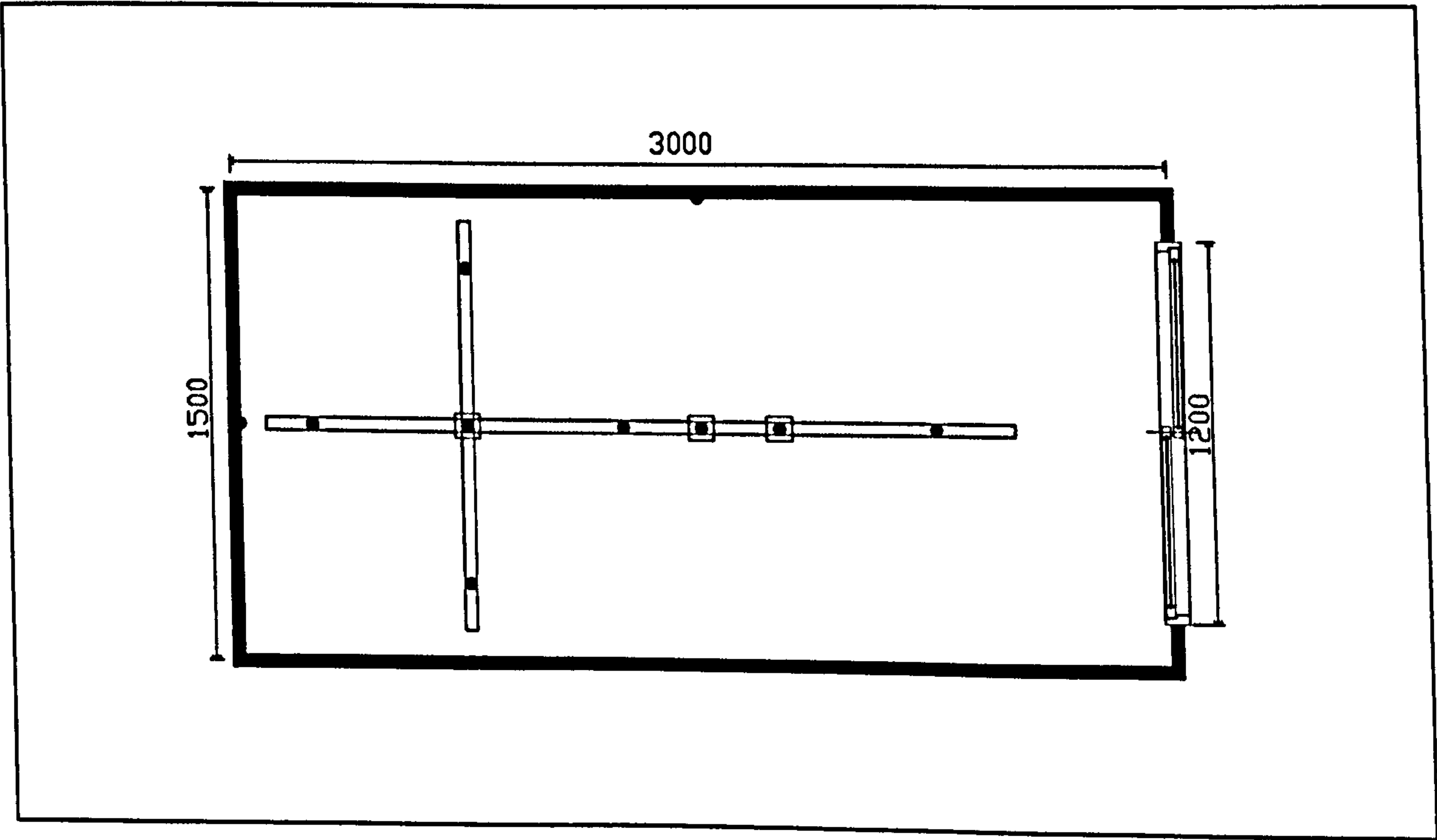
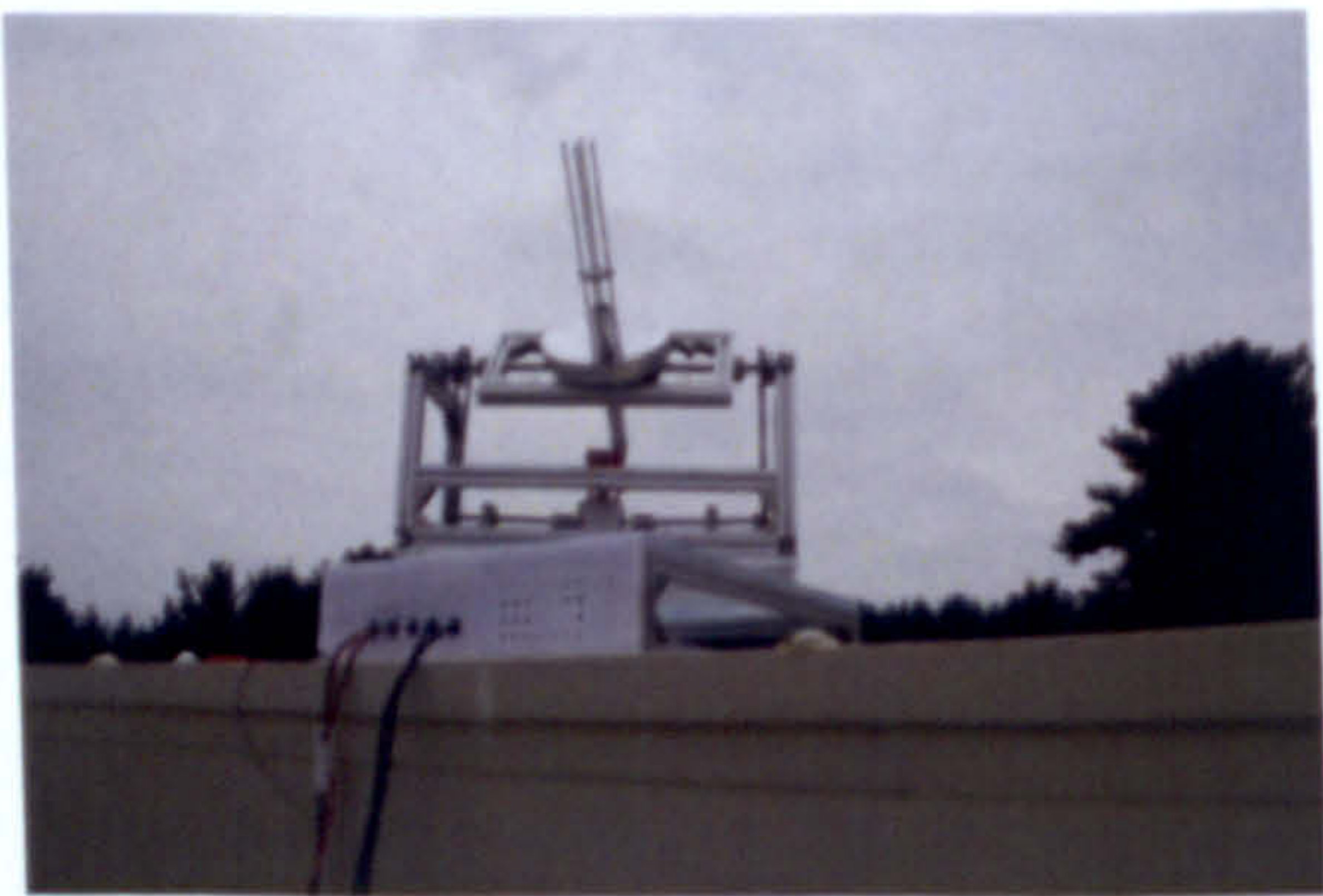


Figure 4.20 Plan view of the test cell

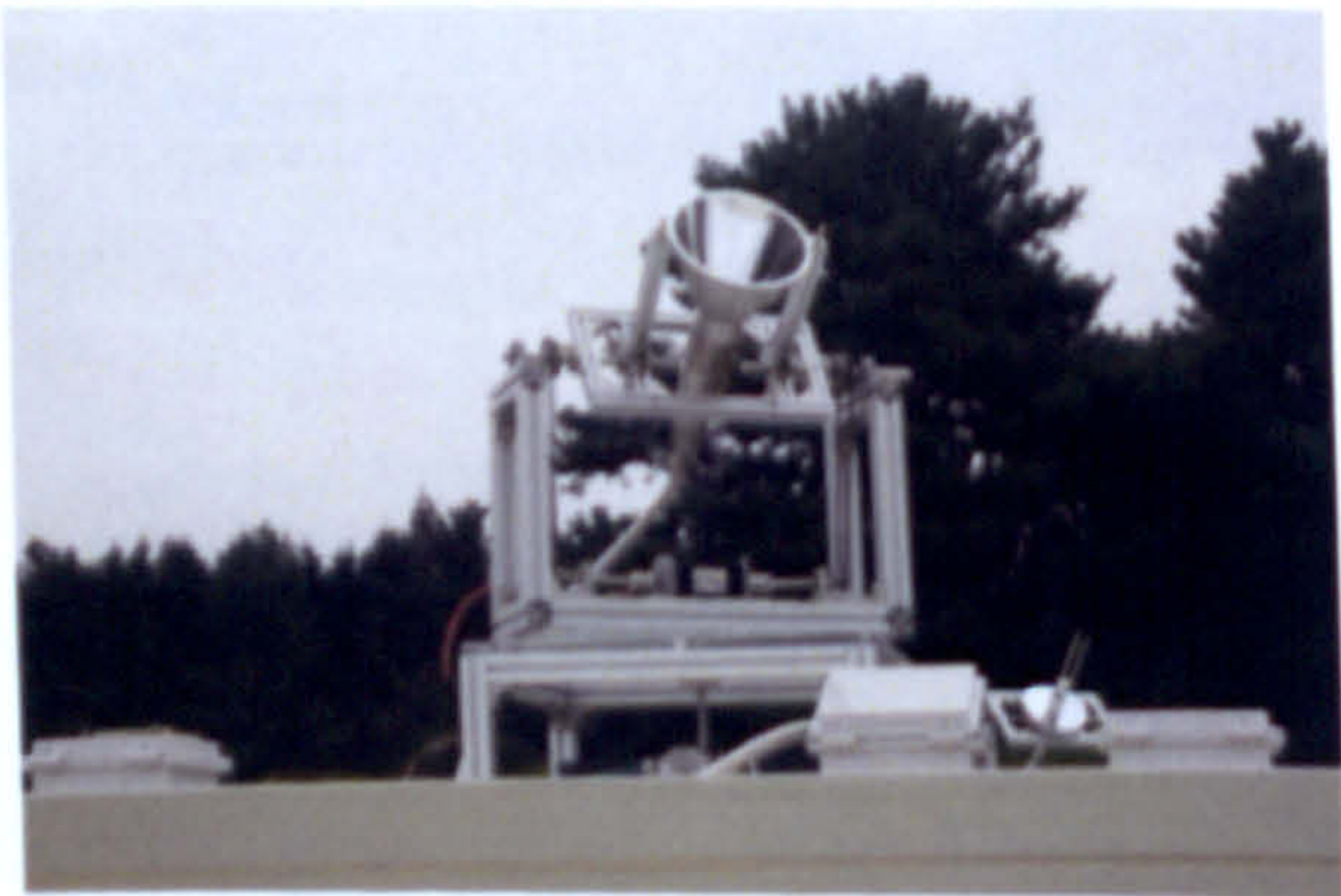
Seven photo sensors (black dots in the figure) were installed at a height of 400 mm above the floor with an interval of 450 mm. A cross shaped adjustable metal mount was prepared and placed on the floor to provide a uniform height for sensors as shown in the figure. Besides on the floor, a photo sensor was mounted at the center of the north wall, east wall (semi-circular black dots), and ceiling. The one on the ceiling is indicated by the circular black dot in a square located as the third one from the right end of the mount.



(a)



(b)



(c)

Figure 4.21 Two identical test cells built for performance assessment of daylighting systems : (a) test cells, (b) daylighting system with dish concentrator installed on top, (c) daylighting system with funnel shaped concentrator installed on top

Figure 4.21 shows the photographs of two identical test cells built with a daylighting system on top of each. They were located on the roof of an office building, which has an unobstructed open view toward south allowing full exposure to sunlight suitable for daylighting measurements. As shown in this figure, the walls (exterior and interior) are painted light beige. Two sets of venetian blinds are installed on the south facing window which has six window panes in three rows and two columns. One set of venetian blinds is to provide shade for the window panes in the top row whereas the other is to cover the window panes in the second and third rows from top.

4.3.2 Basic measurements

Figure 4.22 presents the performance of daylighting systems in terms of illuminance ratio which refers to the ratio between inside and outside illuminance; one with a dish concentrator and the other with a funnel shaped concentrator. This is comparable to the daylight factor which measures the ratio of the illuminance at a select location within a space to the unhindered outdoor illuminance at the same moment, under identical sky conditions. Here, the illuminances used are instantaneously measured values at the point directly below the liminaire (diffuser).

Both concentrators have the same circular projection area of 15 cm in diameter, which results in the same amount of solar rays first striking the reflector's surface. As shown, the daylighting system with a dish concentrator outperforms the one with a funnel shaped concentrator. The former shows a pattern of performance which changes with solar availability. Especially, it performs the best at noon when the air mass is close to 1.

In comparison, the latter almost gives the same performance indifferent to solar availability. A series of tests revealed the occurrence of major reflection losses of incident solar radiation through the homogenizer tube. Except those parallel to and fall through the

straight portion of the homogenizer tube, a great portion of them are lost before entering the optical fiber cable.

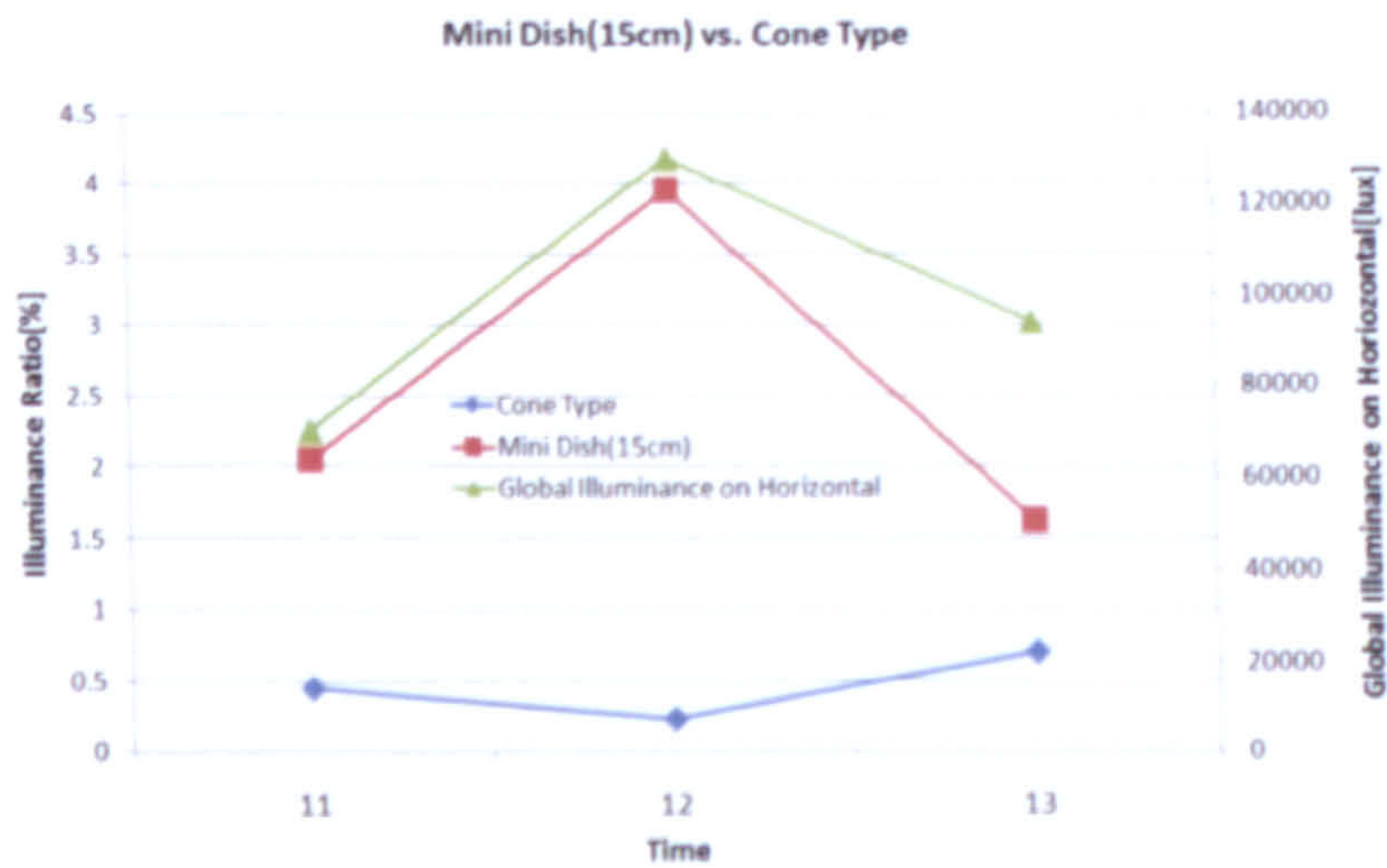


Figure 4.22 Illuminance ratio of daylighting systems with different shapes of solar concentrators : dish, funnel shaped

This was verified with the aid of a Fresnel lens placed at the entrance (conical mouth) of the concentrator, where sufficient amount of sunlight were available to enter the optical fiber cable.

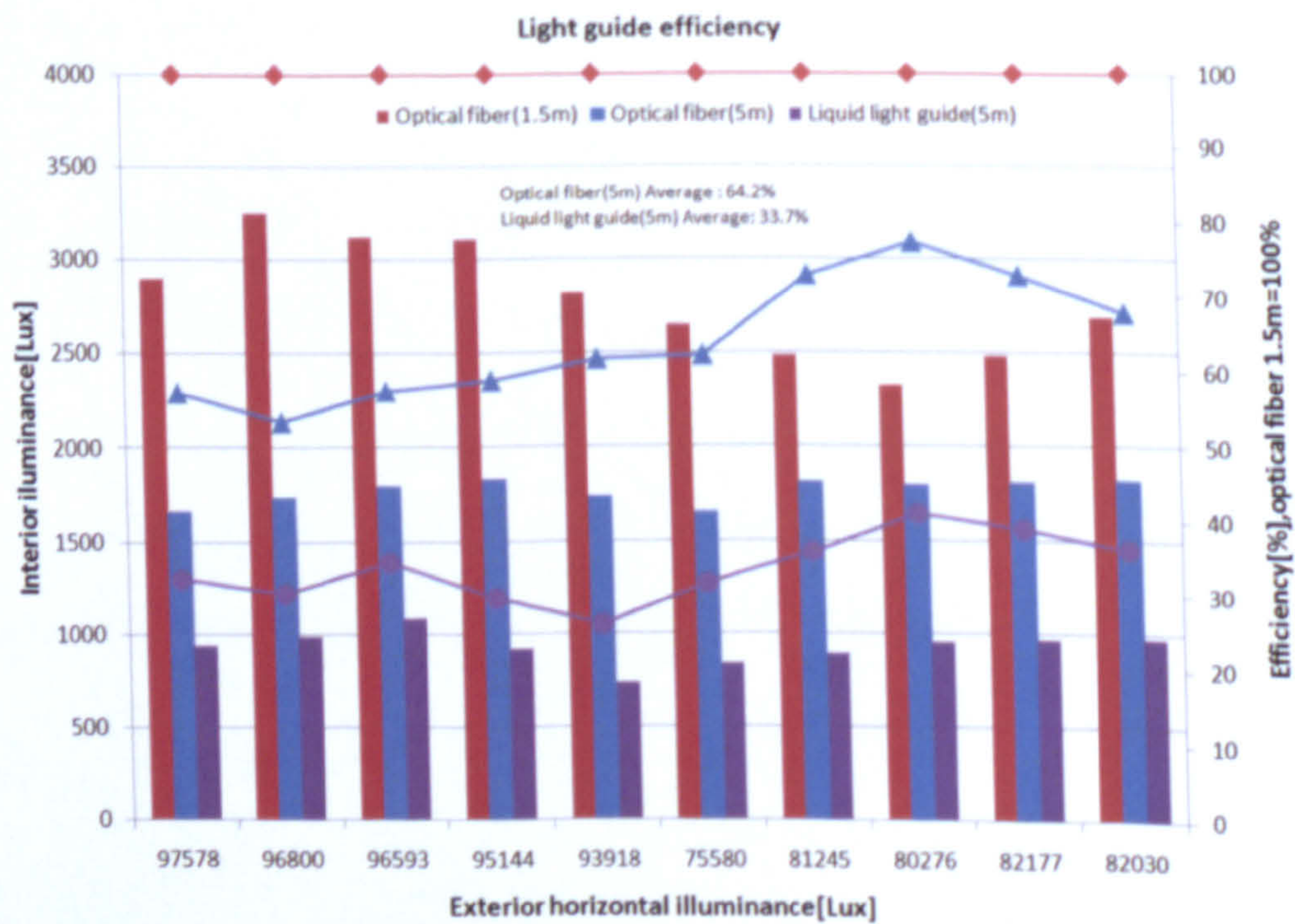


Figure 4.23 Light transmitting efficiency of an optical fiber and liquid light guide cable

Light guides play a very crucial role in the performance of a daylighting system. Figure 4.23 compares the light transmitting efficiency of the optical fiber (glass) and liquid light guide systems. As shown, the performance of the optical fiber cable is about 1.5 to 2 times better than the liquid light guide cable for the same length (5m). Also, light attenuates rather steeply with length (distance of travel), which could limit its application of a daylighting system with the kind of optical fiber cable considered here. When two lengths of 1.5m and 5m are compared at different level of horizontal illuminance due to constant varying sky conditions, there was an average of 35.8% reduction in its performance as shown by the bar graphs. As the daylighting systems considered here mainly utilizes the beam component of solar radiation (illuminance), it is very important to accurately measure the beam and diffuse component at different times of the day during measurements.



(a)

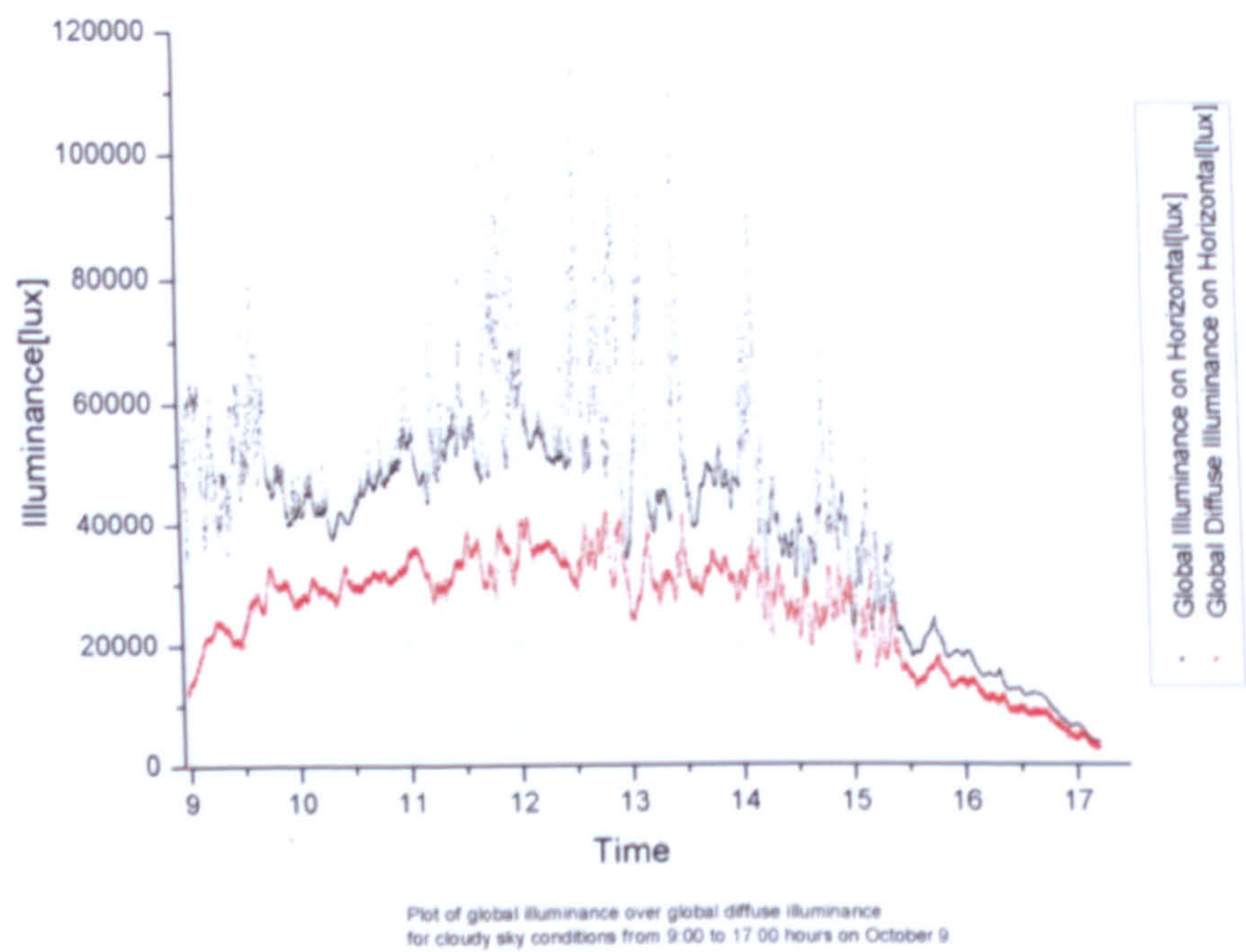


(b)

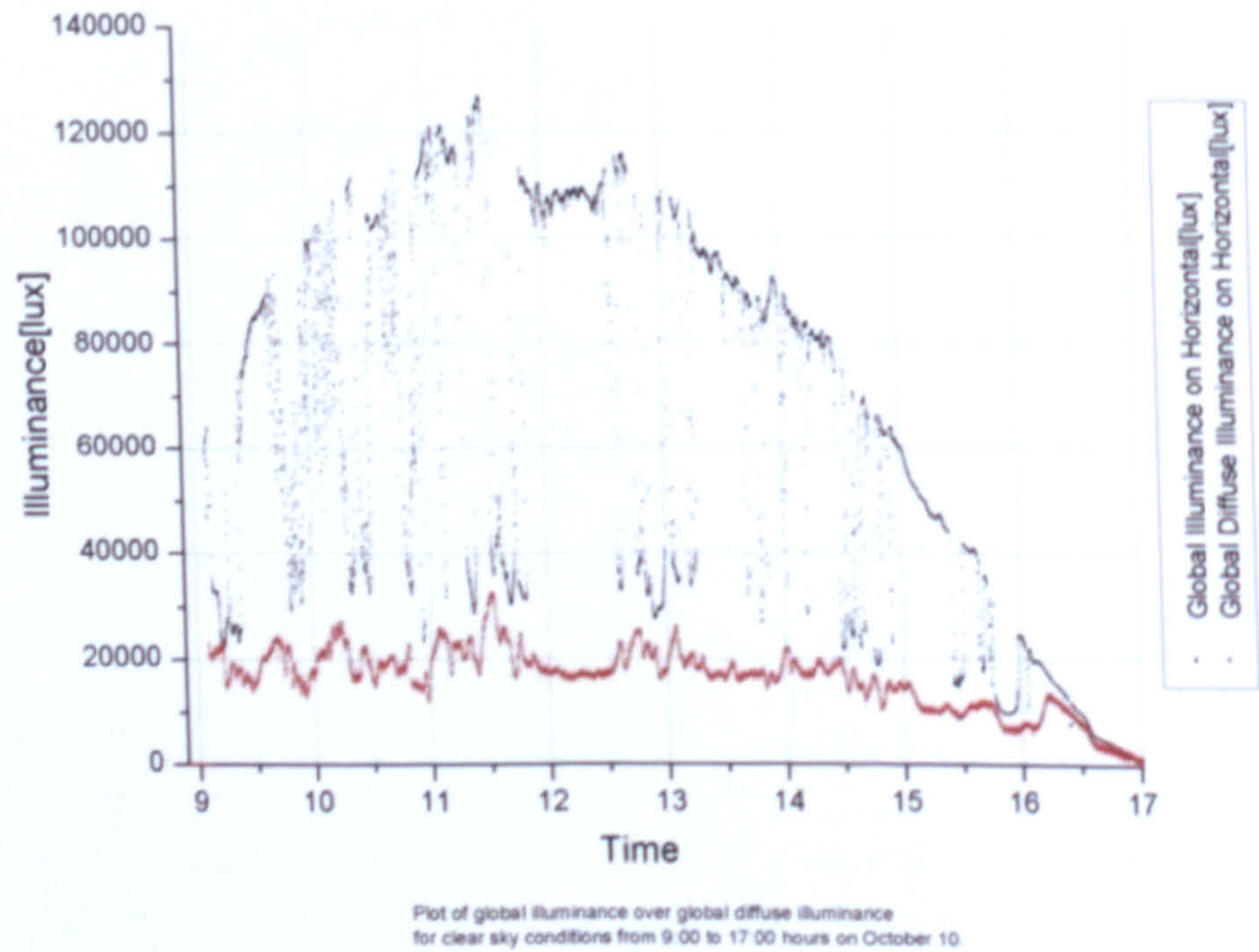
Figure 4.24 Measuring the beam and diffuse component of illuminance (a) solar radiation (b)

Figure 4.24 shows the instruments used to measure these components on a horizontal surface in the present study. As shown, a semicircular curved strip of metal is prepared on the sensor mounting stand to provide shades during measurements. The direct beam component of solar radiation is blocked from impinging on the sensors. To make accurate measurements, sensors must be mounted where they are level and placed at a place with a full view of the sky view without any obstructions.

Figure 4.25 shows how sky conditions affect the global total and diffuse illuminances at different times of the day. On a cloudy day (a), differences between the global and diffuse illuminance are relatively very small when compared to a clear day (b).



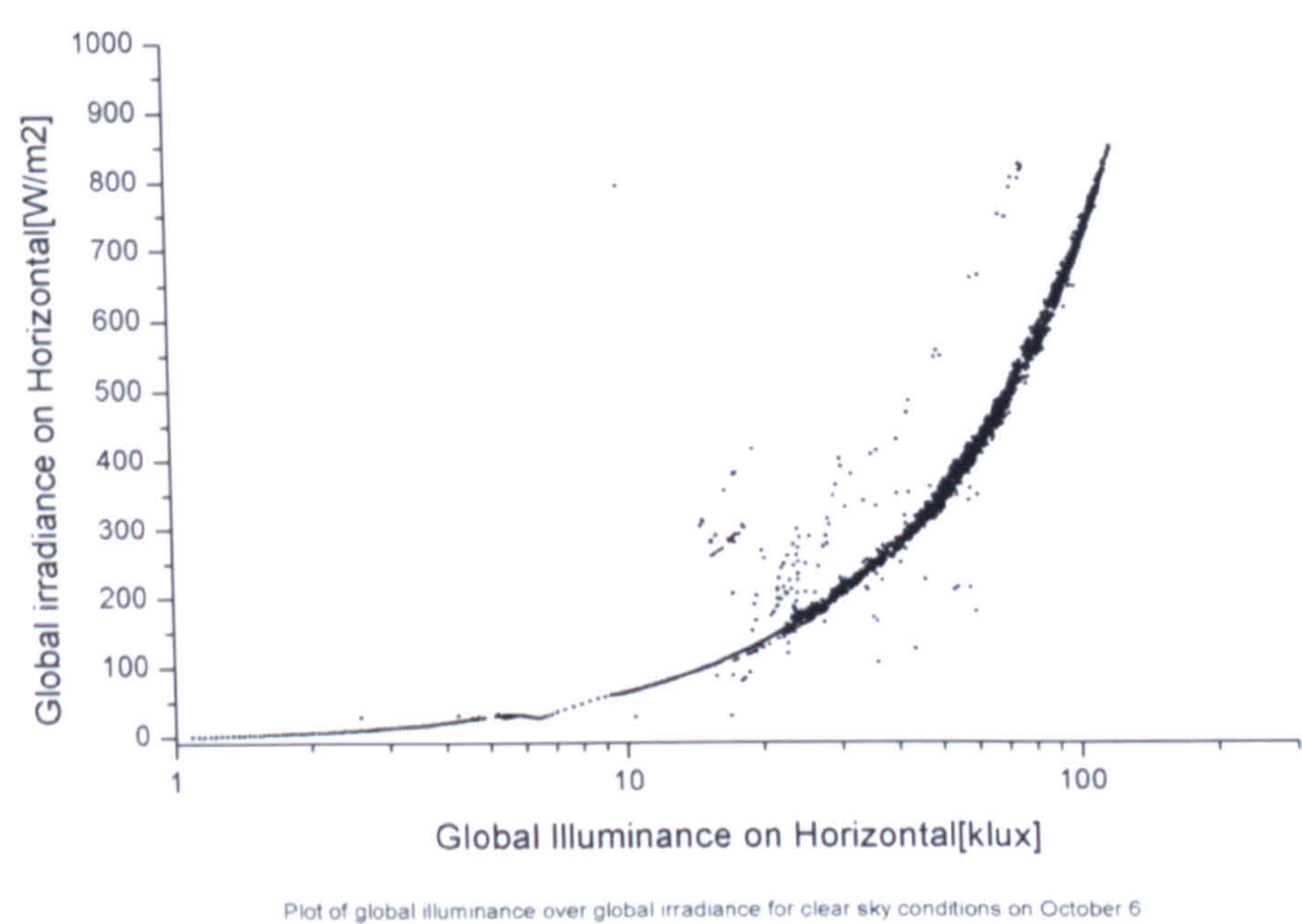
(a)



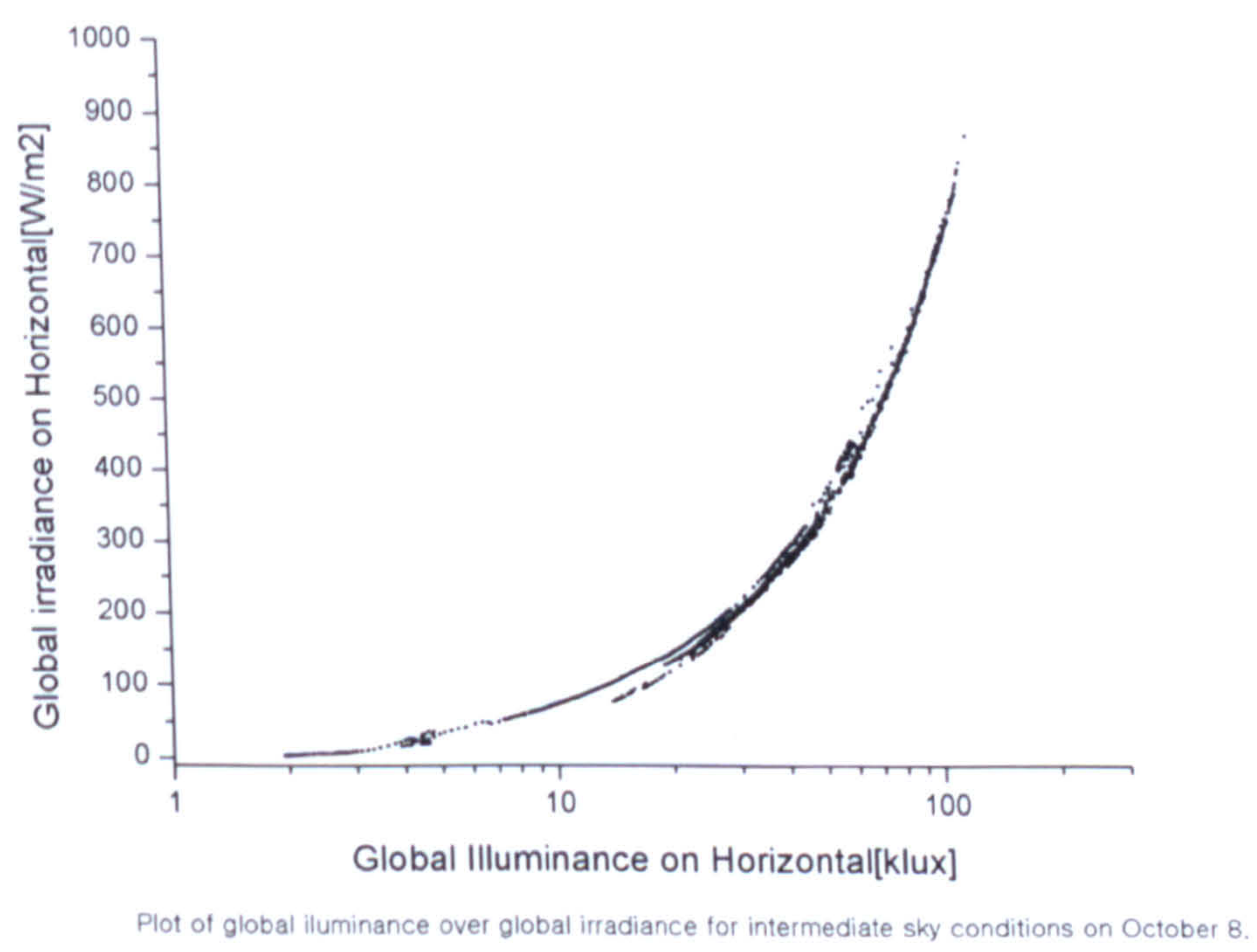
(b)

Figure 4.25 Variation of the global total and diffuse illuminance (outside) at different times on a cloudy(a) and clear day (b)

Figure 4.26 show the global illuminance and irradiance change with the sky conditions. Although there general profile looks similar, greater number of data are shifted in case (a) of the clear sky in comparison to (b) of the intermediate sky condition.



(a)



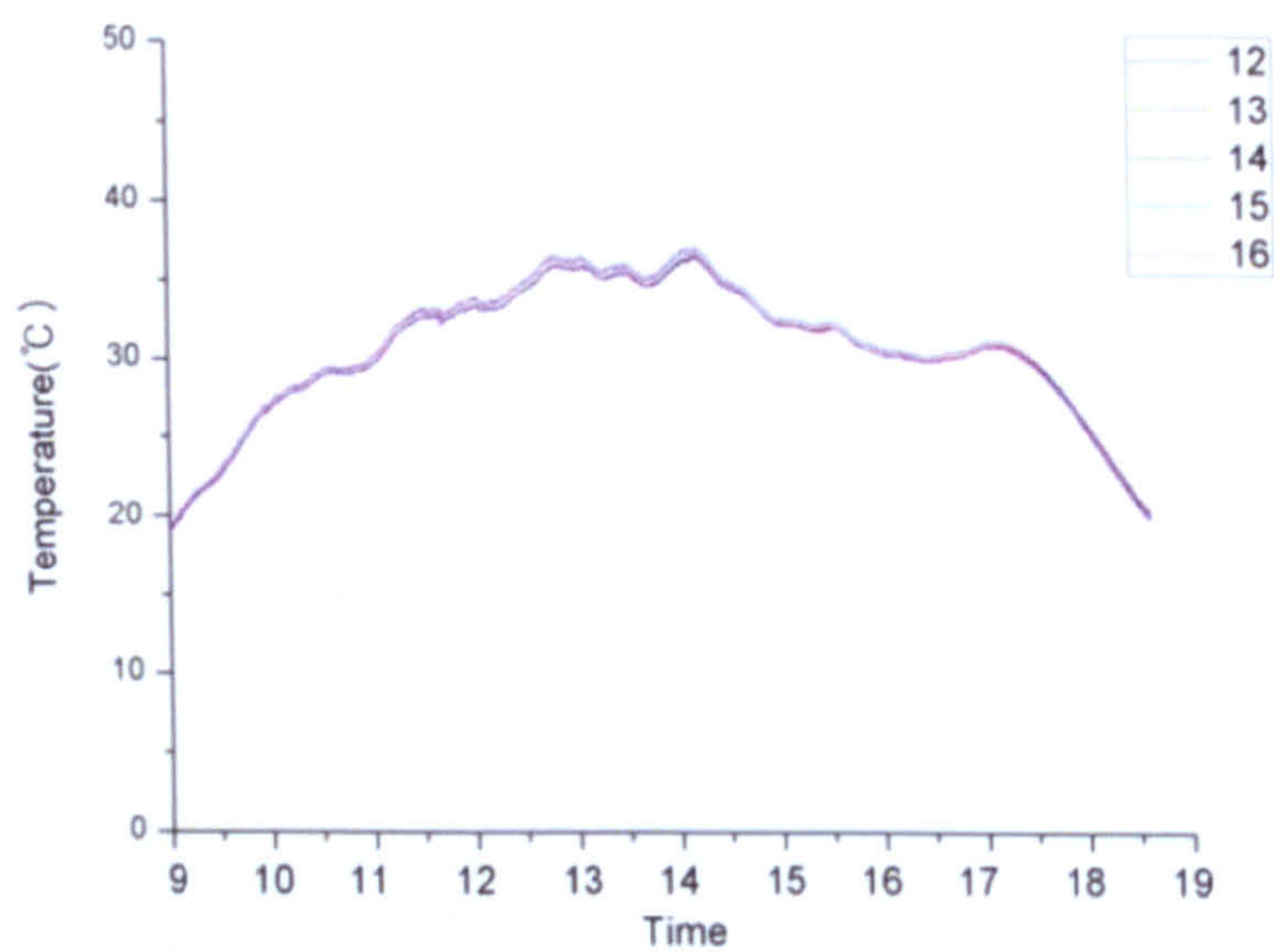
(b)

Figure 4. 26 Global illuminance and irradiance (outside) for different sky conditions:

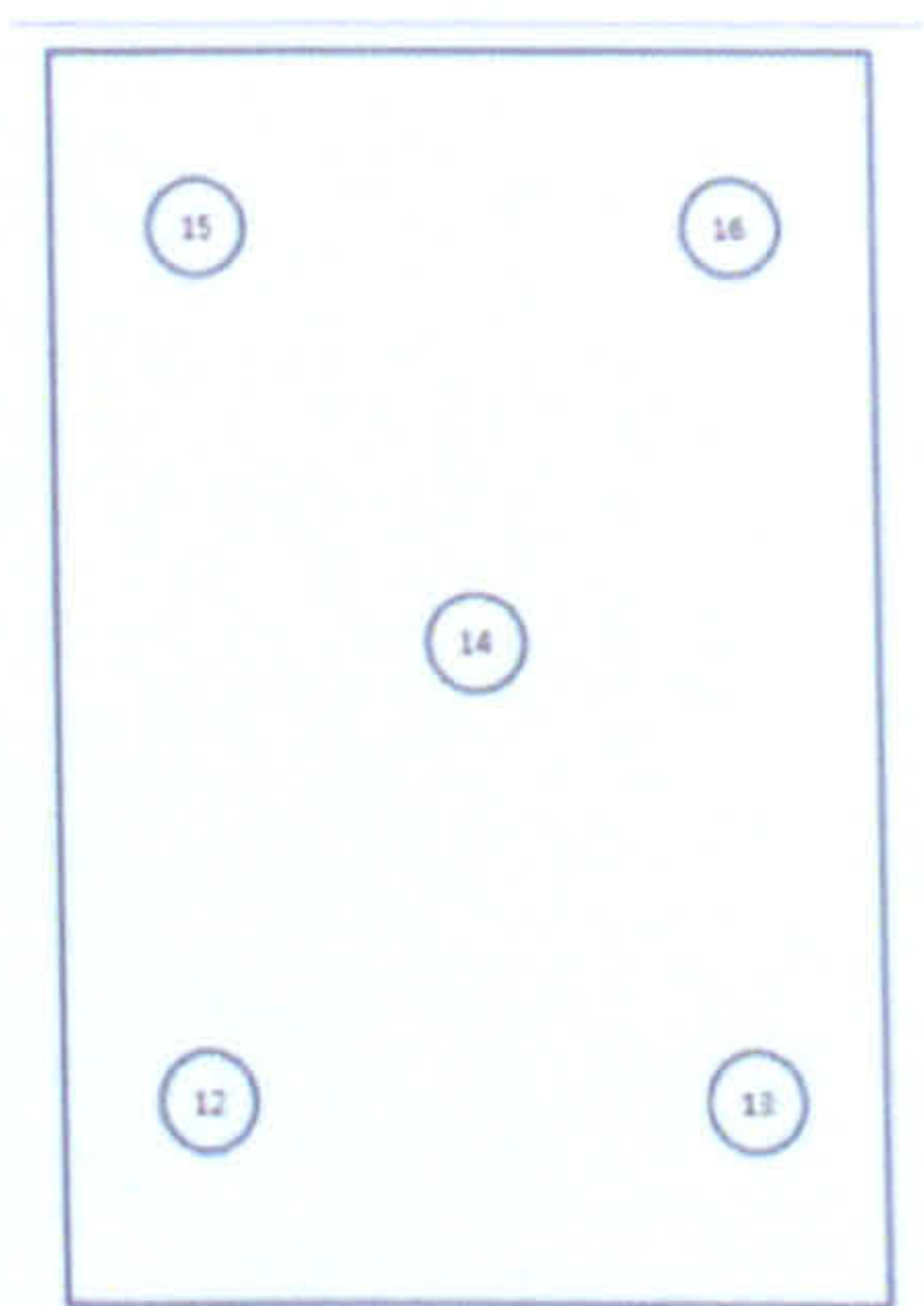
(a) clear sky, (b) intermediate sky

4.3.3 Temperature measurements

When daylight is introduced into a space, it brings warmth with it due to infrared portion of the electromagnetic spectrum. Moreover, sunlight admitted through windows or daylighting systems will eventually converted to heat (thermal energy). In the winter, this heat makes an asset such that there deems no limit to the amount of sunlight that might be introduced as long as glare and excessive brightness ratios are controlled.



(a)



(b)

Figure 4.27 Results of temperature monitoring on a clear day (10/6) : temperature variation of each sensor at various times of the day (a), temperature sensor(k-type thermocouple) location (b)

Heat is, however, a liability in the summer. Especially, for buildings in warm climates requiring no space heating, it is very important to collect the coolest daylight possible. Admitting just enough daylight to turn off electric lighting is the ultimate goal of daylight design.

If a daylight design excludes direct sunlight and thus avoids direct heat gain, clear days will behave similarly to the overcast conditions. If direct sunlight is included, as it generally is in most cases, then it might be desirable to have the design tested by using a scale (mockup) model as in the present analysis or computer simulation.

The problem due to seasonal variations of daylighting is most discernible with skylights. This is because much more sunlight is admitted through horizontal openings in the summer compared to wintertime. One way to alleviate this is to use south-facing vertical glazing instead since it lets in more sunlight in winter than during the summer. As aforementioned, unlike summer, when the amount of daylight let through should not go over a certain limit, it is desirable to collect as much daylight as possible during winter. Consequently, a daylighting system should only be applied after thorough consideration of both visual and thermal effects, and even more so in temperate climates with four seasons.

Thermal measurements deliver crucial data in utilizing daylight for indoor illumination and space conditioning. The figures below present the monitoring results of a test cell when k-type thermocouples were placed at five different locations in its interior. To block any air infiltration from the ambient, the test cell was completely sealed and no air changes were made with the ambient during the hours of monitoring. Figure 4.27 (a) clearly indicates the uniformity of thermal conditions. As shown, no appreciable spatial differences are present between measured points regardless of their relative positions away from the window. This might be due to the relative smallness of the test cell, which enables active mixing of air and no thermal stratification in its interior.

Figure 4.28 presents some FLIR image of two test cells at about 1.5 hours interval. Again, the window was completely sealed and there were no room air changes with the ambient. The effect of the daylighting system is clearly illustrated by the difference in the temperature rise when monitored simultaneously. This, however, does not imply that the use of the present daylighting system would increase energy costs for space cooling. If a window is used instead admitting the same amount of daylight to the interior, it would definitely increase energy costs because of reduced thermal insulation. In addition, if the room air changes per hour are considered as in real situations, this heat accumulation by the daylighting could be readily controlled without undue difficulties.

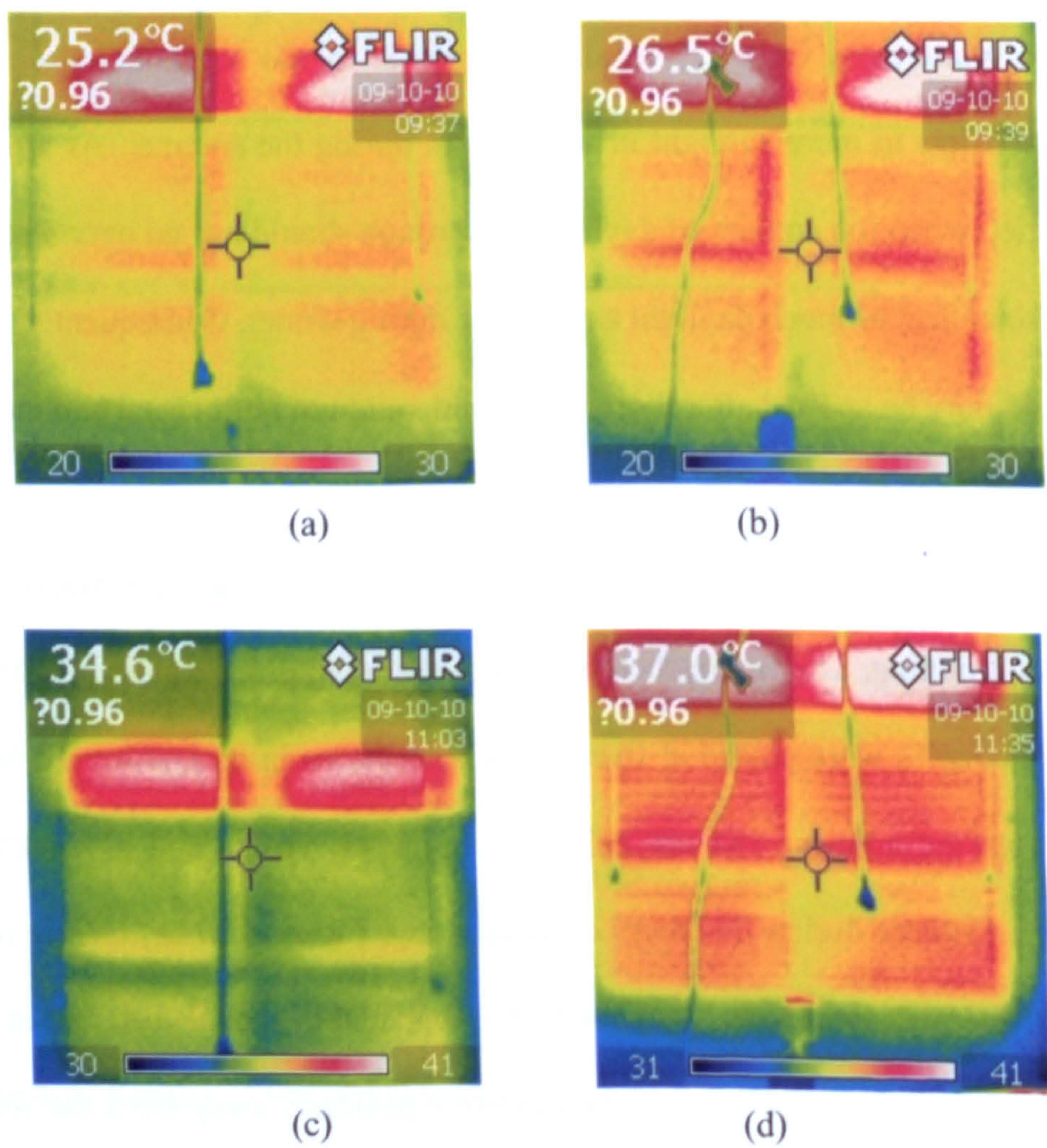
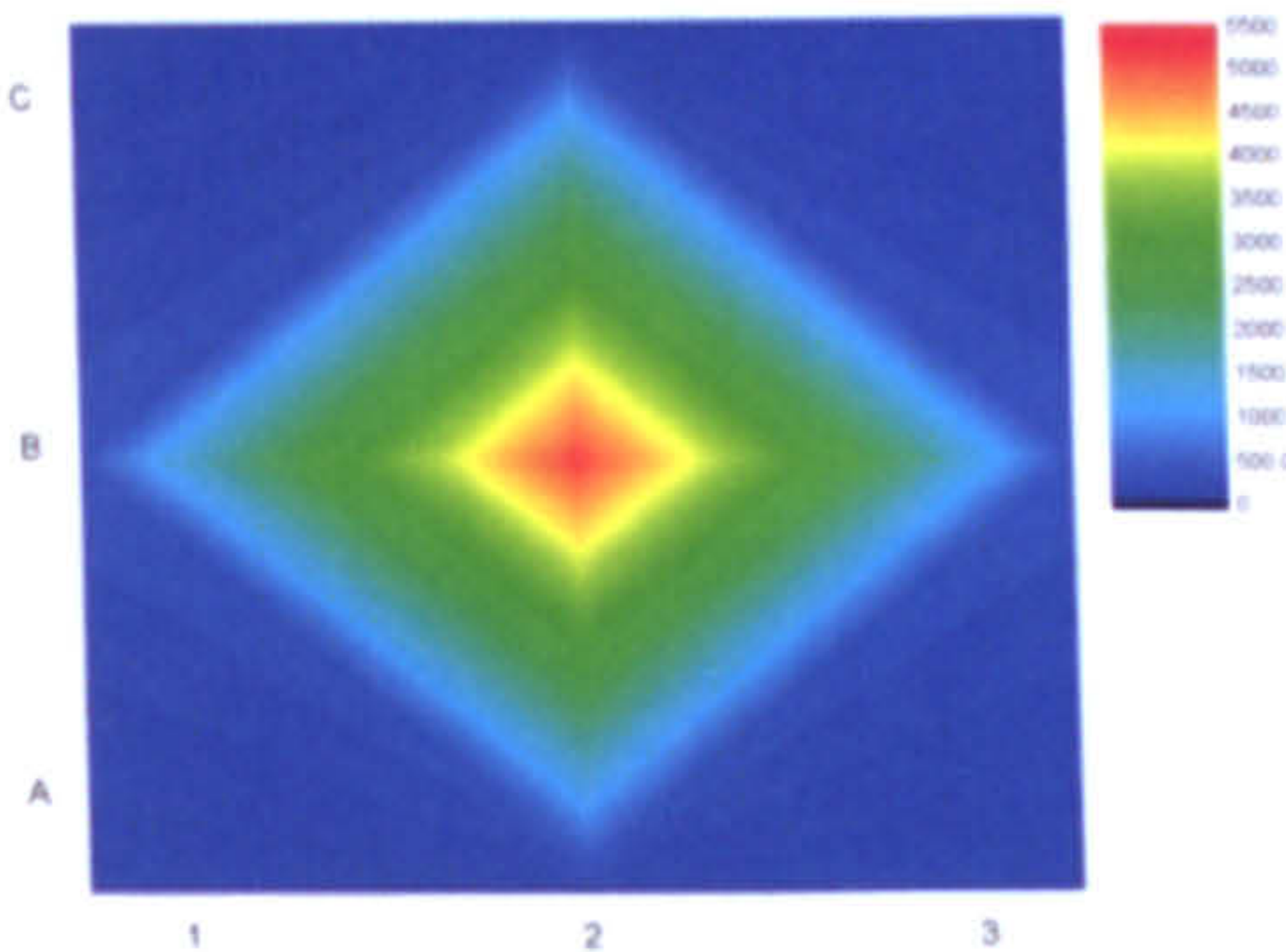


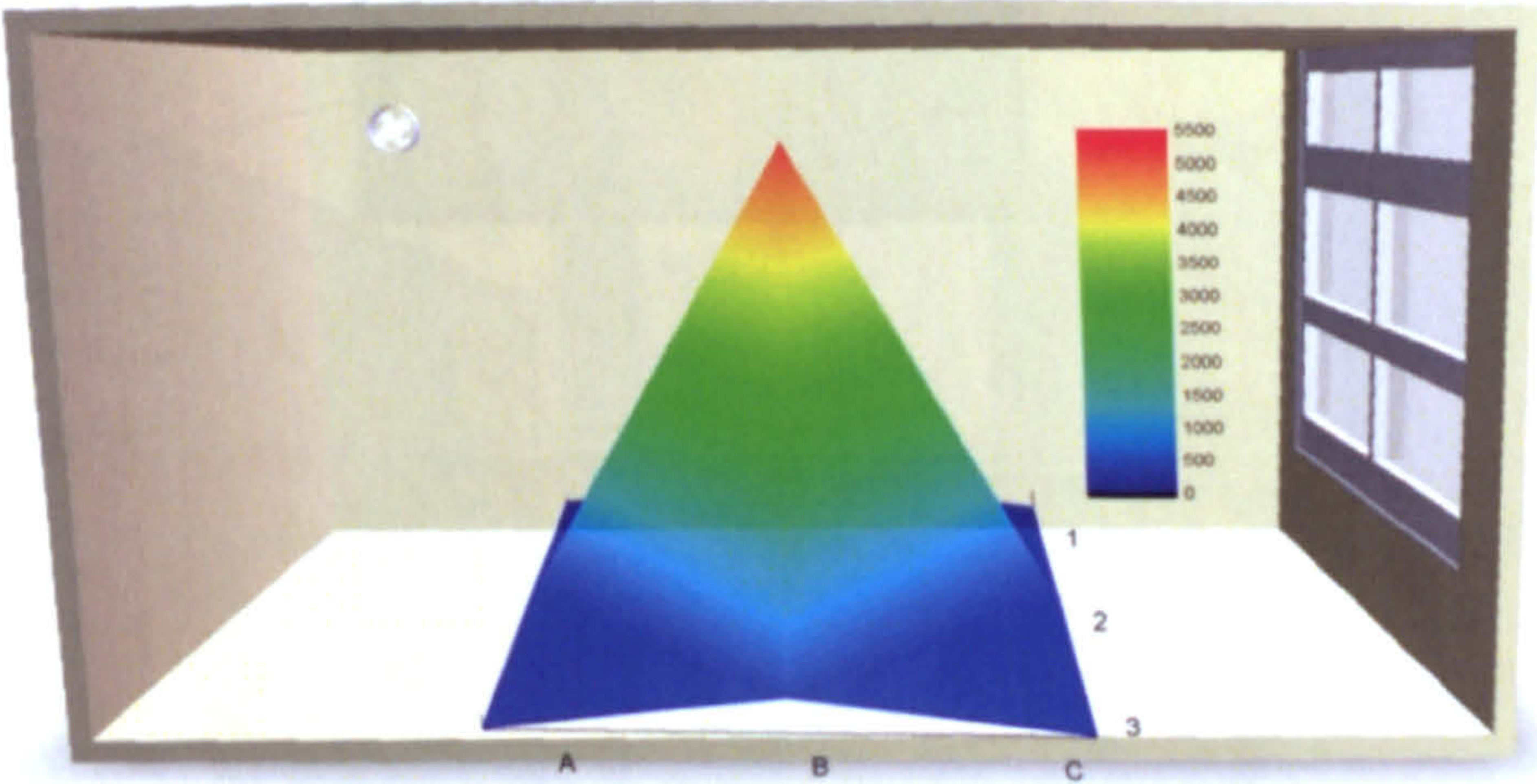
Figure 4.28 Thermal image by FLIR camera for two test cells at 9:37 and 11 :35 hours:
test cell w/o (a), (c) and with the daylighting system (b), (d)

4.3.4 Illuminance measurements

To investigate the indoor illuminance when lighting was solely provided by the present daylighting system (with a 30cm dish concentrator), measurements were made using the test cell where nine photo sensors were placed inside at an interval of 50cm and 40cm above the floor. Data were scanned for every five seconds and recorded with the aid of a data logger (Agilant 34970A). To block any light penetration from outdoors, the window, vent and other possible openings were completely sealed.



(a)



(b)

Figure 4. 29 Iso-illuminance contour plots (in lux) with the convex lens to diffuse sunlight : (a) 2D, (b) 3D.

Figure 4.29 shows the iso-illuminance contour plots when the convex lens (32mm) is applied to diffuse sunlight from the ceiling for indoor illumination. Due to its optical characteristics of a convex lens, light is mostly concentrated near the center reaching about

5,500 lux. This example case implicates the usefulness of the present daylighting system for spot lighting.

When light rods are applied at the end of the optical cable in place of optical lenses, it shows a completely different picture, especially, in illuminance distribution. It is more uniform and less likely to cause any luminance as shown in Figure 4. 30.

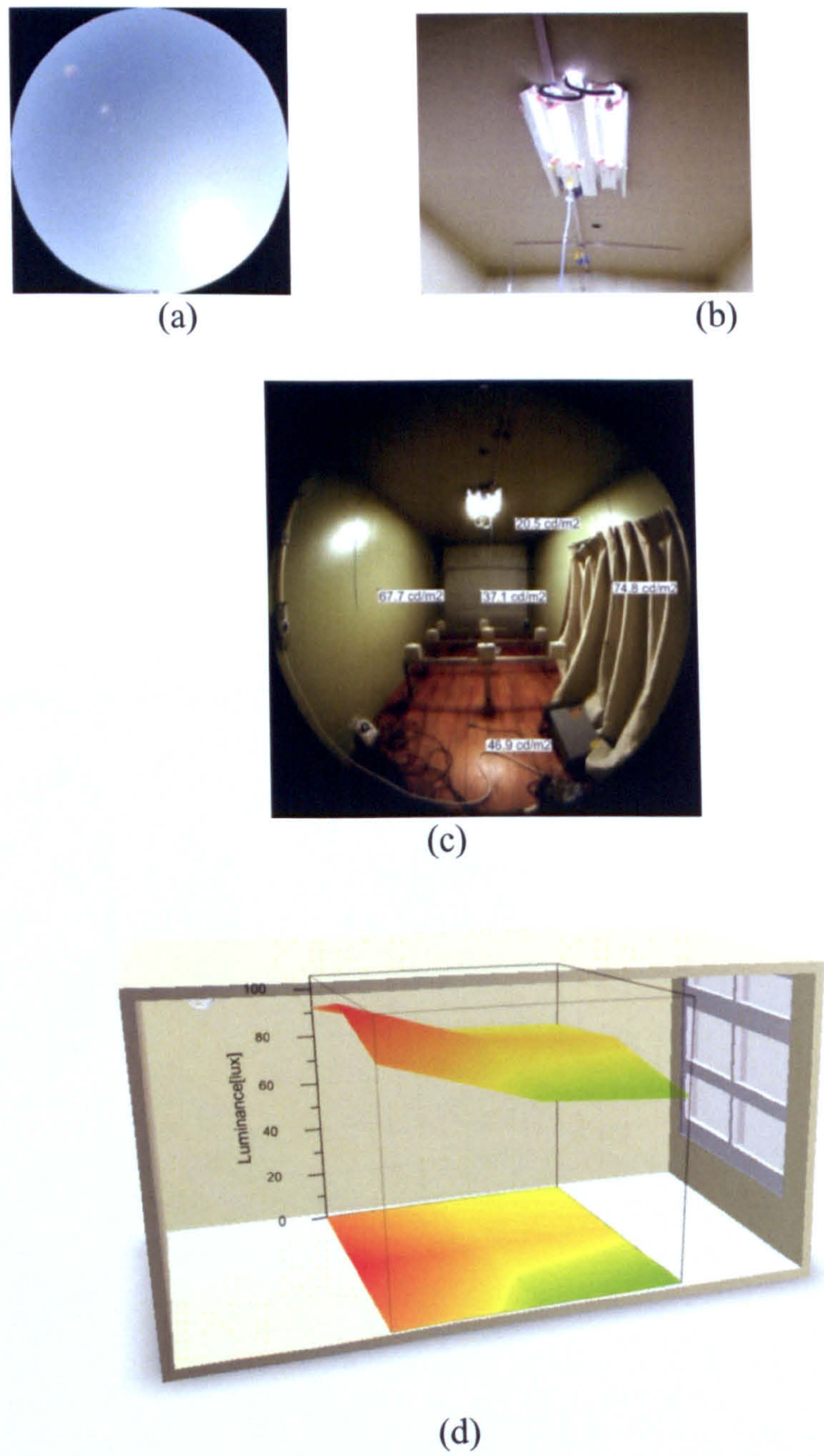
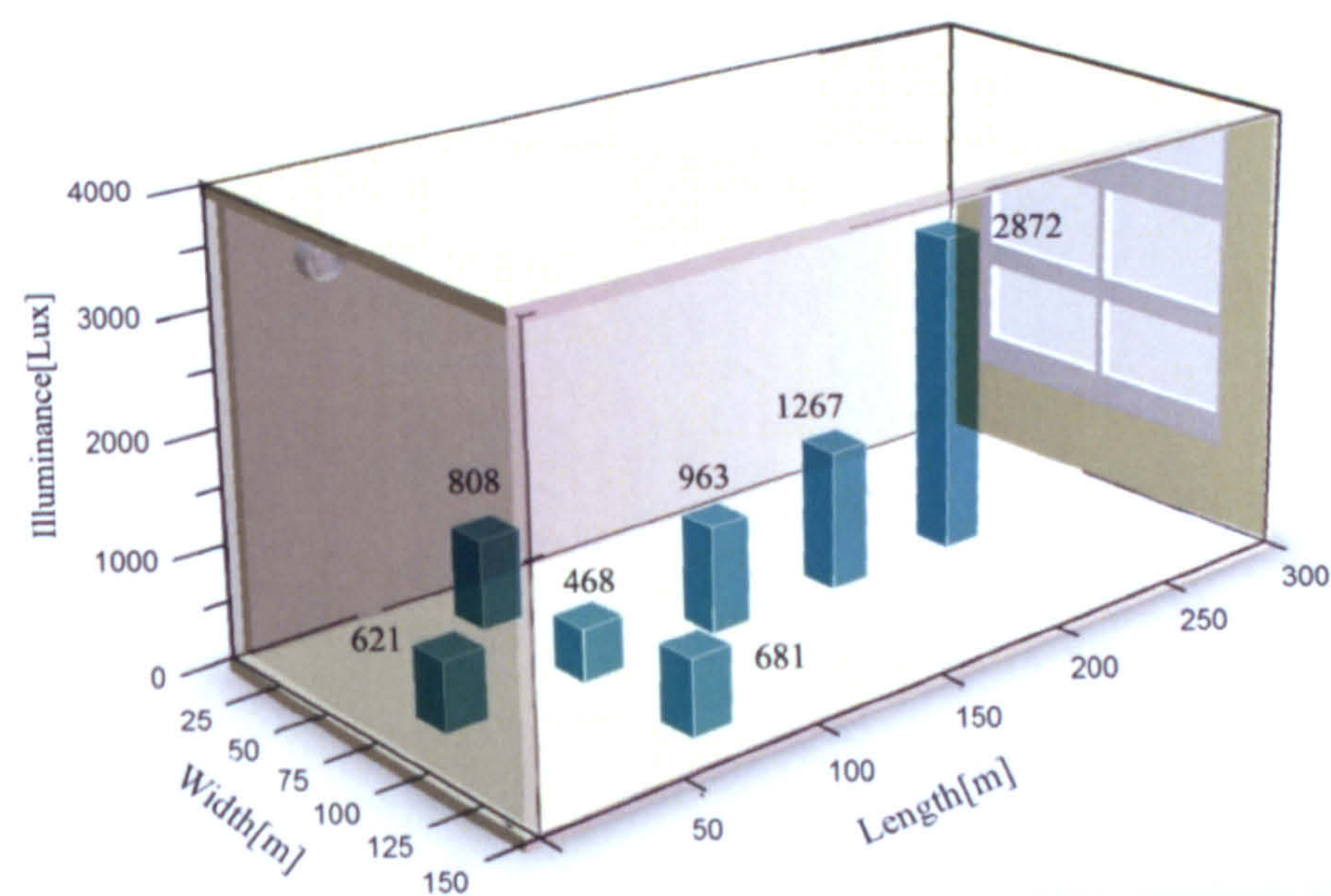
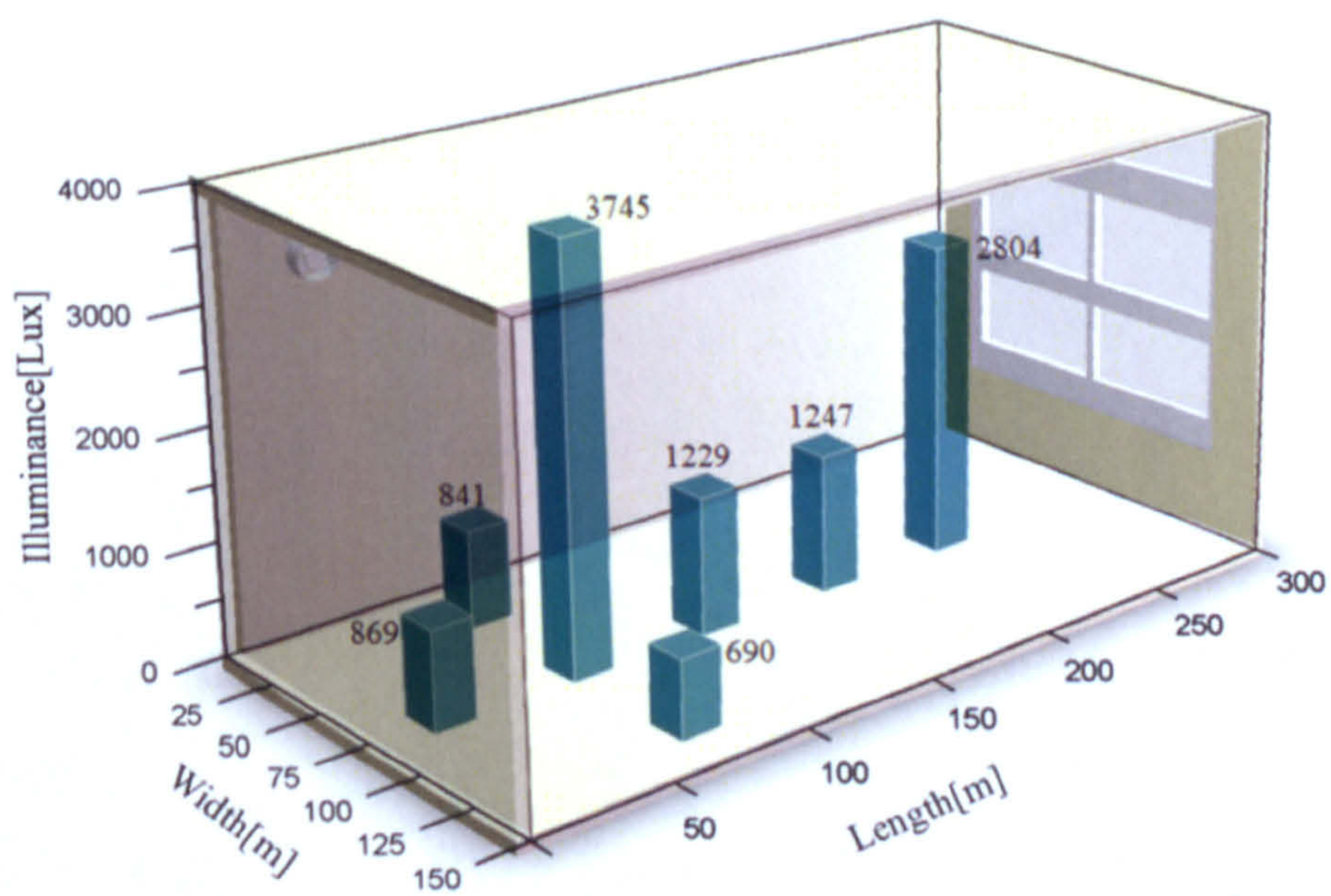


Figure 4.30 Illuminance distribution when two acrylic rods (sand-blasted) are used to diffuse sunlight for indoor illumination: (a) sky condition when measured, (b) light diffused from the rod, (c) and (d) luminance distribution

A series of measurements have been made using two test cells with different amount of sunlight admitted through the south facing window. Figure 4.31 shows the illuminance at each location of the photo sensor at 13:00 hour on a clear day (10/6). Slats of the venetian blinds are tilted downward at 45 degrees for both test cells. Differences are quite patent.



(a)



(b)

Figure 4. 31 Illuminance at each location of the photo sensor at 13:00 hour on a clear day (10/6): without (a) and with (b) a daylighting system

Figure 4.32 shows the average illuminance ratio of the test cells at different times of a day when blinds are tilted 45 degrees toward ground. There is a great difference between the two cells as the daylighting system pours in a great amount of sun rays into one of them. The illuminance ratios at each location of the sensor at different times on a clear day are given in Figure 4.33.

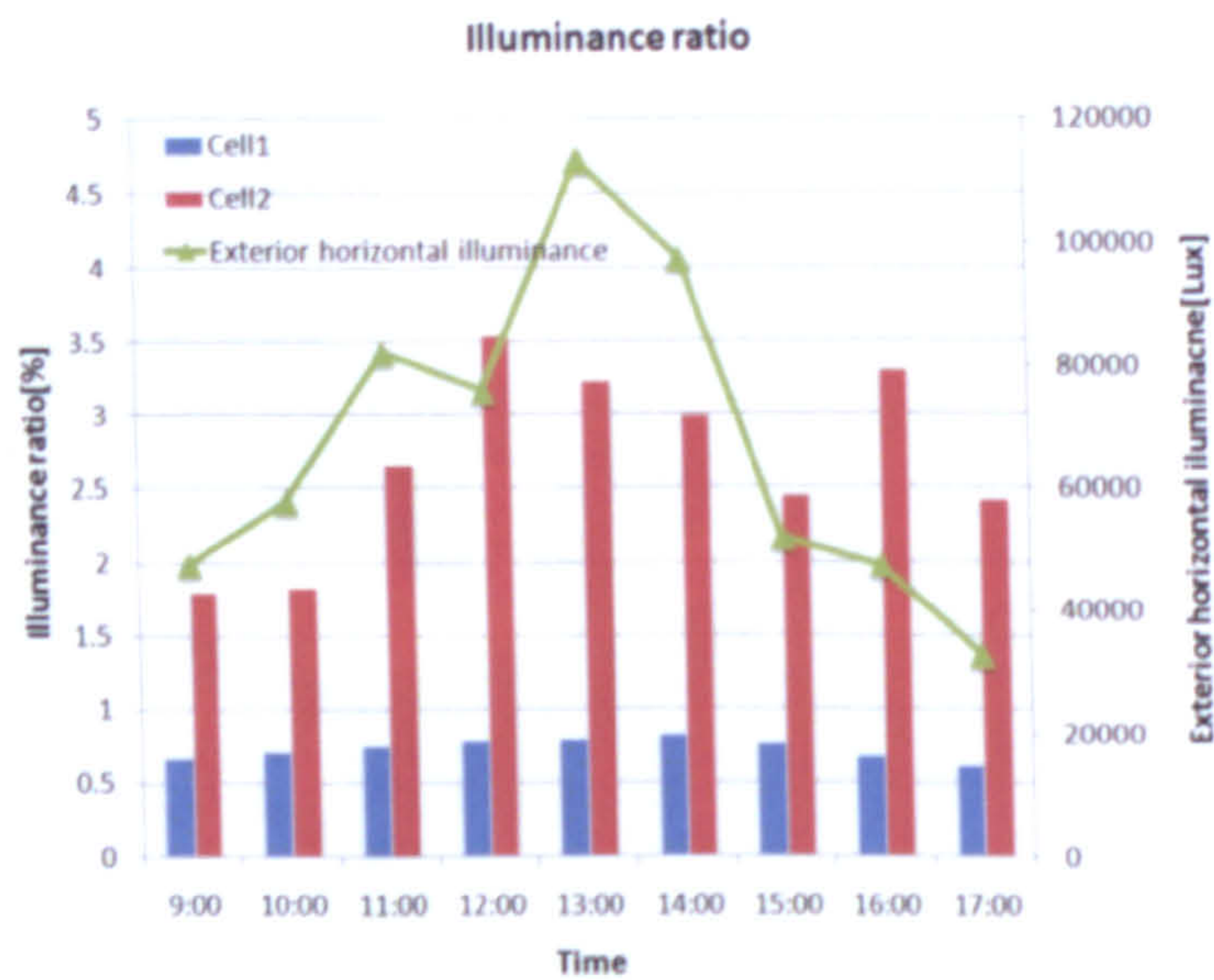


Figure 4.32 Average illuminance ratio of two test cells at different times of the day on a clear day (10/6) : Cell 1 (without a daylighting system), Cell 2 (with a 30cm dish-daylighting system)

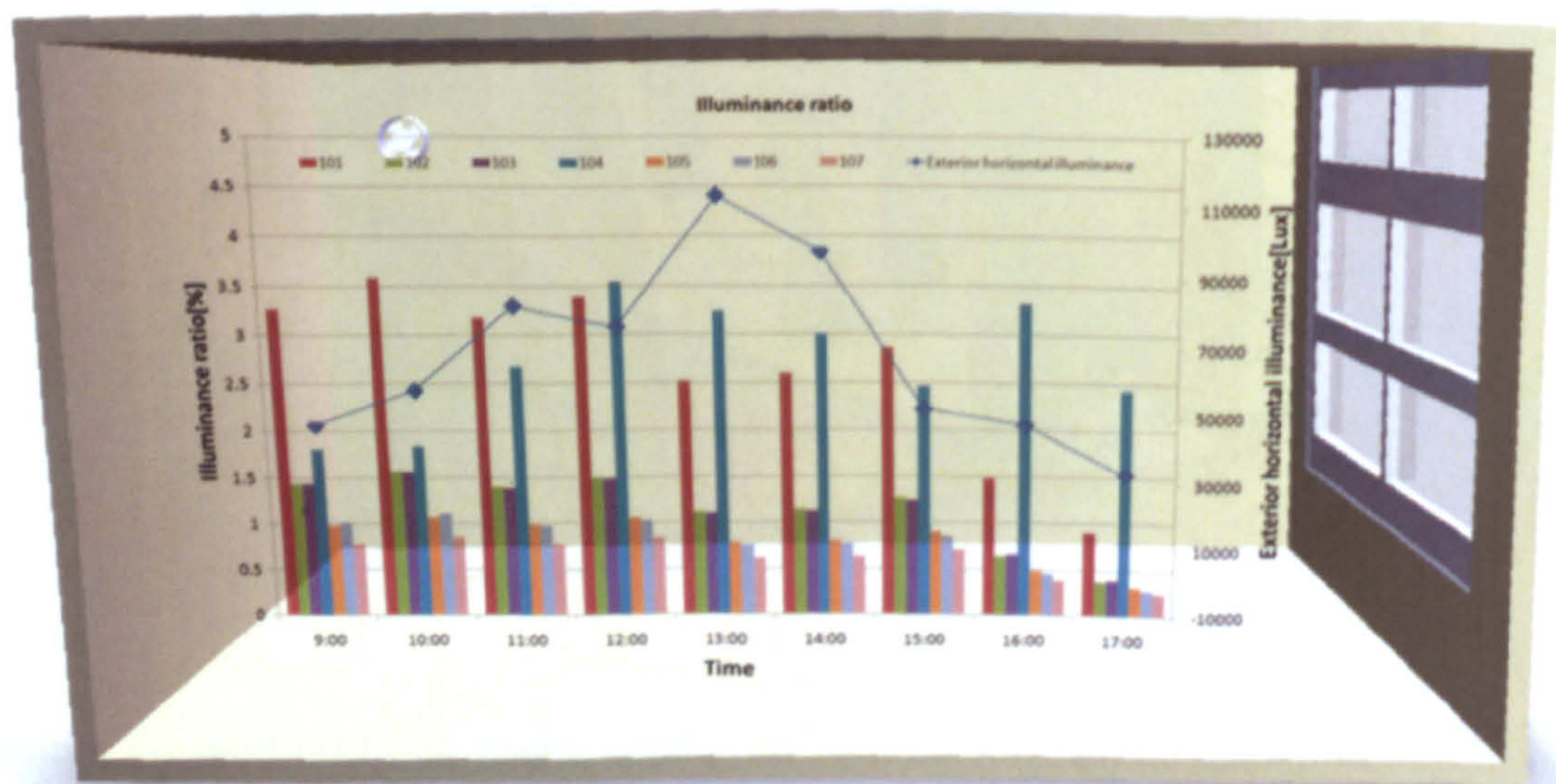


Figure 4.33 Illuminance ratios at each location of the sensor at different times of the day (10/6)

Figures 4.34 through 4.37 show the illuminance at each location of the photo sensor on a clear day for two test cells : without (a) and with (b) a daylighting system for different conditions of slats adjusted for venetian blinds. A concave lens is used for the diffuser in all cases.

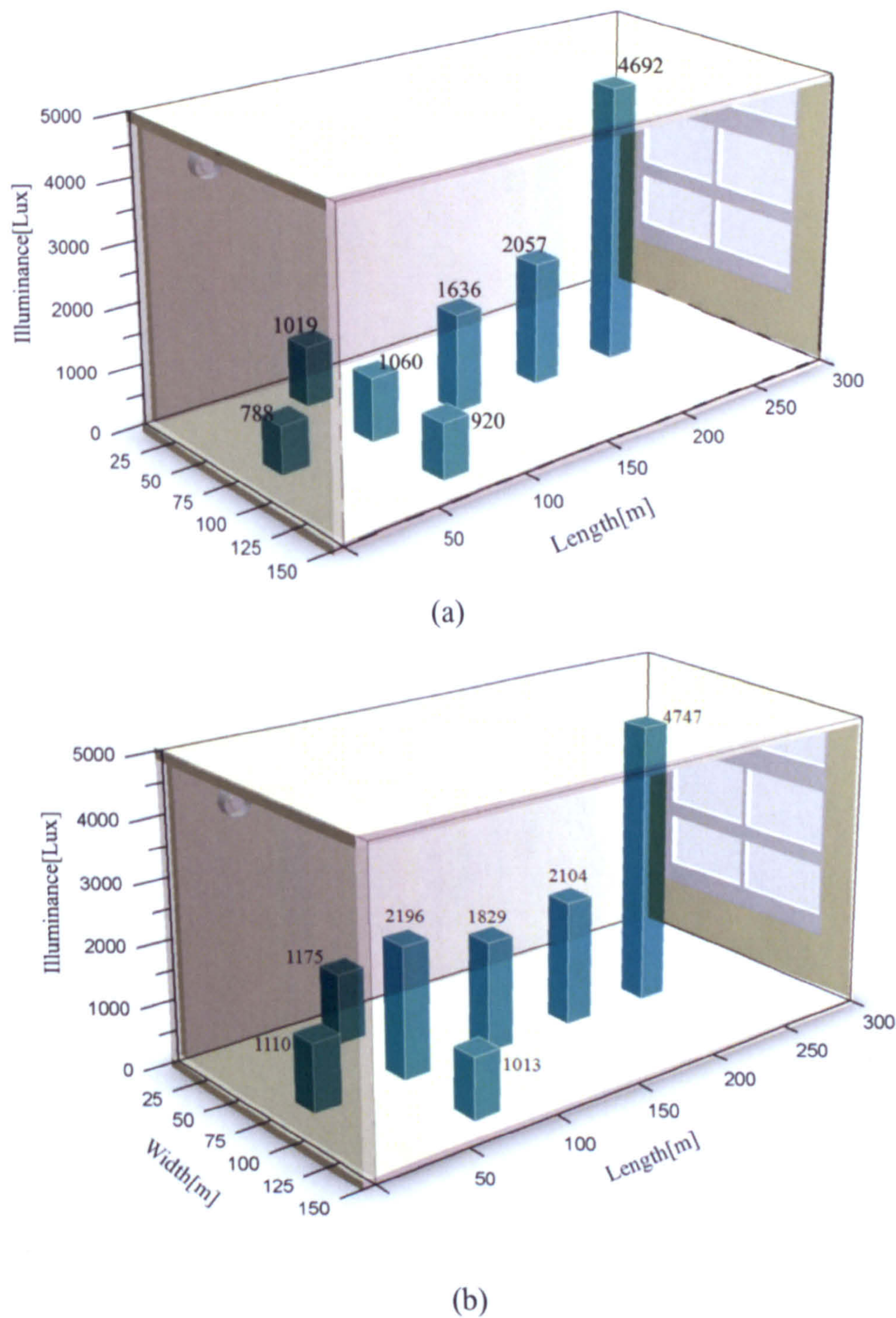
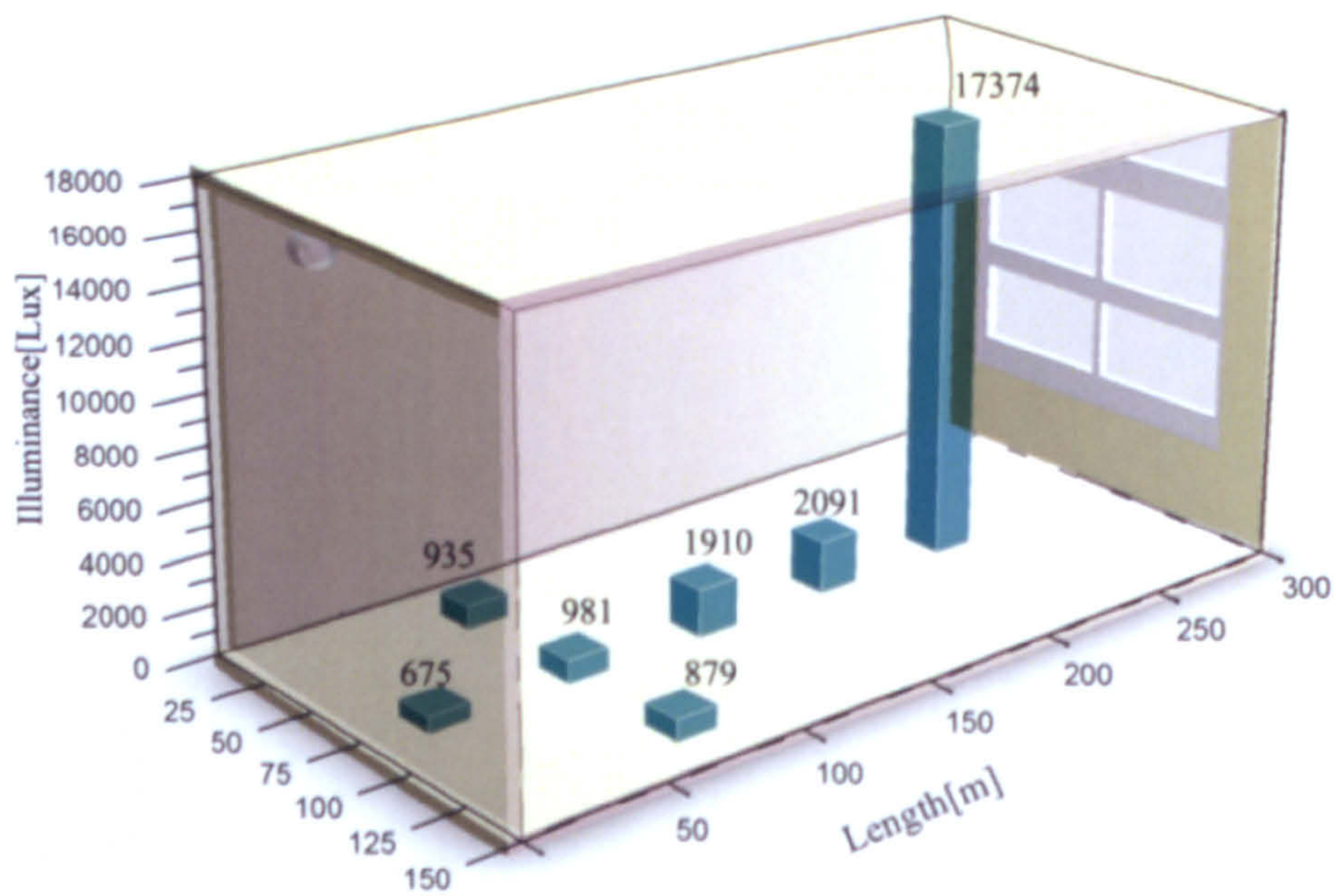
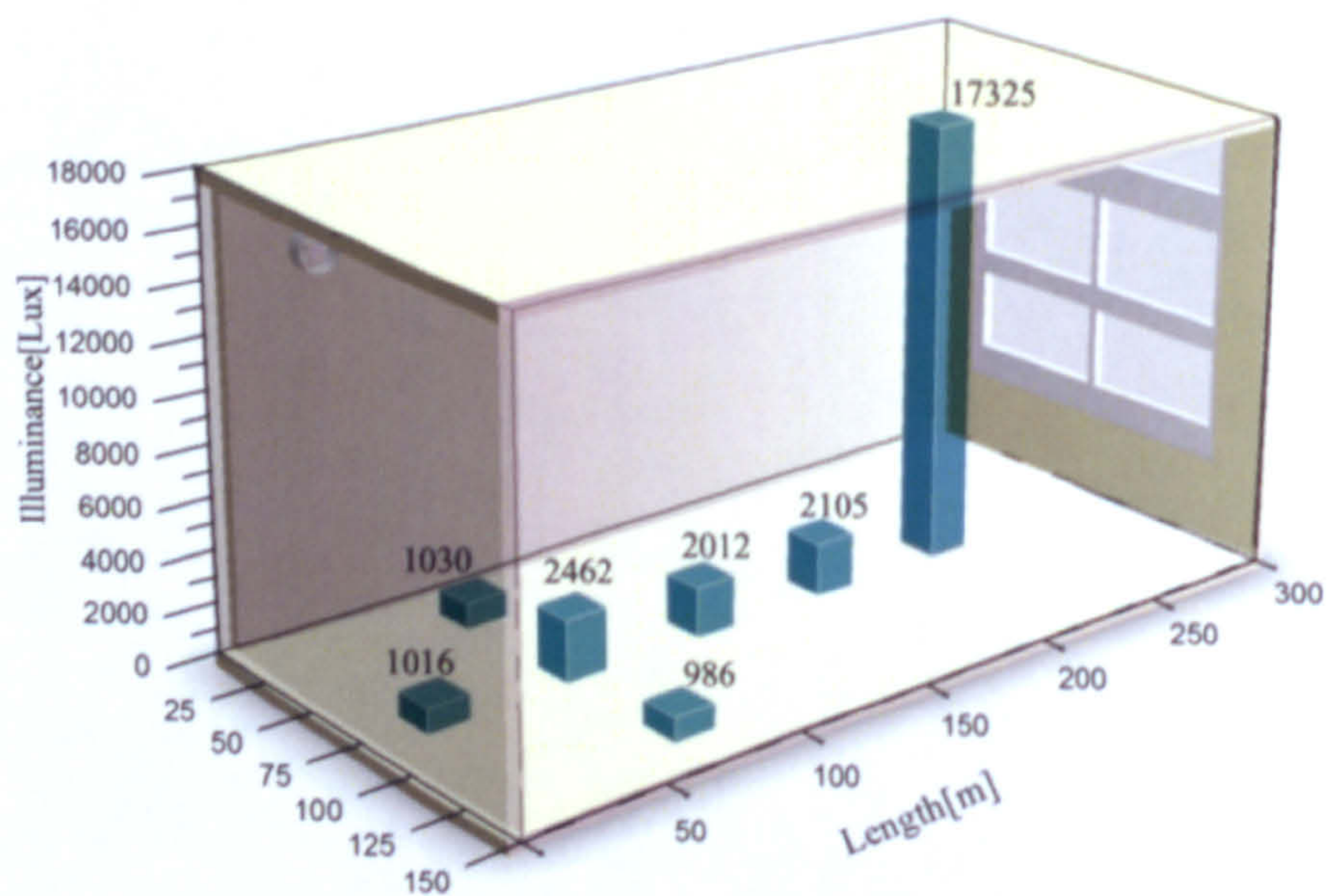


Figure 4. 34 Illuminance at each location of the photo sensor at noon on a clear day (10/4): without (a) and with (b) a daylighting system (slats are adjusted to a horizontal, level position)



(a)



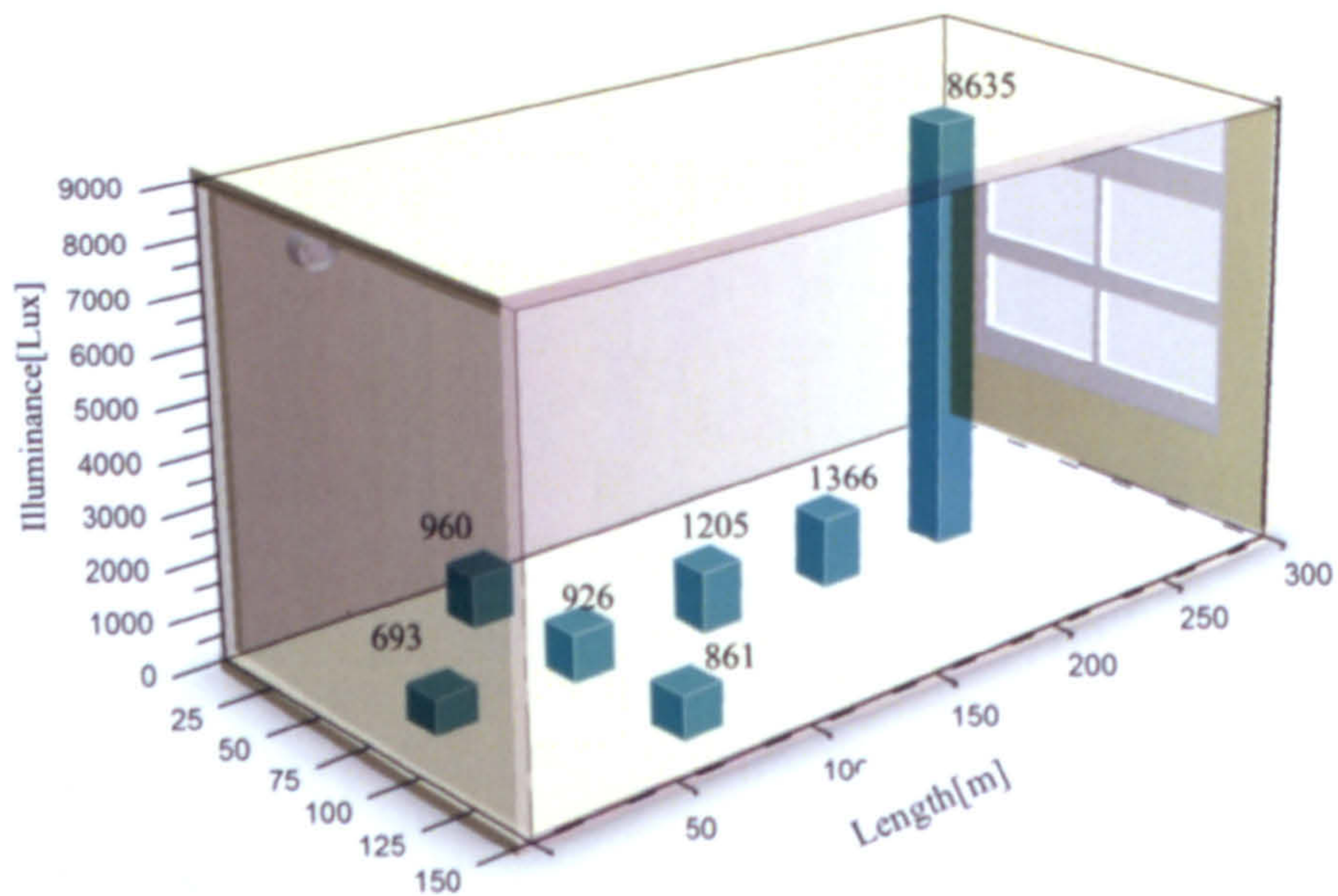
(b)

Figure 4. 35 Illuminance at each location of the photo sensor at 14:00 hours on a clear day (10/5): without (a) and with (b) a daylighting system (tilted upward at 45 degrees for both test cells)

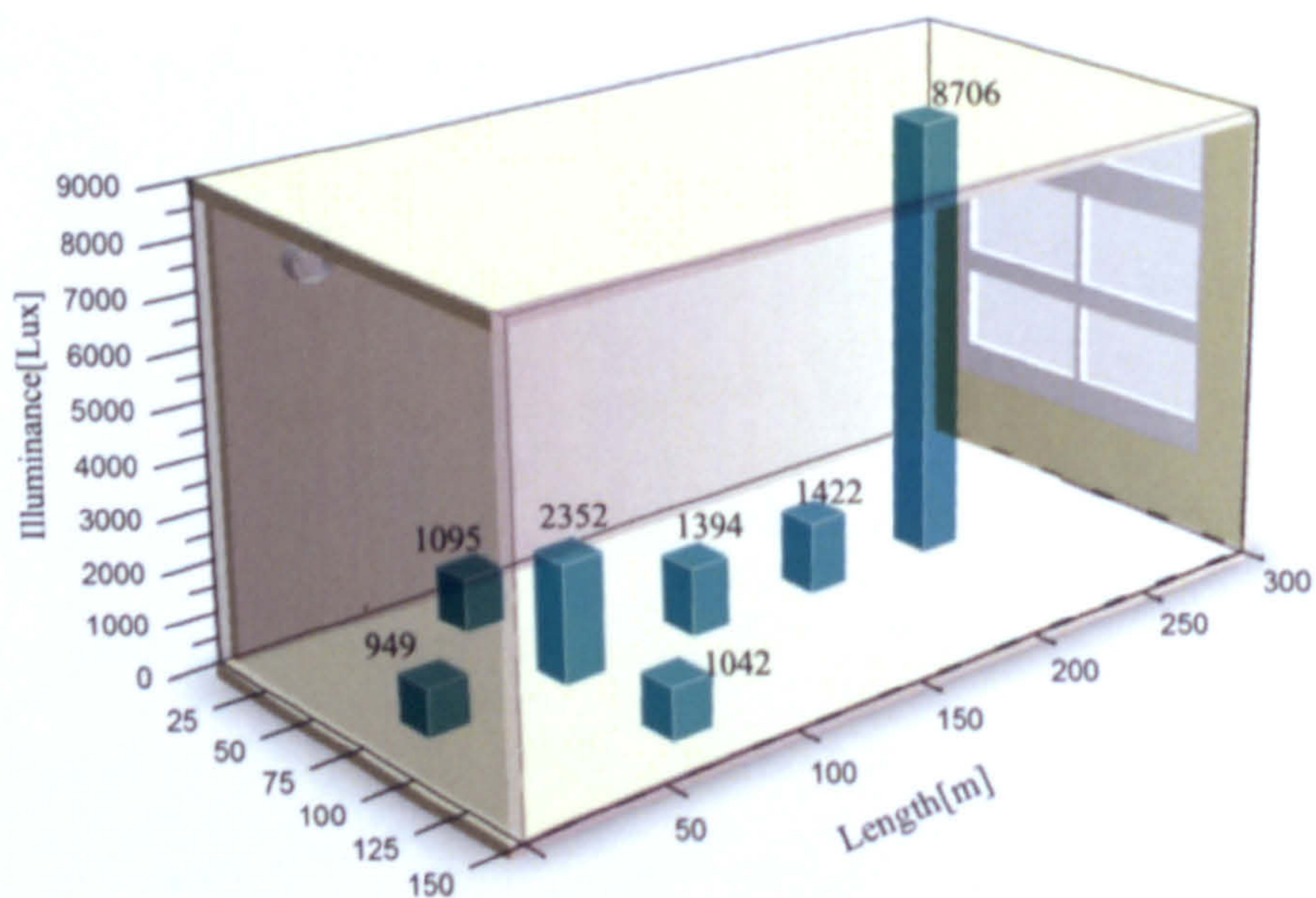
In all figures, interior areas adjacent to the window aperture showed the highest level of illumination due to sunlight admittance from outdoors. This, however, changes and the illuminance rather drops off quite abruptly as measured by those sensors away from the window. The conditions imposed at the window, i.e, pull down and withdrawal of venetian blinds as well as adjustment of blinds' slat angle, also play major roles in the admittance of daylight into the interior space.

In Figure 4.34, there is a deep penetration of sunlight into the interior as the slats in their horizontal position function as light shelves bouncing sun rays up towards the ceiling and reflect it down deeper into the interior space. Different from other cases compared, the maximum illuminance ratio, that exists between the window area and deep space (near the north wall) is measured to be less than 6 : 1. This makes it as the exemplary case in achieving uniformity of lighting, which was further enhanced by employing our daylighting system near the north wall, Figure 4.34 (b).

As shown in Figure 4.21 (a), the window installed on the south wall has three rows of windows with venetian blinds. The top row has a separate set of venetian blinds while the center and bottom rows of windows are covered together with another set of venetian blinds. Figures 4.35 and 4.37 give measured indoor illuminances at 2pm on a clear day where a different condition is imposed on the top row of windows. In Figure 4.35, both venetian blinds were rolled down and the slats were tilted upward at 45 degrees. The same strategy was also applied for the venetian blinds covering the center and bottom rows of windows in Figure 4.37 except the top one which was fully closed (rolled down and slats at vertical position). As shown, the effect of daylight admitted through from top is quite noticeable where the measured illuminance values are almost doubled besides the one located near the south window. It is likely that the reflections from this bright area can negatively affect the quality of indoor visual environment causing glares.

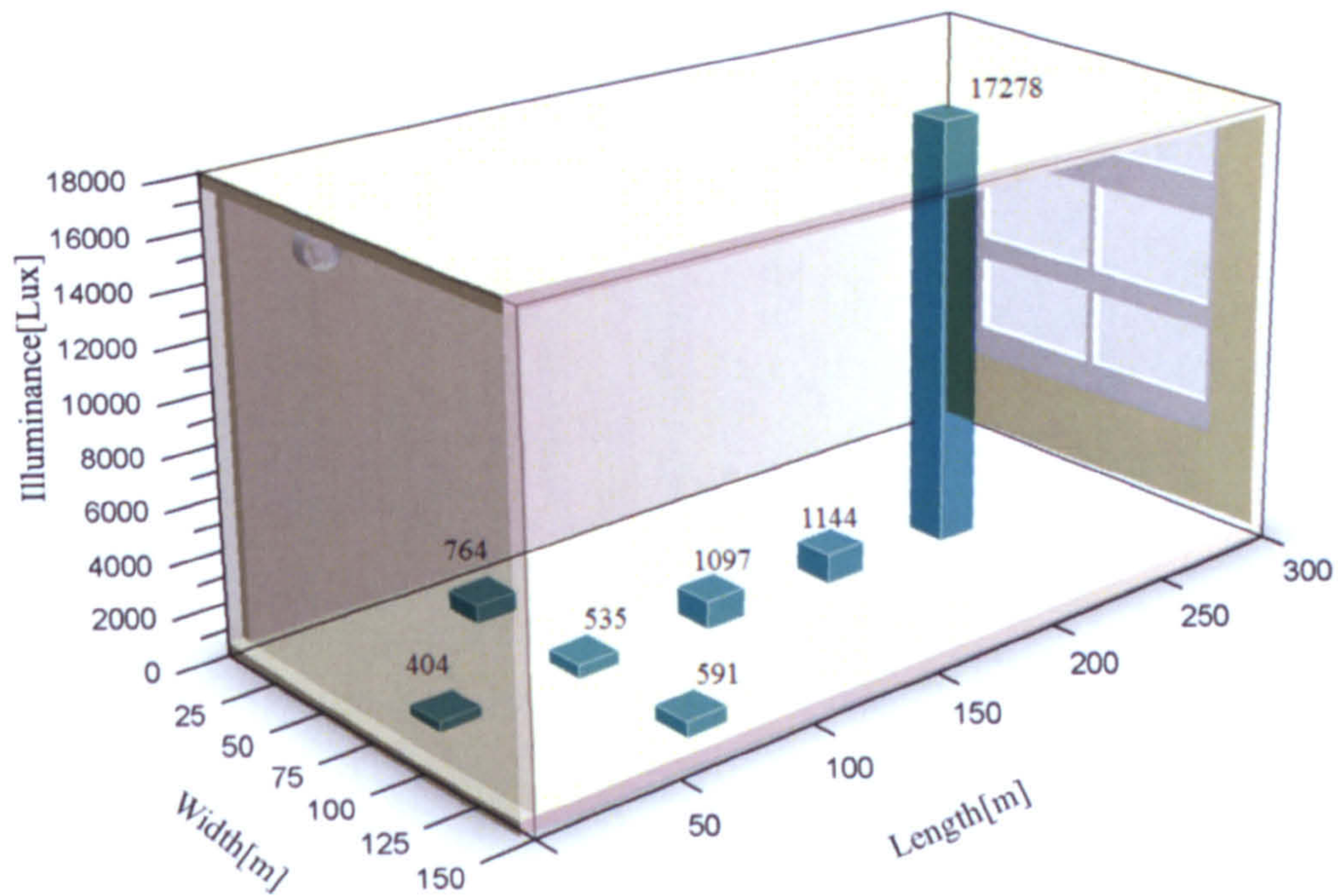


(a)

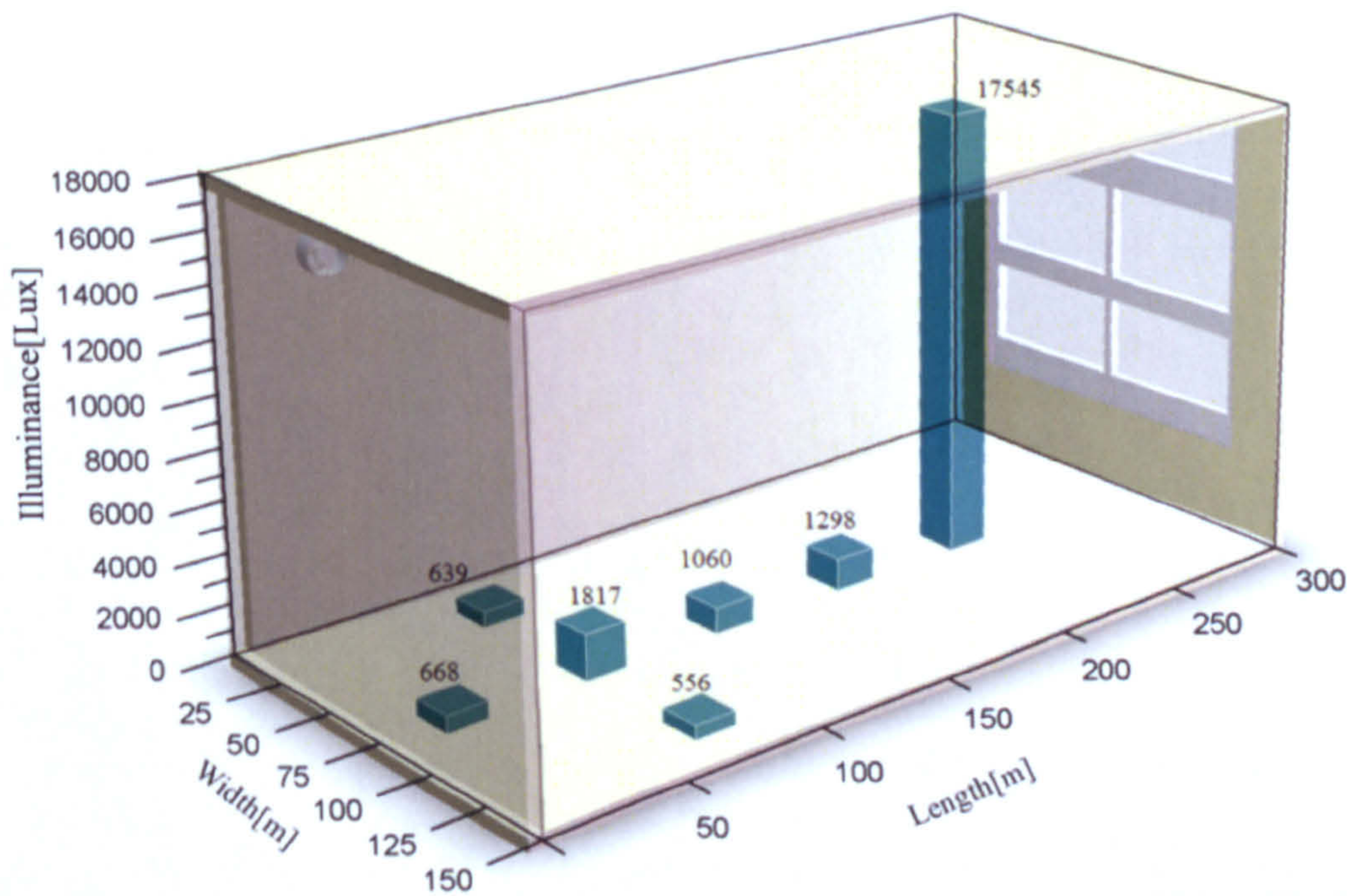


(b)

Figure 4. 36 Illuminance at each location of the photo sensor at 11:40 hours on a clear day (10/8): without (a) and with (b) a daylighting system (For both cells: venetian blinds on top – rolled up, venetian blinds below - slats closed)



(a)



(b)

Figure 4. 37 Illuminance at each location of the photo sensor at 14:00 hours on a clear day (10/9): without (a) and with (b) a daylighting system (For both cells: venetian blinds on top – closed, venetian blinds below - tilted upward at 45 degrees)

4.3.5 Photometric analysis by RADIANCE

Daylight simulation can improve building designs and control applications. However, to reliably predict daylight availability indoors via computational simulation, reasonably detailed and accurate mathematical models are necessary.

RADIANCE is considered as one of the most reliable ray-tracing software capable of producing photo-realistic renderings and calculating illuminance as well as luminance values. It could also generate luminance maps and ratios handy for estimation of visual comfort and glare control. The program's ability to accurately model the interaction between daylight and buildings (both inside and out) makes it an essential tool for designing and evaluating the visual environment of architectural spaces. Especially, its quality renderings in presenting the calculated results, which generally involve sophisticated mathematical procedures to solve various equations with physical constraints, facilitate the use of program in diverse situations of lighting design and simulation. For a successful daylighting design, it is very important to accurately estimate interior illuminance and luminance levels based on daylight penetration through various openings in surrounding walls.

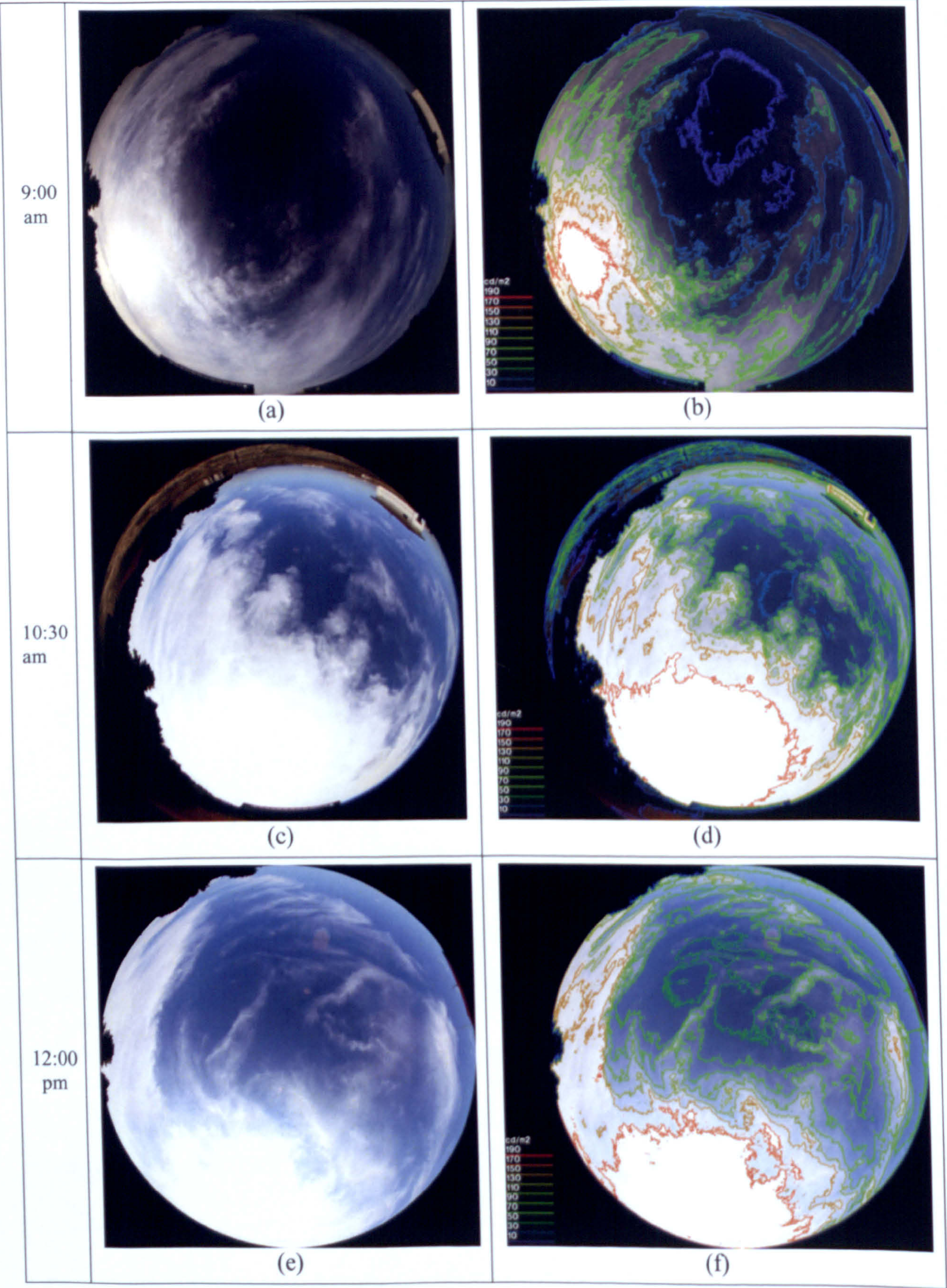
One of the primary concerns of efficient architectural design is the availability of quality daylight indoors. Designers use daylight simulation applications to test and improve daylight solutions. Most of these applications nowadays function with simplified sky luminance models. The standard sky models created with these tools do not, however, accurately represent the state of daylight because such models are not sensitive to luminance variations in different areas of the sky. Generally, the luminance of the sky area viewed from a point in a room is directly related to the illuminance level at that point whereas the other portions of the sky have their influence on the indoor illuminance rather indirectly, i.e., only by reflection.

Figure 4. 38 shows the change in sky conditions at different times of the day (9am, 10:30am, 12:00pm, 2:30pm and 4;pm) with its sky luminance distributions at different hours

using luminance ratio (contrast) maps produced by RADIANCE. As shown, luminances between the lightest and darkest areas of the sky constantly change with the sun's movement and cloud covers. In this figure, the sky images are prepared by a digital camera with fisheye lens, which makes it possible to capture sky images covering a 180° angle. From the pixels of an image, a direct model of the sky distribution luminance is developed by RADIANCE. An image in ttf-format received from a CCD camera (Model : Canon EOS 5D digital camera) is converted to pic-format, which is a default format in RADIANCE. This is readily accomplished by executing a submenu command "Edit Radiance Project" in ECOTECT.

To obtain higher image quality results it is recommended first to change the image's resolution from higher values to 800x800 pixels in any standard image editor (e.g. in Photoshop). Selecting appropriate settings in the 'Render settings' window in the Radiance control panel will give the luminance or illuminance values in the Radiance image viewer. Finally, choosing necessary options from the Radiance image viewer will run the simulation with the desired settings for contour lines/false color, scale, divisions and unit.

As time passes by, sky conditions change, which are reflected by the luminance maps. The digital images of the sky are taken at the same point during its observation. Sky luminance data derived from digital images were converted to luminance map by RADIANCE as shown in (b), (d), (f), (h) and (j) in this figure. The region near the sun is represented by the contours of the highest luminance value. When compared to the rest of the sky, there exists a striking difference in its brightness readily observable to the naked eye. It is not a difficult task to track the change in time as its movement (of this bright region) across the sky is related to the passage of time. Although they do not present the actual luminance values and are generated by using the digital images taken by a camera (that is, based on the contrast ratio between areas), they reveal valuable information regarding the local clearness and brightness of sky conditions.



(continue on the next page)

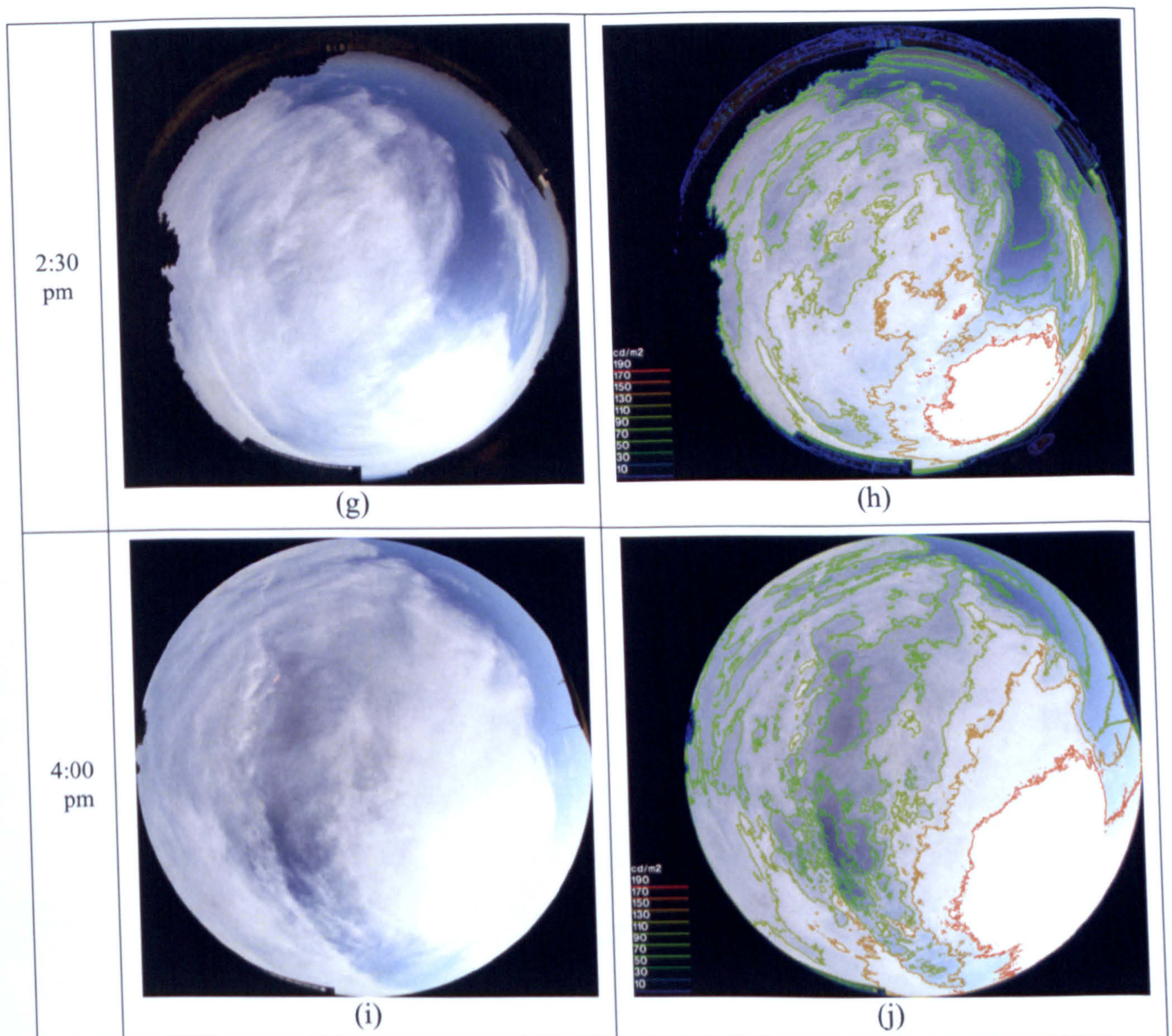


Figure 4. 38 Sky luminance map at different hours : 9:00 am, 10:30 am, noon, 2:30 pm, 4:00pm (produced by Radiance)

Figures 4. 39 ~ 4. 43 show the iso-contour lines superimposed on the original image to demonstrate the spatial distribution of the illuminance and luminance values for test cells with and without the dish-daylighting system at different times of the day : 9am, 10:30am, 12:00pm, 2:30pm and 4:00pm. Slats of the venetian blinds were tilted downward at 45 degrees for both test cells.

The daylighting contribution to indoor illuminance by the present daylighting system appears to be quite palpable as there are some appreciable differences observed for the photometric values measured at the corresponding locations of the test cells. As shown in the

figures, the illuminance and luminance values are given in numbers to the first decimal point for a number of selected locations to compare their relative magnitude on a one-on-one basis. At 9am, the luminance values given range from 69.2 cd/m² to 163.2 cd/m² for the case without any daylighting system (b) whereas the values of 78.2 cd/m² to 165.8 cd/m² were recorded when our daylighting system was introduced (f). These values are quite comparable to their corresponding cases of illuminance values, ranging from 66.7 lux to 164.7 lux (d) and 72.0 lux to 165.2 lux (h), respectively.

When similar comparisons are made for Figures 4. 40, 4. 41, 4. 42 and 4.43, there are some differences readily noticeable among them as the sun moves constantly changing its air mass and altitude with time. Especially, the maximum and minimum of these values were observed at 2:30pm, where the luminance values of 43.1 cd/m² and 169.3 cd/m² were recorded with the corresponding illuminance values of 49.6 lux and 164.7 lux for the case without any daylighting system. In comparison, the luminance values of 79.8.1 cd/m² and 171.5 cd/m² were recorded with the corresponding illuminance values of 78.2 lux and 175.5 lux for the case where our daylighting system was installed.

These kinds of plots (representations) are useful in understanding luminance distribution patterns, luminance ratios and glare assessment. Especially, they make it easier to comprehend and to visualize the spatial luminance (or illuminance) distributions within a space without undue difficulties.

It should also be noted that the maximum and minimum luminance (and illuminance) values given in these figures do not represent the exact maximum or minimum values spatially distributed. They should rather be interpreted as the local representative photometric values for the different areas inside a test cell for comparative analyses. Excessive brightness or uneven distribution in the field of view could be readily perceived (assumed) with varying degrees of light and dark profiles.

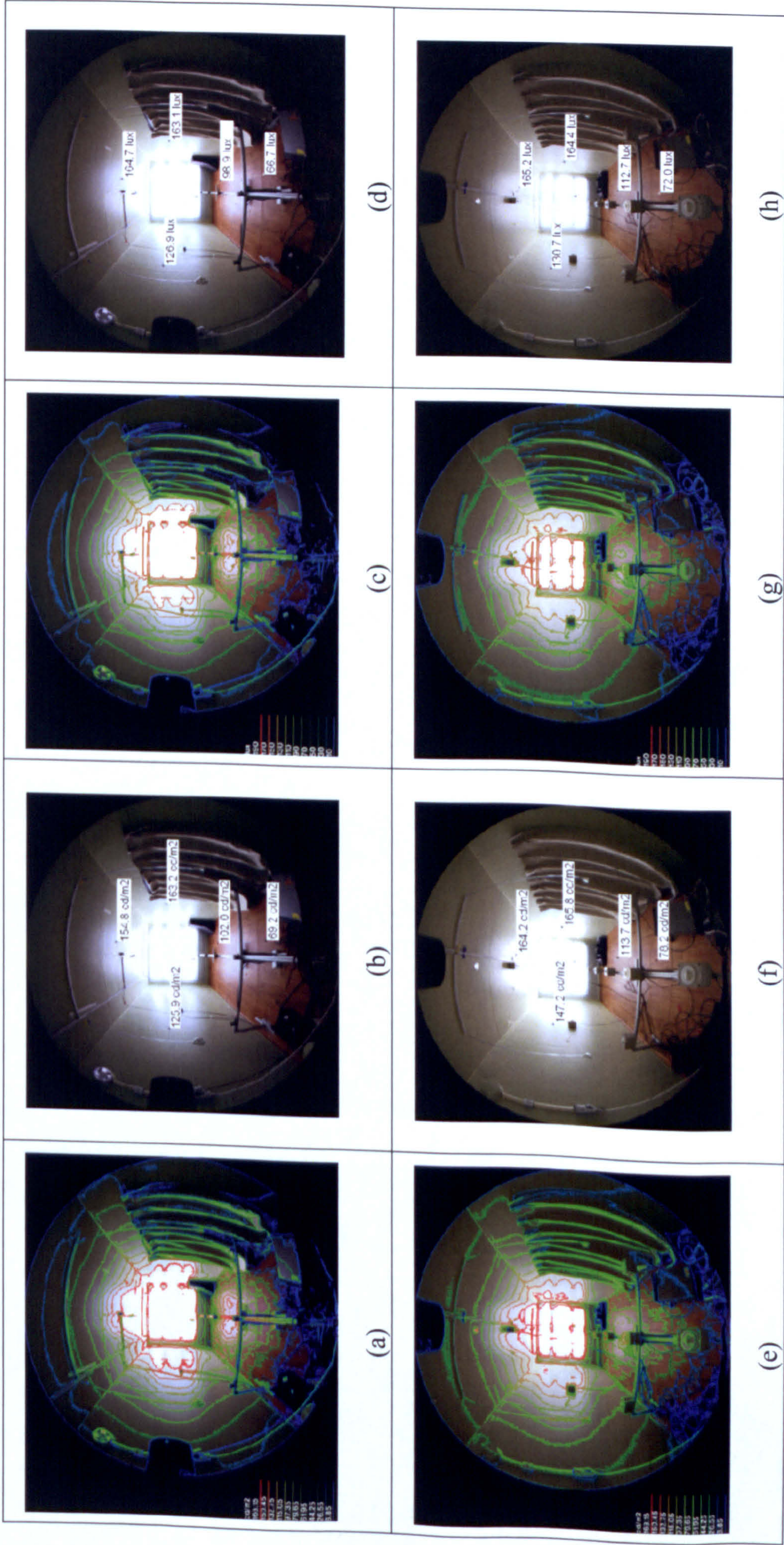


Figure 4.39 Luminance and illuminance distributions without [(a),(b), (c), (d)] and with [(e), (f), (g), (h)] at 9:00am

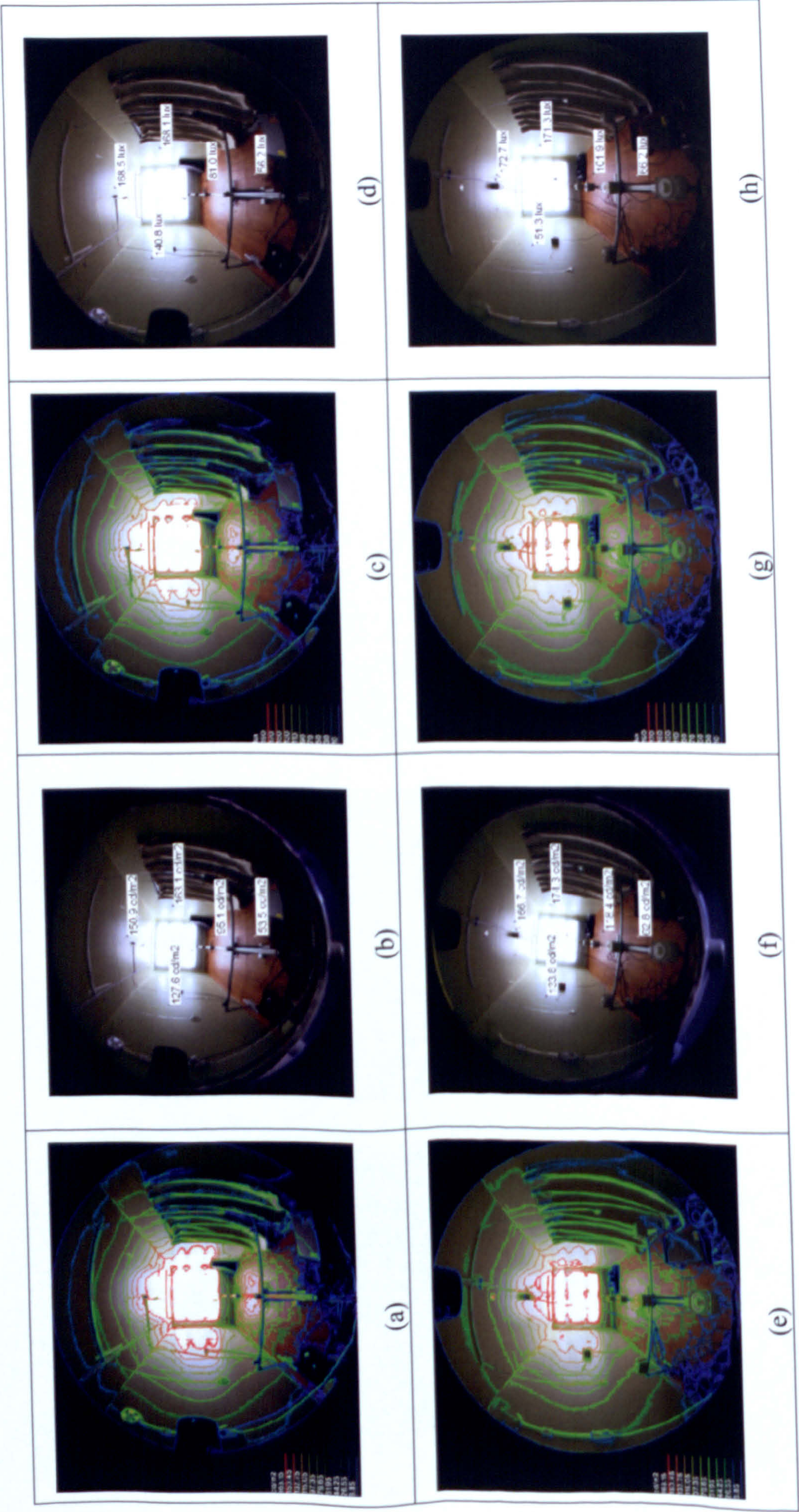


Figure 4. 40 Luminance and illuminance distributions without [(a),(b), (c), (d)] and with [(e), (f), (g), (h)] at 10:30am

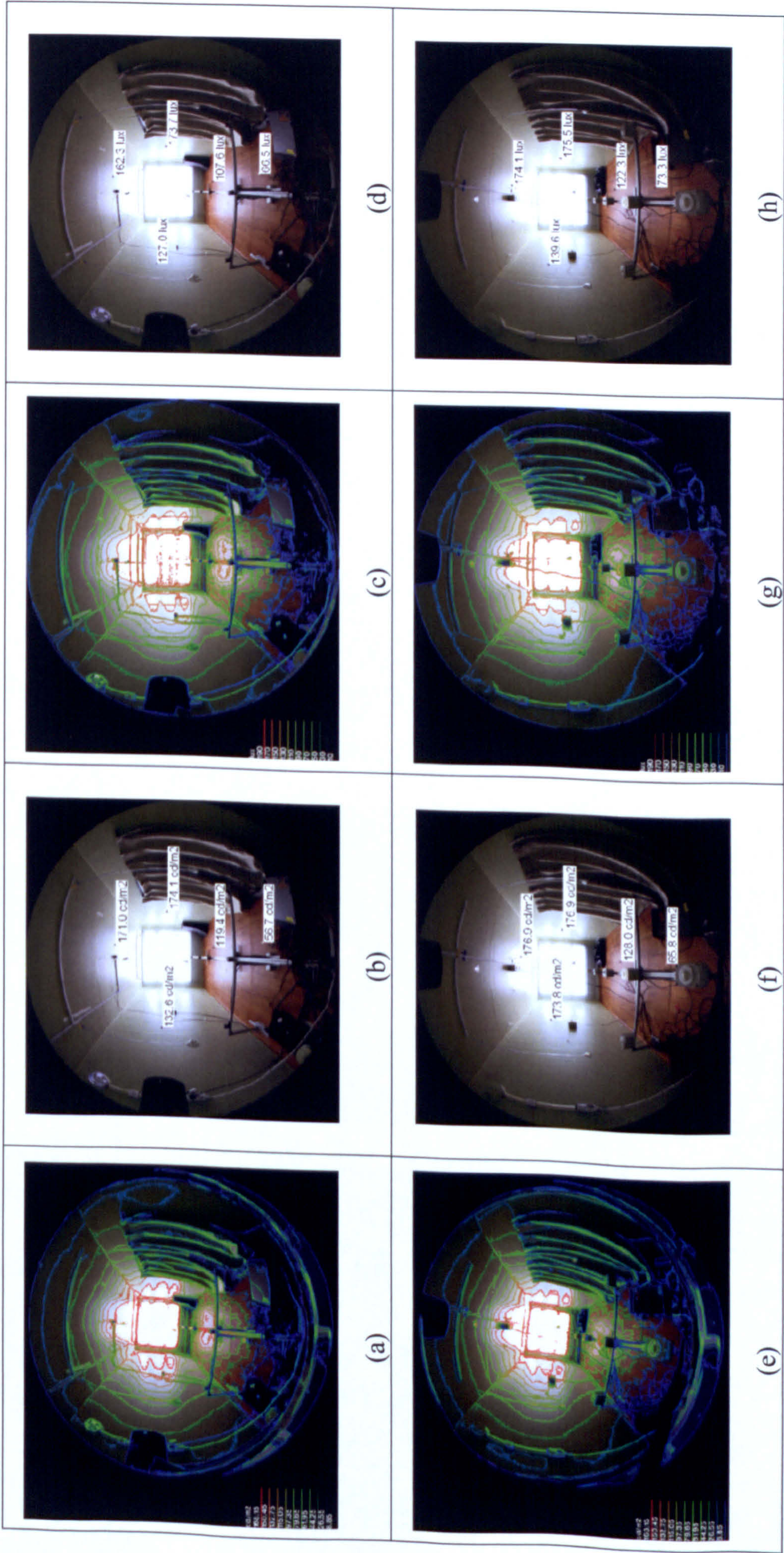


Figure 4.41 Luminance and illuminance distributions without [(a),(b), (c), (d)] and with [(e), (f), (g), (h)] at noon

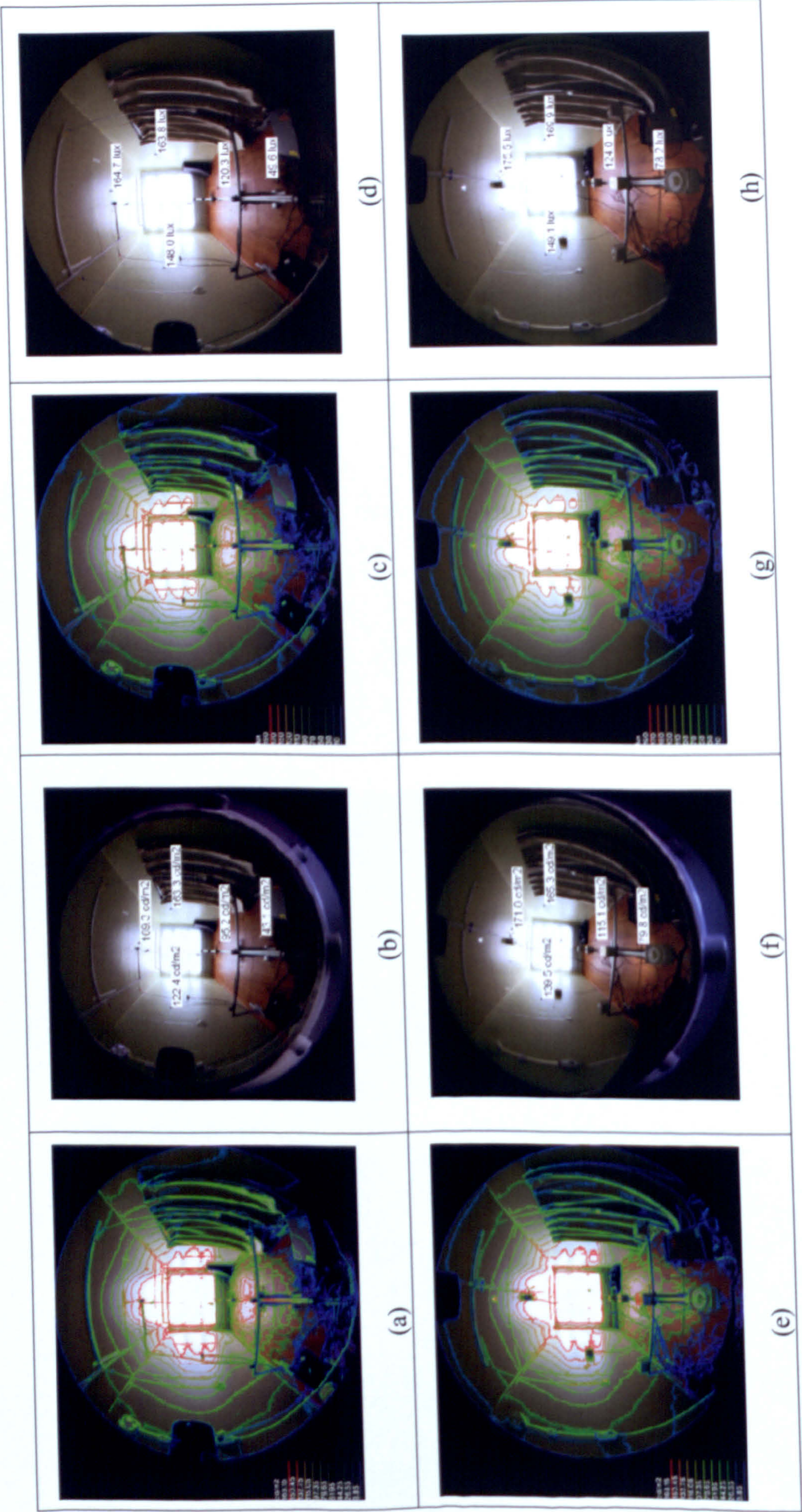


Figure 4.42 Luminance and illuminance distributions without [(a),(b), (c), (d)] and with [(e), (f), (g), (h)] at 2:30pm

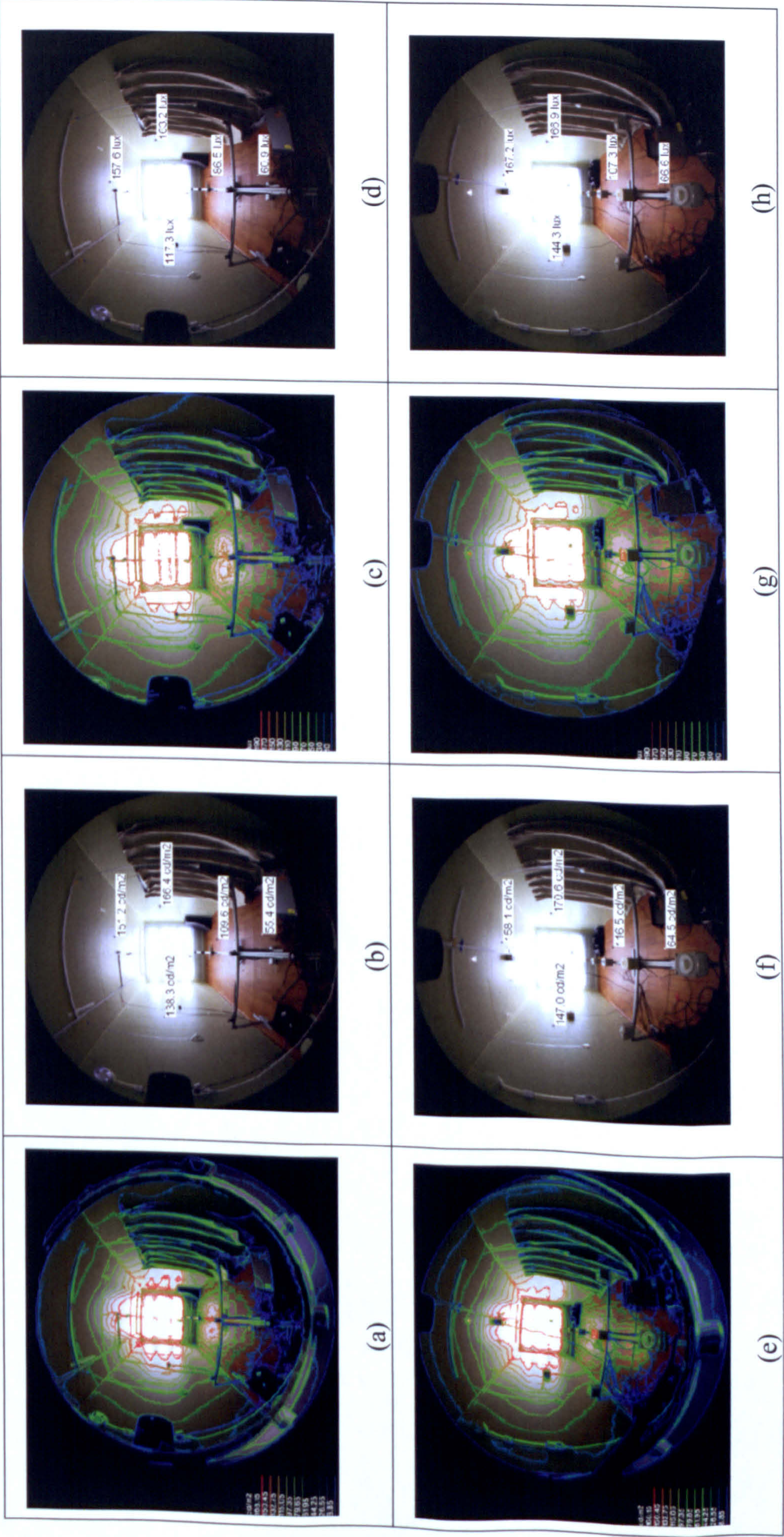


Figure 4. 43 Luminance and illuminance distributions without [(a),(b), (c), (d)] and with [(e), (f), (g), (h)] at 4:00pm

As previously done for the Nottingham test chamber and the office space in Jeju, simulations are performed using RADIANCE. Figure 4. 44 shows a general view of the model image of the test cell to be used for RADIANCE simulation whereas its transparent perspective view is given in Figure 4. 45.

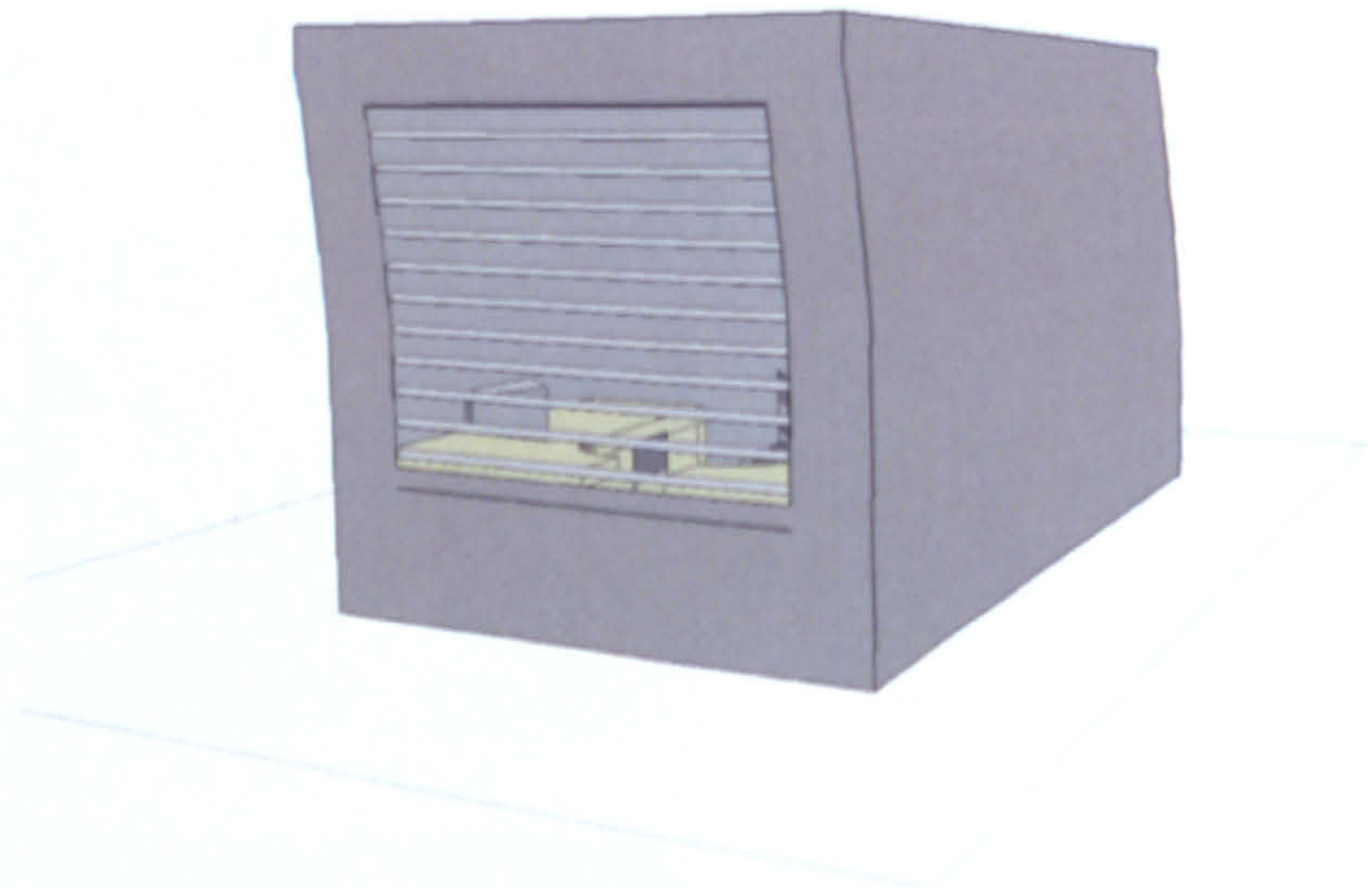


Figure 4. 44 A general view of the model image of the test cell for RADIANCE simulation.

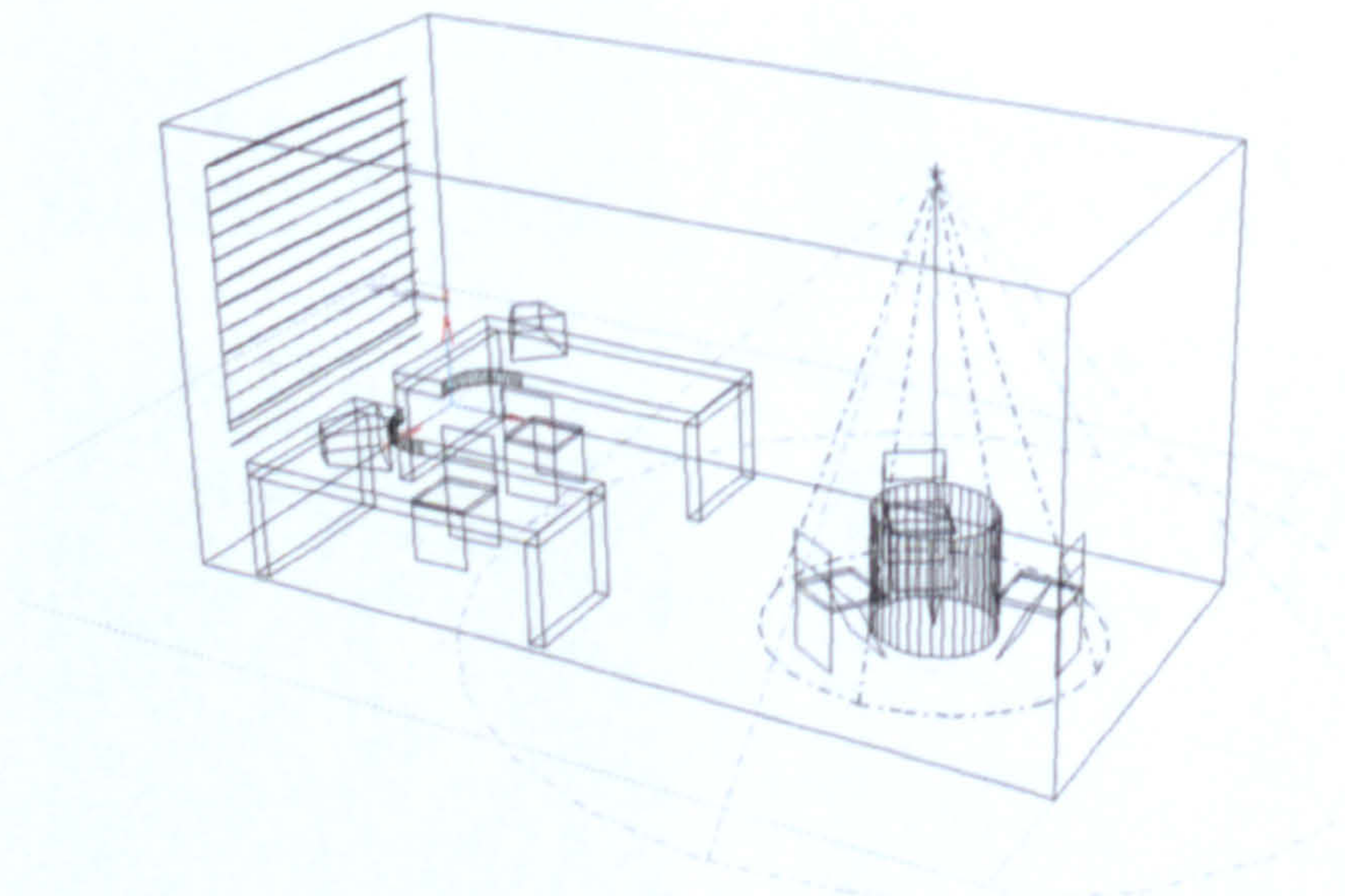


Figure 4. 45 A perspective view of the model image for RADIANCE simulation.

Figures 4. 46 ~ 4. 55 are the results of RADIANCE simulation at different times of the day (9am, 10:30am, 12:00pm, 2:30pm and 4:00pm) with the slats tilted downward at 45 degrees. It is assumed that the test cells are located in Seoul (Latitude: 37.5°, Longitude: 126.9°E) and the amount of light (total lumens) emerging from the diffuser (of the applied daylighting system) is based on the measured values on a typical clear day (October 6, 2009). The figures present spatial distribution of luminance and illuminance values at a number of points on different surfaces along with their contour maps and false color images. The results given are prepared using the images rendered by Radiance. At each hour, the luminance (a) and illuminance (c) contours are given along with their values at a number of selected locations: (b) luminance, (d) illuminance. Also, false color images are given for luminance (e) and illuminance (f) distributions, where a range of colors is assigned to a range of luminance (or illuminance) values. The same set of figures are prepared for both test cells without (Figures 4. 46, 48, 50, 52, 54) and with (Figures 4. 47, 49, 51, 53, 55) the daylighting system (using a 30cm dish concentrator).

Figures 4. 46 and 4. 47 present images of the indoor lighting conditions of the model test cells at 9am. There is quite a contrast in the density of the luminous flux and brightness between the area (on the desk plane) near the window and away from it, especially, on the task plane (round table top), Figure 4. 46. The predicted illuminance of 215.8 lux at the desk plane is more than four times than that at the task plane. It deems impossible to procure a balance between the light levels of these areas if no additional lighting is provided. In Figure 4. 47, some good improvements are shown for the indoor lighting conditions as compared to Figure 4. 46. As sunlight is introduced into the poorly illuminated areas away from the window, both luminance and illuminance values markedly increase to attain 98.8 cd/m² and 374.7 lux, respectively. This is well presented by the false color images, (e) and (f), in these figures.

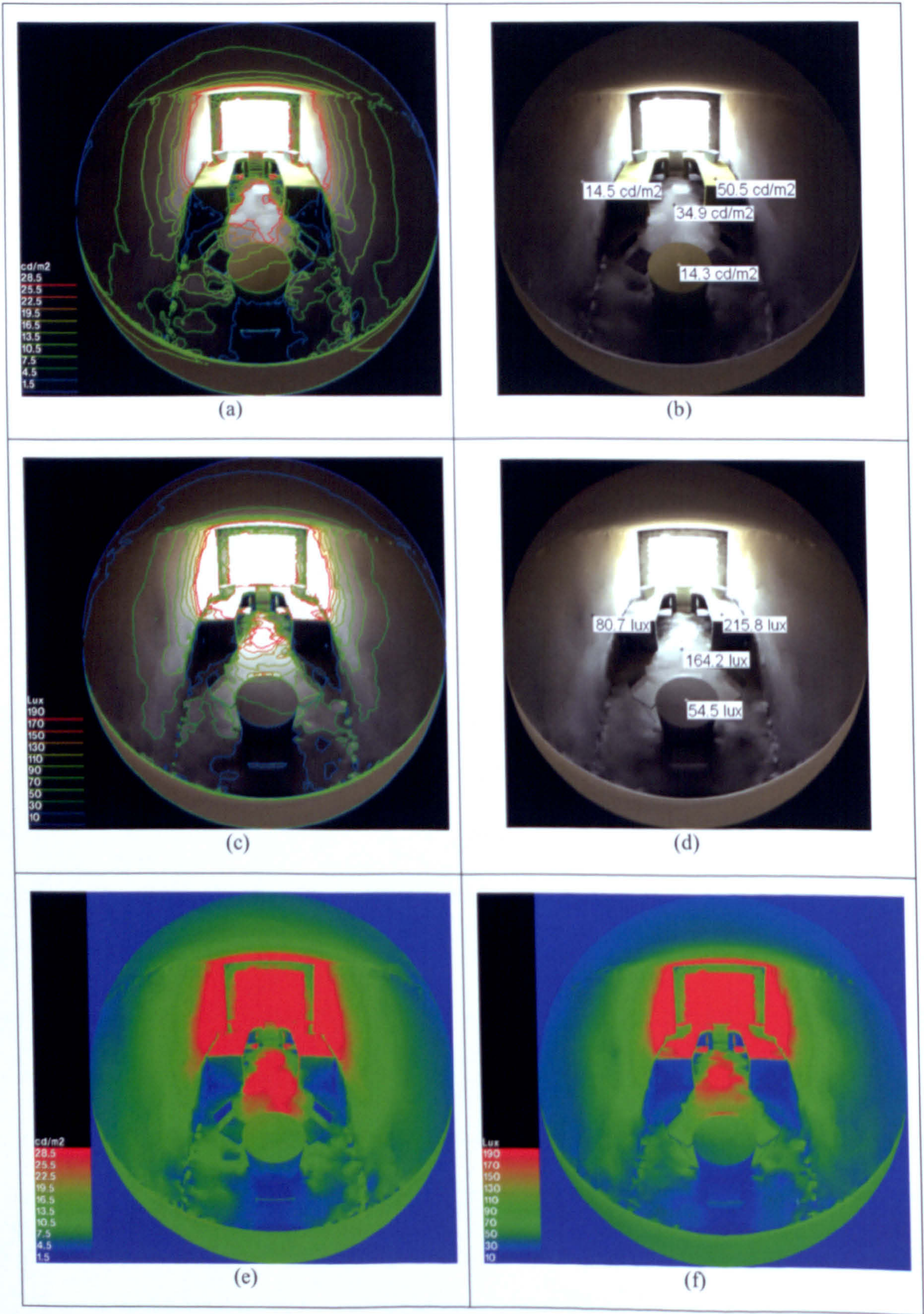


Figure 4. 46 Luminance and illuminance distribution superimposed on the rendered image by RADIANCE (without the daylighting system) : 9:00am

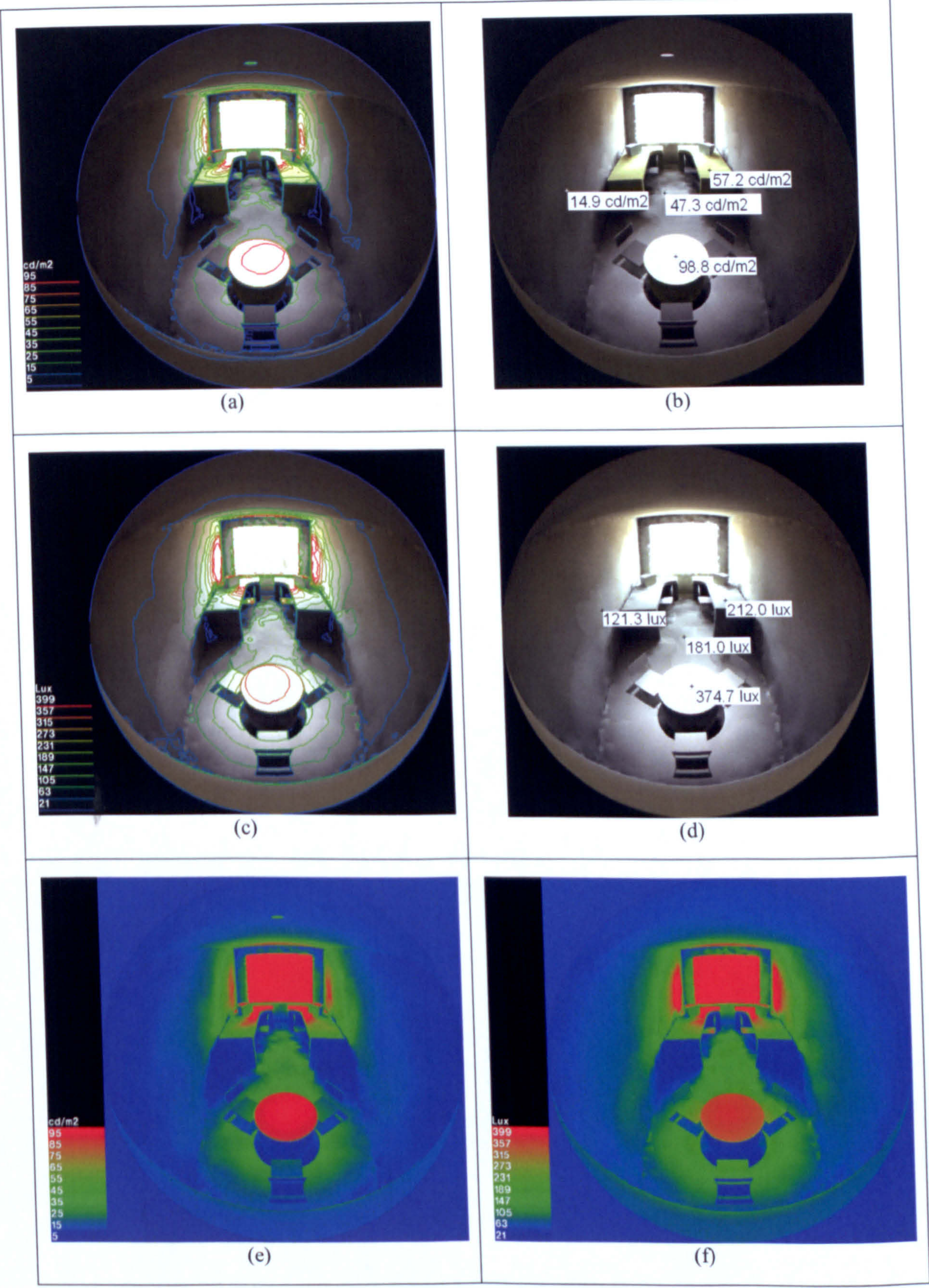


Figure 4. 47 Luminance and illuminance distribution superimposed on the rendered image by RADIANCE (with the daylighting system) : 9:00am

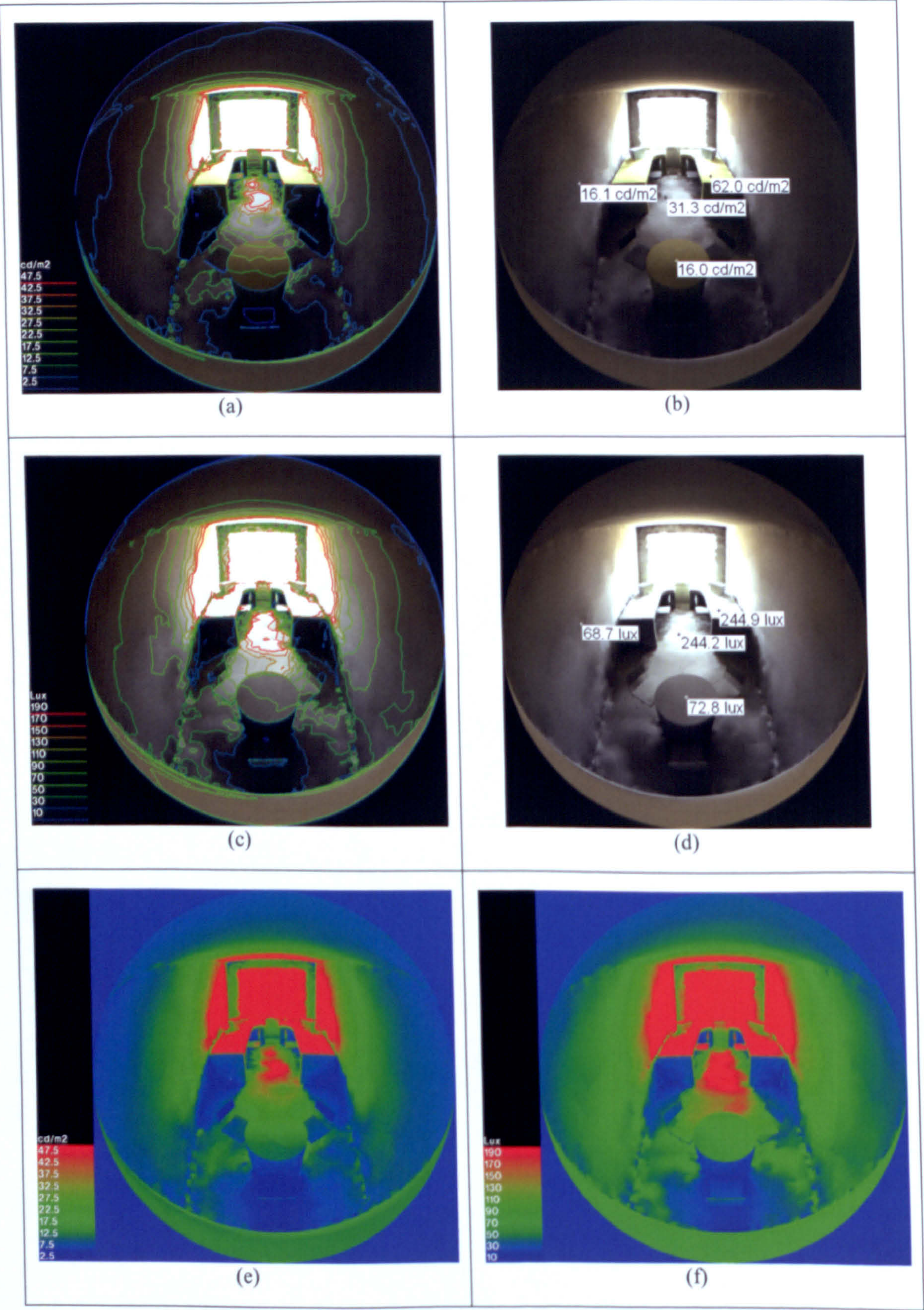


Figure 4. 48 Luminance and illuminance distribution superimposed on the rendered image by RADIANCE (without the daylighting system) : 10:30am

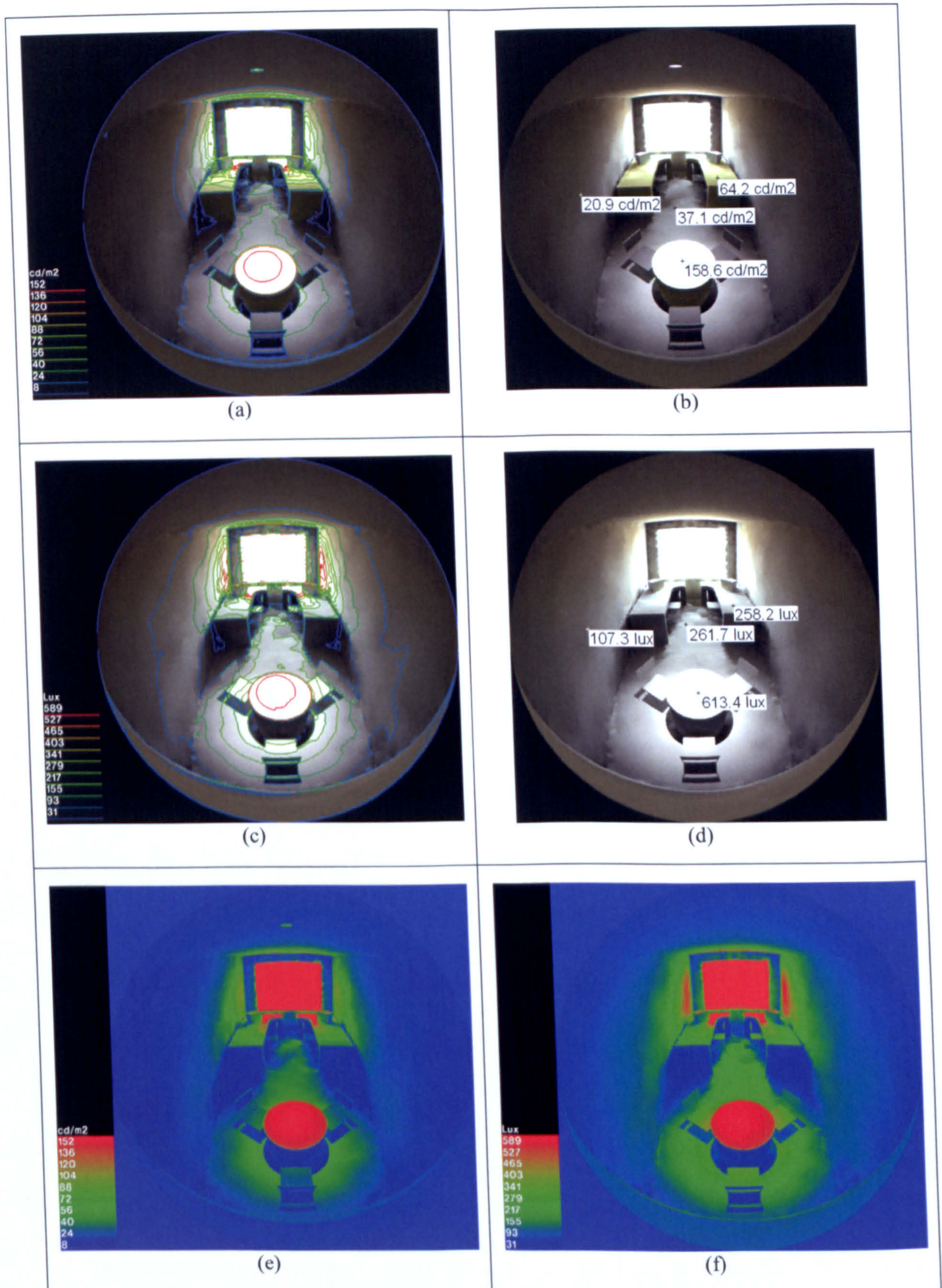


Figure 4. 49 Luminance and illuminance distribution superimposed on the rendered image by RADIANCE (with the daylighting system) : 10:30am

As daylight is captured and introduced from top via the present dish-daylighting system, it provides greater freedom of source placement to achieve more uniform illumination and takes advantage of high wall surfaces and other architectural elements to distribute light where needed. It also adds flexibility in daylight utilization strategy of a deep interior space where light rays admitted through the window fail to furnish adequate lighting conditions despite a number of internal reflections on highly reflective surfaces. Figures 4. 48 and 4. 49 further demonstrate the effect of applying the present daylighting system. As compared to the cases at 9am (in the previous figures), more daylight is available to illuminate the rear space of a room. The predicted luminance and illuminance values reach 158.6 cd/m^2 and 613.4 lux , respectively. This is quite an increase over a span of 1.5 hours, which reflects the effect of reduction in air mass representing the optical path length through which beam radiation takes as it traverses the atmosphere.

In general, the luminance and illuminance values are higher for the cell, which has the daylighting system to introduce additional daylight for indoor illumination. That is, the infusion of daylight by the dish-daylighting system provides a sufficient amount of light to the task plane. Especially, there is quite a difference on the task plane (a round table on the north side of the room). Differences in luminance and illuminance reach their peaks at noon, amounting to 696.5 cd/m^2 and $2,703.5 \text{ lux}$, respectively. Also, since our daylighting system constantly tracks the sun, the illuminance on the working table is kept over 350 lux . It fluctuates from 374 lux at 9:00am to $2,769 \text{ lux}$ at noon. The latter is, of course, too much to establish a healthy visual environment. Some measures are necessary to control its intensity and to prevent any glares developed by surge of sun rays during bright sunshine hours. A simple attenuator could be installed just before the light exits the emitter (optical lens). Rather than using a circular optical lens, other designs could also be considered to spread light more evenly and widely.

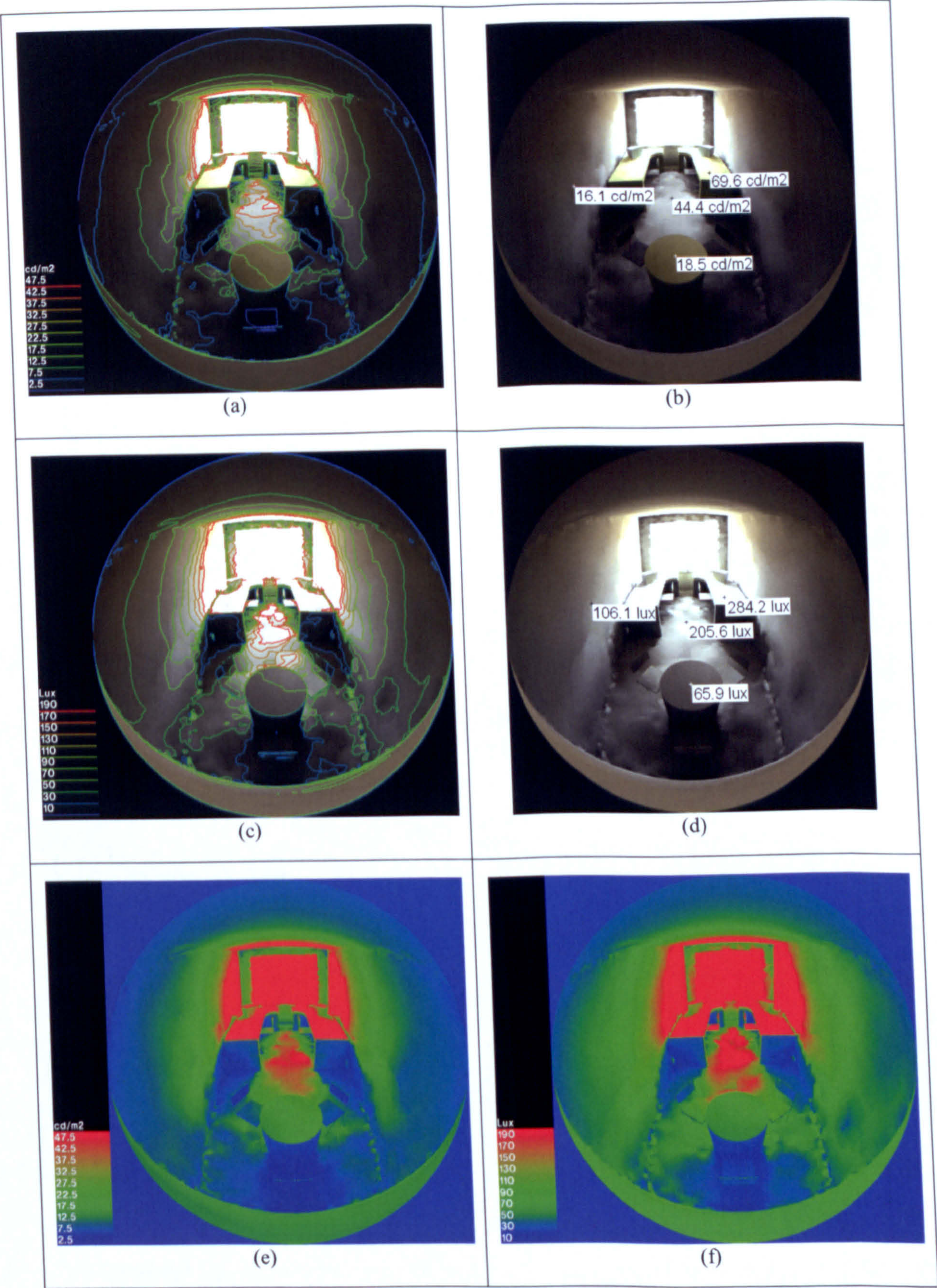


Figure 4. 50 Luminance and illuminance distribution superimposed on the rendered image by RADIANCE (without the daylighting system) : noon

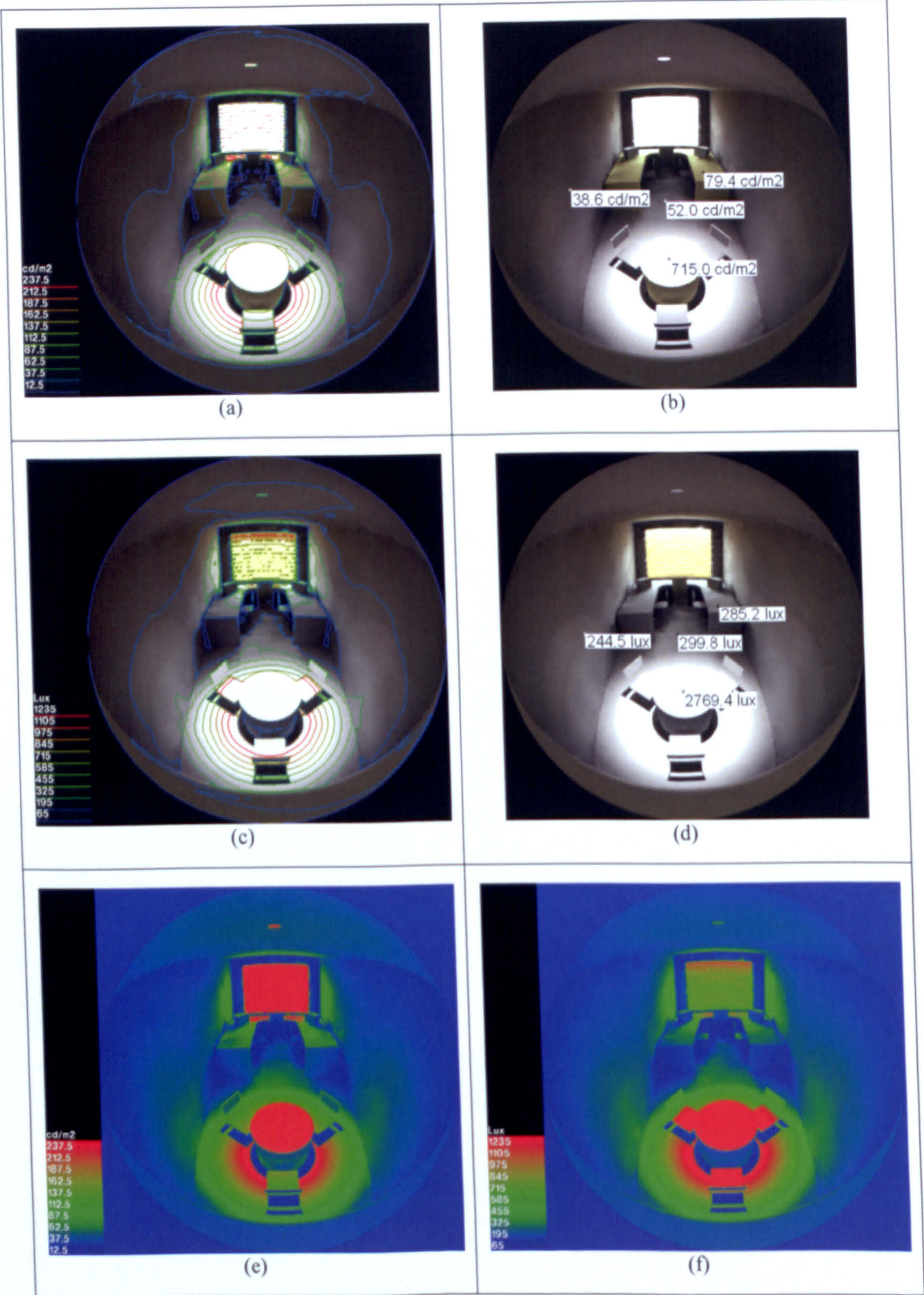


Figure 4. 51 Luminance and illuminance distribution superimposed on the rendered image by RADIANCE (with the daylighting system) : noon

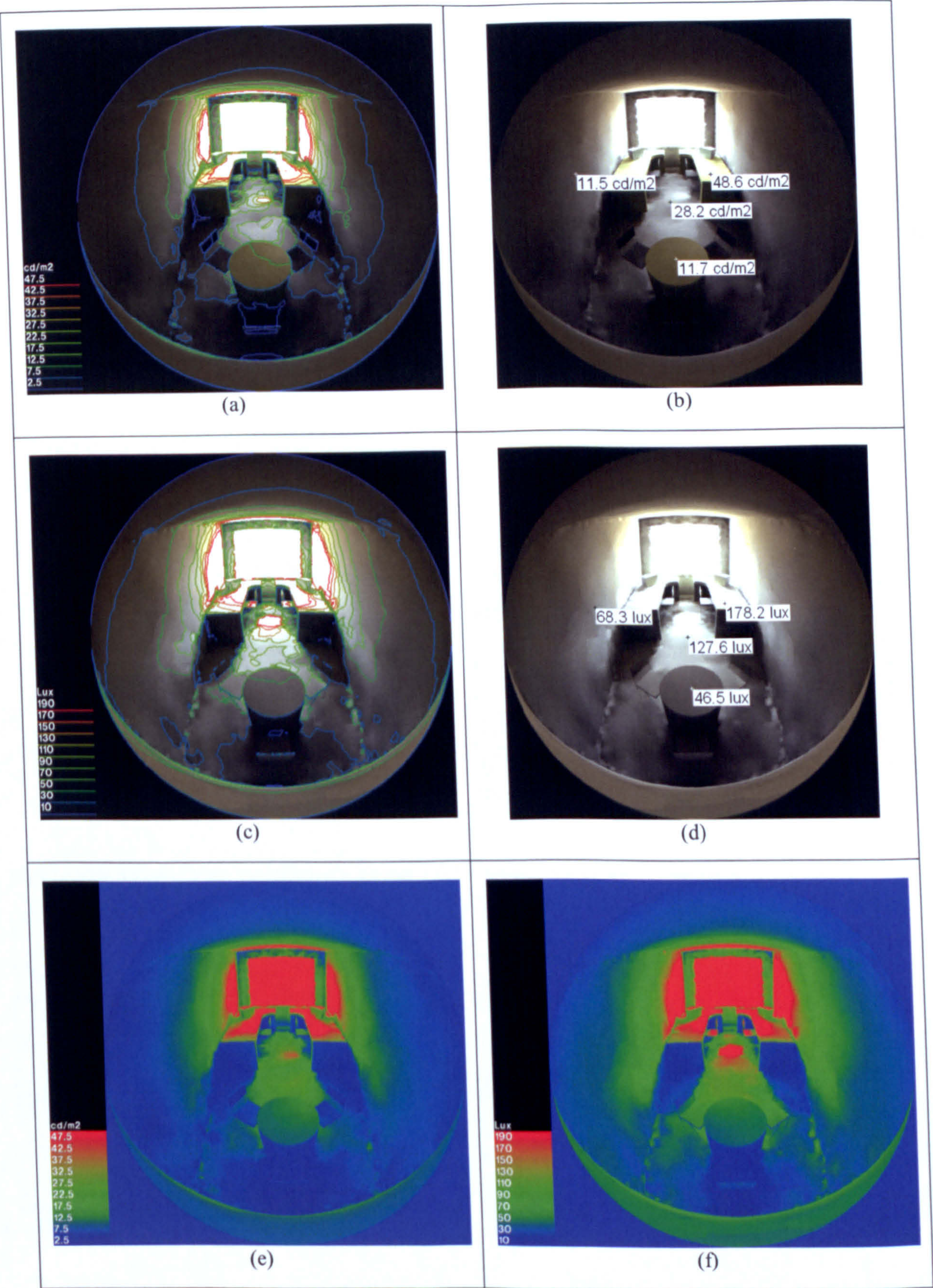


Figure 4. 52 Luminance and illuminance distribution superimposed on the rendered image by RADIANCE (without the daylighting system) : 2:30pm

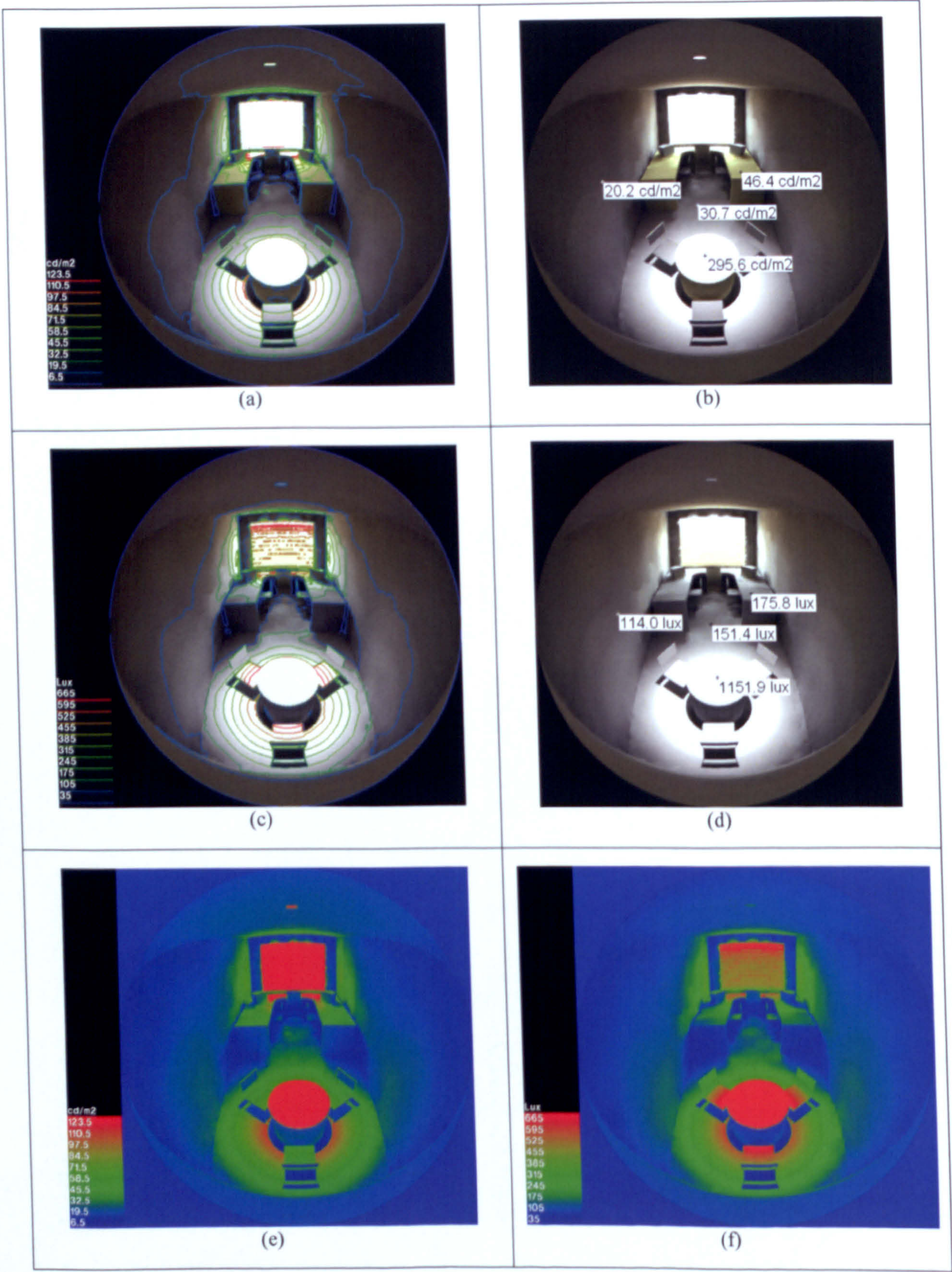


Figure 4. 53 Luminance and illuminance distribution superimposed on the rendered image by RADIANCE (with the daylighting system) : 2:30pm

The present model vividly demonstrates the light transmittance and overall daylighting performance of a window-venetian blind system in relation to the operation of a dish-daylighting system. Throughout the hours of analysis, there isn't enough solar penetration into the space due to the slats of the venetian blinds. Interior areas adjacent to the window aperture showed the highest levels of luminance and illuminance due to sunlight admittance from outdoors. However, moving further away from the window, this changes drastically. The luminance and illuminance values drop off quite sharply as presented by a number of reference point values, countour maps and false color images.

Sunlight is mostly blocked from entering the test cell. Especially, on the working table, the illuminance level is too low for performing any task (for the test cell without the daylighting system). If there were no shading (venetian blinds) installed on the south window, excessive contrast could be developed due to flooding of sun rays through the window.

As shown previously in Figures 4. 31 through 4. 37, venetian blinds used as interior shading devices allow versatility in the control of daylight transmission. Changing the slat angle of the blind should result in varied transmittance, especially on clear days when direct sunlight can be blocked. In addition, pull down and withdrawal of venetian blinds would also affect the indoor visual environment as much as adjustment of blinds' slat angle in link with the functional operation of a daylighting system.

Achieving uniformity and excessive glare control appear to be the most important and pending technical issues to be resolved in applying the present dish-daylighting system as it is likely to develop a brighter area compared to the rest of the room. Deploying a number of units at the PASLI (Permanent Supplementary Artificial Lighting of Interiors) zone could be considered as one of the practical approaches. In addition, there's always the use of the hybrid lighting concept (daylight-linked lighting control systems), which will be discussed in the next section.

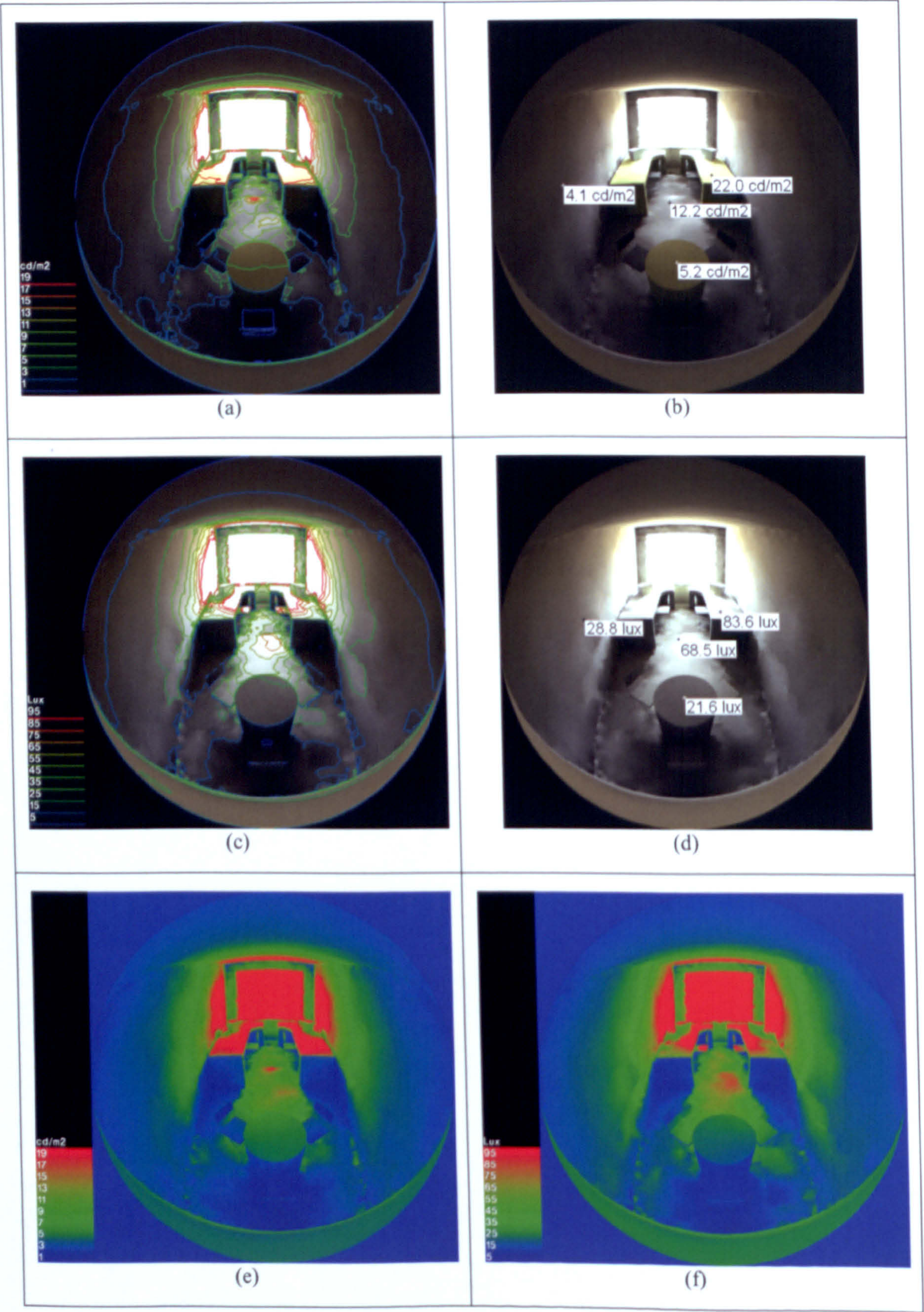


Figure 4. 54 Luminance and illuminance distribution superimposed on the rendered image by RADIANCE (without the daylighting system) : 4:00pm

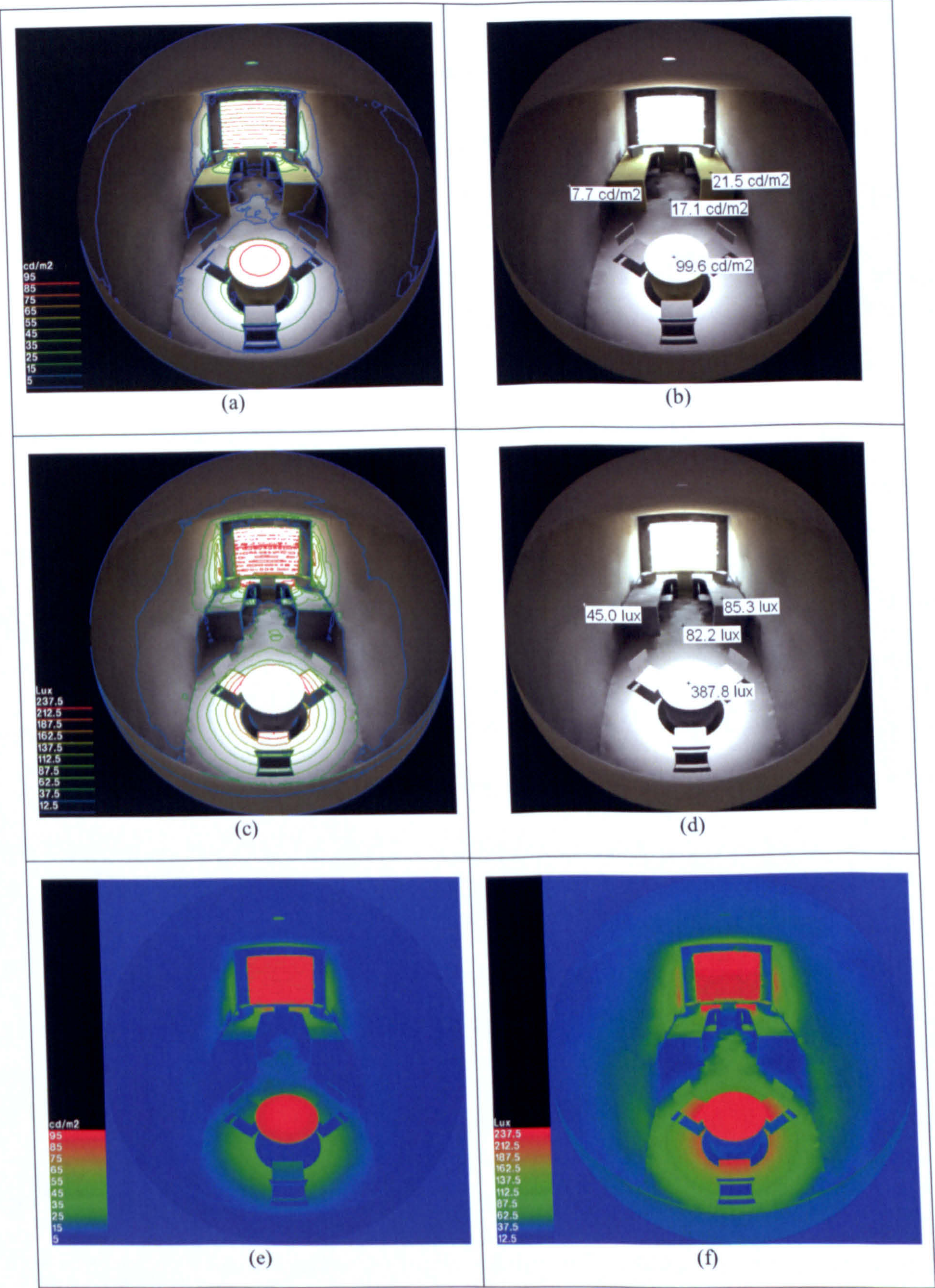


Figure 4. 55 Luminance and illuminance distribution superimposed on the rendered image by RADIANCE (with the daylighting system) : 4:00pm

4.3.6 Hybrid lighting

To find the optimal combination of a building and its lighting control system, one should, first of all, analyze the uses and functions of the said space, and then choose the light control strategy that would support this intent. Although light is indispensable for a space to function properly, providing a sufficient amount is often quite a difficulty. Thus, to promote space flexibility and to save energy, lighting control is an important design tool. This is because applying only the minimal light control would waste energy as unused lights are kept on. The effective combination of the benefits of sunlight with the consistency of conventional electric lighting is thus critical for the improvement of a building's energy efficiency.

Using daylight harvesting is a good way to balance electric and natural lighting. A reason for this is that it automatically lowers electric light levels in the presence of daylight and increases them when there is less daylight. In doing this, daylight harvesting saves energy; it supplements the daylight available with electric lighting, maintaining the visual ergonomics of the space by emitting the appropriate amount of light onto the desktop.

The sensor is essential; it detects the amount of daylight available then signals a controller, which then lowers or heightens the lighting as needed. The desired lighting conditions can be selected for the threshold on and off values. These sensors are able to switch on/off a variety of luminaires (illuminants) or lamps within them. They are also capable of running a continuous dimming system.

The placement of the sensors is important as much as the number of sensors used in achieving adequate control of indoor lighting. The reason is because it influences the type of control algorithm being utilized. In many cases, the photoelectric cell or sensor is often placed on the ceiling and calibrated on site to keep the level of illuminance constant. If a daylighting system is to be innovative, it should simultaneously consider both sky conditions and direct sunlight admitted through various openings of the building.

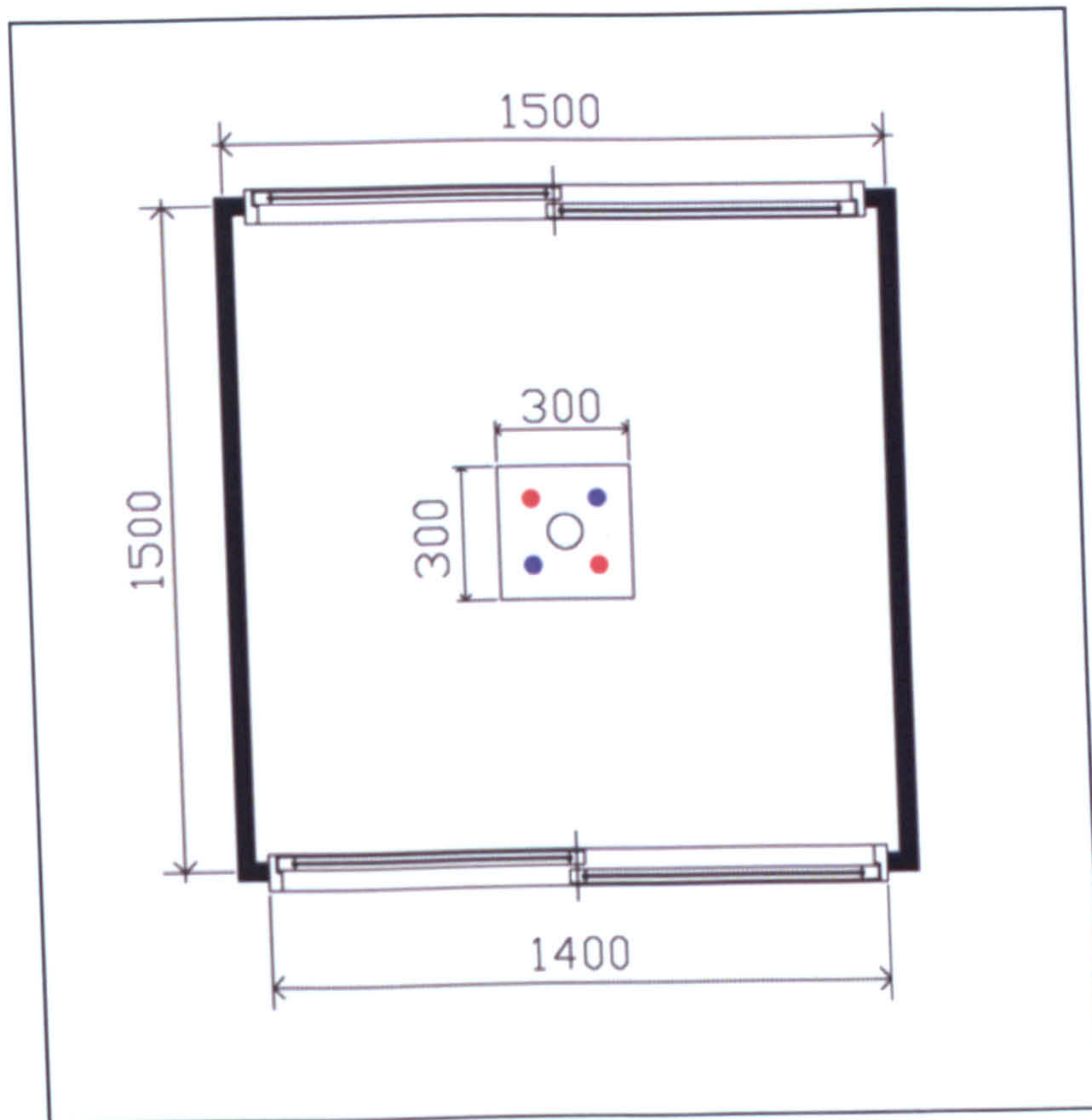


Figure 4.56 A test cell built for hybrid lighting (dimming control) : plan view and venetian blinds installed for the window

Figure 4.56 shows a plan view of the test cell and its actual photo to test dimming control when applying a daylighting system. It has the shape of a cube with a dimension of 1.5m x 1.5 m x 1.5m. The figure shows two dish-daylighting system installed on top of the test cell where its terminal devices (light diffusers) are symmetrically mounted with two 25W halogen lamps on the ceiling. Figure 4.57 shows the location of sensors on the floor and dimming control on the ceiling. Nine sensors are located at a height of 40cm at an interval of 50cm. The dimmer was manually adjusted to find the optimal range of operation with the daylighting system installed.

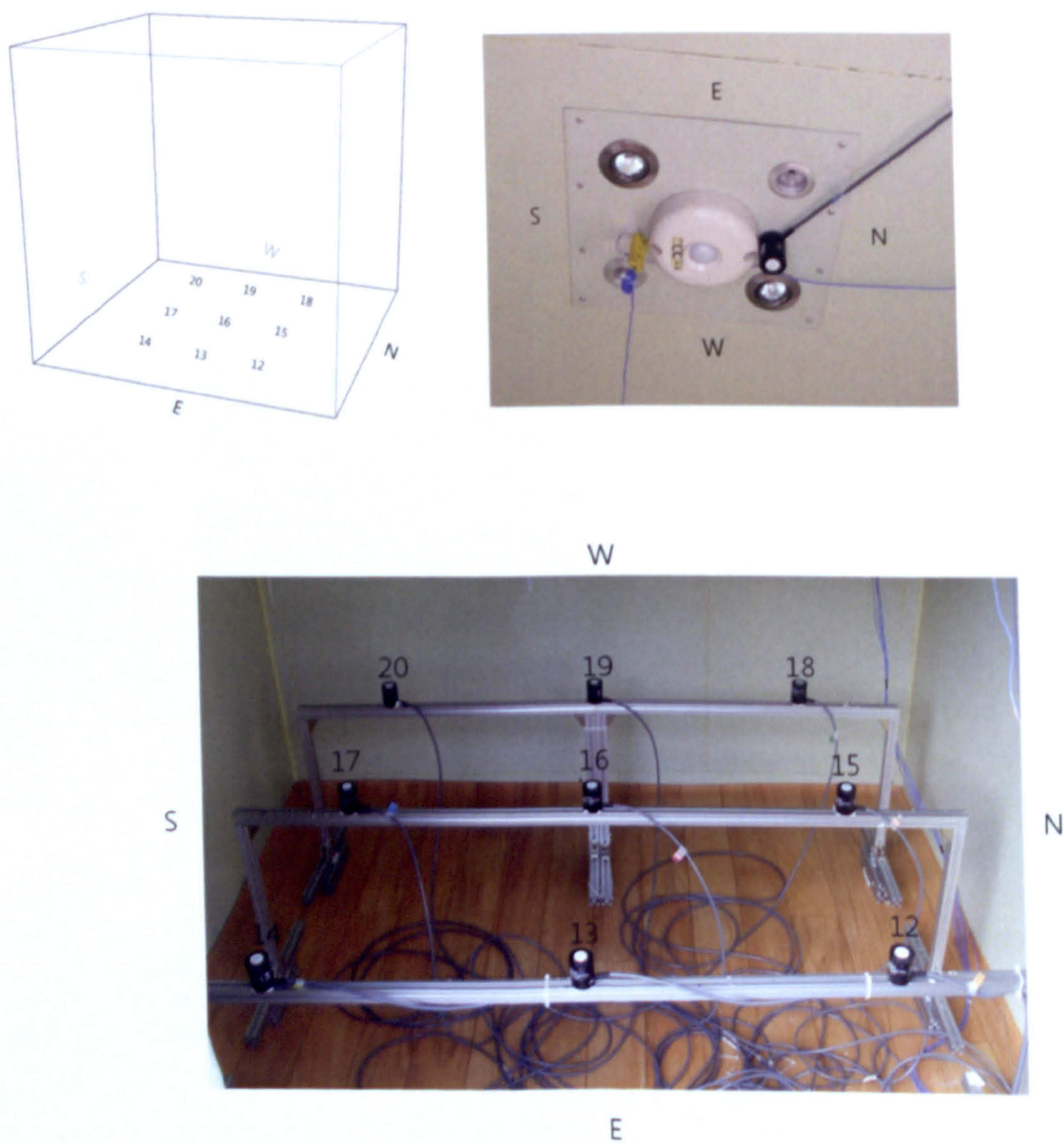
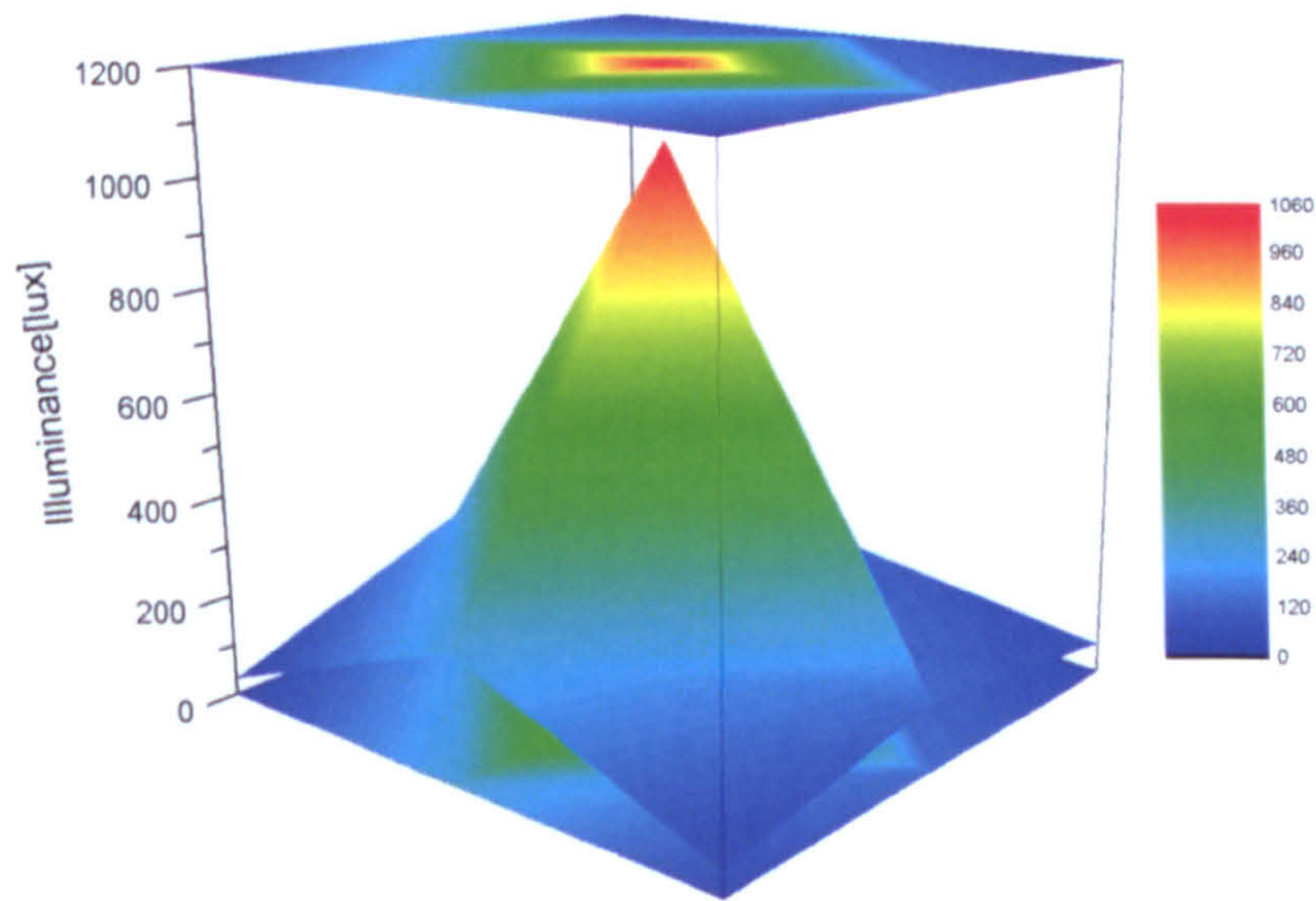
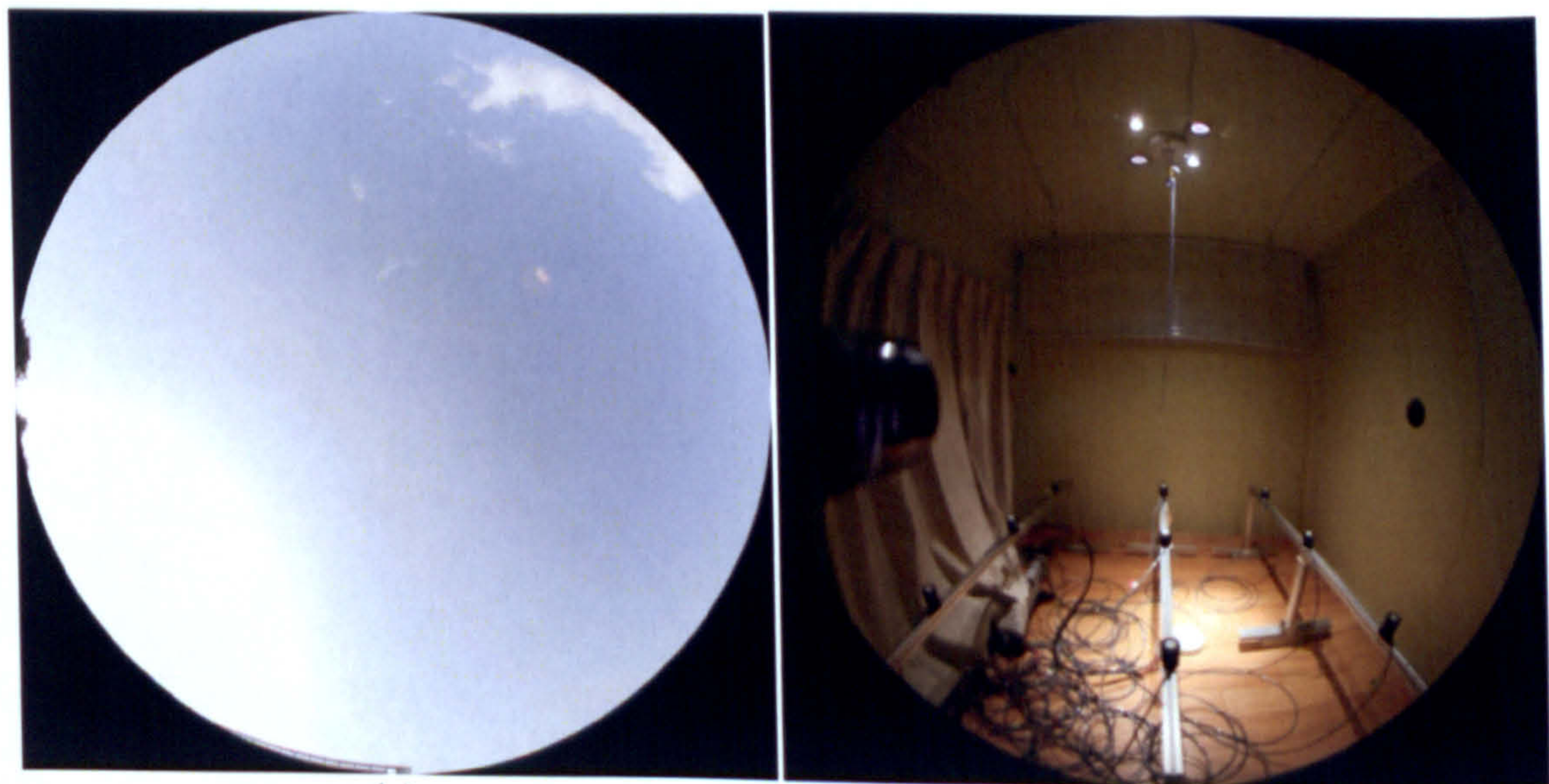


Figure 4.57 Location of sensors on the floor and dimming control on the ceiling

Figure 4.58 gives a 3D contour of iso-illuminance map when the daylighting system was in operation . The plot was prepared when the global Illuminance on a horizontal surface was measured at 99,634 lux.



(a)



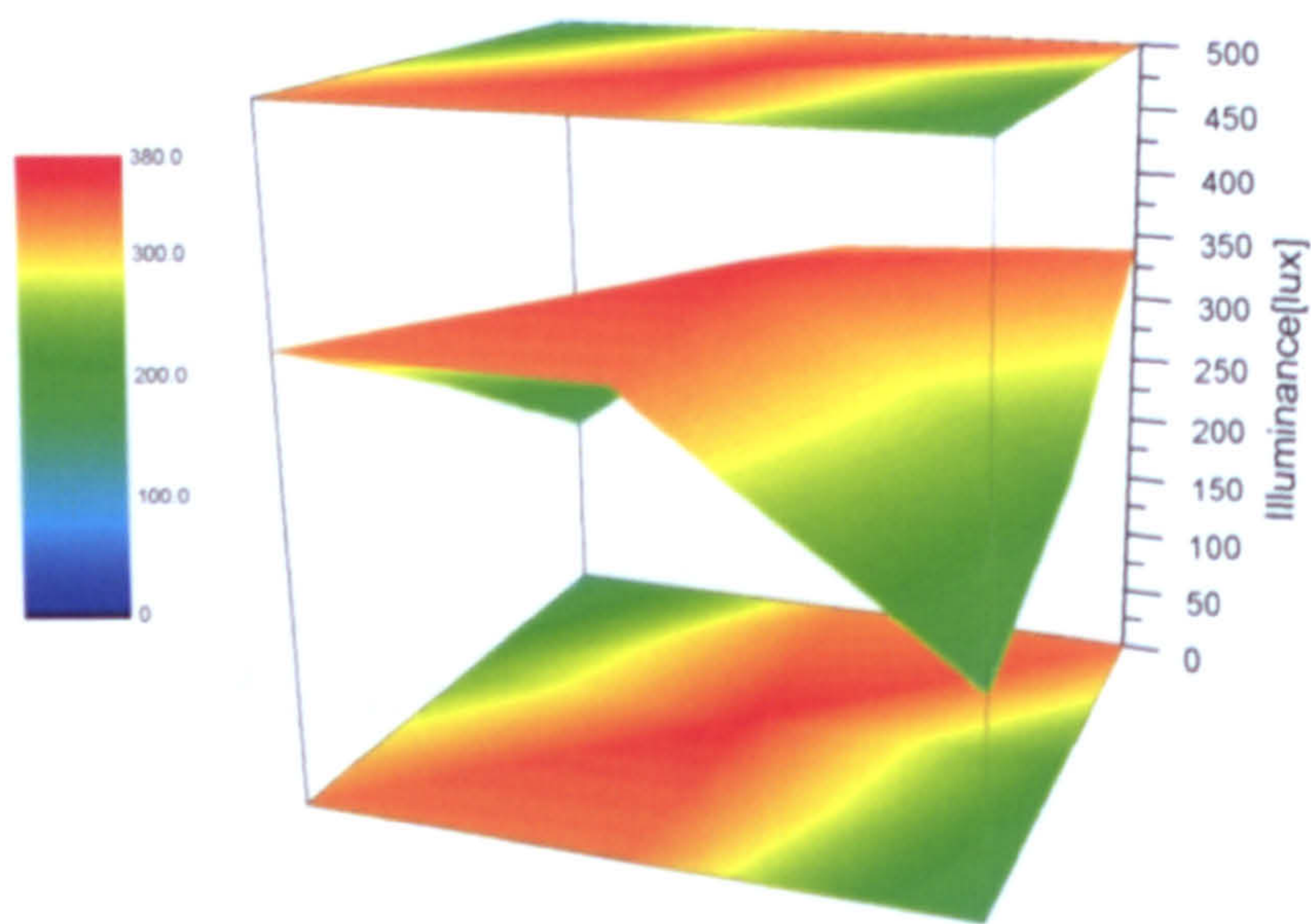
(a)

(c)

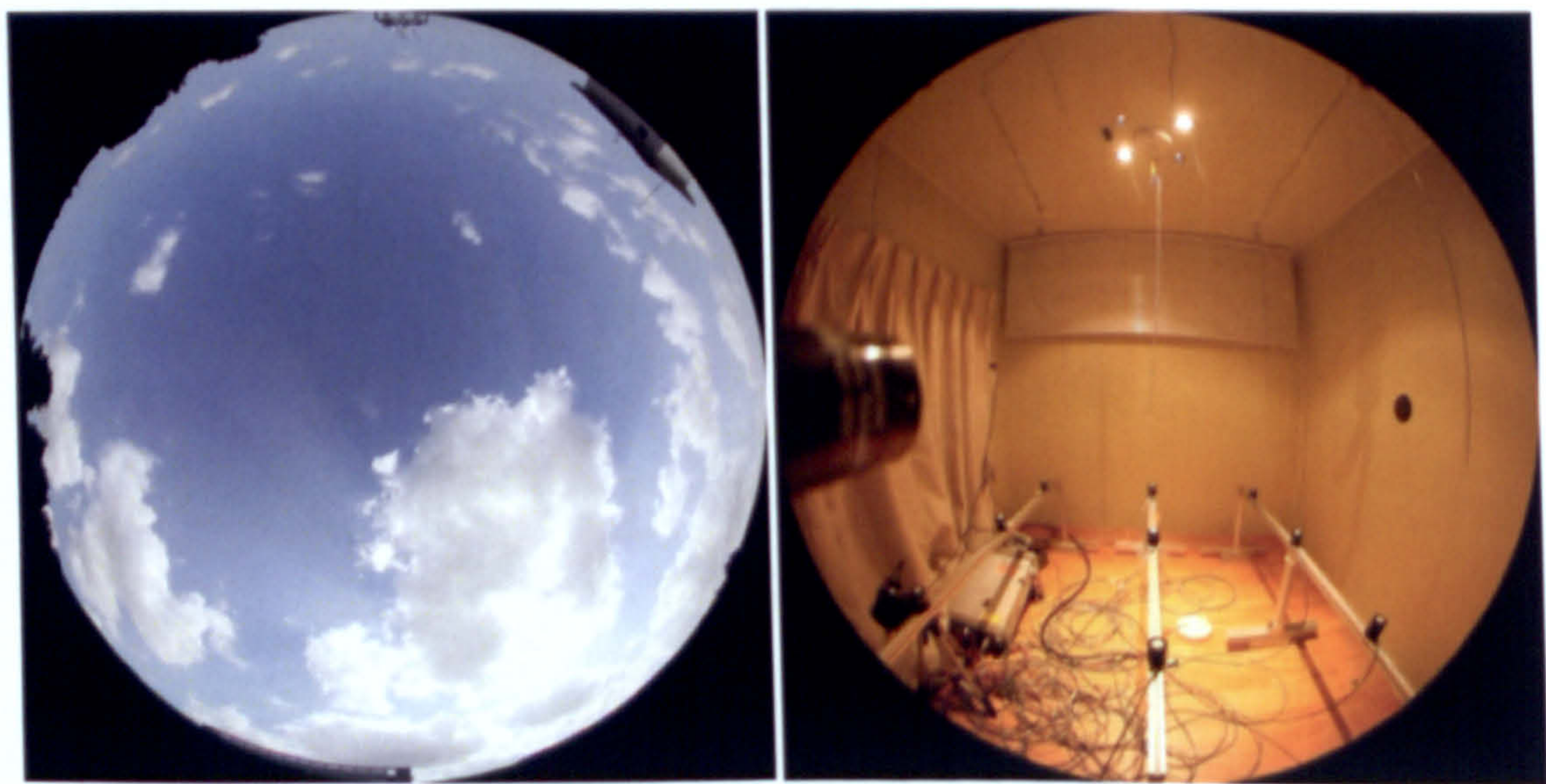
Figure 4.58 Actual illuminance of the test cell when lit by the daylighting system:

- (a) Iso-illuminance contour, (b) sky condition when measured,
- (c) actual interior view when lit

Figure 4.59 shows a 3D contour of iso-illuminance map when the artificial lighting system was in operation for a cloudy sky. The plot was prepared when the global Illuminance on a horizontal surface was measured at 25,288 lux.



(a)



(b)

(c)

Figure 4.59 Actual illuminance of the test cell when lit by the artificial lighting system:
(a) Iso-illuminance contour, (b) sky condition when measured,
(c) actual interior view when lit

As shown in the above figures, Figure 4.58(a) and Figure 4.59(a), there is quite a difference between the indoor lighting environments created by the daylighting and artificial lighting. Especially, the maximum illuminance measured directly below the luminaire shows a fluctuation of more than 500lux, which is definitely beyond an acceptable range. That is, too much sunlight is introduced through the diffuser in clear sky conditions as no measures were considered to control its flow via optical fiber cable.

This, however, could be easily adjusted manually or automatically, which allow more flexibility in fulfilling the needs and requirements of occupants with different preferences. Especially, the illuminance levels could be controlled in accordance with the outdoor conditions by using a number of light sensors and control units to check flow of light streams from the diffuser. The following shows one of such schemes:

- Place a sensor (sensor #1) on the window to measure outdoor illuminance.
- Place a sensor (sensor #2) on the window to measure indoor illuminance.
- Place a sensor (sensor #3) on the opposite side of the wall farthest from the window.
- Install a dimmer unit with four light blocking covers operated by an electronic circuit unit controlling the DC motor to place an appropriate cover for the diffuser on the ceiling:

Figure 4. 60.

- Compare the voltage output from the sensors #1, #2 and #3.

(if the compared reading of sensor outputs is beyond a preset range, it activates the dimmer unit - DC motor control module).

- Control the amount of light emanating from the diffuser
 - When the difference between sensor #1 and #2 is large (beyond a preset value), no blockage (attenuator) is used.
 - If sensor #1 is within a preset range (e.g., 70,000~80,000 lx) or sensors #2 and #3 read output beyond a preset range (too bright), block one diffuser using a cover.

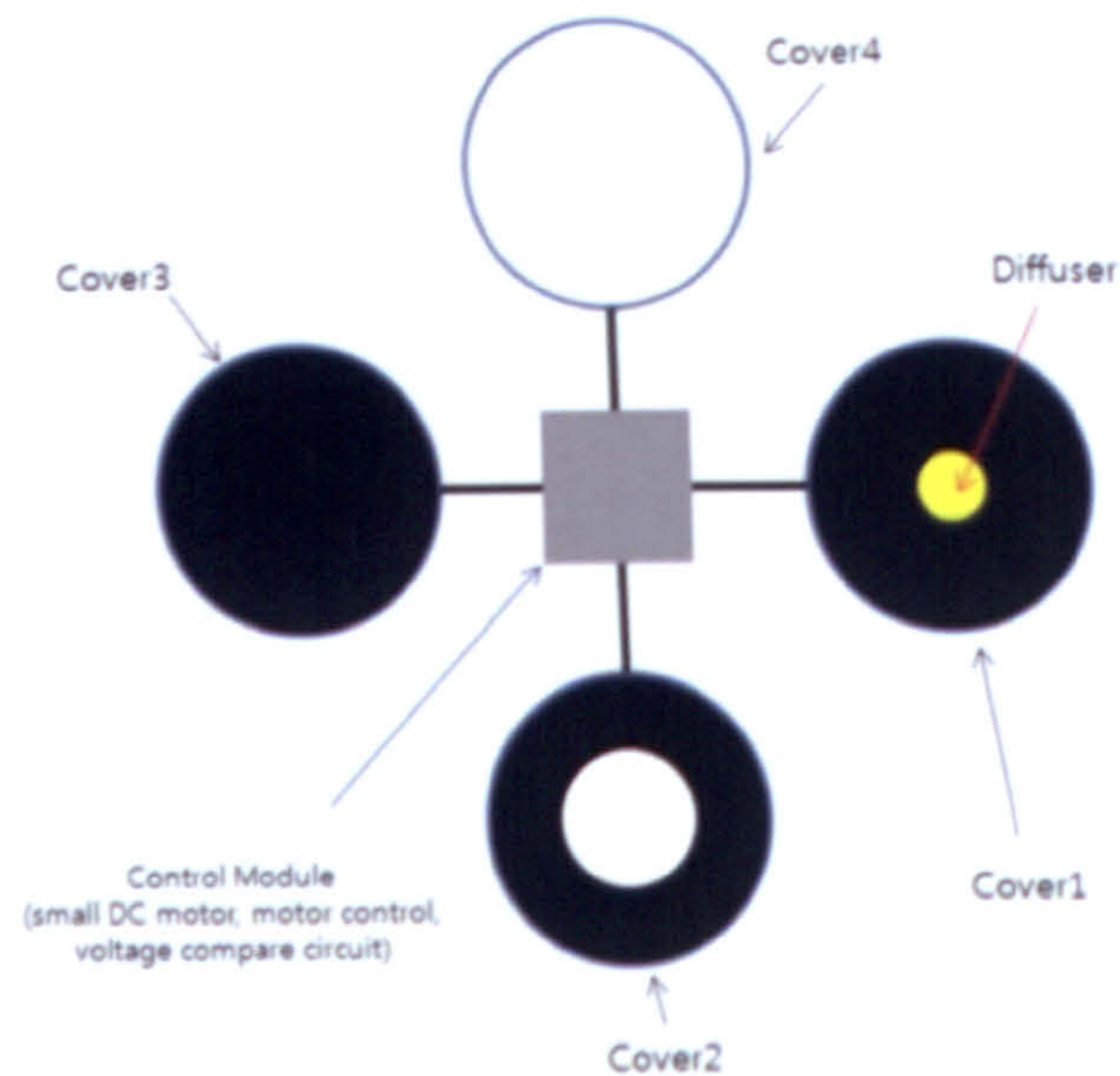


Figure 4. 60 A dimmer unit with four light blocking covers : covers 1 , 2
 – partial blocking, cover 3-complete blocking, cover 4 – no blocking

The system described so far has used a rather simple approach in utilizing daylight in link with a conventional electric lighting system. Apart from this, however, the control system may be designed to regulate the flux output of each source and light from the two sources could be delivered using separate output components whose photometric properties may differ significantly. In any case, daylight is combined with electric light prior to delivery in hybrid lighting and it is very important to select the right electric luminaire (source) that is akin to daylight. Its color temperature (or CRI), light intensity and uniformity should be comparable with daylight to achieve hybrid lighting in an ideal way. Here CRI refers to the color-rendering index, which compares the color content of a light source with daylight. The maximum value of 100 is given for a perfect match with daylight.

Because of the limited dimming capability of our system, variation in output was achieved by manual switching. This, however, put a limit on timely response to match the speed which could compensate in real time for quick variations in the external illuminance. This suggests that the success of hybrid lighting depends on both the nature of light source as well as the technology to synchronize its functional operation in harmony with natural daylight.

4.3.7 A comparative analysis using Radiance (for Seoul and London)

The model now has been extended to predict luminance and illuminance distributions for the model test cell if located in UK (London: 51.5°N, Longitude: 0.126°W) and Korea (Seoul : Latitude: 37.5°N, Longitude: 126.9°E). Seoul and London are chosen here for the seasonal analysis of applying the dish-daylighting system as they are the representative cities of Korea and Seoul. Moreover, the weather data were available for computer simulations.

Figures 4. 61 ~ 4. 76 are the results of RADIANCE simulations at noon for March 20 (vernal equinox), June 21(summer solstice), September 22(autumn equinox) and December 21 (winter solstice). Here it is assumed that venetian blinds are installed inside the south window with slat angles tilted downward at 45 degrees. Also, the amount of light (total lumens) emerging from the diffuser (of the applied daylighting system) is based on the measured values on a typical clear day (October 6, 2009) in link with the beam component of solar radiation from the weather data of ECOTECH (Weather Tool).

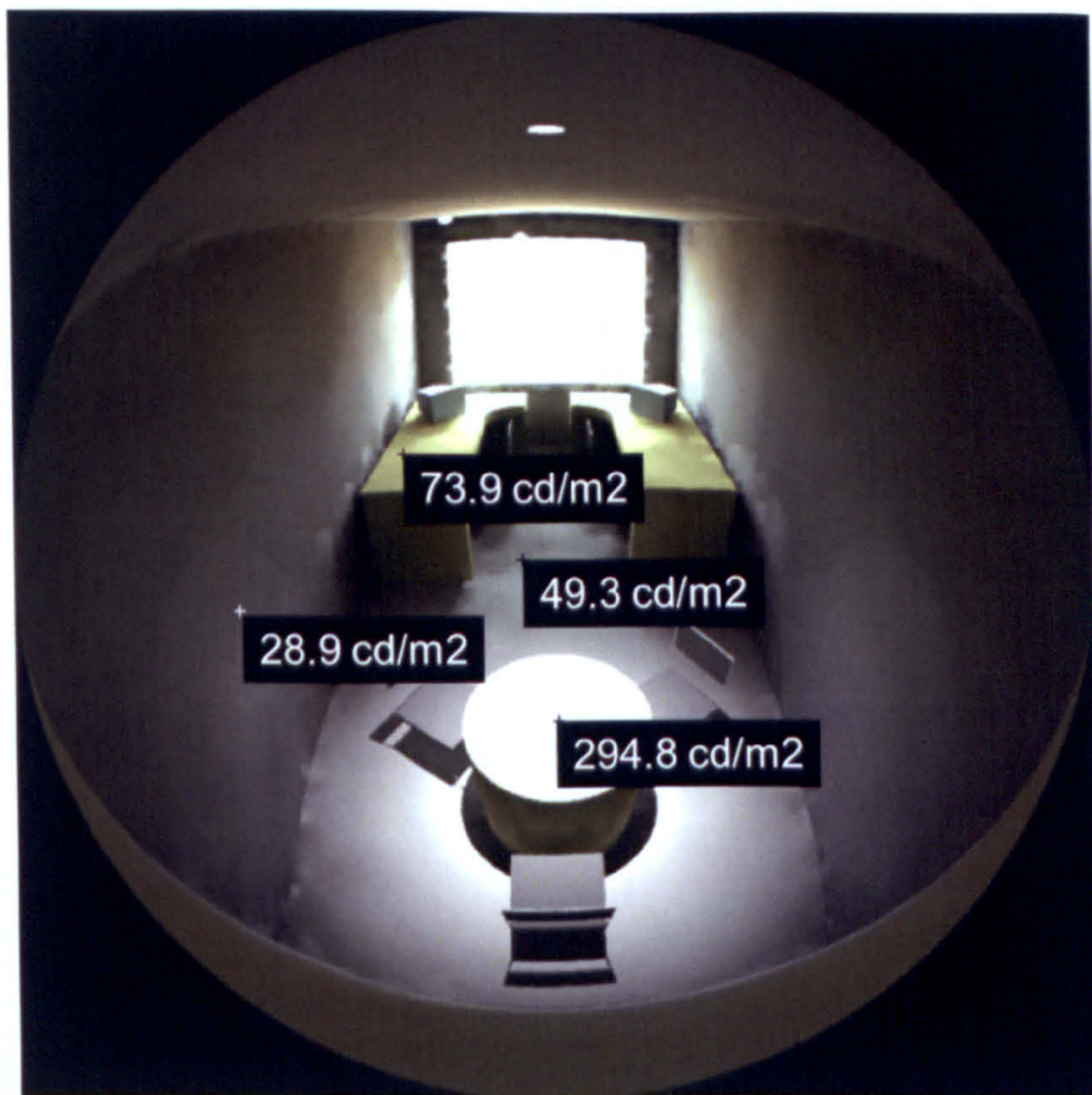
Table 4. 4 Solar radiation data for Seoul and London at equinoxes and solstices at noon

City	Season	Date	Time	Direct Beam Radiation [W/m ²]
Jeju (reference)	Autumn	10/6/2009	12:00	796
Seoul	Spring	3/20	12:00	165
	Summer	6/21	12:00	520
	Autumn	9/22	12:00	395
	Winter	12/21	12:00	150
London	Spring	3/20	12:00	320
	Summer	6/21	12:00	40
	Autumn	9/22	12:00	150
	Winter	12/21	12:00	140

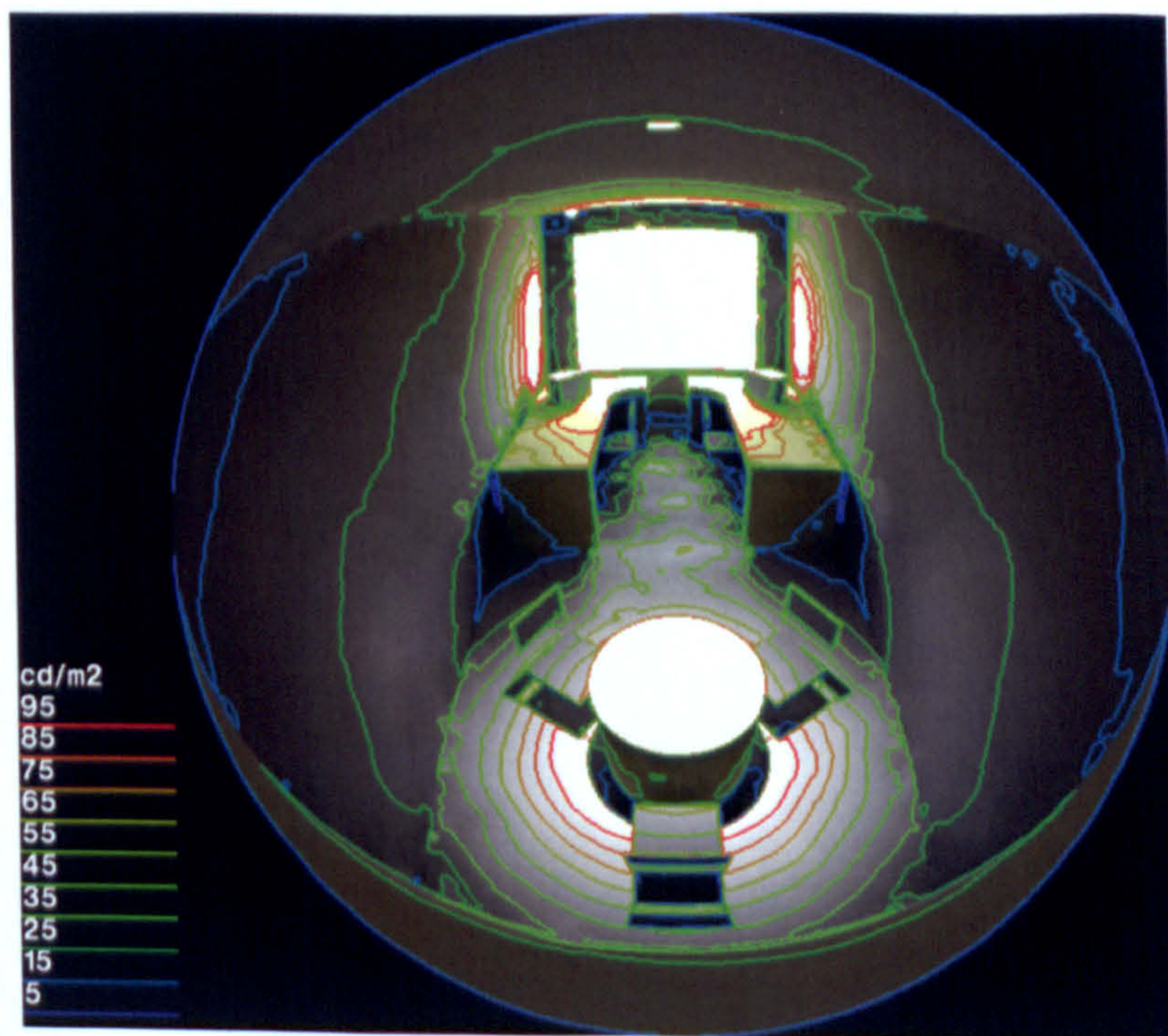
This was the only option available to carry out the simulation for those specific days (equinoxes and solstices) mentioned above as measured illuminance data could not be obtained. In the ECOTECH's weather file library, the beam component of solar radiation is given in terms of energy received on a given surface area in a given time; i.e., W/m^2 . The quantity is measured on a surface directly facing the sun by arranging the measurement surface to track the sun as it moves across the sky. The direction of incident beam radiation is always normal/straight on to it.

As the present system constantly tracks the sun, its output will be definitely proportionate to the beam component of solar radiation and it deems reasonable to predict its performance in this regard. There is currently an immense amount of solar irradiance data for many cities, but measured illuminance data are rarely available. Fortunately, the illuminance can be estimated by using the luminance efficacy values of solar radiation [Szokolay 2005].

Similar to those in Section 4.3.5, the spatial distributions of luminance and illuminance are quantified and presented for a number of selected points on different surfaces followed by the corresponding contour maps. Throughout the figures, there exists a noticeable contrast in the density of the luminous flux and brightness between the area of illumination (round table top) by the daylighting system and its neighboring area. Especially, in most of the cases, the luminance ratios between the task plane (round table top) and its adjacent surroundings are beyond the recommended values, one to one third. The task plane is over-illuminated such that it creates visual discomfort and some measures are necessary to control the sunlight gushing out from the diffuser on the ceiling. As aforementioned, this could be readily achieved by installing a simple optical attenuator prior to the diffuser emitter (optical lens) or by applying a different design for the diffuser, capable of spreading light more evenly and widely. For the latter, a cylindrical shape diffuser could be successfully applied as demonstrated by Figures 3.12 and 3. 13.

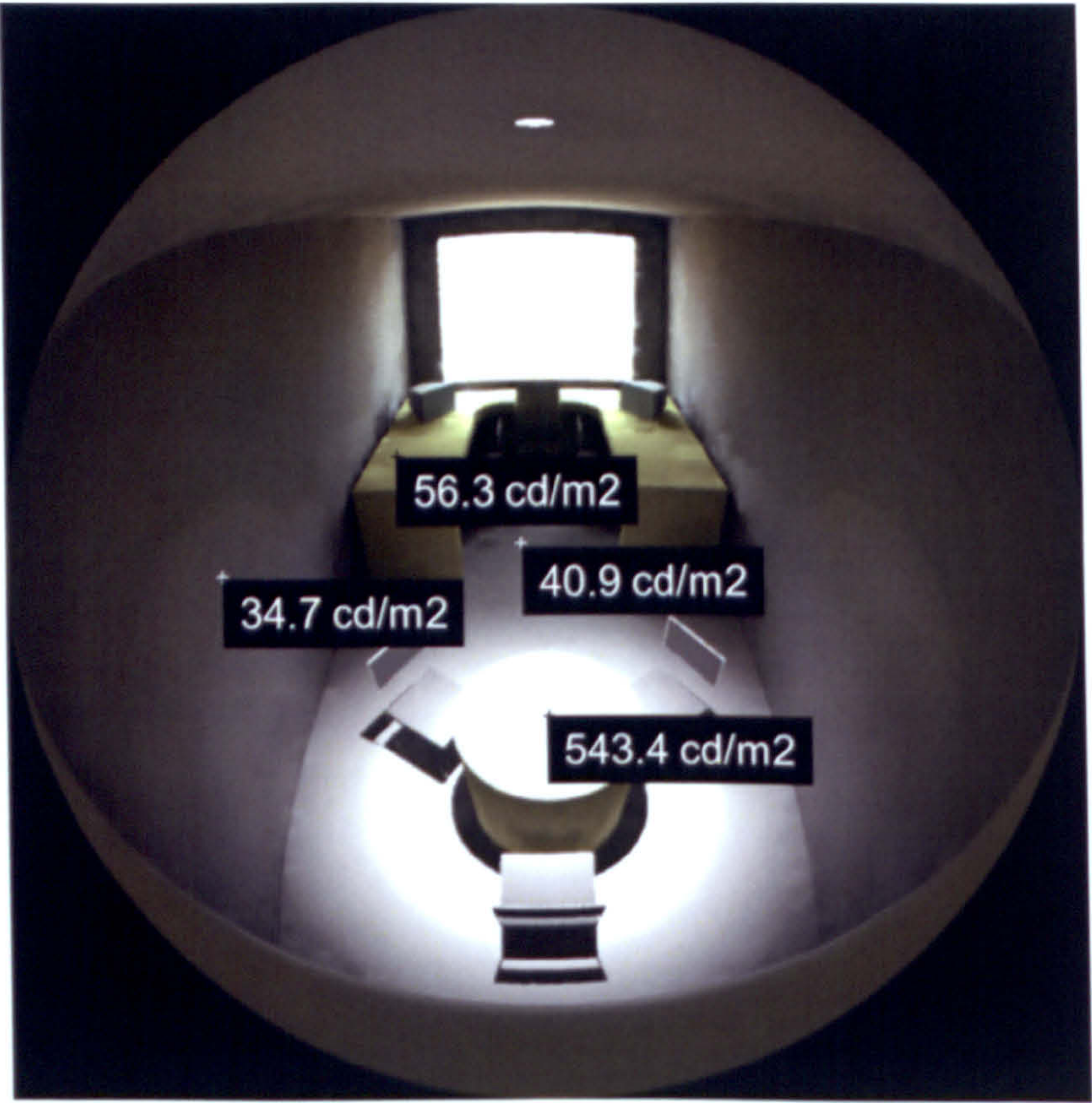


(a)

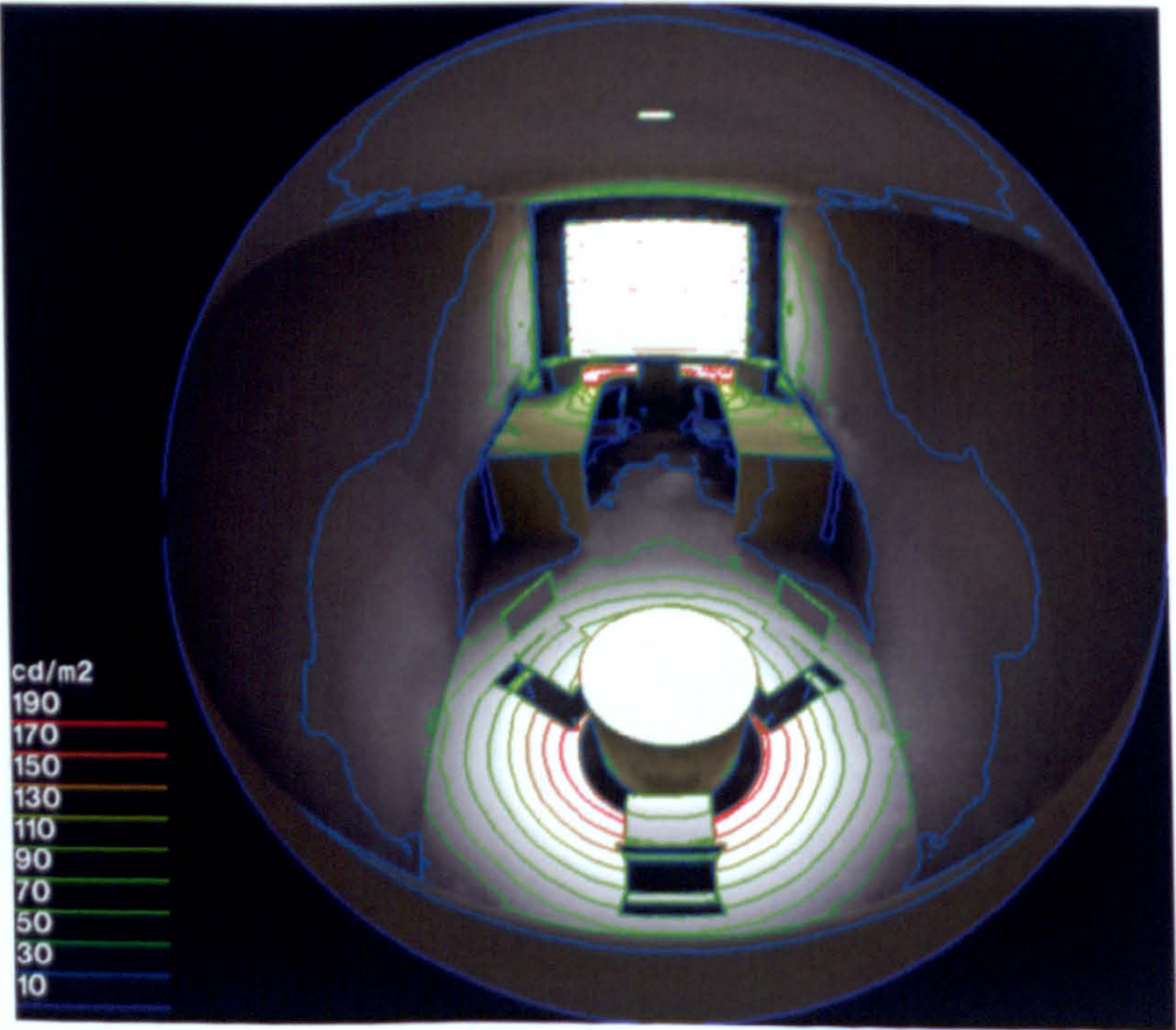


(b)

Figure 4.61 March 20, 12:00 pm, Seoul (luminance)

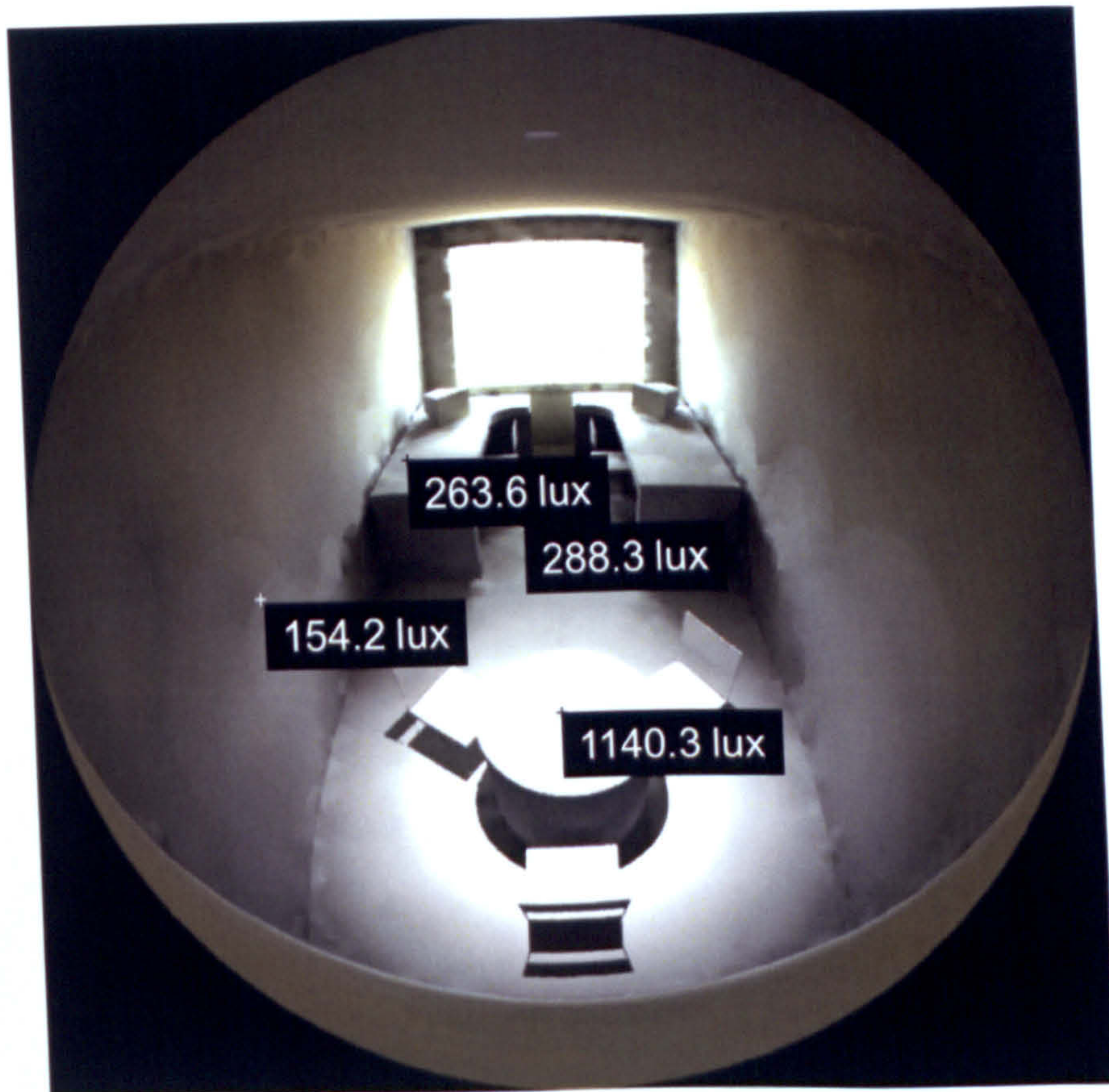


(a)

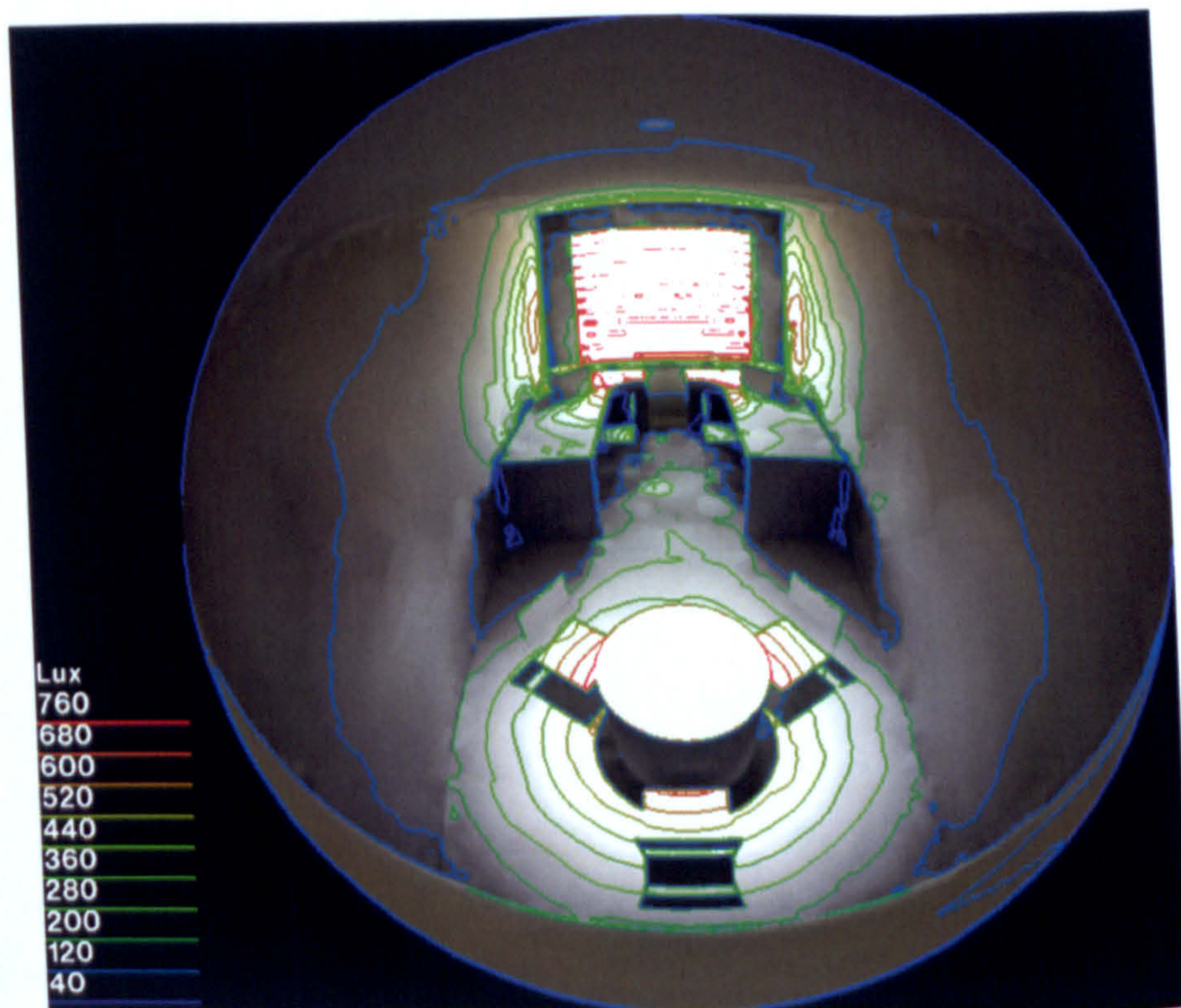


(b)

Figure 4.62 March 20, 12:00 pm, London (luminance)

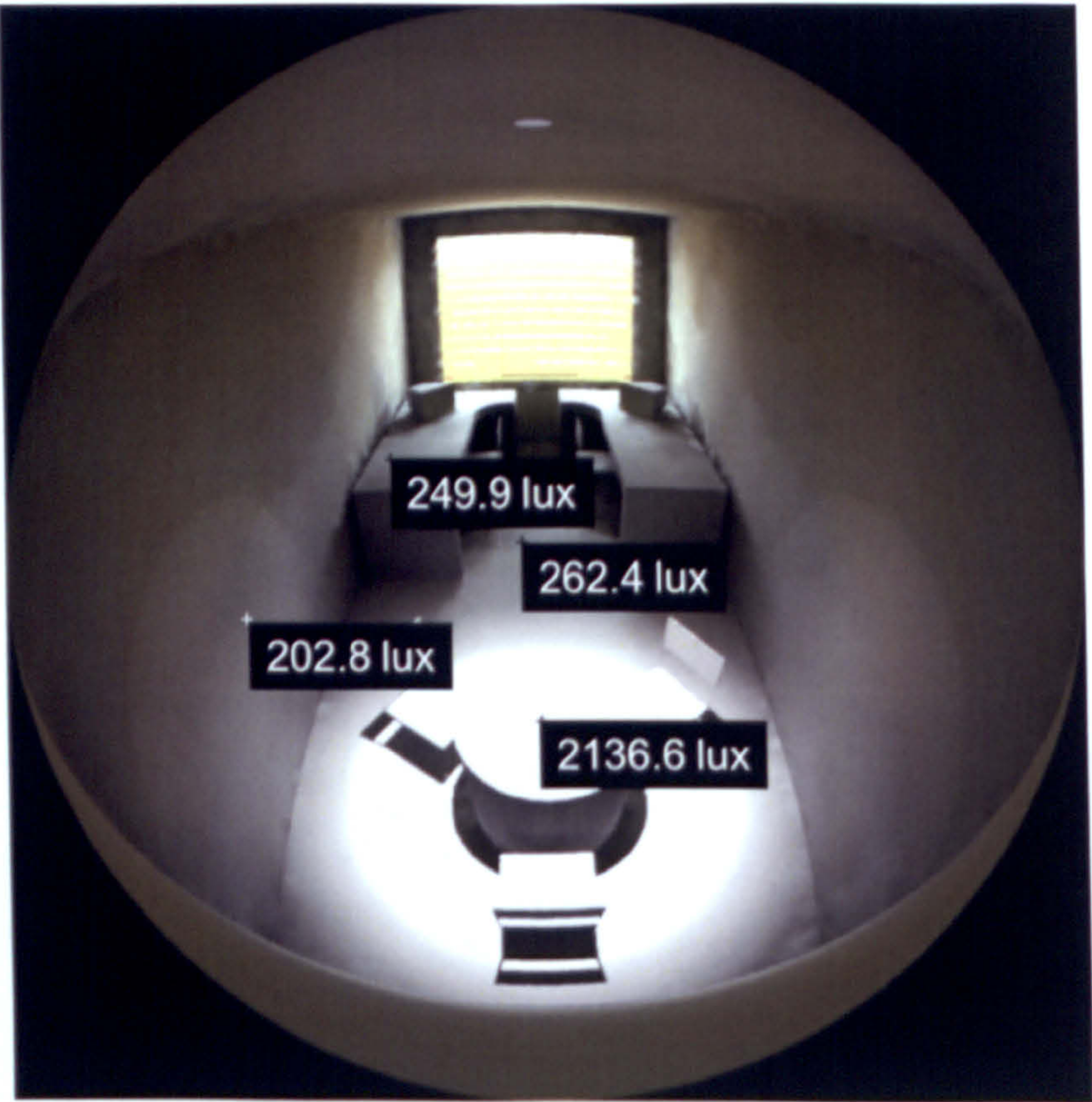


(a)

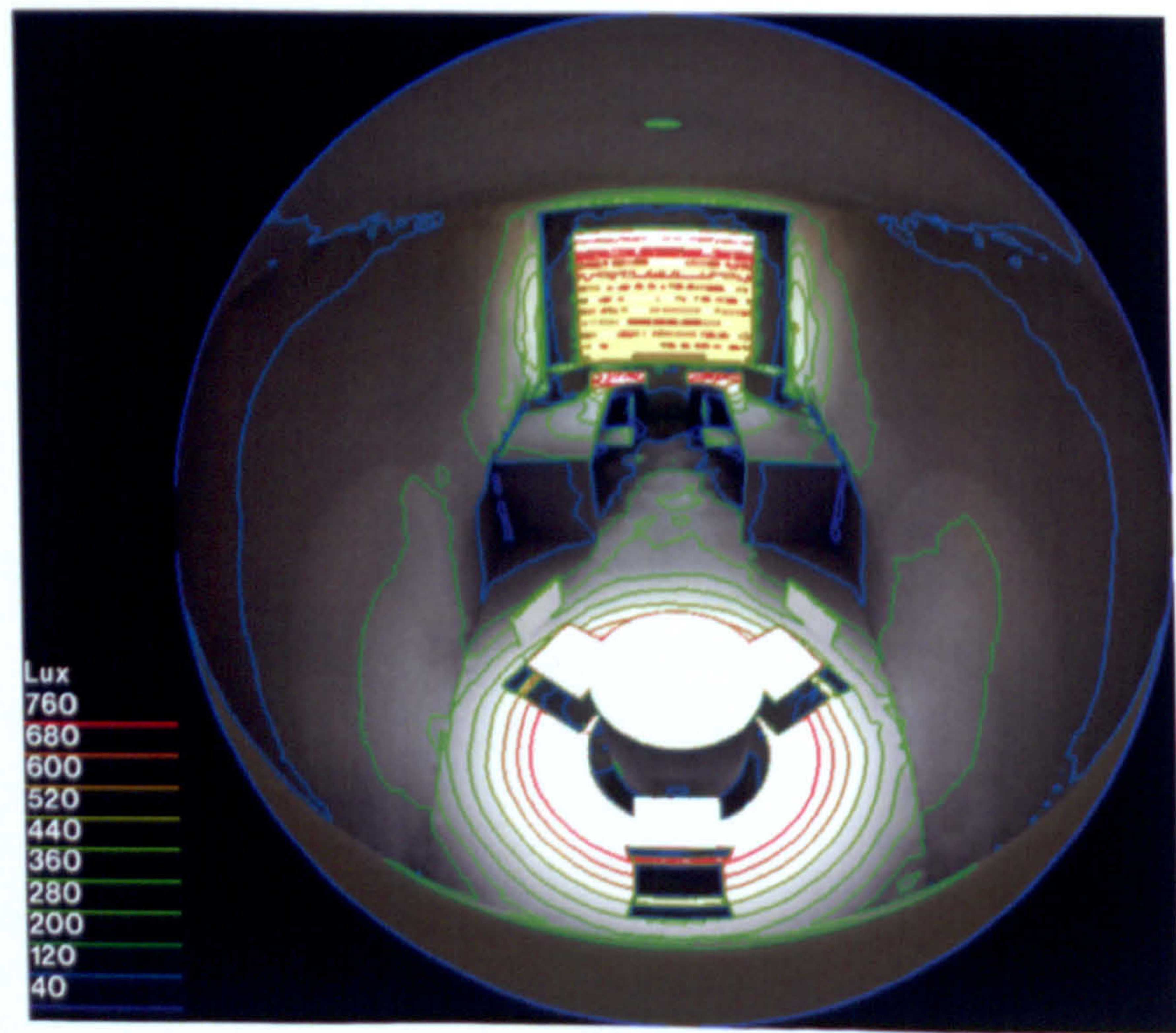


(b)

Figure 4. 63 March 20, 12:00 pm, Seoul (illuminance)

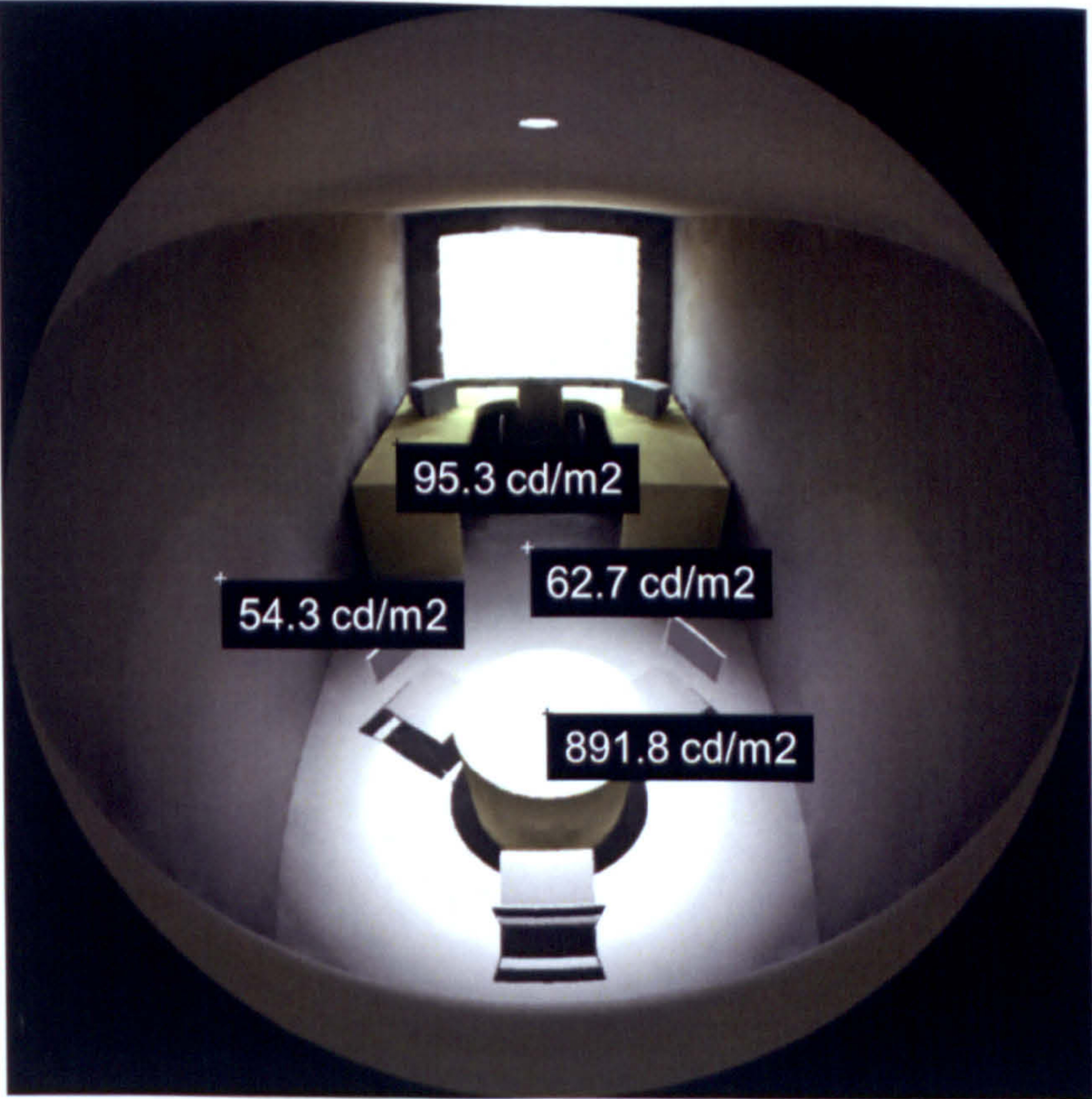


(a)

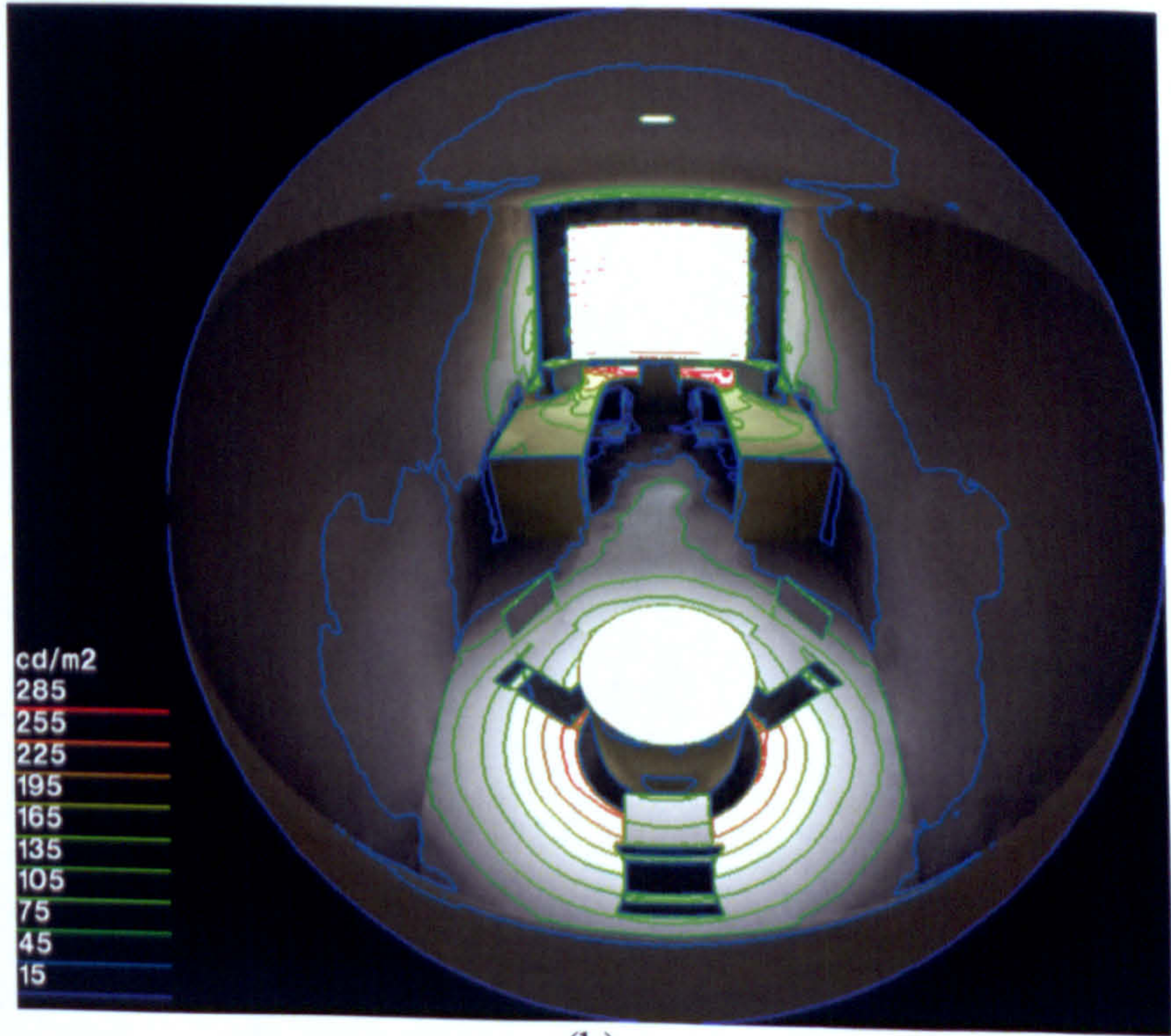


(b)

Figure 4.64 March 20, 12:00 pm, London (illuminance)

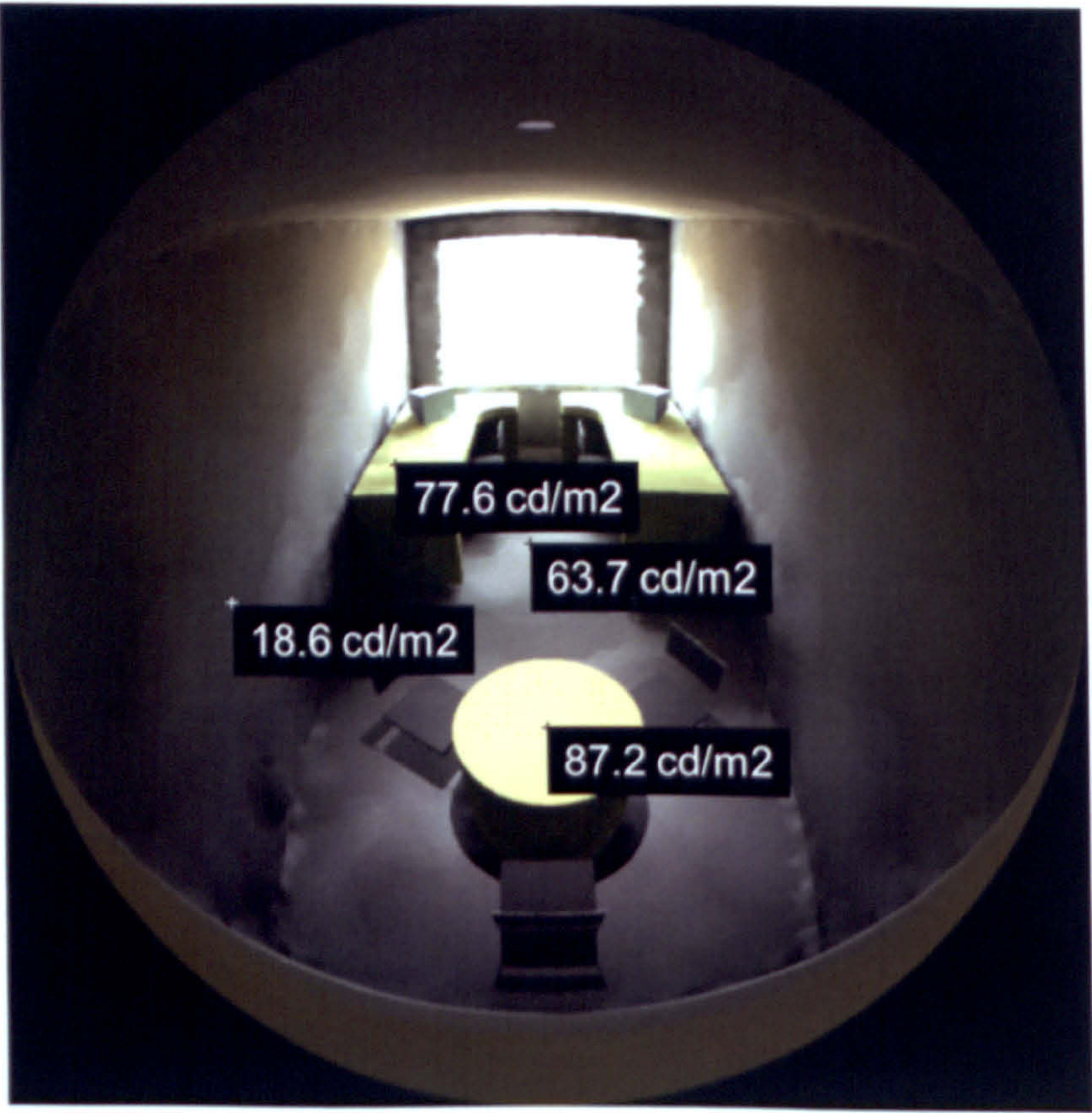


(a)

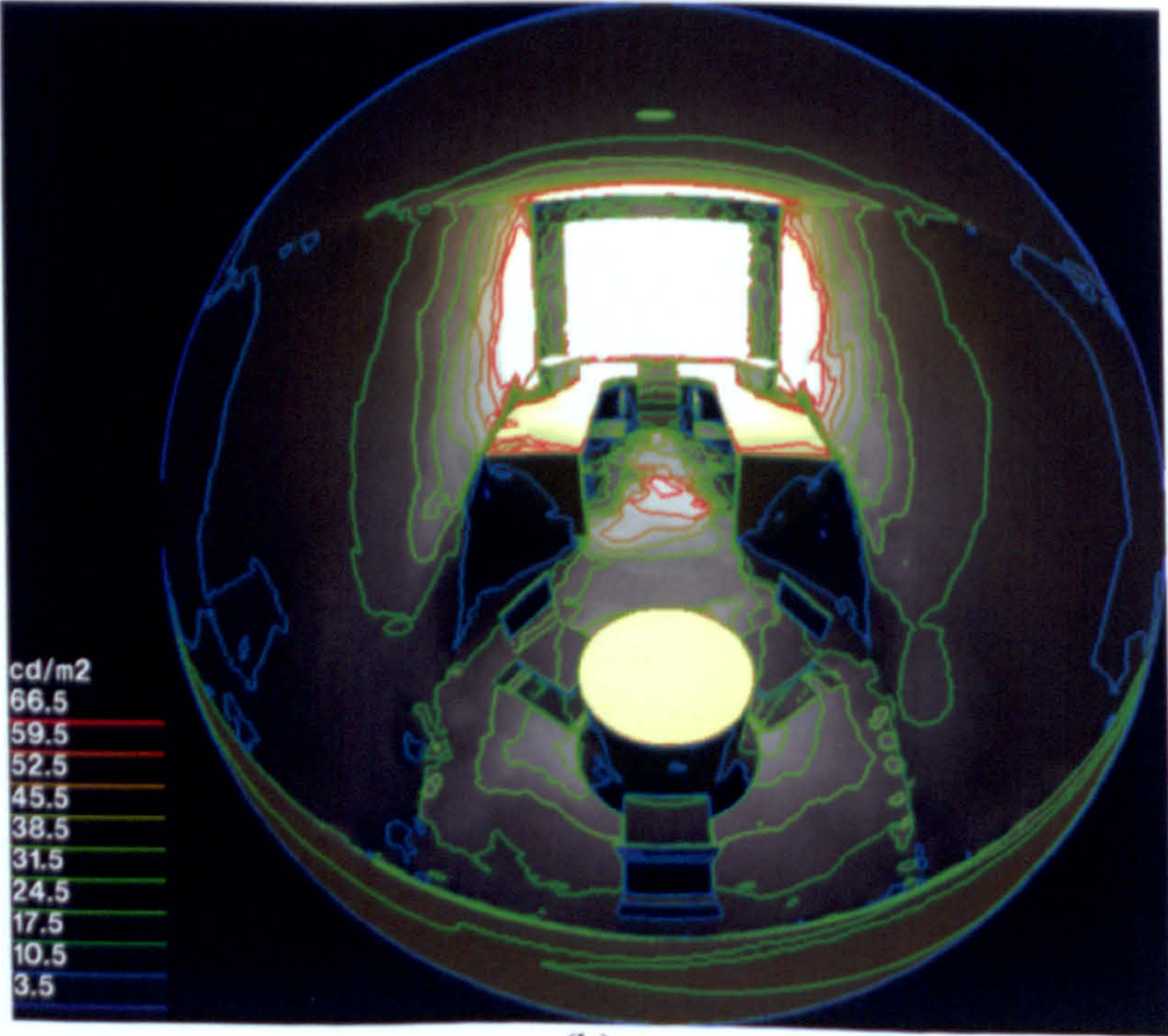


(b)

Figure 4.65 June 21, 12:00 pm, Seoul (luminance)

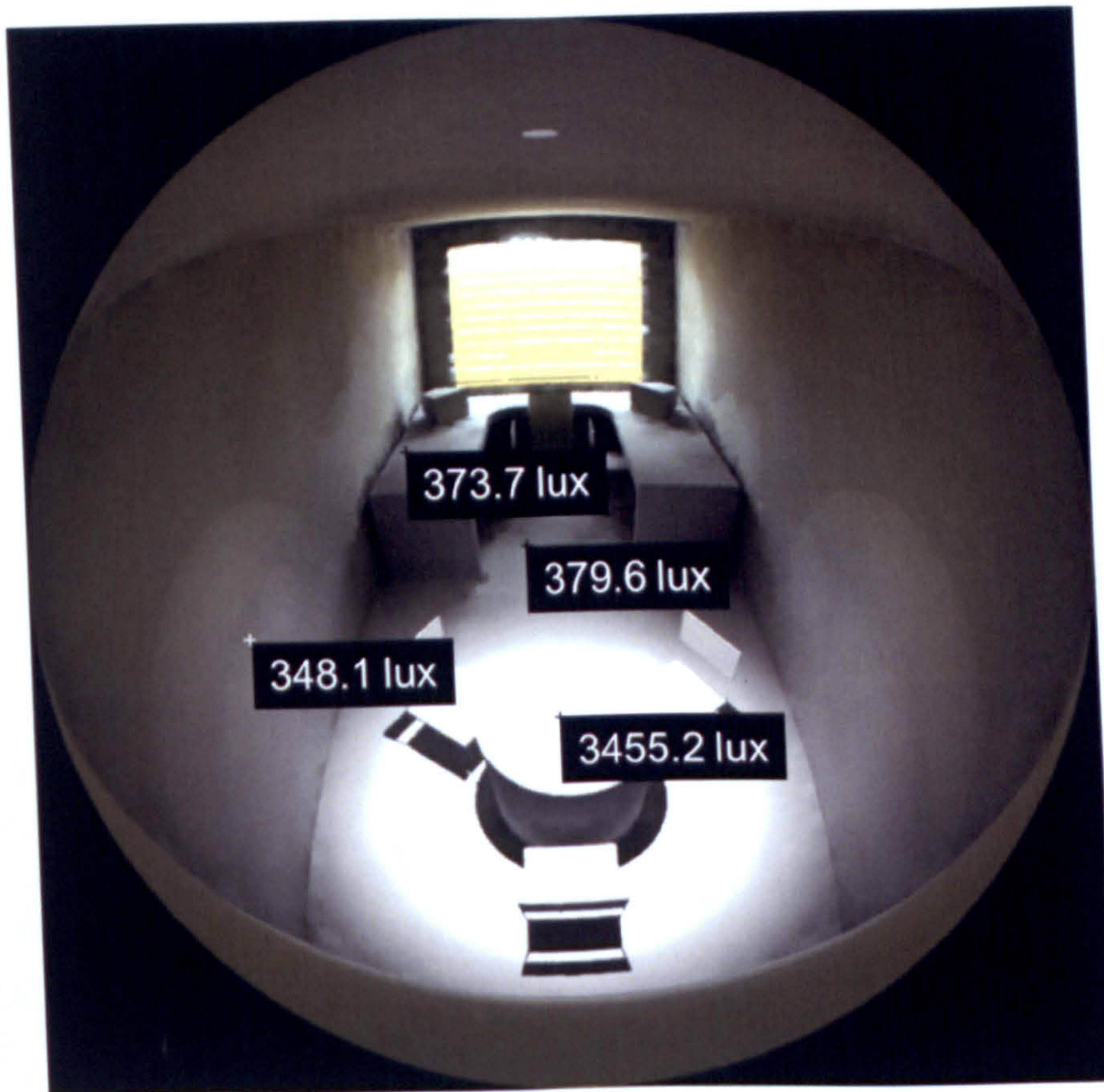


(a)

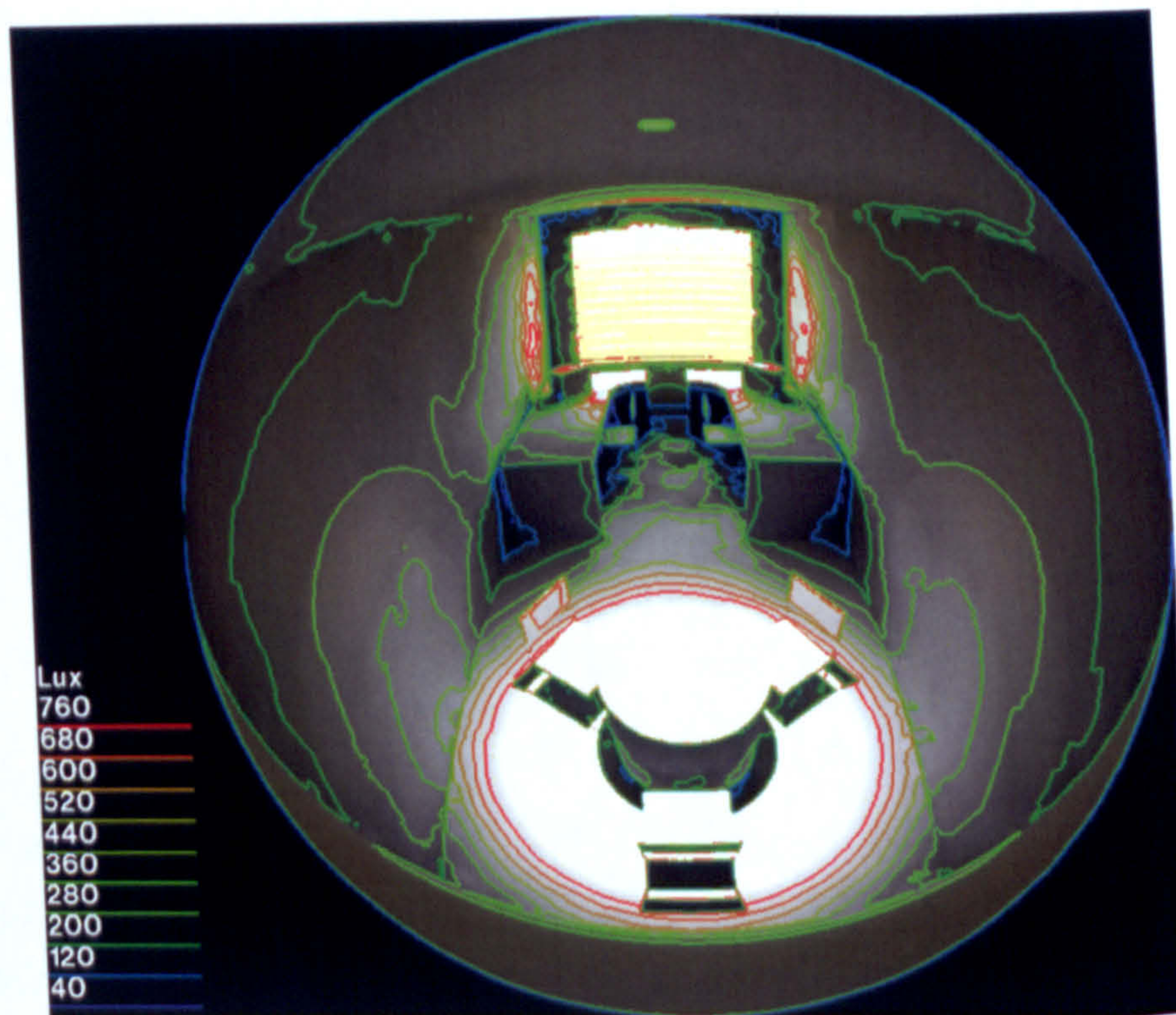


(b)

Figure 4.66 June 21, 12:00 pm, London (luminance)

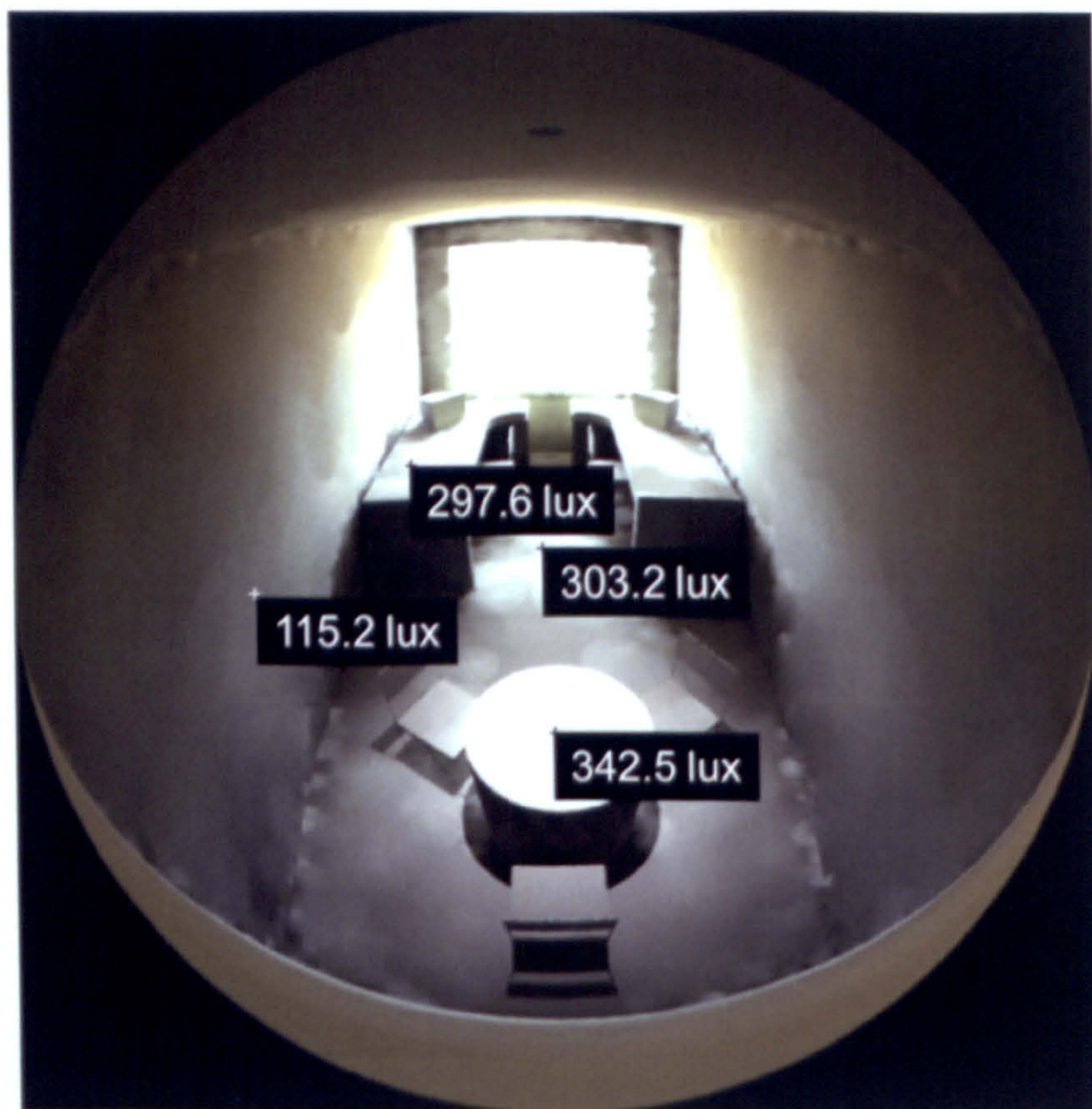


(a)

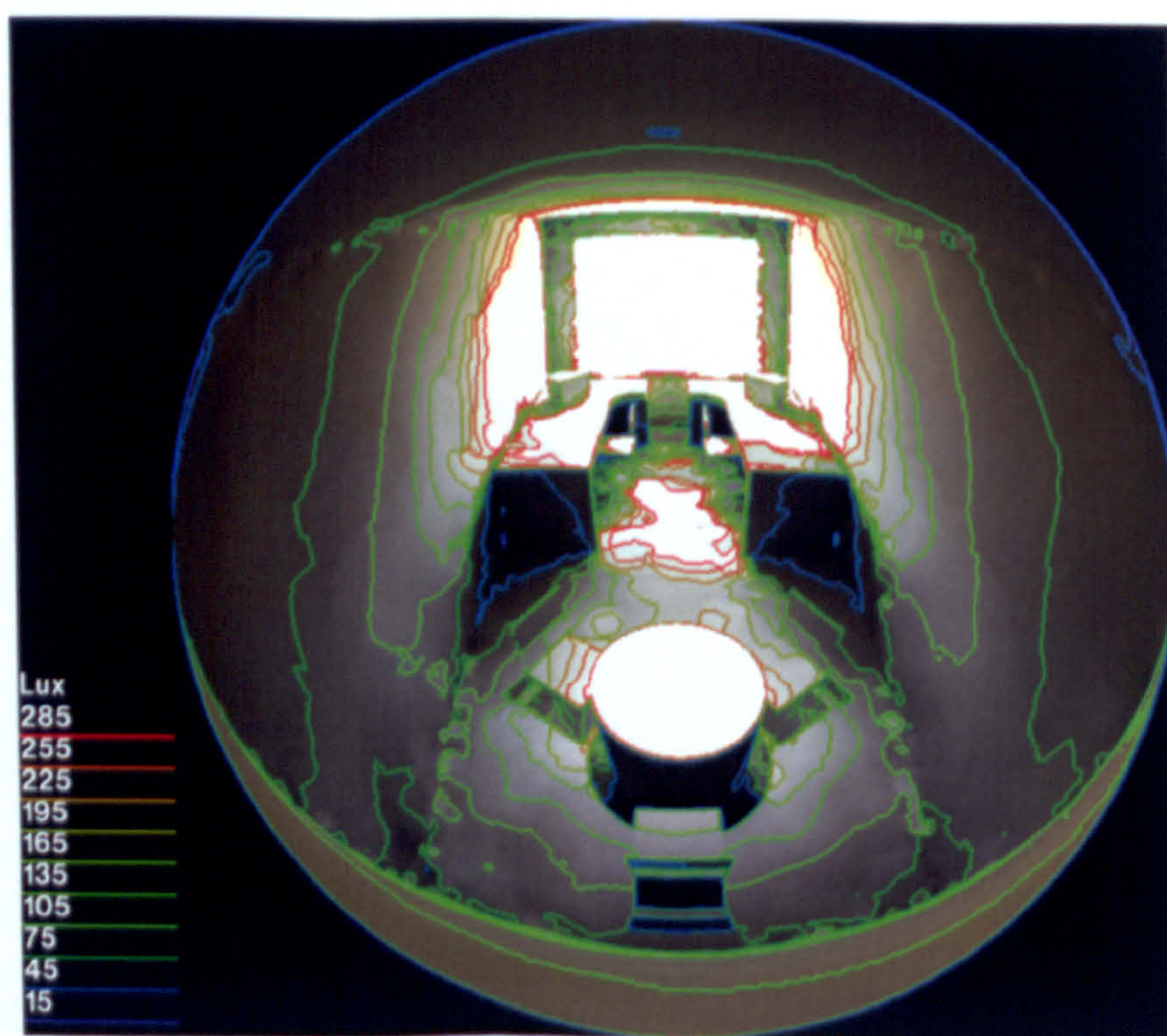


(b)

Figure 4.67 June 21, 12:00 pm, Seoul (illuminance)



(a)

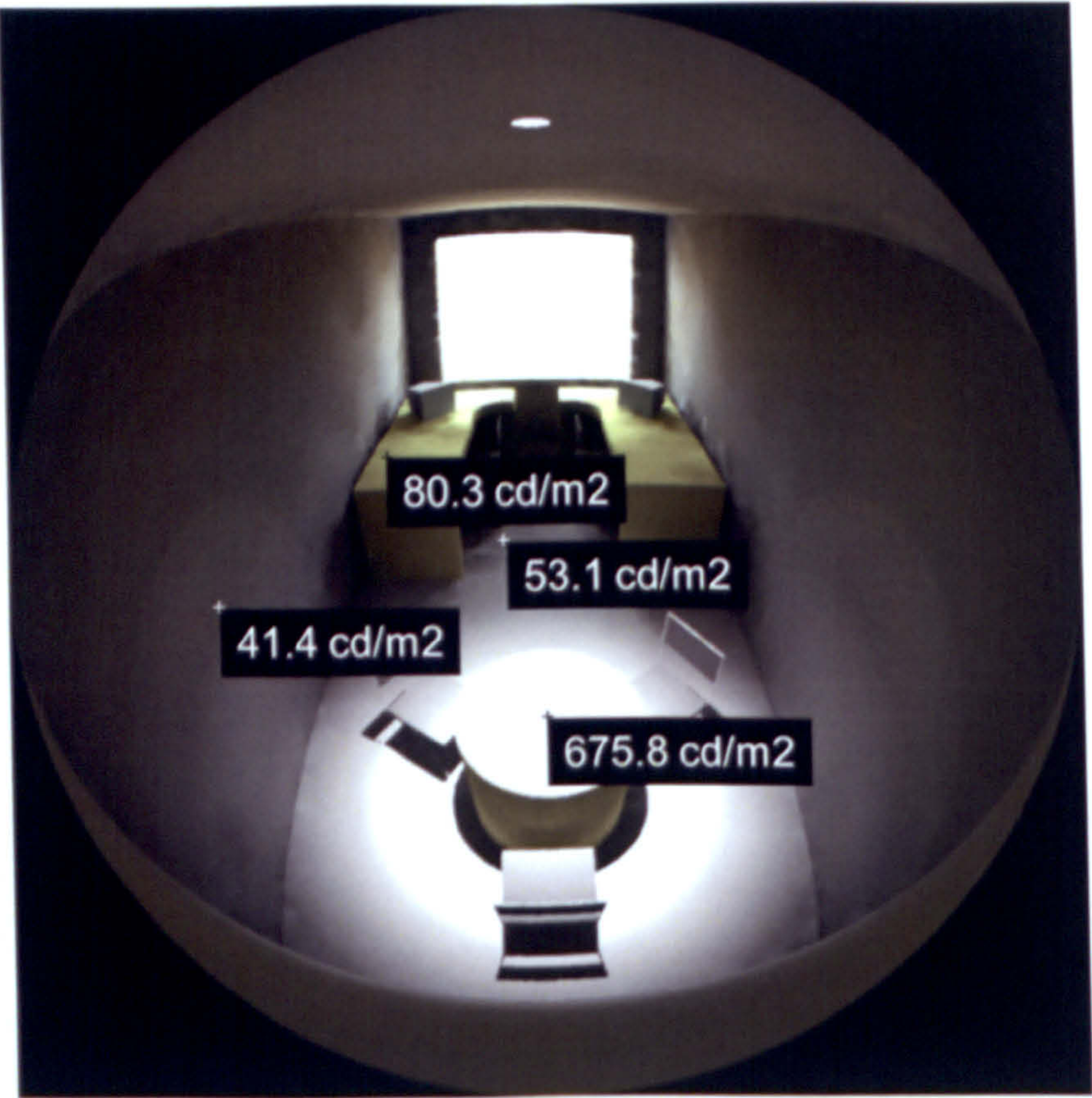


(b)

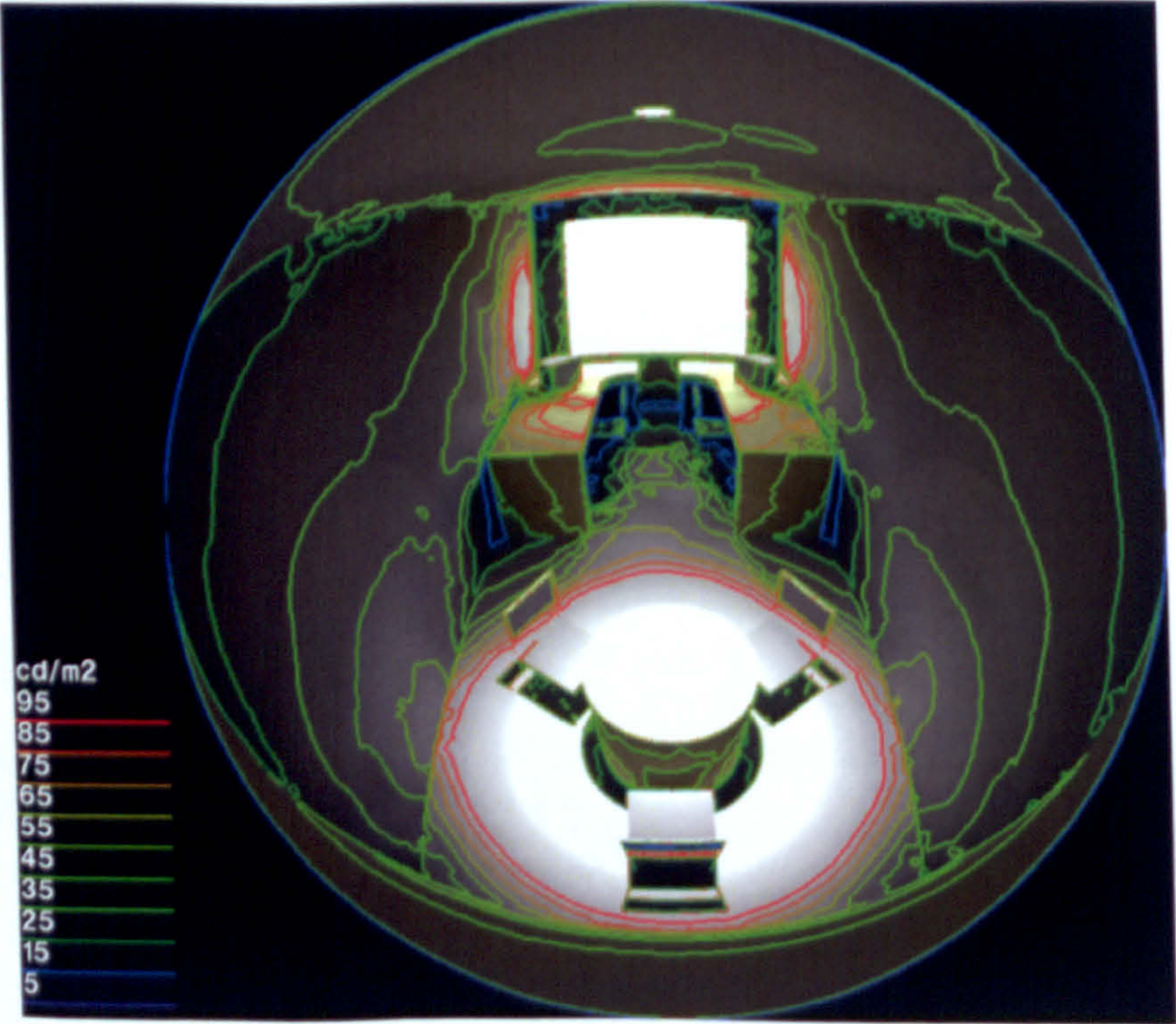
Figure 4.68 June 21, 12:00 pm, London (illuminance)

Figures 4. 61 to 4. 64 show the luminous and illuminance distribution of the model test cell at the vernal equinox. They exhibit quite a difference in the indoor lighting conditions as they are mainly governed by the directed sunrays delivered indoors by the daylighting system and the amount of light entering through the slats of the venetian blinds installed at the south window. When Seoul and London are compared, the sky condition in London allows more direct solar radiation available for the daylighting system and results in brighter but steeper luminance gradients. On the task plane (the round tabletop), the luminance could reach as high as 543.4 cd/m^2 before it decays exponentially to match that of its neighboring area. The concentric circles representing iso-luminance (Figure 4. 65 (b)) and iso-illuminance contours (Figure 4. 67 (b)) near the task plane graphically demonstrates this change in photometric properties. The highest illuminance is also predicted at the corresponding point on the task plane; 2,136.6 lux, which is comparable to 2,618 lux for Seoul in vernal equinox, Figure 4. 71.

Similar patterns are observed for the luminance and illuminance distributions of Seoul, especially, around the task plane but with less intensity. As shown in Figures 4.61 and 4. 63, the maximum luminance and illuminance values are predicted at the center of the task plane directly below the diffuser, which are 294.8 cd/m^2 and 1,140.3 lux, respectively. It should, however, be pointed out that the direct solar radiation values used here do not necessarily represent the typical value for the day. Rather than the values given in Table 4. 4, it might be more realistic to use the average around the day of interest including itself. Also, since the present daylighting system only utilizes the direct beam component of solar radiation, it is more important to have a sky condition with the least amount of suspending particles or gas molecules (H_2O), that is, a high clearness index. The clear sky index is the ratio of the global horizontal solar radiation for a given atmospheric condition to the extraterrestrial horizontal solar radiation. In fact, the present dish-daylighting system would perform most effectively in desert climate conditions.

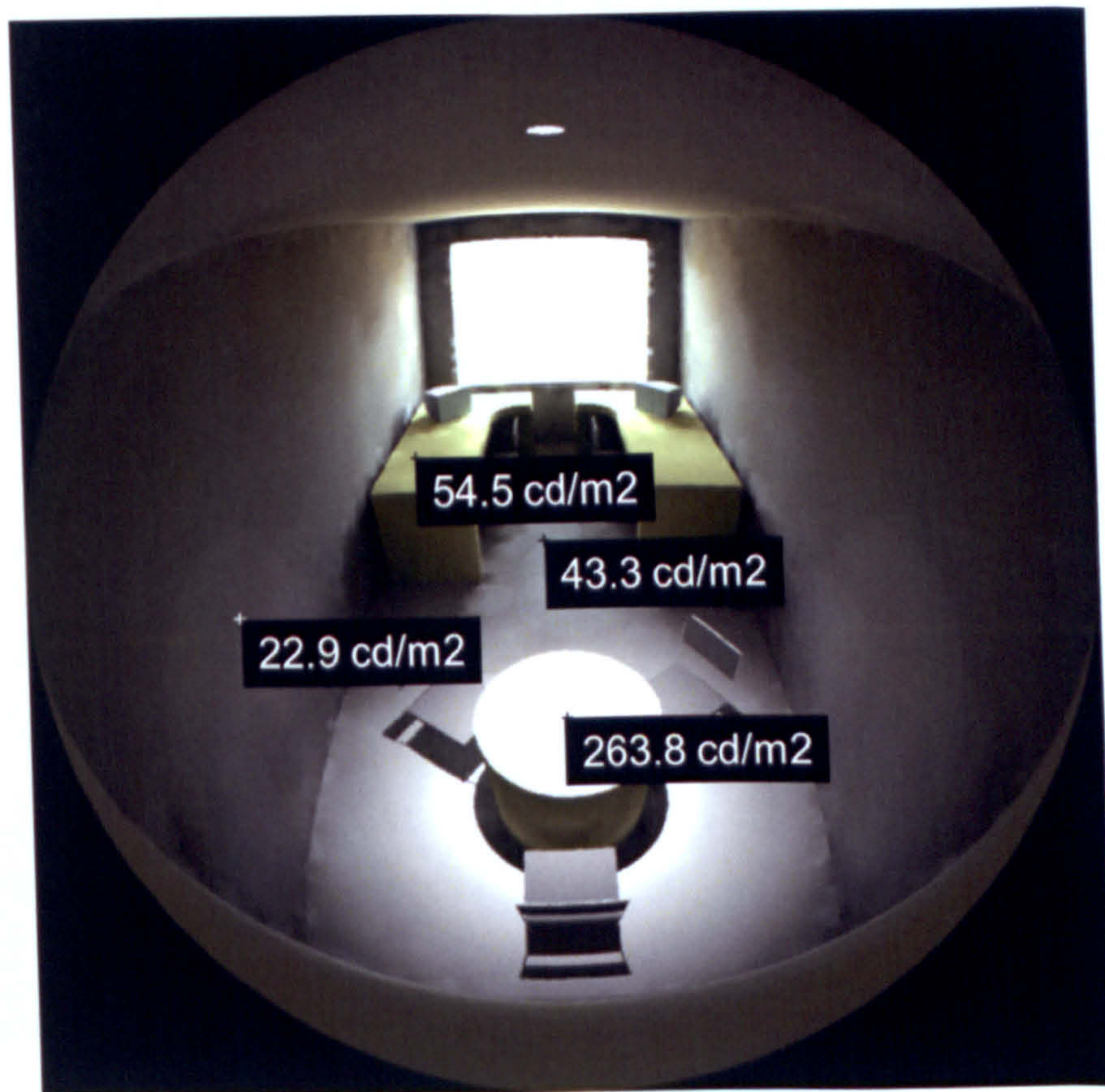


(a)

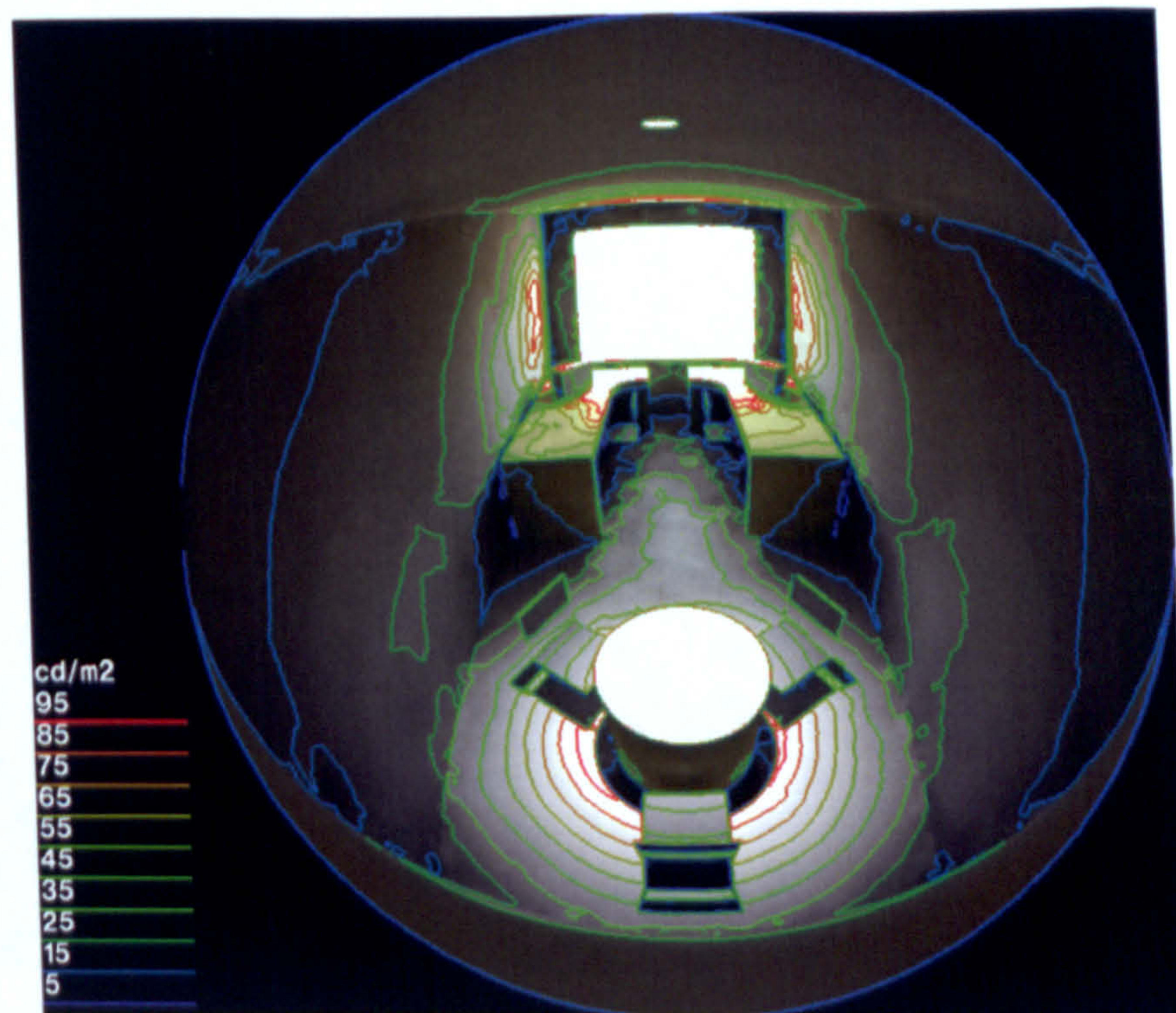


(b)

Figure 4.69 September 22, 12:00 pm, Seoul (luminance)

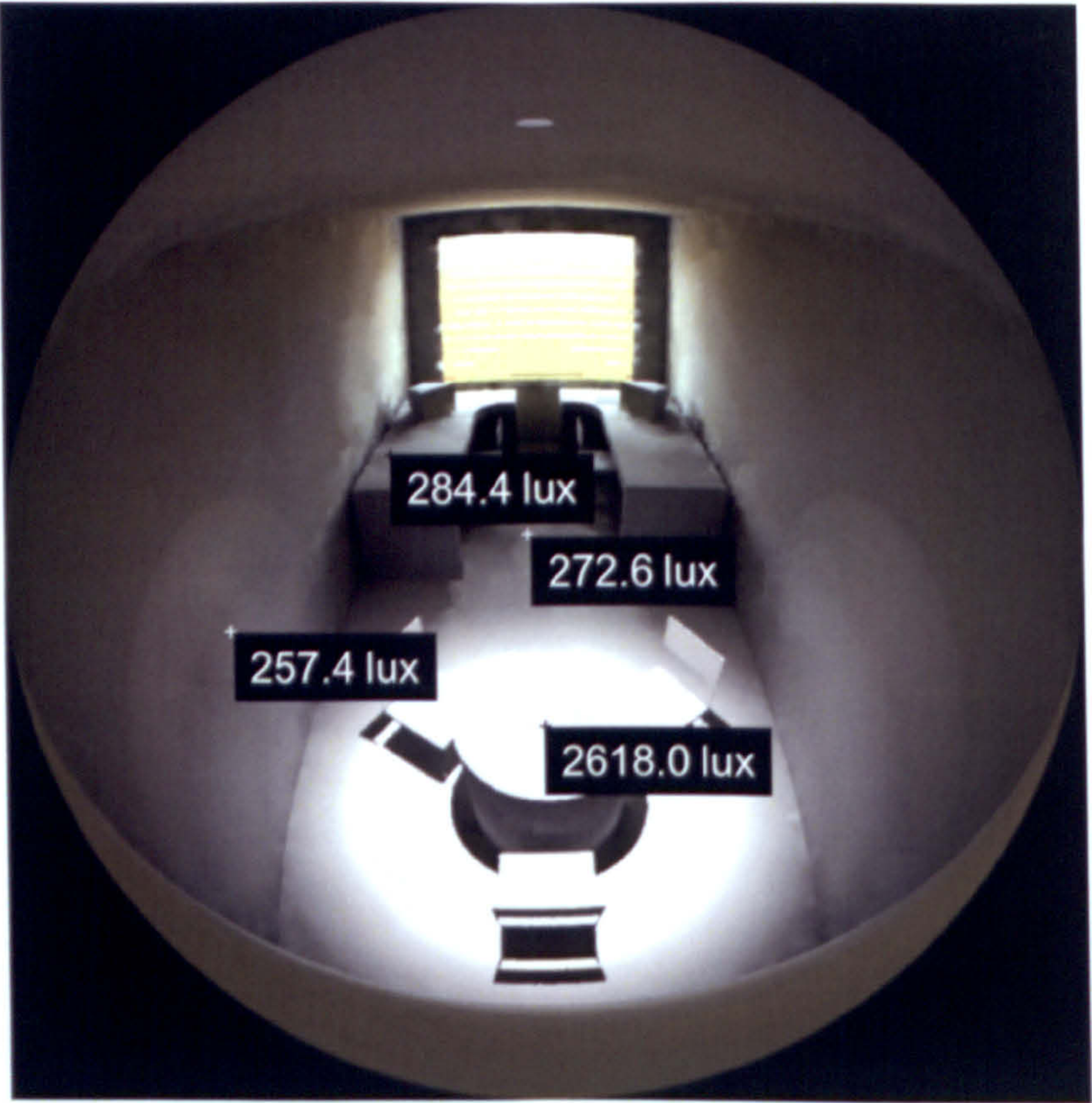


(a)

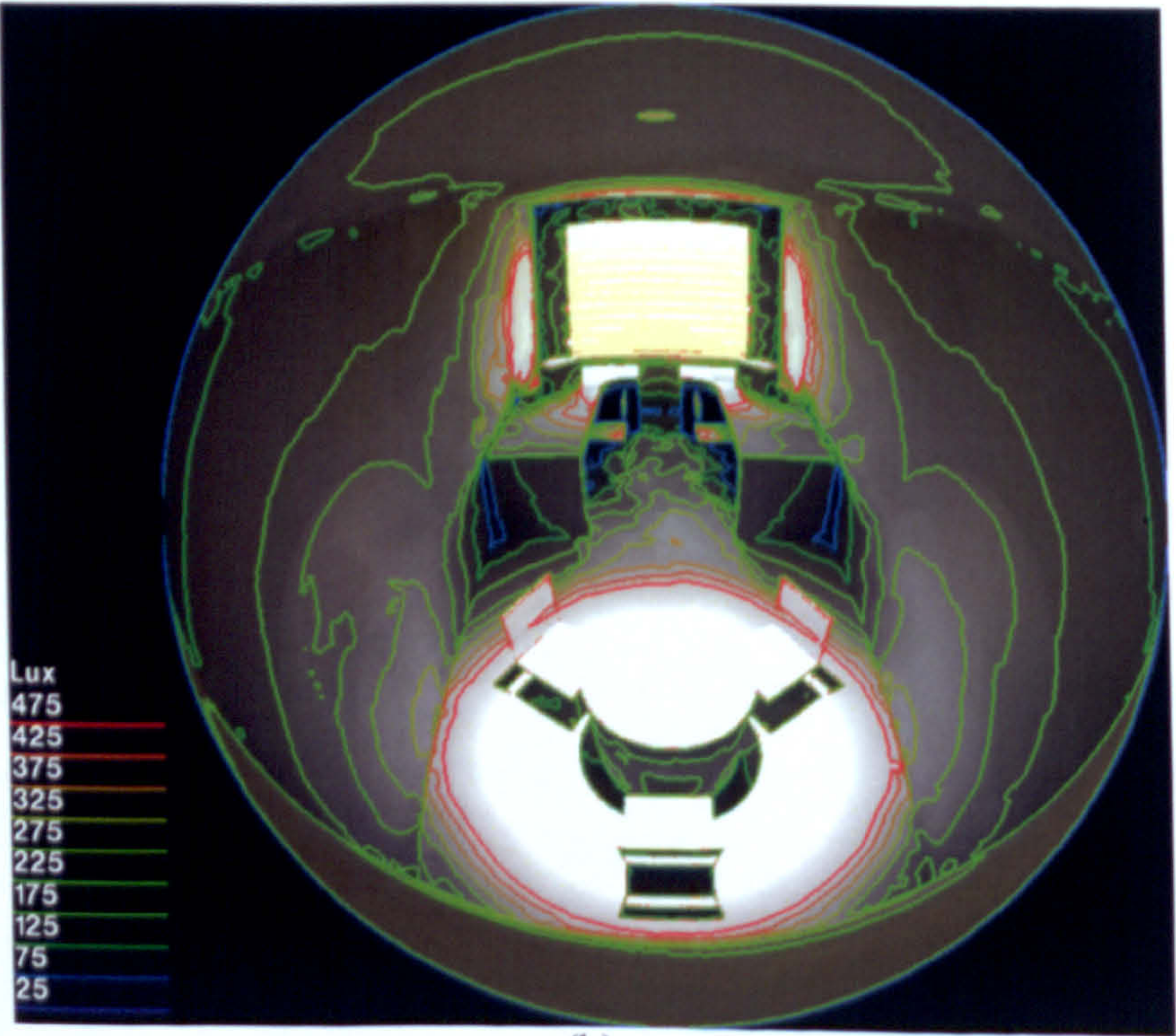


(b)

Figure 4.70 September 22, 12:00 pm, London (luminance)



(a)



(b)

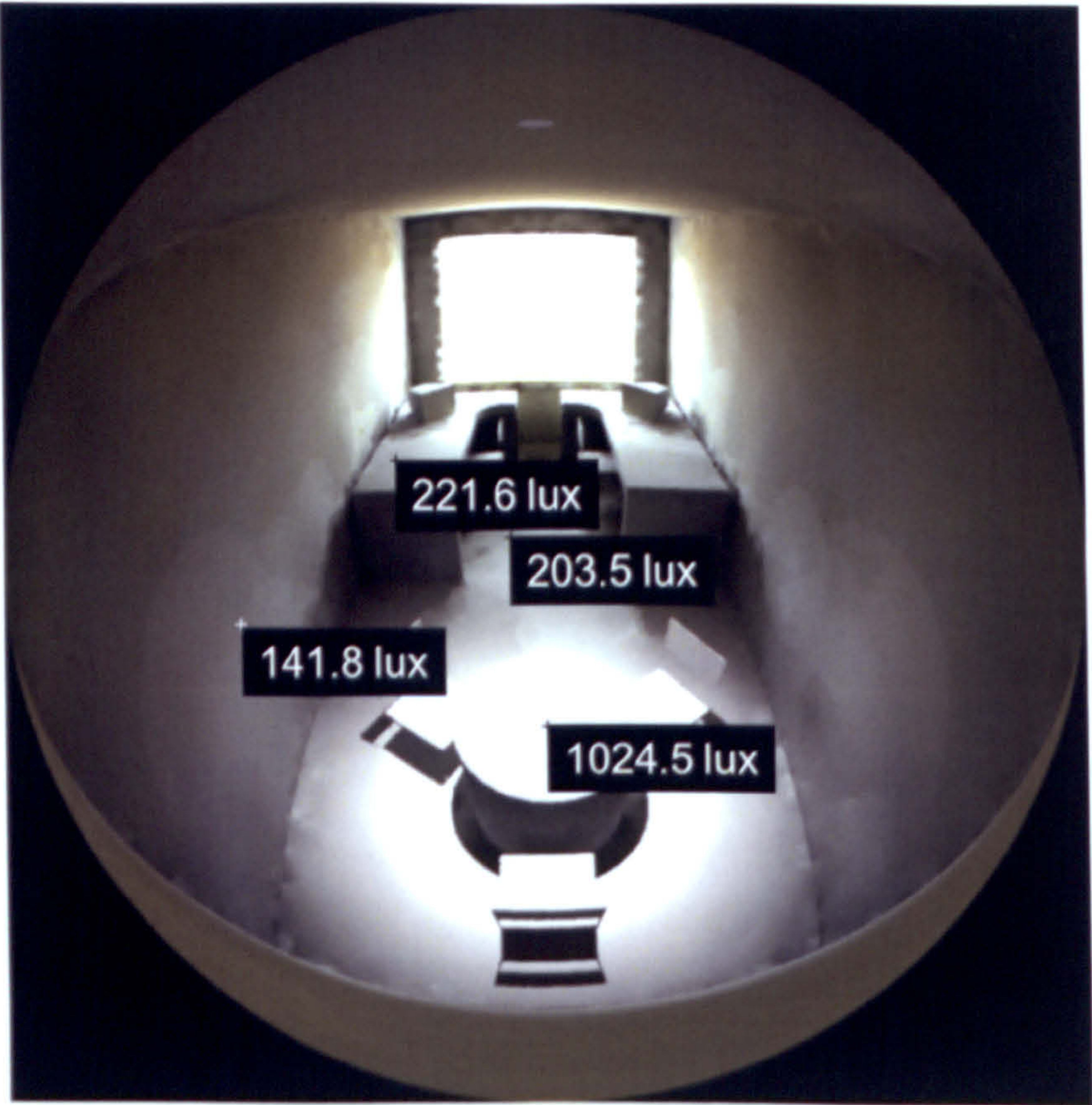
Figure 4.71 September 22, 12:00 pm, Seoul (illuminance)

As for the summer solstice, it shows two extremes of the indoor lighting caused by the present daylighting system. The case for London, Figure 4. 66 (Figure 4. 68), is representative of the meager performance of the daylighting system whereas the case for Seoul gives an example of its outstanding performance, Figure 4. 65 (Figure 4. 67).

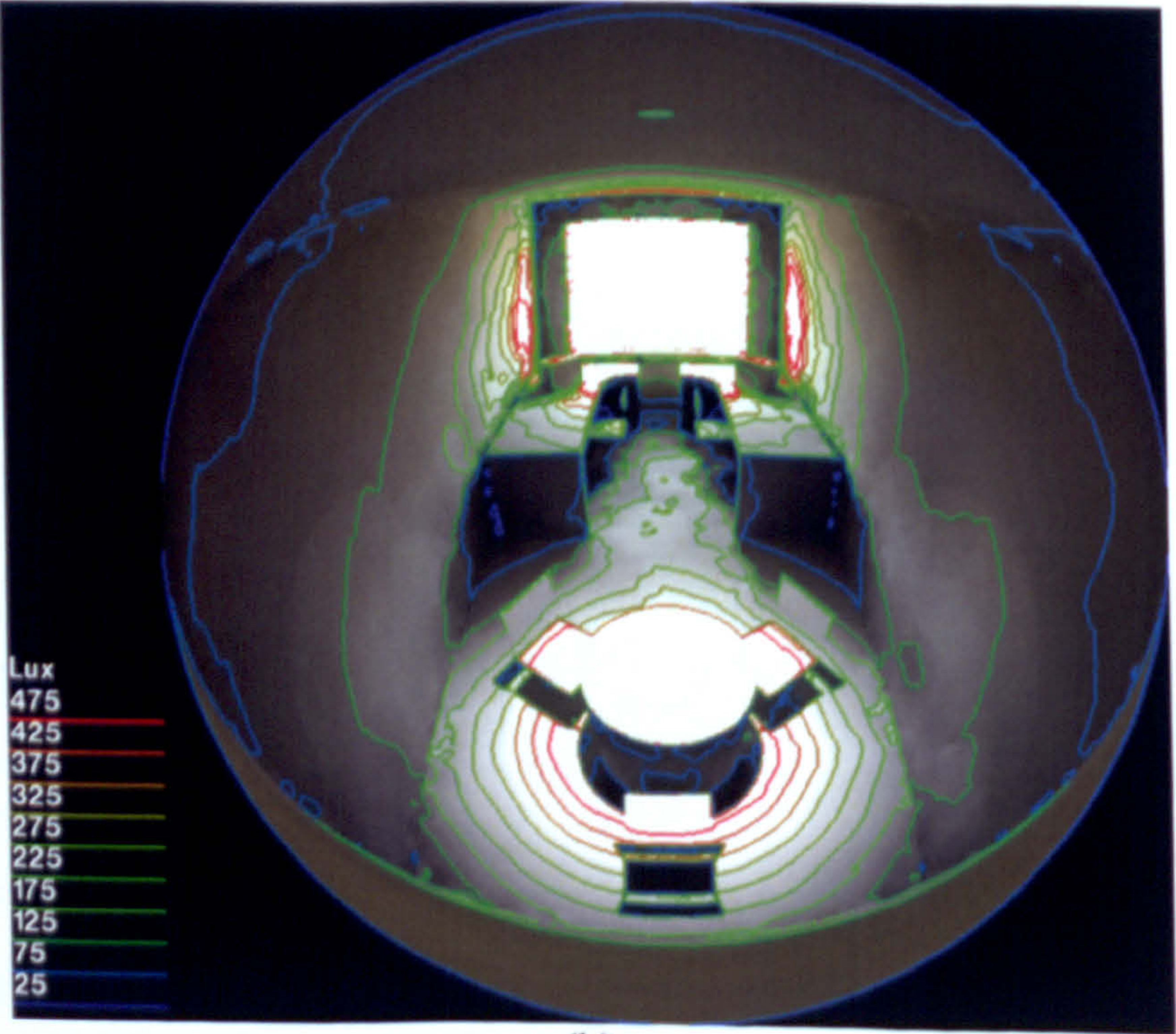
When compared to vernal equinox, there is a turnover in the photometric properties on the illuminated area on the task plane. Figures 4. 69 and 4. 71 clearly demonstrates that both the luminance and illuminance values on the round table top and its vicinity for Seoul are far higher than those for London, Figures 4. 70 and 4. 72. This is quite a change (reversal) since it was the other way around as represented by Figures 4. 61 to 4. 64.

As the winter solstice, both locations display a similar pattern of variations in the indoor lighting conditions. Especially, there are no appreciable differences observed for luminance and illuminance within the area of illumination by the daylighting system. This is well represented by the percentage difference of these values, which falls in within the range of less than ten percent as shown in Figures 4. 73 through 4. 76.

In general, the simulated results again recommend some improvement in uniformity for the lighting design and control of the present dish-daylighting system. Unless the sunlight introduced through the diffuser propagates at an intensity comparable to that admitted through the window, it deems the brightness contrasts are often beyond the acceptable range as witness in the previous cases, i.e., an office building unit, test cells and etc.. As often encountered by other daylighting devices (systems), it should provide functional compatibility and be in harmony with the architecture and local daylight environment which might be sometimes unique or require to meet location-specific characteristics of a place. Along with clearly defined descriptors that are rather readily retrieved, considerations should be made for those factors responsible for specific requirements stemming from architectural design and other local conditions in order to achieve high-quality daylighting applications.

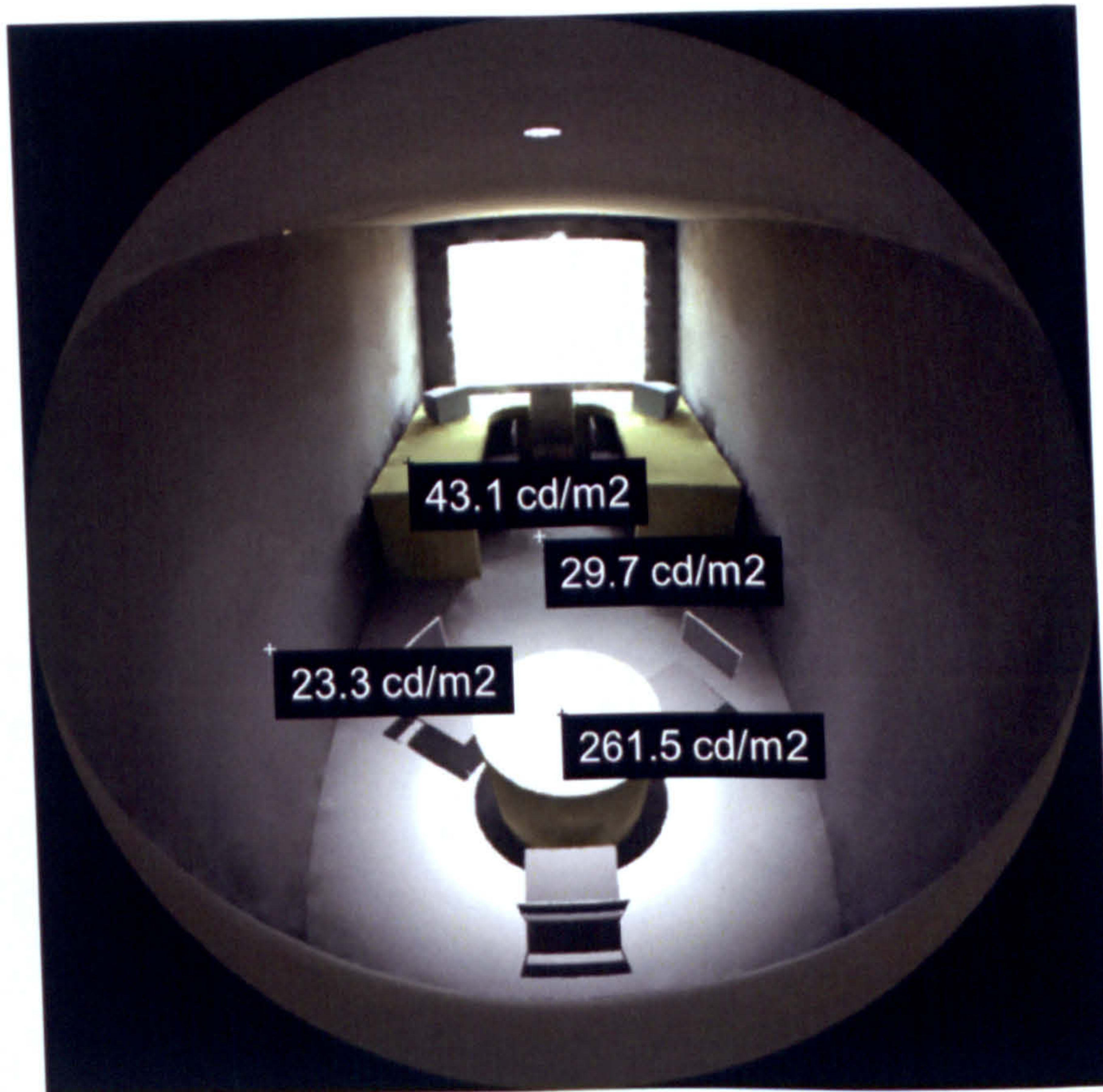


(a)

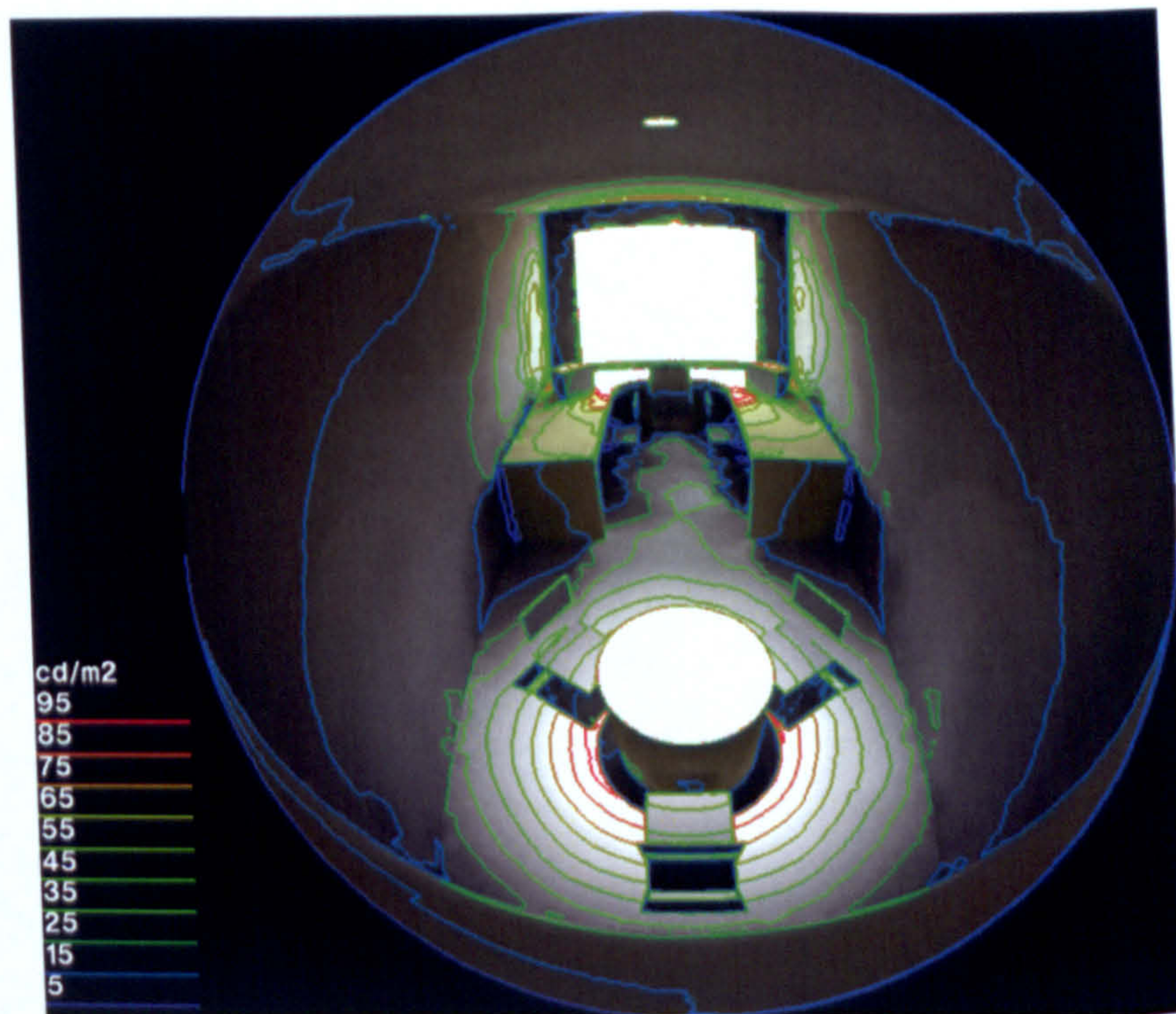


(b)

Figure 4.72 September 22, 12:00 pm, London (illuminance)

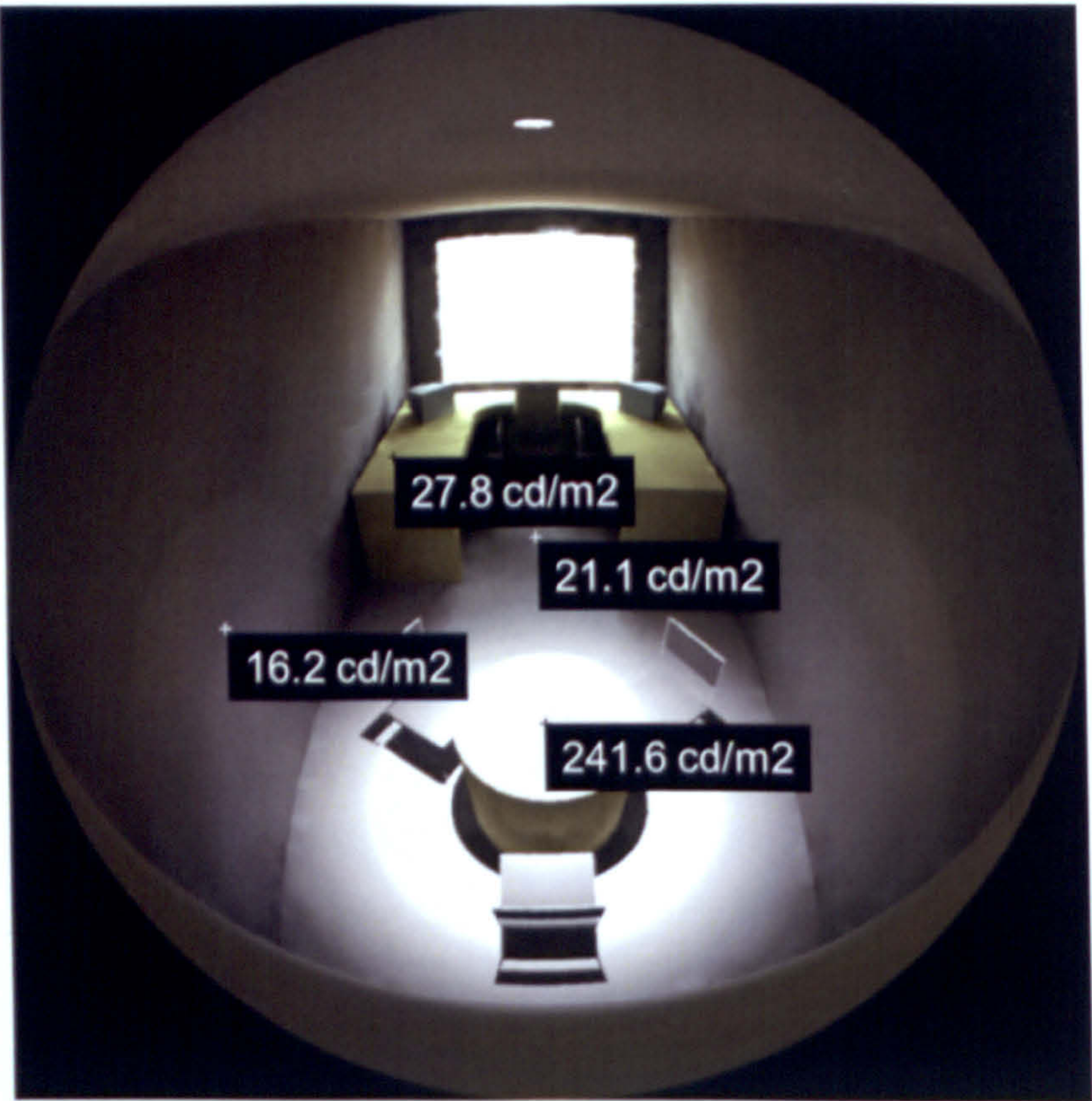


(a)

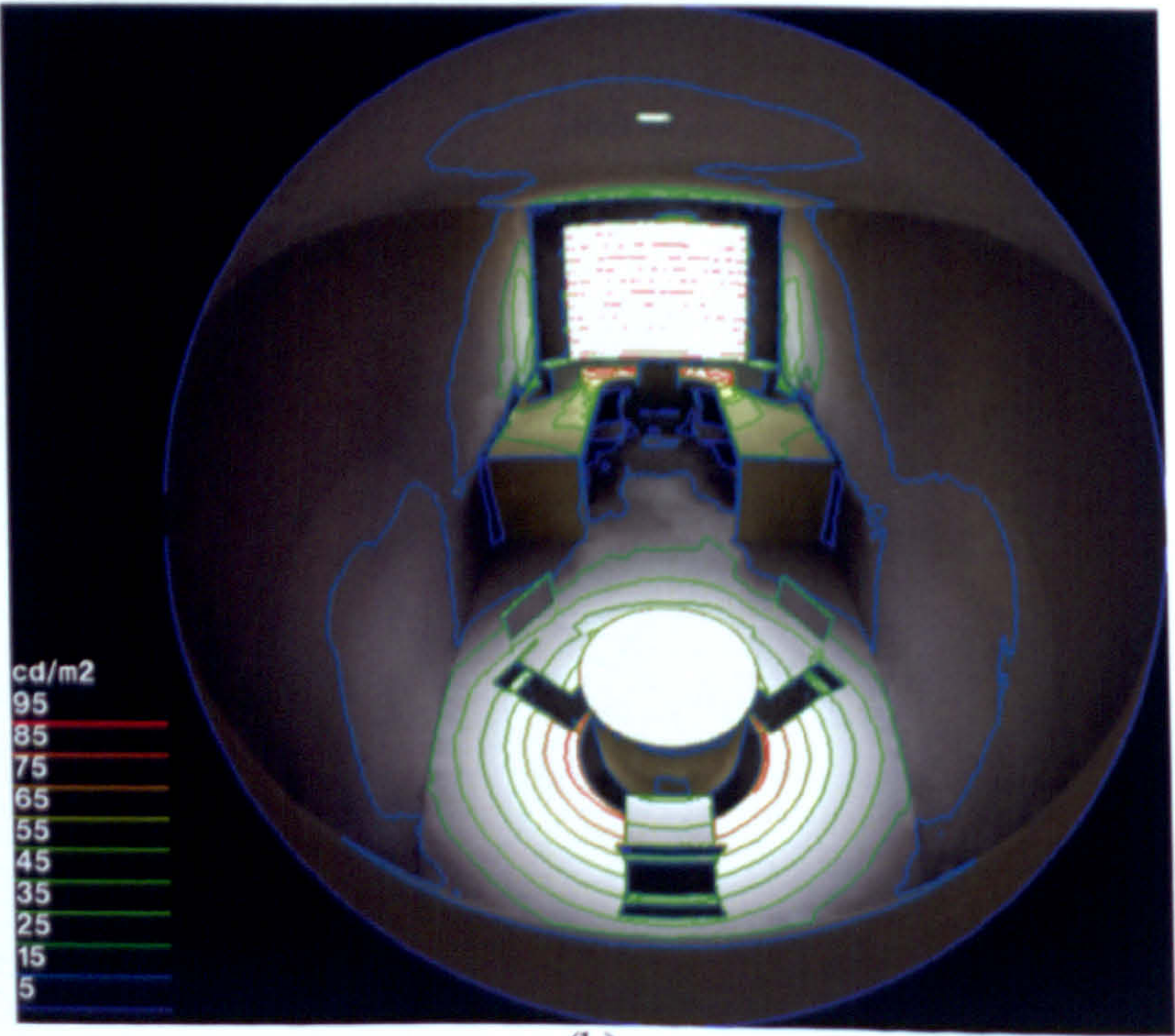


(b)

Figure 4.73 December 21, 12:00 pm, Seoul (luminance)

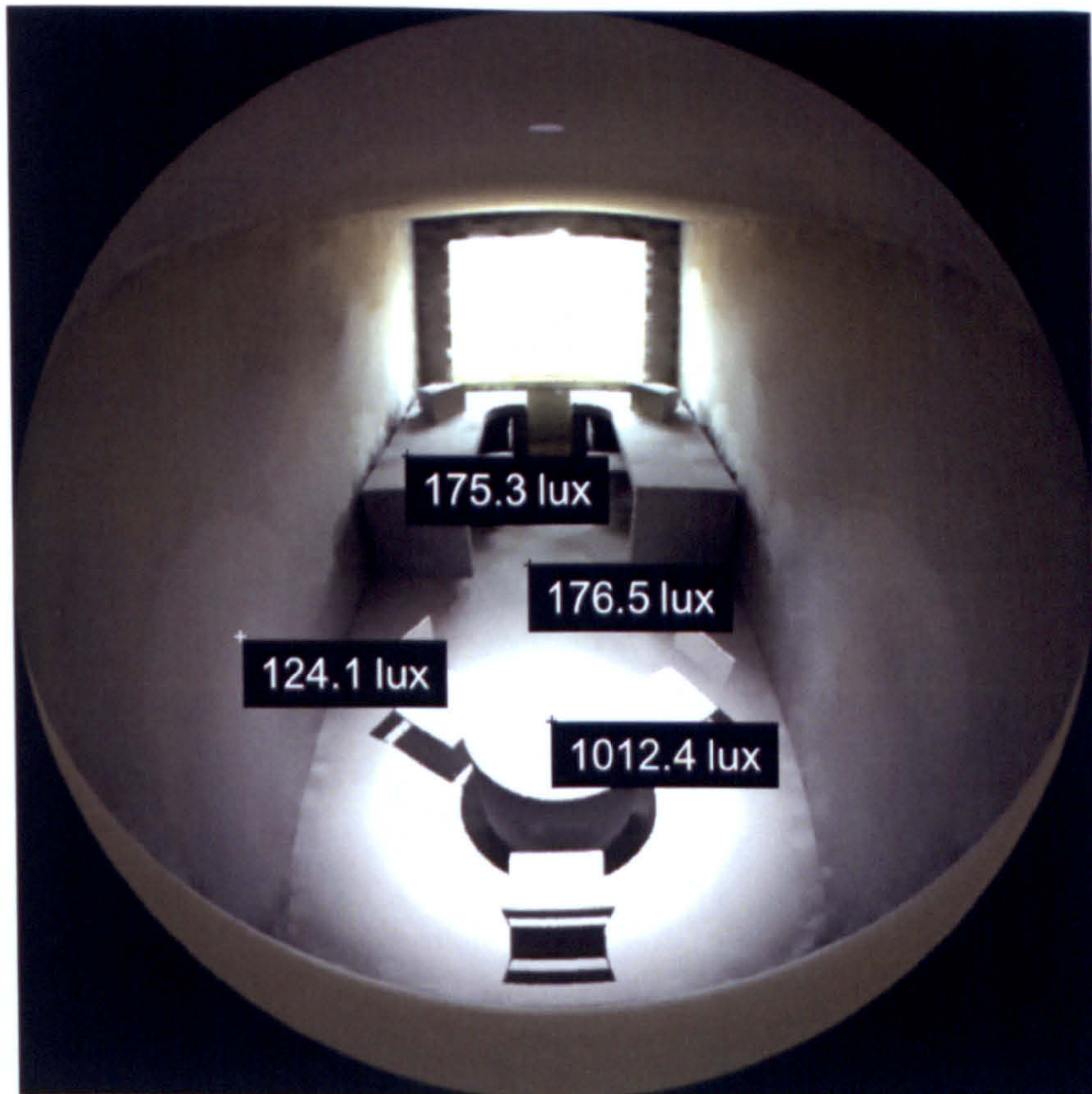


(a)

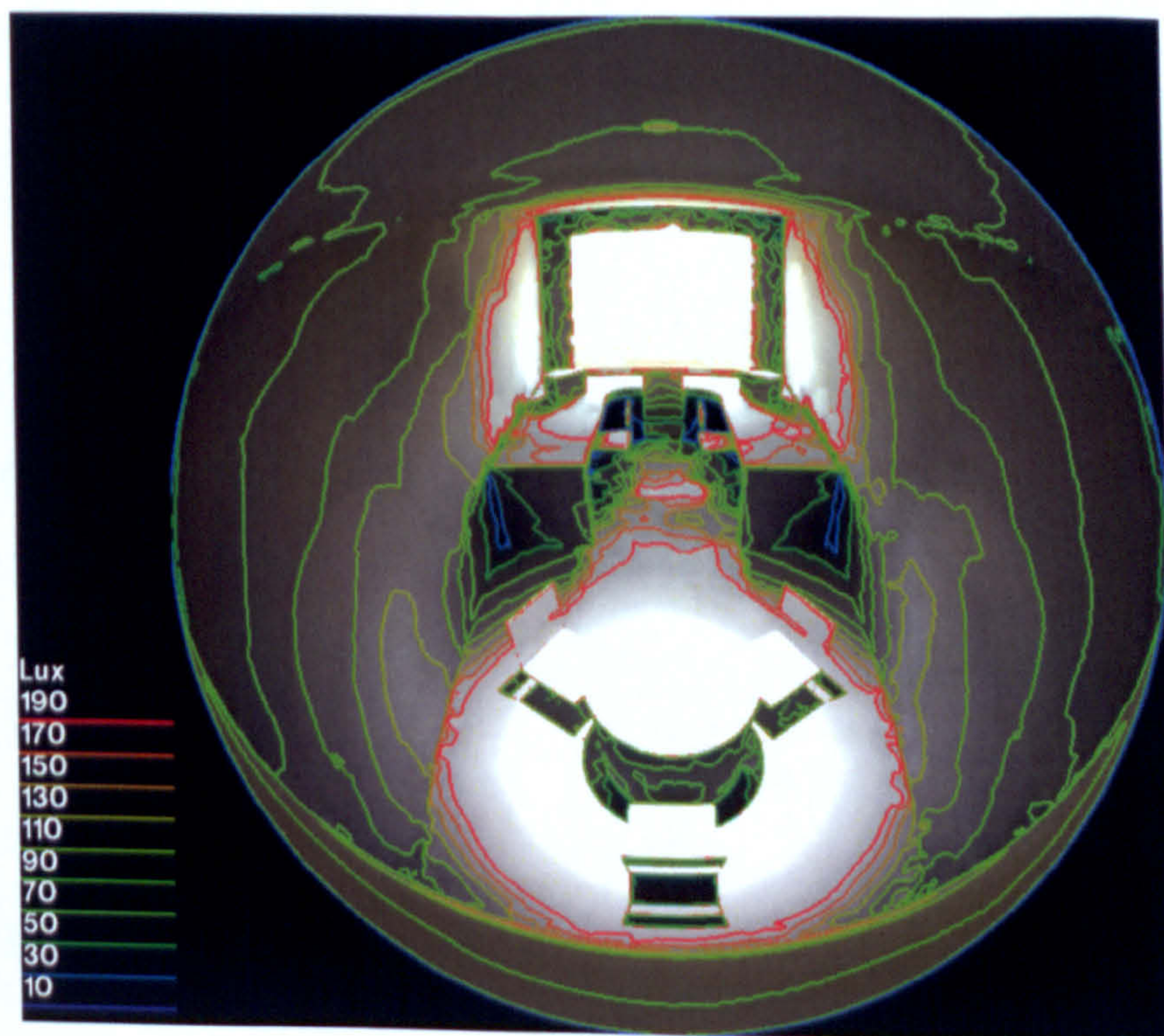


(b)

Figure 4.74 December 21, 12:00 pm, London (luminance)

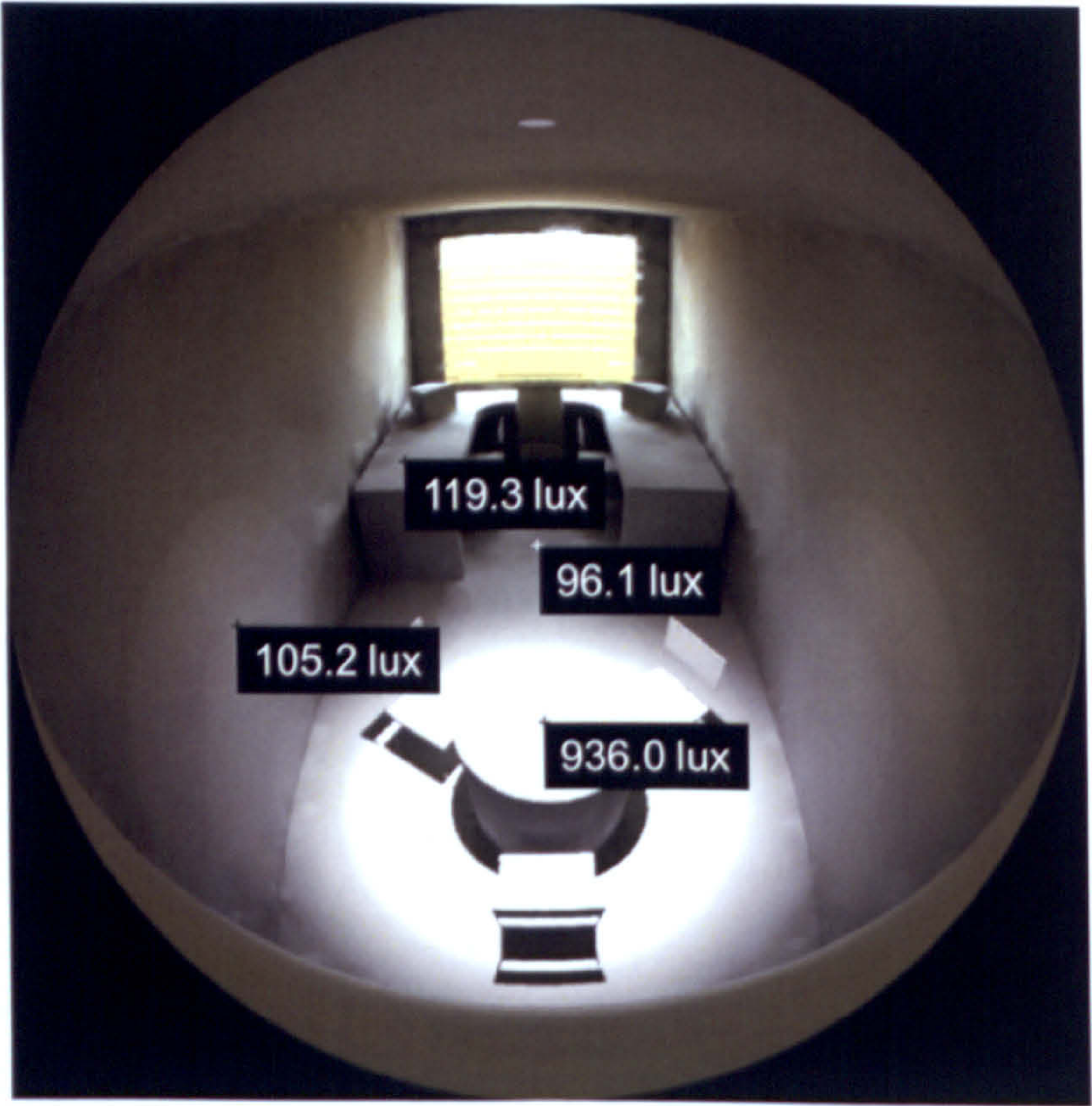


(a)

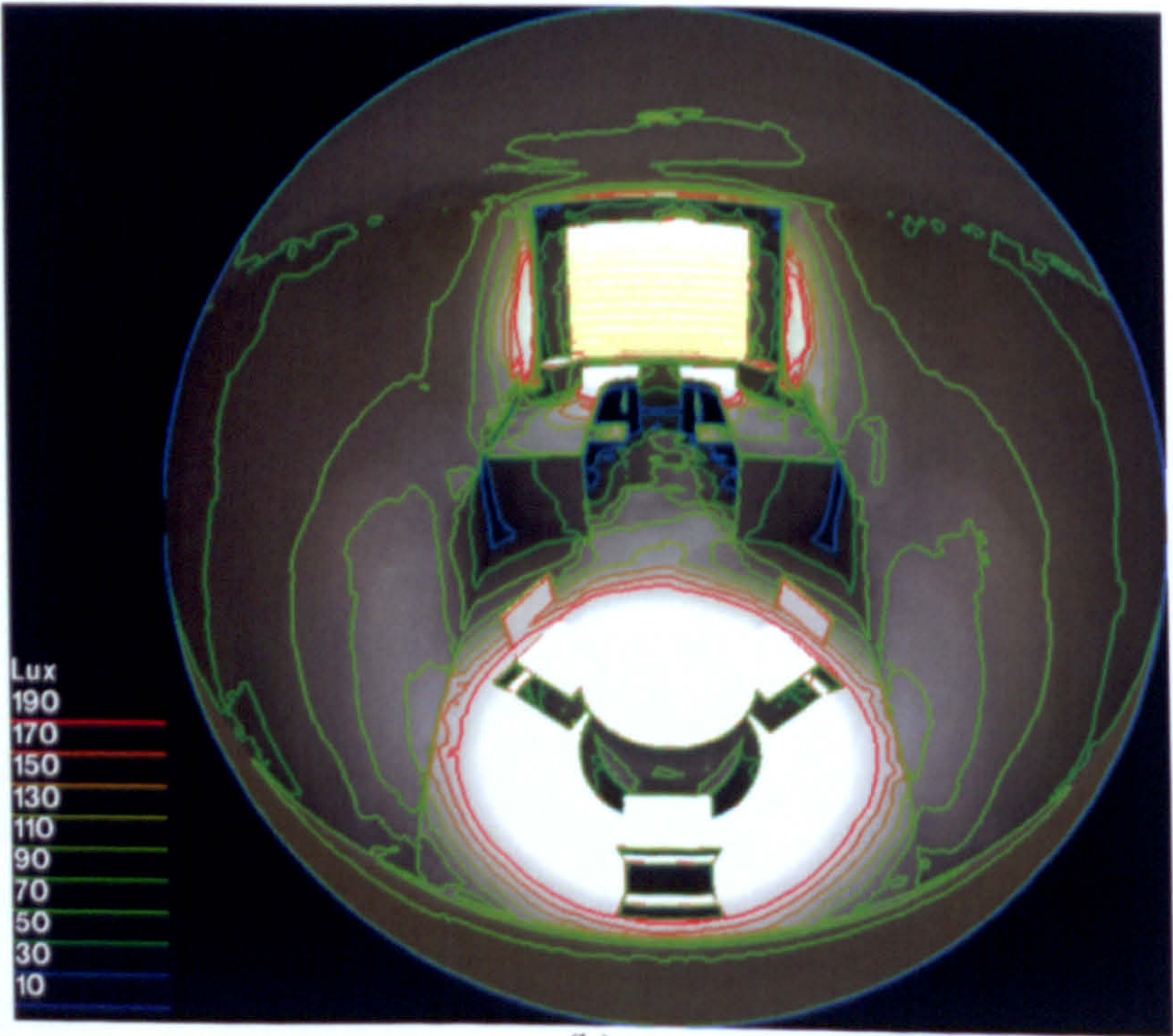


(b)

Figure 4.75 December 21, 12:00 pm, Seoul (illuminance)



(a)



(b)

Figure 4.76 December 21, 12:00 pm, London (illuminance)

4.4 Summary

The applicability of the dish-daylighting daylighting system has been tested for different types of buildings by a series of photometric measurements and simulations. Especially, a number of test cells are designed and built to assess its performance under specified conditions including that in link with a hybrid lighting scheme. A daylighting system with two 15 cm dish concentrators was used in combination with two 25W halogen lamps, which were controlled by a dimmer switch with automatic on-off function. Achieving uniformity and maintaining an adequate level of indoor illumination deem the most important technical issue in applying the present dish-daylighting system. The experiment on actual building has revealed its functional characteristics for different configurations and designs, which are applicable to more realistic situations. Measurements were carried out for buildings in Nottingham (United Kingdom) and Jeju (Korea), which lay the basis for computer simulations under different weather conditions.

5. CONCLUSIONS

Active daylighting systems using different shapes of solar concentrators (dish and funnel shaped) are designed, fabricated and tested for their photometric characteristics and applicability in improving the energy efficiency and lighting conditions of a building. A series of simulations and experimental measurements were carried out to elicit the most effective model and to establish its reliability in reality. The dish-daylighting system proposed here provides an exciting new means of implementing solar lighting not just for energy efficiency itself but for true wellbeing and benefits of the people inside the building.

The models proposed here could be applied to different types of building as long as they could bring sunlight onto the surface of a concentrator. Especially, the dish concentrator design has shown greater potential than the funnel shaped in its design, fabrication, installation and, above all, performance. Since our system constantly tracks the sun, it delivers a rather uniform solar intensity during its hours of operation. Especially, it could be effectively used for hybrid light systems with the aid of a dimmer. The experimental results obtained by its application on a test cell provide practical guidelines for actual implementation of the system.

Also, it deems useful to introduce a ray tracing simulation tool like PHOTOPIA to eliminate extra design variables and fix on a set of essential ones from its initial stage of design procedure. It turned out that this type of simulation offers the experimenter to assess some important design factors such as the shape of the parabolic dish or the size and shape of the reflectors to be tested and analyzed without undue difficulties.

Those results obtained by a series of tests using photometric instruments (such as goniophotometer and etc.) were useful in establishing an informative and comprehensive assessment of the system. In order to determine the workplane illuminance cast by the system, the spatial distribution of light emerging from the terminal device (diffuser) of an optical

fiber cable needs to be verified.

Of the six cases tested, the circular shape acrylic rod spreads out the light most widely followed by semi-concave lens (75 degrees) whereas the semi-convex lens (45 degrees) has shown the smallest light spreading ability. Compared to the optical lenses, the shallow cylindrical acrylic rod(sand-blasted) has shown the possibility of using similar shapes of diffusers to promote uniformity with the application of high concentration daylighting systems considered in the present analysis.

It is noteworthy that the indoor illuminance is not necessarily proportionate to the outdoor illuminance because the present dish-daylighting system tracks the sun utilizing only the beam component of solar irradiation. This was also verified by the luminance ratio maps generated by RADIANCE, which displays various color scales onto the intensity values of a digitized photograph of the object taken with a fish-eye lens. On a clear day, the illuminance ratios of 1.8 ~ 3.5 were recorded at the center of the lighted area by the daylighting system. This is quite a contrast where the illuminance ratios of 0.6 ~ 0.8 were observed when daylight was solely admitted by a window located on the south wall.

When Seoul and London were compared for its performance on one-on-one basis at equinoxes and solstices by RADIANCE, it also showed similar results which totally reflected the availability of direct solar radiation on the day. For London, luminances at the center of the task plane at noon varied from 87.2 cd/m² (summer solstice) to 543.4 cd/m² (vernal equinox) whereas, for Seoul, it fluctuated from 261.5 cd/m² (winter solstice) to 891.8 cd/m² (summer solstice). The corresponding illuminances were 342.5 lux ~ 2,136.6 lux for London and 1,012.4 lux ~ 3,455.2 lux for Seoul, respectively.

It appears the present dish-daylighting system could be effectively applied in bringing natural daylight to non-daylit areas or interior spaces too deep for conventional daylighting apertures. If suitably used with artificial lighting, the daylighting system adds some flexibility

in indoor lighting as it allows individual control over the quality and quantity of light in space. A user can make delicate adjustments selectively to meet his individual preferences for lighting conditions in terms of illuminance level (uniformity), brightness and even color rendition. Most importantly, the system promotes healthy circadian rhythms, reduces stress, and improves productivity in addition to saving energy as sunlight produces less heat per unit of light than electrical lighting.

The present dish-daylighting system is not just functionally reliable but also economically viable as it could be readily integrated with the architecture and is simple in its system configuration. Especially, somewhat different from the existing systems, the modular design of its main components allows the application of off-the-shelf technologies for mass production. It is expected that the system has the potential to save energy use by more than 20 percent if correctly applied to supplement electric lighting with the aid of a suitable controller.

Further extension work is recommended for a complete economical analysis on the system as well as for using numbers of dish concentrators to collect more daylight and to effectively distribute it into building interiors in harmony with the existing light fixtures. Especially, it would be desirable to test its performance with other types of daylighting systems in operation such as light pipes.

BIBLIOGRAPHY

A Report of IEA SHC Task 21 (2000) Daylight in Buildings.

Aarts E and Ruyter BD (2009) “New research perspectives on ambient intelligence”, J. Ambient Intell, Smart Environ 1, pp. 5-14.

Andersen M (2006) “Validation of the performance of a new bidirectional video-goniophotometer”, Lighting Res, Technol 38(4).

ASHRAE (2006) “GreenGuide : the design, construction, and operation of sustainable buildings”, 2nd ed. Atlanta, GA : American Society of Heating, Refrigerating, and Air-Conditioning Engineers.

Atif MR, Love JA and Littlefair P (1997) “Daylighting Monitoring Protocols & Procedures for Buildings”, Daylight in Buildings.

Augustesen C, Brandi U, Dietrich U, Friederici A, Geissmar-Brandi C, Kristensen PT, Madsen M and Storch A (2006) W and B Lighting Design Birkhäuser.

Bonda P and Sosnowchik K (2007) “Sustainable commercial interiors”, Hoboken, NJ : John Wiley & Sons.

Boyce PR et al. (2006) “Occupant use of switching and dimming controls in offices”, Lighting Res. Technol 38(4), pp. 358-378

California Energy Commission (2003. 10) “Modular skylight wells: Design Guidelines for Skylights with Suspended Ceilings”, Design Guidelines (500-03-082-A-13).

Cheng RKC (2007), Inside Rhinoceros 4, McMillan Publishing

Chung B (2008) “Performance evaluation of the wall mounted Hybrid photovoltaic collector combined with Underfloor heating”, MS Thesis, University of Nottingham.

Crone S (1992), RADIANCE User’s Manual.

David Kozlowski (2006. 04) “Using Daylighting To Save On Energy Costs”, Building Operating Management.

Optical & Photometric Technology Pty Ltd. (1999) DP 1600-T Reference & Instruction Manual

Duffie AD and Beckmann WA (2006) “Solar Engineering of Thermal Processes”, John Wiley & Sons.

Dutton S and Shao L (2007) “Ray-tracing simulation for predicting lightpipe transmittance”, Proceedings of the 3rd International Conference on Solar Radiation and Day Lighting, February, India.

ECOTECH Manual (2002), AutoDesk.

Edwards L and Torcellini P (2002) “A literature review of the effects of natural light on build occupants”, NREL.

Egan MD and Olgyay VW (2002) “Architectural Lighting”, 2nd ed McGraw-Hill NY US.

Feuermann D and Gordon JM (2001) “High-concentration Photovoltaic Designs Based on Miniature Parabolic Dishes”, Solar Energy 70(5), pp. 423-430.

Feuermann D and Gordon MG (1999) “Solar fiber-optic mini-dishes: A new approach to the efficient collection of sunlight”, Solar Energy 65(3), UK, pp. 159-170.

FLIR Inc (2009) Getting Started Guide; FLIR iXX

Fontoynt M (1999) “Daylight Performance of Buildings”, Magnum International Printing Co. Ltd., Hong Kong.

Freewan AA (2007. 10) “Optimising the Performance of Innovative Daylighting Systems by Integrating with Ceiling Geometries”, Ph.D Thesis, The school of the Built Environment.

Freewan AA, Shao L and Riffat S (2009) “Interactions between louvers and ceiling geometry for maximum daylighting performance”, Renewable Energy 34, pp. 223-232

Freewan AA, Shao L and Riffat S (2009) “Optimizing performance of the lightshelf by modifying ceiling geometry in highly luminous climates”, Solar Energy 82, pp. 343-353.

Galasiu AD and Atif MR (2002) “Field-performance of daylight-linked lighting controls and window blinds: a pilot study”, 5th European Conference on Energy-Efficient Lighting-Right Light 5 Proceedings (Nice, France).

Galasiu AD and Veitch JA “Occupant preferences and satisfaction with the luminous environment and control systems in daylit offices: a literature review”, Energy and Buildings 38, pp. 728-742.

Garg V and Sarana DC (1997) “Harnessing Sunlight Through Fiber Optics”, TERI Information Digest on Energy [TIDE], 7 (1).

Guzowski M (2000) “Daylighting for Sustainable Design”, McGraw-Hill.

Han H and Kim JT (2006) “Design and Preliminary Performance Test of a Daylighting Device with Mini-dishes”, Proceedings of SET2006, Vicenza Italy.

Han H, Dutton S, Riffat S and Kim JT (2007) “Performance Prediction of Fiber Optic Concentrators for Natural Lighting”, Proceedings of SET2007, Santiago, Chile.

Han HJ and Riffat SB (2009) “Effect of Solar Daylighting on Indoor Visual Environment for an Office Space”, Proceedings of the 8th International Conference on Sustainable Energy Technologies (Aachen, Germany).

Han HJ, Spencer D, Riffat SB and Kim JT (2007) “Performance Prediction of Fiber Optic Concentrators for Natural Lighting”, Proceedings of the 6th International Conference on Sustainable Energy Technologies (Santiago, Chile).

Hecht J (2006) “Understanding Fiber Optics”, Pearson Education, Inc, Upper Saddle River, New Jersey 07458.

Heschong Mahone Group (1999) Daylighting in Schools, “An investigation into the relationship between daylight and human performance”, Detailed Report, Fair Oaks, CA.

Heschong Mahone Group, Inc. (2006) “Scoping Study for Daylight Metrics from Luminance Maps”, Market Research Report.

<http://www.himawari-net.co.jp/>

<http://www.sunlight-direct.com/>

IEA (2000) “Daylight in Buildings”, USA.

Jacobs A UFO (2000. 12) “Universal Fibre Optics (Work Package 1, Deliverable No. 1)”, University of North London.

Kandilli C, Turkoglu AK and Ulgen K (2009) “Transmission performance of fibre-optic bundle for solar lighting”, International Journal of Energy Research 33, pp.194-204.

KIERA (2005) “Report on the Analysis and Planning of Energy & Resource Technologies”.

Koester H (2004) “Dynamic daylighting architecture basics, systems”, projects, Birkhauser.

Kollmann N and Schulz C (2006) “Lighting Design: Principles”, Implementation, Case Studies, Birkhauser, Germany, pp. 6-35.

Konica Minolta (2008) Luminance Meter LS-100/LS-110 Instruction Manual.

Kurian CP, Aithal RS, Bhat J and George VI (2008) “Robust control and optimisation of energy consumption in daylight-artificial light integrated schemes”, Lighting Res. Technol 40, pp. 7-24.

Lee ES and Selkowitz SE (2006) “The New York Times Headquarters daylighting mockup: Monitored performance of the daylighting control system”, Energy and Buildings 38, pp. 914-929.

Lerum V (2008) “High-Performance building”, Hoboken, NJ : John Wiley & Son

Loe DL (2009) “Energy efficiency in lighting-considerations and possibilities”, Lighting Res. Technol 41(3), pp. 209-218.

Lutron (2009) “The Essential Design Element for Any Office Space”, Continuing Education Series, pp. 179-183.

Maamari F, Fontoynt M and Adra N (2006) “Application of the CIE test cases to assess the accuracy of lighting computer programs”, Energy and Buildings 38, pp. 869-877.

Mayhoub MS and Carter DJ (2009) “Towards hybrid lighting systems: A review”, Lighting Res. Technol 00, pp. 1-21.

Michael S, Ross M and Larry K (1998) “Solar Lighting-A New Industry”, Light and Engineering 6, pp. 1-13.

Morad RA, Love JA and Littlefair P (1997) “Daylighting monitoring protocols & procedures for buildings”, IEA Task 21/Annex 29.

Muñoz-Martínez VF, Serón-Barba J, Molina-Mesa R, Gómez-de-Gabriel JM, Fernández-Lozano J and García-Cerezo A (2006) “Double reflection goniophotometer”, Metrologia 43(3), pp. 185-194.

Nabil A and Mardaljevic J (2006) “Useful daylight illuminances: A replacement for daylight factors”, Energy and Buildings 38, pp. 905-913.

Nadal BGMMD (2005. 08) “An Experiment Setup to Evaluate the Daylighting Performance of an Advanced Optical Light Pipe for Deep-plan Office Buildings”, MSc Thesis, Texas A&M University.

Newsham GR, Aries MBC and Mancini S (2009) “Individual control of electric lighting in a daylit space”, Lighting Res. Technol 40, pp. 25-41

Oakley G, Riffat SB and Shao L (2000) "Daylight performance of light pipes. Solar Energy 69(2), pp. 89-98.

PHOTOPIA User's Guide (2002), ver. 2.0.

Photo Research Inc. (1999) PR-680 SpectraScan Colorimeter Brochure

Pohl W and Ansel MC (2000) “Review of Existing Heliostats”, European Commission DG XII.

Pohl W and Anslem C (2002) “Natural room illumination using sunlight. Proceedings of the World Renewable Energy Congress VII (WREC 2002)”, Cologne, Germany.

Pohl W, Zimmermann A and Anslem C (2001. 09) “Review of Coupling Systems (Work Package 7, Deliverable No. 15)”, European Commission DG XII, Austria.

Rea MS (2000) “The IESNA Lighting Handbook Ninth Edition”, IESNA, Publications Department.

- Robbins C (1986)** “Daylighting: Design and Analysis. Van Nostrand Reinhold”, USA, pp 63-86.
- Rosemann A and Kaase H (2004)** “Lightpipe applications for daylighting systems”, Solar Energy 78(6), pp. 772-780.
- Rosemann A and Kasse H (2005)** “Lightpipe applications for daylighting systems”, Solar Energy 8(6), UK, pp 772-780.
- Ross McClunet (1998)** “Advanced Fenestration and DayLighting Systems”, An International Conference on Daylighting Technologies for Energy Efficiency in Buildings, Ph. D. Ottawa, Canada.
- Schlegel GO, Burkholder FW, Klein SA, Beckman WA, Wood BD and Muhs JD (2003)** “Analysis of a full spectrum hybrid lighting system”, 76(4), pp. 359-368.
- Sebe N (2009)** “Multimodal interfaces:Challenges and perspectives”, J. Ambient Intell, Smart Environ 1, pp. 23-30.
- Shao L and Callow JM (2003)** “Daylighting performance of optical rods”, Solar Energy 75, pp. 439-445.
- Sinco (2009)** S-3100 System Manual User’s Guide
- Szokolay SV (2005)** “Introduction to Architectural Science – The Basis of Sustainable Design”, Architectural Press.
- The European Commission(Directorate-General for Energy) (1994)** Daylighting in Buildings.
- Thomas R and Fordham M (2005)** “Taylor & Francis”, USA, pp. 96-109.
- Tsangrassoulis A, Doulos L, Santamouris M, Fontoynt M, Maamari F, Wilson M, Jacobs A, Solomon J, Zimmerman A, Pohl W and Mihalakakou G (2005)** “On the energy efficiency of a prototype hybrid daylighting system”, Solar Energy 79(1), pp. 56-64.
- Wienold J and Christoffersen J (2006)** “Evaluation methods and development of a new glare prediction model for daylight environments with the use of CCD cameras”, Energy and Buildings 38, pp. 743-757.
- Wilson M, Jacobs A and Solomon J (2002)** “Creating sunlight rooms in non-daylight spaces”, RighLight 5, Nice, France.
- Wilson M, Jacobs A, Solomon J, Pohl W, Zimmermann A, Tsangrassoulis J and Fontoynt M (2002)** “Sunlight, fibres and liquid optics : the UFO project”, EPIC 2002 AIVC : Energy Efficient & Healthy Buildings in Sustainable Cities, Lyon, France, 3, pp. 649-654.

Wong N and Agustinus D (2004) “Effect of external shading devices on daylighting penetration in residential buildings”, Lighting Research and Technology 36(4), pp. 317-333.

Xue X, Zheng H, He K, Chen Z, Tao T and Xie G N (2010) “Experimental study on a new solar boiling water system with holistic track solar funnel concentrator”, Energy 35, pp. 692-697.

Yudelson J (2007) “Green building A to Z”, Gabriola Island, BC. Canada : New Society Publishers.

Yudelson J (2008) “The green building revolution”, Washington DC : Island Press.

http://archrecord.construction.com/resources/conteduc/article_pdf/0511lutron.pdf

http://www.sunoptics.com/_pdfs/Sunoptics-Sacramento-Bec-Article-030208.pdf

<http://www.informedesign.umn.edu/>

APPENDIX

**(Goniophotometer
Measurements)**

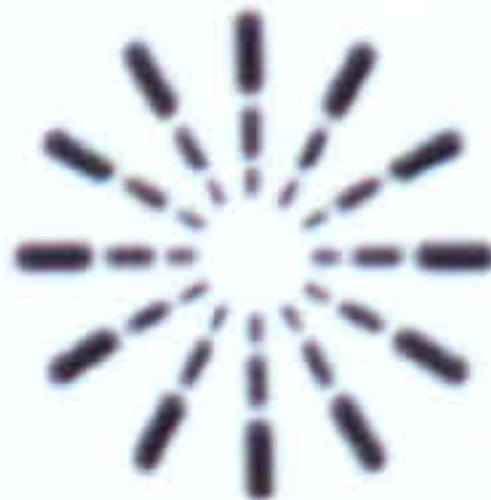
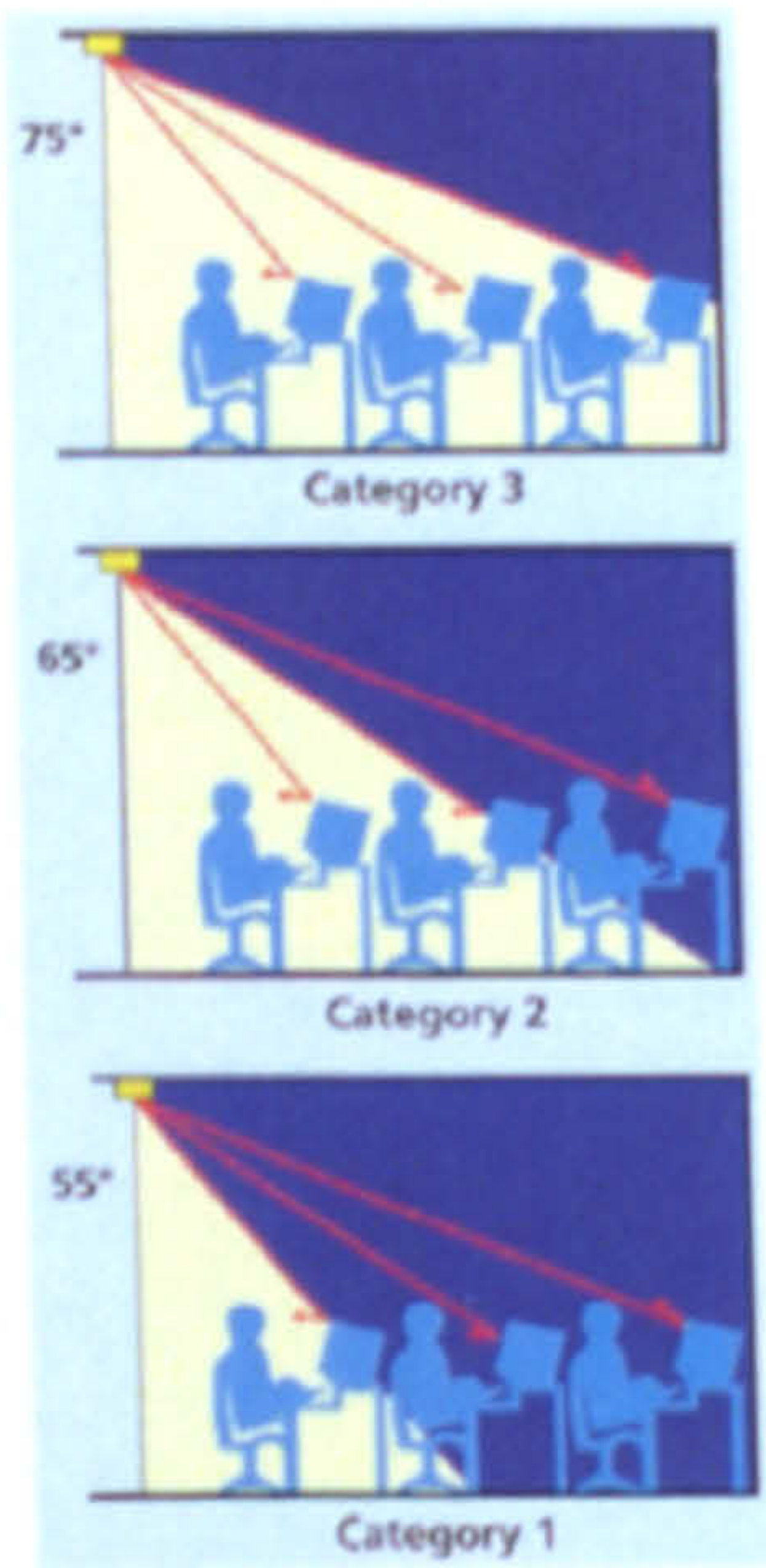
7.1 Semi-concave Lens

Report Number:
Catalog Number:
Description: je-1
Correction Factor Used: White

Date: 18/12/2009

CIBSE LG3 VDT Category

	Category 1	Category 2	Category 3
Starting Gamma Angle (°):	55.0	65.0	75.0
Final Gamma Angle (°):	90.0	90.0	90.0
Avg Luminance Found (cd/m²):	1341	1428	1638
Max. Permissible (cd/m²):	200.0	200.0	200.0
Max Luminance Found (cd/m²):	50700	50700	50700
Max. Permissible (cd/m²):	500.0	500.0	500.0
Result:	-	-	-



Distribution Photometry Report

Report Number:

Date: 18/12/2009

Catalog Number:

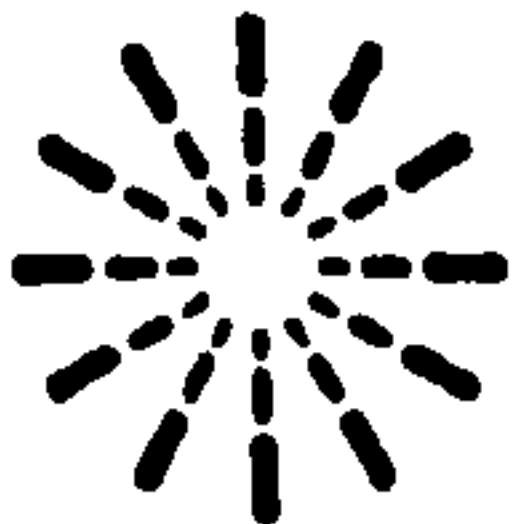
Description: *Je-1*
Correction Factor Used: White

Filename: *Je-1.IES*

Results For: *Test Details*
Luminous Intensity Distribution
LID (Lowest 10%)
Luminous Intensity Data
Luminous Flux Data
Luminaire Luminance
IsoCandela Diagram
IsoLux Diagram
IsoLux 3D
Illuminance Grid
IESNA CoU Table
TM5 UF Table
TM5 UF Table (Variation)
Roadway UF Graph
Zonal Flux Diagram
Luminance Limiting Curve
CIBSE LG3 Rating
Photometric Solid

Page 1 of 23

PhotometricCentre v4.03 Copyright (C) Photometric Solutions International 2004-2008



Photometric Solutions International Pty Ltd
Factory Two, 21-29 Railway Ave
Huntingdale, Vic, 3166, AUSTRALIA
Tel: +61 3 9568 1879
Fax: +61 3 9568 4667
www.PhotometricSolutions.com

IESNA Coefficients of Utilisation Table

Ceiling Cavity Reflect.:	80%			70%			50%			30%			10%			0%
Wall Reflect.:	50%	30%	10%	50%	30%	10%	50%	30%	10%	50%	30%	10%	50%	30%	10%	0%
Room Cavity Ratio	Coefficients of Utilisation for 20% Effective Floor Cavity Reflectance															
0	0.06	0.06	0.06	0.05	0.05	0.05	0.05	0.05	0.05	0.05	0.05	0.05	0.05	0.05	0.05	0.05
1	0.05	0.05	0.05	0.05	0.05	0.04	0.05	0.04	0.04	0.04	0.04	0.04	0.04	0.04	0.04	0.04
2	0.05	0.04	0.04	0.05	0.04	0.04	0.04	0.04	0.04	0.04	0.04	0.04	0.04	0.04	0.04	0.04
3	0.04	0.04	0.04	0.04	0.04	0.04	0.04	0.04	0.04	0.04	0.04	0.04	0.04	0.04	0.04	0.04
4	0.04	0.04	0.04	0.04	0.04	0.04	0.04	0.04	0.04	0.04	0.04	0.04	0.04	0.04	0.04	0.04
5	0.04	0.04	0.04	0.04	0.04	0.04	0.04	0.04	0.04	0.04	0.04	0.04	0.04	0.04	0.03	0.03
6	0.04	0.04	0.03	0.04	0.04	0.03	0.04	0.04	0.03	0.04	0.04	0.03	0.04	0.04	0.03	0.03
7	0.04	0.04	0.03	0.04	0.04	0.03	0.04	0.03	0.03	0.04	0.03	0.03	0.04	0.03	0.03	0.03
8	0.04	0.03	0.03	0.04	0.03	0.03	0.04	0.03	0.03	0.04	0.03	0.03	0.03	0.03	0.03	0.03
9	0.04	0.03	0.03	0.04	0.03	0.03	0.03	0.03	0.03	0.03	0.03	0.03	0.03	0.03	0.03	0.03
10	0.03	0.03	0.03	0.03	0.03	0.03	0.03	0.03	0.03	0.03	0.03	0.03	0.03	0.03	0.03	0.03

Report Number:
Catalog Number:
Description: Je-1
Correction Factor Used: White

Date: 18/12/2009

Illumination Levels

y (m)	0.01	0.01	0.01	0.01	0.02	0.02	0.02	0.03	0.04	0.04	0.04	0.04	0.04	0.03	0.02	0.02	0.01	0.01	0.01	0.01	0.01
3.0	0.01	0.01	0.01	0.02	0.02	0.04	0.05	0.07	0.08	0.09	0.09	0.09	0.08	0.06	0.05	0.03	0.02	0.01	0.01	0.01	0.01
2.4	0.01	0.01	0.02	0.03	0.05	0.07	0.10	0.16	0.21	0.24	0.24	0.23	0.20	0.15	0.09	0.06	0.04	0.02	0.02	0.01	0.01
1.8	0.01	0.02	0.03	0.05	0.08	0.15	0.24	0.33	0.46	0.56	0.59	0.55	0.45	0.32	0.22	0.14	0.07	0.05	0.02	0.02	0.01
1.2	0.01	0.02	0.05	0.08	0.17	0.30	0.50	0.75	0.99	1.18	1.24	1.16	0.95	0.71	0.46	0.27	0.15	0.07	0.04	0.02	0.01
0.6	0.02	0.04	0.07	0.15	0.31	0.57	0.94	1.40	1.84	2.16	2.31	2.15	1.80	1.34	0.87	0.52	0.26	0.13	0.06	0.03	0.02
0.0	0.02	0.05	0.10	0.25	0.52	0.94	1.55	2.33	3.16	3.73	3.93	3.61	3.02	2.23	1.47	0.85	0.44	0.21	0.09	0.04	0.02
-0.6	0.03	0.06	0.16	0.36	0.77	1.39	2.31	3.58	4.89	5.72	5.94	5.53	4.50	3.35	2.16	1.26	0.66	0.29	0.14	0.06	0.03
-1.2	0.04	0.07	0.21	0.48	0.98	1.80	3.16	4.90	6.23	7.08	7.69	7.46	6.06	4.37	2.91	1.65	0.85	0.41	0.18	0.07	0.03
-1.8	0.04	0.08	0.25	0.58	1.19	2.20	3.77	5.80	6.69	7.45	8.57	8.82	7.19	5.05	3.47	1.96	1.01	0.48	0.21	0.07	0.04
-2.4	0.04	0.08	0.26	0.61	1.26	2.32	3.95	5.86	6.72	7.54	8.72	8.97	7.49	5.33	3.67	2.08	1.08	0.52	0.22	0.07	0.04
-3.0	0.04	0.07	0.24	0.58	1.19	2.11	3.63	5.51	6.75	7.53	8.49	8.39	6.80	4.93	3.44	1.92	1.01	0.49	0.21	0.07	0.03
-3.6	0.03	0.07	0.20	0.47	0.98	1.76	2.98	4.48	5.85	6.86	7.37	6.85	5.53	4.17	2.85	1.62	0.84	0.40	0.18	0.06	0.03
-4.2	0.03	0.05	0.14	0.33	0.77	1.39	2.16	3.25	4.32	5.09	5.38	4.93	4.14	3.19	2.05	1.22	0.64	0.29	0.13	0.05	0.02
-4.8	0.02	0.04	0.08	0.23	0.49	0.90	1.46	2.12	2.83	3.32	3.52	3.36	2.82	2.07	1.36	0.79	0.42	0.21	0.08	0.04	0.02
-5.4	0.02	0.03	0.06	0.13	0.27	0.55	0.87	1.28	1.69	1.99	2.11	1.98	1.66	1.22	0.78	0.48	0.25	0.12	0.05	0.03	0.02
-6.0	0.01	0.02	0.04	0.06	0.16	0.27	0.45	0.68	0.87	1.04	1.11	1.02	0.84	0.64	0.42	0.25	0.14	0.06	0.04	0.02	0.01
-6.6	0.01	0.01	0.02	0.04	0.08	0.17	0.22	0.29	0.40	0.48	0.51	0.48	0.40	0.28	0.20	0.12	0.06	0.04	0.02	0.01	0.01
-7.2	0.01	0.01	0.02	0.02	0.06	0.09	0.08	0.13	0.17	0.20	0.21	0.20	0.17	0.12	0.07	0.05	0.04	0.02	0.01	0.01	0.01
-7.8	0.01	0.01	0.01	0.02	0.04	0.06	0.05	0.05	0.06	0.06	0.06	0.06	0.06	0.05	0.04	0.03	0.02	0.01	0.01	0.01	0.01
-8.4	0.01	0.01	0.01	0.01	0.04	0.04	0.03	0.03	0.03	0.03	0.03	0.03	0.03	0.03	0.02	0.01	0.01	0.01	0.01	0.01	0.01
-9.0	-3.0	-2.4	-1.8	-1.2	-0.6	0.0	0.6	1.2	1.8	2.4	3.0										
																					x (m)

Horizontal Illuminance
All illuminance values in lux / 1000 lm
Table Average: 1.15 Table Maximum: 8.97 Table Minimum: 0.01
Mounting Height = 2.7 m

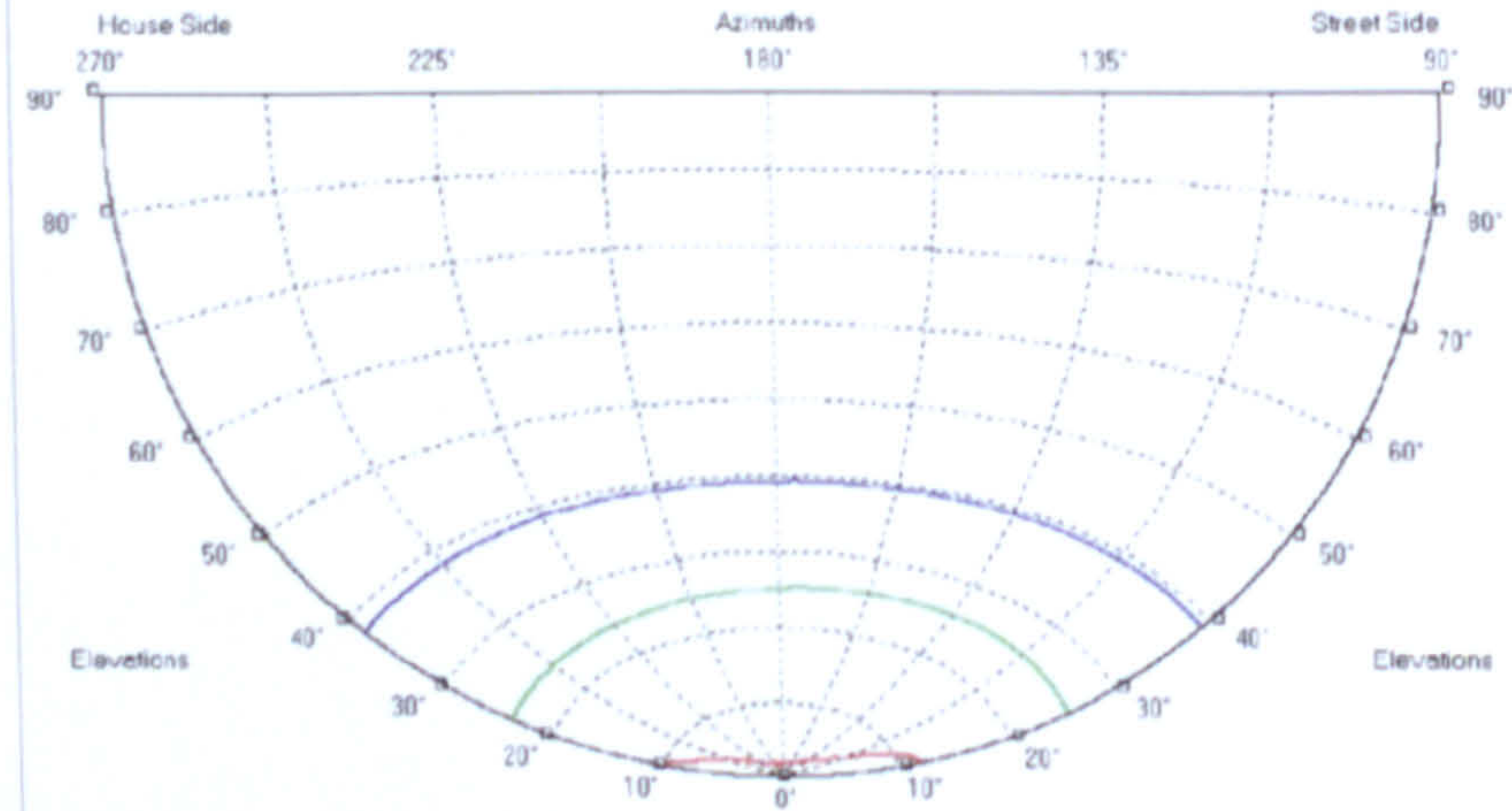
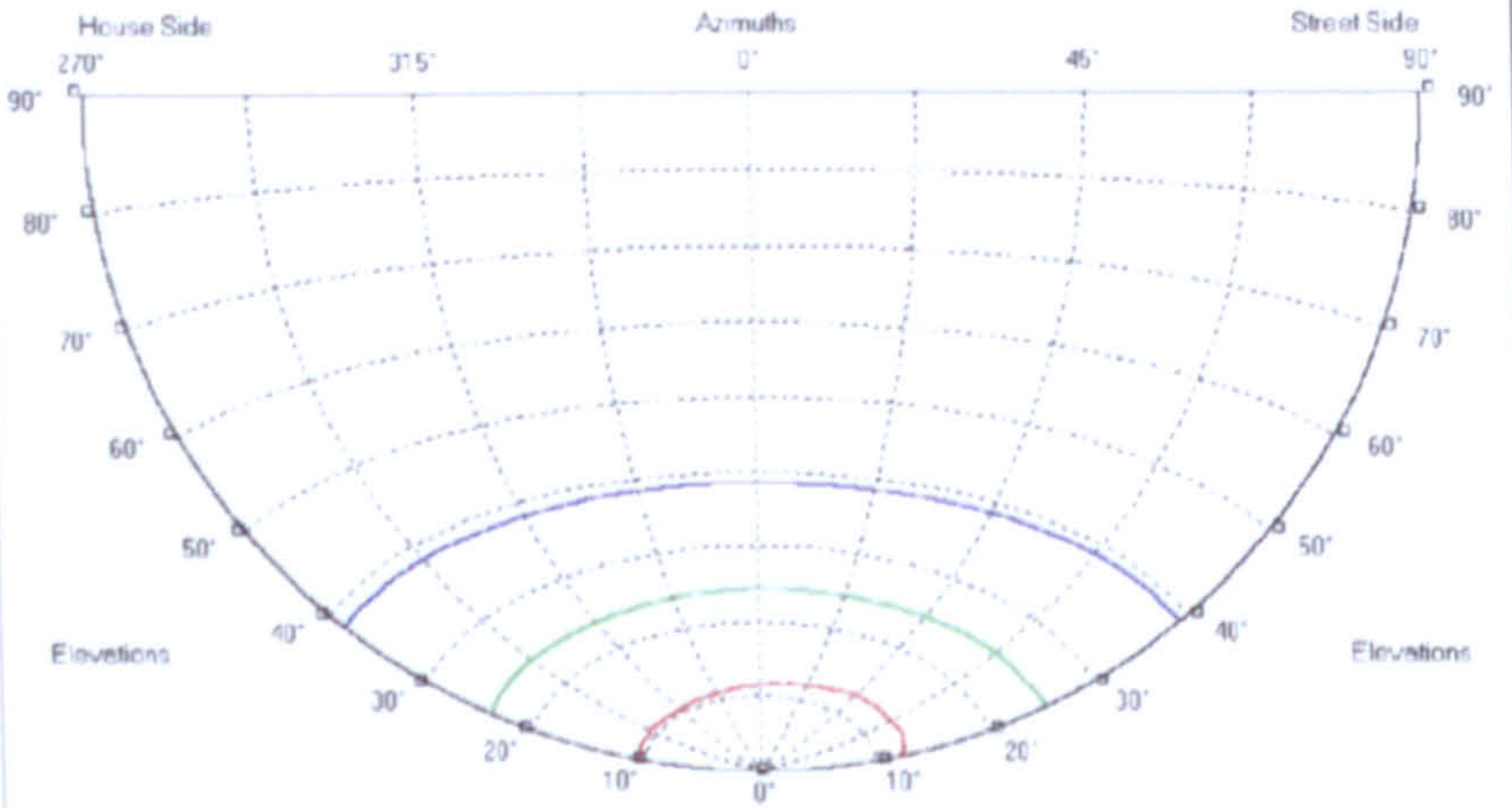


Photometric Solutions International Pty Ltd
Factory Two, 21-29 Railway Ave
Huntingdale, Vic, 3166, AUSTRALIA
Tel: +61 3 9568 1879
Fax: +61 3 9568 4667
www.PhotometricSolutions.com

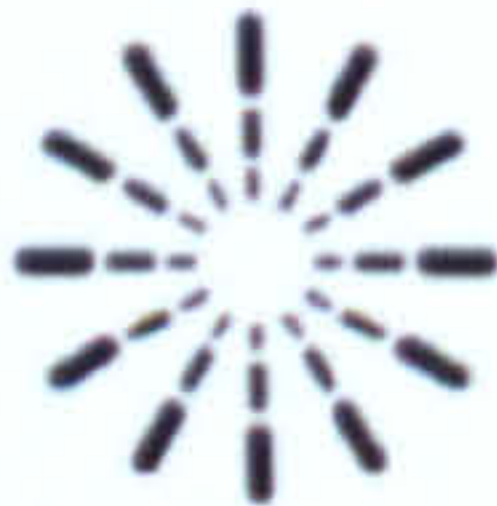
IsoCandela Diagram

Legend
(cd / 1000 lm)
Max = 67.5

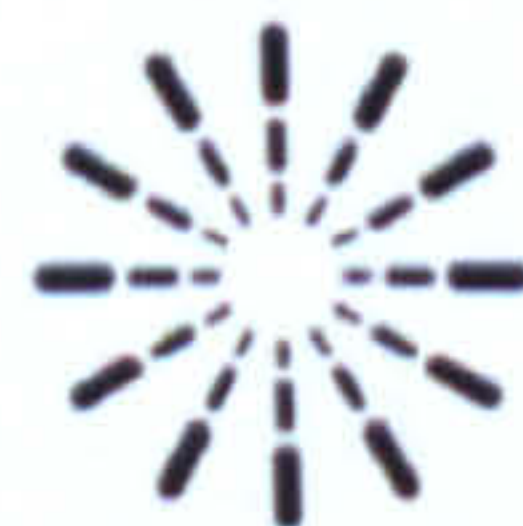
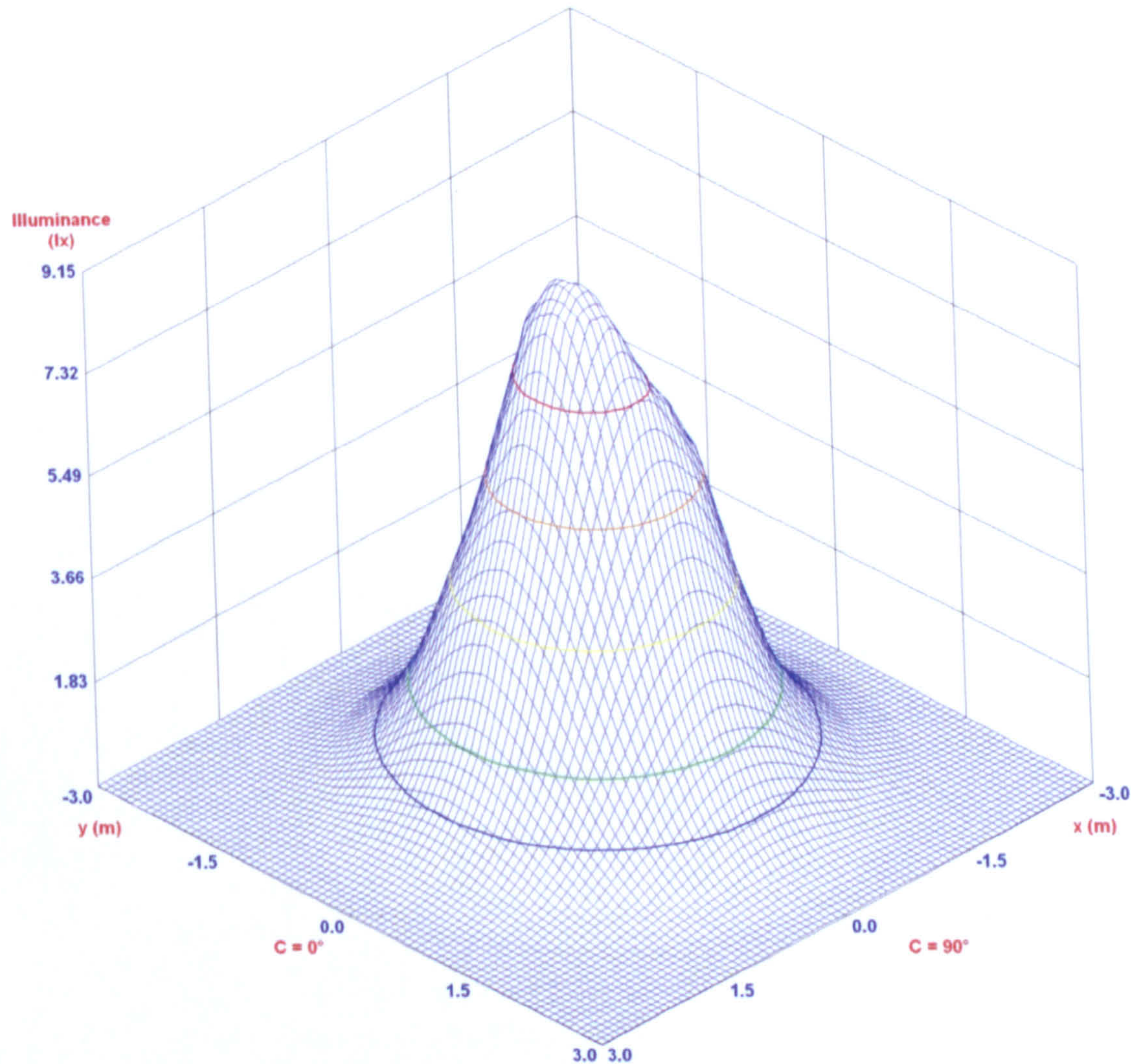
- 60.8 (90.0%)
- 33.8 (50.0%)
- 6.8 (10.0%)



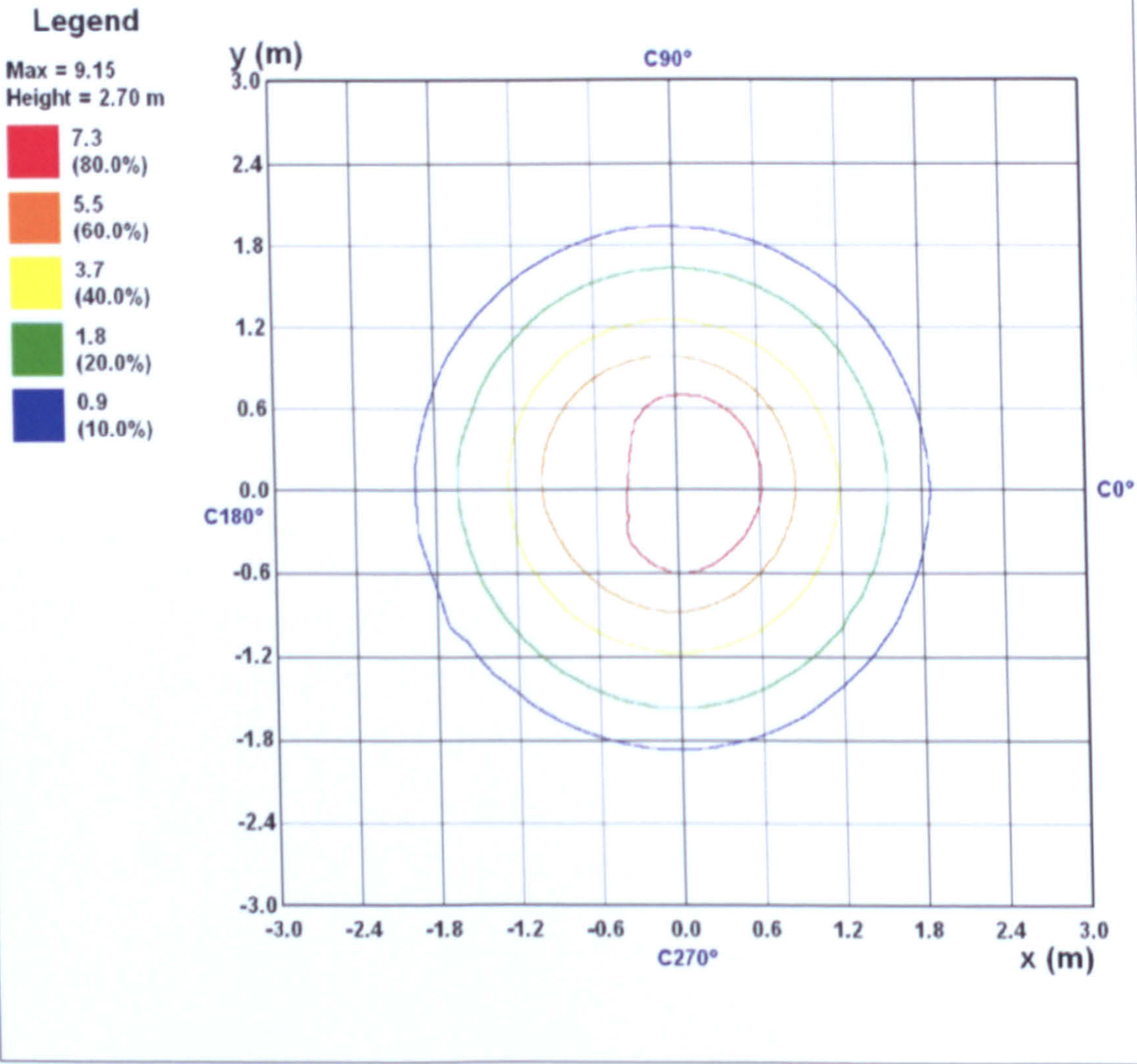
All luminous intensity values in cd / 1000 lm



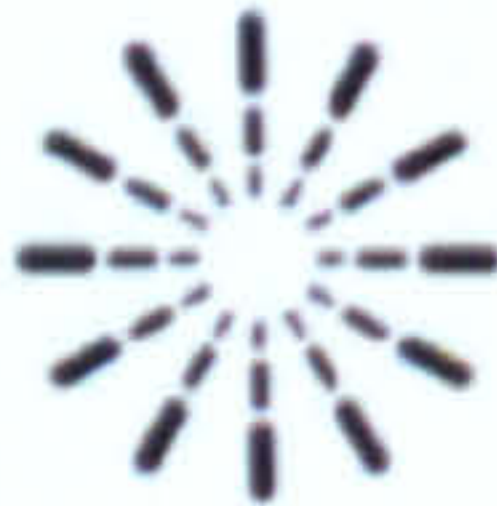
IsoLux 3D



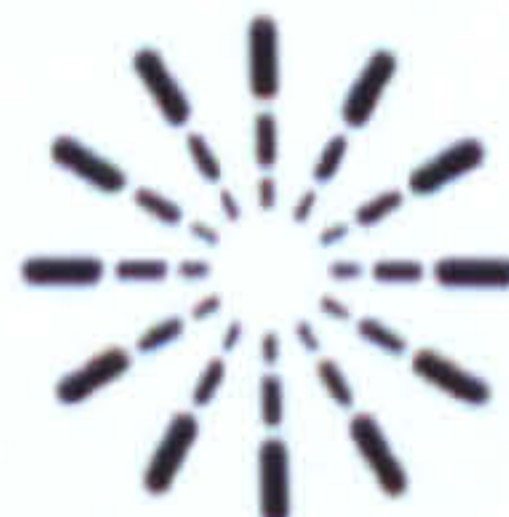
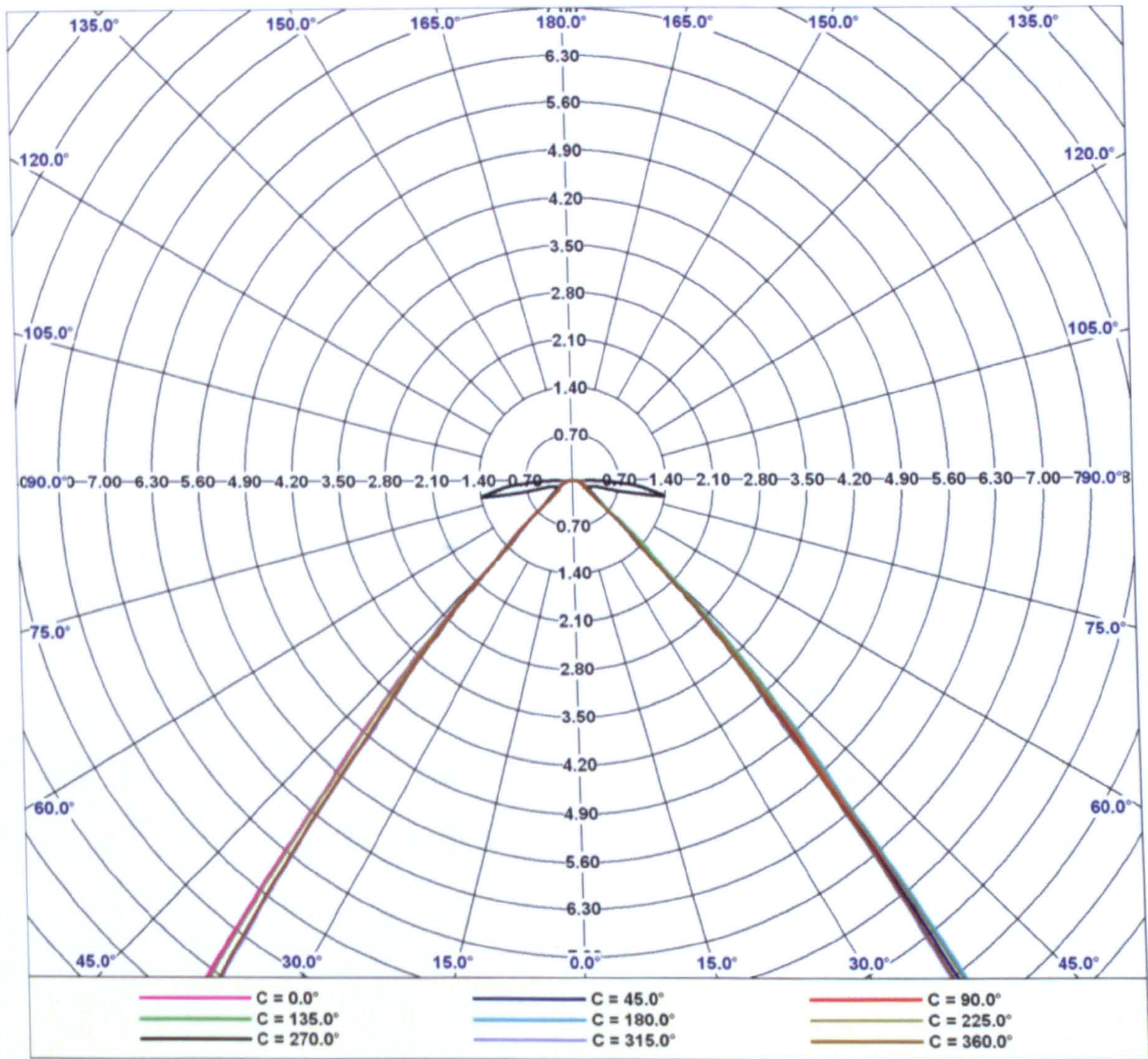
IsoLux Diagram



All illuminance values in lx / 1000 lm



Luminous Intensity Distribution (Lowest 10%)



Report Number:
Catalog Number:
Description: *je-1*
Correction Factor Used: White

Date: 18/12/2009

Average Luminance Table

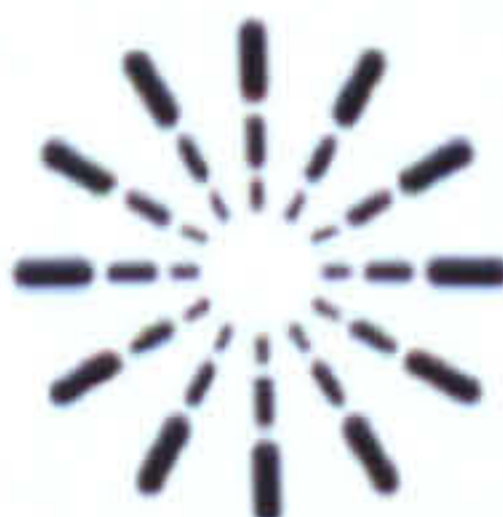
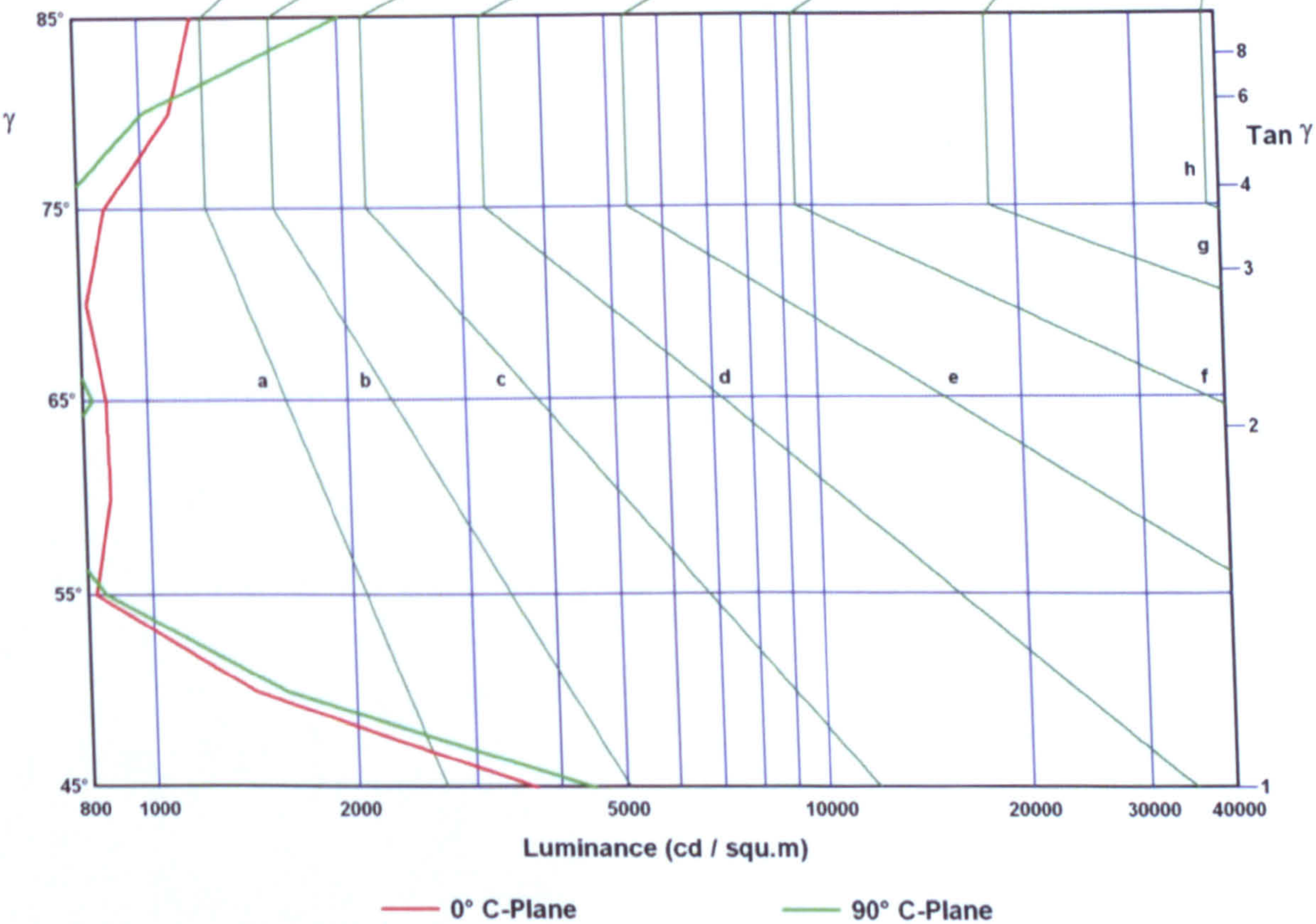
All luminance values expressed in cd / squ.m / 1000 lm

Azimuth:	0	45	90	135	180	235	270	315
Elevation								
0	111000	111000	111000	111000	111000	111000	111000	111000
45	3680	4220	4500	4690	4050	6640	3290	3480
55	822	914	853	944	761	944	1160	944
65	868	951	827	992	909	909	909	909
75	877	675	742	945	675	1150	2360	945
85	1200	1600	2000	200	1000	2000	19000	401



Luminance Limiting Curve

Glare Rating	Quality Class	Service Values of Illuminance (lx)							
		2000	1000	500	<300	e	f	g	h
1.15	A								
1.5	B		2000	1000	500	<300			
1.85	C			2000	1000	500	<300		
2.2	D				2000	1000	500	<300	
2.55	E	a	b	c	d	2000	1000	500	<300



Report Number:
Catalog Number:
Description: *Je-1*
Correction Factor Used: White

Date: 18/12/2009

Luminous Flux Table

Elevation	Cone	Lumens	Cumulative	Lamp %	Luminaire %
0°	0.00° - 2.50°	0.4	0.4	0.0	0.8
5°	2.50° - 7.50°	3.0	3.4	0.3	7.3
10°	7.50° - 12.50°	5.7	9.1	0.9	19.7
15°	12.50° - 17.50°	7.7	16.8	1.7	36.3
20°	17.50° - 22.50°	8.4	25.3	2.5	54.4
25°	22.50° - 27.50°	7.8	33.0	3.3	71.2
30°	27.50° - 32.50°	5.9	39.0	3.9	83.9
35°	32.50° - 37.50°	3.9	42.8	4.3	92.3
40°	37.50° - 42.50°	1.9	44.7	4.5	96.3
45°	42.50° - 47.50°	0.6	45.3	4.5	97.7
50°	47.50° - 52.50°	0.2	45.6	4.6	98.2
55°	52.50° - 57.50°	0.1	45.7	4.6	98.5
60°	57.50° - 62.50°	0.2	45.9	4.6	98.9
65°	62.50° - 67.50°	0.1	46.0	4.6	99.1
70°	67.50° - 72.50°	0.1	46.1	4.6	99.3
75°	72.50° - 77.50°	0.1	46.2	4.6	99.5
80°	77.50° - 82.50°	0.1	46.3	4.6	99.7
85°	82.50° - 87.50°	0.1	46.4	4.6	100.0
90°	87.50° - 90.00°	0.0	46.4	4.6	100.0

Light Output Ratio = 4.6% (DLOR = 4.6% , ULOR = 0.0%)



Report Number:
Catalog Number:
Description: *Je-1*
Correction Factor Used: White

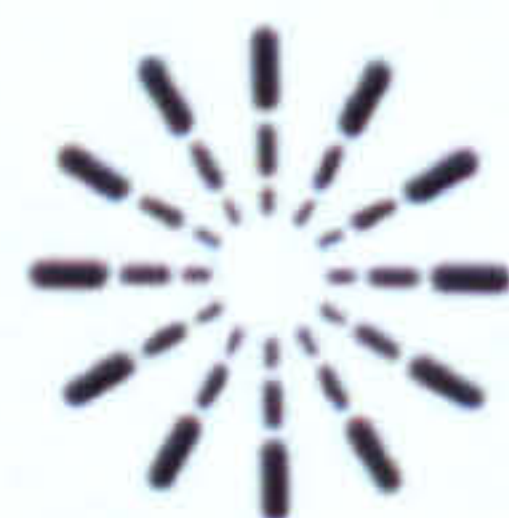
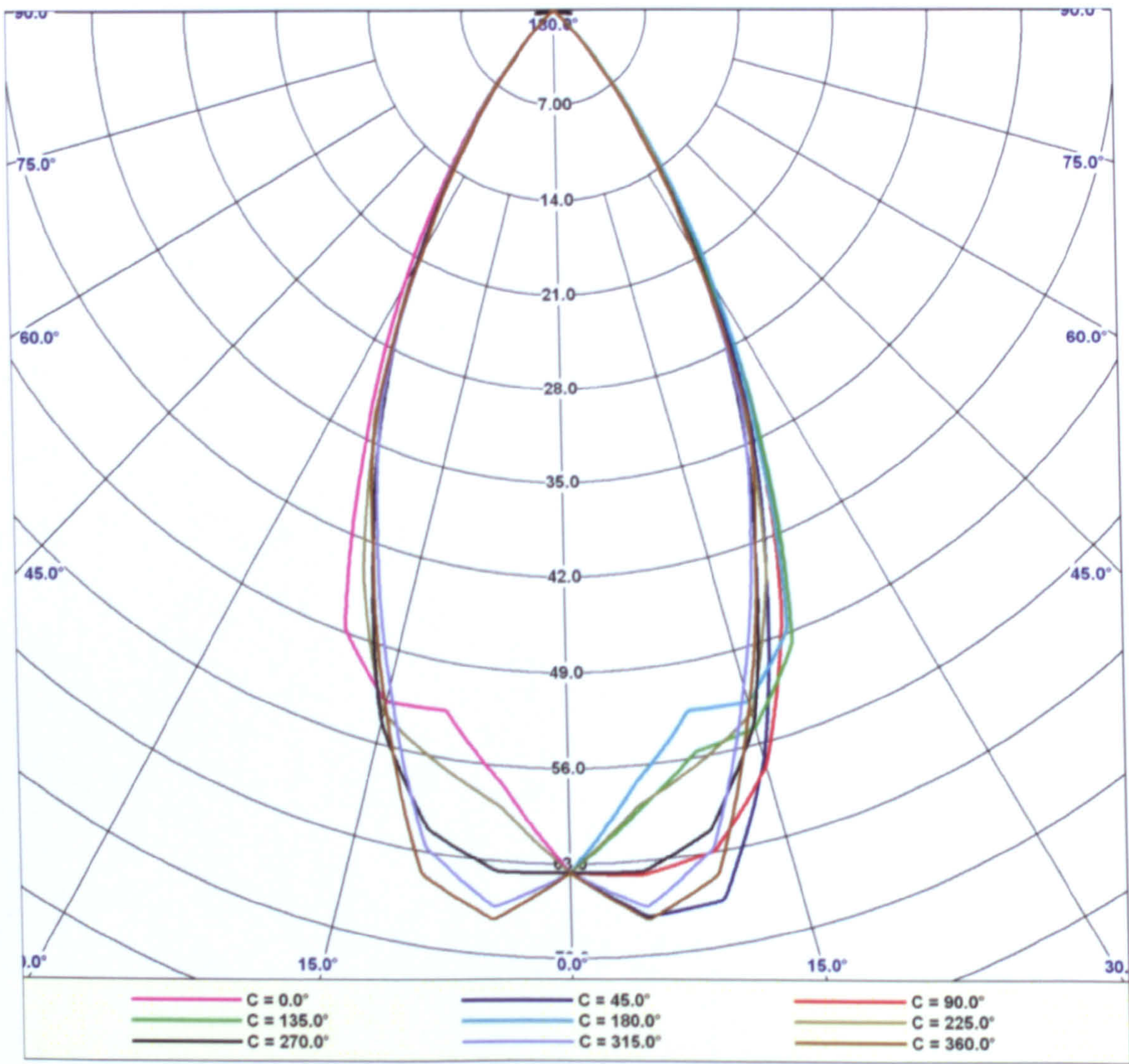
Date: 18/12/2009

Luminous Intensity Table (cd / 1000 lm) (Continued)

$\gamma \setminus C$	320.0	325.0	330.0	335.0	340.0	345.0	350.0	355.0	360.0
0.0	63.6	63.6	63.6	63.6	63.6	63.6	63.6	63.6	63.6
5.0	66.2	66.8	66.7	67.0	67.0	67.3	67.5	67.4	67.3
10.0	62.5	62.9	62.8	63.3	63.6	63.7	64.3	64.4	64.6
15.0	51.4	52.2	52.0	51.8	51.7	52.6	52.5	52.9	53.0
20.0	41.1	41.6	41.2	41.7	41.4	41.6	41.8	41.9	42.1
25.0	32.1	32.0	32.5	32.4	32.6	32.6	32.8	32.7	33.2
30.0	20.6	19.7	20.5	20.0	20.4	20.1	20.1	20.4	20.2
35.0	11.1	11.1	11.4	11.1	11.3	11.2	11.2	11.4	11.4
40.0	4.8	4.8	4.9	4.9	4.9	5.0	5.0	4.9	5.0
45.0	1.4	1.4	1.4	1.5	1.4	1.5	1.5	1.5	1.5
50.0	0.5	0.5	0.5	0.5	0.5	0.5	0.5	0.5	0.5
55.0	0.3	0.3	0.3	0.3	0.3	0.3	0.3	0.3	0.3
60.0	0.3	0.3	0.3	0.3	0.2	0.2	0.3	0.2	0.3
65.0	0.2	0.2	0.2	0.2	0.2	0.3	0.2	0.2	0.2
70.0	0.2	0.2	0.2	0.2	0.1	0.2	0.2	0.2	0.2
75.0	0.1	0.1	0.1	0.2	0.1	0.2	0.1	0.1	0.1
80.0	0.0	0.1	0.1	0.1	0.1	0.1	0.1	0.1	0.1
85.0	0.0	0.0	0.0	0.1	0.1	0.0	0.1	0.1	0.1
90.0	0.0	0.0	0.0	0.0	0.0	0.0	0.0	0.0	0.0



Luminous Intensity Distribution



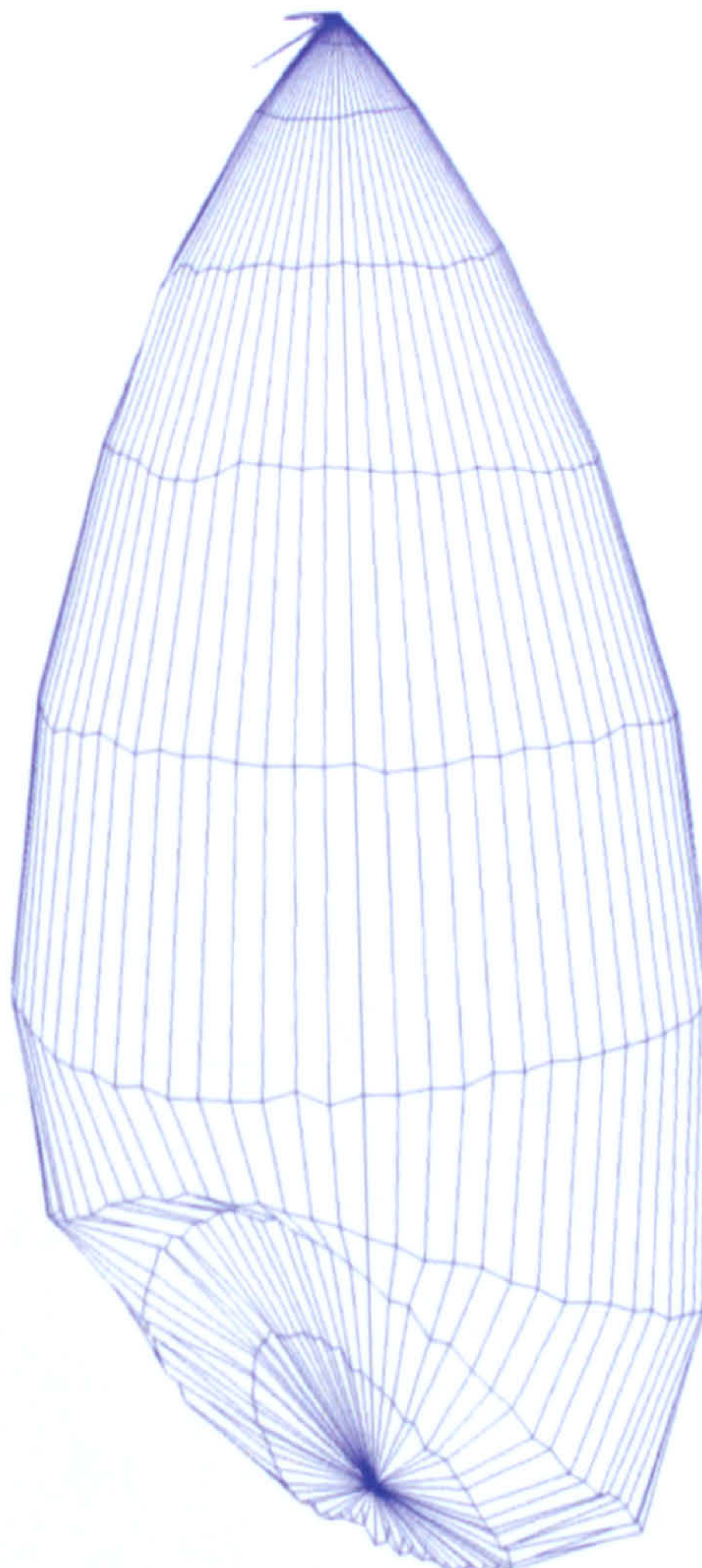
Report Number:

Date: 18/12/2009

Catalog Number:

Description: *je-1*
Correction Factor Used: White

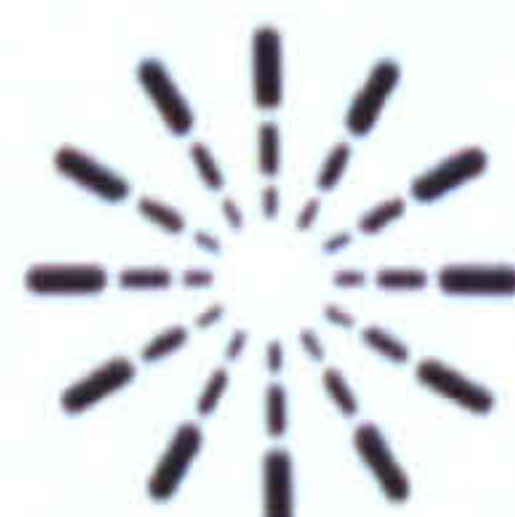
Photometric Solid



Viewing Angle: C = 315°

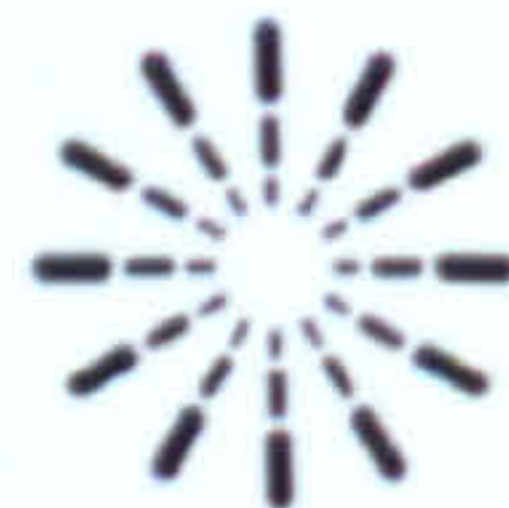
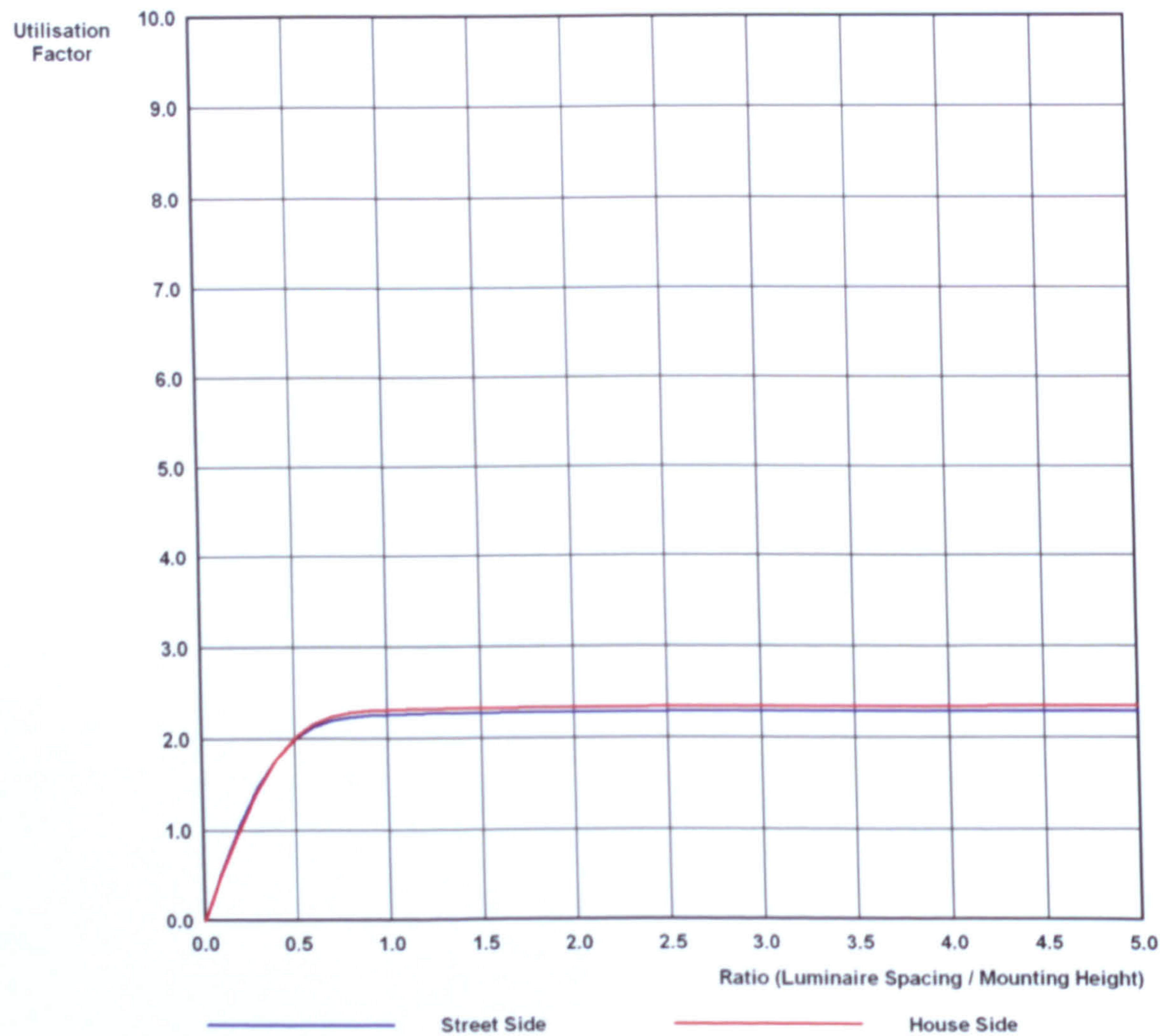
Page 23 of 23

PhotometricCentre v4.03 Copyright (C) Photometric Solutions International 2004-2008



Photometric Solutions International Pty Ltd
Factory Two, 21-29 Railway Ave
Huntingdale, Vic, 3166, AUSTRALIA
Tel: +61 3 9568 1879
Fax: +61 3 9568 4667
www.PhotometricSolutions.com

Roadway Utilisation Factor Graph



Report Number:
Catalog Number:
Description: *Je-1*
Correction Factor Used: White

Date: 18/12/2009

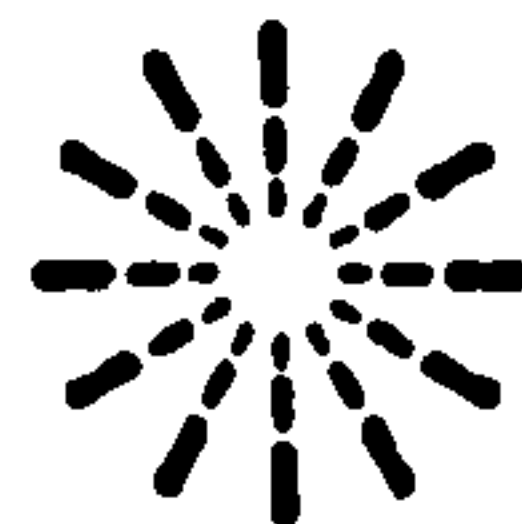
Luminaire Details

Luminaire Test Details:

Photometry Type: *Type C/Gamma*
Number of Lamps: *1*
Lumens per Lamp: *1000*

Luminous Dimensions:

Base Area: *0.027 m Diameter*
Side Area: *N/A*
End Area: *N/A*
Luminous Shape: *Circular*



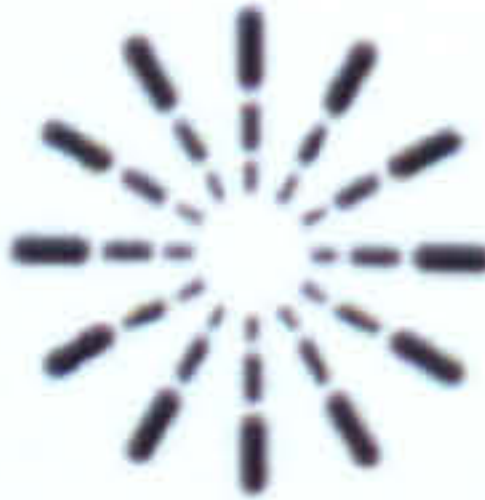
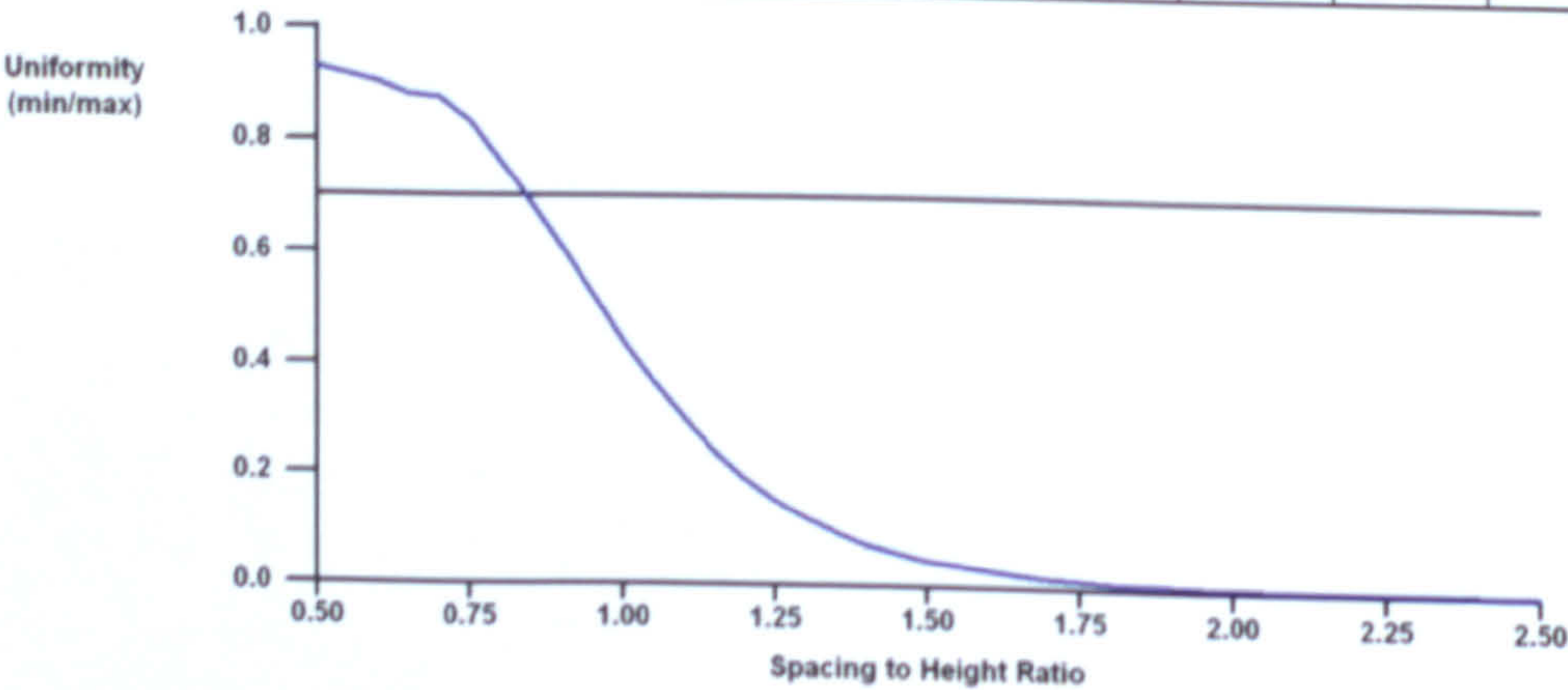
Report Number:
Catalog Number:
Description: je-1
Correction Factor Used: White

Date: 18/12/2009

TM5 Utilisation Factor Table

SHR Nominal = 0.75:1 SHR Maximum = 0.84:1

Reflectance			Room Index (K)								
Ceiling	Wall	Floor	0.75	1.00	1.25	1.50	2.00	2.50	3.00	4.00	5.00
0.70	0.50	0.20	0.04	0.04	0.04	0.05	0.05	0.05	0.05	0.05	0.05
0.70	0.30	0.20	0.04	0.04	0.04	0.04	0.05	0.05	0.05	0.05	0.05
0.70	0.10	0.20	0.04	0.04	0.04	0.04	0.04	0.05	0.05	0.05	0.05
0.50	0.50	0.20	0.04	0.04	0.04	0.04	0.05	0.05	0.05	0.05	0.05
0.50	0.30	0.20	0.04	0.04	0.04	0.04	0.05	0.05	0.05	0.05	0.05
0.50	0.10	0.20	0.04	0.04	0.04	0.04	0.04	0.05	0.05	0.05	0.05
0.30	0.50	0.20	0.04	0.04	0.04	0.04	0.05	0.05	0.05	0.05	0.05
0.30	0.30	0.20	0.04	0.04	0.04	0.04	0.04	0.05	0.05	0.05	0.05
0.30	0.10	0.20	0.04	0.04	0.04	0.04	0.04	0.04	0.05	0.05	0.05
0.00	0.00	0.00	0.03	0.04	0.04	0.04	0.04	0.04	0.04	0.04	0.04
Distribution Factors			Floor:	0.03	0.04	0.04	0.04	0.04	0.04	0.04	0.04
			Wall:	0.01	0.01	0.01	0.01	0.00	0.00	0.00	0.00
			Ceiling:	0.00	0.00	0.00	0.00	0.00	0.00	0.00	0.00
BZ Numbers:				1	1	1	1	1	1	1	1



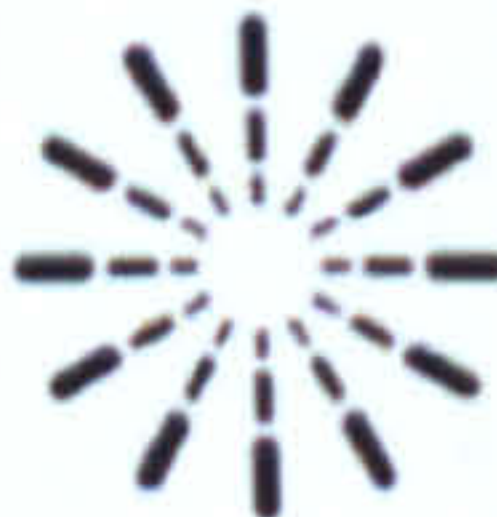
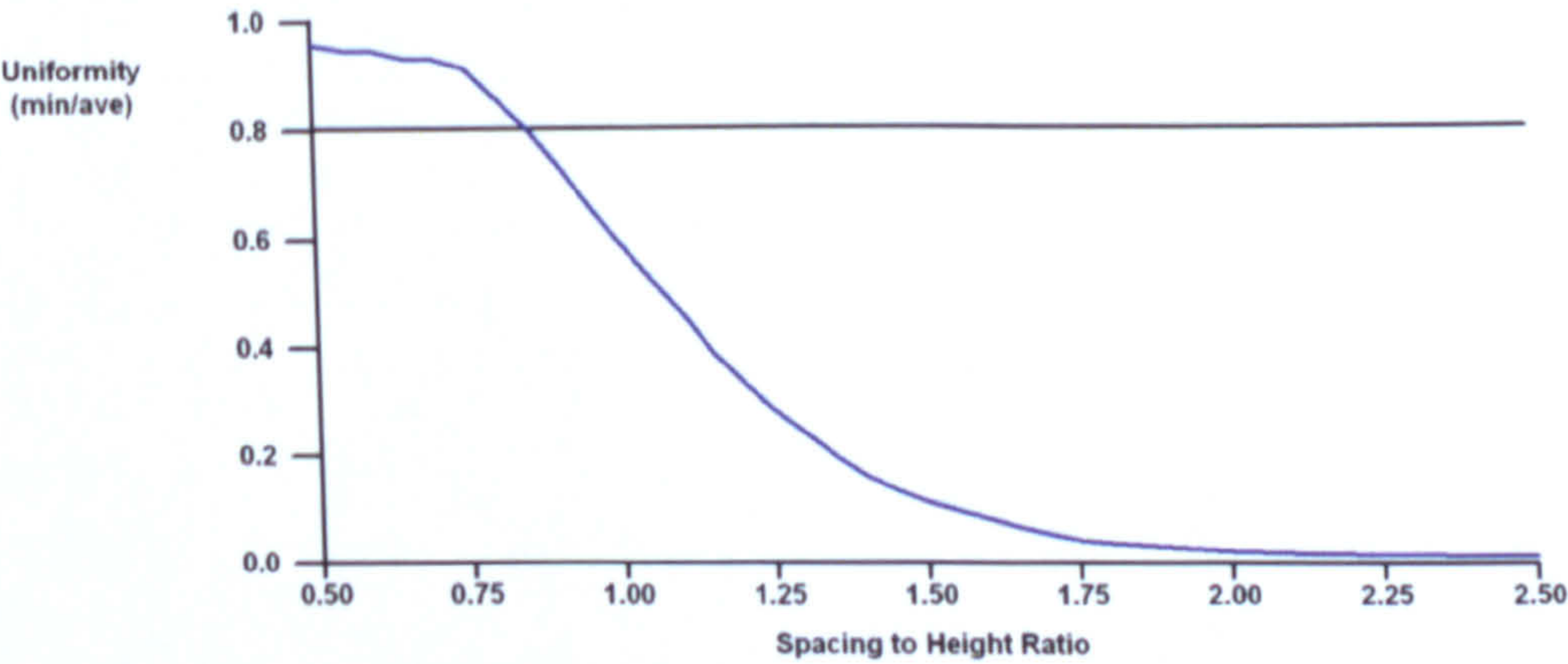
Report Number:
Catalog Number:
Description: je-1
Correction Factor Used: White

Date: 18/12/2009

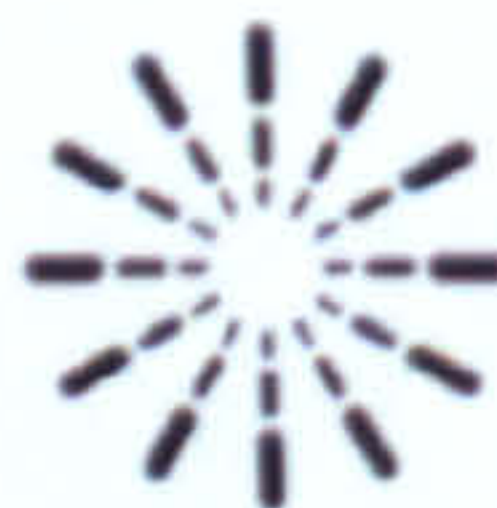
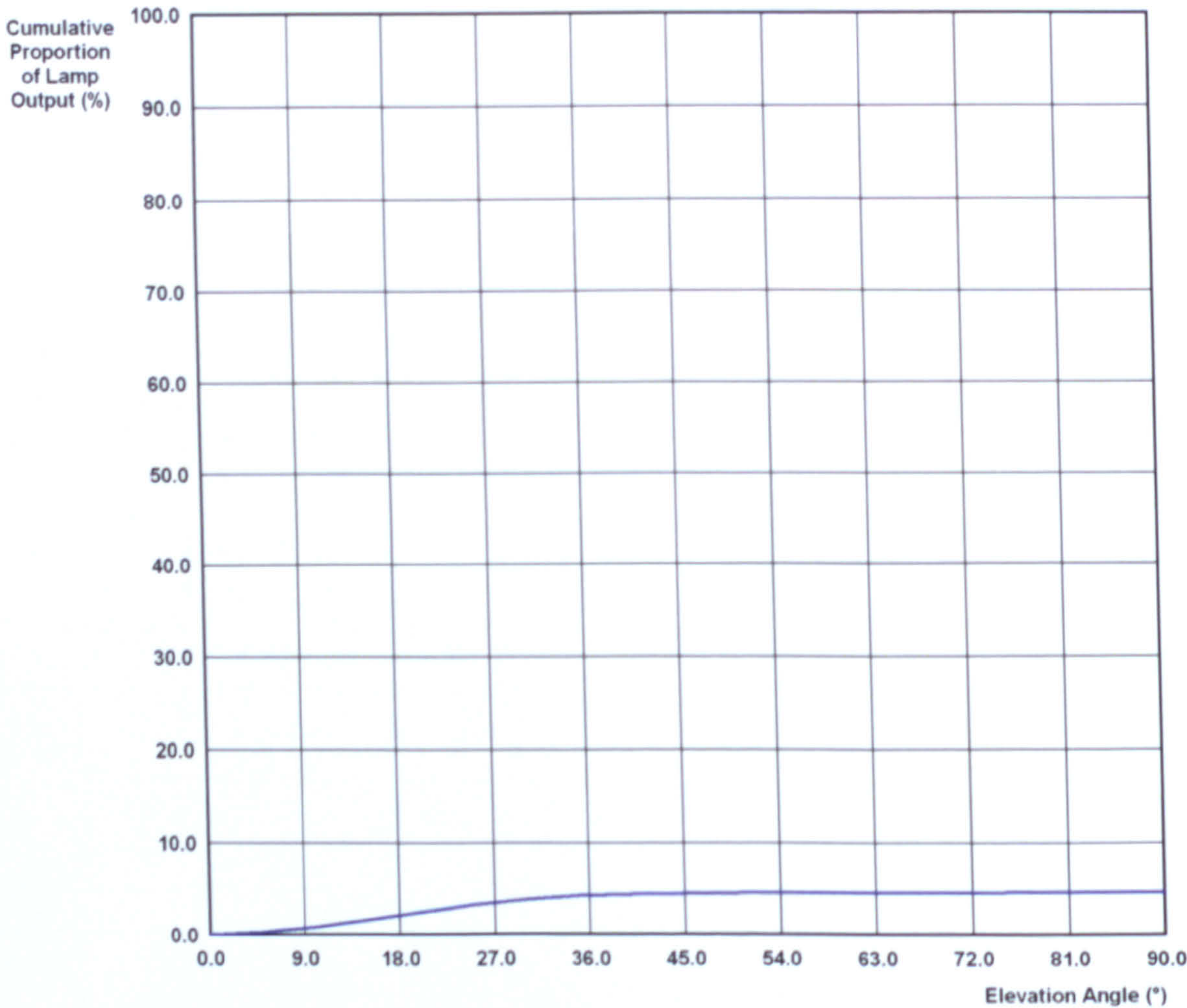
TM5* Utilisation Factor Table

* Based on TM5, except using Min / Ave = 0.8 as Spacing Criteria
SHR Nominal = 0.75:1 SHR Maximum = 0.90:1

Reflectance			Room Index (K)								
Ceiling	Wall	Floor	0.75	1.00	1.25	1.50	2.00	2.50	3.00	4.00	5.00
0.70	0.50	0.20	0.04	0.04	0.04	0.05	0.05	0.05	0.05	0.05	0.05
0.70	0.30	0.20	0.04	0.04	0.04	0.04	0.05	0.05	0.05	0.05	0.05
0.70	0.10	0.20	0.04	0.04	0.04	0.04	0.04	0.05	0.05	0.05	0.05
0.50	0.50	0.20	0.04	0.04	0.04	0.04	0.05	0.05	0.05	0.05	0.05
0.50	0.30	0.20	0.04	0.04	0.04	0.04	0.05	0.05	0.05	0.05	0.05
0.50	0.10	0.20	0.04	0.04	0.04	0.04	0.04	0.05	0.05	0.05	0.05
0.30	0.50	0.20	0.04	0.04	0.04	0.04	0.05	0.05	0.05	0.05	0.05
0.30	0.30	0.20	0.04	0.04	0.04	0.04	0.04	0.05	0.05	0.05	0.05
0.30	0.10	0.20	0.04	0.04	0.04	0.04	0.04	0.04	0.05	0.05	0.05
0.00	0.00	0.00	0.03	0.04	0.04	0.04	0.04	0.04	0.04	0.04	0.04
Distribution Factors			Floor:	0.03	0.04	0.04	0.04	0.04	0.04	0.04	0.04
			Wall:	0.01	0.01	0.01	0.01	0.00	0.00	0.00	0.00
			Ceiling:	0.00	0.00	0.00	0.00	0.00	0.00	0.00	0.00
BZ Numbers:				1	1	1	1	1	1	1	1



Zonal Flux Diagram



7.2 Concave Lens

Report Number:

Catalog Number:

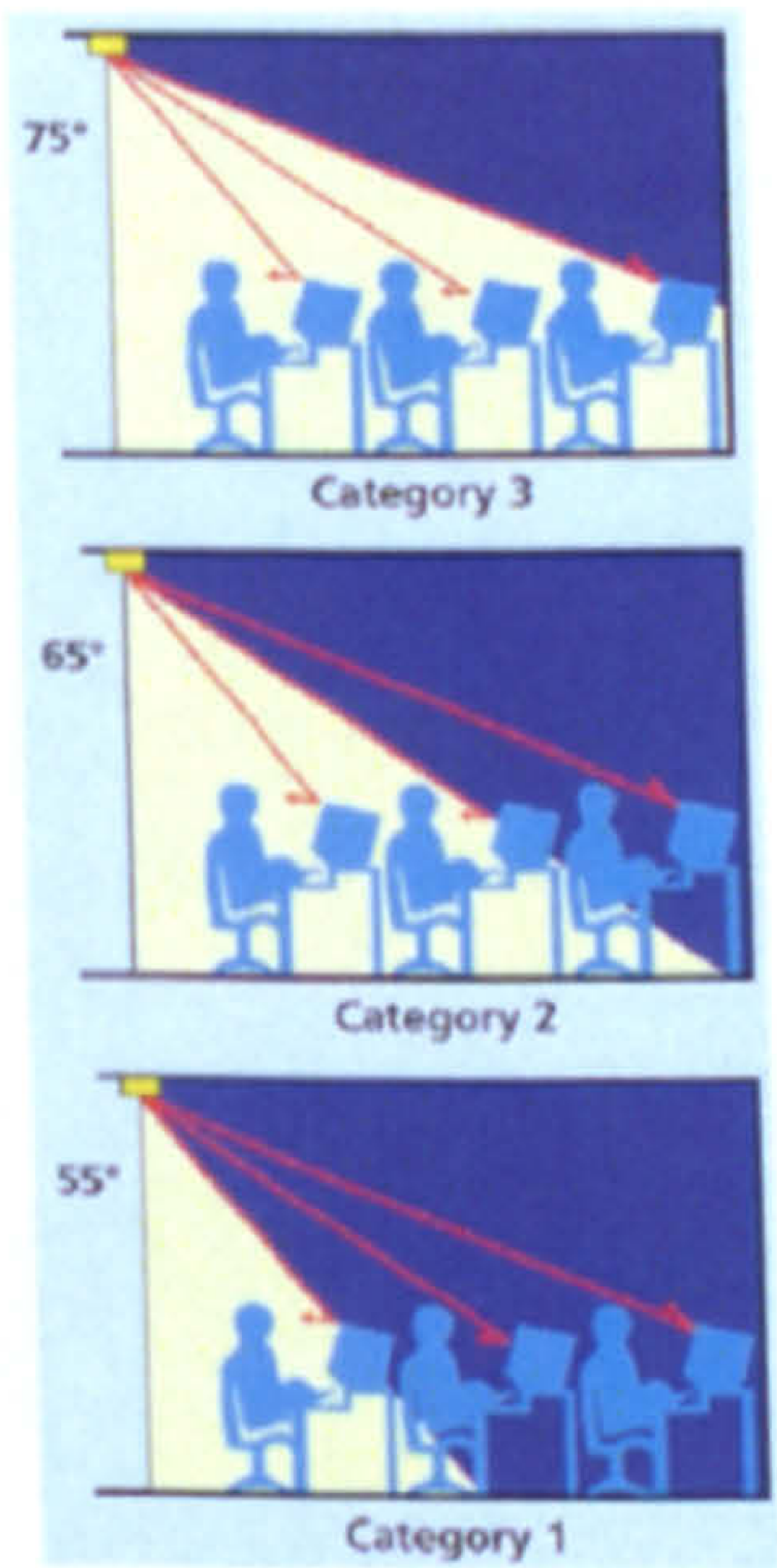
Description: je-2

Correction Factor Used: White

Date: 18/12/2009

CIBSE LG3 VDT Category

	Category 1	Category 2	Category 3
Starting Gamma Angle (°):	55.0	65.0	75.0
Final Gamma Angle (°):	90.0	90.0	90.0
Avg Luminance Found (cd/m²):	543.3	500.5	628.1
Max. Permissible (cd/m²):	200.0	200.0	200.0
Max Luminance Found (cd/m²):	32100	32100	32100
Max. Permissible (cd/m²):	500.0	500.0	500.0
Result:	-	-	-



Distribution Photometry Report

Report Number:

Date: 18/12/2009

Catalog Number:

Description: *Je-2*
Correction Factor Used: White

Filename: *Je-2.IES*

Results For: *Test Details*
Luminous Intensity Distribution
LID (Lowest 10%)
Luminous Intensity Data
Luminous Flux Data
Luminaire Luminance
IsoCandela Diagram
IsoLux Diagram
IsoLux 3D
Illuminance Grid
IESNA CoU Table
TM5 UF Table
TM5 UF Table (Variation)
Roadway UF Graph
Zonal Flux Diagram
Luminance Limiting Curve
CIBSE LG3 Rating
Photometric Solid

Page 1 of 23

PhotometricCentre v4.03 Copyright (C) Photometric Solutions International 2004-2008



Photometric Solutions International Pty Ltd
Factory Two, 21-29 Railway Ave
Huntingdale, Vic, 3166, AUSTRALIA
Tel: +61 3 9568 1879
Fax: +61 3 9568 4667
www.PhotometricSolutions.com

Report Number:
Catalog Number:
Description: *Je-2*
Correction Factor Used: White

Date: 18/12/2009

IESNA Coefficients of Utilisation Table

Ceiling Cavity Reflect.:	80%			70%			50%			30%			10%			0%
Wall Reflect.:	50%	30%	10%	50%	30%	10%	50%	30%	10%	50%	30%	10%	50%	30%	10%	0%
Room Cavity Ratio	Coefficients of Utilisation for 20% Effective Floor Cavity Reflectance															
0	0.06	0.06	0.06	0.06	0.06	0.06	0.06	0.06	0.06	0.05	0.05	0.05	0.05	0.05	0.05	0.05
1	0.05	0.05	0.05	0.05	0.05	0.05	0.05	0.05	0.04	0.05	0.04	0.04	0.04	0.04	0.04	0.04
2	0.05	0.05	0.04	0.05	0.05	0.04	0.05	0.04	0.04	0.04	0.04	0.04	0.04	0.04	0.04	0.04
3	0.05	0.04	0.04	0.05	0.04	0.04	0.04	0.04	0.04	0.04	0.04	0.04	0.04	0.04	0.04	0.04
4	0.04	0.04	0.04	0.04	0.04	0.04	0.04	0.04	0.04	0.04	0.04	0.04	0.04	0.04	0.04	0.04
5	0.04	0.04	0.04	0.04	0.04	0.04	0.04	0.04	0.04	0.04	0.04	0.04	0.04	0.04	0.04	0.04
6	0.04	0.04	0.04	0.04	0.04	0.04	0.04	0.04	0.04	0.04	0.04	0.04	0.04	0.04	0.04	0.04
7	0.04	0.04	0.04	0.04	0.04	0.04	0.04	0.04	0.04	0.04	0.04	0.04	0.04	0.04	0.04	0.04
8	0.04	0.04	0.04	0.04	0.04	0.04	0.04	0.04	0.04	0.04	0.04	0.04	0.04	0.04	0.03	0.03
9	0.04	0.04	0.03	0.04	0.04	0.03	0.04	0.04	0.03	0.04	0.04	0.03	0.04	0.04	0.03	0.03
10	0.04	0.04	0.03	0.04	0.04	0.03	0.04	0.04	0.03	0.04	0.03	0.03	0.04	0.03	0.03	0.03



Report Number:
Catalog Number:
Description: Je-2
Correction Factor Used: White

Date: 18/12/2009

Illumination Levels

y (m)																						
3.0	0.00	0.01	0.01	0.01	0.01	0.02	0.02	0.03	0.03	0.03	0.03	0.03	0.03	0.03	0.02	0.02	0.01	0.01	0.01	0.01	0.01	
	0.01	0.01	0.01	0.02	0.02	0.03	0.04	0.05	0.05	0.06	0.06	0.06	0.06	0.05	0.04	0.03	0.02	0.02	0.01	0.01	0.01	
2.4	0.01	0.01	0.02	0.02	0.04	0.05	0.07	0.10	0.13	0.15	0.15	0.15	0.13	0.10	0.07	0.05	0.04	0.02	0.02	0.01	0.01	
	0.01	0.02	0.02	0.04	0.06	0.09	0.14	0.20	0.29	0.36	0.38	0.35	0.28	0.20	0.15	0.10	0.06	0.04	0.02	0.02	0.01	
1.8	0.02	0.02	0.04	0.06	0.10	0.17	0.31	0.50	0.66	0.84	0.89	0.80	0.61	0.45	0.29	0.17	0.11	0.06	0.04	0.02	0.02	
	0.02	0.03	0.05	0.09	0.17	0.35	0.62	1.06	1.48	1.82	1.94	1.75	1.36	0.94	0.53	0.32	0.17	0.10	0.06	0.03	0.02	
1.2	0.02	0.04	0.07	0.14	0.30	0.60	1.23	2.02	2.97	3.72	4.09	3.65	2.78	1.81	1.05	0.51	0.27	0.14	0.07	0.04	0.02	
	0.03	0.05	0.10	0.19	0.46	1.04	2.03	3.44	5.50	7.14	7.66	6.91	5.15	3.13	1.75	0.85	0.40	0.19	0.10	0.05	0.03	
0.6	0.03	0.06	0.12	0.27	0.60	1.49	2.99	5.38	8.14	9.84	10.2	9.90	7.77	4.88	2.58	1.17	0.50	0.25	0.13	0.06	0.04	
	0.04	0.06	0.14	0.33	0.80	1.91	3.74	6.73	9.82	10.9	11.6	11.6	9.60	6.10	3.25	1.44	0.63	0.29	0.14	0.07	0.04	
0.0	0.04	0.06	0.15	0.35	0.85	2.02	4.01	7.15	10.4	12.3	13.0	12.6	10.2	6.52	3.49	1.54	0.67	0.30	0.15	0.07	0.04	
	0.04	0.06	0.13	0.32	0.75	1.72	3.64	6.34	9.58	12.1	13.3	12.1	9.15	5.92	3.12	1.38	0.61	0.29	0.14	0.07	0.04	
-0.6	0.03	0.06	0.12	0.25	0.54	1.29	2.78	4.85	7.26	9.25	10.1	9.07	6.97	4.52	2.36	1.07	0.48	0.24	0.13	0.06	0.04	
	0.03	0.05	0.09	0.18	0.43	0.92	1.72	3.15	4.72	6.05	6.57	6.03	4.57	2.72	1.48	0.76	0.37	0.18	0.10	0.06	0.03	
-1.2	0.02	0.04	0.07	0.14	0.29	0.51	0.96	1.63	2.52	3.19	3.44	3.05	2.32	1.47	0.87	0.45	0.26	0.14	0.08	0.05	0.02	
	0.02	0.03	0.05	0.09	0.17	0.32	0.47	0.80	1.10	1.38	1.51	1.36	1.07	0.75	0.45	0.29	0.16	0.10	0.06	0.03	0.02	
-1.8	0.02	0.02	0.04	0.06	0.12	0.17	0.26	0.38	0.48	0.62	0.67	0.61	0.48	0.38	0.26	0.17	0.11	0.06	0.04	0.02	0.02	
	0.01	0.02	0.03	0.05	0.08	0.14	0.14	0.18	0.24	0.29	0.31	0.29	0.25	0.19	0.14	0.10	0.06	0.04	0.03	0.02	0.01	
-2.4	0.01	0.01	0.02	0.03	0.06	0.09	0.08	0.10	0.12	0.14	0.15	0.14	0.13	0.10	0.08	0.06	0.04	0.03	0.02	0.01	0.01	
	0.01	0.01	0.01	0.02	0.04	0.06	0.06	0.05	0.06	0.07	0.07	0.07	0.06	0.06	0.05	0.03	0.02	0.02	0.01	0.01	0.01	
-3.0	0.01	0.01	0.01	0.02	0.04	0.04	0.03	0.03	0.04	0.04	0.04	0.04	0.04	0.03	0.03	0.02	0.02	0.01	0.01	0.01	0.01	
	-3.0	-2.4	-1.8	-1.2	-0.6	0.0	0.6	1.2	1.8	2.4	3.0											
																					x (m)	

Horizontal Illuminance
All Illuminance values in lux / 1000 lm
Table Average: 1.25 Table Maximum: 13.3 Table Minimum: 0.00
Mounting Height = 2.7 m



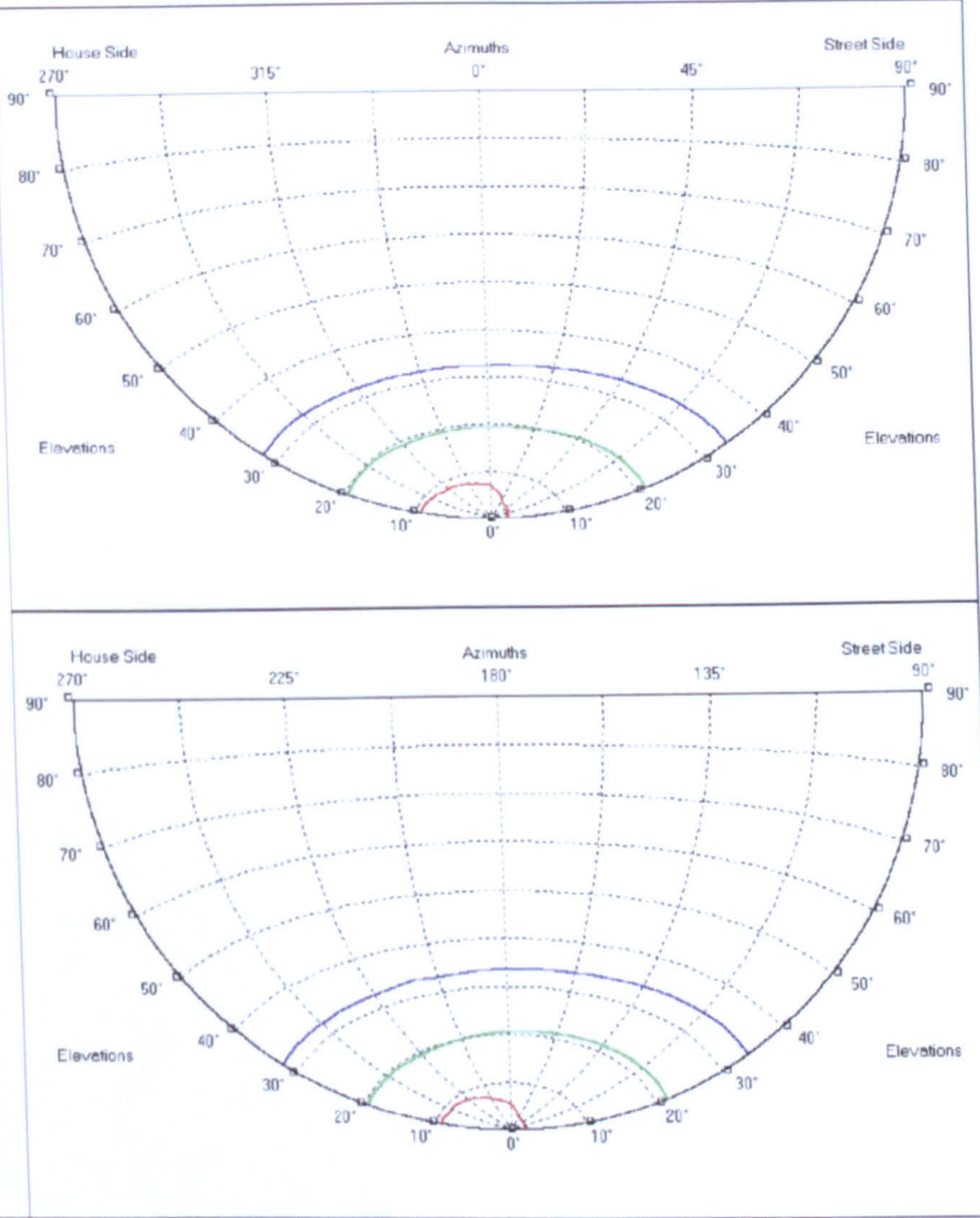
IsoCandela Diagram

Legend
(cd / 1000 lm)
Max = 102.5

92.3 (90.0%)

51.3 (50.0%)

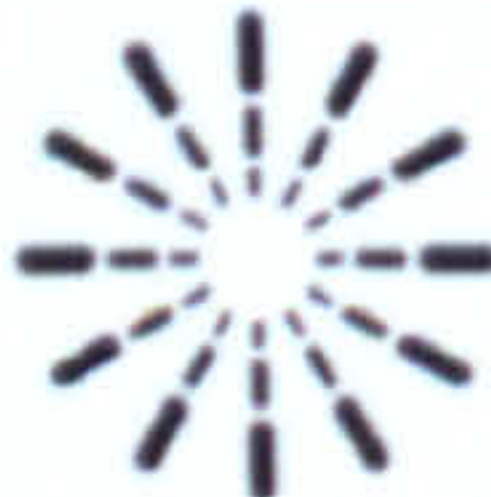
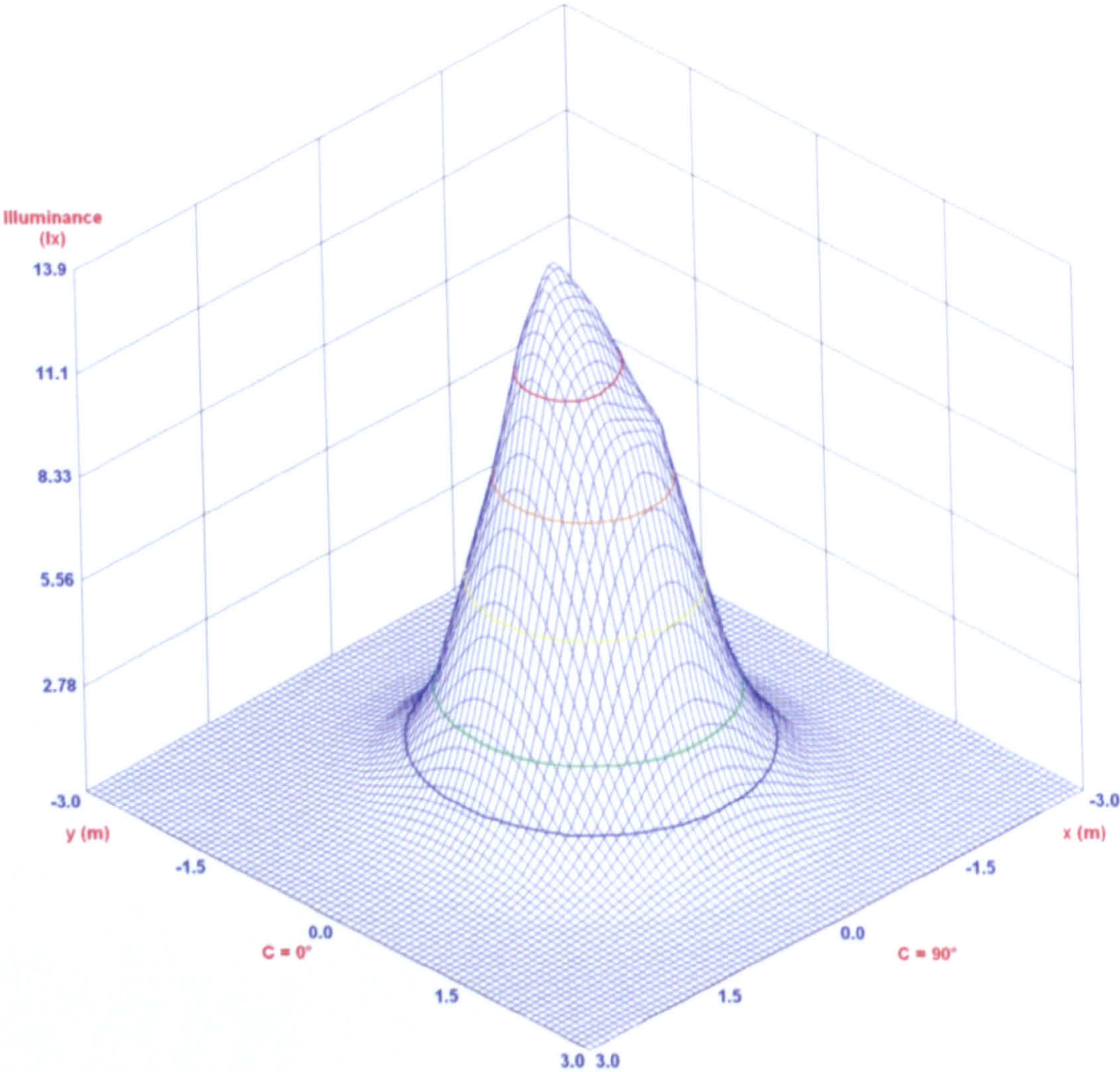
10.3 (10.0%)



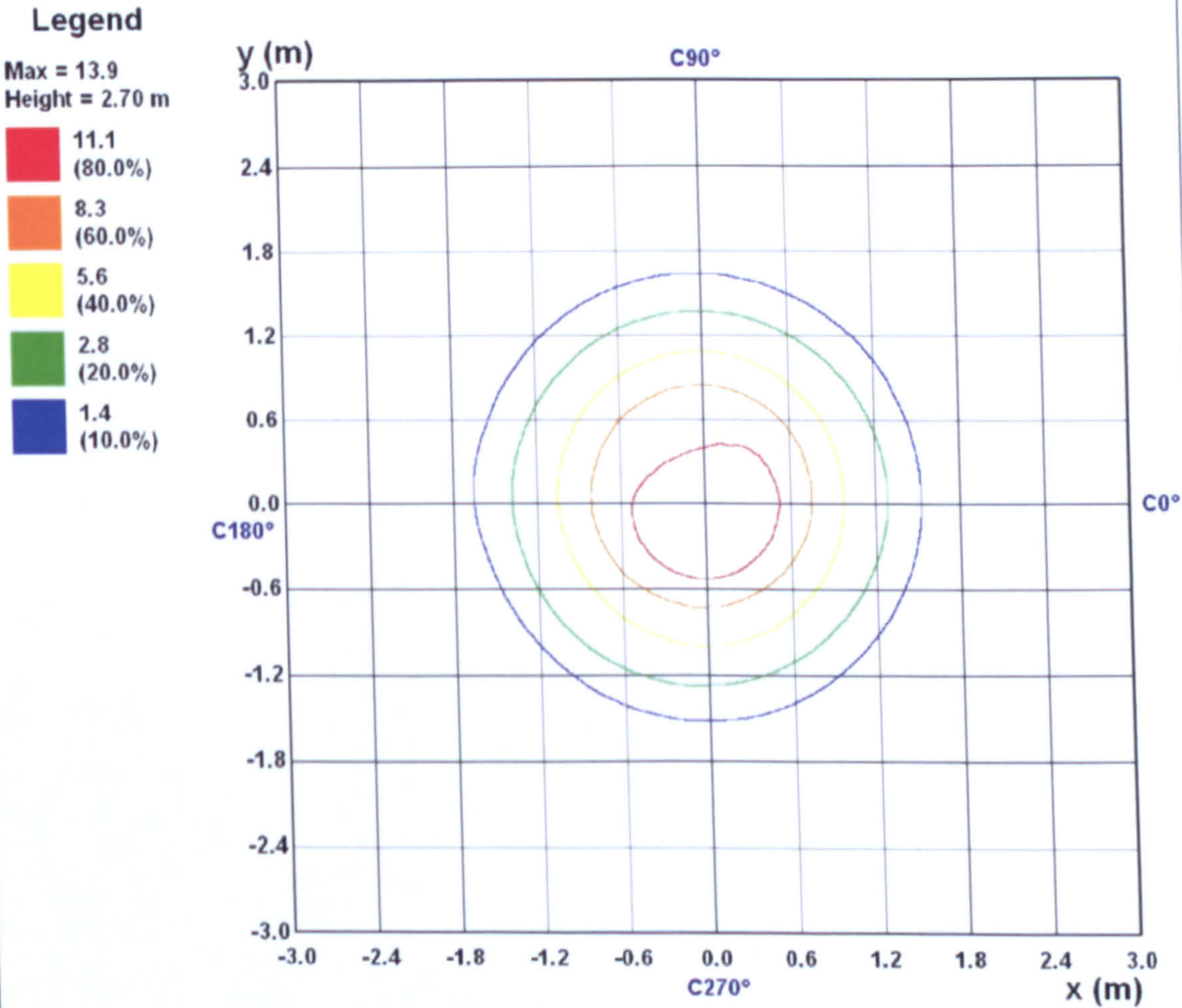
All luminous intensity values in cd / 1000 lm

Photometric Solutions International Pty Ltd
Factory Two, 21-29 Railway Ave
Huntingdale, Vic, 3166, AUSTRALIA
Tel: +61 3 9568 1879
Fax: +61 3 9568 4667
www.PhotometricSolutions.com

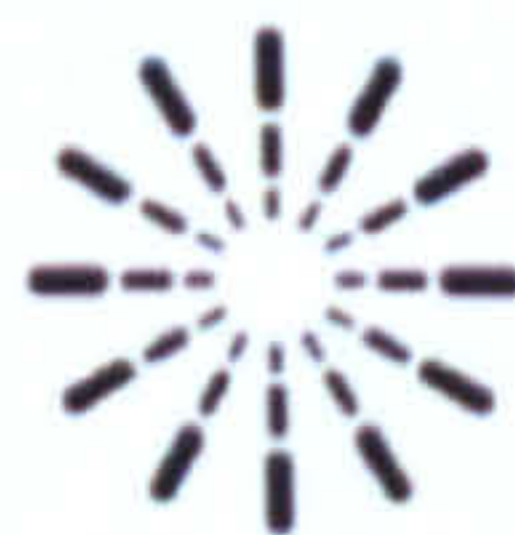
IsoLux 3D



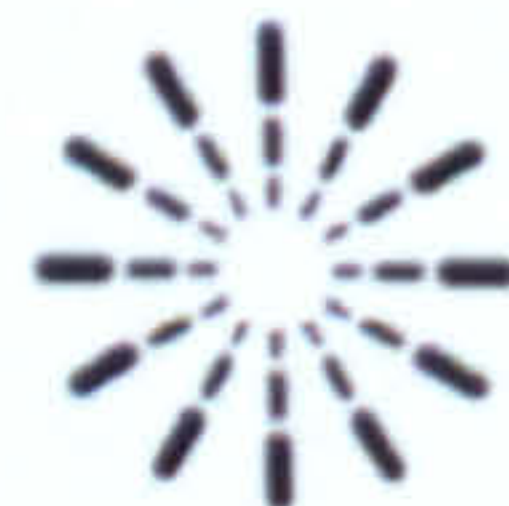
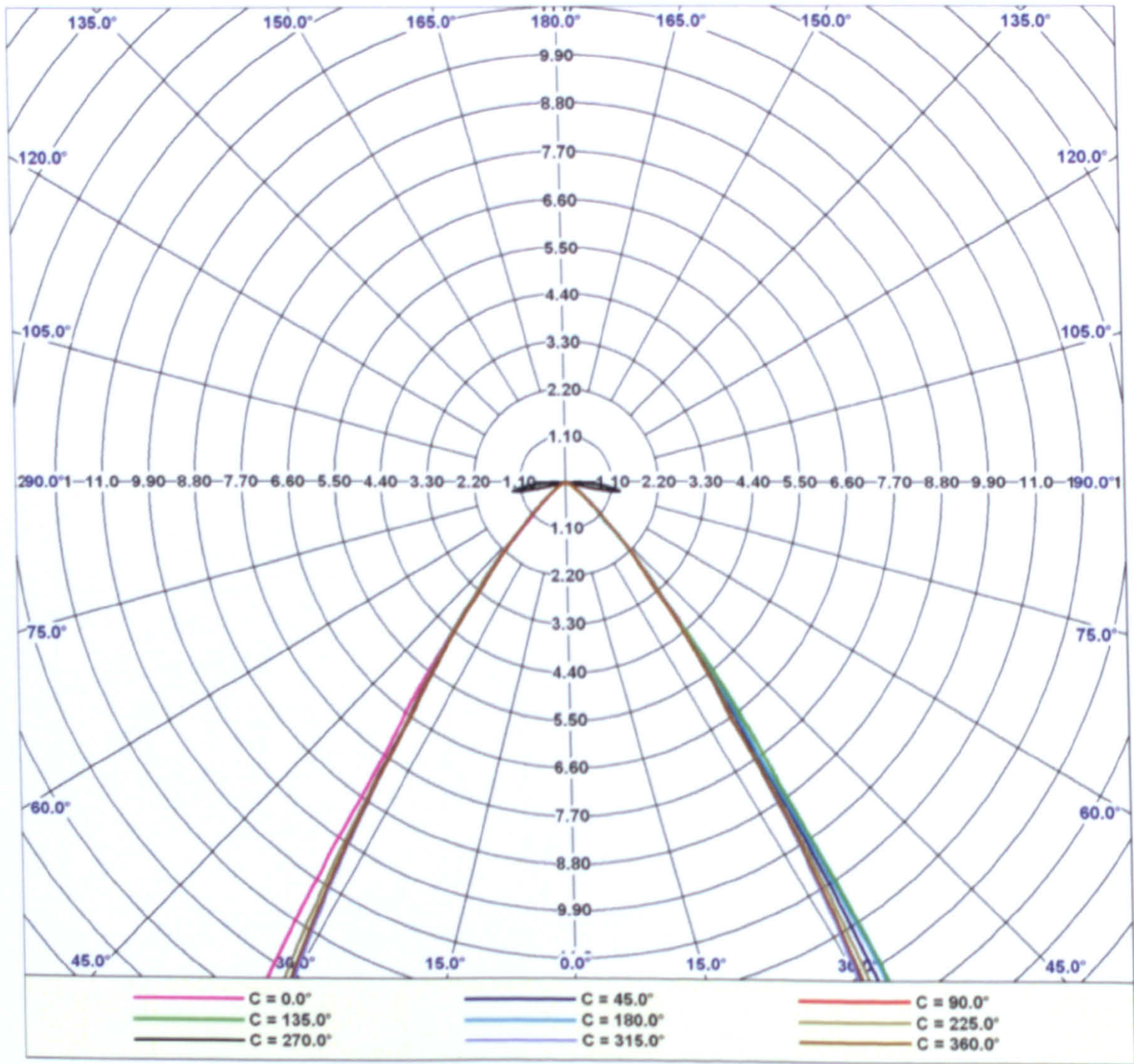
IsoLux Diagram



All illuminance values in lx / 1000 lm



Luminous Intensity Distribution (Lowest 10%)



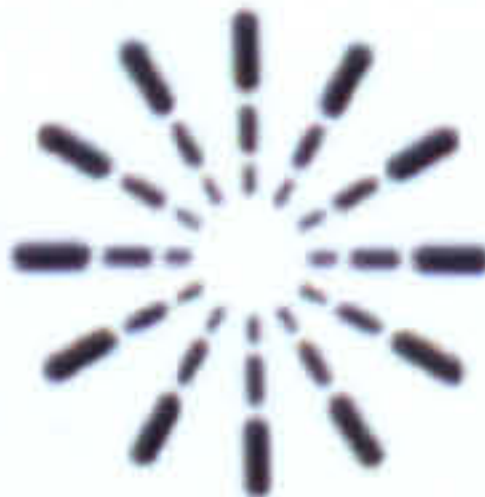
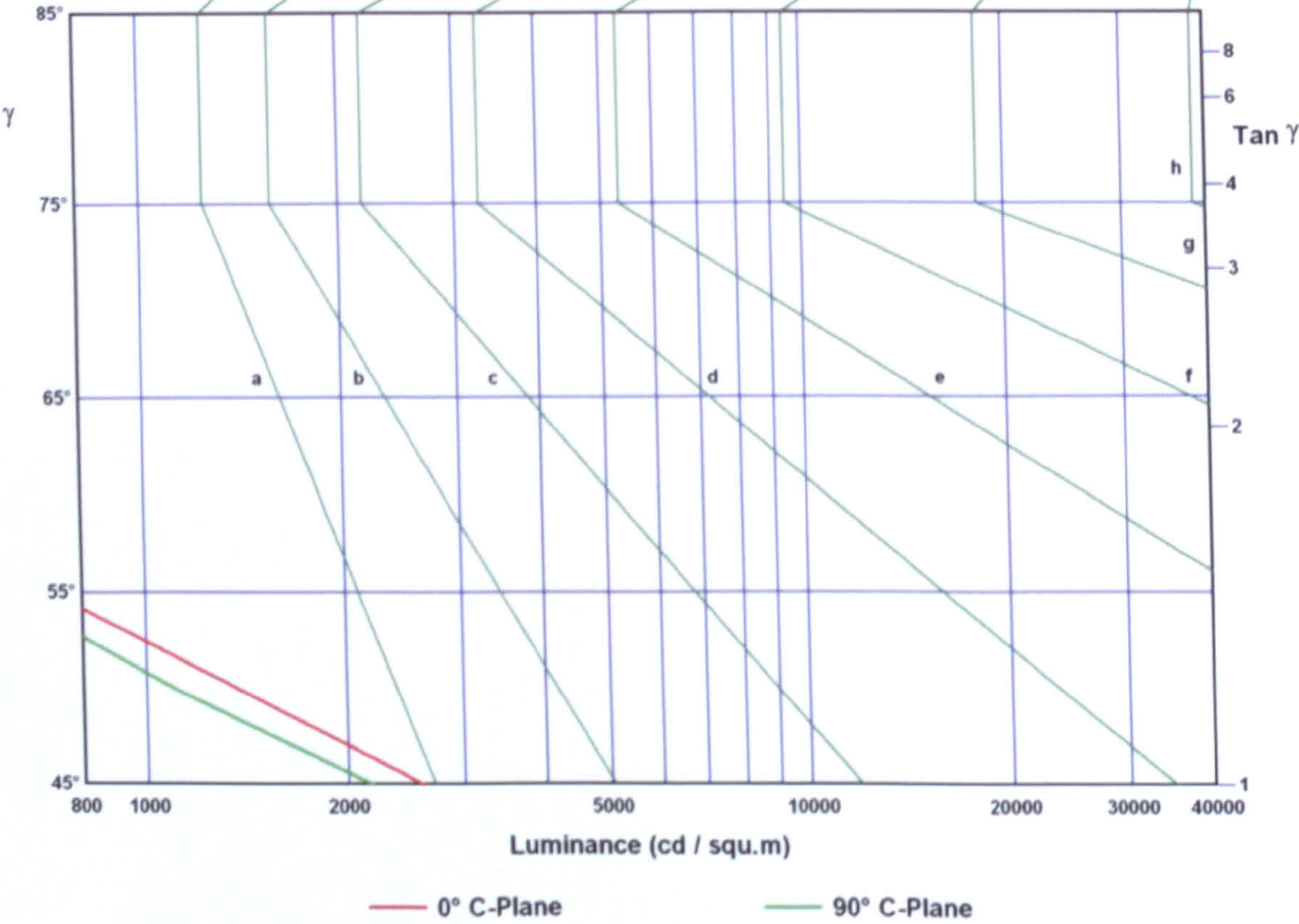
Average Luminance Table

All luminance values expressed in cd / squ.m / 1000 lm

Azimuth:	0	45	90	135	180	235	270	315
Elevation								
0	118000	118000	118000	118000	118000	118000	118000	118000
45	2600	2500	2180	2270	2290	4660	2580	2580
55	715	715	607	672	759	824	802	802
65	147	265	147	265	235	235	88.3	88.3
75	48.0	192	0.0	192	0.0	144	1010	96.1
85	0.0	0.0	0.0	285	0.0	571	12000	285

Luminance Limiting Curve

Glare Rating	Quality Class	Service Values of Illuminance (lx)							
		2000	1000	500	<300	e	f	g	h
1.15	A								
1.5	B		2000	1000	500	<300			
1.85	C			2000	1000	500	<300		
2.2	D				2000	1000	500	<300	
2.55	E	a	b	c	d	2000	1000	500	<300



Report Number:
Catalog Number:
Description: Je-2
Correction Factor Used: White

Date: 18/12/2009

Luminous Flux Table

Elevation	Cone	Lumens	Cumulative	Lamp %	Luminaire %
0°	0.00° - 2.50°	0.6	0.6	0.1	1.1
5°	2.50° - 7.50°	4.5	5.1	0.5	10.1
10°	7.50° - 12.50°	8.3	13.3	1.3	26.6
15°	12.50° - 17.50°	10.4	23.7	2.4	47.3
20°	17.50° - 22.50°	9.9	33.7	3.4	67.1
25°	22.50° - 27.50°	7.3	41.0	4.1	81.7
30°	27.50° - 32.50°	4.4	45.4	4.5	90.5
35°	32.50° - 37.50°	2.3	47.7	4.8	95.1
40°	37.50° - 42.50°	1.1	48.8	4.9	97.3
45°	42.50° - 47.50°	0.5	49.4	4.9	98.4
50°	47.50° - 52.50°	0.3	49.7	5.0	99.0
55°	52.50° - 57.50°	0.2	49.8	5.0	99.3
60°	57.50° - 62.50°	0.1	49.9	5.0	99.5
65°	62.50° - 67.50°	0.0	50.0	5.0	99.6
70°	67.50° - 72.50°	0.0	50.0	5.0	99.7
75°	72.50° - 77.50°	0.0	50.0	5.0	99.7
80°	77.50° - 82.50°	0.1	50.1	5.0	99.8
85°	82.50° - 87.50°	0.1	50.2	5.0	100.0
90°	87.50° - 90.00°	0.0	50.2	5.0	100.0

Light Output Ratio = 5.0% (DLOR = 5.0% , ULOR = 0.0%)



Report Number:
Catalog Number:
Description: *Je-2*
Correction Factor Used: White

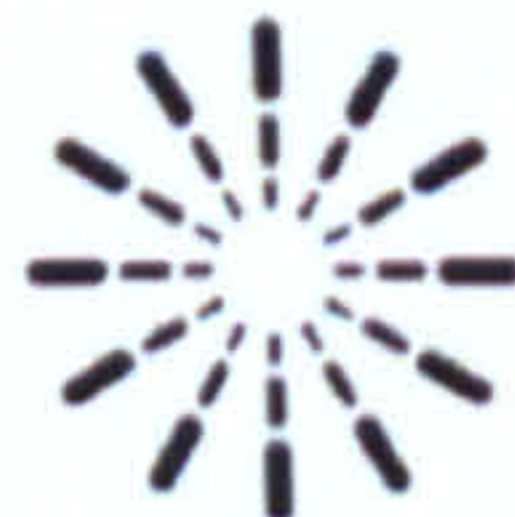
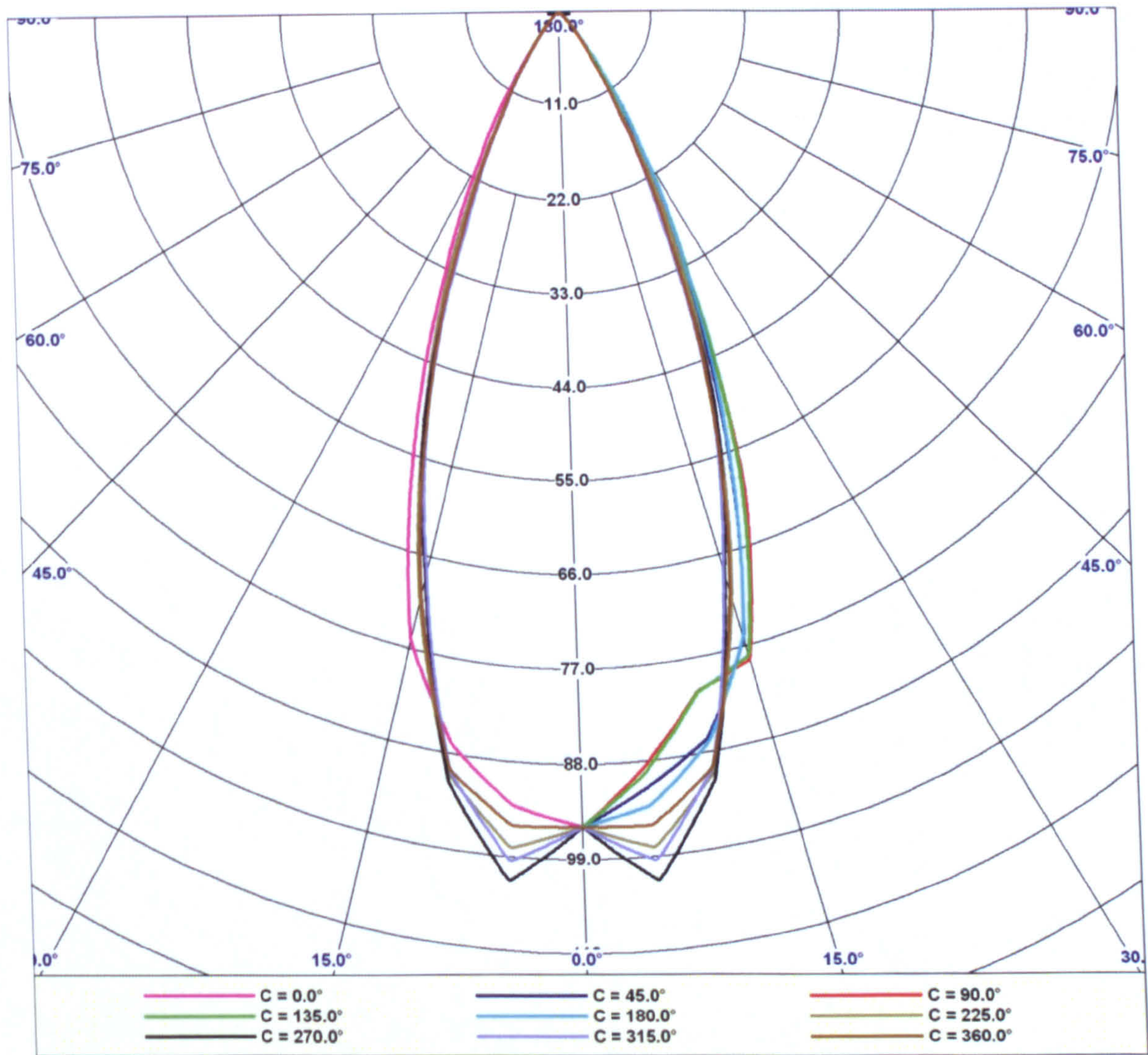
Date: 18/12/2009

Luminous Intensity Table (cd / 1000 lm) (Continued)

$\gamma \setminus C$	360.0
0.0	95.1
5.0	95.3
10.0	89.6
15.0	70.5
20.0	48.9
25.0	29.2
30.0	13.9
35.0	6.5
40.0	3.1
45.0	1.5
50.0	0.7
55.0	0.3
60.0	0.2
65.0	0.1
70.0	0.0
75.0	0.0
80.0	0.0
85.0	0.0
90.0	-0.1



Luminous Intensity Distribution



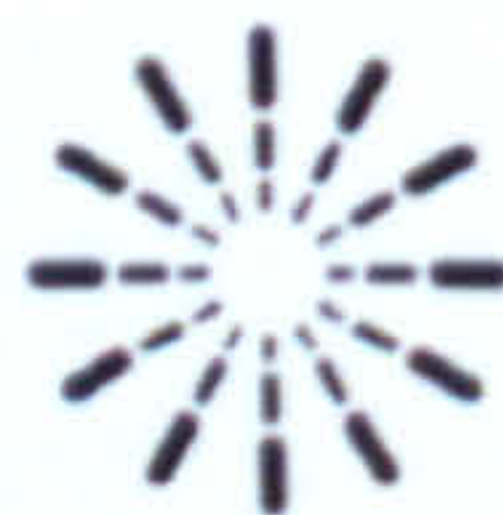
Report Number:
Catalog Number:
Description: *je-2*
Correction Factor Used: White

Date: 18/12/2009

Photometric Solid



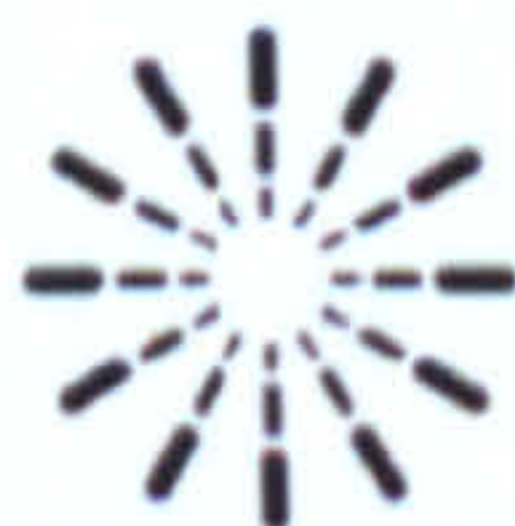
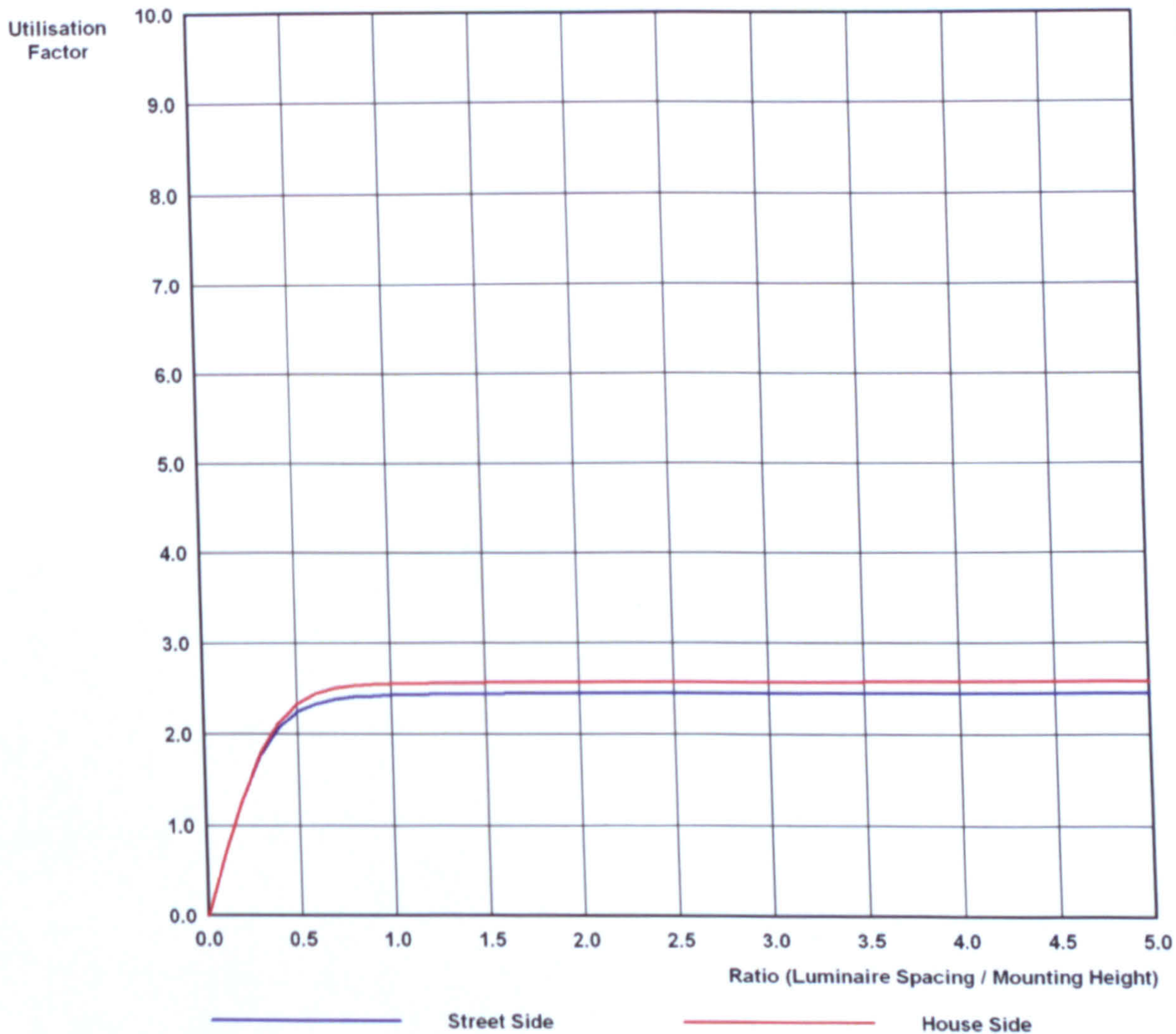
Viewing Angle: C = 315°



Report Number:
Catalog Number:
Description: je-2
Correction Factor Used: White

Date: 18/12/2009

Roadway Utilisation Factor Graph



Report Number:
Catalog Number:
Description: *Je-2*
Correction Factor Used: White

Date: 18/12/2009

Luminaire Details

Luminaire Test Details:

Photometry Type:	<i>Type C/Gamma</i>
Number of Lamps:	<i>1</i>
Lumens per Lamp:	<i>1000</i>

Luminous Dimensions:

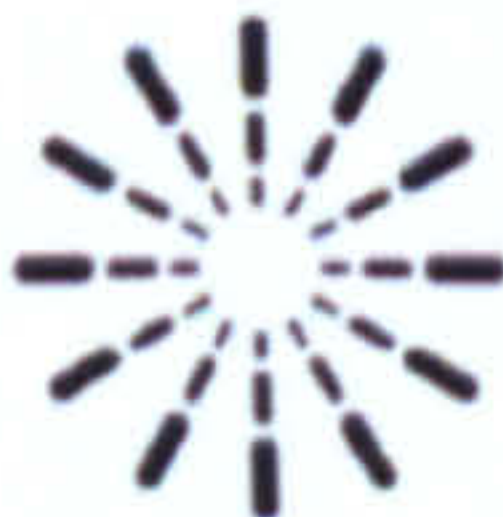
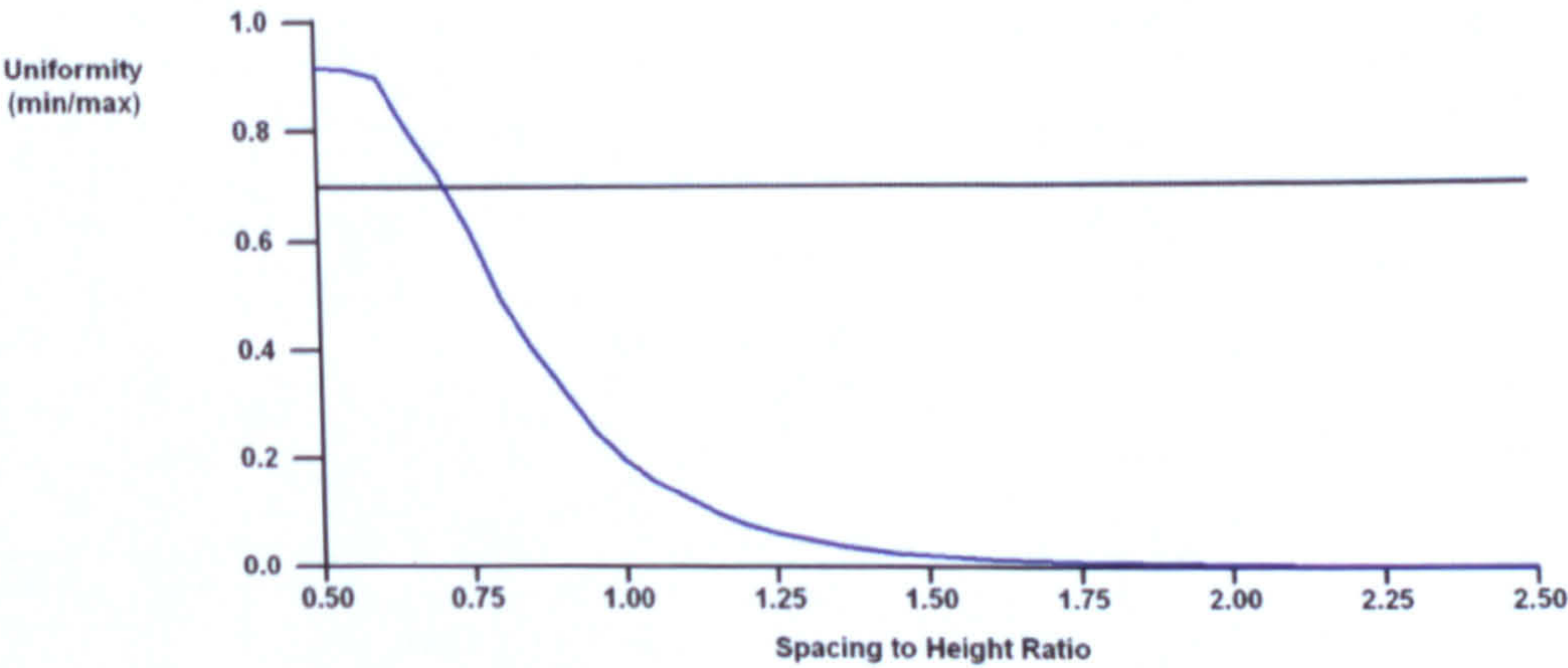
Base Area:	<i>0.032 m Diameter</i>
Side Area:	<i>N/A</i>
End Area:	<i>N/A</i>
Luminous Shape:	<i>Circular</i>



TM5 Utilisation Factor Table

SHR Nominal = 0.50:1 SHR Maximum = 0.71:1

Reflectance			Room Index (K)								
Ceiling	Wall	Floor	0.75	1.00	1.25	1.50	2.00	2.50	3.00	4.00	5.00
0.70	0.50	0.20	0.04	0.05	0.05	0.05	0.05	0.05	0.05	0.05	0.06
0.70	0.30	0.20	0.04	0.04	0.05	0.05	0.05	0.05	0.05	0.05	0.05
0.70	0.10	0.20	0.04	0.04	0.04	0.05	0.05	0.05	0.05	0.05	0.05
0.50	0.50	0.20	0.04	0.05	0.05	0.05	0.05	0.05	0.05	0.05	0.05
0.50	0.30	0.20	0.04	0.04	0.05	0.05	0.05	0.05	0.05	0.05	0.05
0.50	0.10	0.20	0.04	0.04	0.04	0.05	0.05	0.05	0.05	0.05	0.05
0.30	0.50	0.20	0.04	0.04	0.05	0.05	0.05	0.05	0.05	0.05	0.05
0.30	0.30	0.20	0.04	0.04	0.04	0.05	0.05	0.05	0.05	0.05	0.05
0.30	0.10	0.20	0.04	0.04	0.04	0.05	0.05	0.05	0.05	0.05	0.05
0.00	0.00	0.00	0.04	0.04	0.04	0.04	0.05	0.05	0.05	0.05	0.05
Distribution Factors		Floor:	0.04	0.04	0.04	0.04	0.05	0.05	0.05	0.05	0.05
		Wall:	0.01	0.01	0.01	0.01	0.00	0.00	0.00	0.00	0.00
		Ceiling:	0.00	0.00	0.00	0.00	0.00	0.00	0.00	0.00	0.00
BZ Numbers:			1	1	1	1	1	1	1	1	1



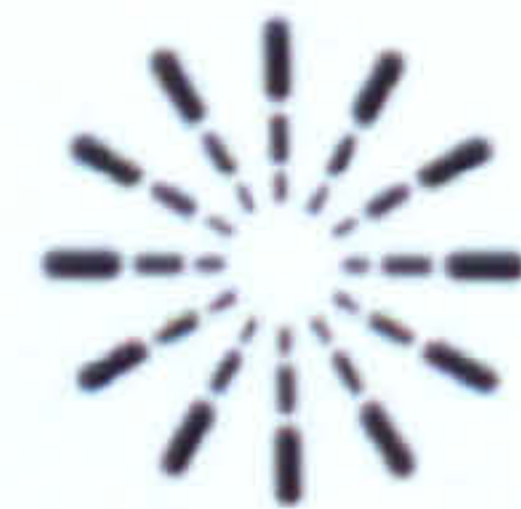
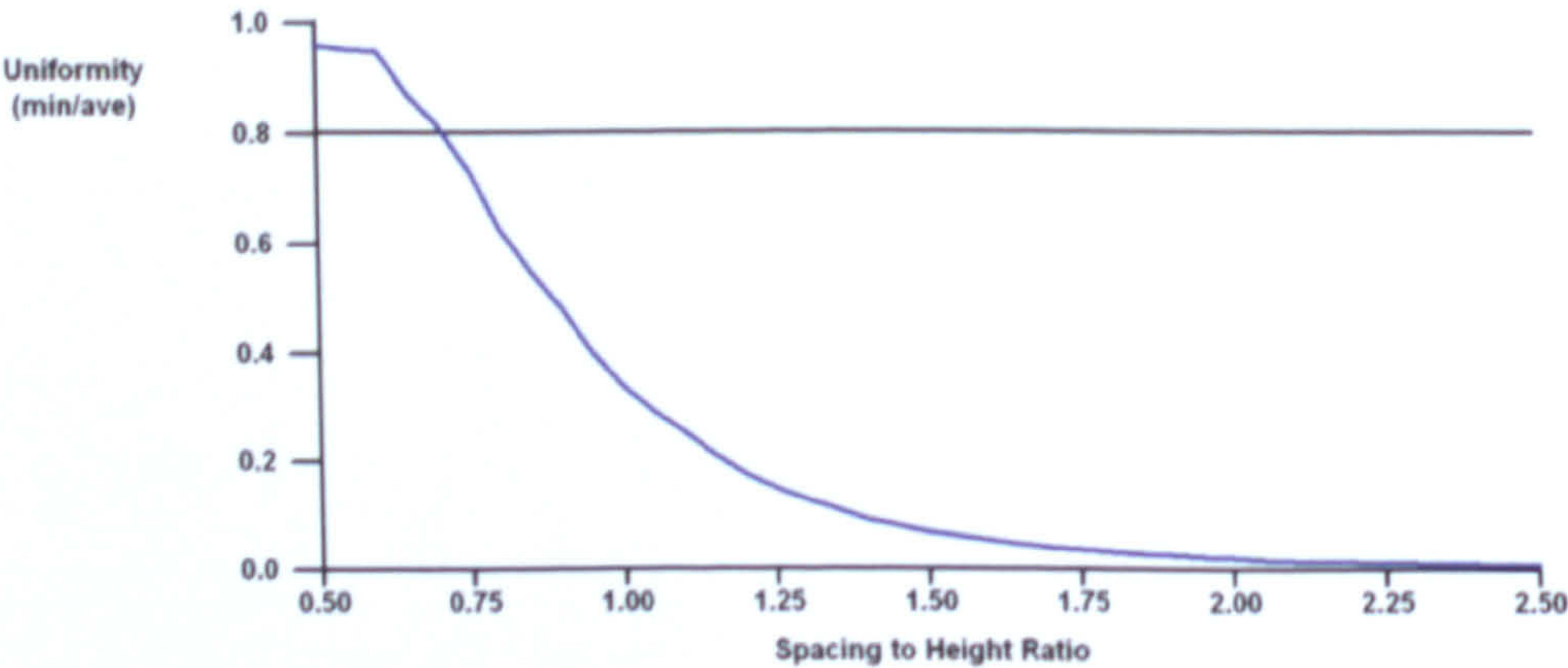
Report Number:
Catalog Number:
Description: je-2
Correction Factor Used: White

Date: 18/12/2009

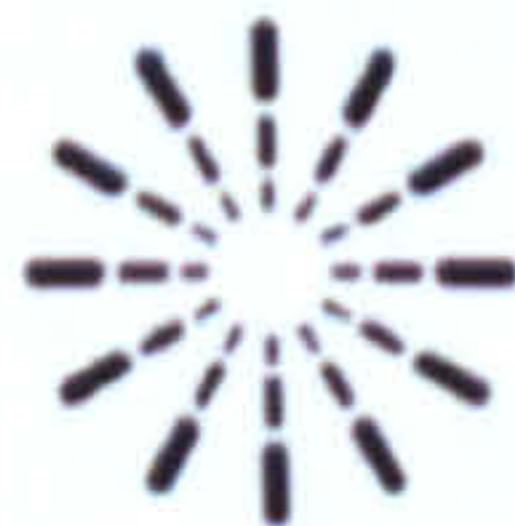
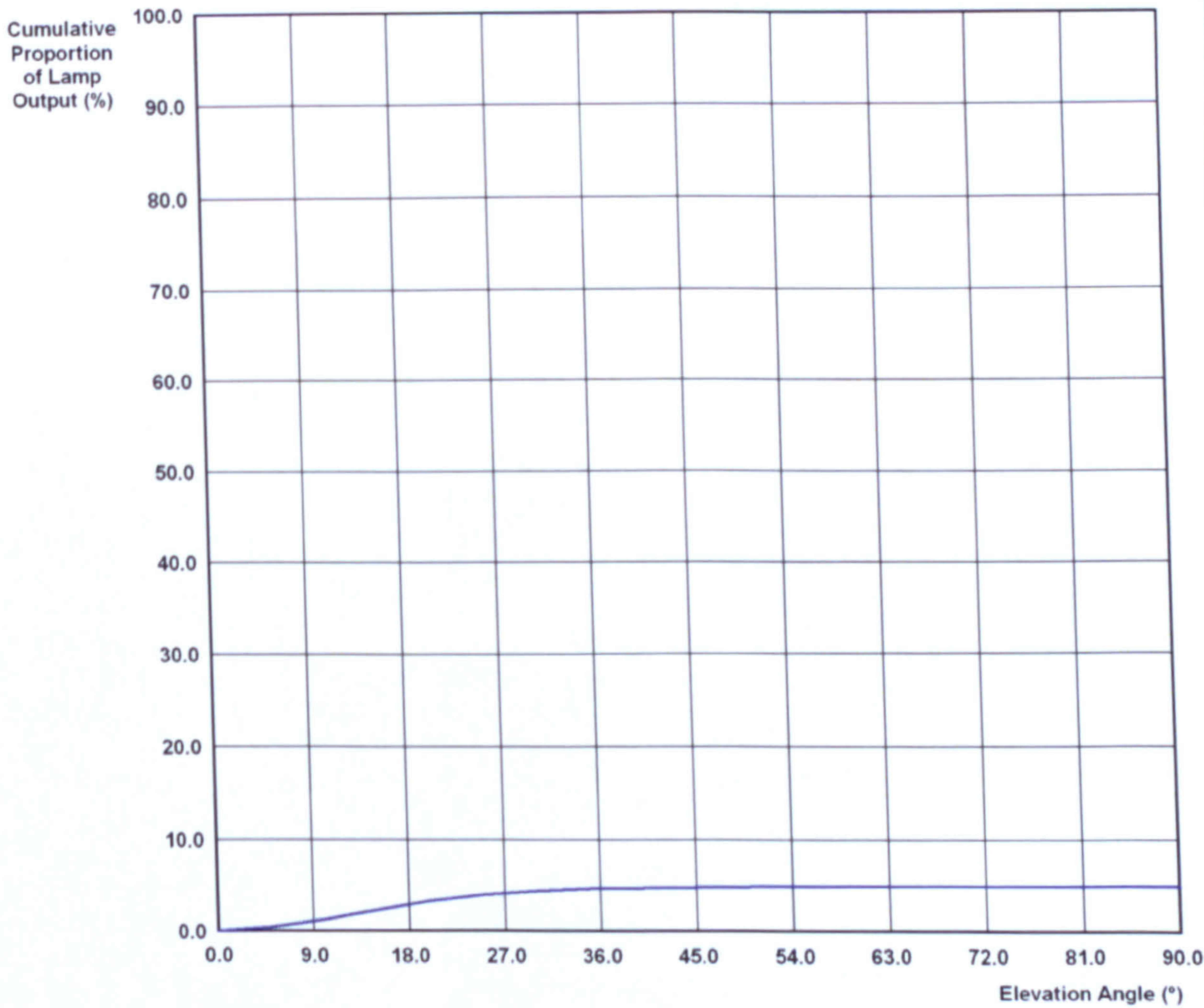
TM5* Utilisation Factor Table

* Based on TM5, except using Min / Ave = 0.8 as Spacing Criteria
SHR Nominal = 0.75:1 SHR Maximum = 0.75:1

Reflectance			Room Index (K)								
Ceiling	Wall	Floor	0.75	1.00	1.25	1.50	2.00	2.50	3.00	4.00	5.00
0.70	0.50	0.20	0.05	0.05	0.05	0.05	0.05	0.05	0.05	0.06	0.06
0.70	0.30	0.20	0.04	0.05	0.05	0.05	0.05	0.05	0.05	0.05	0.06
0.70	0.10	0.20	0.04	0.05	0.05	0.05	0.05	0.05	0.05	0.05	0.05
0.50	0.50	0.20	0.05	0.05	0.05	0.05	0.05	0.05	0.05	0.05	0.05
0.50	0.30	0.20	0.04	0.05	0.05	0.05	0.05	0.05	0.05	0.05	0.05
0.50	0.10	0.20	0.04	0.04	0.05	0.05	0.05	0.05	0.05	0.05	0.05
0.30	0.50	0.20	0.04	0.05	0.05	0.05	0.05	0.05	0.05	0.05	0.05
0.30	0.30	0.20	0.04	0.05	0.05	0.05	0.05	0.05	0.05	0.05	0.05
0.30	0.10	0.20	0.04	0.04	0.05	0.05	0.05	0.05	0.05	0.05	0.05
0.00	0.00	0.00	0.04	0.04	0.04	0.05	0.05	0.05	0.05	0.05	0.05
Distribution Factors			Floor:	0.04	0.04	0.04	0.05	0.05	0.05	0.05	0.05
			Wall:	0.01	0.01	0.01	0.00	0.00	0.00	0.00	0.00
			Ceiling:	0.00	0.00	0.00	0.00	0.00	0.00	0.00	0.00
BZ Numbers:				1	1	1	1	1	1	1	1



Zonal Flux Diagram



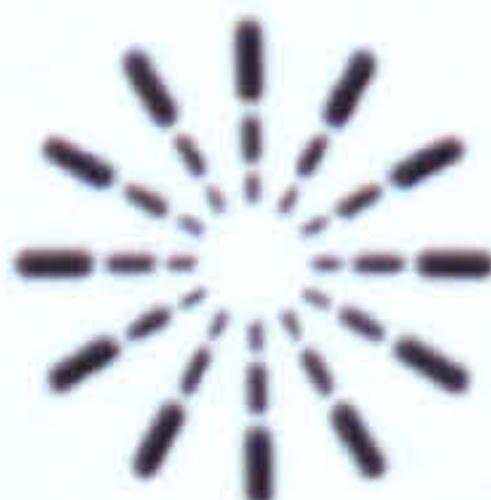
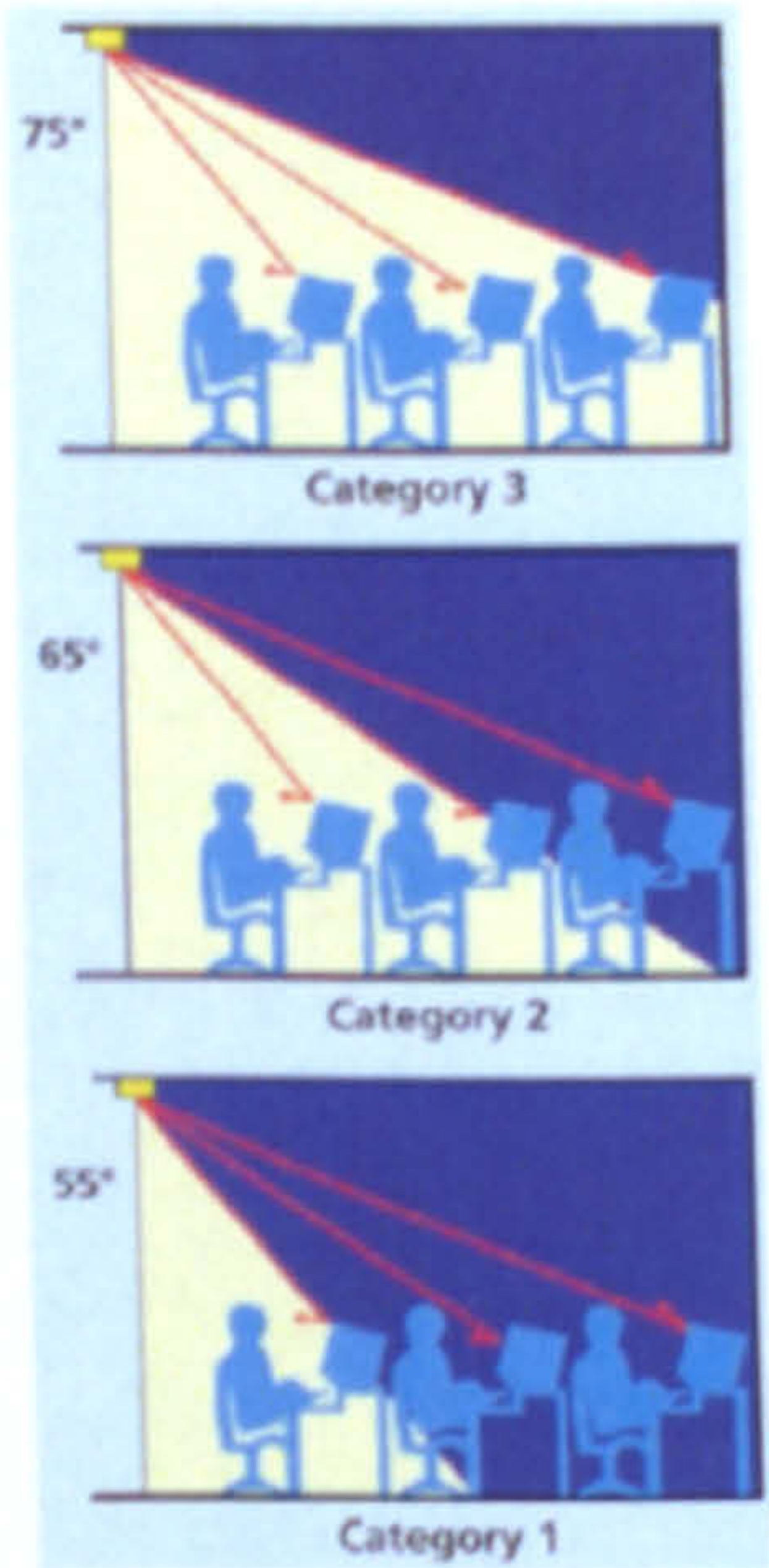
7. 3 Semi-convex Lens

Report Number:
Catalog Number:
Description: je-3
Correction Factor Used: White

Date: 18/12/2009

CIBSE LG3 VDT Category

	Category 1	Category 2	Category 3
Starting Gamma Angle (°):	55.0	65.0	75.0
Final Gamma Angle (°):	90.0	90.0	90.0
Avg Luminance Found (cd/m²):	368.7	429.6	576.7
Max. Permissible (cd/m²):	200.0	200.0	200.0
Max Luminance Found (cd/m²):	31670	31670	31670
Max. Permissible (cd/m²):	500.0	500.0	500.0
Result:	-	-	-



Distribution Photometry Report

Report Number:

Date: 18/12/2009

Catalog Number:

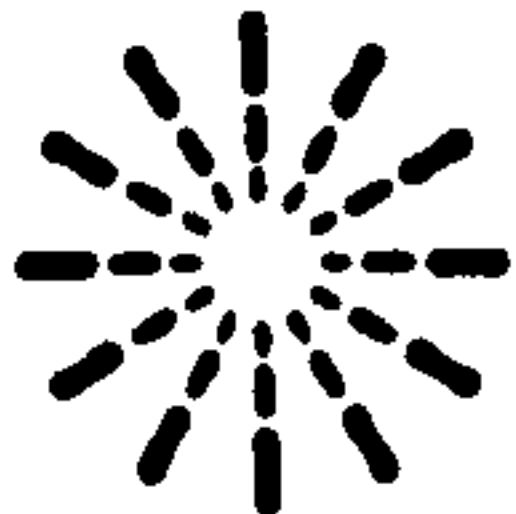
Description: **Je-3**
Correction Factor Used: White

Filename: **Je-3.IES**

Results For: **Test Details**
Luminous Intensity Distribution
LID (Lowest 10%)
Luminous Intensity Data
Luminous Flux Data
Luminaire Luminance
IsoCandela Diagram
IsoLux Diagram
IsoLux 3D
Illuminance Grid
IESNA CoU Table
TM5 UF Table
TM5 UF Table (Variation)
Roadway UF Graph
Zonal Flux Diagram
Luminance Limiting Curve
CIBSE LG3 Rating
Photometric Solid

Page 1 of 23

PhotometricCentre v4.03 Copyright (C) Photometric Solutions International 2004-2008



Photometric Solutions International Pty Ltd
Factory Two, 21-29 Railway Ave
Huntingdale, Vic. 3166, AUSTRALIA
Tel: +61 3 9568 1879
Fax: +61 3 9568 4667
www.PhotometricSolutions.com

Report Number:
Catalog Number:
Description: *Je-3*
Correction Factor Used: White

Date: 18/12/2009

IESNA Coefficients of Utilisation Table

Ceiling Cavity Reflect.:	80%			70%			50%			30%			10%			0%
Wall Reflect.:	50%	30%	10%	50%	30%	10%	50%	30%	10%	50%	30%	10%	50%	30%	10%	0%
Room Cavity Ratio	Coefficients of Utilisation for 20% Effective Floor Cavity Reflectance															
0	0.06	0.06	0.06	0.05	0.05	0.05	0.05	0.05	0.05	0.05	0.05	0.05	0.05	0.05	0.05	0.05
1	0.04	0.04	0.03	0.04	0.04	0.03	0.04	0.03	0.03	0.04	0.03	0.03	0.03	0.03	0.03	0.03
2	0.04	0.04	0.03	0.04	0.03	0.03	0.04	0.03	0.03	0.03	0.03	0.03	0.03	0.03	0.03	0.03
3	0.04	0.03	0.03	0.04	0.03	0.03	0.04	0.03	0.03	0.03	0.03	0.03	0.03	0.03	0.03	0.03
4	0.04	0.03	0.03	0.04	0.03	0.03	0.03	0.03	0.03	0.03	0.03	0.03	0.03	0.03	0.03	0.03
5	0.04	0.03	0.03	0.03	0.03	0.03	0.03	0.03	0.03	0.03	0.03	0.03	0.03	0.03	0.03	0.03
6	0.03	0.03	0.03	0.03	0.03	0.03	0.03	0.03	0.03	0.03	0.03	0.03	0.03	0.03	0.03	0.03
7	0.03	0.03	0.03	0.03	0.03	0.03	0.03	0.03	0.03	0.03	0.03	0.03	0.03	0.03	0.03	0.03
8	0.03	0.03	0.03	0.03	0.03	0.03	0.03	0.03	0.03	0.03	0.03	0.03	0.03	0.03	0.03	0.03
9	0.03	0.03	0.03	0.03	0.03	0.03	0.03	0.03	0.03	0.03	0.03	0.03	0.03	0.03	0.03	0.03
10	0.03	0.03	0.03	0.03	0.03	0.03	0.03	0.03	0.03	0.03	0.03	0.03	0.03	0.03	0.03	0.03

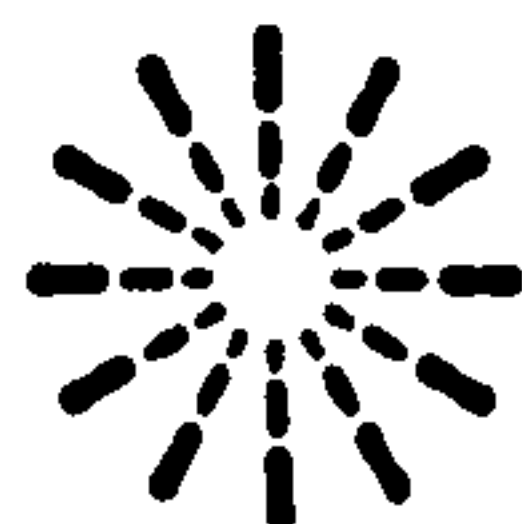


Date: 18/12/2009

Description: Je-3
Correction Factor Used: White

y (m)																					x (m)	
3.0	0.00	0.00	0.00	0.00	0.00	0.00	0.00	0.00	0.00	0.00	0.00	0.00	0.00	0.00	0.00	0.00	0.00	0.00	0.00	0.00	0.00	
2.4	0.00	0.00	0.00	0.00	0.00	0.00	0.00	0.00	0.00	0.00	0.00	0.00	0.00	0.00	0.00	0.00	0.00	0.00	0.00	0.00	0.00	
	0.00	0.00	0.00	0.00	0.00	0.01	0.01	0.01	0.01	0.01	0.01	0.01	0.01	0.01	0.01	0.00	0.00	0.00	0.00	0.00	0.00	
1.8	0.00	0.00	0.00	0.00	0.01	0.01	0.01	0.02	0.03	0.04	0.04	0.04	0.02	0.02	0.01	0.01	0.01	0.00	0.00	0.00	0.00	
	0.00	0.00	0.00	0.01	0.01	0.01	0.03	0.06	0.09	0.16	0.22	0.16	0.09	0.05	0.02	0.01	0.01	0.01	0.00	0.00	0.00	
1.2	0.00	0.00	0.00	0.01	0.01	0.03	0.07	0.19	0.50	0.96	1.40	0.99	0.57	0.22	0.07	0.02	0.01	0.01	0.00	0.00	0.00	
	0.00	0.00	0.01	0.01	0.02	0.06	0.18	0.57	2.84	5.18	6.57	4.88	2.59	0.74	0.22	0.05	0.01	0.01	0.01	0.00	0.00	
0.6	0.00	0.00	0.01	0.01	0.03	0.09	0.41	2.73	8.06	14.3	17.3	14.1	7.58	2.40	0.55	0.08	0.02	0.01	0.00	0.00	0.00	
	0.00	0.00	0.01	0.02	0.07	0.21	0.76	4.87	13.8	22.3	24.4	22.7	13.1	4.19	0.89	0.15	0.03	0.01	0.01	0.00	0.00	
0.0	0.00	0.00	0.01	0.02	0.08	0.26	1.11	5.92	16.2	23.0	26.6	25.6	14.9	5.28	1.15	0.19	0.04	0.01	0.01	0.00	0.00	
	0.00	0.00	0.01	0.02	0.07	0.16	0.69	4.10	12.6	20.9	24.7	20.5	11.8	3.84	0.81	0.13	0.03	0.01	0.01	0.00	0.00	
-0.6	0.00	0.00	0.01	0.02	0.03	0.09	0.36	1.97	6.55	11.9	14.3	11.7	6.20	1.99	0.46	0.07	0.02	0.01	0.00	0.00	0.00	
	0.00	0.00	0.01	0.01	0.05	0.11	0.16	0.45	1.84	3.55	4.85	3.56	1.91	0.56	0.17	0.04	0.01	0.01	0.00	0.00	0.00	
-1.2	0.00	0.00	0.01	0.01	0.04	0.05	0.06	0.15	0.35	0.63	0.92	0.68	0.41	0.16	0.05	0.02	0.01	0.01	0.00	0.00	0.00	
	0.00	0.00	0.00	0.01	0.02	0.04	0.02	0.05	0.07	0.11	0.15	0.11	0.06	0.04	0.02	0.01	0.01	0.01	0.00	0.00	0.00	
-1.8	0.00	0.00	0.00	0.01	0.03	0.02	0.02	0.02	0.02	0.03	0.03	0.03	0.02	0.01	0.01	0.01	0.00	0.00	0.00	0.00	0.00	
	0.00	0.00	0.00	0.01	0.02	0.05	0.02	0.01	0.01	0.01	0.01	0.01	0.01	0.01	0.01	0.01	0.00	0.00	0.00	0.00	0.00	
-2.4	0.00	0.00	0.00	0.00	0.02	0.04	0.01	0.01	0.01	0.01	0.00	0.01	0.00	0.00	0.00	0.00	0.00	0.00	0.00	0.00	0.00	
	0.00	0.00	0.00	0.00	0.02	0.03	0.02	0.01	0.00	0.00	0.00	0.00	0.00	0.00	0.00	0.00	0.00	0.00	0.00	0.00	0.00	
-3.0	0.00	0.00	0.00	0.00	0.02	0.03	0.01	0.00	0.00	0.00												

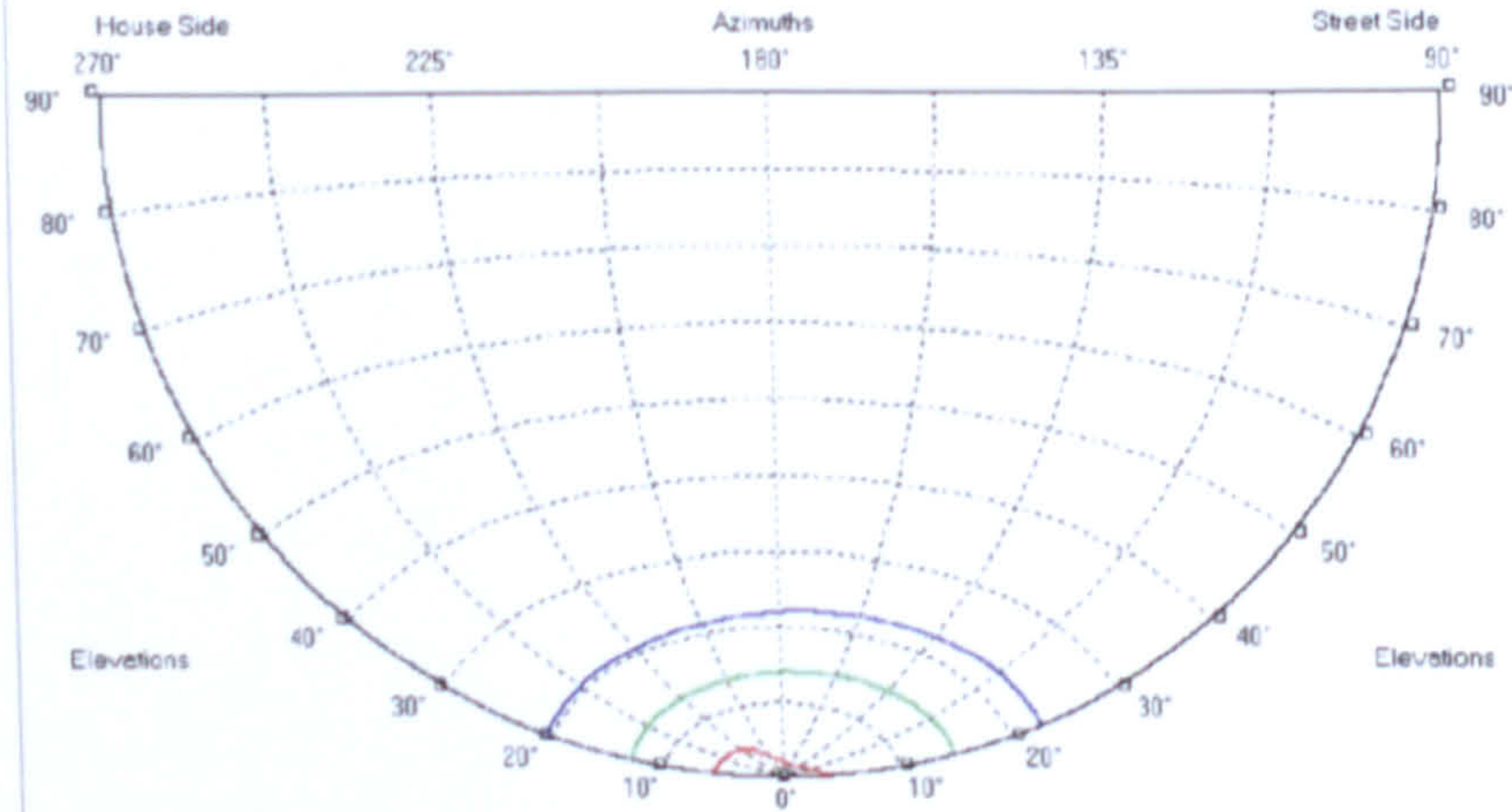
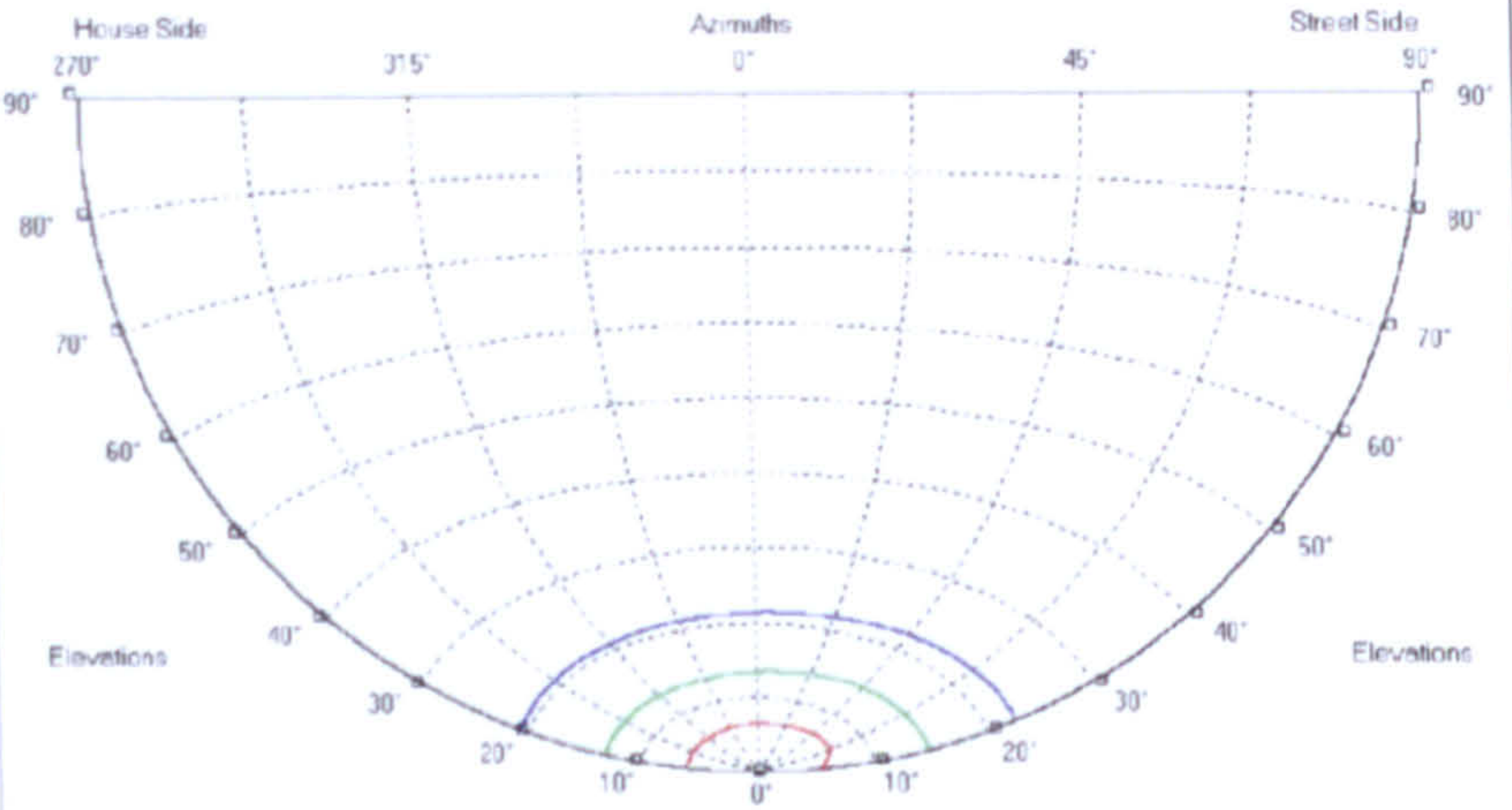
Horizontal Illuminance
All illuminance values in lux / 1000 lm
Table Average: 1.14 Table Maximum: 26.6 Table Minimum: 0.00
Mounting Height = 2.7 m



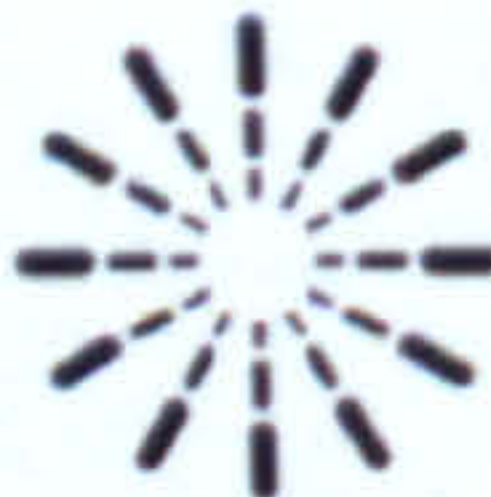
IsoCandela Diagram

Legend
(cd / 1000 lm)
Max = 204.7

- 184.2 (90.0%)
- 102.4 (50.0%)
- 20.5 (10.0%)



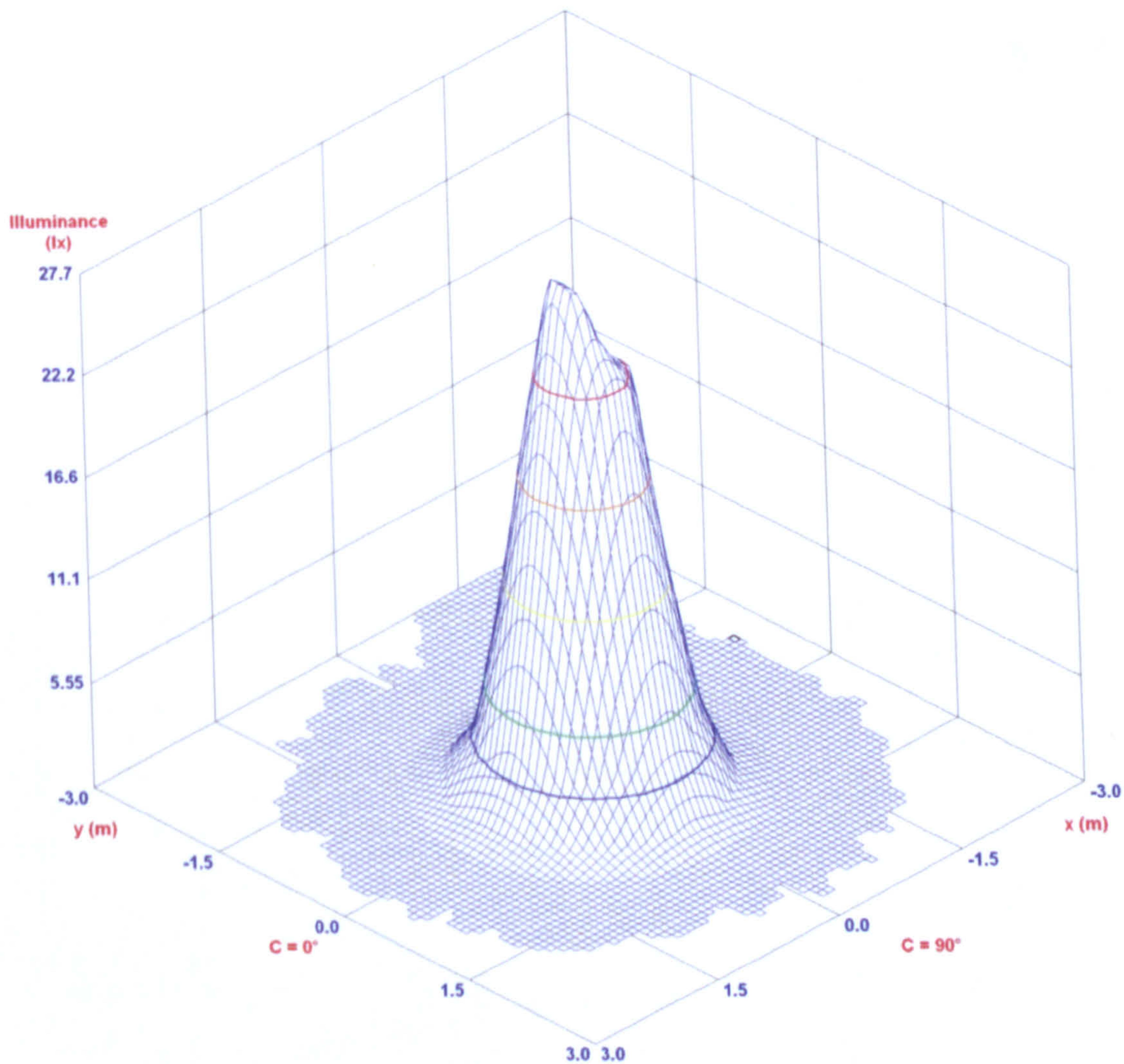
All luminous intensity values in cd / 1000 lm



Report Number:
Catalog Number:
Description: je-3
Correction Factor Used: White

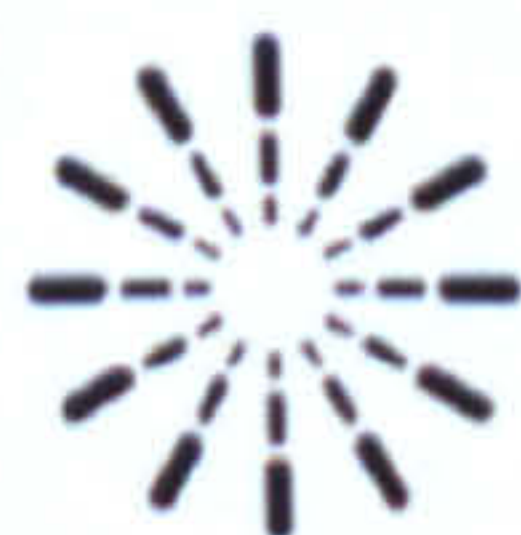
Date: 18/12/2009

IsoLux 3D



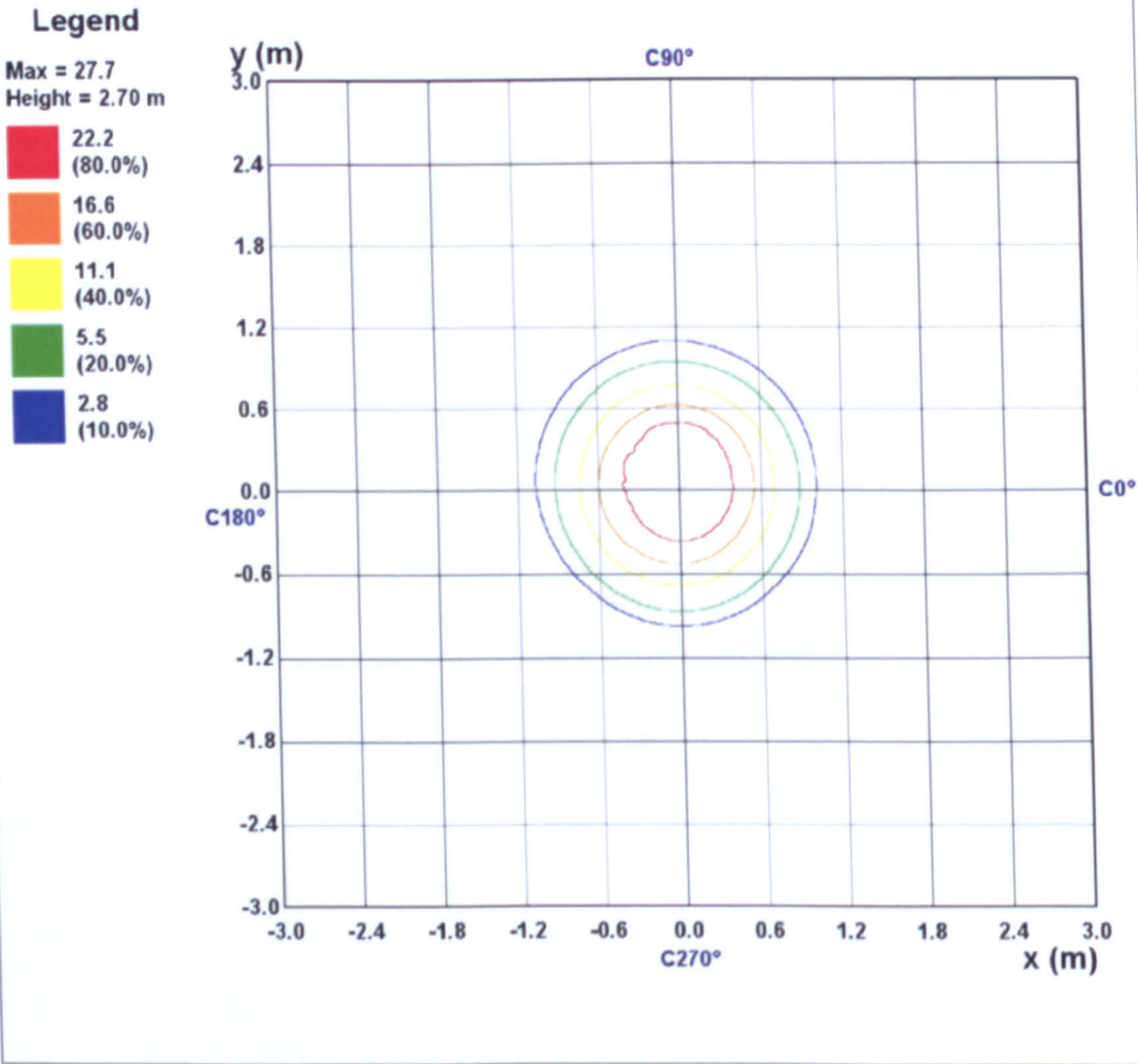
Page 14 of 23

PhotometricCentre v4.03 Copyright (C) Photometric Solutions International 2004-2008

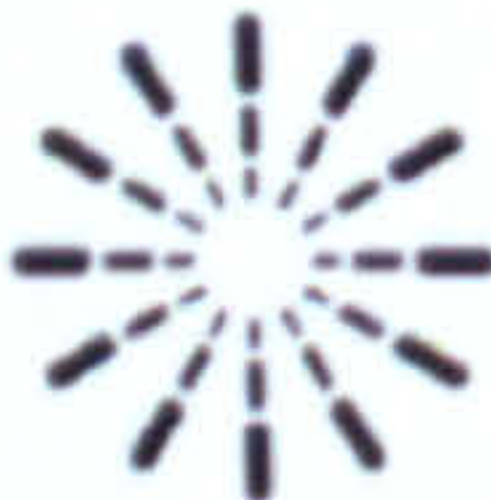


Photometric Solutions International Pty Ltd
Factory Two, 21-29 Railway Ave
Huntingdale, Vic, 3166, AUSTRALIA
Tel: +61 3 9568 1879
Fax: +61 3 9568 4667
www.PhotometricSolutions.com

IsoLux Diagram



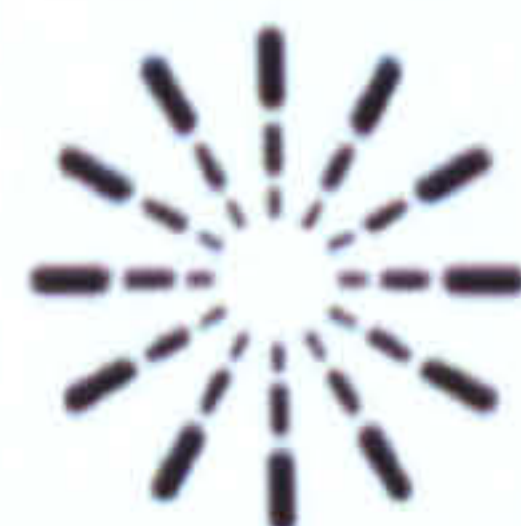
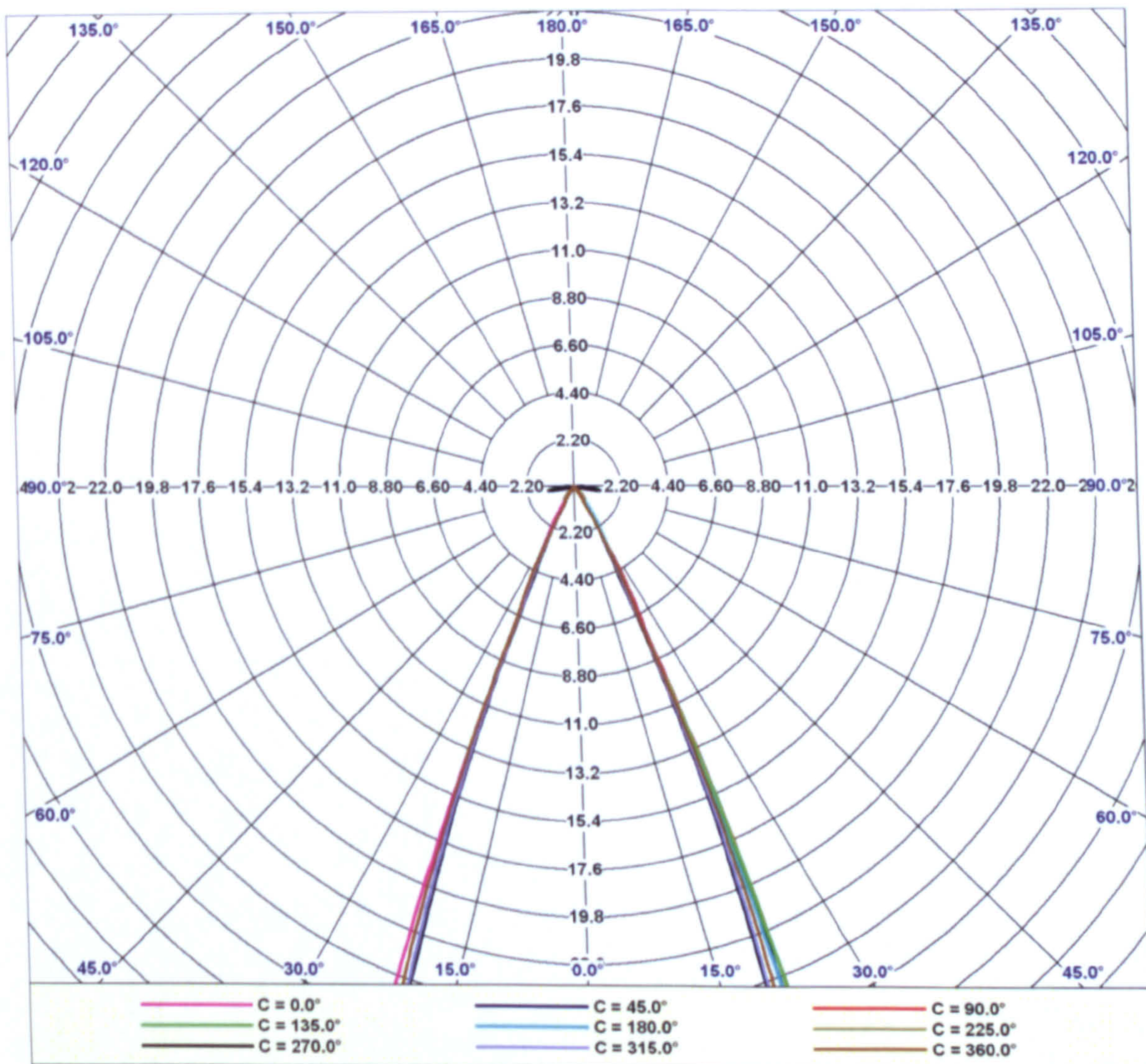
All illuminance values in lx / 1000 lm



Report Number:
 Catalog Number:
 Description: *je-3*
 Correction Factor Used: *White*

Date: 18/12/2009

Luminous Intensity Distribution (Lowest 10%)



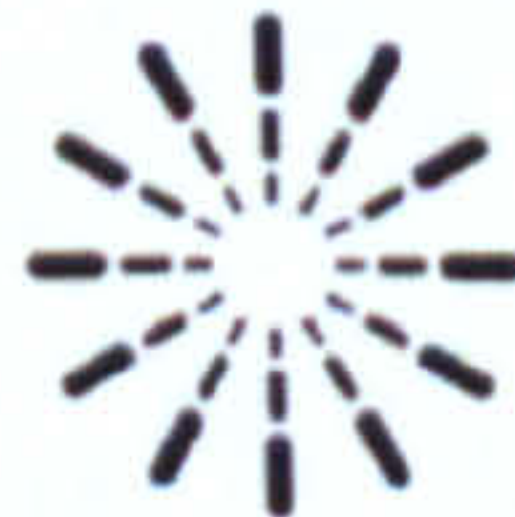
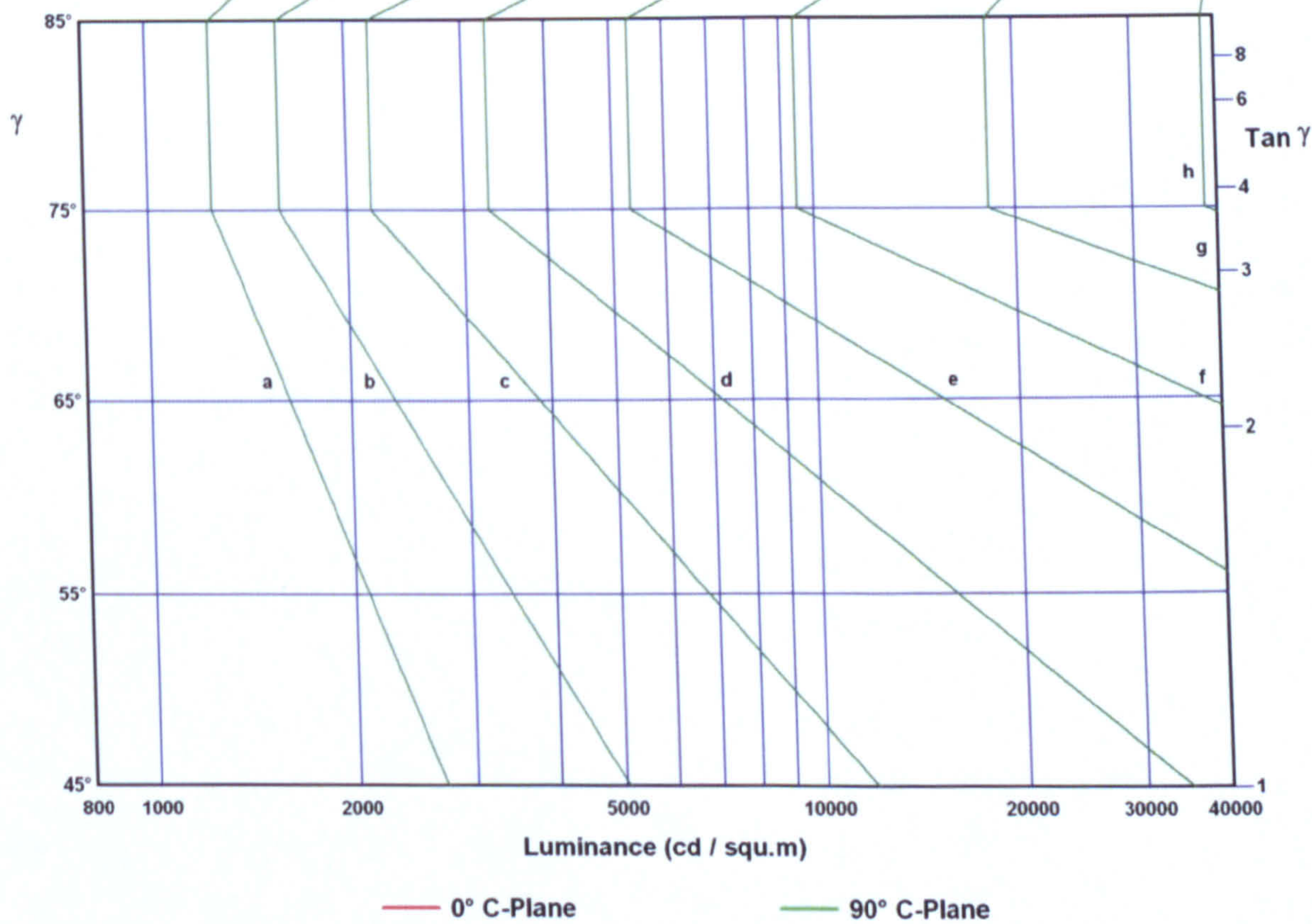
Average Luminance Table

All luminance values expressed in cd / squ.m / 1000 lm

Azimuth:	0	45	90	135	180	235	270	315
Elevation	0	241000	241000	241000	241000	241000	241000	241000
45	158	176	141	158	158	2370	176	123
55	21.7	65.0	21.7	152	108	130	86.7	0.0
65	58.8	58.8	58.8	118	0.0	29.4	29.4	88.3
75	48.0	48.0	240	144	0.0	240	769	0.0
85	-428	0.0	0.0	571	285	0.0	11800	0.0

Luminance Limiting Curve

Glare Rating	Quality Class	Service Values of Illuminance (lx)							
		2000	1000	500	<300	e	f	g	h
1.15	A								
1.5	B		2000	1000	500	<300			
1.85	C			2000	1000	500	<300		
2.2	D				2000	1000	500	<300	
2.55	E	a	b	c	d	2000	1000	500	<300



Report Number:
Catalog Number:
Description: Je-3
Correction Factor Used: White

Date: 18/12/2009

Luminous Flux Table

Elevation	Cone	Lumens	Cumulative	Lamp %	Luminaire %
0°	0.00° - 2.50°	1.2	1.2	0.1	2.5
5°	2.50° - 7.50°	9.0	10.2	1.0	22.4
10°	7.50° - 12.50°	14.9	25.1	2.5	55.3
15°	12.50° - 17.50°	12.6	37.7	3.8	83.0
20°	17.50° - 22.50°	5.5	43.3	4.3	95.1
25°	22.50° - 27.50°	1.4	44.7	4.5	98.2
30°	27.50° - 32.50°	0.3	45.0	4.5	98.9
35°	32.50° - 37.50°	0.1	45.1	4.5	99.1
40°	37.50° - 42.50°	0.1	45.1	4.5	99.2
45°	42.50° - 47.50°	0.0	45.2	4.5	99.3
50°	47.50° - 52.50°	0.0	45.2	4.5	99.4
55°	52.50° - 57.50°	0.0	45.2	4.5	99.5
60°	57.50° - 62.50°	0.0	45.3	4.5	99.6
65°	62.50° - 67.50°	0.0	45.3	4.5	99.6
70°	67.50° - 72.50°	0.0	45.3	4.5	99.7
75°	72.50° - 77.50°	0.0	45.4	4.5	99.7
80°	77.50° - 82.50°	0.0	45.4	4.5	99.8
85°	82.50° - 87.50°	0.1	45.5	4.5	100.0
90°	87.50° - 90.00°	0.0	45.5	4.5	100.0

Light Output Ratio = 4.5% (DLOR = 4.5% , ULOR = 0.0%)



Report Number:
Catalog Number:
Description: *Je-3*
Correction Factor Used: White

Date: 18/12/2009

Luminous Intensity Table (cd / 1000 lm) (Continued)

$\gamma \setminus C$	360.0
0.0	194
5.0	204
10.0	150
15.0	84.3
20.0	27.3
25.0	6.7
30.0	1.0
35.0	0.3
40.0	0.1
45.0	0.1
50.0	0.0
55.0	0.0
60.0	0.0
65.0	0.0
70.0	0.0
75.0	0.0
80.0	0.0
85.0	0.0
90.0	0.0

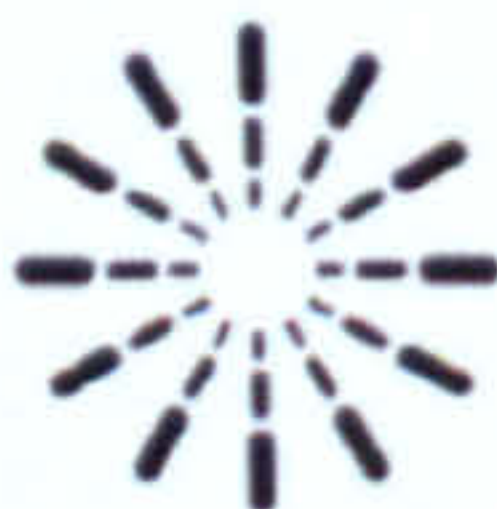
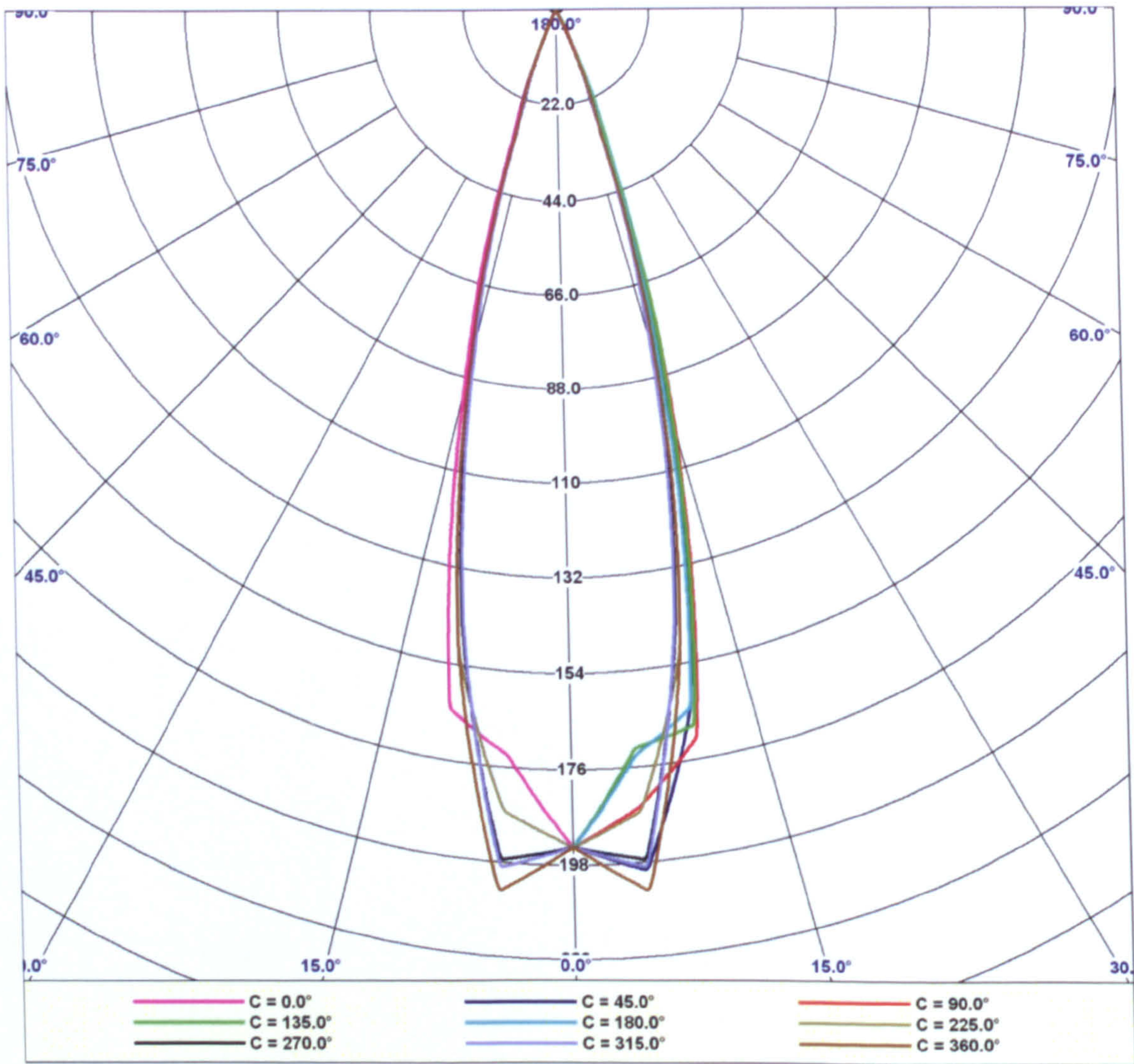


Photometric Solutions International Pty Ltd
Factory Two, 21-29 Railway Ave
Huntingdale, Vic, 3166, AUSTRALIA
Tel: +61 3 9568 1879
Fax: +61 3 9568 4667
www.PhotometricSolutions.com

Report Number:
Catalog Number:
Description: je-3
Correction Factor Used: White

Date: 18/12/2009

Luminous Intensity Distribution

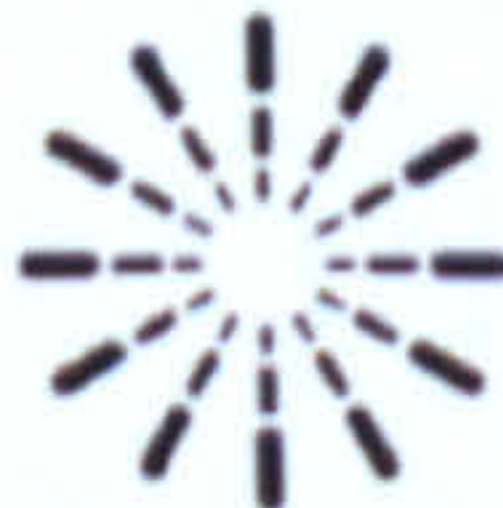


Photometric Solutions International Pty Ltd
Factory Two, 21-29 Railway Ave
Huntingdale, Vic, 3166, AUSTRALIA
Tel: +61 3 9568 1879
Fax: +61 3 9568 4667
www.PhotometricSolutions.com

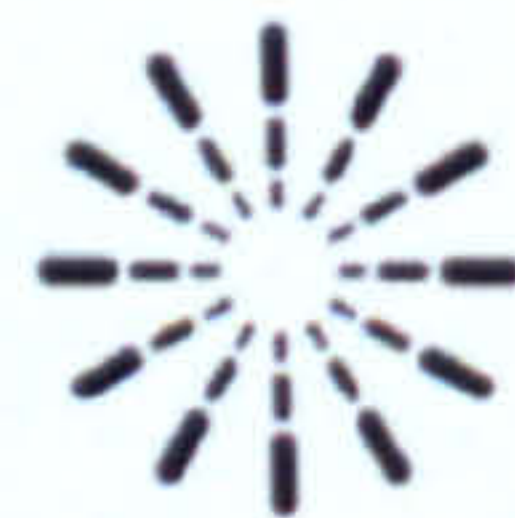
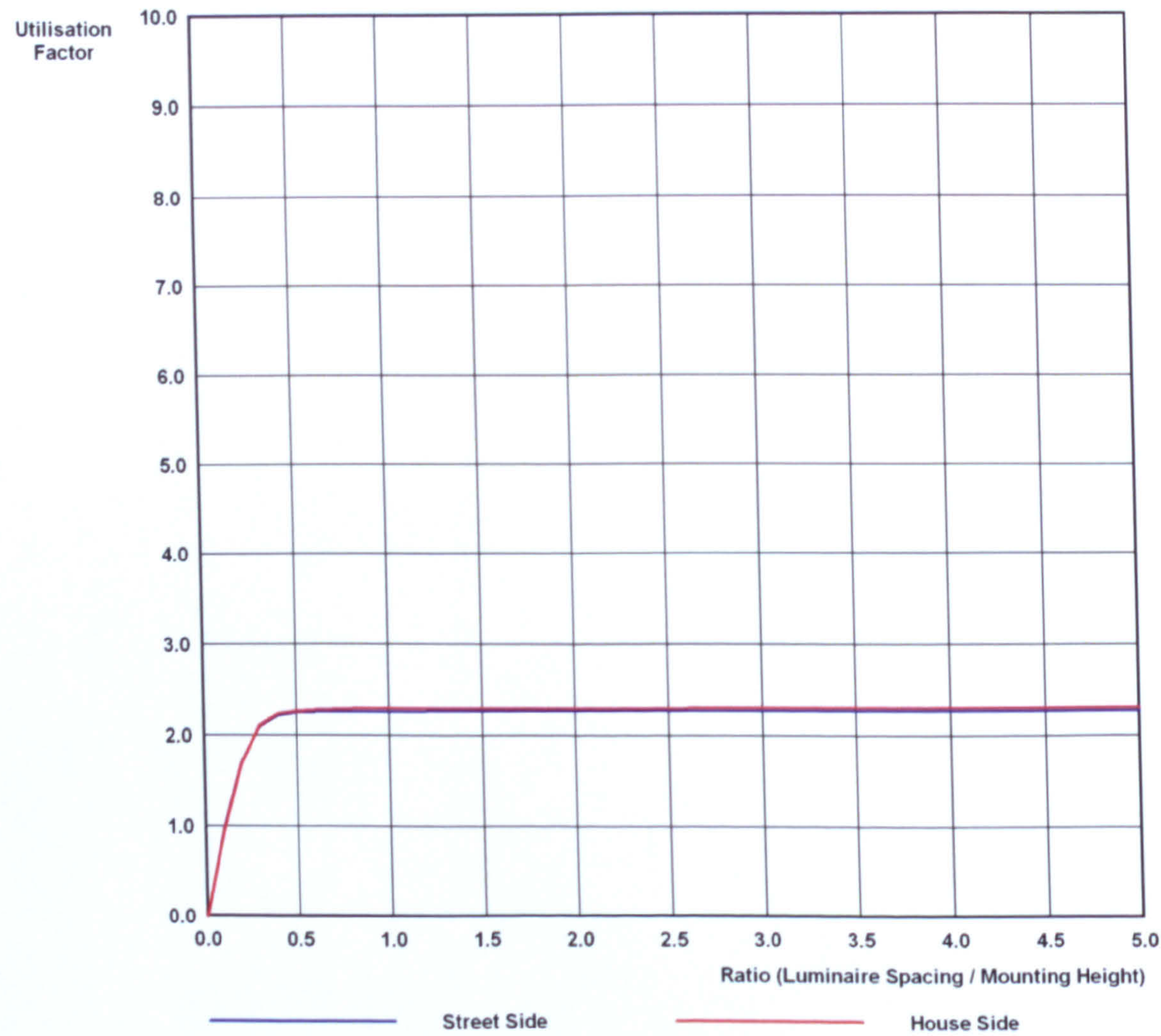
Photometric Solid



Viewing Angle: C = 315°



Roadway Utilisation Factor Graph



Report Number:
Catalog Number:
Description: *Je-3*
Correction Factor Used: White

Date: 18/12/2009

Luminaire Details

Luminaire Test Details:

Photometry Type: *Type C/Gamma*
Number of Lamps: *1*
Lumens per Lamp: *1000*

Luminous Dimensions:

Base Area: *0.032 m Diameter*
Side Area: *N/A*
End Area: *N/A*
Luminous Shape: *Circular*



Report Number:
Catalog Number:
Description: *Je-3*
Correction Factor Used: White

Date: 18/12/2009

TM5 Utilisation Factor Table

SHR < 0.5 - No UF Table or Graph can be Produced

Page 17 of 23

PhotometricCentre v4.03 Copyright (C) Photometric Solutions International 2004-2008



Photometric Solutions International Pty Ltd
Factory Two, 21-29 Railway Ave
Huntingdale, Vic, 3166, AUSTRALIA
Tel: +61 3 9568 1879
Fax: +61 3 9568 4667
www.PhotometricSolutions.com

Report Number:
Catalog Number:
Description: Jc-3
Correction Factor Used: White

Date: 18/12/2009

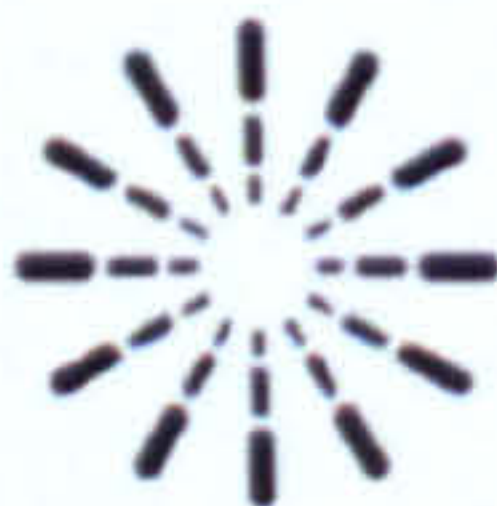
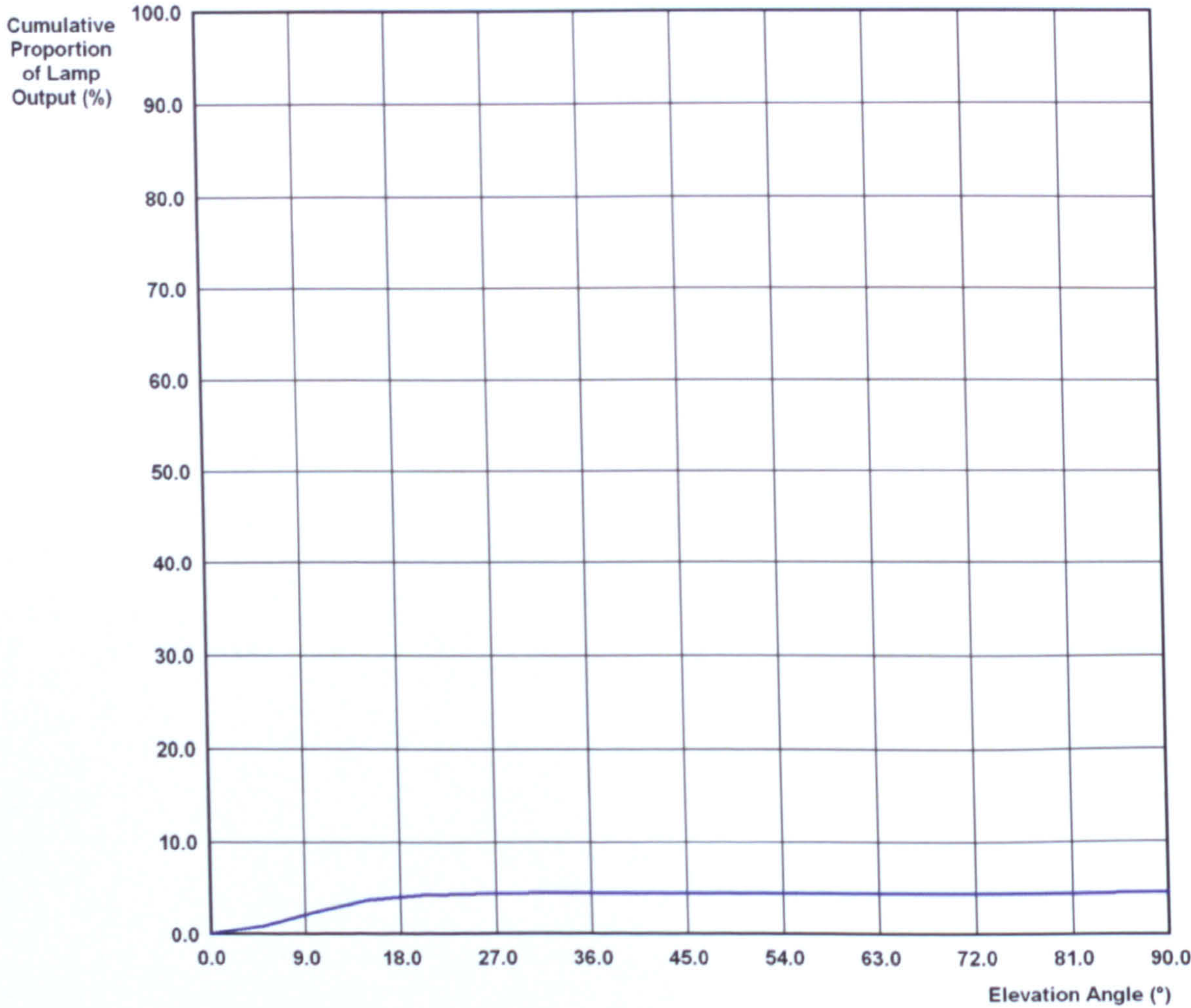
TM5* Utilisation Factor Table

* Based on TM5, except using Min / Ave = 0.8 as Spacing Criteria
SHR < 0.5 - No UF Table or Graph can be Produced



Photometric Solutions International Pty Ltd
Factory Two, 21-29 Railway Ave
Huntingdale, Vic, 3166, AUSTRALIA
Tel: +61 3 9568 1879
Fax: +61 3 9568 4667
www.PhotometricSolutions.com

Zonal Flux Diagram



7.4 Convex Lens

Report Number:

Catalog Number:

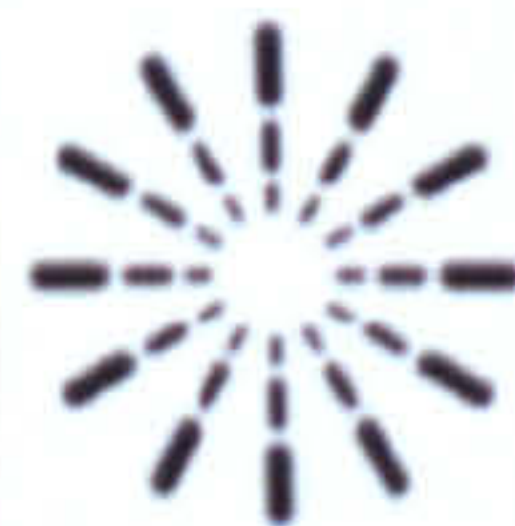
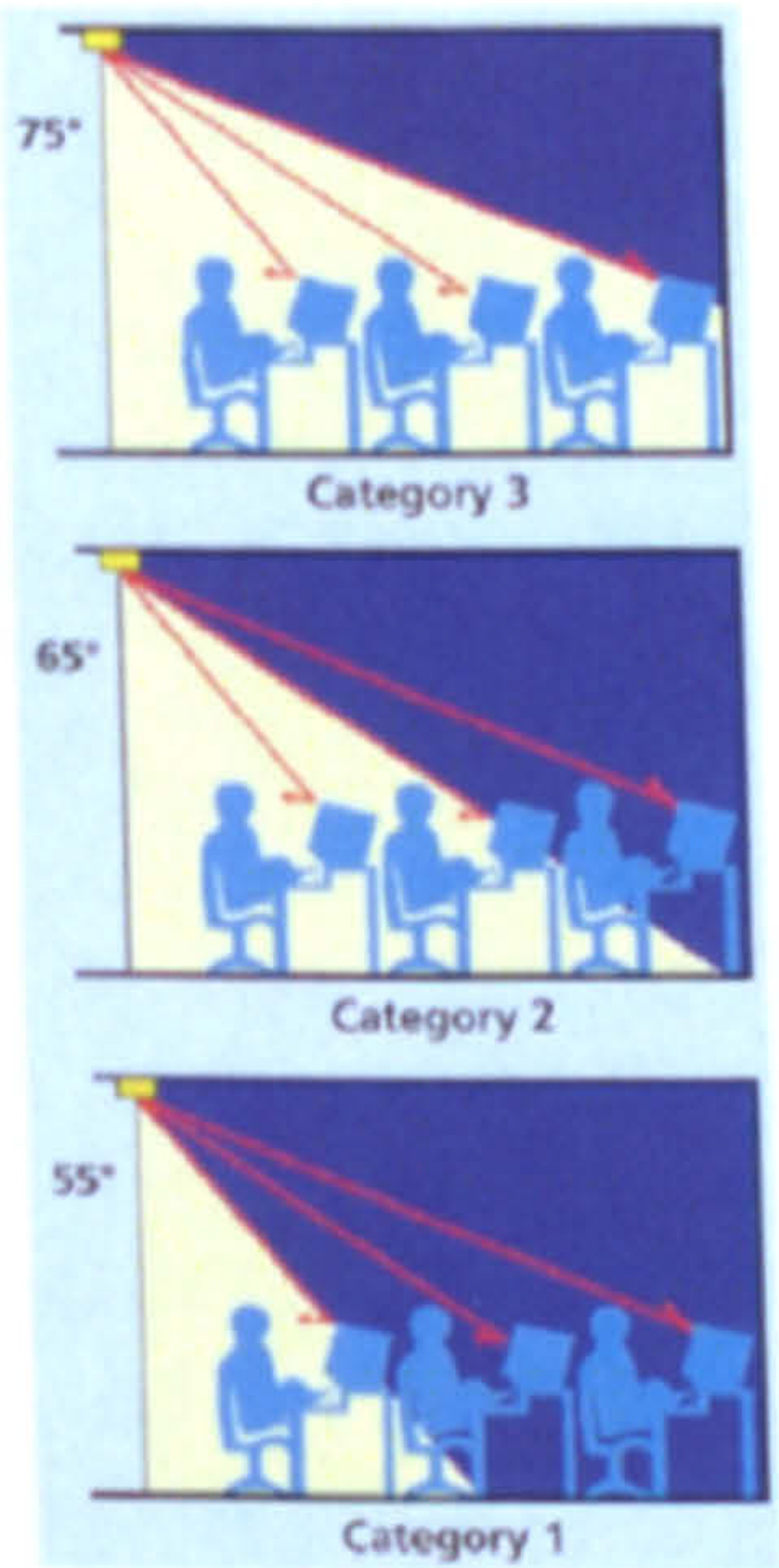
Description: je-4

Date: 17/12/2009

Correction Factor Used: White

CIBSE LG3 VDT Category

	Category 1	Category 2	Category 3
Starting Gamma Angle (°):	55.0	65.0	75.0
Final Gamma Angle (°):	90.0	90.0	90.0
Avg Luminance Found (cd/m²):	566.3	635.4	828.1
Max. Permissible (cd/m²):	200.0	200.0	200.0
Max Luminance Found (cd/m²):	43890	43890	43890
Max. Permissible (cd/m²):	500.0	500.0	500.0
Result:	-	-	-



Distribution Photometry Report

Report Number:

Date: 17/12/2009

Catalog Number:

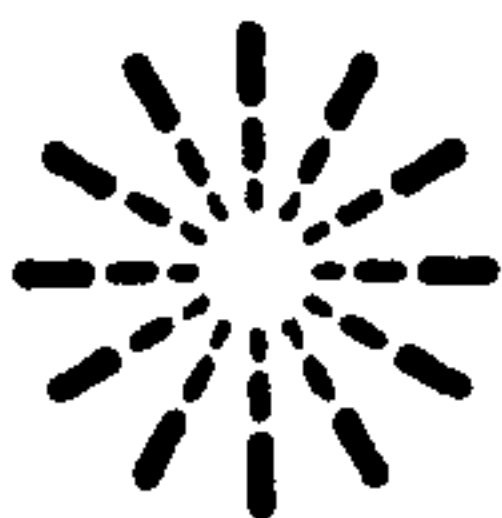
Description: **Je-4**
Correction Factor Used: White

Filename: **Je-4.IES**

Results For: **Test Details**
Luminous Intensity Distribution
LID (Lowest 10%)
Luminous Intensity Data
Luminous Flux Data
Luminaire Luminance
IsoCandela Diagram
IsoLux Diagram
IsoLux 3D
Illuminance Grid
IESNA CoU Table
TM5 UF Table
TM5 UF Table (Variation)
Roadway UF Graph
Zonal Flux Diagram
Luminance Limiting Curve
CIBSE LG3 Rating
Photometric Solid

Page 1 of 23

PhotometricCentre v4.03 Copyright (C) Photometric Solutions International 2004-2008



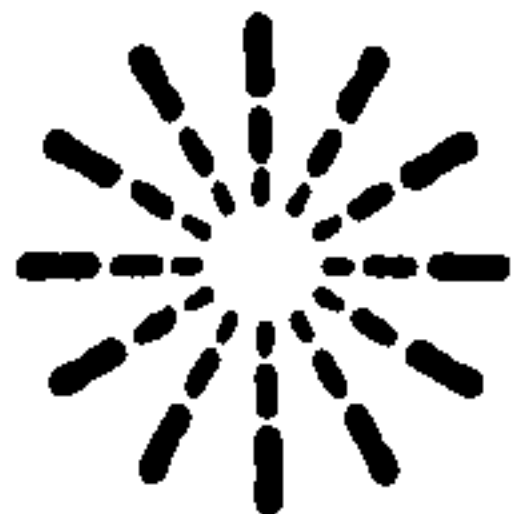
Photometric Solutions International Pty Ltd
Factory Two, 21-29 Railway Ave
Huntingdale, Vic, 3166, AUSTRALIA
Tel: +61 3 9568 1879
Fax: +61 3 9568 4667
www.PhotometricSolutions.com

Date: 17/12/2009

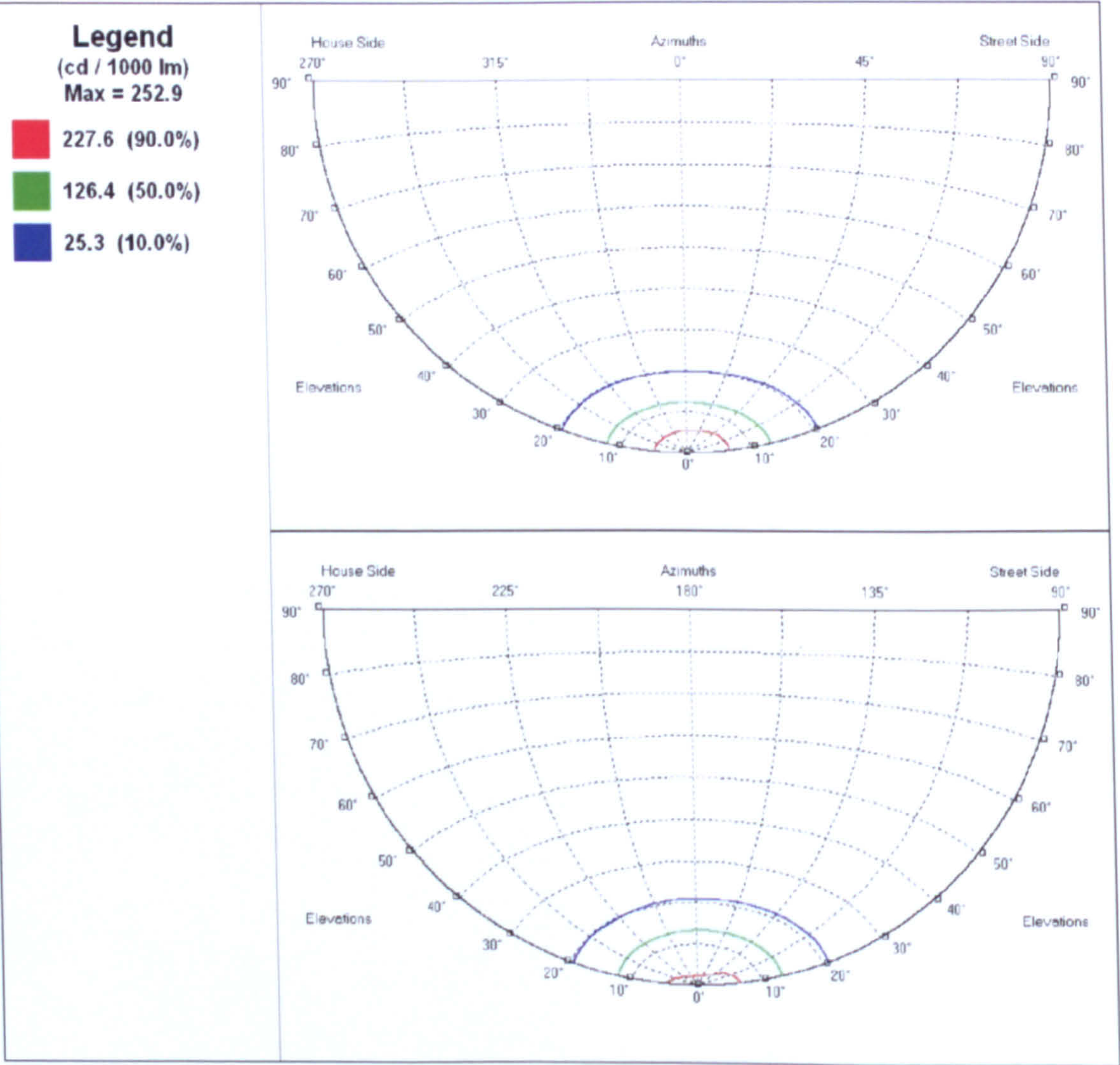
Description: *Je-4*
Correction Factor Used: *White*

y (m)																					x (m)
3.0	0.00	0.00	0.00	0.00	0.00	0.00	0.00	0.00	0.00	0.00	0.00	0.00	0.00	0.00	0.00	0.00	0.00	0.00	0.00	0.00	0.00
	0.00	0.00	0.00	0.00	0.00	0.00	0.00	0.00	0.00	0.00	0.00	0.01	0.00	0.01	0.00	0.00	0.00	0.00	0.00	0.00	0.00
2.4	0.00	0.00	0.00	0.00	0.00	0.00	0.01	0.01	0.01	0.01	0.01	0.01	0.01	0.01	0.01	0.00	0.00	0.00	0.00	0.00	0.00
	0.00	0.00	0.00	0.00	0.00	0.01	0.01	0.01	0.01	0.01	0.01	0.01	0.01	0.01	0.01	0.01	0.01	0.00	0.00	0.00	0.00
1.8	0.00	0.00	0.00	0.01	0.01	0.01	0.01	0.01	0.01	0.01	0.02	0.03	0.02	0.01	0.01	0.01	0.01	0.01	0.00	0.00	0.00
	0.00	0.00	0.01	0.01	0.01	0.01	0.01	0.03	0.06	0.12	0.17	0.12	0.06	0.04	0.01	0.01	0.01	0.01	0.01	0.00	0.00
1.2	0.00	0.00	0.01	0.01	0.01	0.02	0.04	0.15	0.45	0.84	1.18	0.83	0.46	0.16	0.04	0.02	0.01	0.01	0.01	0.01	0.00
	0.00	0.00	0.01	0.01	0.01	0.04	0.14	0.53	2.39	4.49	5.88	4.28	2.23	0.58	0.16	0.03	0.01	0.01	0.01	0.01	0.00
0.6	0.00	0.00	0.01	0.01	0.02	0.06	0.35	2.41	7.92	14.7	18.0	13.7	6.91	2.13	0.42	0.05	0.01	0.01	0.01	0.01	0.00
	0.00	0.01	0.01	0.02	0.05	0.17	0.66	4.68	15.0	26.2	31.2	25.4	12.7	3.85	0.72	0.10	0.02	0.01	0.01	0.01	0.00
0.0	0.00	0.00	0.01	0.02	0.06	0.21	1.01	6.16	18.3	27.2	33.9	29.4	16.0	5.06	0.99	0.15	0.03	0.01	0.01	0.01	0.00
	0.00	0.00	0.01	0.02	0.06	0.12	0.61	4.43	14.2	24.4	28.7	23.8	12.5	3.73	0.68	0.10	0.02	0.01	0.01	0.01	0.00
-0.6	0.00	0.00	0.01	0.01	0.03	0.07	0.28	2.03	7.18	13.6	16.4	12.8	6.43	1.91	0.35	0.05	0.02	0.01	0.01	0.00	0.00
	0.00	0.00	0.01	0.01	0.04	0.10	0.12	0.34	1.88	3.74	5.16	3.64	1.84	0.43	0.13	0.03	0.01	0.01	0.01	0.01	0.00
-1.2	0.00	0.00	0.01	0.01	0.04	0.04	0.05	0.12	0.27	0.52	0.83	0.57	0.31	0.13	0.04	0.02	0.01	0.01	0.01	0.00	0.00
	0.00	0.00	0.01	0.01	0.02	0.04	0.02	0.04	0.05	0.09	0.12	0.09	0.05	0.03	0.02	0.01	0.01	0.01	0.00	0.00	0.00
-1.8	0.00	0.00	0.00	0.01	0.03	0.02	0.01	0.02	0.02	0.03	0.03	0.03	0.02	0.02	0.01	0.01	0.01	0.00	0.00	0.00	0.00
	0.00	0.00	0.00	0.01	0.02	0.05	0.02	0.01	0.01	0.01	0.02	0.01	0.01	0.01	0.01	0.01	0.01	0.00	0.00	0.00	0.00
-2.4	0.00	0.00	0.00	0.01	0.02	0.04	0.02	0.01	0.01	0.01	0.01	0.01	0.01	0.01	0.01	0.00	0.00	0.00	0.00	0.00	0.00
	0.00	0.00	0.00	0.01	0.02	0.03	0.02	0.01	0.01	0.01	0.01	0.01	0.01	0.01	0.00	0.00	0.00	0.00	0.00	0.00	0.00
-3.0	0.00	0.00	0.00	0.00	0.02	0.03	0.01	0.01	0.00												

Horizontal Illuminance
All illuminance values in lux / 1000 lm
Table Average: 1.24 Table Maximum: 33.9 Table Minimum: 0.00
Mounting Height = 2.7 m



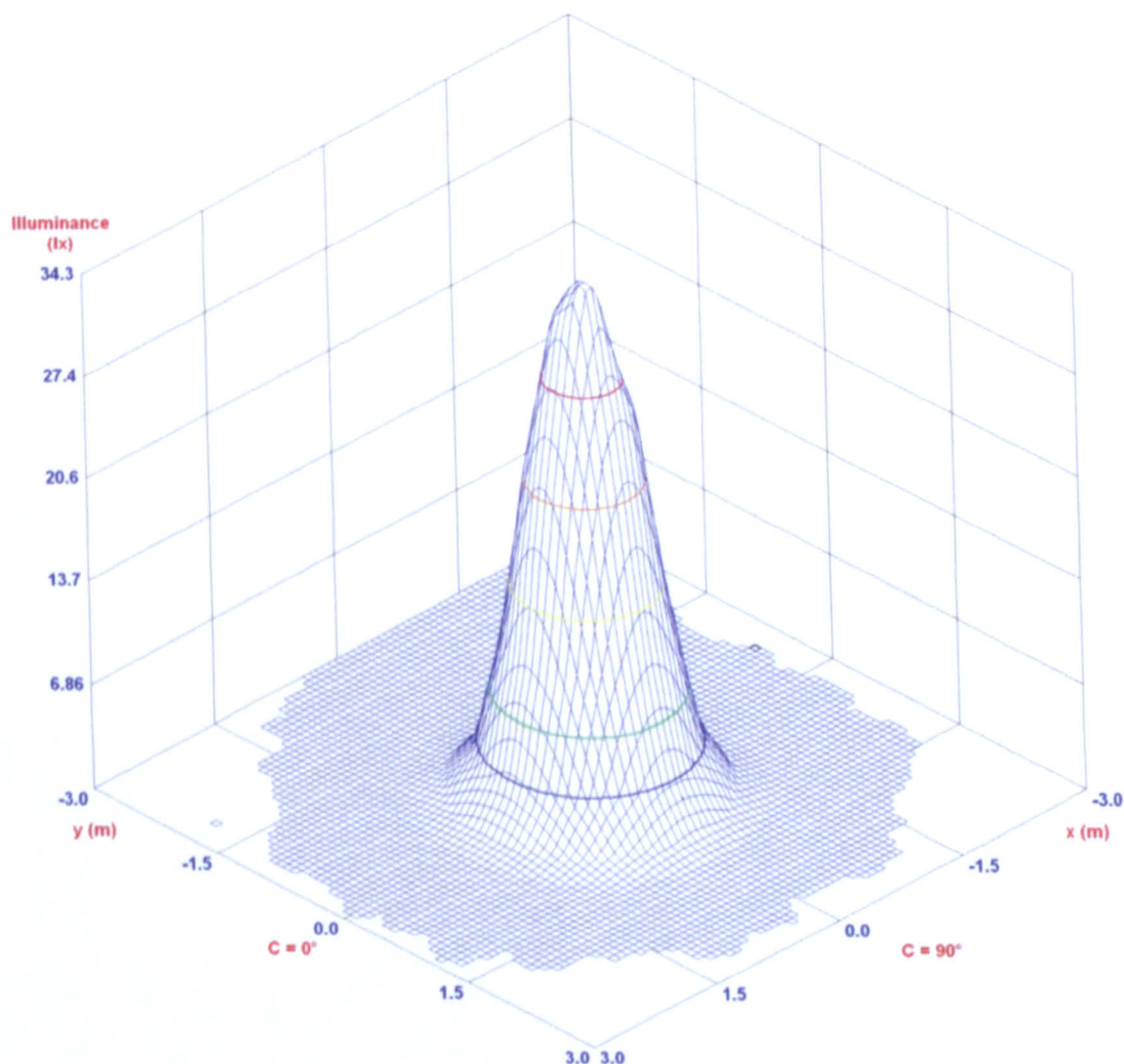
IsoCandela Diagram



Report Number:
Catalog Number:
Description: *Je-4*
Correction Factor Used: *White*

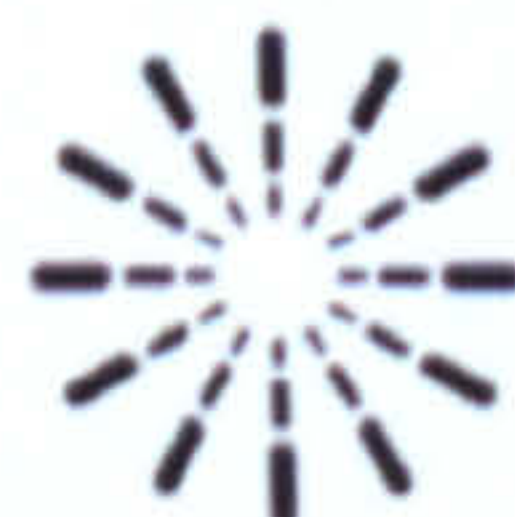
Date: 17/12/2009

IsoLux 3D



PhotometricCentre v4.03 Copyright (C) Photometric Solutions International 2004-2008

Page 14 of 23



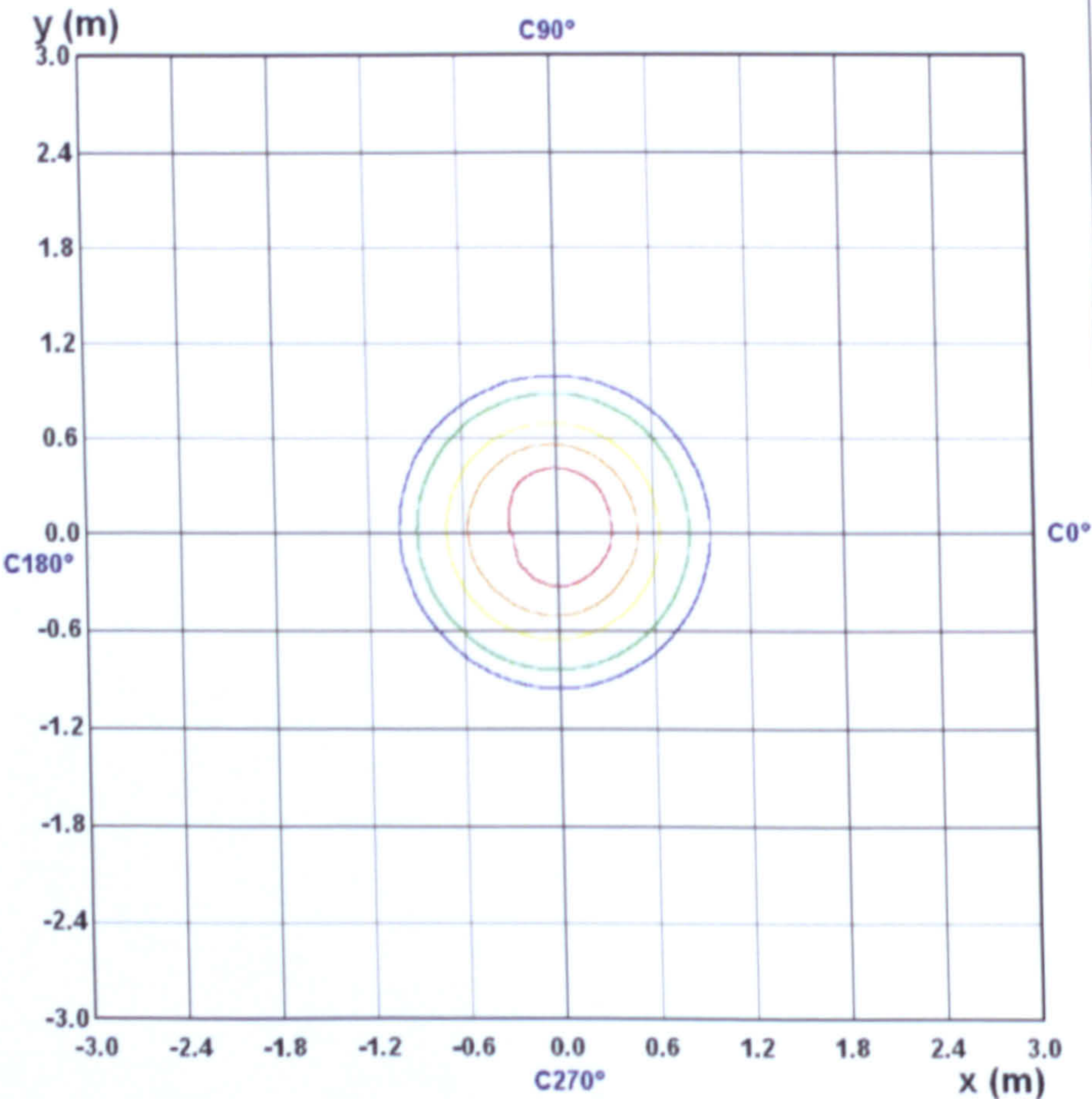
Photometric Solutions International Pty Ltd
Factory Two, 21-29 Railway Ave
Huntingdale, Vic, 3166, AUSTRALIA
Tel: +61 3 9568 1879
Fax: +61 3 9568 4667
www.PhotometricSolutions.com

IsoLux Diagram

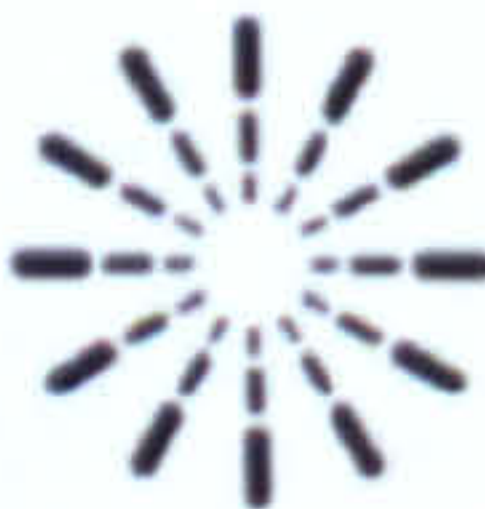
Legend

Max = 34.3
Height = 2.70 m

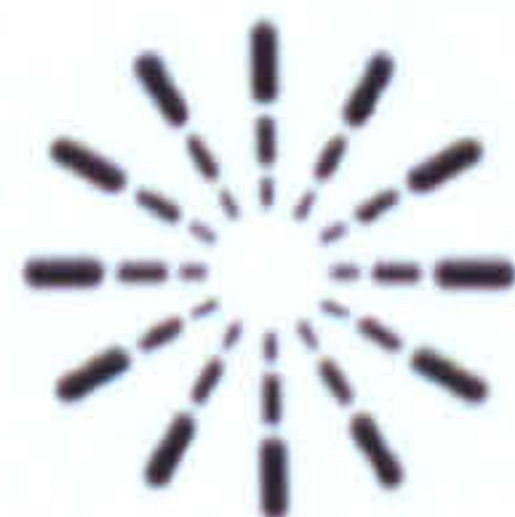
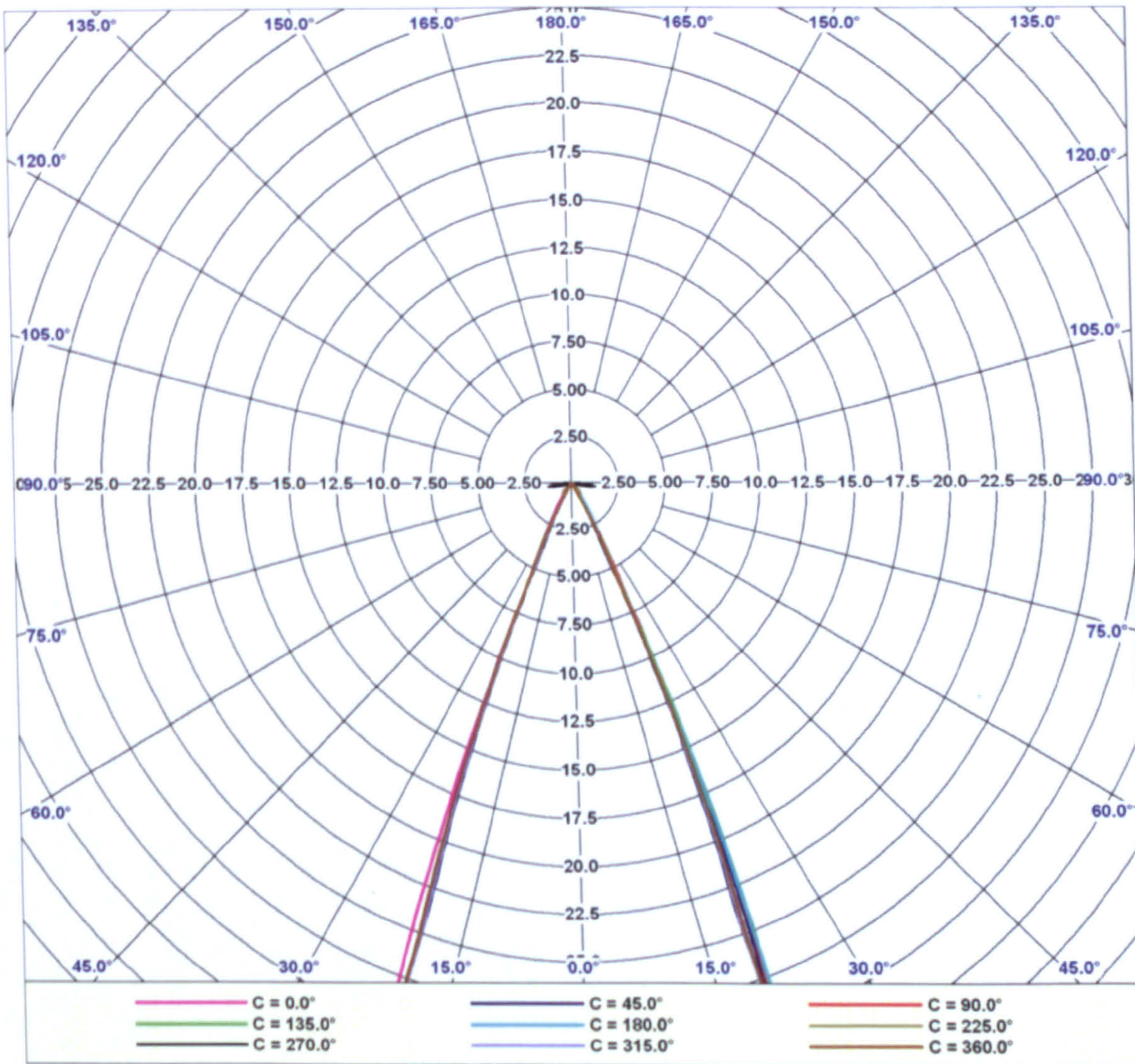
- 27.4 (80.0%)
- 20.6 (60.0%)
- 13.7 (40.0%)
- 6.9 (20.0%)
- 3.4 (10.0%)



All illuminance values in lx / 1000 lm



Luminous Intensity Distribution (Lowest 10%)



Report Number:
Catalog Number:
Description: **Je-4**
Correction Factor Used: White

Date: 17/12/2009

Average Luminance Table

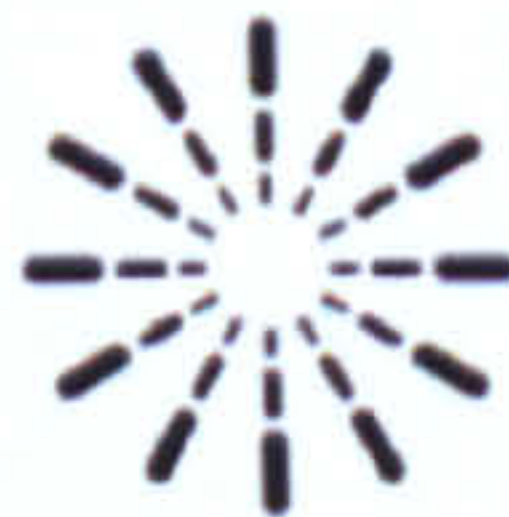
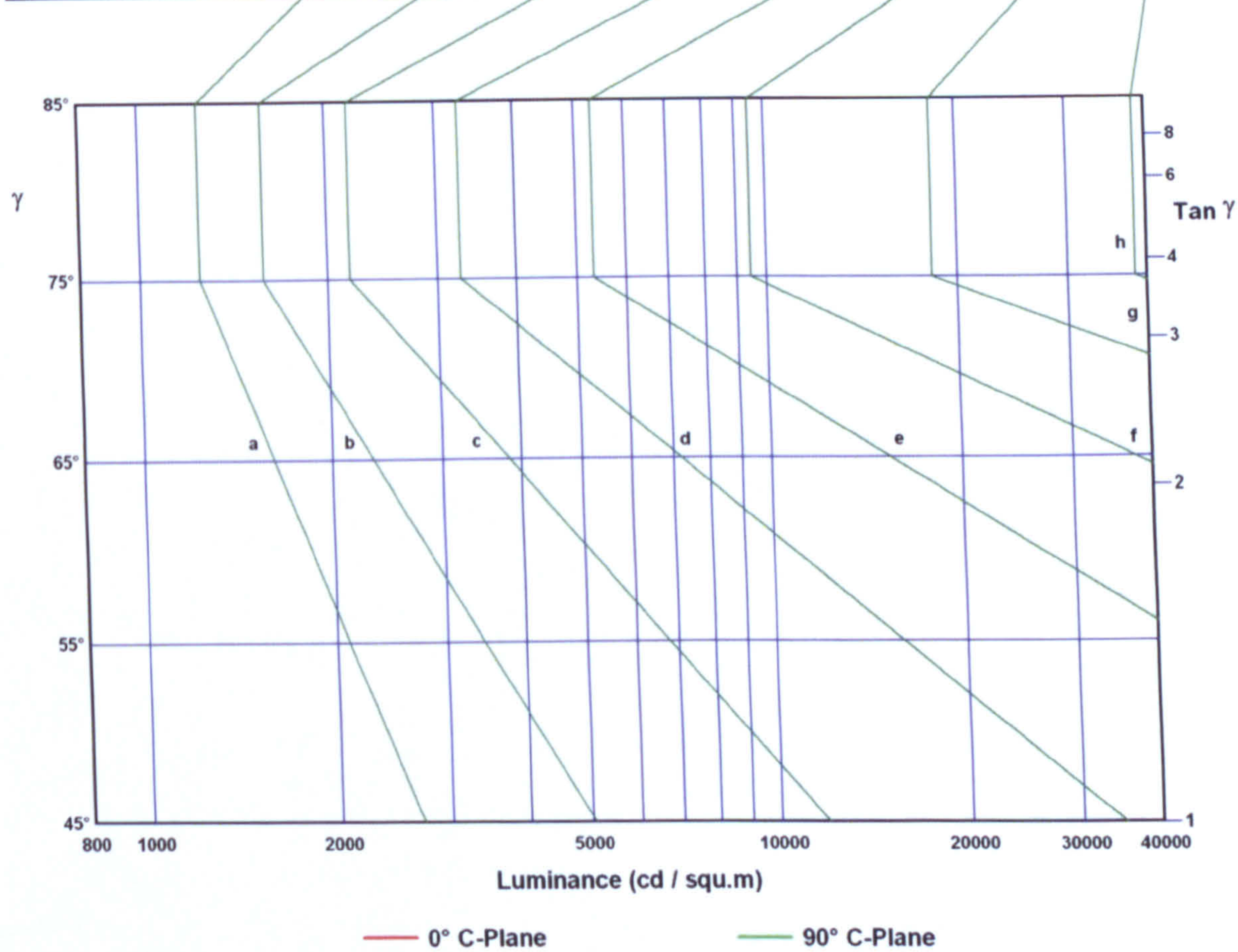
All luminance values expressed in cd / squ.m / 1000 lm

Azimuth:	0	45	90	135	180	235	270	315
Elevation								
0	432000	432000	432000	432000	432000	432000	432000	432000
45	321	247	173	247	247	3260	371	222
55	183	274	274	122	213	183	213	274
65	165	165	207	82.7	165	248	207	207
75	67.5	0.0	0.0	0.0	67.5	405	1080	0.0
85	0.0	0.0	0.0	0.0	401	0.0	15800	0.0



Luminance Limiting Curve

Glare Rating	Quality Class	Service Values of Illuminance (lx)							
		2000	1000	500	<300	e	f	g	h
1.15	A								
1.5	B		2000	1000	500	<300			
1.85	C			2000	1000	500	<300		
2.2	D				2000	1000	500	<300	
2.55	E	a	b	c	d	2000	1000	500	<300



Report Number:
Catalog Number:
Description: Jc-4
Correction Factor Used: White

Date: 17/12/2009

Luminous Flux Table

Elevation	Cone	Lumens	Cumulative	Lamp %	Luminaire %
0°	0.00° - 2.50°	1.5	1.5	0.1	3.0
5°	2.50° - 7.50°	10.9	12.4	1.2	25.2
10°	7.50° - 12.50°	16.9	29.4	2.9	59.6
15°	12.50° - 17.50°	12.9	42.2	4.2	85.7
20°	17.50° - 22.50°	5.2	47.4	4.7	96.1
25°	22.50° - 27.50°	1.1	48.5	4.9	98.4
30°	27.50° - 32.50°	0.2	48.7	4.9	98.8
35°	32.50° - 37.50°	0.1	48.8	4.9	99.0
40°	37.50° - 42.50°	0.1	48.9	4.9	99.2
45°	42.50° - 47.50°	0.1	49.0	4.9	99.3
50°	47.50° - 52.50°	0.0	49.0	4.9	99.4
55°	52.50° - 57.50°	0.0	49.0	4.9	99.5
60°	57.50° - 62.50°	0.1	49.1	4.9	99.6
65°	62.50° - 67.50°	0.0	49.1	4.9	99.6
70°	67.50° - 72.50°	0.0	49.2	4.9	99.7
75°	72.50° - 77.50°	0.0	49.2	4.9	99.7
80°	77.50° - 82.50°	0.0	49.2	4.9	99.8
85°	82.50° - 87.50°	0.1	49.3	4.9	100.0
90°	87.50° - 90.00°	0.0	49.3	4.9	100.0

Light Output Ratio = 4.9% (DLOR = 4.9% , ULOR = 0.0%)



Report Number:
Catalog Number:
Description: *Je-4*
Correction Factor Used: White

Date: 17/12/2009

Luminous Intensity Table (cd / 1000 lm) (Continued)

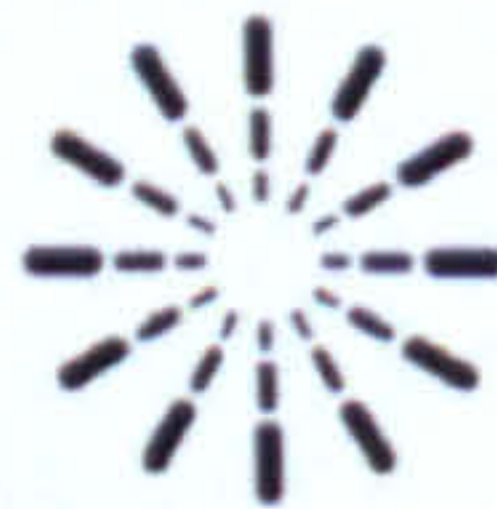
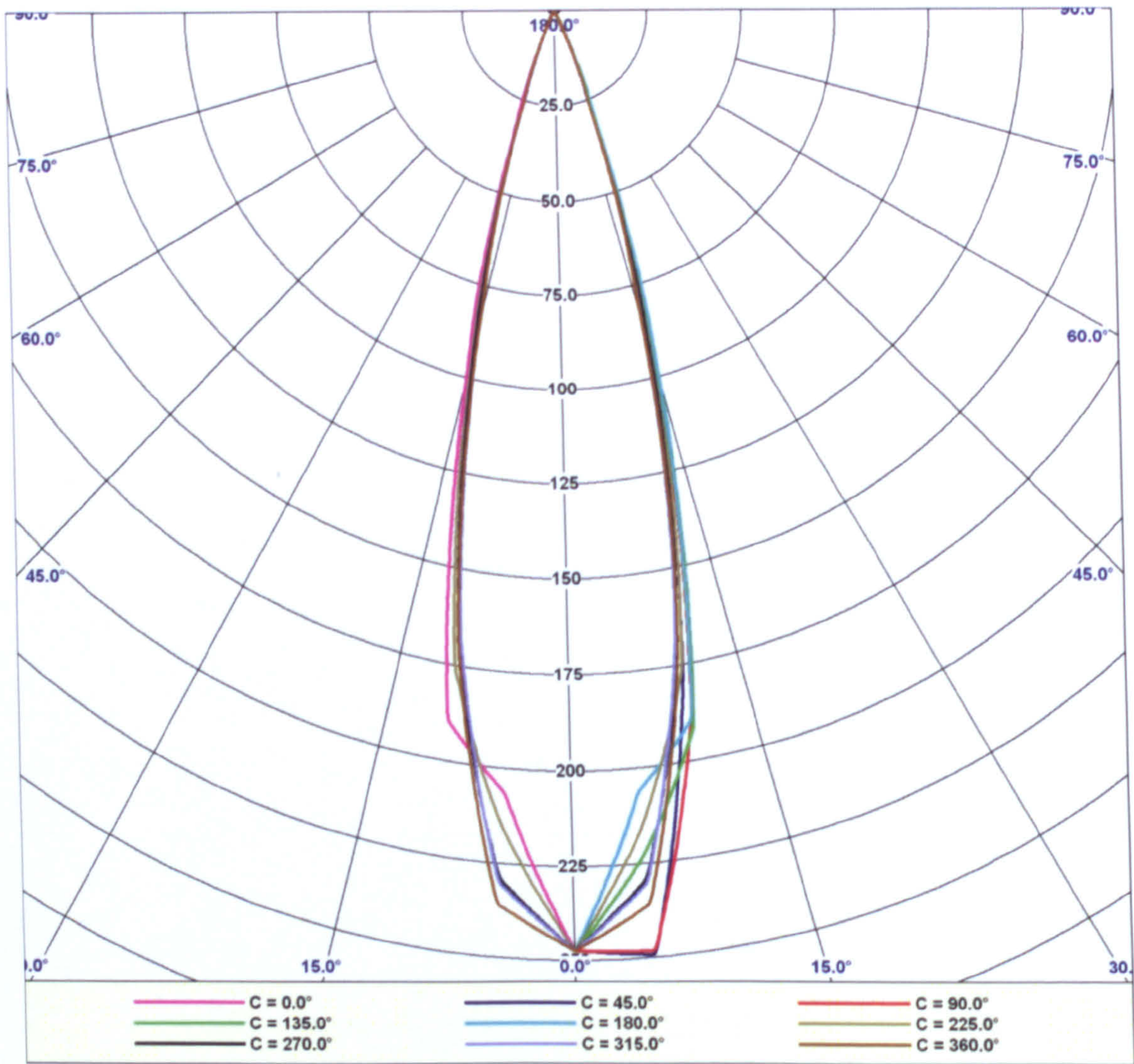
γ \ C	360.0
0.0	247
5.0	236
10.0	170
15.0	81.8
20.0	25.6
25.0	5.2
30.0	0.8
35.0	0.2
40.0	0.2
45.0	0.1
50.0	0.1
55.0	0.1
60.0	0.1
65.0	0.0
70.0	0.0
75.0	0.0
80.0	0.0
85.0	0.0
90.0	0.0



Report Number:
Catalog Number:
Description: je-4
Correction Factor Used: White

Date: 17/12/2009

Luminous Intensity Distribution

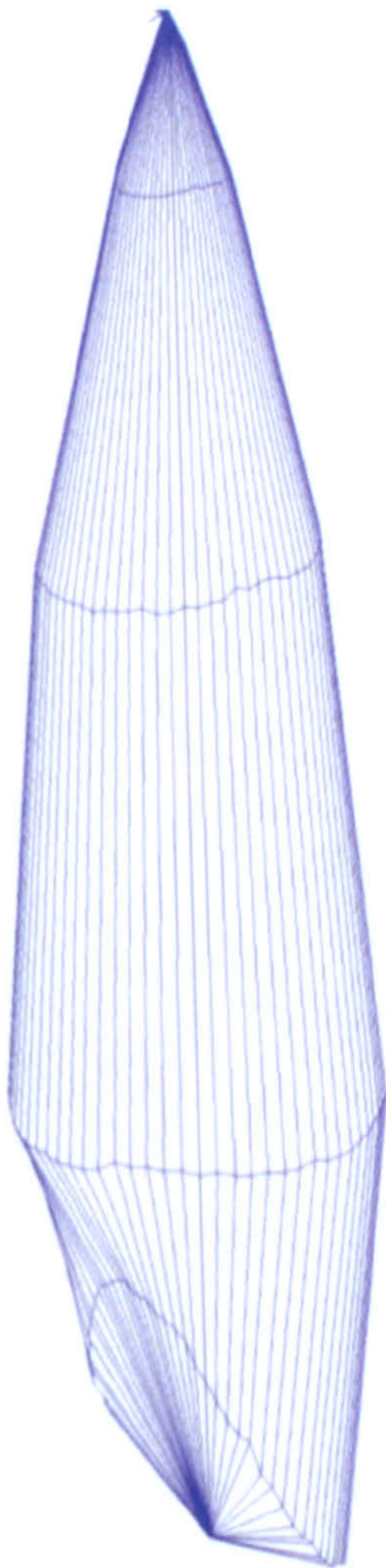


Photometric Solutions International Pty Ltd
Factory Two, 21-29 Railway Ave
Huntingdale, Vic, 3166, AUSTRALIA
Tel: +61 3 9568 1879
Fax: +61 3 9568 4667
www.PhotometricSolutions.com

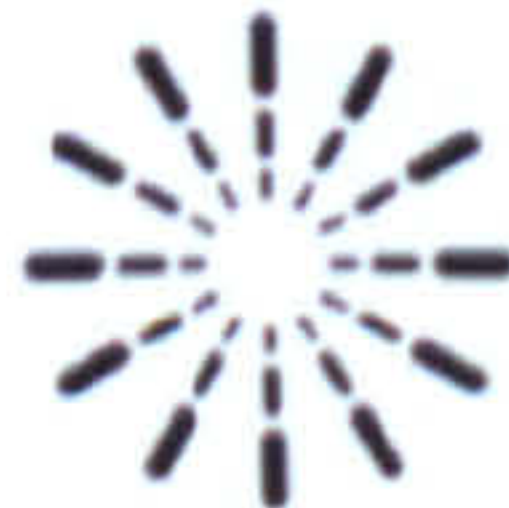
Report Number:
Catalog Number:
Description: *je-4*
Correction Factor Used: *White*

Date: 17/12/2009

Photometric Solid

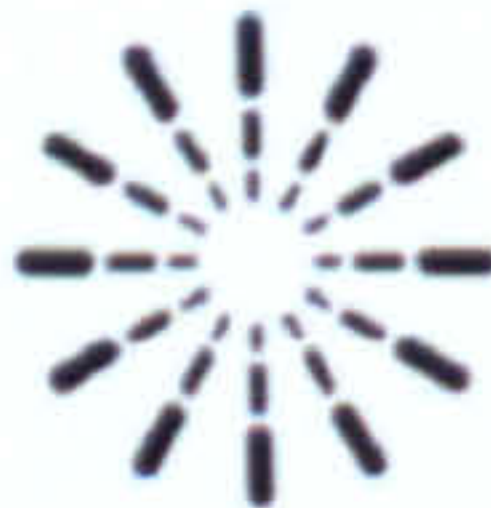
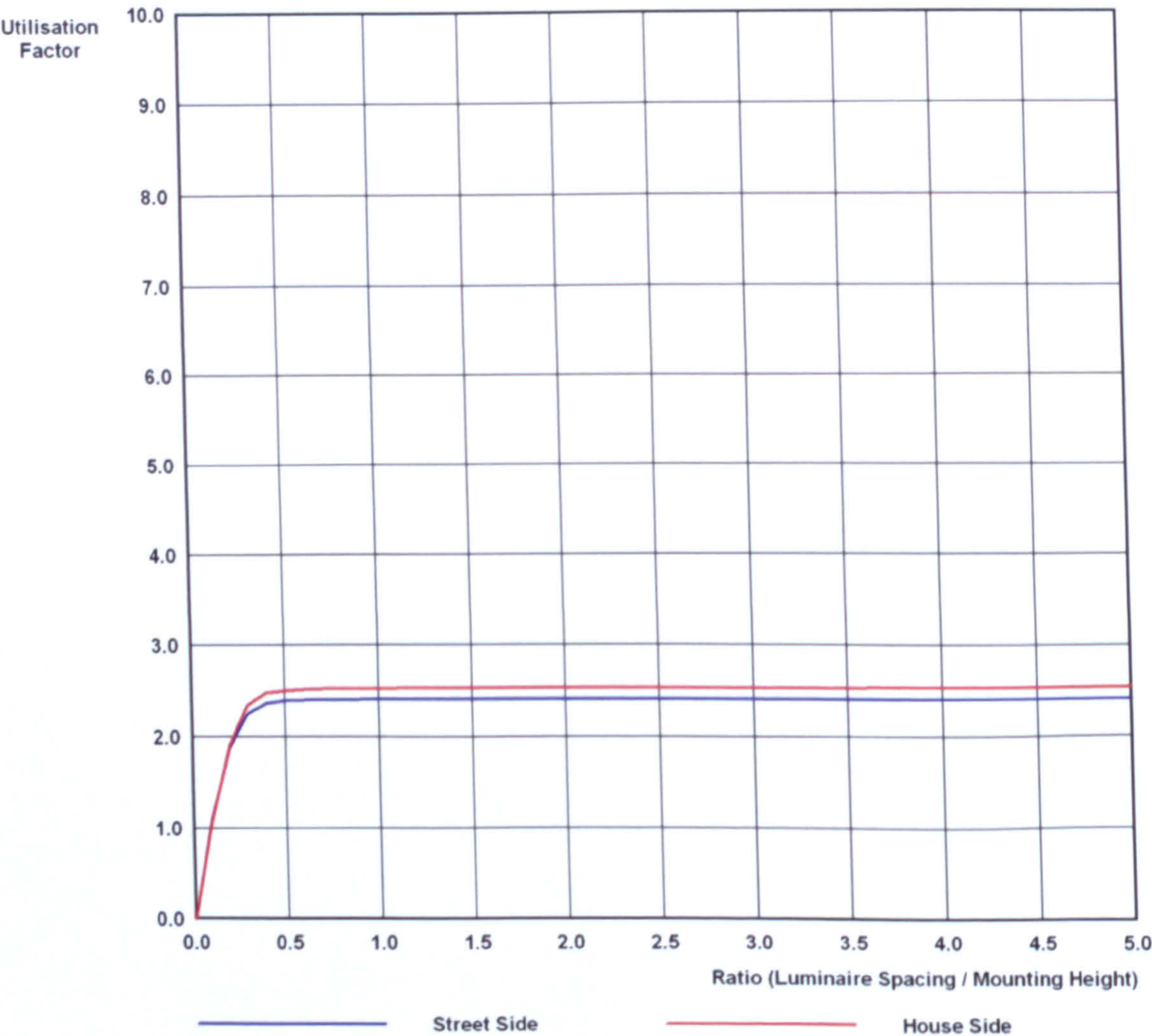


Viewing Angle: C = 315°



Photometric Solutions International Pty Ltd
Factory Two, 21-29 Railway Ave
Huntingdale, Vic, 3166, AUSTRALIA
Tel: +61 3 9568 1879
Fax: +61 3 9568 4667
www.PhotometricSolutions.com

Roadway Utilisation Factor Graph



Report Number:
Catalog Number:
Description: *Je-4*
Correction Factor Used: White

Date: 17/12/2009

Luminaire Details

Luminaire Test Details:
Photometry Type: *Type C/Gamma*
Number of Lamps: *1*
Lumens per Lamp: *1000*

Luminous Dimensions:
Base Area: *0.027 m Diameter*
Side Area: *N/A*
End Area: *N/A*
Luminous Shape: *Circular*



Report Number:
Catalog Number:
Description: *Je-4*
Correction Factor Used: White

Date: 17/12/2009

TM5 Utilisation Factor Table

SHR < 0.5 - No UF Table or Graph can be Produced



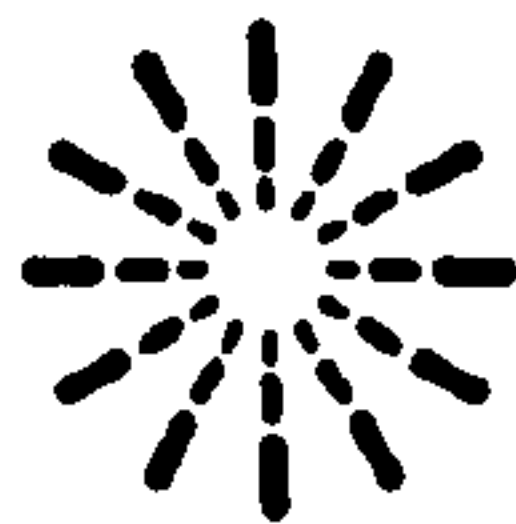
Photometric Solutions International Pty Ltd
Factory Two, 21-29 Railway Ave
Huntingdale, Vic, 3166, AUSTRALIA
Tel: +61 3 9568 1879
Fax: +61 3 9568 4667
www.PhotometricSolutions.com

Report Number:
Catalog Number:
Description: **Je-4**
Correction Factor Used: White

Date: 17/12/2009

TM5* Utilisation Factor Table

* Based on TM5, except using Min / Ave = 0.8 as Spacing Criteria
SHR < 0.5 - No UF Table or Graph can be Produced

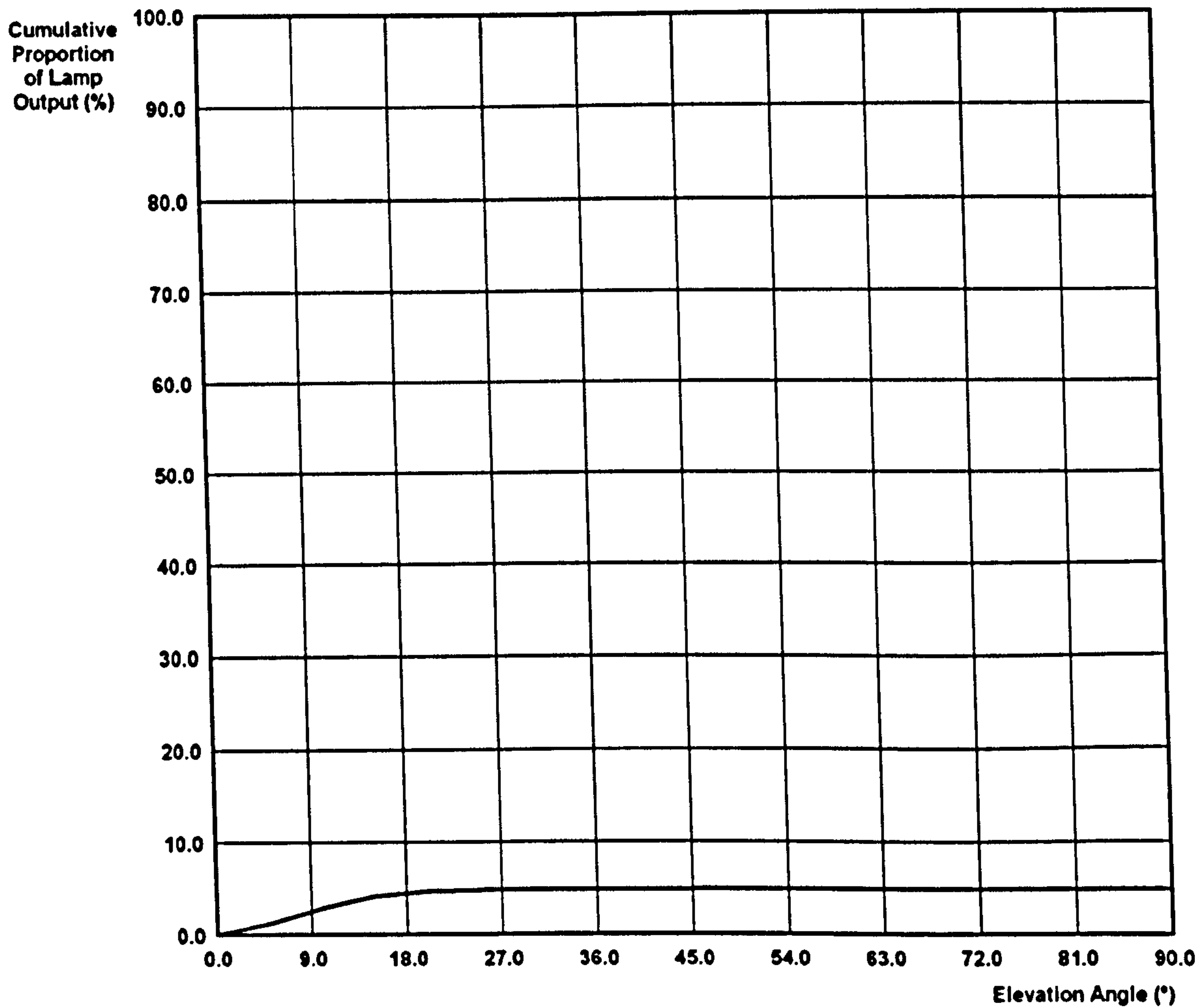


Photometric Solutions International Pty Ltd
Factory Two, 21-29 Railway Ave
Huntingdale, Vic, 3168, AUSTRALIA
Tel: +61 3 9568 1879
Fax: +61 3 9568 4667
www.PhotometricSolutions.com

Report Number:
Catalog Number:
Description: *Je-4*
Correction Factor Used: *White*

Date: 17/12/2009

Zonal Flux Diagram



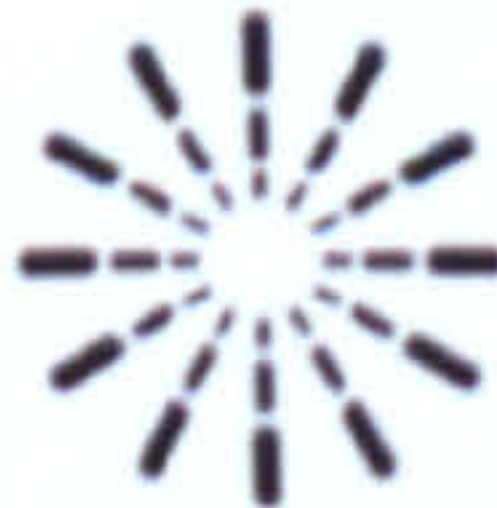
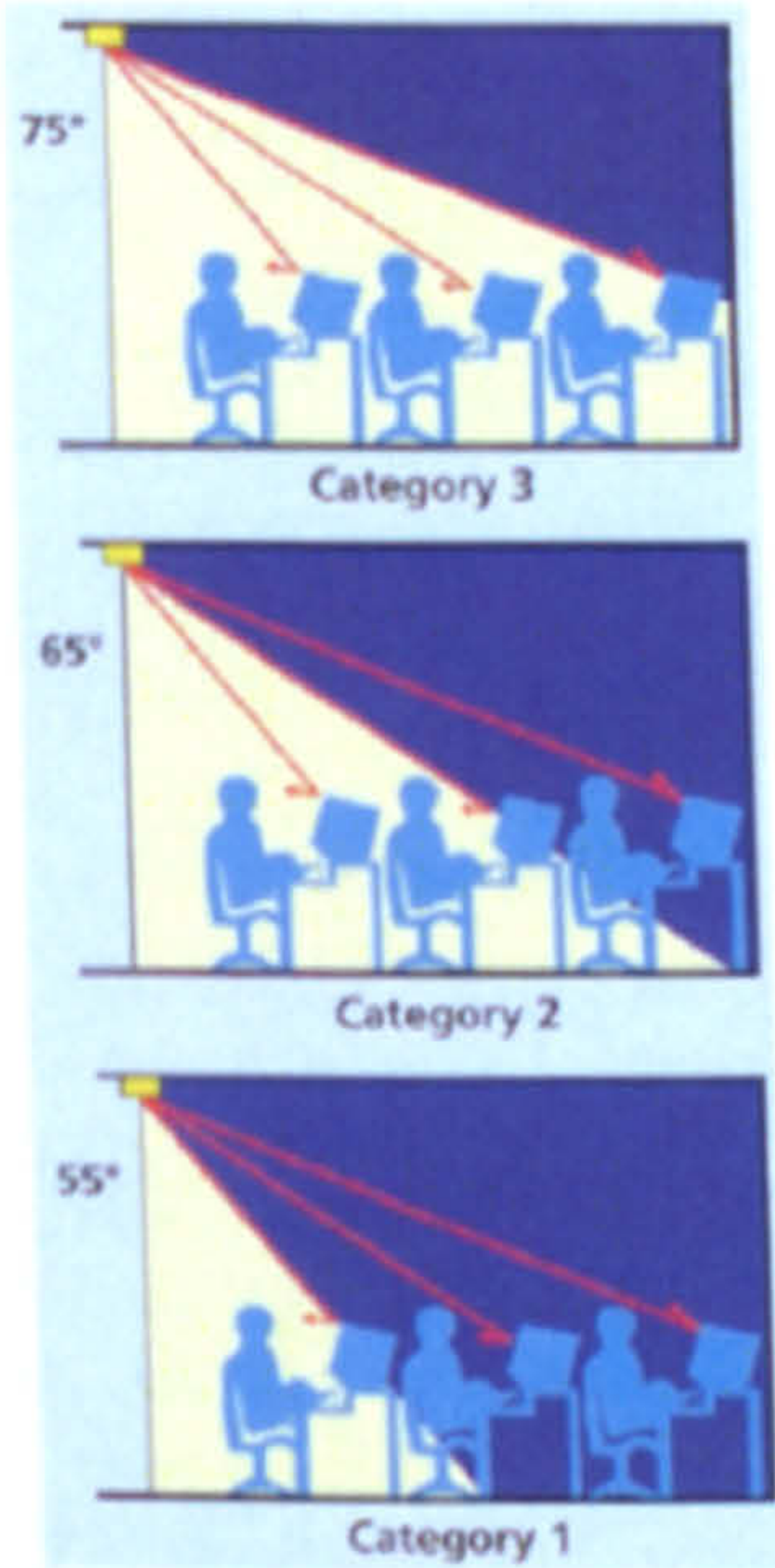
Photometric Solutions International Pty Ltd
Factory Two, 21-28 Railway Ave
Huntingdale, Vic, 3166, AUSTRALIA
Tel: +61 3 9568 1879
Fax: +61 3 9568 4667
www.PhotometricSolutions.com

Report Number:
Catalog Number:
Description: *je-6*
Correction Factor Used: White

Date: 17/12/2009

CIBSE LG3 VDT Category

	Category 1	Category 2	Category 3
Starting Gamma Angle (°):	55.0	65.0	75.0
Final Gamma Angle (°):	90.0	90.0	90.0
Avg Luminance Found (cd/m²):	1747	2072	2532
Max. Permissible (cd/m²):	200.0	200.0	200.0
Max Luminance Found (cd/m²):	12680	12680	12680
Max. Permissible (cd/m²):	500.0	500.0	500.0
Result:	-	-	-



Distribution Photometry Report

Report Number:

Date: 17/12/2009

Catalog Number:

Description: **Je-6**
Correction Factor Used: White

Filename: **Je-6.IES**

Results For: **Test Details**
Luminous Intensity Distribution
LID (Lowest 10%)
Luminous Intensity Data
Luminous Flux Data
Luminaire Luminance
IsoCandela Diagram
IsoLux Diagram
IsoLux 3D
Illuminance Grid
IESNA CoU Table
TM5 UF Table
TM5 UF Table (Variation)
Roadway UF Graph
Zonal Flux Diagram
Luminance Limiting Curve
CIBSE LG3 Rating
Photometric Solid

Page 1 of 23

PhotometricCentre v4.03 Copyright (C) Photometric Solutions International 2004-2008



Photometric Solutions International Pty Ltd
Factory Two, 21-29 Railway Ave
Huntingdale, Vic, 3166, AUSTRALIA
Tel: +61 3 9568 1879
Fax: +61 3 9568 4667
www.PhotometricSolutions.com

Report Number:
Catalog Number:
Description: *Je-6*
Correction Factor Used: White

Date: 17/12/2009

IESNA Coefficients of Utilisation Table

Ceiling Cavity Reflect.:	80%			70%			50%			30%			10%			0%
Wall Reflect.:	50%	30%	10%	50%	30%	10%	50%	30%	10%	50%	30%	10%	50%	30%	10%	0%
Room Cavity Ratio	Coefficients of Utilisation for 20% Effective Floor Cavity Reflectance															
0	0.02	0.02	0.02	0.02	0.02	0.02	0.02	0.02	0.02	0.02	0.02	0.02	0.02	0.02	0.02	0.02
1	0.02	0.02	0.02	0.02	0.02	0.02	0.02	0.02	0.02	0.02	0.02	0.02	0.02	0.02	0.01	0.01
2	0.02	0.01	0.01	0.02	0.01	0.01	0.01	0.01	0.01	0.01	0.01	0.01	0.01	0.01	0.01	0.01
3	0.01	0.01	0.01	0.01	0.01	0.01	0.01	0.01	0.01	0.01	0.01	0.01	0.01	0.01	0.01	0.01
4	0.01	0.01	0.01	0.01	0.01	0.01	0.01	0.01	0.01	0.01	0.01	0.01	0.01	0.01	0.01	0.01
5	0.01	0.01	0.01	0.01	0.01	0.01	0.01	0.01	0.01	0.01	0.01	0.01	0.01	0.01	0.01	0.01
6	0.01	0.01	0.01	0.01	0.01	0.01	0.01	0.01	0.01	0.01	0.01	0.01	0.01	0.01	0.01	0.01
7	0.01	0.01	0.01	0.01	0.01	0.01	0.01	0.01	0.00	0.01	0.01	0.00	0.01	0.01	0.00	0.00
8	0.01	0.01	0.00	0.01	0.01	0.00	0.01	0.01	0.00	0.01	0.01	0.00	0.01	0.01	0.00	0.00
9	0.01	0.01	0.00	0.01	0.01	0.00	0.01	0.00	0.00	0.01	0.00	0.00	0.01	0.00	0.00	0.00
10	0.01	0.00	0.00	0.01	0.00	0.00	0.01	0.00	0.00	0.01	0.00	0.00	0.01	0.00	0.00	0.00



Report Number:
Catalog Number:
Description: Je-6
Correction Factor Used: White

Date: 17/12/2009

Illumination Levels

y (m)																						
3.0	0.03	0.03	0.04	0.04	0.05	0.05	0.06	0.07	0.08	0.08	0.09	0.10	0.10	0.11	0.11	0.11	0.11	0.11	0.11	0.10	0.10	
	0.03	0.03	0.04	0.05	0.05	0.06	0.07	0.08	0.09	0.10	0.11	0.12	0.12	0.13	0.13	0.14	0.13	0.13	0.12	0.12	0.11	
2.4	0.03	0.04	0.04	0.05	0.06	0.07	0.08	0.09	0.10	0.11	0.13	0.14	0.15	0.15	0.16	0.16	0.16	0.15	0.14	0.13	0.12	
	0.03	0.04	0.05	0.06	0.07	0.08	0.09	0.11	0.12	0.13	0.15	0.17	0.17	0.18	0.19	0.18	0.18	0.17	0.16	0.15	0.14	
1.8	0.04	0.04	0.05	0.06	0.08	0.09	0.10	0.12	0.14	0.16	0.18	0.20	0.21	0.21	0.22	0.22	0.21	0.20	0.18	0.17	0.15	
	0.04	0.05	0.06	0.07	0.08	0.10	0.12	0.14	0.16	0.18	0.21	0.23	0.24	0.25	0.25	0.25	0.24	0.22	0.21	0.19	0.17	
1.2	0.04	0.05	0.06	0.07	0.09	0.11	0.13	0.16	0.18	0.21	0.24	0.26	0.28	0.29	0.29	0.28	0.27	0.25	0.22	0.20	0.18	
	0.04	0.05	0.06	0.08	0.10	0.12	0.14	0.17	0.20	0.23	0.26	0.29	0.31	0.32	0.32	0.31	0.29	0.27	0.24	0.21	0.19	
0.6	0.04	0.05	0.07	0.08	0.11	0.13	0.15	0.18	0.22	0.25	0.29	0.32	0.34	0.35	0.34	0.33	0.31	0.28	0.25	0.22	0.20	
	0.04	0.05	0.06	0.09	0.13	0.20	0.15	0.19	0.23	0.26	0.31	0.34	0.36	0.36	0.36	0.35	0.32	0.29	0.26	0.23	0.20	
0.0	0.04	0.05	0.06	0.09	0.14	0.22	0.16	0.19	0.23	0.26	0.31	0.35	0.36	0.37	0.37	0.35	0.33	0.30	0.26	0.23	0.20	
	0.04	0.05	0.07	0.10	0.14	0.16	0.16	0.19	0.23	0.26	0.31	0.33	0.36	0.37	0.37	0.35	0.32	0.29	0.26	0.23	0.20	
-0.6	0.04	0.05	0.07	0.09	0.12	0.14	0.16	0.18	0.22	0.25	0.29	0.32	0.34	0.35	0.35	0.33	0.31	0.28	0.25	0.22	0.20	
	0.04	0.05	0.07	0.08	0.13	0.19	0.16	0.18	0.21	0.24	0.27	0.30	0.32	0.33	0.32	0.31	0.29	0.27	0.24	0.21	0.19	
-1.2	0.04	0.05	0.06	0.08	0.12	0.14	0.14	0.16	0.19	0.21	0.24	0.27	0.28	0.29	0.29	0.28	0.27	0.25	0.22	0.20	0.18	
	0.04	0.05	0.06	0.08	0.10	0.13	0.13	0.15	0.17	0.19	0.21	0.23	0.25	0.26	0.26	0.25	0.24	0.22	0.20	0.19	0.17	
-1.8	0.04	0.05	0.05	0.07	0.10	0.11	0.11	0.13	0.14	0.17	0.19	0.20	0.21	0.22	0.22	0.22	0.21	0.20	0.18	0.17	0.15	
	0.04	0.04	0.05	0.06	0.09	0.13	0.10	0.11	0.13	0.14	0.16	0.17	0.18	0.19	0.19	0.19	0.18	0.18	0.16	0.15	0.14	
-2.4	0.03	0.04	0.05	0.06	0.08	0.11	0.09	0.10	0.11	0.12	0.14	0.15	0.16	0.16	0.16	0.16	0.16	0.15	0.15	0.14	0.12	
	0.03	0.04	0.04	0.05	0.08	0.10	0.09	0.09	0.09	0.11	0.12	0.13	0.13	0.14	0.14	0.14	0.14	0.13	0.13	0.12	0.11	
-3.0	0.03	0.03	0.04	0.05	0.07	0.08	0.08	0.07	0.08	0.09	0.10	0.11	0.11	0.12	0.12	0.12	0.12	0.12	0.11	0.11	0.10	
	-3.0	-2.4	-1.8	-1.2	-0.6	0.0	0.6	1.2	1.8	2.4	3.0											
																					x (m)	

Horizontal Illuminance
All Illuminance values in lux / 1000 lm
Table Average: 0.16 Table Maximum: 0.37 Table Minimum: 0.03
Mounting Height = 2.7 m

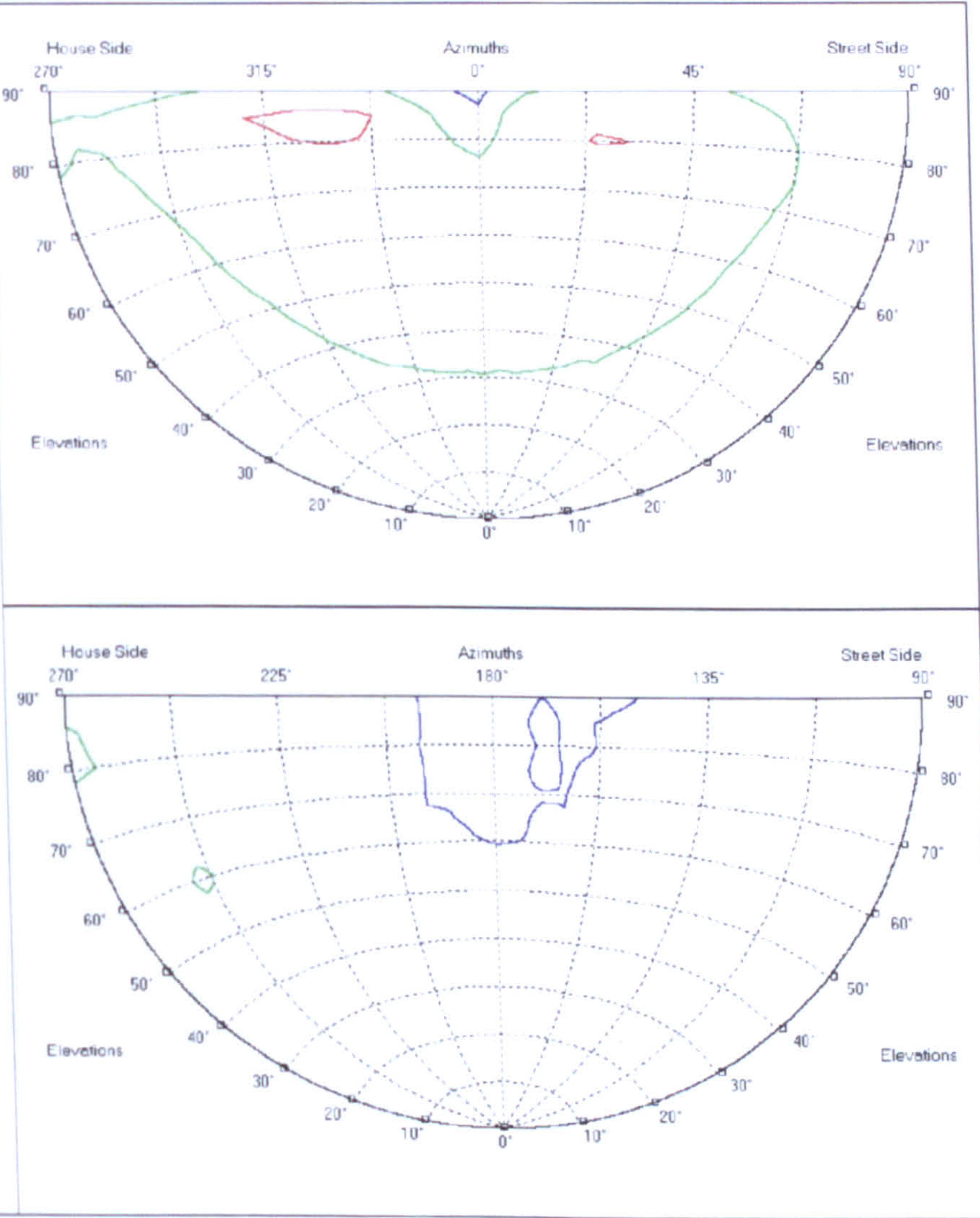


Photometric Solutions International Pty Ltd
Factory Two, 21-29 Railway Ave
Huntingdale, Vic, 3166, AUSTRALIA
Tel: +61 3 9568 1879
Fax: +61 3 9568 4667
www.PhotometricSolutions.com

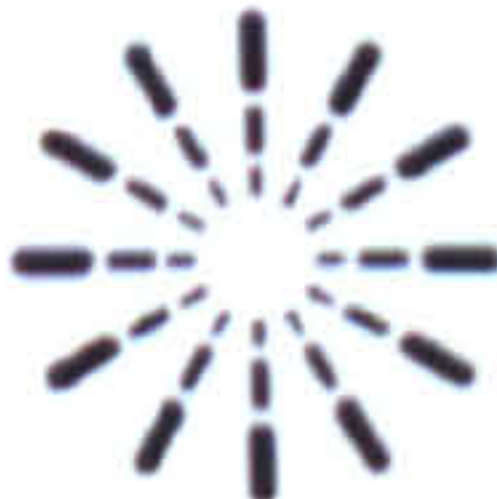
IsoCandela Diagram

Legend
(cd / 1000 lm)
Max = 7.9

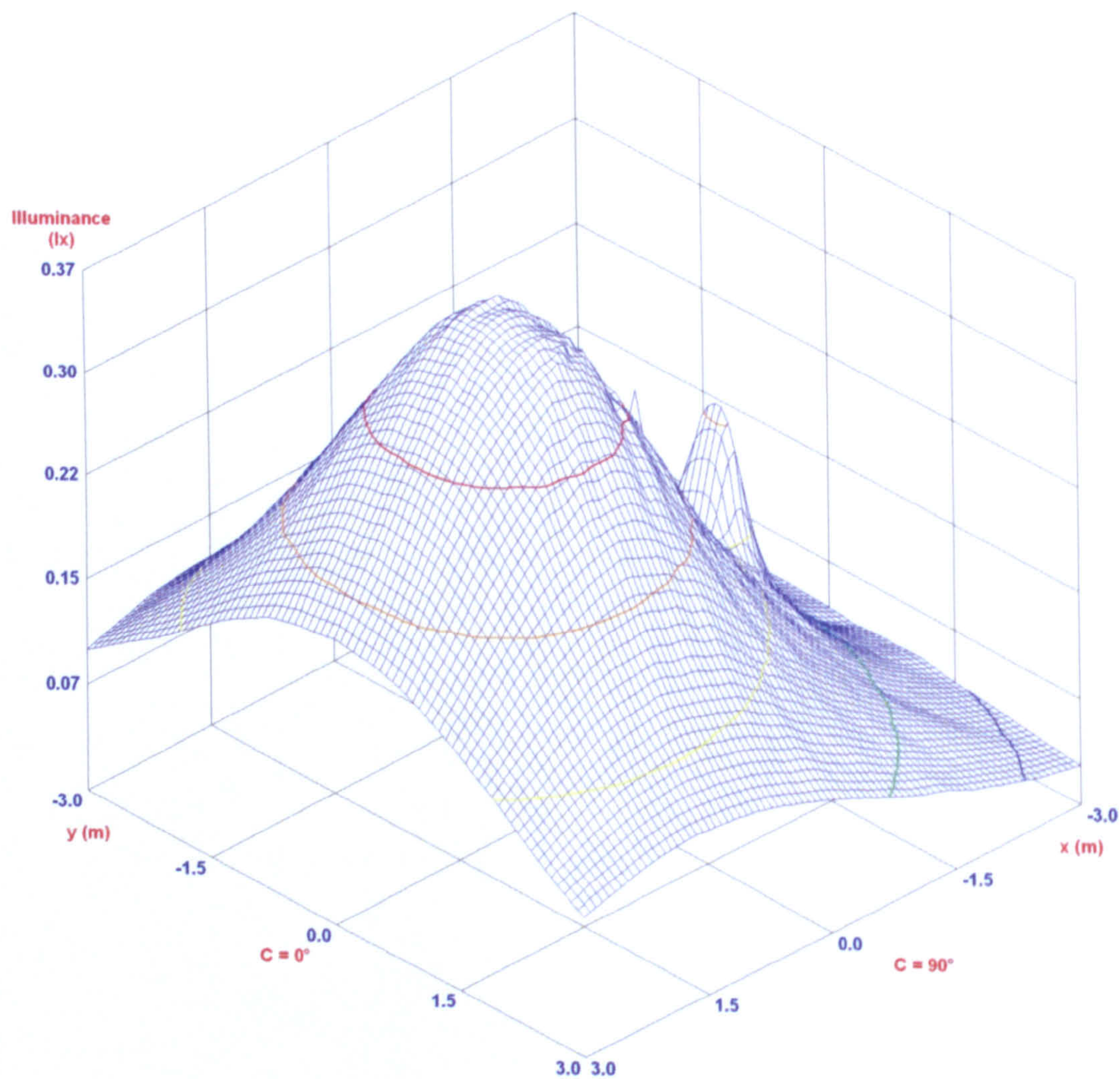
7.1 (90.0%)
3.9 (50.0%)
0.8 (10.0%)



All luminous intensity values in cd / 1000 lm



IsoLux 3D



Report Number:

Date: 17/12/2009

Catalog Number:

Description: je-6
Correction Factor Used: White

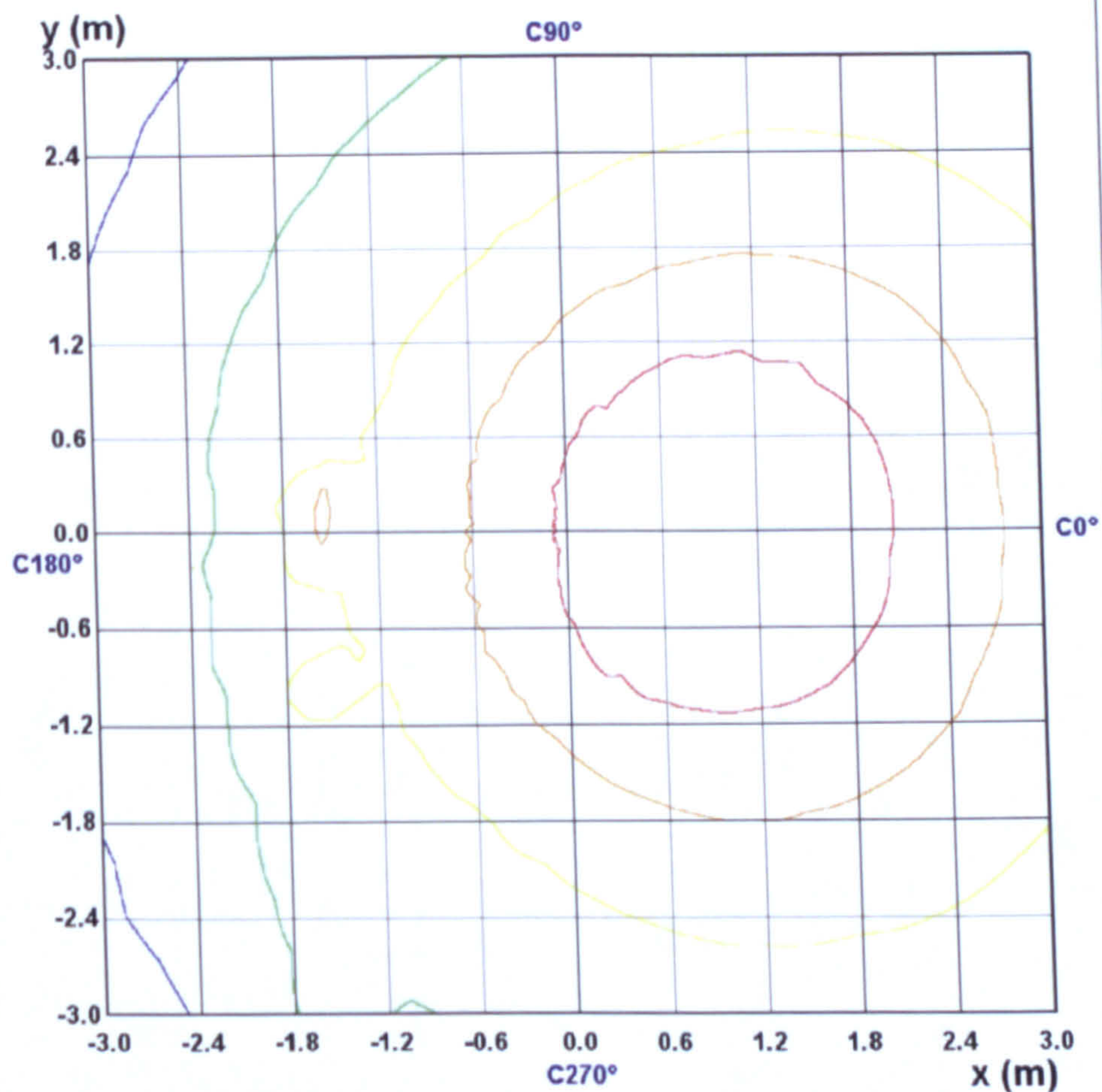
IsoLux Diagram

Legend

Max = 0.37

Height = 2.70 m

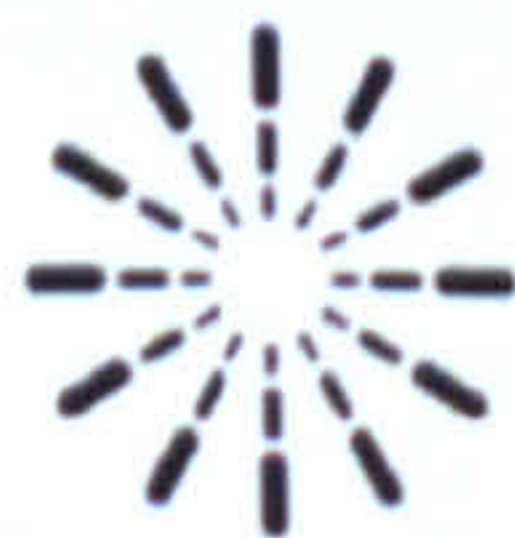
0.3	(80.0%)
0.2	(60.0%)
0.1	(40.0%)
0.1	(20.0%)
0.0	(10.0%)



All illuminance values in lx / 1000 lm

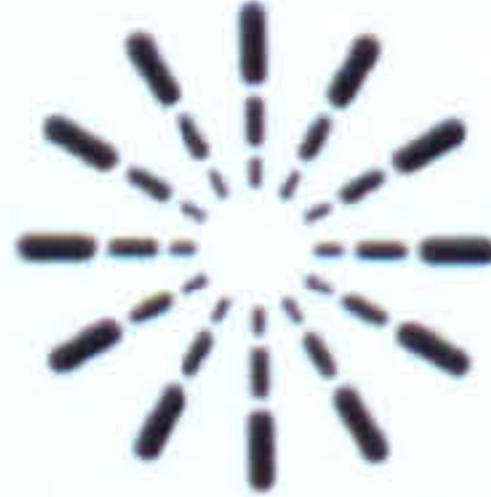
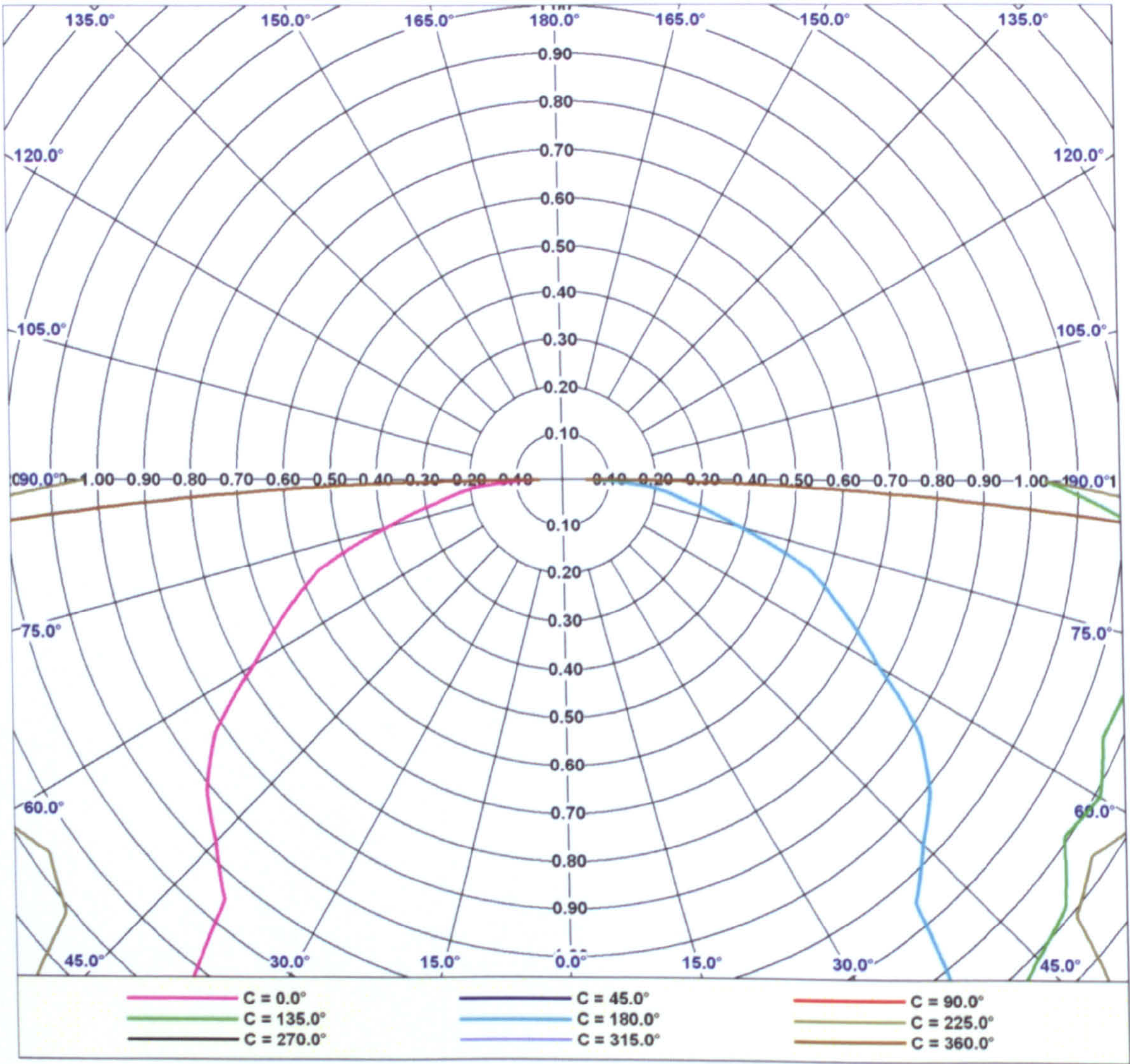
Page 13 of 23

PhotometricCentre v4.03 Copyright (C) Photometric Solutions International 2004-2008



Photometric Solutions International Pty Ltd
Factory Two, 21-29 Railway Ave
Huntingdale, Vic, 3166, AUSTRALIA
Tel: +61 3 9568 1879
Fax: +61 3 9568 4667
www.PhotometricSolutions.com

Luminous Intensity Distribution (Lowest 10%)



Report Number:
Catalog Number:
Description: *Je-6*
Correction Factor Used: White

Date: 17/12/2009

Average Luminance Table

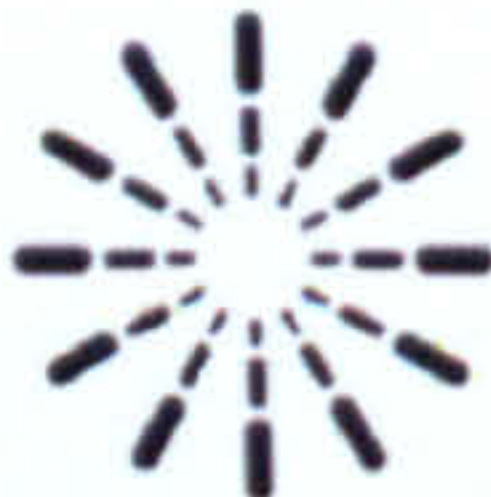
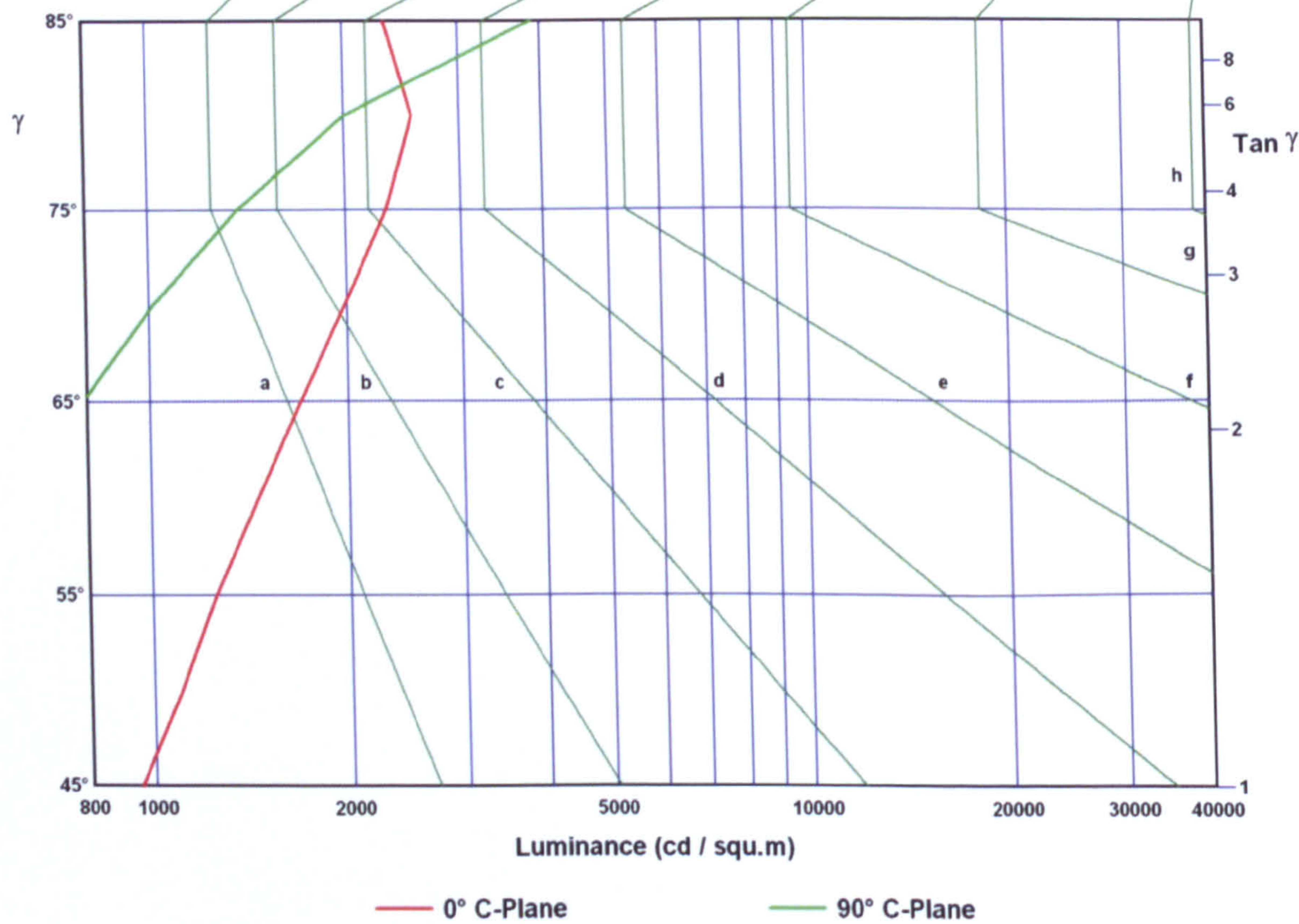
All luminance values expressed in cd / squ.m / 1000 lm

Azimuth: 0	45	90	135	180	235	270	315
Elevation							
0	317	317	317	317	317	317	317
45	949	804	452	281	213	561	484
55	1240	1100	552	317	226	385	599
65	1690	1700	786	420	220	516	863
75	2310	3210	1360	734	212	914	1660
85	2310	9110	3860	2020	307	2940	6910



Luminance Limiting Curve

Glare Rating	Quality Class	Service Values of Illuminance (lx)							
		2000	1000	500	<300	e	f	g	h
1.15	A								
1.5	B		2000	1000	500	<300			
1.85	C			2000	1000	500	<300		
2.2	D				2000	1000	500	<300	
2.55	E	a	b	c	d	2000	1000	500	<300



Report Number:
Catalog Number:
Description: Je-6
Correction Factor Used: White

Date: 17/12/2009

Luminous Flux Table

Elevation	Cone	Lumens	Cumulative	Lamp %	Luminaire %
0°	0.00° - 2.50°	0.0	0.0	0.0	0.1
5°	2.50° - 7.50°	0.1	0.1	0.0	0.7
10°	7.50° - 12.50°	0.2	0.3	0.0	1.8
15°	12.50° - 17.50°	0.3	0.7	0.1	3.6
20°	17.50° - 22.50°	0.4	1.1	0.1	6.1
25°	22.50° - 27.50°	0.6	1.7	0.2	9.2
30°	27.50° - 32.50°	0.7	2.4	0.2	13.0
35°	32.50° - 37.50°	0.8	3.2	0.3	17.5
40°	37.50° - 42.50°	0.9	4.1	0.4	22.6
45°	42.50° - 47.50°	1.1	5.2	0.5	28.4
50°	47.50° - 52.50°	1.2	6.4	0.6	34.8
55°	52.50° - 57.50°	1.3	7.6	0.8	41.8
60°	57.50° - 62.50°	1.4	9.0	0.9	49.5
65°	62.50° - 67.50°	1.5	10.5	1.1	57.6
70°	67.50° - 72.50°	1.6	12.1	1.2	66.4
75°	72.50° - 77.50°	1.7	13.9	1.4	76.0
80°	77.50° - 82.50°	1.9	15.7	1.6	86.2
85°	82.50° - 87.50°	1.9	17.6	1.8	96.5
90°	87.50° - 90.00°	0.6	18.3	1.8	100.0

Light Output Ratio = 1.8% (DLOR = 1.8% , ULOR = 0.0%)



Photometric Solutions International Pty Ltd
Factory Two, 21-29 Railway Ave
Huntingdale, Vic, 3166, AUSTRALIA
Tel: +61 3 9568 1879
Fax: +61 3 9568 4667
www.PhotometricSolutions.com

Report Number:
Catalog Number:
Description: *Je-6*
Correction Factor Used: White

Date: 17/12/2009

Luminous Intensity Table (cd / 1000 lm) (Continued)

$\gamma \setminus C$	320.0	325.0	330.0	335.0	340.0	345.0	350.0	355.0	360.0
0.0	2.3	2.3	2.3	2.3	2.3	2.3	2.3	2.3	2.3
5.0	2.5	2.4	2.4	2.5	2.5	2.5	2.5	2.5	2.5
10.0	2.7	2.7	2.7	2.7	2.7	2.7	2.7	2.7	2.7
15.0	2.8	2.9	2.9	2.9	3.0	3.0	3.0	3.0	3.0
20.0	3.0	3.1	3.1	3.2	3.3	3.3	3.2	3.3	3.3
25.0	3.3	3.4	3.4	3.5	3.5	3.6	3.6	3.6	3.6
30.0	3.5	3.6	3.7	3.7	3.8	3.9	3.9	3.9	3.9
35.0	3.8	3.9	4.0	4.0	4.1	4.2	4.2	4.2	4.2
40.0	4.0	4.2	4.2	4.4	4.4	4.5	4.5	4.5	4.5
45.0	4.3	4.4	4.5	4.6	4.7	4.7	4.8	4.7	4.8
50.0	4.5	4.6	4.8	4.9	5.0	5.0	5.0	5.0	5.0
55.0	4.8	4.8	5.0	5.1	5.1	5.2	5.2	5.0	5.1
60.0	5.0	5.2	5.3	5.4	5.4	5.4	5.3	5.1	5.2
65.0	5.3	5.5	5.6	5.7	5.6	5.5	5.3	5.1	5.1
70.0	5.7	5.9	6.0	6.0	5.9	5.6	5.3	5.0	4.8
75.0	6.3	6.4	6.4	6.4	6.2	5.9	5.2	4.6	4.2
80.0	6.9	7.1	7.1	7.0	6.6	5.9	4.9	3.8	3.1
85.0	7.7	7.9	7.8	7.5	6.8	5.4	4.0	2.5	1.4
90.0	4.8	5.0	4.9	4.6	4.2	3.0	2.2	0.9	0.1

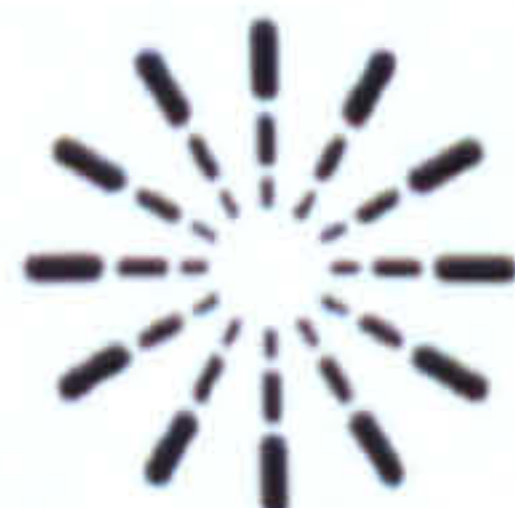
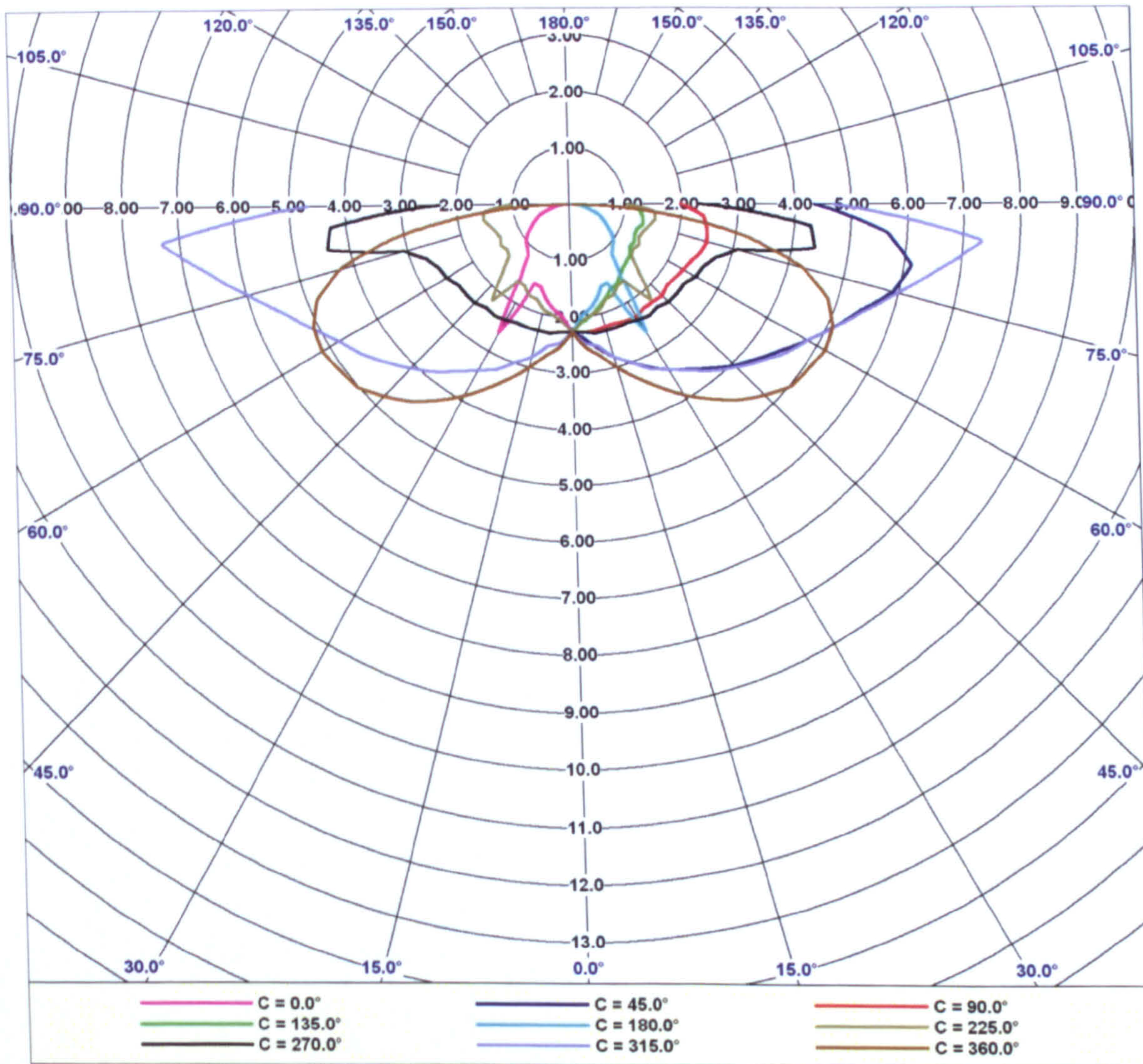


Photometric Solutions International Pty Ltd
Factory Two, 21-29 Railway Ave
Huntingdale, Vic, 3166, AUSTRALIA
Tel: +61 3 9568 1879
Fax: +61 3 9568 4667
www.PhotometricSolutions.com

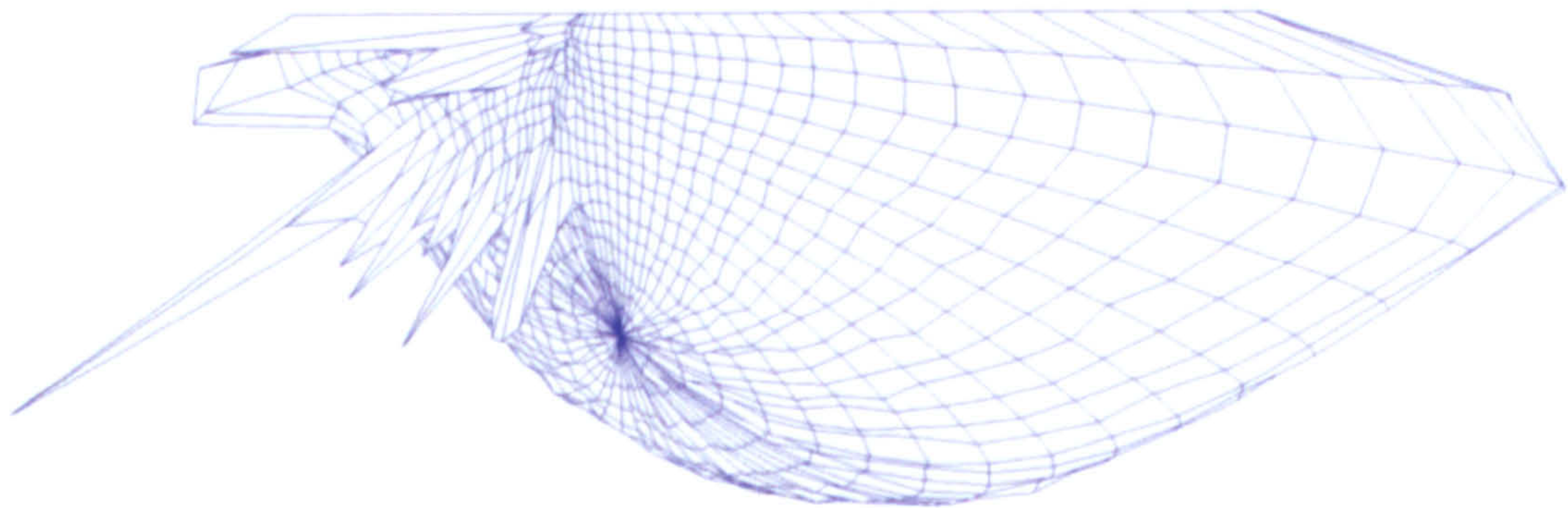
Report Number:
Catalog Number:
Description: Je-6
Correction Factor Used: White

Date: 17/12/2009

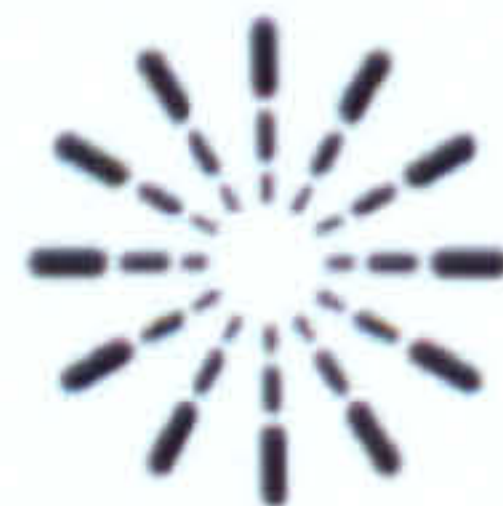
Luminous Intensity Distribution



Photometric Solid



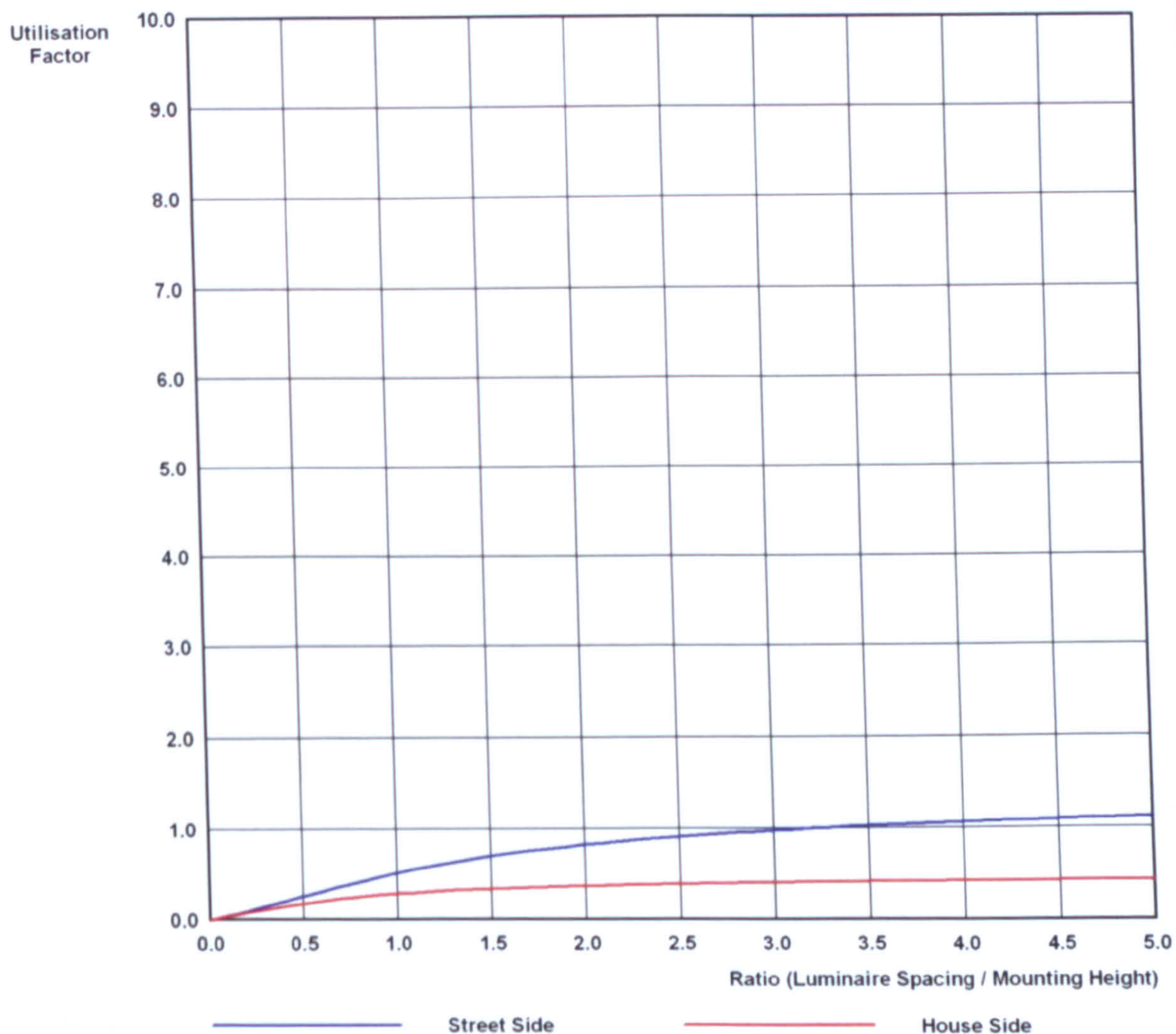
Viewing Angle: C = 315°



Report Number:
Catalog Number:
Description: *je-6*
Correction Factor Used: White

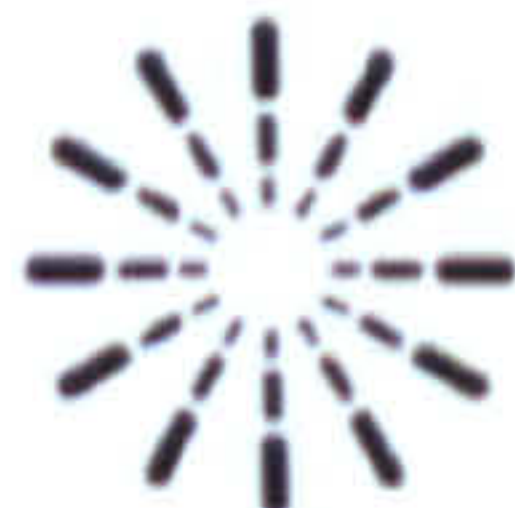
Date: 17/12/2009

Roadway Utilisation Factor Graph



Page 19 of 23

PhotometricCentre v4.03 Copyright (C) Photometric Solutions International 2004-2008



Photometric Solutions International Pty Ltd
Factory Two, 21-29 Railway Ave
Huntingdale, Vic, 3166, AUSTRALIA
Tel: +61 3 9568 1879
Fax: +61 3 9568 4667
www.PhotometricSolutions.com

Report Number:
Catalog Number:
Description: *Je-6*
Correction Factor Used: White

Date: 17/12/2009

Luminaire Details

Luminaire Test Details:

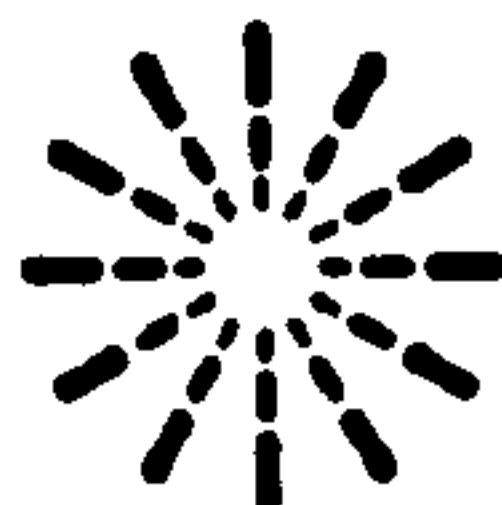
Photometry Type:	<i>Type C/Gamma</i>
Number of Lamps:	<i>1</i>
Lumens per Lamp:	<i>1000</i>

Luminous Dimensions:

Base Area:	<i>0.025 m X 0.290 m</i>
Side Area:	<i>N/A</i>
End Area:	<i>N/A</i>
Luminous Shape:	<i>2D Rectangle</i>

Page 2 of 23

PhotometricCentre v4.03 Copyright (C) Photometric Solutions International 2004-2008



Photometric Solutions International Pty Ltd
Factory Two, 21-29 Railway Ave
Huntingdale, Vic, 3166, AUSTRALIA
Tel: +61 3 9568 1879
Fax: +61 3 9568 4667
www.PhotometricSolutions.com

Report Number:
Catalog Number:
Description: *Je-6*
Correction Factor Used: White

Date: 17/12/2009

TM5 Utilisation Factor Table

SHR < 0.5 - No UF Table or Graph can be Produced



Report Number:
Catalog Number:
Description: *Je-6*
Correction Factor Used: White

Date: 17/12/2009

TM5* Utilisation Factor Table

* Based on TM5, except using Min / Ave = 0.8 as Spacing Criteria
SHR < 0.5 - No UF Table or Graph can be Produced



Photometric Solutions International Pty Ltd
Factory Two, 21-29 Railway Ave
Huntingdale, Vic, 3168, AUSTRALIA
Tel: +61 3 9568 1878
Fax: +61 3 9568 4667
www.PhotometricSolutions.com

Zonal Flux Diagram

